

Averages of b -hadron, c -hadron, and τ -lepton properties as of early 2012

Heavy Flavor Averaging Group (HFAG):

Y. Amhis¹, Sw. Banerjee², R. Bernhard³, S. Blyth⁴, A. Bozek⁵, C. Bozzi⁶,
A. Carbone^{7,8}, A. Oyanguren Campos⁹, R. Chistov¹⁰, G. Cibinetto⁶,
J. Coleman¹¹, J. Dingfelder¹², W. Dungel¹³, M. Gersabeck¹⁴,
T. J. Gershon^{14,15}, L. Gibbons¹⁶, B. Golob¹⁷, R. Harr¹⁸, K. Hayasaka¹⁹,
H. Hayashii²⁰, O. Leroy²¹, D. Lopes Pegna²², R. Louvot²³, A. Lusiani²⁴,
V. Lüth²⁵, B. Meadows²⁶, S. Nishida²⁷, M. Patel²⁸, D. Pedrini²⁹, M. Rama³⁰,
M. Roney², M. Rotondo³¹, O. Schneider²³, C. Schwanda¹³, A. J. Schwartz²⁵,
B. Shwartz³², J. G. Smith³³, R. Tesarek³⁴, D. Tonelli^{14,34}, K. Trabelsi²⁶,
P. Urquijo¹², and R. Van Kooten³⁵

¹*LAL, Université Paris-Sud, France*

²*University of Victoria, Canada*

³*University of Freiburg, Germany*

⁴*National United University, Taiwan*

⁵*H. Niewodniczanski Institute of Nuclear Physics, Krakow, Poland*

⁶*INFN Ferrara, Italy*

⁷*INFN Bologna, Italy*

⁸*Università di Bologna, Italy*

⁹*IFIC, University of Valencia, Spain*

¹⁰*Institute for Theoretical and Experimental Physics, Russia*

¹¹*University of Liverpool, UK*

¹²*Bonn University, Germany*

¹³*Austrian Academy of Sciences, Austria*

¹⁴*European Organization for Nuclear Research (CERN), Switzerland*

¹⁵*University of Warwick, UK*

¹⁶*Cornell University, USA*

¹⁷*University of Ljubljana, Slovenia*

¹⁸*Wayne State University, USA*

¹⁹*Nagoya University, Japan*

²⁰*Nara Women's University, Japan*

²¹*CPPM, Aix-Marseille Université, CNRS/IN2P3, Marseille, France*

²²*Princeton University, USA*

²³*Ecole Polytechnique Fédérale de Lausanne (EPFL), Switzerland*

²⁴*Scuola Normale Superiore and INFN, Pisa, Italy*

²⁵*SLAC National Accelerator Laboratory, USA*

²⁶*University of Cincinnati, USA*

²⁷*KEK, Tsukuba, Japan*

²⁸*Imperial College London, UK*

²⁹*INFN Milano-Bicocca, Italy*

³⁰*INFN Frascati, Italy*

³¹*INFN Padova, Italy*

³²*Budker Institute of Nuclear Physics, Russia*

³³*University of Colorado, USA*

³⁴*Fermilab, USA*

³⁵*Indiana University, USA*

May 9, 2013

Abstract

This article reports world averages of measurements of b -hadron, c -hadron, and τ -lepton properties obtained by the Heavy Flavor Averaging Group (HFAG) using results available through the end of 2011. In some cases results available in the early part of 2012 are included. For the averaging, common input parameters used in the various analyses are adjusted (rescaled) to common values, and known correlations are taken into account. The averages include branching fractions, lifetimes, neutral meson mixing parameters, CP violation parameters, parameters of semileptonic decays and CKM matrix elements.

Contents

1	Introduction	6
2	Methodology	7
3	b-hadron production fractions, lifetimes and mixing parameters	15
3.1	b -hadron production fractions	15
3.1.1	b -hadron production fractions in $\Upsilon(4S)$ decays	15
3.1.2	b -hadron production fractions in $\Upsilon(5S)$ decays	17
3.1.3	b -hadron production fractions at high energy	19
3.2	b -hadron lifetimes	24
3.2.1	Lifetime measurements, uncertainties and correlations	25
3.2.2	Inclusive b -hadron lifetimes	26
3.2.3	B^0 and B^+ lifetimes and their ratio	29
3.2.4	B_s^0 lifetimes	30
3.2.5	B_c^+ lifetime	33
3.2.6	Λ_b^0 and b -baryon lifetimes	33
3.2.7	Summary and comparison with theoretical predictions	35
3.3	Neutral B -meson mixing	37
3.3.1	B^0 mixing parameters $\Delta\Gamma_d$ and Δm_d	37
3.3.2	B_s^0 mixing parameters $\Delta\Gamma_s$ and Δm_s	42
3.3.3	CP violation in B^0 and B_s^0 mixing	46
3.3.4	Mixing-induced CP violation in B_s^0 decays	51
4	Measurements related to Unitarity Triangle angles	54
4.1	Introduction	54
4.2	Notations	56
4.2.1	CP asymmetries	56
4.2.2	Time-dependent CP asymmetries in decays to CP eigenstates	56
4.2.3	Time-dependent distributions with non-zero decay width difference	57
4.2.4	Time-dependent CP asymmetries in decays to vector-vector final states	58
4.2.5	Time-dependent asymmetries: self-conjugate multiparticle final states	59
4.2.6	Time-dependent CP asymmetries in decays to non- CP eigenstates	62
4.2.7	Asymmetries in $B \rightarrow D^{(*)}K^{(*)}$ decays	67
4.3	Common inputs and error treatment	70
4.4	Time-dependent asymmetries in $b \rightarrow c\bar{c}s$ transitions	72
4.4.1	Time-dependent CP asymmetries in $b \rightarrow c\bar{c}s$ decays to CP eigenstates	72
4.4.2	Time-dependent transversity analysis of $B^0 \rightarrow J/\psi K^{*0}$	73
4.4.3	Time-dependent CP asymmetries in $B^0 \rightarrow D^{*+}D^{*-}K_s^0$ decays	74
4.4.4	Time-dependent analysis of $B_s^0 \rightarrow J/\psi\phi$	74
4.5	Time-dependent CP asymmetries in colour-suppressed $b \rightarrow c\bar{u}d$ transitions	76
4.6	Time-dependent CP asymmetries in charmless $b \rightarrow q\bar{q}s$ transitions	78
4.6.1	Time-dependent CP asymmetries: $b \rightarrow q\bar{q}s$ decays to CP eigenstates	78
4.6.2	Time-dependent Dalitz plot analyses: $B^0 \rightarrow K^+K^-K^0$ and $B^0 \rightarrow \pi^+\pi^-K_s^0$	79
4.6.3	Time-dependent analyses of $B^0 \rightarrow \phi K_s^0\pi^0$	81
4.6.4	Time-dependent CP asymmetries in $B_s^0 \rightarrow K^+K^-$	84

4.7	Time-dependent CP asymmetries in $b \rightarrow c\bar{c}d$ transitions	88
4.8	Time-dependent CP asymmetries in $b \rightarrow q\bar{q}d$ transitions	93
4.9	Time-dependent asymmetries in $b \rightarrow s\gamma$ transitions	94
4.10	Time-dependent asymmetries in $b \rightarrow d\gamma$ transitions	95
4.11	Time-dependent CP asymmetries in $b \rightarrow u\bar{u}d$ transitions	97
4.12	Time-dependent CP asymmetries in $b \rightarrow c\bar{u}d/u\bar{c}d$ transitions	104
4.13	Time-dependent CP asymmetries in $b \rightarrow c\bar{u}s/u\bar{c}s$ transitions	105
4.14	Rates and asymmetries in $B^\mp \rightarrow D^{(*)}K^{(*)\mp}$ decays	107
4.14.1	D decays to CP eigenstates	107
4.14.2	D decays to suppressed final states	107
4.14.3	D decays to multiparticle self-conjugate final states	108
5	Semileptonic B decays	116
5.1	Exclusive CKM-favored decays	116
5.1.1	$\bar{B} \rightarrow D^*\ell^-\bar{\nu}_\ell$	116
5.1.2	$\bar{B} \rightarrow D\ell^-\bar{\nu}_\ell$	119
5.1.3	$\bar{B} \rightarrow D^{(*)}\pi\ell^-\bar{\nu}_\ell$	122
5.1.4	$\bar{B} \rightarrow D^{**}\ell^-\bar{\nu}_\ell$	124
5.2	Inclusive CKM-favored decays	127
5.2.1	Global analysis of $\bar{B} \rightarrow X_c\ell^-\bar{\nu}_\ell$	127
5.2.2	Analysis in the kinetic scheme	128
5.2.3	Analysis in the 1S scheme	129
5.3	Exclusive CKM-suppressed decays	130
5.4	Inclusive CKM-suppressed decays	132
5.4.1	BLNP	134
5.4.2	DGE	134
5.4.3	GGOU	135
5.4.4	ADFR	136
5.4.5	BLL	138
5.4.6	Summary	138
6	B decays to charmed hadrons	143
7	B decays to charmless final states	193
7.1	Mesonic charmless decays	193
7.2	Radiative and leptonic decays	201
7.3	$B \rightarrow X_s\gamma$	204
7.4	Baryonic decays	206
7.5	B_s decays	209
7.6	Charge asymmetries	209
7.7	Polarization measurements	214
8	D decays	217
8.1	D^0 - \bar{D}^0 mixing and CP violation	217
8.1.1	Introduction	217
8.1.2	Input observables	218
8.1.3	Fit results	218

8.1.4	Conclusions	220
8.2	Semileptonic decays	230
8.2.1	Introduction	230
8.2.2	$D \rightarrow P\bar{\ell}\nu_\ell$ decays	230
8.2.3	Form factor parameterizations	230
8.2.4	Experimental techniques and results	232
8.2.5	$D \rightarrow V\bar{\ell}\nu_\ell$ decays	234
8.2.6	S -wave component	237
8.2.7	Model-independent form factor measurement	237
8.2.8	Detailed measurements of the $D^+ \rightarrow K^-\pi^+e^+\nu_e$ decay channel	238
8.3	CP asymmetries	245
8.4	T -violating asymmetries	249
8.5	World average for the D_s^+ decay constant f_{D_s}	250
8.6	Two-body hadronic D^0 decays and final state radiation	254
8.6.1	Branching fraction corrections	254
8.6.2	Average branching fractions	257
8.7	Direct CP violation	261
8.8	Charm baryons	264
8.9	Rare and forbidden decays	267
9	Tau lepton properties	276
9.1	Branching fractions fit	276
9.1.1	Correlation between base nodes uncertainties	284
9.1.2	Equality constraints	287
9.1.3	Fit procedure	289
9.2	Tests of lepton universality	289
9.3	Universality improved $B(\tau \rightarrow e\nu\bar{\nu})$ and R_{had}	290
9.4	$ V_{us} $ measurement	290
9.4.1	Inclusive tau partial width to strange	291
9.4.2	$ V_{us} $ from $B(\tau \rightarrow K\nu)/B(\tau \rightarrow \pi\nu)$ and from $B(\tau \rightarrow K\nu)$	291
9.4.3	$ V_{us} $ from tau summary	293
9.5	Upper limits on tau LFV branching fractions	293
10	Summary	298
11	Acknowledgments	302

1 Introduction

Flavor dynamics is an important element in understanding the nature of particle physics. The accurate knowledge of properties of heavy flavor hadrons, especially b hadrons, plays an essential role for determining the elements of the Cabibbo-Kobayashi-Maskawa (CKM) weak-mixing matrix [1, 2]. The operation of the Belle and BABAR $e^+e^- B$ factory experiments led to a large increase in the size of available B meson, D hadron and τ lepton samples, enabling dramatic improvement in the accuracies of related measurements. The CDF and D0 experiments at the Fermilab Tevatron have also provided important results in heavy flavor physics, most notably in the B_s^0 sector. The CERN Large Hadron Collider is now delivering high luminosity, enabling the collection of even higher statistics samples of b and c hadrons at the ATLAS, CMS, and (especially) LHCb experiments.

The Heavy Flavor Averaging Group (HFAG) was formed in 2002 to continue the activities of the LEP Heavy Flavor Steering group [3]. This group was responsible for calculating averages of measurements of b -flavor related quantities. HFAG has evolved since its inception and currently consists of seven subgroups:

- the “ B Lifetime and Oscillations” subgroup provides averages for b -hadron lifetimes, b -hadron fractions in $\Upsilon(4S)$ decay and $p\bar{p}$ collisions, and various parameters governing B^0 - \bar{B}^0 and B_s^0 - \bar{B}_s^0 mixing;
- the “Unitarity Triangle Parameters” subgroup provides averages for time-dependent CP asymmetry parameters and resulting determinations of the angles of the CKM unitarity triangle;
- the “Semileptonic B Decays” subgroup provides averages for inclusive and exclusive B -decay branching fractions, and subsequent determinations of the CKM matrix elements $|V_{cb}|$ and $|V_{ub}|$;
- the “ B to Charm Decays” subgroup provides averages of branching fractions for B decays to final states involving open charm or charmonium mesons;
- the “Rare Decays” subgroup provides averages of branching fractions and CP asymmetries for charmless, radiative, leptonic, and baryonic B meson decays;
- the “Charm Physics” subgroup provides averages of branching fractions for D meson hadronic and semileptonic decays, averages of D^0 - \bar{D}^0 mixing and CP and T violation parameters, and an average value for the D_s decay constant f_{D_s} . The subgroup also documents properties of charm baryons, and upper limits for rare and forbidden D^0 , $D_{(s)}^+$, and A_c^+ decays.
- the “Tau Physics” subgroup provides documentation and averages for the τ lepton branching fractions and the resulting determination of the CKM matrix element $|V_{us}|$, and documents upper limits for τ lepton-flavor-violating decays.

The “Lifetime and Oscillations” and “Semileptonic” subgroups were formed from the merger of four LEP working groups. The “Unitarity Triangle,” “ B to Charm Decays,” and “Rare Decays” subgroups were formed to provide averages for new results obtained from the B factory experiments (and now also from the Fermilab Tevatron and CERN LHC experiments). The

“Charm” and “Tau” subgroups were formed more recently in response to the wealth of new data concerning D and τ decays. Subgroup typically include representatives from Belle and BABAR and, when relevant, CLEO, CDF, D0 and LHCb.

This article is an update of the last HFAG preprint, which used results available at least through the end of 2009 [4]. Here we report world averages using results available at least through the end of 2011. In some cases results available in the early part of 2012 have been included.¹ In general, we use all publicly available results that have written documentation. These include preliminary results presented at conferences or workshops. However, we do not use preliminary results that remain unpublished for an extended period of time, or for which no publication is planned. Close contacts have been established between representatives from the experiments and members of subgroups that perform averaging to ensure that the data are prepared in a form suitable for combinations.

In the case of obtaining a world average for which $\chi^2/\text{dof} > 1$, where dof is the number of degrees of freedom in the average calculation, we do not scale the resulting error, as is presently done by the Particle Data Group [5]. Rather, we examine the systematics of each measurement to better understand them. Unless we find possible systematic discrepancies between the measurements, we do not apply any additional correction to the calculated error. We provide the confidence level of the fit as an indicator for the consistency of the measurements included in the average. In case some special treatment was necessary to calculate an average, or if an approximation used in an average calculation might not be sufficiently accurate (*e.g.*, assuming Gaussian errors when the likelihood function indicates non-Gaussian behavior), we include a warning message.

Chapter 2 describes the methodology used for calculating averages. In the averaging procedure, common input parameters used in the various analyses are adjusted (rescaled) to common values, and, where possible, known correlations are taken into account. Chapters 3–9 present world average values from each of the subgroups listed above. A brief summary of the averages presented is given in Chapter 10. A complete listing of the averages and plots, including updates since this document was prepared, are also available on the HFAG web site:

<http://www.slac.stanford.edu/xorg/hfag>

2 Methodology

The general averaging problem that HFAG faces is to combine information provided by different measurements of the same parameter to obtain our best estimate of the parameter’s value and uncertainty. The methodology described here focuses on the problems of combining measurements performed with different systematic assumptions and with potentially-correlated systematic uncertainties. Our methodology relies on the close involvement of the people performing the measurements in the averaging process.

Consider two hypothetical measurements of a parameter x , which might be summarized as

$$\begin{aligned} x &= x_1 \pm \delta x_1 \pm \Delta x_{1,1} \pm \Delta x_{2,1} \dots \\ x &= x_2 \pm \delta x_2 \pm \Delta x_{1,2} \pm \Delta x_{2,2} \dots , \end{aligned}$$

¹ The precise cut-off date for including results in the averages varies between subgroups.

where the δx_k are statistical uncertainties, and the $\Delta x_{i,k}$ are contributions to the systematic uncertainty. One popular approach is to combine statistical and systematic uncertainties in quadrature

$$\begin{aligned}x &= x_1 \pm (\delta x_1 \oplus \Delta x_{1,1} \oplus \Delta x_{2,1} \oplus \dots) \\x &= x_2 \pm (\delta x_2 \oplus \Delta x_{1,2} \oplus \Delta x_{2,2} \oplus \dots)\end{aligned}$$

and then perform a weighted average of x_1 and x_2 , using their combined uncertainties, as if they were independent. This approach suffers from two potential problems that we attempt to address. First, the values of the x_k may have been obtained using different systematic assumptions. For example, different values of the B^0 lifetime may have been assumed in separate measurements of the oscillation frequency Δm_d . The second potential problem is that some contributions of the systematic uncertainty may be correlated between experiments. For example, separate measurements of Δm_d may both depend on an assumed Monte-Carlo branching fraction used to model a common background.

The problems mentioned above are related since, ideally, any quantity y_i that x_k depends on has a corresponding contribution $\Delta x_{i,k}$ to the systematic error which reflects the uncertainty Δy_i on y_i itself. We assume that this is the case and use the values of y_i and Δy_i assumed by each measurement explicitly in our averaging (we refer to these values as $y_{i,k}$ and $\Delta y_{i,k}$ below). Furthermore, since we do not lump all the systematics together, we require that each measurement used in an average have a consistent definition of the various contributions to the systematic uncertainty. Different analyses often use different decompositions of their systematic uncertainties, so achieving consistent definitions for any potentially correlated contributions requires close coordination between HFAG and the experiments. In some cases, a group of systematic uncertainties must be combined to obtain a coarser description that is consistent between measurements. Systematic uncertainties that are uncorrelated with any other sources of uncertainty appearing in an average are lumped together with the statistical error, so that the only systematic uncertainties treated explicitly are those that are correlated with at least one other measurement via a consistently-defined external parameter y_i . When asymmetric statistical or systematic uncertainties are quoted, we symmetrize them since our combination method implicitly assumes parabolic likelihoods for each measurement.

The fact that a measurement of x is sensitive to the value of y_i indicates that, in principle, the data used to measure x could equally-well be used for a simultaneous measurement of x and y_i , as illustrated by the large contour in Fig. 1(a) for a hypothetical measurement. However, we often have an external constraint Δy_i on the value of y_i (represented by the horizontal band in Fig. 1(a)) that is more precise than the constraint $\sigma(y_i)$ from our data alone. Ideally, in such cases we would perform a simultaneous fit to x and y_i , including the external constraint, obtaining the filled (x, y) contour and corresponding dashed one-dimensional estimate of x shown in Fig. 1(a). Throughout, we assume that the external constraint Δy_i on y_i is Gaussian.

In practice, the added technical complexity of a constrained fit with extra free parameters is not justified by the small increase in sensitivity, as long as the external constraints Δy_i are sufficiently precise when compared with the sensitivities $\sigma(y_i)$ to each y_i of the data alone. Instead, the usual procedure adopted by the experiments is to perform a baseline fit with all y_i fixed to nominal values $y_{i,0}$, obtaining $x = x_0 \pm \delta x$. This baseline fit neglects the uncertainty due to Δy_i , but this error can be mostly recovered by repeating the fit separately for each external parameter y_i with its value fixed at $y_i = y_{i,0} + \Delta y_i$ to obtain $x = \tilde{x}_{i,0} \pm \delta \tilde{x}$, as illustrated in Fig. 1(b). The absolute shift, $|\tilde{x}_{i,0} - x_0|$, in the central value of x is what the experiments

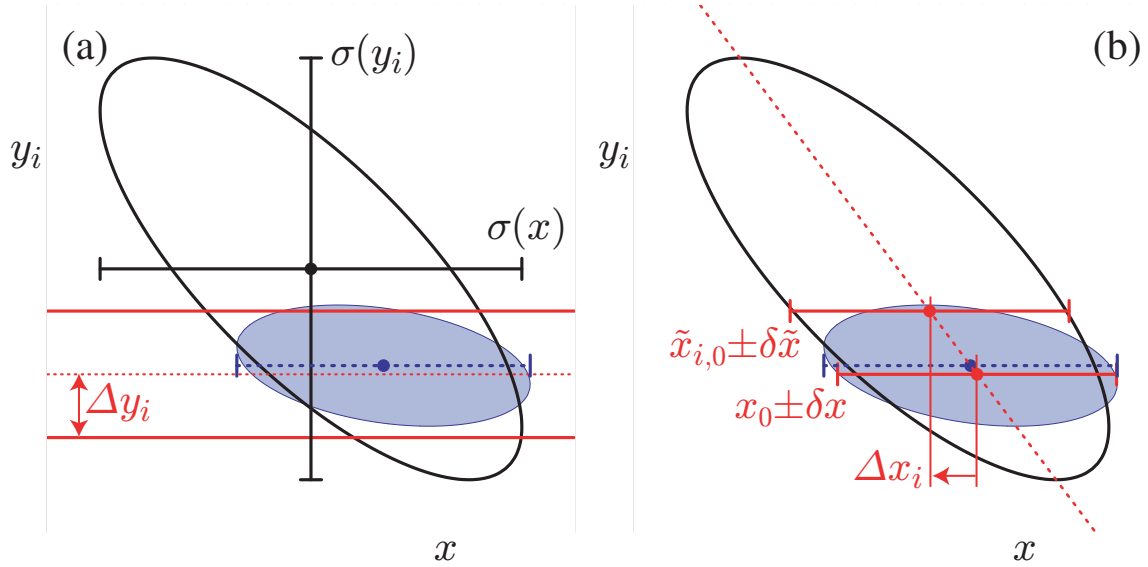


Figure 1: The left-hand plot (a) compares the 68% confidence-level contours of a hypothetical measurement's unconstrained (large ellipse) and constrained (filled ellipse) likelihoods, using the Gaussian constraint on y_i represented by the horizontal band. The solid error bars represent the statistical uncertainties $\sigma(x)$ and $\sigma(y_i)$ of the unconstrained likelihood. The dashed error bar shows the statistical error on x from a constrained simultaneous fit to x and y_i . The right-hand plot (b) illustrates the method described in the text of performing fits to x with y_i fixed at different values. The dashed diagonal line between these fit results has the slope $\rho(x, y_i)\sigma(y_i)/\sigma(x)$ in the limit of a parabolic unconstrained likelihood. The result of the constrained simultaneous fit from (a) is shown as a dashed error bar on x .

usually quote as their systematic uncertainty Δx_i on x due to the unknown value of y_i . Our procedure requires that we know not only the magnitude of this shift but also its sign. In the limit that the unconstrained data is represented by a parabolic likelihood, the signed shift is given by

$$\Delta x_i = \rho(x, y_i) \frac{\sigma(x)}{\sigma(y_i)} \Delta y_i, \quad (1)$$

where $\sigma(x)$ and $\rho(x, y_i)$ are the statistical uncertainty on x and the correlation between x and y_i in the unconstrained data. While our procedure is not equivalent to the constrained fit with extra parameters, it yields (in the limit of a parabolic unconstrained likelihood) a central value x_0 that agrees to $\mathcal{O}(\Delta y_i/\sigma(y_i))^2$ and an uncertainty $\delta x \oplus \Delta x_i$ that agrees to $\mathcal{O}(\Delta y_i/\sigma(y_i))^4$.

In order to combine two or more measurements that share systematics due to the same external parameters y_i , we would ideally perform a constrained simultaneous fit of all data samples to obtain values of x and each y_i , being careful to only apply the constraint on each y_i once. This is not practical since we generally do not have sufficient information to reconstruct the unconstrained likelihoods corresponding to each measurement. Instead, we perform the two-step approximate procedure described below.

Figs. 2(a,b) illustrate two statistically-independent measurements, $x_1 \pm (\delta x_1 \oplus \Delta x_{i,1})$ and $x_2 \pm (\delta x_2 \oplus \Delta x_{i,2})$, of the same hypothetical quantity x (for simplicity, we only show the contribution of a single correlated systematic due to an external parameter y_i). As our knowledge of the external parameters y_i evolves, it is natural that the different measurements of x will assume different nominal values and ranges for each y_i . The first step of our procedure is to adjust the values of each measurement to reflect the current best knowledge of the values y'_i and ranges $\Delta y'_i$ of the external parameters y_i , as illustrated in Figs. 2(c,b). We adjust the central values x_k and correlated systematic uncertainties $\Delta x_{i,k}$ linearly for each measurement (indexed by k) and each external parameter (indexed by i):

$$x'_k = x_k + \sum_i \frac{\Delta x_{i,k}}{\Delta y_{i,k}} (y'_i - y_{i,k}) \quad (2)$$

$$\Delta x'_{i,k} = \Delta x_{i,k} \cdot \frac{\Delta y'_i}{\Delta y_{i,k}}. \quad (3)$$

This procedure is exact in the limit that the unconstrained likelihoods of each measurement is parabolic.

The second step of our procedure is to combine the adjusted measurements, $x'_k \pm (\delta x_k \oplus \Delta x'_{k,1} \oplus \Delta x'_{k,2} \oplus \dots)$ using the chi-square

$$\chi_{\text{comb}}^2(x, y_1, y_2, \dots) \equiv \sum_k \frac{1}{\delta x_k^2} \left[x'_k - \left(x + \sum_i (y_i - y'_i) \frac{\Delta x'_{i,k}}{\Delta y'_i} \right) \right]^2 + \sum_i \left(\frac{y_i - y'_i}{\Delta y'_i} \right)^2, \quad (4)$$

and then minimize this χ^2 to obtain the best values of x and y_i and their uncertainties, as illustrated in Fig. 3. Although this method determines new values for the y_i , we do not report them since the $\Delta x_{i,k}$ reported by each experiment are generally not intended for this purpose (for example, they may represent a conservative upper limit rather than a true reflection of a 68% confidence level).

For comparison, the exact method we would perform if we had the unconstrained likelihoods $\mathcal{L}_k(x, y_1, y_2, \dots)$ available for each measurement is to minimize the simultaneous constrained

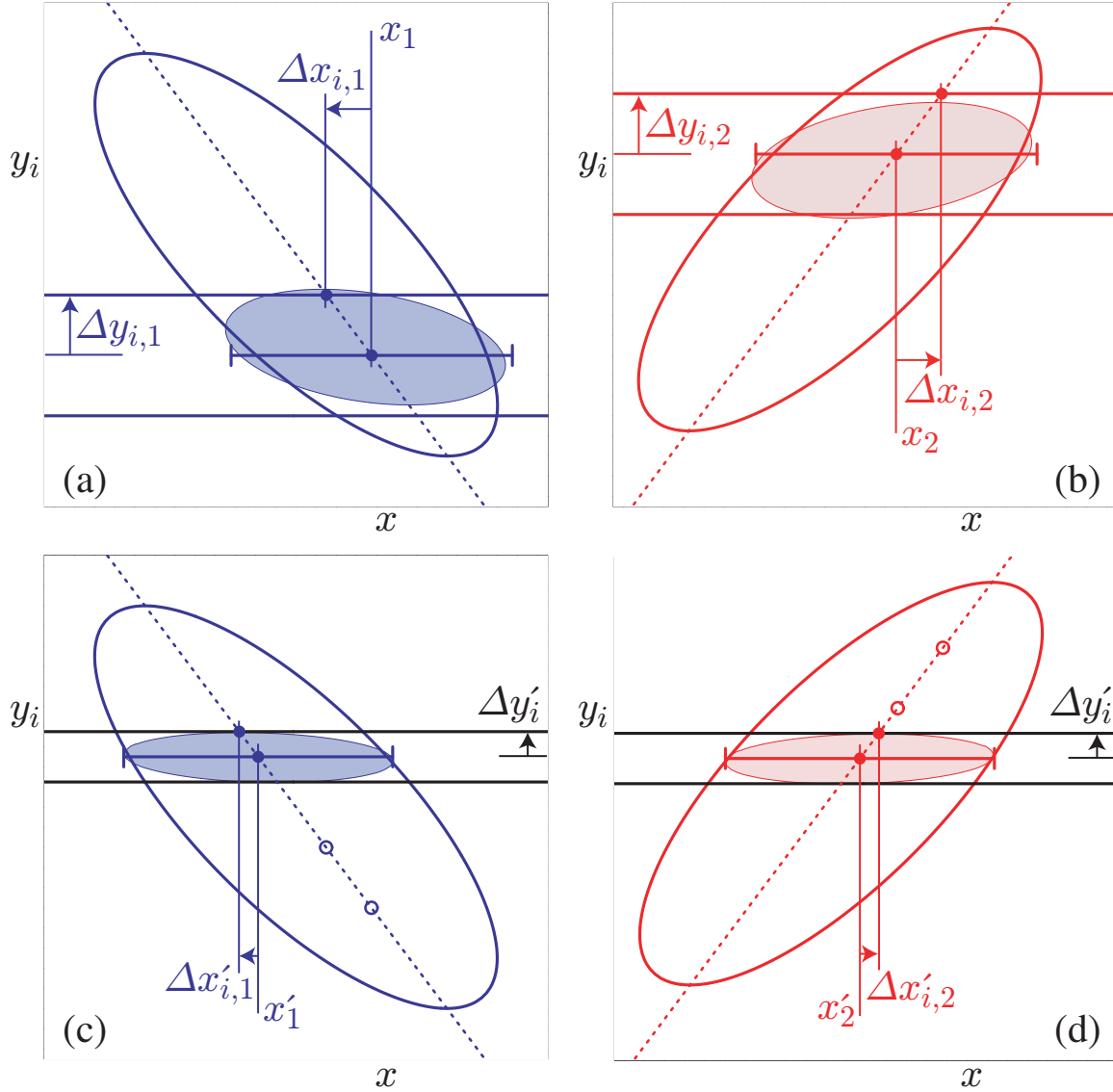


Figure 2: The upper plots (a) and (b) show examples of two individual measurements to be combined. The large ellipses represent their unconstrained likelihoods, and the filled ellipses represent their constrained likelihoods. Horizontal bands indicate the different assumptions about the value and uncertainty of y_i used by each measurement. The error bars show the results of the approximate method described in the text for obtaining x by performing fits with y_i fixed to different values. The lower plots (c) and (d) illustrate the adjustments to accommodate updated and consistent knowledge of y_i as described in the text. Open circles mark the central values of the unadjusted fits to x with y fixed; these determine the dashed line used to obtain the adjusted values.

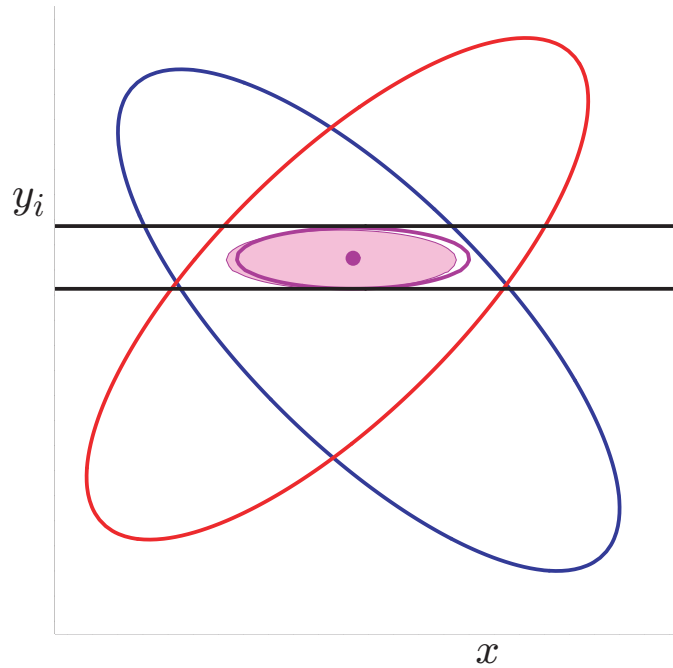


Figure 3: An illustration of the combination of two hypothetical measurements of x using the method described in the text. The ellipses represent the unconstrained likelihoods of each measurement, and the horizontal band represents the latest knowledge about y_i that is used to adjust the individual measurements. The filled small ellipse shows the result of the exact method using $\mathcal{L}_{\text{comb}}$, and the hollow small ellipse and dot show the result of the approximate method using χ_{comb}^2 .

likelihood

$$\mathcal{L}_{\text{comb}}(x, y_1, y_2, \dots) \equiv \prod_k \mathcal{L}_k(x, y_1, y_2, \dots) \prod_i \mathcal{L}_i(y_i), \quad (5)$$

with an independent Gaussian external constraint on each y_i

$$\mathcal{L}_i(y_i) \equiv \exp \left[-\frac{1}{2} \left(\frac{y_i - y'_i}{\Delta y'_i} \right)^2 \right]. \quad (6)$$

The results of this exact method are illustrated by the filled ellipses in Figs. 3(a,b) and agree with our method in the limit that each \mathcal{L}_k is parabolic and that each $\Delta y'_i \ll \sigma(y_i)$. In the case of a non-parabolic unconstrained likelihood, experiments would have to provide a description of \mathcal{L}_k itself to allow an improved combination. In the case of $\sigma(y_i) \simeq \Delta y'_i$, experiments are advised to perform a simultaneous measurement of both x and y so that their data will improve the world knowledge about y .

The algorithm described above is used as a default in the averages reported in the following sections. For some cases, somewhat simplified or more complex algorithms are used and noted in the corresponding sections. Some examples for extensions of the standard method for extracting averages are given here. These include the case where measurement errors depend on the measured value, i.e. are relative errors, unknown correlation coefficients and the breakdown of error sources.

For measurements with Gaussian errors, the usual estimator for the average of a set of measurements is obtained by minimizing the following χ^2 :

$$\chi^2(t) = \sum_i^N \frac{(y_i - t)^2}{\sigma_i^2}, \quad (7)$$

where y_i is the measured value for input i and σ_i^2 is the variance of the distribution from which y_i was drawn. The value \hat{t} of t at minimum χ^2 is our estimator for the average. (This discussion is given for independent measurements for the sake of simplicity; the generalization to correlated measurements is straightforward, and has been used when averaging results.) The true σ_i are unknown but typically the error as assigned by the experiment σ_i^{raw} is used as an estimator for it. Caution is advised, however, in the case where σ_i^{raw} depends on the value measured for y_i . Examples of this include an uncertainty in any multiplicative factor (like an acceptance) that enters the determination of y_i , i.e. the \sqrt{N} dependence of Poisson statistics, where $y_i \propto N$ and $\sigma_i \propto \sqrt{N}$. Failing to account for this type of dependence when averaging leads to a biased average. Biases in the average can be avoided (or at least reduced) by minimizing the following χ^2 :

$$\chi^2(t) = \sum_i^N \frac{(y_i - t)^2}{\sigma_i^2(\hat{t})}. \quad (8)$$

In the above $\sigma_i(\hat{t})$ is the uncertainty assigned to input i that includes the assumed dependence of the stated error on the value measured. As an example, consider a pure acceptance error, for which $\sigma_i(\hat{t}) = (\hat{t}/y_i) \times \sigma_i^{\text{raw}}$. It is easily verified that solving Eq. 8 leads to the correct behavior, namely

$$\hat{t} = \frac{\sum_i^N y_i^3 / (\sigma_i^{\text{raw}})^2}{\sum_i^N y_i^2 / (\sigma_i^{\text{raw}})^2},$$

i.e. weighting by the inverse square of the fractional uncertainty, $\sigma_i^{\text{raw}}/y_i$. It is sometimes difficult to assess the dependence of σ_i^{raw} on \hat{t} from the errors quoted by experiments.

Another issue that needs careful treatment is the question of correlation among different measurements, e.g. due to using the same theory for calculating acceptances. A common practice is to set the correlation coefficient to unity to indicate full correlation. However, this is not a “conservative” thing to do, and can in fact lead to a significantly underestimated uncertainty on the average. In the absence of better information, the most conservative choice of correlation coefficient between two measurements i and j is the one that maximizes the uncertainty on \hat{t} due to that pair of measurements:

$$\sigma_{\hat{t}(i,j)}^2 = \frac{\sigma_i^2 \sigma_j^2 (1 - \rho_{ij}^2)}{\sigma_i^2 + \sigma_j^2 - 2 \rho_{ij} \sigma_i \sigma_j}, \quad (9)$$

namely

$$\rho_{ij} = \min \left(\frac{\sigma_i}{\sigma_j}, \frac{\sigma_j}{\sigma_i} \right), \quad (10)$$

which corresponds to setting $\sigma_{\hat{t}(i,j)}^2 = \min(\sigma_i^2, \sigma_j^2)$. Setting $\rho_{ij} = 1$ when $\sigma_i \neq \sigma_j$ can lead to a significant underestimate of the uncertainty on \hat{t} , as can be seen from Eq. 9.

Finally, we carefully consider the various sources of error contributing to the overall uncertainty of an average. The overall covariance matrix is constructed from a number of individual sources, e.g. $\mathbf{V} = \mathbf{V}_{\text{stat}} + \mathbf{V}_{\text{sys}} + \mathbf{V}_{\text{th}}$. The variance on the average \hat{t} can be written

$$\sigma_{\hat{t}}^2 = \frac{\sum_{i,j} (\mathbf{V}^{-1} [\mathbf{V}_{\text{stat}} + \mathbf{V}_{\text{sys}} + \mathbf{V}_{\text{th}}] \mathbf{V}^{-1})_{ij}}{\left(\sum_{i,j} V_{ij}^{-1} \right)^2} = \sigma_{\text{stat}}^2 + \sigma_{\text{sys}}^2 + \sigma_{\text{th}}^2. \quad (11)$$

Written in this form, one can readily determine the contribution of each source of uncertainty to the overall uncertainty on the average. This breakdown of the uncertainties is used in the following sections.

Following the prescription described above, the central values and errors are rescaled to a common set of input parameters in the averaging procedures according to the dependency on any of these input parameters. We try to use the most up-to-date values for these common inputs and the same values among the HFAG subgroups. For the parameters whose averages are produced by HFAG, we use the values in the current update cycle. For other external parameters, we use the most recent PDG values available (usually Ref. [5]). The parameters and values used are listed in each subgroup section.

3 b -hadron production fractions, lifetimes and mixing parameters

Quantities such as b -hadron production fractions, b -hadron lifetimes, and neutral B -meson oscillation frequencies have been studied in the nineties at LEP and SLC (e^+e^- colliders at $\sqrt{s} = m_Z$) as well as at the first version of the Tevatron ($p\bar{p}$ collider at $\sqrt{s} = 1.8$ TeV). Since then precise measurements of the B^0 and B^+ mesons have also been performed at the asymmetric B factories, KEKB and PEP-II (e^+e^- colliders at $\sqrt{s} = m_{\Upsilon(4S)}$) while measurements related to the other b -hadrons, in particular B_s^0 , B_c^+ and A_b^0 , have been performed at the upgraded Tevatron ($\sqrt{s} = 1.96$ TeV) and are continuing at the LHC (pp collider at $\sqrt{s} = 7$ TeV). In most cases, these basic quantities, although interesting by themselves, became necessary ingredients for the more complicated and refined analyses at the asymmetric B factories, the Tevatron and the LHC, in particular the time-dependent CP asymmetry measurements. It is therefore important that the best experimental values of these quantities continue to be kept up-to-date and improved.

In several cases, the averages presented in this chapter are needed and used as input for the results given in the subsequent chapters. Within this chapter, some averages need the knowledge of other averages in a circular way. This coupling, which appears through the b -hadron fractions whenever inclusive or semi-exclusive measurements have to be considered, has reduced drastically in the past several years with increasingly precise exclusive measurements becoming available and dominating practically all averages.

In addition to b -hadron fractions, lifetimes and mixing parameters, this chapter also deals with the CP -violating phase $\phi_s^{c\bar{c}s} \simeq -2\beta_s$, which is the phase difference between the B_s^0 mixing amplitude and the $b \rightarrow c\bar{c}s$ decay amplitude. The angle β , which is the equivalent of β_s for the B^0 system, is discussed in Chapter 4.

3.1 b -hadron production fractions

We consider here the relative fractions of the different b -hadron species found in an unbiased sample of weakly-decaying b hadrons produced under some specific conditions. The knowledge of these fractions is useful to characterize the signal composition in inclusive b -hadron analyses, to predict the background composition in exclusive analyses, or to convert (relative) observe rates into (relative) branching fraction measurements. Many B -physics analyses need these fractions as input. We distinguish here the following three conditions: $\Upsilon(4S)$ decays, $\Upsilon(5S)$ decays, and high-energy collisions (including Z^0 decays).

3.1.1 b -hadron production fractions in $\Upsilon(4S)$ decays

Only pairs of the two lightest (charged and neutral) B mesons can be produced in $\Upsilon(4S)$ decays, and it is enough to determine the following branching fractions:

$$f^{+-} = \Gamma(\Upsilon(4S) \rightarrow B^+B^-)/\Gamma_{\text{tot}}(\Upsilon(4S)), \quad (12)$$

$$f^{00} = \Gamma(\Upsilon(4S) \rightarrow B^0\bar{B}^0)/\Gamma_{\text{tot}}(\Upsilon(4S)). \quad (13)$$

In practice, most analyses measure their ratio

$$R^{+/-00} = f^{+-}/f^{00} = \Gamma(\Upsilon(4S) \rightarrow B^+B^-)/\Gamma(\Upsilon(4S) \rightarrow B^0\bar{B}^0), \quad (14)$$

Table 1: Published measurements of the B^+/B^0 production ratio in $\mathcal{T}(4S)$ decays, together with their average (see text). Systematic uncertainties due to the imperfect knowledge of $\tau(B^+)/\tau(B^0)$ are included. The latest *BABAR* result [6] supersedes the earlier *BABAR* measurements [7, 8].

Experiment and year	Ref.	Decay modes or method	Published value of $R^{+-/00} = f^{+-/} / f^{00}$	Assumed value of $\tau(B^+)/\tau(B^0)$
CLEO, 2001	[9]	$J/\psi K^{(*)}$	$1.04 \pm 0.07 \pm 0.04$	1.066 ± 0.024
<i>BABAR</i> , 2002	[7]	$(c\bar{c})K^{(*)}$	$1.10 \pm 0.06 \pm 0.05$	1.062 ± 0.029
CLEO, 2002	[10]	$D^* \ell \nu$	$1.058 \pm 0.084 \pm 0.136$	1.074 ± 0.028
Belle, 2003	[11]	dilepton events	$1.01 \pm 0.03 \pm 0.09$	1.083 ± 0.017
<i>BABAR</i> , 2004	[8]	$J/\psi K$	$1.006 \pm 0.036 \pm 0.031$	1.083 ± 0.017
<i>BABAR</i> , 2005	[6]	$(c\bar{c})K^{(*)}$	$1.06 \pm 0.02 \pm 0.03$	1.086 ± 0.017
Average			1.056 ± 0.028 (tot)	1.079 ± 0.007

which is easier to access experimentally. Since an inclusive (but separate) reconstruction of B^+ and B^0 is difficult, specific exclusive decay modes, $B^+ \rightarrow x^+$ and $B^0 \rightarrow x^0$, are usually considered to perform a measurement of $R^{+-/00}$, whenever they can be related by isospin symmetry (for example $B^+ \rightarrow J/\psi K^+$ and $B^0 \rightarrow J/\psi K^0$). Under the assumption that $\Gamma(B^+ \rightarrow x^+) = \Gamma(B^0 \rightarrow x^0)$, *i.e.* that isospin invariance holds in these B decays, the ratio of the number of reconstructed $B^+ \rightarrow x^+$ and $B^0 \rightarrow x^0$ mesons is proportional to

$$\frac{f^{+-} \mathcal{B}(B^+ \rightarrow x^+)}{f^{00} \mathcal{B}(B^0 \rightarrow x^0)} = \frac{f^{+-} \Gamma(B^+ \rightarrow x^+) \tau(B^+)}{f^{00} \Gamma(B^0 \rightarrow x^0) \tau(B^0)} = \frac{f^{+-}}{f^{00}} \frac{\tau(B^+)}{\tau(B^0)}, \quad (15)$$

where $\tau(B^+)$ and $\tau(B^0)$ are the B^+ and B^0 lifetimes respectively. Hence the primary quantity measured in these analyses is $R^{+-/00} \tau(B^+)/\tau(B^0)$, and the extraction of $R^{+-/00}$ with this method therefore requires the knowledge of the $\tau(B^+)/\tau(B^0)$ lifetime ratio.

The published measurements of $R^{+-/00}$ are listed in Table 1 together with the corresponding assumed values of $\tau(B^+)/\tau(B^0)$. All measurements are based on the above-mentioned method, except the one from Belle, which is a by-product of the B^0 mixing frequency analysis using dilepton events (but note that it also assumes isospin invariance, namely $\Gamma(B^+ \rightarrow \ell^+ X) = \Gamma(B^0 \rightarrow \ell^+ X)$). The latter is therefore treated in a slightly different manner in the following procedure used to combine these measurements:

- each published value of $R^{+-/00}$ from CLEO and *BABAR* is first converted back to the original measurement of $R^{+-/00} \tau(B^+)/\tau(B^0)$, using the value of the lifetime ratio assumed in the corresponding analysis;
- a simple weighted average of these original measurements of $R^{+-/00} \tau(B^+)/\tau(B^0)$ from CLEO and *BABAR* (which do not depend on the assumed value of the lifetime ratio) is then computed, assuming no statistical or systematic correlations between them;
- the weighted average of $R^{+-/00} \tau(B^+)/\tau(B^0)$ is converted into a value of $R^{+-/00}$, using the latest average of the lifetime ratios, $\tau(B^+)/\tau(B^0) = 1.079 \pm 0.007$ (see Sec. 3.2.3);

- the Belle measurement of $R^{+-/00}$ is adjusted to the current values of $\tau(B^0) = 1.519 \pm 0.007$ ps and $\tau(B^+)/\tau(B^0) = 1.079 \pm 0.007$ (see Sec. 3.2.3), using the quoted systematic uncertainties due to these parameters;
- the combined value of $R^{+-/00}$ from CLEO and *BABAR* is averaged with the adjusted value of $R^{+-/00}$ from Belle, assuming a 100% correlation of the systematic uncertainty due to the limited knowledge on $\tau(B^+)/\tau(B^0)$; no other correlation is considered.

The resulting global average,

$$R^{+-/00} = \frac{f^{+-}}{f^{00}} = 1.056 \pm 0.028, \quad (16)$$

is consistent with an equal production of charged and neutral B mesons, although only at the 2.0σ level.

On the other hand, the *BABAR* collaboration has performed a direct measurement of the f^{00} fraction using an original method, which does not rely on isospin symmetry nor requires the knowledge of $\tau(B^+)/\tau(B^0)$. Its analysis, based on a comparison between the number of events where a single $B^0 \rightarrow D^{*-}\ell^+\nu$ decay could be reconstructed and the number of events where two such decays could be reconstructed, yields [12]

$$f^{00} = 0.487 \pm 0.010 \text{ (stat)} \pm 0.008 \text{ (syst)}. \quad (17)$$

The two results of Eqs. (16) and (17) are of very different natures and completely independent of each other. Their product is equal to $f^{+-} = 0.514 \pm 0.019$, while another combination of them gives $f^{+-} + f^{00} = 1.001 \pm 0.030$, compatible with unity. Assuming² $f^{+-} + f^{00} = 1$, also consistent with CLEO's observation that the fraction of $\Upsilon(4S)$ decays to $B\bar{B}$ pairs is larger than 0.96 at 95% CL [14], the results of Eqs. (16) and (17) can be averaged (first converting Eq. (16) into a value of $f^{00} = 1/(R^{+-/00} + 1)$) to yield the following more precise estimates:

$$f^{00} = 0.487 \pm 0.006, \quad f^{+-} = 1 - f^{00} = 0.513 \pm 0.006, \quad \frac{f^{+-}}{f^{00}} = 1.055 \pm 0.025. \quad (18)$$

The latter ratio differs from one by 2.2σ .

3.1.2 b -hadron production fractions in $\Upsilon(5S)$ decays

Hadronic events produced in e^+e^- collisions at the $\Upsilon(5S)$ energy can be classified into three categories: light-quark (u, d, s, c) continuum events, $b\bar{b}$ continuum events, and $\Upsilon(5S)$ events. The latter two cannot be distinguished and will be called $b\bar{b}$ events in the following. These $b\bar{b}$ events, which also include $b\bar{b}\gamma$ events because of possible initial-state radiation, can hadronize in different final states. We define $f_{u,d}^{\Upsilon(5S)}$ as the fraction of $b\bar{b}$ events with a pair of non-strange bottom mesons ($B\bar{B}, B\bar{B}^*, B^*\bar{B}, B^*\bar{B}^*, B\bar{B}\pi, B\bar{B}^*\pi, B^*\bar{B}\pi, B^*\bar{B}^*\pi$, and $B\bar{B}\pi\pi$ final states, where B denotes a B^0 or B^+ meson and \bar{B} denotes a \bar{B}^0 or B^- meson), $f_s^{\Upsilon(5S)}$ as the fraction

²A few non- $B\bar{B}$ decay modes of the $\Upsilon(4S)$ ($\Upsilon(1S)\pi^+\pi^-$, $\Upsilon(2S)\pi^+\pi^-$, $\Upsilon(1S)\eta$) have been observed with branching fractions of the order of 10^{-4} [13], corresponding to a partial width several times larger than that in the e^+e^- channel. However, this can still be neglected and the assumption $f^{+-} + f^{00} = 1$ remains valid in the present context of the determination of f^{+-} and f^{00} .

Table 2: Published measurements of $f_s^{\Upsilon(5S)}$. All values have been obtained assuming $f_{\mathcal{B}}^{\Upsilon(5S)} = 0$. They are quoted as in the original publications, except for the most recent measurement which is quoted as $1 - f_{u,d}^{\Upsilon(5S)}$, with $f_{u,d}^{\Upsilon(5S)}$ from Ref. [15]. The last line gives our average of $f_s^{\Upsilon(5S)}$ assuming $f_{\mathcal{B}}^{\Upsilon(5S)} = 0$.

Experiment, year, dataset	Decay mode or method	Value of $f_s^{\Upsilon(5S)}$
CLEO, 2006, 0.42 fb ⁻¹ [16]	$\Upsilon(5S) \rightarrow D_s X$	$0.168 \pm 0.026^{+0.067}_{-0.034}$
	$\Upsilon(5S) \rightarrow \phi X$	$0.246 \pm 0.029^{+0.110}_{-0.053}$
	$\Upsilon(5S) \rightarrow B\bar{B}X$	$0.411 \pm 0.100 \pm 0.092$
	CLEO average of above 3	$0.21^{+0.06}_{-0.03}$
Belle, 2006, 1.86 fb ⁻¹ [17]	$\Upsilon(5S) \rightarrow D_s X$	$0.179 \pm 0.014 \pm 0.041$
	$\Upsilon(5S) \rightarrow D^0 X$	$0.181 \pm 0.036 \pm 0.075$
	Belle average of above 2	$0.180 \pm 0.013 \pm 0.032$
Belle, 2010, 23.6 fb ⁻¹ [15]	$\Upsilon(5S) \rightarrow B\bar{B}X$	$0.263 \pm 0.032 \pm 0.051$
Average of all above after adjustments to inputs of Table 3		0.215 ± 0.032

Table 3: External inputs on which the $f_s^{\Upsilon(5S)}$ averages are based.

Branching fraction	Value	Explanation and reference
$\mathcal{B}(B \rightarrow D_s X) \times \mathcal{B}(D_s \rightarrow \phi\pi)$	0.00374 ± 0.00014	derived from [18]
$\mathcal{B}(B_s^0 \rightarrow D_s X)$	0.92 ± 0.11	model-dependent estimate [19]
$\mathcal{B}(D_s \rightarrow \phi\pi)$	0.045 ± 0.004	[18]
$\mathcal{B}(B \rightarrow D^0 X) \times \mathcal{B}(D^0 \rightarrow K\pi)$	0.0243 ± 0.0011	derived from [18]
$\mathcal{B}(B_s^0 \rightarrow D^0 X)$	0.08 ± 0.07	model-dependent estimate [17, 19]
$\mathcal{B}(D^0 \rightarrow K\pi)$	0.0387 ± 0.0005	[18]
$\mathcal{B}(B \rightarrow \phi X)$	0.0343 ± 0.0012	world average [16, 18]
$\mathcal{B}(B_s^0 \rightarrow \phi X)$	0.161 ± 0.024	model-dependent estimate [16]

of $b\bar{b}$ events with a pair of strange bottom mesons ($B_s^0\bar{B}_s^0$, $B_s^0\bar{B}_s^{0*}$, $B_s^{0*}\bar{B}_s^0$, and $B_s^{0*}\bar{B}_s^{0*}$ final states), and $f_{\mathcal{B}}^{\Upsilon(5S)}$ as the fraction of $b\bar{b}$ events without bottom meson in the final state. Note that the excited bottom-meson states decay via $B^* \rightarrow B\gamma$ and $B_s^{0*} \rightarrow B_s^0\gamma$. These fractions satisfy

$$f_{u,d}^{\Upsilon(5S)} + f_s^{\Upsilon(5S)} + f_{\mathcal{B}}^{\Upsilon(5S)} = 1. \quad (19)$$

The CLEO and Belle collaborations have published in 2006 measurements of several inclusive $\Upsilon(5S)$ branching fractions, $\mathcal{B}(\Upsilon(5S) \rightarrow D_s X)$, $\mathcal{B}(\Upsilon(5S) \rightarrow \phi X)$ and $\mathcal{B}(\Upsilon(5S) \rightarrow D^0 X)$, from which they extracted the model-dependent estimates of $f_s^{\Upsilon(5S)}$ reported in Table 2. This extraction was performed under the implicit assumption $f_{\mathcal{B}}^{\Upsilon(5S)} = 0$, using the relation

$$\frac{1}{2}\mathcal{B}(\Upsilon(5S) \rightarrow D_s X) = f_s^{\Upsilon(5S)} \times \mathcal{B}(B_s^0 \rightarrow D_s X) + \left(1 - f_s^{\Upsilon(5S)} - f_{\mathcal{B}}^{\Upsilon(5S)}\right) \times \mathcal{B}(B \rightarrow D_s X), \quad (20)$$

and similar relations for $\mathcal{B}(\Upsilon(5S) \rightarrow D^0 X)$ and $\mathcal{B}(\Upsilon(5S) \rightarrow \phi X)$. We list also in Table 2 the

values of $f_s^{\Upsilon(5S)}$ derived from measurements of $f_{u,d}^{\Upsilon(5S)} = \mathcal{B}(\Upsilon(5S) \rightarrow B\bar{B}X)$ [15, 16], as well as our average value of $f_s^{\Upsilon(5S)}$, all obtained under the assumption $f_{\mathcal{B}}^{\Upsilon(5S)} = 0$.

However, the assumption $f_{\mathcal{B}}^{\Upsilon(5S)} = 0$ is no longer valid since the observation of $\Upsilon(5S)$ decays to $\Upsilon(1S)\pi^+\pi^-$, $\Upsilon(2S)\pi^+\pi^-$, $\Upsilon(3S)\pi^+\pi^-$ and $\Upsilon(1S)K^+K^-$ [20], and more recently to $h_b(1P)\pi^+\pi^-$ and $h_b(2P)\pi^+\pi^-$ [21]. The sum of these measured branching fractions, adding also the contributions of the $\Upsilon(1S)\pi^0\pi^0$, $\Upsilon(2S)\pi^0\pi^0$, $\Upsilon(3S)\pi^0\pi^0$, $\Upsilon(1S)K^0\bar{K}^0$, $h_b(1P)\pi^0\pi^0$ and $h_b(2P)\pi^0\pi^0$ final states assuming isospin conservation, amounts to

$$\mathcal{B}(\Upsilon(5S) \rightarrow (b\bar{b})hh) = 0.042 \pm 0.006, \quad \text{for } (b\bar{b}) = \Upsilon(1S, 2S, 3S), h_b(1P, 2P) \text{ and } hh = \pi\pi, KK,$$

which is to be considered as a lower bound for $f_{\mathcal{B}}^{\Upsilon(5S)}$. Following the method described in Ref. [22], we perform a χ^2 fit of the original measurements of the $\Upsilon(5S)$ branching fractions of Refs. [15–17], using the inputs of Table 3, the relations of Eqs. (19) and (20) and the one-sided Gaussian constraint $f_{\mathcal{B}}^{\Upsilon(5S)} \geq \mathcal{B}(\Upsilon(5S) \rightarrow (b\bar{b})hh)$, to simultaneously extract $f_{u,d}^{\Upsilon(5S)}$, $f_s^{\Upsilon(5S)}$ and $f_{\mathcal{B}}^{\Upsilon(5S)}$. Taking all known correlations into account, the best fit values are

$$f_{u,d}^{\Upsilon(5S)} = 0.759_{-0.040}^{+0.027}, \quad (21)$$

$$f_s^{\Upsilon(5S)} = 0.199 \pm 0.030, \quad (22)$$

$$f_{\mathcal{B}}^{\Upsilon(5S)} = 0.042_{-0.006}^{+0.046}, \quad (23)$$

where the strongly asymmetric uncertainty on $f_{\mathcal{B}}^{\Upsilon(5S)}$ is due to the one-sided constraint from the observed $(b\bar{b})hh$ decays. These results, together with their correlation, imply

$$f_s^{\Upsilon(5S)}/f_{u,d}^{\Upsilon(5S)} = 0.262_{-0.043}^{+0.051}, \quad (24)$$

in fair agreement with the results of a *BABAR* analysis [23] performed as a function of centre-of-mass energy³.

The production of B_s^0 mesons at the $\Upsilon(5S)$ is observed to be dominated by the $B_s^{0*}\bar{B}_s^{0*}$ channel, with $\sigma(e^+e^- \rightarrow B_s^{0*}\bar{B}_s^{0*})/\sigma(e^+e^- \rightarrow B_s^{0(*)}\bar{B}_s^{0(*)}) = (87.0 \pm 1.7)\%$ [24, 25]. The proportion of the various production channels for non-strange B mesons have also been measured [15].

3.1.3 b -hadron production fractions at high energy

At high energy, all species of weakly-decaying b hadrons may be produced, either directly or in strong and electromagnetic decays of excited b hadrons. It is often assumed that the fractions of these different species are the same in unbiased samples of high- p_T b jets originating from Z^0 decays, from $p\bar{p}$ collisions at the Tevatron, or from pp collisions at the LHC. This hypothesis is plausible under the condition that the square of the momentum transfer to the produced b quarks, Q^2 , is large compared with the square of the hadronization energy scale, $Q^2 \gg \Lambda_{\text{QCD}}^2$. On the other hand, there is no strong argument to claim that the fractions at different machines should be strictly equal, so this assumption should be checked experimentally. Although the available data is not sufficient at this time to perform a definitive check, it is expected that more refined analyses of the Tevatron Run II data and new analyses from LHC experiments may

³ This has not been included in the average, since no numerical value is given for $f_s^{\Upsilon(5S)}/f_{u,d}^{\Upsilon(5S)}$ in Ref. [23].

improve this situation and allow one to confirm or disprove this assumption with reasonable confidence. Meanwhile, the attitude adopted here is that these fractions are assumed to be equal at all high-energy colliders until demonstrated otherwise by experiment. However, both CDF and LHCb report a p_T dependence for Λ_b production relative to B^+ and B^0 ; the number of Λ_b baryons observed at low p_T is enhanced with respect to that seen at LEP at higher p_T . Therefore we present three sets of complete averages: one set including only measurements performed at LEP, a second set including only measurements performed at the Tevatron, a third set including measurements performed at LEP, Tevatron and LHCb. The LHCb production fractions results, by themselves, are still incomplete, lacking measurements on the production of other weakly decaying heavy flavour baryons, Ξ_b and Ω_b , and a measurement of $\bar{\chi}$ giving an extra constraint between f_d and f_s .

Contrary to what happens in the charm sector where the fractions of D^+ and D^0 are different, the relative amount of B^+ and B^0 is not affected by the electromagnetic decays of excited B^{+*} and B^{0*} states and strong decays of excited B^{+**} and B^{0**} states. Decays of the type $B_s^{0**} \rightarrow B^{(*)}K$ also contribute to the B^+ and B^0 rates, but with the same magnitude if mass effects can be neglected. We therefore assume equal production of B^+ and B^0 . We also neglect the production of weakly-decaying states made of several heavy quarks (like B_c^+ and other heavy baryons) which is known to be very small. Hence, for the purpose of determining the b -hadron fractions, we use the constraints

$$f_u = f_d \quad \text{and} \quad f_u + f_d + f_s + f_{\text{baryon}} = 1, \quad (25)$$

where f_u , f_d , f_s and f_{baryon} are the unbiased fractions of B^+ , B^0 , B_s^0 and b baryons, respectively.

The LEP experiments have measured $f_s \times \mathcal{B}(B_s^0 \rightarrow D_s^- \ell^+ \nu_\ell X)$ [26], $\mathcal{B}(b \rightarrow \Lambda_b^0) \times \mathcal{B}(\Lambda_b^0 \rightarrow \Lambda_c^+ \ell^- \bar{\nu}_\ell X)$ [27, 28] and $\mathcal{B}(b \rightarrow \Xi_b^-) \times \mathcal{B}(\Xi_b^- \rightarrow \Xi^- \ell^- \bar{\nu}_\ell X)$ [29, 30]⁴ from partially reconstructed final states including a lepton, f_{baryon} from protons identified in b events [32], and the production rate of charged b hadrons [33]. Ratios of b -hadron fractions have been measured at CDF using lepton+charm final states [34–36]⁵ and double semileptonic decays with $K^* \mu \mu$ and $\phi \mu \mu$ final states [37]. Measurements of the production of other heavy flavour baryons at the Tevatron are included in the determination of f_{baryon} [38–40]⁶ using the constraint

$$\begin{aligned} f_{\text{baryon}} &= f_{\Lambda_b} + f_{\Xi_b^0} + f_{\Xi_b^-} + f_{\Omega_b^-} \\ &= f_{\Lambda_b} \left(1 + 2 \frac{f_{\Xi_b^-}}{f_{\Lambda_b}} + \frac{f_{\Omega_b^-}}{f_{\Lambda_b}} \right), \end{aligned} \quad (26)$$

where isospin invariance is assumed in the production of Ξ_b^0 and Ξ_b^- . Other b -baryons are expected to decay strongly or electromagnetically to those baryons listed. For the production measurements, both CDF and D0 reconstruct their b -baryons exclusively to final states which include a J/ψ and a hyperon ($\Lambda_b \rightarrow J/\psi \Lambda$, $\Xi_b^- \rightarrow J/\psi \Xi^-$ and $\Omega_b^- \rightarrow J/\psi \Omega^-$). We assume that the partial decay width of a b -baryon to a J/ψ and the corresponding hyperon is equal to the partial width of any other b -baryon to a J/ψ and the corresponding hyperon. LHCb has also

⁴The DELPHI result of Ref. [30] is considered to supersede an older one [31].

⁵CDF updated their measurement of f_{Λ_b}/f_d [34] to account for a measured p_T dependence between exclusively reconstructed Λ_b and B^0 [36].

⁶D0 reports $f_{\Omega_b^-}/f_{\Xi_b^-}$. We use the CDF+D0 average of $f_{\Xi_b^-}/f_{\Lambda_b}$ to obtain $f_{\Omega_b^-}/f_{\Lambda_b}$ and then combine with the CDF result.

Table 4: Comparison of average production fraction ratios from CDF and LHCb. The kinematic regime of the lepton+charm system reconstructed in each experiment is also shown.

Quantity	CDF	LHCb
$f_s/(f_u + f_d)$	0.140 ± 0.022	0.132 ± 0.010
$f_{\Lambda_b}/(f_u + f_d)$	0.290 ± 0.109	0.305 ± 0.022
Average lepton+charm p_T	$\sim 13 \text{ GeV}/c$	$\sim 7 \text{ GeV}/c$
Pseudo-rapidity range	$-1 < \eta < 1$	$2 < \eta < 5$

measured ratios of b -hadron fractions, $f_s/(f_u + f_d)$ and $f_{\Lambda_b}/(f_u + f_d)$, in lepton+charm final states [41] and f_s/f_d in fully reconstructed hadronic final states using theoretical values for the branching fractions of two-body B_s^0 and B^0 decays [42].

Both CDF and LHCb observe a p_T dependence in the relative fractions f_{Λ_b}/f_d [36, 41]⁷. No p_T dependence is yet observed for $f_s/(f_u + f_d)$. CDF chose to correct an older result to account for the p_T dependence whereas LHCb chose to report a linear dependence of $f_{\Lambda_b}/(f_u + f_d)$, which yields unphysical results for $p_T > 32 \text{ GeV}/c$. In a second result, CDF binned their data in p_T of the electron+charm system. Figure 4 shows the ratio $R_{\Lambda_b} = f_{\Lambda_b}/(f_u + f_d)$ as a function of this p_T , as measured by both CDF and LHCb. Two fits are performed. The first fit using the LHCb parameterization yields $R_{\Lambda_b} = (0.386 \pm 0.21) [1 - (0.0270 \pm 0.0056) \times p_T]$. A second fit using a simple exponential yields $R_{\Lambda_b} = \exp \{(-0.928 \pm 0.066) - (0.0344 \pm 0.0086) \times p_T\}$. A common systematic uncertainty of 26% on the scale of both results arises from the $\Lambda_c^+ \rightarrow pK^-\pi^+$ branching fraction. The quality of the two fits are similar, but the second parameterization gives a physical result for all p_T . A value of R_{Λ_b} is also calculated for LEP and placed at the approximate p_T for the lepton+charm system, but this value does not participate in any fit. Note that the p_T dependence of R_{Λ_b} combined with the constraint in Eq. (25) implies a compensating p_T dependence in one or more of the production fractions, f_u , f_d , or f_s .

In order to combine or compare LHCb results with other experiments, the p_T -dependent $f_{\Lambda_b}/(f_u + f_d)$ is weighted by the p_T spectrum⁸. Table 4 compares the p_T -weighted LHCb data with comparable averages from the CDF. The average CDF and LHCb data are in good agreement despite the b hadrons being produced in different kinematic regimes.

All these published results have been combined following the procedure and assumptions described in Ref. [3], to yield $f_u = f_d = 0.400 \pm 0.008$, $f_s = 0.103 \pm 0.007$ and $f_{\text{baryon}} = 0.097 \pm 0.016$ under the constraints of Eq. (25). Repeating the combinations, for LEP and the Tevatron, we obtain $f_u = f_d = 0.407 \pm 0.009$, $f_s = 0.087 \pm 0.014$ and $f_{\text{baryon}} = 0.099 \pm 0.016$ when using the LEP data only, $f_u = f_d = 0.322 \pm 0.032$, $f_s = 0.094 \pm 0.016$ $f_{\text{baryon}} = 0.262 \pm 0.073$ when using the Tevatron data only. As noted previously, the LHCb data are insufficient to determine a complete set of b -hadron production fractions. The world averages (LEP, Tevatron and LHCb) for the various fractions are presented here for comparison with previous averages.

⁷CDF compares the p_T distribution of fully reconstructed $\Lambda_b \rightarrow \Lambda_c^+ \pi^-$ with $\overline{B^0} \rightarrow D^+ \pi^-$ which compares f_{Λ_b}/f_d up to a scale factor. LHCb compares the p_T in the lepton+charm system between Λ_b and B^0 and B^+ comparing $R_{\Lambda_b} = f_{\Lambda_b}/(f_u + f_d) = f_{\Lambda_b}/2f_d$.

⁸In practice the LHCb data are given in 14 bins in p_T and η with a full covariance matrix [41]. The weighted average is calculated as $D^T C^{-1} M / \sigma$, where $\sigma = D^T C^{-1} D$, M is a vector of measurements, C^{-1} is the inverse covariance matrix and D^T is the transpose of the design matrix (vector of 1's)

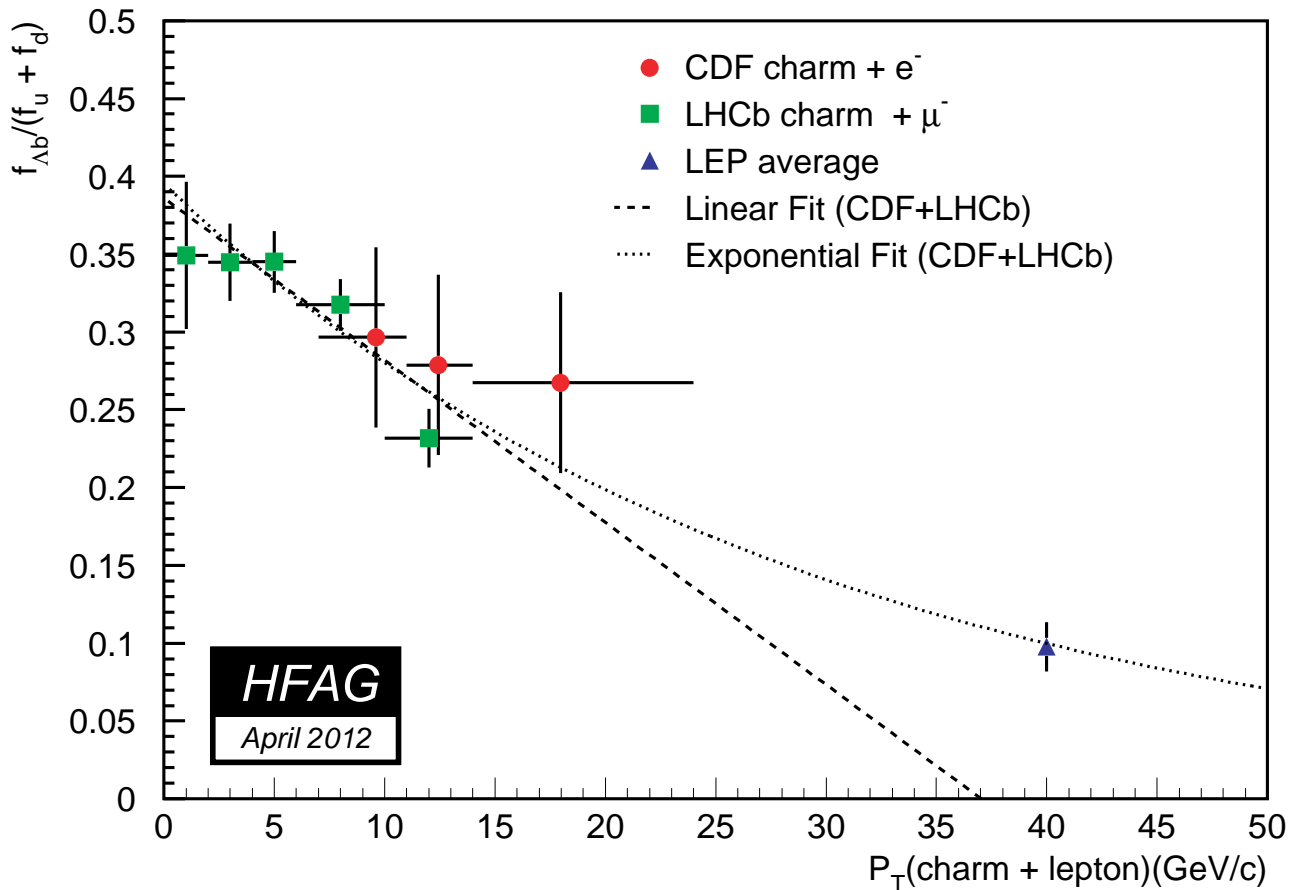


Figure 4: Ratio of production fractions $f_{\Lambda_b}/(f_u + f_d)$ as a function of p_T of the lepton+charm system for CDF [36] and LHCb [41] data. A scale uncertainty due to the common systematic uncertainty from the $\Lambda_c^+ \rightarrow pK^-\pi^+$ branching fraction is omitted. The curves represent fits to the data: a linear fit using the LHCb parameterization (dashed), and an exponential fit described in the text (dotted). The computed LEP ratio is included at an approximate p_T in Z decays, but does not participate in any fit.

Significant differences exist between the LEP and Tevatron fractions, therefore use of the world averages should be taken with some care. For these combinations other external inputs are used, *e.g.* the branching ratios of B mesons to final states with a D , D^* or D^{**} in semileptonic decays, which are needed to evaluate the fraction of semileptonic B_s^0 decays with a D_s^- in the final state.

Time-integrated mixing analyses performed with lepton pairs from $b\bar{b}$ events produced at high-energy colliders measure the quantity

$$\bar{\chi} = f'_d \chi_d + f'_s \chi_s, \quad (27)$$

where f'_d and f'_s are the fractions of B^0 and B_s^0 hadrons in a sample of semileptonic b -hadron decays, and where χ_d and χ_s are the B^0 and B_s^0 time-integrated mixing probabilities. Assuming that all b hadrons have the same semileptonic decay width implies $f'_i = f_i R_i$, where $R_i = \tau_i/\tau_b$ is the ratio of the lifetime τ_i of species i to the average b -hadron lifetime $\tau_b = \sum_i f_i \tau_i$. Hence

Table 5: Time-integrated mixing probability $\bar{\chi}$ (defined in Eq. (27)), and fractions of the different b -hadron species in an unbiased sample of weakly-decaying b hadrons, obtained from both direct and mixing measurements. The correlation coefficients between the fractions are also given. The last column includes measurements performed at LEP, Tevatron and LHCb.

Quantity		Z decays	Tevatron	LHCb [41]	all
Mixing probability	$\bar{\chi}$	0.1259 ± 0.0042	0.127 ± 0.008		0.1260 ± 0.0037
B^+ or B^0 fraction	$f_u = f_d$	0.403 ± 0.009	0.330 ± 0.030		0.401 ± 0.007
B_s^0 fraction	f_s	0.103 ± 0.009	0.103 ± 0.012		0.107 ± 0.005
b -baryon fraction	f_{baryon}	0.090 ± 0.015	0.236 ± 0.067		0.091 ± 0.015
B_s^0/B^0 ratio	f_s/f_d	0.256 ± 0.025	0.311 ± 0.037	$0.267^{+0.021}_{-0.020}$	0.266 ± 0.015
$\rho(f_s, f_u) = \rho(f_s, f_d)$		-0.521	$+0.379$		-0.224
$\rho(f_{\text{baryon}}, f_u) = \rho(f_{\text{baryon}}, f_d)$		-0.871	-0.986		-0.935
$\rho(f_{\text{baryon}}, f_s)$		$+0.036$	-0.530		-0.136

measurements of the mixing probabilities $\bar{\chi}$, χ_d and χ_s can be used to improve our knowledge of f_u , f_d , f_s and f_{baryon} . In practice, the above relations yield another determination of f_s obtained from f_{baryon} and mixing information,

$$f_s = \frac{1}{R_s} \frac{(1+r)\bar{\chi} - (1-f_{\text{baryon}}R_{\text{baryon}})\chi_d}{(1+r)\chi_s - \chi_d}, \quad (28)$$

where $r = R_u/R_d = \tau(B^+)/\tau(B^0)$.

The published measurements of $\bar{\chi}$ performed by the LEP experiments have been combined by the LEP Electroweak Working Group to yield $\bar{\chi} = 0.1259 \pm 0.0042$ [43]. This can be compared with the Tevatron average, $\bar{\chi} = 0.127 \pm 0.008$, obtained from D0 [44] and CDF [45] measurements with Run II data.⁹ The two averages agree, showing no evidence that the production fractions of B^0 and B_s^0 mesons at the Z peak or at the Tevatron are different. We combine these two results in a simple weighted average, assuming no correlations, and obtain $\bar{\chi} = 0.1260 \pm 0.0037$.

Introducing the $\bar{\chi}$ average in Eq. (28), together with our world average $\chi_d = 0.1862 \pm 0.0023$ (see Eq. (57) of Sec. 3.3.1), the assumption $\chi_s = 1/2$ (justified by Eq. (66) in Sec. 3.3.2), the best knowledge of the lifetimes (see Sec. 3.2) and the estimate of f_{baryon} given above, yields $f_s = 0.115 \pm 0.011$ (or $f_s = 0.115 \pm 0.012$ using only LEP data, or $f_s = 0.117 \pm 0.020$ using only Tevatron data), an estimate dominated by the mixing information. Taking into account all known correlations (including the one introduced by f_{baryon}), this result is then combined with the set of fractions obtained from direct measurements (given above), to yield the improved estimates of Table 5, still under the constraints of Eq. (25). As can be seen, our knowledge on the mixing parameters substantially reduces the uncertainty on f_s . It should be noted that the results are correlated, as indicated in Table 5.

⁹ As explained in Ref. [45], a previous CDF analysis [46] performed with Run I data overlooked a background component, so the corresponding result is not included in the average.

3.2 b -hadron lifetimes

In the spectator model the decay of b -flavoured hadrons H_b is governed entirely by the flavour changing $b \rightarrow Wq$ transition ($q = c, u$). For this very reason, lifetimes of all b -flavoured hadrons are the same in the spectator approximation regardless of the (spectator) quark content of the H_b . In the early 1990's experiments became sophisticated enough to start seeing the differences of the lifetimes among various H_b species. The first theoretical calculations of the spectator quark effects on H_b lifetime emerged only few years earlier.

Currently, most of such calculations are performed in the framework of the Heavy Quark Expansion, HQE. In the HQE, under certain assumptions (most important of which is that of quark-hadron duality), the decay rate of an H_b to an inclusive final state f is expressed as the sum of a series of expectation values of operators of increasing dimension, multiplied by the correspondingly higher powers of Λ_{QCD}/m_b :

$$\Gamma_{H_b \rightarrow f} = |CKM|^2 \sum_n c_n^{(f)} \left(\frac{\Lambda_{\text{QCD}}}{m_b} \right)^n \langle H_b | O_n | H_b \rangle, \quad (29)$$

where $|CKM|^2$ is the relevant combination of the CKM matrix elements. Coefficients $c_n^{(f)}$ of this expansion, known as Operator Product Expansion [47], can be calculated perturbatively. Hence, the HQE predicts $\Gamma_{H_b \rightarrow f}$ in the form of an expansion in both Λ_{QCD}/m_b and $\alpha_s(m_b)$. The precision of current experiments makes it mandatory to go to the next-to-leading order in QCD, *i.e.* to include correction of the order of $\alpha_s(m_b)$ to the $c_n^{(f)}$'s. All non-perturbative physics is shifted into the expectation values $\langle H_b | O_n | H_b \rangle$ of operators O_n . These can be calculated using lattice QCD or QCD sum rules, or can be related to other observables via the HQE [48]. One may reasonably expect that powers of Λ_{QCD}/m_b provide enough suppression that only the first few terms of the sum in Eq. (29) matter.

Theoretical predictions are usually made for the ratios of the lifetimes (with $\tau(B^0)$ chosen as the common denominator) rather than for the individual lifetimes, for this allows several uncertainties to cancel. The precision of the current HQE calculations (see Refs. [49–51] for the latest updates) is in some instances already surpassed by the measurements, *e.g.* in the case of $\tau(B^+)/\tau(B^0)$. Also, HQE calculations are not assumption-free. More accurate predictions are a matter of progress in the evaluation of the non-perturbative hadronic matrix elements and verifying the assumptions that the calculations are based upon. However, the HQE, even in its present shape, draws a number of important conclusions, which are in agreement with experimental observations:

- The heavier the mass of the heavy quark the smaller is the variation in the lifetimes among different hadrons containing this quark, which is to say that as $m_b \rightarrow \infty$ we retrieve the spectator picture in which the lifetimes of all H_b 's are the same. This is well illustrated by the fact that lifetimes are rather similar in the b sector, while they differ by large factors in the c sector ($m_c < m_b$).
- The non-perturbative corrections arise only at the order of $\Lambda_{\text{QCD}}^2/m_b^2$, which translates into differences among H_b lifetimes of only a few percent.
- It is only the difference between meson and baryon lifetimes that appears at the $\Lambda_{\text{QCD}}^2/m_b^2$ level. The splitting of the meson lifetimes occurs at the $\Lambda_{\text{QCD}}^3/m_b^3$ level, yet it is enhanced by a phase space factor $16\pi^2$ with respect to the leading free b decay.

To ensure that certain sources of systematic uncertainty cancel, lifetime analyses are sometimes designed to measure a ratio of lifetimes. However, because of the differences in decay topologies, abundance (or lack thereof) of decays of a certain kind, *etc.*, measurements of the individual lifetimes are more common. In the following section we review the most common types of the lifetime measurements. This discussion is followed by the presentation of the averaging of the various lifetime measurements, each with a brief description of its particularities.

3.2.1 Lifetime measurements, uncertainties and correlations

In most cases lifetime of an H_b is estimated from a flight distance and a $\beta\gamma$ factor which is used to convert the geometrical distance into the proper decay time. Methods of accessing lifetime information can roughly be divided in the following five categories:

1. ***Inclusive (flavour-blind) measurements.*** These measurements are aimed at extracting the lifetime from a mixture of b -hadron decays, without distinguishing the decaying species. Often the knowledge of the mixture composition is limited, which makes these measurements experiment-specific. Also, these measurements have to rely on Monte Carlo for estimating the $\beta\gamma$ factor, because the decaying hadrons are not fully reconstructed. On the bright side, these usually are the largest statistics b -hadron lifetime measurements that are accessible to a given experiment, and can, therefore, serve as an important performance benchmark.
2. ***Measurements in semileptonic decays of a specific H_b .*** W from $b \rightarrow Wc$ produces $\ell\nu_\ell$ pair ($\ell = e, \mu$) in about 21% of the cases. Electron or muon from such decays is usually a well-detected signature, which provides for clean and efficient trigger. c quark from $b \rightarrow Wc$ transition and the other quark(s) making up the decaying H_b combine into a charm hadron, which is reconstructed in one or more exclusive decay channels. Knowing what this charmed hadron is allows one to separate, at least statistically, different H_b species. The advantage of these measurements is in statistics, which usually is superior to that of the exclusively reconstructed H_b decays. Some of the main disadvantages are related to the difficulty of estimating lepton+charm sample composition and Monte Carlo reliance for the $\beta\gamma$ factor estimate.
3. ***Measurements in exclusively reconstructed hadronic decays.*** These have the advantage of complete reconstruction of decaying H_b , which allows one to infer the decaying species as well as to perform precise measurement of the $\beta\gamma$ factor. Both lead to generally smaller systematic uncertainties than in the above two categories. The downsides are smaller branching ratios, larger combinatoric backgrounds, especially in $H_b \rightarrow H_c\pi(\pi\pi)$ and multi-body H_c decays, or in a hadron collider environment with non-trivial underlying event. $H_b \rightarrow J/\psi H_s$ are relatively clean and easy to trigger on $J/\psi \rightarrow \ell^+\ell^-$, but their branching fraction is only about 1%.
4. ***Measurements at asymmetric B factories.***

In the $\Upsilon(4S) \rightarrow B\bar{B}$ decay, the B mesons (B^+ or B^0) are essentially at rest in the $\Upsilon(4S)$ frame. This makes direct lifetime measurements impossible in experiments at symmetric colliders producing $\Upsilon(4S)$ at rest. At asymmetric B factories the $\Upsilon(4S)$ meson is boosted resulting in B and \bar{B} moving nearly parallel to each other with the same boost. The

lifetime is inferred from the distance Δz separating the B and \bar{B} decay vertices along the beam axis and from the $\Upsilon(4S)$ boost known from the beam energies. This boost is equal to $\beta\gamma \approx 0.55$ (0.43) in the *BABAR* (*Belle*) experiment, resulting in an average B decay length of approximately 250 (190) μm .

In order to determine the charge of the B mesons in each event, one of the them is fully reconstructed in a semileptonic or hadronic decay mode. The other B is typically not fully reconstructed, only the position of its decay vertex is determined from the remaining tracks in the event. These measurements benefit from large statistics, but suffer from poor proper time resolution, comparable to the B lifetime itself. This resolution is dominated by the uncertainty on the decay vertices, which is typically 50 (100) μm for a fully (partially) reconstructed B meson. With very large future statistics, the resolution and purity could be improved (and hence the systematics reduced) by fully reconstructing both B mesons in the event.

5. ***Direct measurement of lifetime ratios.*** This method has so far been only applied in the measurement of $\tau(B^+)/\tau(B^0)$. The ratio of the lifetimes is extracted from the dependence of the observed relative number of B^+ and B^0 candidates (both reconstructed in semileptonic decays) on the proper decay time.

In some of the latest analyses, measurements of two (*e.g.* $\tau(B^+)$ and $\tau(B^+)/\tau(B^0)$) or three (*e.g.* $\tau(B^+)$, $\tau(B^+)/\tau(B^0)$, and Δm_d) quantities are combined. This introduces correlations among measurements. Another source of correlations among the measurements are the systematic effects, which could be common to an experiment or to an analysis technique across the experiments. When calculating the averages, such correlations are taken into account per general procedure, described in Ref. [52].

3.2.2 Inclusive b -hadron lifetimes

The inclusive b hadron lifetime is defined as $\tau_b = \sum_i f_i \tau_i$ where τ_i are the individual species lifetimes and f_i are the fractions of the various species present in an unbiased sample of weakly-decaying b hadrons produced at a high-energy collider.¹⁰ This quantity is certainly less fundamental than the lifetimes of the individual species, the latter being much more useful in comparisons of the measurements with the theoretical predictions. Nonetheless, we perform the averaging of the inclusive lifetime measurements for completeness as well as for the reason that they might be of interest as “technical numbers.”

In practice, an unbiased measurement of the inclusive lifetime is difficult to achieve, because it would imply an efficiency which is guaranteed to be the same across species. So most of the measurements are biased. In an attempt to group analyses which are expected to select the same mixture of b hadrons, the available results (given in Table 6) are divided into the following three sets:

1. measurements at LEP and SLD that accept any b -hadron decay, based on topological reconstruction (secondary vertex or track impact parameters);
2. measurements at LEP based on the identification of a lepton from a b decay; and

¹⁰In principle such a quantity could be slightly different in Z decays and at the Tevatron, in case the fractions of b -hadron species are not exactly the same; see the discussion in Sec. 3.1.3.

Table 6: Measurements of average b -hadron lifetimes.

Experiment	Method	Data set	τ_b (ps)	Ref.
ALEPH	Dipole	91	$1.511 \pm 0.022 \pm 0.078$	[53]
DELPHI	All track i.p. (2D)	91–92	$1.542 \pm 0.021 \pm 0.045$	[54] ^a
DELPHI	Sec. vtx	91–93	$1.582 \pm 0.011 \pm 0.027$	[55] ^a
DELPHI	Sec. vtx	94–95	$1.570 \pm 0.005 \pm 0.008$	[56]
L3	Sec. vtx + i.p.	91–94	$1.556 \pm 0.010 \pm 0.017$	[57] ^b
OPAL	Sec. vtx	91–94	$1.611 \pm 0.010 \pm 0.027$	[58]
SLD	Sec. vtx	93	$1.564 \pm 0.030 \pm 0.036$	[59]
Average set 1 (b vertex)			1.572 ± 0.009	
ALEPH	Lepton i.p. (3D)	91–93	$1.533 \pm 0.013 \pm 0.022$	[60]
L3	Lepton i.p. (2D)	91–94	$1.544 \pm 0.016 \pm 0.021$	[57] ^b
OPAL	Lepton i.p. (2D)	90–91	$1.523 \pm 0.034 \pm 0.038$	[61]
Average set 2 ($b \rightarrow \ell$)			1.537 ± 0.020	
CDF1	J/ψ vtx	92–95	$1.533 \pm 0.015_{-0.031}^{+0.035}$	[62]
ATLAS	J/ψ vtx	2010	$1.489 \pm 0.016 \pm 0.043$	[63]
Average set 3 ($b \rightarrow J/\psi$)			1.516 ± 0.028	
Average of all above			1.566 ± 0.009	

^a The combined DELPHI result quoted in [55] is $1.575 \pm 0.010 \pm 0.026$ ps.

^b The combined L3 result quoted in [57] is $1.549 \pm 0.009 \pm 0.015$ ps.

3. measurements at the Tevatron based on inclusive $H_b \rightarrow J/\psi X$ reconstruction, where the J/ψ is fully reconstructed.

The measurements of the first set are generally considered as estimates of τ_b , although the efficiency to reconstruct a secondary vertex most probably depends, in an analysis-specific way, on the number of tracks coming from the vertex, thereby depending on the type of the H_b . Even though these efficiency variations can in principle be accounted for using Monte Carlo simulations (which inevitably contain assumptions on branching fractions), the H_b mixture in that case can remain somewhat ill-defined and could be slightly different among analyses in this set.

On the contrary, the mixtures corresponding to the other two sets of measurements are better defined in the limit where the reconstruction and selection efficiency of a lepton or a J/ψ from an H_b does not depend on the decaying hadron type. These mixtures are given by the production fractions and the inclusive branching fractions for each H_b species to give a lepton or a J/ψ . In particular, under the assumption that all b hadrons have the same semileptonic decay width, the analyses of the second set should measure $\tau(b \rightarrow \ell) = (\sum_i f_i \tau_i^2) / (\sum_i f_i \tau_i)$ which is necessarily larger than τ_b if lifetime differences exist. Given the present knowledge on τ_i and f_i , $\tau(b \rightarrow \ell) - \tau_b$ is expected to be of the order of 0.01 ps.

Measurements by SLC and LEP experiments are subject to a number of common systematic uncertainties, such as those due to (lack of knowledge of) b and c fragmentation, b and c decay models, $\mathcal{B}(B \rightarrow \ell)$, $\mathcal{B}(B \rightarrow c \rightarrow \ell)$, $\mathcal{B}(c \rightarrow \ell)$, τ_c , and H_b decay multiplicity. In the averaging, these systematic uncertainties are assumed to be 100% correlated. The averages for the sets

Table 7: Measurements of the B^0 lifetime.

Experiment	Method	Data set	$\tau(B^0)$ (ps)	Ref.
ALEPH	$D^{(*)}\ell$	91–95	$1.518 \pm 0.053 \pm 0.034$	[64]
ALEPH	Exclusive	91–94	$1.25_{-0.13}^{+0.15} \pm 0.05$	[65]
ALEPH	Partial rec. $\pi^+\pi^-$	91–94	$1.49_{-0.15-0.06}^{+0.17+0.08}$	[65]
DELPHI	$D^{(*)}\ell$	91–93	$1.61_{-0.13}^{+0.14} \pm 0.08$	[66]
DELPHI	Charge sec. vtx	91–93	$1.63 \pm 0.14 \pm 0.13$	[67]
DELPHI	Inclusive $D^*\ell$	91–93	$1.532 \pm 0.041 \pm 0.040$	[68]
DELPHI	Charge sec. vtx	94–95	$1.531 \pm 0.021 \pm 0.031$	[56]
L3	Charge sec. vtx	94–95	$1.52 \pm 0.06 \pm 0.04$	[69]
OPAL	$D^{(*)}\ell$	91–93	$1.53 \pm 0.12 \pm 0.08$	[70]
OPAL	Charge sec. vtx	93–95	$1.523 \pm 0.057 \pm 0.053$	[71]
OPAL	Inclusive $D^*\ell$	91–00	$1.541 \pm 0.028 \pm 0.023$	[72]
SLD	Charge sec. vtx ℓ	93–95	$1.56_{-0.13}^{+0.14} \pm 0.10$	[73] ^a
SLD	Charge sec. vtx	93–95	$1.66 \pm 0.08 \pm 0.08$	[73] ^a
CDF1	$D^{(*)}\ell$	92–95	$1.474 \pm 0.039_{-0.051}^{+0.052}$	[74]
CDF1	Excl. $J/\psi K^{*0}$	92–95	$1.497 \pm 0.073 \pm 0.032$	[75]
CDF2	Excl. $J/\psi K_S, J/\psi K^{*0}$	02–09	$1.507 \pm 0.010 \pm 0.008$	[76]
D0	Excl. $J/\psi K^{*0}$	03–07	$1.414 \pm 0.018 \pm 0.034$	[77]
D0	Excl. $J/\psi K_S$	02–11	$1.508 \pm 0.025 \pm 0.043$	[78]
BABAR	Exclusive	99–00	$1.546 \pm 0.032 \pm 0.022$	[79]
BABAR	Inclusive $D^*\ell$	99–01	$1.529 \pm 0.012 \pm 0.029$	[80]
BABAR	Exclusive $D^*\ell$	99–02	$1.523_{-0.023}^{+0.024} \pm 0.022$	[81]
BABAR	Incl. $D^*\pi, D^*\rho$	99–01	$1.533 \pm 0.034 \pm 0.038$	[82]
BABAR	Inclusive $D^*\ell$	99–04	$1.504 \pm 0.013_{-0.013}^{+0.018}$	[83]
Belle	Exclusive	00–03	$1.534 \pm 0.008 \pm 0.010$	[84]
ATLAS	Excl. $J/\psi K^{*0}$	2010	$1.51 \pm 0.04 \pm 0.04$	[85] ^p
LHCb	Excl. $J/\psi K^{*0}$	2010	$1.512 \pm 0.032 \pm 0.042$	[86] ^p
LHCb	Excl. $J/\psi K_S$	2010	$1.558 \pm 0.056 \pm 0.022$	[86] ^p
Average			1.519 ± 0.007	

^a The combined SLD result quoted in [73] is $1.64 \pm 0.08 \pm 0.08$ ps.

^p Preliminary.

defined above (also given in Table 6) are

$$\tau(b \text{ vertex}) = 1.572 \pm 0.009 \text{ ps}, \quad (30)$$

$$\tau(b \rightarrow \ell) = 1.537 \pm 0.020 \text{ ps}, \quad (31)$$

$$\tau(b \rightarrow J/\psi) = 1.516 \pm 0.028 \text{ ps}, \quad (32)$$

whereas an average of all measurements, ignoring mixture differences, yields 1.566 ± 0.009 ps.

Table 8: Measurements of the B^+ lifetime.

Experiment	Method	Data set	$\tau(B^+)$ (ps)	Ref.
ALEPH	$D^{(*)}\ell$	91–95	$1.648 \pm 0.049 \pm 0.035$	[64]
ALEPH	Exclusive	91–94	$1.58^{+0.21+0.04}_{-0.18-0.03}$	[65]
DELPHI	$D^{(*)}\ell$	91–93	$1.61 \pm 0.16 \pm 0.12$	[66] ^a
DELPHI	Charge sec. vtx	91–93	$1.72 \pm 0.08 \pm 0.06$	[67] ^a
DELPHI	Charge sec. vtx	94–95	$1.624 \pm 0.014 \pm 0.018$	[56]
L3	Charge sec. vtx	94–95	$1.66 \pm 0.06 \pm 0.03$	[69]
OPAL	$D^{(*)}\ell$	91–93	$1.52 \pm 0.14 \pm 0.09$	[70]
OPAL	Charge sec. vtx	93–95	$1.643 \pm 0.037 \pm 0.025$	[71]
SLD	Charge sec. vtx ℓ	93–95	$1.61^{+0.13}_{-0.12} \pm 0.07$	[73] ^b
SLD	Charge sec. vtx	93–95	$1.67 \pm 0.07 \pm 0.06$	[73] ^b
CDF1	$D^{(*)}\ell$	92–95	$1.637 \pm 0.058^{+0.045}_{-0.043}$	[74]
CDF1	Excl. $J/\psi K$	92–95	$1.636 \pm 0.058 \pm 0.025$	[75]
CDF2	Excl. $J/\psi K$	02–09	$1.639 \pm 0.009 \pm 0.009$	[76]
CDF2	Excl. $D^0\pi$	02–06	$1.663 \pm 0.023 \pm 0.015$	[87]
<i>BABAR</i>	Exclusive	99–00	$1.673 \pm 0.032 \pm 0.023$	[79]
Belle	Exclusive	00–03	$1.635 \pm 0.011 \pm 0.011$	[84]
LHCb	Excl. $J/\psi K$	2010	$1.689 \pm 0.022 \pm 0.047$	[86] ^p
Average			1.642 ± 0.008	

^a The combined DELPHI result quoted in [67] is 1.70 ± 0.09 ps.

^b The combined SLD result quoted in [73] is $1.66 \pm 0.06 \pm 0.05$ ps.

^p Preliminary.

3.2.3 B^0 and B^+ lifetimes and their ratio

After a number of years of dominating these averages the LEP experiments yielded the scene to the asymmetric B factories and the Tevatron experiments. The B factories have been very successful in utilizing their potential – in only a few years of running, *BABAR* and, to a greater extent, Belle, have struck a balance between the statistical and the systematic uncertainties, with both being close to (or even better than) the impressive 1%. In the meanwhile, CDF and D0 have emerged as significant contributors to the field as the Tevatron Run II data flowed in, with CDF eventually providing the most precise results.

At present time we are in an interesting position of having three sets of measurements (from LEP/SLC, B factories and the Tevatron) that originate from different environments, obtained using substantially different techniques and are precise enough for incisive comparison.

The averaging of $\tau(B^+)$, $\tau(B^0)$ and $\tau(B^+)/\tau(B^0)$ measurements is summarized¹¹ in Tables 7, 8, and 9. For $\tau(B^+)/\tau(B^0)$ we averaged only the measurements of this quantity provided by experiments rather than using all available knowledge, which would have included, for example, $\tau(B^+)$ and $\tau(B^0)$ measurements which did not contribute to any of the ratio measurements.

The following sources of correlated (within experiment/machine) systematic uncertainties have been considered:

¹¹ We do not include the old unpublished measurements of Refs. [89,90].

Table 9: Measurements of the ratio $\tau(B^+)/\tau(B^0)$.

Experiment	Method	Data set	Ratio $\tau(B^+)/\tau(B^0)$	Ref.
ALEPH	$D^{(*)}\ell$	91–95	$1.085 \pm 0.059 \pm 0.018$	[64]
ALEPH	Exclusive	91–94	$1.27^{+0.23+0.03}_{-0.19-0.02}$	[65]
DELPHI	$D^{(*)}\ell$	91–93	$1.00^{+0.17}_{-0.15} \pm 0.10$	[66]
DELPHI	Charge sec. vtx	91–93	$1.06^{+0.13}_{-0.11} \pm 0.10$	[67]
DELPHI	Charge sec. vtx	94–95	$1.060 \pm 0.021 \pm 0.024$	[56]
L3	Charge sec. vtx	94–95	$1.09 \pm 0.07 \pm 0.03$	[69]
OPAL	$D^{(*)}\ell$	91–93	$0.99 \pm 0.14^{+0.05}_{-0.04}$	[70]
OPAL	Charge sec. vtx	93–95	$1.079 \pm 0.064 \pm 0.041$	[71]
SLD	Charge sec. vtx ℓ	93–95	$1.03^{+0.16}_{-0.14} \pm 0.09$	[73] ^a
SLD	Charge sec. vtx	93–95	$1.01^{+0.09}_{-0.08} \pm 0.05$	[73] ^a
CDF1	$D^{(*)}\ell$	92–95	$1.110 \pm 0.056^{+0.033}_{-0.030}$	[74]
CDF1	Excl. $J/\psi K$	92–95	$1.093 \pm 0.066 \pm 0.028$	[75]
CDF2	Excl. $J/\psi K^{(*)}$	02–09	$1.088 \pm 0.009 \pm 0.004$	[76]
D0	$D^{*+}\mu D^0\mu$ ratio	02–04	$1.080 \pm 0.016 \pm 0.014$	[88]
BABAR	Exclusive	99–00	$1.082 \pm 0.026 \pm 0.012$	[79]
Belle	Exclusive	00–03	$1.066 \pm 0.008 \pm 0.008$	[84]
Average			1.079 ± 0.007	

^a The combined SLD result quoted in [73] is $1.01 \pm 0.07 \pm 0.06$.

- for SLC/LEP measurements – D^{**} branching ratio uncertainties [3], momentum estimation of b mesons from Z^0 decays (b -quark fragmentation parameter $\langle X_E \rangle = 0.702 \pm 0.008$ [3]), B_s^0 and b baryon lifetimes (see Secs. 3.2.4 and 3.2.6), and b -hadron fractions at high energy (see Table 5);
- for BABAR measurements – alignment, z scale, PEP-II boost, sample composition (where applicable);
- for D0 and CDF Run II measurements – alignment (separately within each experiment).

The resultant averages are:

$$\tau(B^0) = 1.519 \pm 0.007 \text{ ps}, \quad (33)$$

$$\tau(B^+) = 1.642 \pm 0.008 \text{ ps}, \quad (34)$$

$$\tau(B^+)/\tau(B^0) = 1.079 \pm 0.007. \quad (35)$$

3.2.4 B_s^0 lifetimes

Like neutral kaons, neutral B mesons contain short- and long-lived components, since the light (L) and heavy (H) eigenstates, B_L and B_H , differ not only in their masses, but also in their total decay widths, with a decay width difference defined as $\Delta\Gamma = \Gamma_L - \Gamma_H$. Neglecting CP violation in $B - \bar{B}$ mixing, which is expected to be very small [91, 92], the mass eigenstates are also CP eigenstates, with the light B_L state being CP -even and the heavy B_H state being

CP -odd. While the decay width difference $\Delta\Gamma_d$ can be neglected in the B^0 system, the B_s^0 system exhibits a significant value of $\Delta\Gamma_s$: the sign of $\Delta\Gamma_s$ is known to be positive [93], *i.e.* the heavy eigenstates lives longer than the light eigenstate. Specific measurements of $\Delta\Gamma_s$ and $\Gamma_s = (\Gamma_L + \Gamma_H)/2$ are explained and averaged in Sec. 3.3.2, but the results for $1/\Gamma_L$, $1/\Gamma_H$ and the mean B_s^0 lifetime, defined as $\tau(B_s^0) = 1/\Gamma_s$, are also quoted at the end of this section.

Many B_s^0 lifetime analyses, in particular the early ones performed before the non-zero value of $\Delta\Gamma_s$ was firmly established, ignore $\Delta\Gamma_s$ and fit the proper time distribution of a sample of B_s^0 candidates reconstructed in a certain final state f with a model assuming a single exponential function for the signal. We denote such effective lifetime measurements as $\tau_{\text{single}}(B_s^0 \rightarrow f)$; their true values may lie *a priori* anywhere between $1/\Gamma_L = 1/(\Gamma_s + \Delta\Gamma_s/2)$ and $1/\Gamma_H = 1/(\Gamma_s - \Delta\Gamma_s/2)$, depending on the proportion of B_L and B_H in the final state f . Table 10 summarizes the effective lifetime measurements.

Averaging measurements of $\tau_{\text{single}}(B_s^0 \rightarrow f)$ over several final states f will yield a result corresponding to an ill-defined observable when the proportions of B_L and B_H differ. Therefore, the effective B_s^0 lifetime measurements are broken down into several categories and averaged separately.

- **Flavour-specific decays**, such as semileptonic $B_s^0 \rightarrow D_s^- \ell^+ \nu$ or $B_s^0 \rightarrow D_s^- \pi^+$, have equal fractions of B_L and B_H at time zero. If the resulting superposition of two exponential distributions is fitted with a single exponential function, one obtains a measure of the so-called *flavour-specific lifetime* [108]:

$$\tau_{\text{single}}(B_s^0 \rightarrow \text{flavour specific}) = \frac{1}{\Gamma_s} \frac{1 + \left(\frac{\Delta\Gamma_s}{2\Gamma_s}\right)^2}{1 - \left(\frac{\Delta\Gamma_s}{2\Gamma_s}\right)^2}. \quad (36)$$

The average of all flavour-specific B_s^0 lifetime measurements¹² is

$$\tau_{\text{single}}(B_s^0 \rightarrow \text{flavour specific}) = 1.463 \pm 0.032 \text{ ps}. \quad (37)$$

- **$B_s^0 \rightarrow D_s^\mp X$ decays** include flavour-specific decays but also decays with a less known mixture of light and heavy components. The corresponding effective lifetime average,

$$\tau_{\text{single}}(B_s^0 \rightarrow D_s^\mp X) = 1.466 \pm 0.031 \text{ ps}, \quad (38)$$

can still be a useful input for analyses examining an inclusive D_s sample. The following correlated systematic errors were considered: average B lifetime used in backgrounds, B_s^0 decay multiplicity, and branching ratios used to determine backgrounds (*e.g.* $\mathcal{B}(B \rightarrow D_s D)$). A knowledge of the multiplicity of B_s^0 decays is important for measurements that partially reconstruct the final state such as $B \rightarrow D_s X$ (where X is not a lepton). The boost deduced from Monte Carlo simulation depends on the multiplicity used. Since this is not well known, the multiplicity in the simulation is varied and this range of values observed is taken to be a systematic. Similarly not all the branching ratios for the potential background processes are measured. Where they are available, the PDG values are used for the error estimate. Where no measurements are available estimates can usually be made by using measured branching ratios of related processes and using some reasonable extrapolation.

¹² An old unpublished measurement [109] is not included.

Table 10: Measurements of the effective B_s^0 lifetimes obtained from single exponential fits, without attempting to separate the CP -even and CP -odd components.

Experiment	Final state f	Data set	$\tau_{\text{single}}(B_s^0 \rightarrow f)$ (ps)	Ref.
ALEPH	$D_s \ell$	91–95	$1.54^{+0.14}_{-0.13} \pm 0.04$	[94]
CDF1	$D_s \ell$	92–96	$1.36 \pm 0.09^{+0.06}_{-0.05}$	[95]
DELPHI	$D_s \ell$	91–95	$1.42^{+0.14}_{-0.13} \pm 0.03$	[96]
OPAL	$D_s \ell$	90–95	$1.50^{+0.16}_{-0.15} \pm 0.04$	[97]
D0	$D_s \mu$	02–04	$1.398 \pm 0.044^{+0.028}_{-0.025}$	[98]
CDF2	$D_s \pi(X)$	02–06	1.3 fb $^{-1}$	$1.518 \pm 0.041 \pm 0.027$ [99]
Average of above 6 flavour-specific measurements			1.463 ± 0.032	
ALEPH	$D_s h$	91–95	$1.47 \pm 0.14 \pm 0.08$	[100]
DELPHI	$D_s h$	91–95	$1.53^{+0.16}_{-0.15} \pm 0.07$	[101]
OPAL	D_s incl.	90–95	$1.72^{+0.20+0.18}_{-0.19-0.17}$	[102]
Average of above 9 D_s measurements			1.466 ± 0.031	
CDF1	$J/\psi \phi$	92–95	$1.34^{+0.23}_{-0.19} \pm 0.05$	[62]
D0	$J/\psi \phi$	02–04	$1.444^{+0.098}_{-0.090} \pm 0.02$	[103]
ATLAS	$J/\psi \phi$	2010	40 pb $^{-1}$	$1.41 \pm 0.08 \pm 0.05$ [85] ^p
LHCb	$J/\psi \phi$	2010	36 pb $^{-1}$	$1.447 \pm 0.064 \pm 0.056$ [86] ^p
Average of above 4 $J/\psi \phi$ measurements			1.430 ± 0.050	
ALEPH	$D_s^{(*)+} D_s^{(*)-}$	91–95	4M $Z \rightarrow q\bar{q}$	$1.27 \pm 0.33 \pm 0.08$ [104]
LHCb	$K^+ K^-$	10	0.037 fb $^{-1}$	$1.440 \pm 0.096 \pm 0.009$ [105]
LHCb	$K^+ K^-$	11	1.0 fb $^{-1}$	$1.468 \pm 0.046 \pm 0.006$ [106] ^p
Average of above 2 $K^+ K^-$ measurements			1.463 ± 0.042	
CDF2	$J/\psi f_0(980)$	02–08	3.8 fb $^{-1}$	$1.70^{+0.12}_{-0.11} \pm 0.03$ [107]
Average of above 1 $J/\psi f_0(980)$ measurement			1.70 ± 0.12	

^p Preliminary.

- $B_s^0 \rightarrow J/\psi \phi$ *decays* contain a well-defined mixture of CP -even and CP -odd states. There are no known correlations between the existing $B_s^0 \rightarrow J/\psi \phi$ effective lifetime measurements; these are combined into the average¹³

$$\tau_{\text{single}}(B_s^0 \rightarrow J/\psi \phi) = 1.430 \pm 0.050 \text{ ps}. \quad (39)$$

A caveat is that different experimental acceptances may lead to different admixtures of the CP -even and CP -odd states, and simple fits to a single exponential may result in inherently different values of $\tau_{\text{single}}(B_s^0 \rightarrow J/\psi \phi)$. Analyses that separate the CP -even and CP -odd components in this decay through a full angular study, outlined in Sec. 3.3.2, provide directly measurements of $1/\Gamma_s$ and $\Delta\Gamma_s$ (see Table 21).

- *Decays to (almost) pure CP -even eigenstates* have also been measured, in the modes $B_s^0 \rightarrow D_s^{(*)+} D_s^{(*)-}$ by ALEPH [104], $B_s^0 \rightarrow K^+ K^-$ by LHCb [105, 106]¹⁴, and

¹³ An old unpublished measurement [110] is not included.

¹⁴ An old unpublished measurement of the $B_s^0 \rightarrow K^+ K^-$ effective lifetime by CDF [111] is no longer considered.

$B_s^0 \rightarrow J/\psi f_0(980)$ by CDF [107]. The $B_s^0 \rightarrow D_s^{(*)+} D_s^{(*)-}$ decays are expected to be mostly CP -even, but a small CP -odd component is most probably present. The decays $B_s^0 \rightarrow K^+ K^-$ and $B_s^0 \rightarrow J/\psi f_0(980)$ have CP -even and CP -odd final states, respectively; if these decays are dominated by a single weak phase and if CP violation can be neglected, then $\tau_{\text{single}}(B_s^0 \rightarrow K^+ K^-) \sim 1/\Gamma_L$ and $\tau_{\text{single}}(B_s^0 \rightarrow J/\psi f_0(980)) \sim 1/\Gamma_H$ (see Eqs. (61) and (62) for approximate relations in presence of CP violation in the mixing). The averages for these two effective lifetimes are

$$\tau_{\text{single}}(B_s^0 \rightarrow K^+ K^-) = 1.463 \pm 0.042 \text{ ps}, \quad (40)$$

$$\tau_{\text{single}}(B_s^0 \rightarrow J/\psi f_0(980)) = 1.70 \pm 0.12 \text{ ps}. \quad (41)$$

As described in Sec. 3.3.2, the effective lifetime averages of Eqs. (37), (40), and (41) are used as ingredients to improve the determination of $1/\Gamma_s$ and $\Delta\Gamma_s$ obtained from the full angular analyses of $B_s^0 \rightarrow J/\psi \phi$ decays. The resulting world averages for the B_s^0 lifetimes are

$$\frac{1}{\Gamma_L} = \frac{1}{\Gamma_s + \Delta\Gamma_s/2} = 1.408 \pm 0.017 \text{ ps}, \quad (42)$$

$$\frac{1}{\Gamma_H} = \frac{1}{\Gamma_s - \Delta\Gamma_s/2} = 1.626 \pm 0.023 \text{ ps}, \quad (43)$$

$$\tau(B_s^0) = \frac{1}{\Gamma_s} = \frac{2}{\Gamma_L + \Gamma_H} = 1.509 \pm 0.012 \text{ ps}. \quad (44)$$

3.2.5 B_c^+ lifetime

Early measurements of the B_c^+ meson lifetime, from CDF [112, 113] and D0 [114], use the semileptonic decay mode $B_c^+ \rightarrow J/\psi \ell$ and are based on a simultaneous fit to the mass and lifetime using the vertex formed with the leptons from the decay of the J/ψ and the third lepton. Correction factors to estimate the boost due to the missing neutrino are used. In the analysis of the CDF Run I data [112], a mass value of $6.40 \pm 0.39 \pm 0.13 \text{ GeV}/c^2$ is found by fitting to the tri-lepton invariant mass spectrum. In the CDF and D0 Run II results [113, 114], the B_c^+ mass is assumed to be $6285.7 \pm 5.3 \pm 1.2 \text{ MeV}/c^2$, taken from a CDF result [115]. These mass measurements are consistent within uncertainties, and also consistent with the most recent precision determination from CDF of $6275.6 \pm 2.9 \pm 2.5 \text{ MeV}/c^2$ [116]. Correlated systematic errors include the impact of the uncertainty of the B_c^+ p_T spectrum on the correction factors, the level of feed-down from $\psi(2S)$, Monte-Carlo modeling of the decay model varying from phase space to the ISGW model, and mass variations.

The most recent determination of the B_c^+ lifetime, from CDF2 [117], is based on fully reconstructed $B_c^+ \rightarrow J/\psi \pi$ decays and does not suffer from a missing neutrino. All the measurements are summarized in Table 11 and the world average is determined to be

$$\tau(B_c^+) = 0.458 \pm 0.030 \text{ ps}. \quad (45)$$

3.2.6 Λ_b^0 and b -baryon lifetimes

The first measurements of b -baryon lifetimes originate from two classes of partially reconstructed decays. In the first class, decays with an exclusively reconstructed Λ_c^+ baryon and a lepton of

Table 11: Measurements of the B_c^+ lifetime.

Experiment	Method	Data set		$\tau(B_c^+)$ (ps)	Ref.
CDF1	$J/\psi \ell$	92–95	0.11 fb^{-1}	$0.46_{-0.16}^{+0.18} \pm 0.03$	[112]
CDF2	$J/\psi \ell$	02–06	1.0 fb^{-1}	$0.475_{-0.049}^{+0.053} \pm 0.018$	[113] ^p
D0	$J/\psi \mu$	02–06	1.3 fb^{-1}	$0.448_{-0.036}^{+0.038} \pm 0.032$	[114]
CDF2	$J/\psi \pi$		6.7 fb^{-1}	$0.452 \pm 0.048 \pm 0.027$	[117] ^p
Average				0.458 ± 0.030	

^p Preliminary.

opposite charge are used. These products are more likely to occur in the decay of Λ_b^0 baryons. In the second class, more inclusive final states with a baryon (p , \bar{p} , Λ , or $\bar{\Lambda}$) and a lepton have been used, and these final states can generally arise from any b baryon. With the large b -hadron samples available at the Tevatron, the most precise measurements of b -baryons now come from fully reconstructed exclusive decays.

The following sources of correlated systematic uncertainties have been considered: experimental time resolution within a given experiment, b -quark fragmentation distribution into weakly decaying b baryons, Λ_b^0 polarization, decay model, and evaluation of the b -baryon purity in the selected event samples. In computing the averages the central values of the masses are scaled to $M(\Lambda_b^0) = 5620 \pm 2 \text{ MeV}/c^2$ [118] and $M(b\text{-baryon}) = 5670 \pm 100 \text{ MeV}/c^2$.

For the semi-inclusive lifetime measurements, the meaning of decay model systematic uncertainties and the correlation of these uncertainties between measurements are not always clear. Uncertainties related to the decay model are dominated by assumptions on the fraction of n -body semileptonic decays. To be conservative it is assumed that these are 100% correlated whenever given as an error. DELPHI varies the fraction of 4-body decays from 0.0 to 0.3. In computing the average, the DELPHI result is corrected to a value of 0.2 ± 0.2 for this fraction.

Furthermore, in computing the average, the semileptonic decay results from LEP are corrected for a polarization of $-0.45_{-0.17}^{+0.19}$ [3] and a Λ_b^0 fragmentation parameter $\langle X_E \rangle = 0.70 \pm 0.03$ [119].

Inputs to the averages are given in Table 12. The CDF $\Lambda_b \rightarrow J/\psi \Lambda$ lifetime result [76] is 3.4σ larger than the world average computed excluding this result. It is nonetheless combined with the rest without adjustment of input errors. The world average lifetime of b baryons is then

$$\langle \tau(b\text{-baryon}) \rangle = 1.378 \pm 0.027 \text{ ps} . \quad (46)$$

Keeping only $\Lambda_c^\pm \ell^\mp$, $\Lambda \ell^- \ell^+$, and fully exclusive final states, as representative of the Λ_b^0 baryon, the following lifetime is obtained:

$$\tau(\Lambda_b^0) = 1.413 \pm 0.030 \text{ ps} . \quad (47)$$

Averaging the measurements based on the $\Xi^\mp \ell^\mp$ [29–31] and $J/\psi \Xi^\mp$ [40] final states gives a lifetime value for a sample of events containing Ξ_b^0 and Ξ_b^- baryons:

$$\langle \tau(\Xi_b) \rangle = 1.49_{-0.18}^{+0.19} \text{ ps} . \quad (48)$$

Table 12: Measurements of the b -baryon lifetimes.

Experiment	Method	Data set	Lifetime (ps)	Ref.
ALEPH	$\Lambda_c^+ \ell$	91–95	$1.18_{-0.12}^{+0.13} \pm 0.03$	[28] ^a
ALEPH	$\Lambda \ell^- \ell^+$	91–95	$1.30_{-0.21}^{+0.26} \pm 0.04$	[28] ^a
DELPHI	$\Lambda_c^+ \ell$	91–94	$1.11_{-0.18}^{+0.19} \pm 0.05$	[120] ^b
OPAL	$\Lambda_c^+ \ell, \Lambda \ell^- \ell^+$	90–95	$1.29_{-0.22}^{+0.24} \pm 0.06$	[97]
CDF1	$\Lambda_c^+ \ell$	91–95	$1.32 \pm 0.15 \pm 0.07$	[121]
CDF2	$\Lambda_c^+ \pi$	02–06	$1.401 \pm 0.046 \pm 0.035$	[122]
CDF2	$J/\psi \Lambda$	02–09	$1.537 \pm 0.045 \pm 0.014$	[76]
D0	$\Lambda_c^+ \mu$	02–06	$1.290_{-0.110-0.091}^{+0.119+0.087}$	[123]
D0	$J/\psi \Lambda$	02–11	$1.303 \pm 0.075 \pm 0.035$	[78]
LHCb	$J/\psi \Lambda$	2010	$1.353 \pm 0.108 \pm 0.035$	[86] ^p
Average of above 10:		Λ_b^0 lifetime =	1.413 ± 0.030	
ALEPH	$\Lambda \ell$	91–95	$1.20 \pm 0.08 \pm 0.06$	[28]
DELPHI	$\Lambda \ell \pi$ vtx	91–94	$1.16 \pm 0.20 \pm 0.08$	[120] ^b
DELPHI	$\Lambda \mu$ i.p.	91–94	$1.10_{-0.17}^{+0.19} \pm 0.09$	[124] ^b
DELPHI	$p \ell$	91–94	$1.19 \pm 0.14 \pm 0.07$	[120] ^b
OPAL	$\Lambda \ell$ i.p.	90–94	$1.21_{-0.13}^{+0.15} \pm 0.10$	[125] ^c
OPAL	$\Lambda \ell$ vtx	90–94	$1.15 \pm 0.12 \pm 0.06$	[125] ^c
Average of above 16: mean b -baryon lifetime =			1.378 ± 0.027	
CDF2	$J/\psi \Xi^-$	02–09	$1.56_{-0.25}^{+0.27} \pm 0.02$	[40]
Average of above 1:		Ξ_b^- lifetime =	$1.56_{-0.25}^{+0.27}$	
ALEPH	$\Xi \ell$	90–95	$1.35_{-0.28-0.17}^{+0.37+0.15}$	[29]
DELPHI	$\Xi \ell$	91–93	$1.5_{-0.4}^{+0.7} \pm 0.3$	[31] ^d
DELPHI	$\Xi \ell$	92–95	$1.45_{-0.43}^{+0.55} \pm 0.13$	[30] ^d
Average of above 4:		mean Ξ_b^- lifetime =	$1.49_{-0.18}^{+0.19}$	
CDF2	$J/\psi \Omega^-$	02–09	$1.13_{-0.40}^{+0.53} \pm 0.02$	[40]
Average of above 1:		Ω_b^- lifetime =	$1.13_{-0.40}^{+0.53}$	

^a The combined ALEPH result quoted in [28] is 1.21 ± 0.11 ps.

^b The combined DELPHI result quoted in [120] is $1.14 \pm 0.08 \pm 0.04$ ps.

^c The combined OPAL result quoted in [125] is $1.16 \pm 0.11 \pm 0.06$ ps.

^d The combined DELPHI result quoted in [30] is $1.48_{-0.31}^{+0.40} \pm 0.12$ ps.

^p Preliminary.

First measurements of fully reconstructed $\Xi_b^- \rightarrow J/\psi \Xi^-$ and $\Omega_b^- \rightarrow J/\psi \Omega^-$ baryons yield [40]

$$\tau(\Xi_b^-) = 1.56_{-0.25}^{+0.27} \text{ ps}, \quad (49)$$

$$\tau(\Omega_b^-) = 1.13_{-0.40}^{+0.53} \text{ ps}. \quad (50)$$

3.2.7 Summary and comparison with theoretical predictions

Averages of lifetimes of specific b -hadron species are collected in Table 13. As described in Sec. 3.2, Heavy Quark Effective Theory can be employed to explain the hierarchy of $\tau(B_c^+) \ll \tau(\Lambda_b^0) < \tau(B_s^0) \approx \tau(B^0) < \tau(B^+)$, and used to predict the ratios between lifetimes. Typical

Table 13: Summary of lifetimes of different b -hadron species.

b -hadron species	Measured lifetime
B^+	1.642 ± 0.008 ps
B^0	1.519 ± 0.007 ps
B_s^0 ($1/\Gamma_s$)	1.509 ± 0.012 ps
B_c^+	0.458 ± 0.030 ps
Λ_b^0	1.413 ± 0.030 ps
Ξ_b mixture	$1.49_{-0.18}^{+0.19}$ ps
b -baryon mixture	1.378 ± 0.027 ps
b -hadron mixture	1.566 ± 0.009 ps

Table 14: Measured ratios of b -hadron lifetimes relative to the B^0 lifetime and ranges predicted by theory [50, 51].

Lifetime ratio	Measured value	Predicted range
$\tau(B^+)/\tau(B^0)$	1.079 ± 0.007	$1.04 - 1.08$
$\tau(B_s^0)/\tau(B^0)$	0.993 ± 0.009	$0.99 - 1.01$
$\tau(\Lambda_b^0)/\tau(B^0)$	0.930 ± 0.020	$0.86 - 0.95$
$\tau(b\text{-baryon})/\tau(B^0)$	0.907 ± 0.018	$0.86 - 0.95$

predictions are compared to the measured lifetime ratios in Table 14. The prediction of the ratio between the B^+ and B^0 lifetimes, 1.06 ± 0.02 [50], is in good agreement with experiment.

The total widths of the B_s^0 and B^0 mesons are expected to be very close and differ by at most 1% [51, 126]. This prediction is consistent with the experimental ratio $\tau(B_s^0)/\tau(B^0) = \Gamma_d/\Gamma_s$, which is smaller than 1 by $(0.7 \pm 0.9)\%$.

The ratio $\tau(\Lambda_b^0)/\tau(B^0)$ has particularly been the source of theoretical scrutiny since earlier calculations using Heavy Quark Effective Theory [47, 127] predicted a value larger than 0.90, almost 2σ above the world average at the time. Many predictions cluster around a most likely central value of 0.94 [128]. More recent calculations of this ratio that include higher-order effects predict a lower ratio between the Λ_b^0 and B^0 lifetimes [50, 51] and reduce this difference. References [50, 51] present probability density functions of their predictions with variation of theoretical inputs, and the indicated ranges in Table 14 are the RMS of the distributions from the most probable values, and for $\tau(\Lambda_b^0)/\tau(B^0)$, also encompass the earlier theoretical predictions [47, 127, 128]. Note that in contrast to the B mesons, complete NLO QCD corrections and fully reliable lattice determinations of the matrix elements for Λ_b^0 are not yet available. As already mentioned, the CDF measurement of the Λ_b lifetime in the exclusive decay mode $J/\psi \Lambda$ [76] is significantly higher than the world average before inclusion, with a ratio to the $\tau(B^0)$ world average of $\tau(\Lambda_b^0)/\tau(B^0) = 1.012 \pm 0.031$, resulting in continued interest in lifetimes of b baryons.

3.3 Neutral B -meson mixing

The $B^0 - \bar{B}^0$ and $B_s^0 - \bar{B}_s^0$ systems both exhibit the phenomenon of particle-antiparticle mixing. For each of them, there are two mass eigenstates which are linear combinations of the two flavour states, B and \bar{B} . The heaviest (lightest) of these mass states is denoted B_H (B_L), with mass m_H (m_L) and total decay width Γ_H (Γ_L). We define

$$\Delta m = m_H - m_L, \quad x = \Delta m / \Gamma, \quad (51)$$

$$\Delta \Gamma = \Gamma_L - \Gamma_H, \quad y = \Delta \Gamma / (2\Gamma), \quad (52)$$

where $\Gamma = (\Gamma_H + \Gamma_L) / 2 = 1 / \bar{\tau}(B)$ is the average decay width. Δm is positive by definition, and $\Delta \Gamma$ is expected to be positive within the Standard Model.¹⁵

There are four different time-dependent probabilities describing the case of a neutral B meson produced as a flavour state and decaying to a flavour-specific final state. If CPT is conserved (which will be assumed throughout), they can be written as

$$\begin{cases} \mathcal{P}(B \rightarrow B) &= \frac{e^{-\Gamma t}}{2} \left[\cosh\left(\frac{\Delta \Gamma}{2} t\right) + \cos(\Delta m t) \right] \\ \mathcal{P}(B \rightarrow \bar{B}) &= \frac{e^{-\Gamma t}}{2} \left[\cosh\left(\frac{\Delta \Gamma}{2} t\right) - \cos(\Delta m t) \right] \left| \frac{q}{p} \right|^2 \\ \mathcal{P}(\bar{B} \rightarrow B) &= \frac{e^{-\Gamma t}}{2} \left[\cosh\left(\frac{\Delta \Gamma}{2} t\right) - \cos(\Delta m t) \right] \left| \frac{p}{q} \right|^2 \\ \mathcal{P}(\bar{B} \rightarrow \bar{B}) &= \frac{e^{-\Gamma t}}{2} \left[\cosh\left(\frac{\Delta \Gamma}{2} t\right) + \cos(\Delta m t) \right] \end{cases}, \quad (53)$$

where t is the proper time of the system (*i.e.* the time interval between the production and the decay in the rest frame of the B meson). At the B factories, only the proper-time difference Δt between the decays of the two neutral B mesons from the $\Upsilon(4S)$ can be determined, but, because the two B mesons evolve coherently (keeping opposite flavours as long as none of them has decayed), the above formulae remain valid if t is replaced with Δt and the production flavour is replaced by the flavour at the time of the decay of the accompanying B meson in a flavour-specific state. As can be seen in the above expressions, the mixing probabilities depend on three mixing observables: Δm , $\Delta \Gamma$, and $|q/p|^2$ which signals CP violation in the mixing if $|q/p|^2 \neq 1$.

In the next sections we review in turn the experimental knowledge on the B^0 decay-width and mass differences, the B_s^0 decay-width and mass differences, CP violation in B^0 and B_s^0 mixing, and mixing-induced CP violation in B_s^0 decays.

3.3.1 B^0 mixing parameters $\Delta \Gamma_d$ and Δm_d

Many time-dependent $B^0 - \bar{B}^0$ oscillation analyses have been performed by the ALEPH, BABAR, Belle, CDF, D0, DELPHI, L3 and OPAL collaborations. The corresponding measurements of Δm_d are summarized in Table 15, where only the most recent results are listed (*i.e.* measurements superseded by more recent ones are omitted)¹⁶. Although a variety of different techniques have been used, the individual Δm_d results obtained at high-energy colliders have remarkably

¹⁵For reason of symmetry in Eqs. (51) and (52), $\Delta \Gamma$ is sometimes defined with the opposite sign. The definition adopted here, *i.e.* Eq. (52), is the one used by most experimentalists and many phenomenologists in B physics.

¹⁶Two old unpublished CDF2 measurements [145, 146] are also omitted from our averages, Table 15 and Fig. 5.

Table 15: Time-dependent measurements included in the Δm_d average. The results obtained from multi-dimensional fits involving also the B^0 (and B^+) lifetimes as free parameter(s) [81, 83, 84] have been converted into one-dimensional measurements of Δm_d . All the measurements have then been adjusted to a common set of physics parameters before being combined.

Experiment and Ref.	Method		Δm_d in ps^{-1}	Δm_d in ps^{-1}
	rec.	tag	before adjustment	after adjustment
ALEPH [129]	ℓ	Q_{jet}	$0.404 \pm 0.045 \pm 0.027$	
ALEPH [129]	ℓ	ℓ	$0.452 \pm 0.039 \pm 0.044$	
ALEPH [129]	above two combined		$0.422 \pm 0.032 \pm 0.026$	$0.442 \pm 0.032 \begin{smallmatrix} +0.020 \\ -0.019 \end{smallmatrix}$
ALEPH [129]	D^*	ℓ, Q_{jet}	$0.482 \pm 0.044 \pm 0.024$	$0.482 \pm 0.044 \pm 0.024$
DELPHI [130]	ℓ	Q_{jet}	$0.493 \pm 0.042 \pm 0.027$	$0.503 \pm 0.042 \pm 0.024$
DELPHI [130]	$\pi^* \ell$	Q_{jet}	$0.499 \pm 0.053 \pm 0.015$	$0.501 \pm 0.053 \pm 0.015$
DELPHI [130]	ℓ	ℓ	$0.480 \pm 0.040 \pm 0.051$	$0.497 \pm 0.040 \begin{smallmatrix} +0.042 \\ -0.041 \end{smallmatrix}$
DELPHI [130]	D^*	Q_{jet}	$0.523 \pm 0.072 \pm 0.043$	$0.518 \pm 0.072 \pm 0.043$
DELPHI [131]	vtx	comb	$0.531 \pm 0.025 \pm 0.007$	$0.527 \pm 0.025 \pm 0.006$
L3 [132]	ℓ	ℓ	$0.458 \pm 0.046 \pm 0.032$	$0.467 \pm 0.046 \pm 0.028$
L3 [132]	ℓ	Q_{jet}	$0.427 \pm 0.044 \pm 0.044$	$0.439 \pm 0.044 \pm 0.042$
L3 [132]	ℓ	$\ell(\text{IP})$	$0.462 \pm 0.063 \pm 0.053$	$0.473 \pm 0.063 \begin{smallmatrix} +0.045 \\ -0.044 \end{smallmatrix}$
OPAL [133]	ℓ	ℓ	$0.430 \pm 0.043 \begin{smallmatrix} +0.028 \\ -0.030 \end{smallmatrix}$	$0.466 \pm 0.043 \begin{smallmatrix} +0.017 \\ -0.016 \end{smallmatrix}$
OPAL [134]	ℓ	Q_{jet}	$0.444 \pm 0.029 \begin{smallmatrix} +0.020 \\ -0.017 \end{smallmatrix}$	$0.475 \pm 0.029 \begin{smallmatrix} +0.014 \\ -0.013 \end{smallmatrix}$
OPAL [135]	$D^* \ell$	Q_{jet}	$0.539 \pm 0.060 \pm 0.024$	$0.544 \pm 0.060 \pm 0.023$
OPAL [135]	D^*	ℓ	$0.567 \pm 0.089 \begin{smallmatrix} +0.029 \\ -0.023 \end{smallmatrix}$	$0.572 \pm 0.089 \begin{smallmatrix} +0.028 \\ -0.022 \end{smallmatrix}$
OPAL [72]	$\pi^* \ell$	Q_{jet}	$0.497 \pm 0.024 \pm 0.025$	$0.496 \pm 0.024 \pm 0.025$
CDF1 [136]	$D \ell$	SST	$0.471 \begin{smallmatrix} +0.078 \\ -0.068 \end{smallmatrix} \begin{smallmatrix} +0.033 \\ -0.034 \end{smallmatrix}$	$0.470 \begin{smallmatrix} +0.078 \\ -0.068 \end{smallmatrix} \begin{smallmatrix} +0.033 \\ -0.034 \end{smallmatrix}$
CDF1 [137]	μ	μ	$0.503 \pm 0.064 \pm 0.071$	$0.515 \pm 0.064 \pm 0.070$
CDF1 [138]	ℓ	ℓ, Q_{jet}	$0.500 \pm 0.052 \pm 0.043$	$0.545 \pm 0.052 \pm 0.036$
CDF1 [139]	$D^* \ell$	ℓ	$0.516 \pm 0.099 \begin{smallmatrix} +0.029 \\ -0.035 \end{smallmatrix}$	$0.523 \pm 0.099 \begin{smallmatrix} +0.028 \\ -0.035 \end{smallmatrix}$
D0 [140]	$D^{(*)} \mu$	OST	$0.506 \pm 0.020 \pm 0.016$	$0.506 \pm 0.020 \pm 0.016$
BABAR [141]	B^0	ℓ, K, NN	$0.516 \pm 0.016 \pm 0.010$	$0.521 \pm 0.016 \pm 0.008$
BABAR [142]	ℓ	ℓ	$0.493 \pm 0.012 \pm 0.009$	$0.487 \pm 0.012 \pm 0.006$
BABAR [83]	$D^* \ell \nu(\text{part})$	ℓ	$0.511 \pm 0.007 \pm 0.007$	$0.512 \pm 0.007 \pm 0.007$
BABAR [81]	$D^* \ell \nu$	ℓ, K, NN	$0.492 \pm 0.018 \pm 0.014$	$0.493 \pm 0.018 \pm 0.013$
Belle [143]	$D^* \pi(\text{part})$	ℓ	$0.509 \pm 0.017 \pm 0.020$	$0.513 \pm 0.017 \pm 0.019$
Belle [11]	ℓ	ℓ	$0.503 \pm 0.008 \pm 0.010$	$0.506 \pm 0.008 \pm 0.008$
Belle [84]	$B^0, D^* \ell \nu$	comb	$0.511 \pm 0.005 \pm 0.006$	$0.513 \pm 0.005 \pm 0.006$
LHCb [144]	B^0	OST	$0.499 \pm 0.032 \pm 0.003$	$0.499 \pm 0.032 \pm 0.003$
World average (all above measurements included):				$0.507 \pm 0.003 \pm 0.003$
– ALEPH, DELPHI, L3, OPAL and CDF1 only:				$0.496 \pm 0.010 \pm 0.009$
– Above measurements of BABAR and Belle only:				$0.508 \pm 0.003 \pm 0.003$

similar precision. Their average is compatible with the recent and more precise measurements from the asymmetric B factories. The systematic uncertainties are not negligible; they are often dominated by sample composition, mistag probability, or b -hadron lifetime contributions. Before being combined, the measurements are adjusted on the basis of a common set of input values, including the averages of the b -hadron fractions and lifetimes given in this report (see Secs. 3.1 and 3.2). Some measurements are statistically correlated. Systematic correlations arise both from common physics sources (fractions, lifetimes, branching ratios of b hadrons), and from purely experimental or algorithmic effects (efficiency, resolution, flavour tagging, background description). Combining all published measurements listed in Table 15 and accounting for all identified correlations as described in Ref. [3] yields $\Delta m_d = 0.507 \pm 0.003 \pm 0.003 \text{ ps}^{-1}$.

On the other hand, ARGUS and CLEO have published measurements of the time-integrated mixing probability χ_d [147–149], which average to $\chi_d = 0.182 \pm 0.015$. Following Ref. [149], the width difference $\Delta\Gamma_d$ could in principle be extracted from the measured value of $\Gamma_d = 1/\tau(B^0)$ and the above averages for Δm_d and χ_d (provided that $\Delta\Gamma_d$ has a negligible impact on the $\Delta m_d \tau(B^0)$ analyses that have assumed $\Delta\Gamma_d = 0$), using the relation

$$\chi_d = \frac{x_d^2 + y_d^2}{2(x_d^2 + 1)} \quad \text{with} \quad x_d = \frac{\Delta m_d}{\Gamma_d} \quad \text{and} \quad y_d = \frac{\Delta\Gamma_d}{2\Gamma_d}. \quad (54)$$

However, direct time-dependent studies provide much stronger constraints: $|\Delta\Gamma_d|/\Gamma_d < 18\%$ at 95% CL from DELPHI [131], and $-6.8\% < \text{sign}(\text{Re}\lambda_{CP})\Delta\Gamma_d/\Gamma_d < 8.4\%$ at 90% CL from BABAR [150], where $\lambda_{CP} = (q/p)_d(\overline{A}_{CP}/A_{CP})$ is defined for a CP -even final state (the sensitivity to the overall sign of $\text{sign}(\text{Re}\lambda_{CP})\Delta\Gamma_d/\Gamma_d$ comes from the use of B^0 decays to CP final states). Recently Belle has measured $\text{sign}(\text{Re}\lambda_{CP}) = 0.017 \pm 0.018 \pm 0.011$ [151]. A combination of these three results (after adjusting the DELPHI and BABAR ones to $1/\Gamma_d = \tau(B^0) = 1.519 \pm 0.007 \text{ ps}$) yields

$$\text{sign}(\text{Re}\lambda_{CP})\Delta\Gamma_d/\Gamma_d = 0.015 \pm 0.018. \quad (55)$$

The sign of $\text{Re}\lambda_{CP}$ is not measured, but expected to be positive from the global fits of the Unitarity Triangle within the Standard Model [152].

Assuming $\Delta\Gamma_d = 0$ and using $1/\Gamma_d = \tau(B^0) = 1.519 \pm 0.007 \text{ ps}$, the Δm_d and χ_d results are combined through Eq. (54) to yield the world average

$$\Delta m_d = 0.507 \pm 0.004 \text{ ps}^{-1}, \quad (56)$$

or, equivalently,

$$x_d = 0.770 \pm 0.008 \quad \text{and} \quad \chi_d = 0.1862 \pm 0.0023. \quad (57)$$

Figure 5 compares the Δm_d values obtained by the different experiments.

The B^0 mixing averages given in Eqs. (56) and (57) and the b -hadron fractions of Table 5 have been obtained in a fully consistent way, taking into account the fact that the fractions are computed using the χ_d value of Eq. (57) and that many individual measurements of Δm_d at high energy depend on the assumed values for the b -hadron fractions. Furthermore, this set of averages is consistent with the lifetime averages of Sec. 3.2.

It should be noted that the most recent (and precise) analyses at the asymmetric B factories measure Δm_d as a result of a multi-dimensional fit. Two BABAR analyses [81, 83], based on fully and partially reconstructed $B^0 \rightarrow D^* \ell \nu$ decays respectively, extract simultaneously Δm_d and $\tau(B^0)$ while the latest Belle analysis [84], based on fully reconstructed hadronic B^0 decays

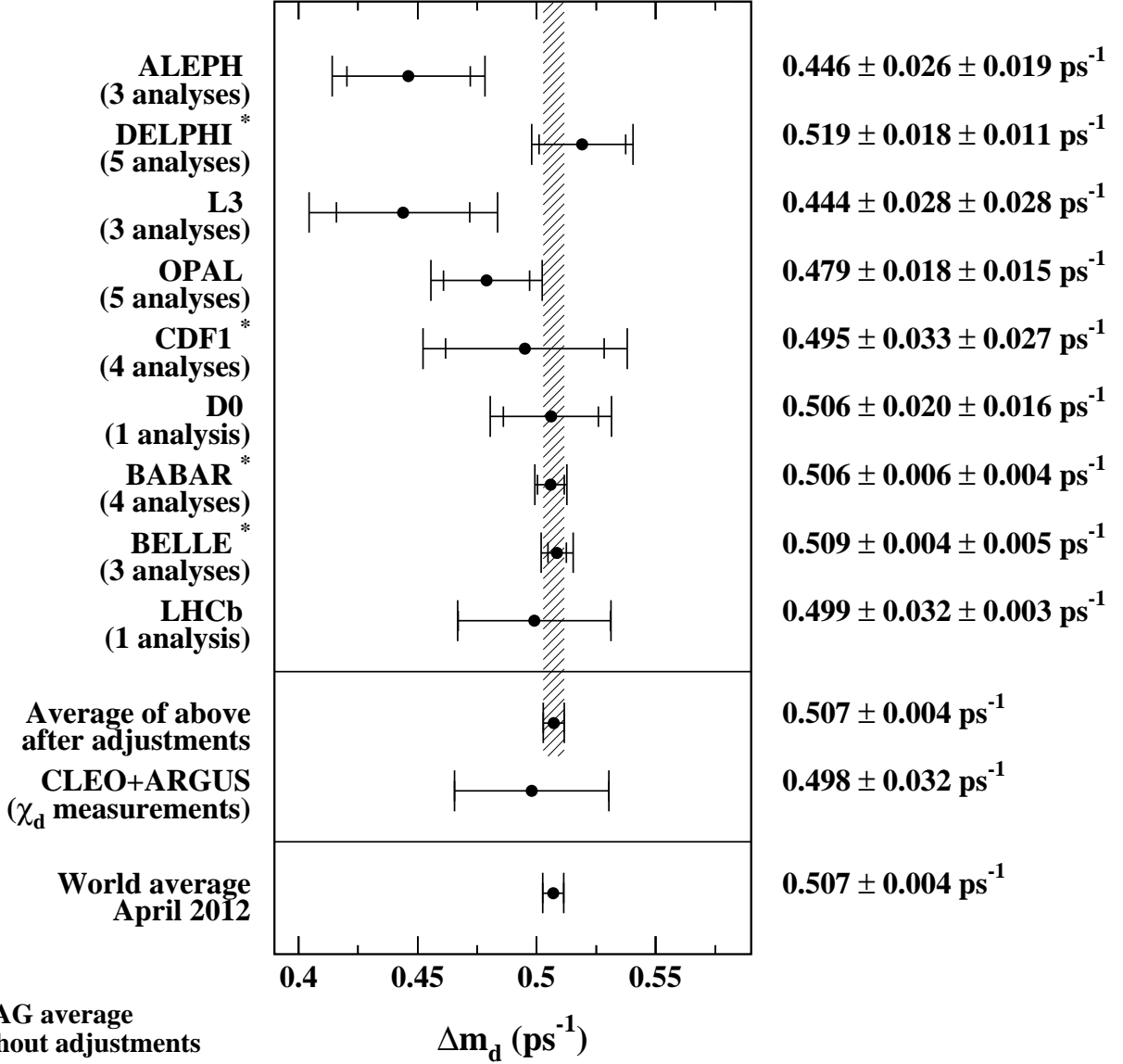


Figure 5: The $B^0-\bar{B}^0$ oscillation frequency Δm_d as measured by the different experiments. The averages quoted for ALEPH, L3 and OPAL are taken from the original publications, while the ones for DELPHI, CDF, *BABAR*, and Belle have been computed from the individual results listed in Table 15 without performing any adjustments. The time-integrated measurements of χ_d from the symmetric B factory experiments ARGUS and CLEO have been converted to a Δm_d value using $\tau(B^0) = 1.519 \pm 0.007$ ps. The two global averages have been obtained after adjustments of all the individual Δm_d results of Table 15 (see text).

Table 16: Simultaneous measurements of Δm_d and $\tau(B^0)$, and their average. The Belle analysis also measures $\tau(B^+)$ at the same time, but it is converted here into a two-dimensional measurement of Δm_d and $\tau(B^0)$, for an assumed value of $\tau(B^+)$. The first quoted error on the measurements is statistical and the second one systematic; in the case of adjusted measurements, the latter includes a contribution obtained from the variation of $\tau(B^+)$ or $\tau(B^+)/\tau(B^0)$ in the indicated range. Units are ps^{-1} for Δm_d and ps for lifetimes. The three different values of $\rho(\Delta m_d, \tau(B^0))$ correspond to the statistical, systematic and total correlation coefficients between the adjusted measurements of Δm_d and $\tau(B^0)$.

Exp. & Ref.	Measured Δm_d	Measured $\tau(B^0)$	Measured $\tau(B^+)$	Assumed $\tau(B^+)$
BABAR [81]	$0.492 \pm 0.018 \pm 0.013$	$1.523 \pm 0.024 \pm 0.022$	—	$(1.083 \pm 0.017)\tau(B^0)$
BABAR [83]	$0.511 \pm 0.007 \begin{smallmatrix} +0.007 \\ -0.006 \end{smallmatrix}$	$1.504 \pm 0.013 \begin{smallmatrix} +0.018 \\ -0.013 \end{smallmatrix}$	—	1.671 ± 0.018
Belle [84]	$0.511 \pm 0.005 \pm 0.006$	$1.534 \pm 0.008 \pm 0.010$	$1.635 \pm 0.011 \pm 0.011$	—
	Adjusted Δm_d	Adjusted $\tau(B^0)$	$\rho(\Delta m_d, B^0)$	Assumed $\tau(B^+)$
BABAR [81]	$0.492 \pm 0.018 \pm 0.013$	$1.523 \pm 0.024 \pm 0.022$	$-0.22 \ +0.71 \ +0.16$	$(1.079 \pm 0.007)\tau(B^0)$
BABAR [83]	$0.512 \pm 0.007 \pm 0.007$	$1.506 \pm 0.013 \pm 0.018$	$+0.01 \ -0.85 \ -0.48$	1.642 ± 0.008
Belle [84]	$0.511 \pm 0.005 \pm 0.006$	$1.535 \pm 0.008 \pm 0.011$	$-0.27 \ -0.14 \ -0.19$	1.642 ± 0.008
Average	$0.509 \pm 0.004 \pm 0.004$	$1.527 \pm 0.006 \pm 0.008$	$-0.19 \ -0.26 \ -0.23$	1.642 ± 0.008

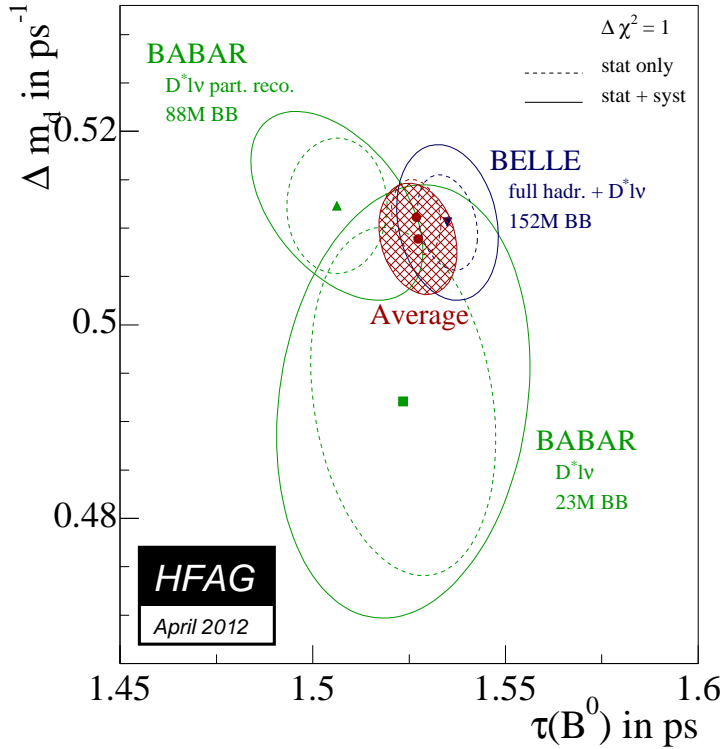


Figure 6: Simultaneous measurements of Δm_d and $\tau(B^0)$ [81, 83, 84], after adjustment to a common set of parameters (see text). Statistical and total uncertainties are represented as dashed and solid contours respectively. The average of the three measurements is indicated by a hatched ellipse.

Table 17: Averages of $\Delta\Gamma_s$, $1/\Gamma_s$ and related quantities, obtained from $B_s^0 \rightarrow J/\psi \phi$ alone (first column), adding the constraints from the effective lifetime measured in $B_s^0 \rightarrow K^+K^-$ and $B_s^0 \rightarrow J/\psi f_0(980)$ (second column), and adding the constraint from the average flavour-specific lifetime (third column, recommended world averages).

	$J/\psi \phi$	$J/\psi \phi, K^+K^-, J/\psi f_0$	$J/\psi \phi, K^+K^-, J/\psi f_0, D_s^- \ell^+, D_s^- \pi^+$
$\Delta\Gamma_s$	$+0.105 \pm 0.015 \text{ ps}^{-1}$	$+0.100 \pm 0.014 \text{ ps}^{-1}$	$+0.095 \pm 0.014 \text{ ps}^{-1}$
$1/\Gamma_s$	$1.514 \pm 0.013 \text{ ps}$	$1.520 \pm 0.013 \text{ ps}$	$1.509 \pm 0.012 \text{ ps}$
$1/\Gamma_L$	$1.403 \pm 0.019 \text{ ps}$	$1.412 \pm 0.017 \text{ ps}$	$1.408 \pm 0.017 \text{ ps}$
$1/\Gamma_H$	$1.645 \pm 0.027 \text{ ps}$	$1.644 \pm 0.025 \text{ ps}$	$1.626 \pm 0.023 \text{ ps}$
$\Delta\Gamma_s/\Gamma_s$	$+0.159 \pm 0.023$	$+0.152 \pm 0.021$	$+0.144 \pm 0.021$

and $B^0 \rightarrow D^* \ell \nu$ decays, extracts simultaneously Δm_d , $\tau(B^0)$ and $\tau(B^+)$. The measurements of Δm_d and $\tau(B^0)$ of these three analyses are displayed in Table 16 and in Fig. 6. Their two-dimensional average, taking into account all statistical and systematic correlations, and expressed at $\tau(B^+) = 1.642 \pm 0.008 \text{ ps}$, is

$$\left. \begin{array}{l} \Delta m_d = 0.509 \pm 0.006 \text{ ps}^{-1} \\ \tau(B^0) = 1.527 \pm 0.010 \text{ ps} \end{array} \right\} \text{ with a total correlation of } -0.23. \quad (58)$$

3.3.2 B_s^0 mixing parameters $\Delta\Gamma_s$ and Δm_s

Definitions and an introduction to $\Delta\Gamma_s$ have been given in Sec. 3.2.4. Neglecting CP violation, the mass eigenstates are also CP eigenstates, with the short-lived state being CP -even and the long-lived state being CP -odd.

The best sensitivity to $\Delta\Gamma_s$ is currently achieved by the recent time-dependent measurements of the $B_s^0 \rightarrow J/\psi \phi$ decay rates performed at CDF [153,154], D0 [155] and LHCb [156,157], where the CP -even and CP -odd amplitudes are statistically separated through a full angular analysis (see last two columns of Table 21). In particular LHCb obtained the first observation of a non-zero value of $\Delta\Gamma_s$ [156]. These studies use both untagged and tagged B_s^0 candidates and are optimized for the measurement of the CP -violating phase $\phi_s^{c\bar{c}s}$, defined later in Sec. 3.3.4. Recently the LHCb collaboration analyzed the $B_s^0 \rightarrow J/\psi K^+K^-$ decay, considering that the K^+K^- system can be in a P -wave or S -wave state, and measured the dependence of the strong phase difference between the P -wave and S -wave amplitudes as a function of the K^+K^- invariant mass [93]. This allowed, for the first time, the unambiguous determination of the sign of $\Delta\Gamma_s$, which was found to be positive at the 4.7σ level and the following averages present only the $\Delta\Gamma_s > 0$ solutions.

The combined fit procedure used to extract simultaneously $\Delta\Gamma_s$ and $\phi_s^{c\bar{c}s}$ is described in Sec. 3.3.4. The results, displayed as the red contours labelled “ $B_s^0 \rightarrow J/\psi \phi$ measurements” in the plots of Fig. 7, are given in the first column of numbers of Table 17. In those averages, the correlation between $\Delta\Gamma_s$ and Γ_s has been neglected.

An alternative approach, which is directly sensitive to first order in $\Delta\Gamma_s/\Gamma_s$, is to determine the effective lifetime of untagged B_s^0 candidates decaying to CP eigenstates; measurements

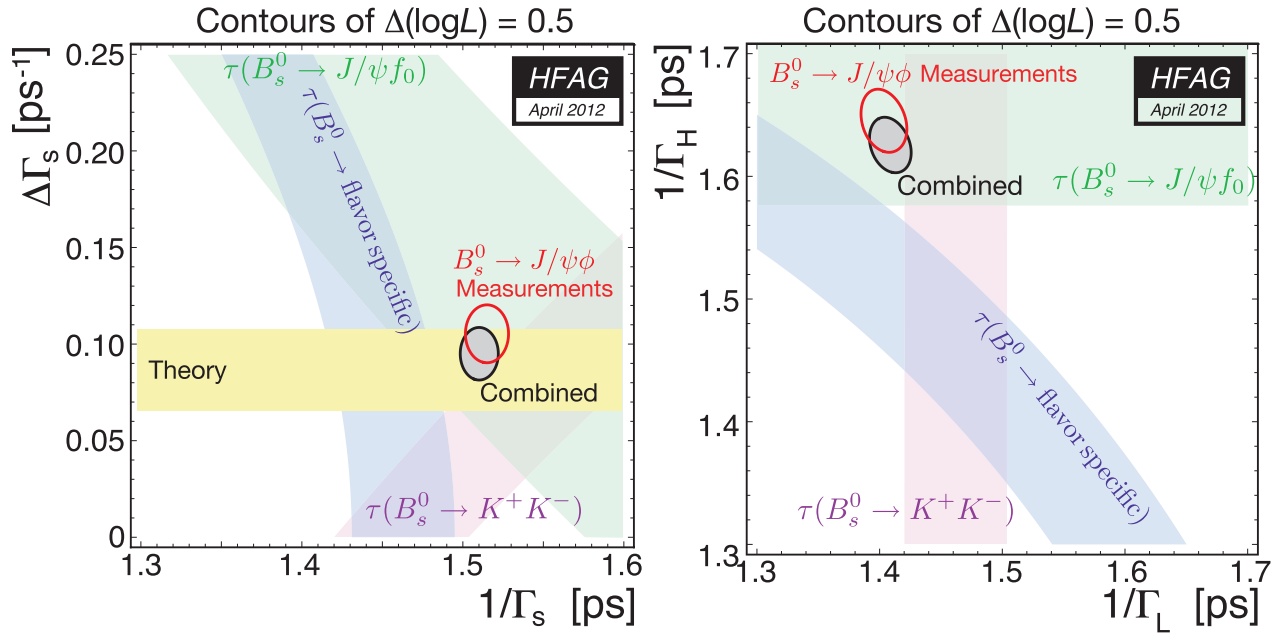


Figure 7: Contours of $\Delta \ln L = 0.5$ (39% CL for the enclosed 2D regions, 68% CL for the bands) shown in the $(1/\Gamma_s, \Delta\Gamma_s)$ plane on the left and in the $(1/\Gamma_L, 1/\Gamma_H)$ plane on the right. The average of all the $B_s^0 \rightarrow J/\psi\phi$ results is shown as the red contour, and the constraints given by the effective lifetime measurements of B_s^0 to flavour-specific final states, $B_s^0 \rightarrow J/\psi f_0(980)$ and $B_s^0 \rightarrow K^+K^-$ are shown as the blue, green and purple bands, respectively. The average taking all constraints into account is shown as the gray-filled contour. The yellow band is a theory prediction $\Delta\Gamma_s = 0.087 \pm 0.021 \text{ ps}^{-1}$ [91] that assumes no new physics in B_s^0 mixing.

exist for $B_s^0 \rightarrow K^+K^-$ [105, 106]¹⁷, and $B_s^0 \rightarrow J/\psi f_0(980)$ [107]. The precise extraction of $1/\Gamma_s$ and $\Delta\Gamma_s$ from such measurements, discussed in detail in Ref. [158], requires additional information in the form of theoretical assumptions or external inputs on weak phases and hadronic parameters. If f designates a final state in which both B_s^0 and \bar{B}_s^0 can decay, the ratio of the effective B_s^0 lifetime decaying to f relative to the mean B_s^0 lifetime is [158]¹⁸

$$\frac{\tau_{\text{single}}(B_s^0 \rightarrow f)}{\tau(B_s^0)} = \frac{1}{1 - y_s^2} \left[\frac{1 - 2A_f^{\Delta\Gamma} y_s + y_s^2}{1 - A_f^{\Delta\Gamma} y_s} \right], \quad (59)$$

where

$$A_f^{\Delta\Gamma} = -\frac{2\text{Re}(\lambda_f)}{1 + |\lambda_f|^2}. \quad (60)$$

To include the measurements of the effective $B_s^0 \rightarrow K^+K^-$ and $B_s^0 \rightarrow J/\psi f_0(980)$ lifetimes as constraints in the $\Delta\Gamma_s$ fit, we neglect sub-leading penguin contributions and possible direct CP violation. Explicitly, in Eq. (60), we set $A_{KK}^{\Delta\Gamma} = \cos \phi_s^{c\bar{c}s}$ and $A_{J/\psi f_0}^{\Delta\Gamma} = -\cos \phi_s^{c\bar{c}s}$. Given the

¹⁷An old unpublished measurement of the $B_s^0 \rightarrow K^+K^-$ effective lifetime by CDF [111] is no longer considered.

¹⁸The definition of $A_f^{\Delta\Gamma}$ given in Eq. (60) has the sign opposite to that given in Ref. [158].

small value of $\phi_s^{c\bar{c}s}$, we have, to first order in y_s :

$$\tau_{\text{single}}(B_s^0 \rightarrow K^+ K^-) \approx \frac{1}{\Gamma_L} \left(1 + \frac{(\phi_s^{c\bar{c}s})^2 y_s}{2} \right), \quad (61)$$

$$\tau_{\text{single}}(B_s^0 \rightarrow J/\psi f_0(980)) \approx \frac{1}{\Gamma_H} \left(1 - \frac{(\phi_s^{c\bar{c}s})^2 y_s}{2} \right). \quad (62)$$

The numerical inputs are taken from Eqs. (40) and (41) and the resulting averages, combined with the $B_s^0 \rightarrow J/\psi \phi$ information, are indicated in the second column of numbers of Table 17.

Information on $\Delta\Gamma_s$ can also be obtained from the study of the proper time distribution of untagged samples of flavour-specific B_s^0 decays [108]. In the case of flavour-specific B_s^0 decays where the flavour, *i.e.* B_s^0 or \bar{B}_s^0 , at the time of decay can be determined by the decay products. In such decays, *e.g.* semileptonic B_s^0 decays, there is an equal mix of the heavy and light mass eigenstates at time zero. The proper time distribution is then a superposition of two exponential functions with decay constants $\Gamma_{L,H} = \Gamma_s \pm \Delta\Gamma_s/2$. This provides sensitivity to both $1/\Gamma_s$ and $(\Delta\Gamma_s/\Gamma_s)^2$. Ignoring $\Delta\Gamma_s$ and fitting for a single exponential leads to an estimate of Γ_s with a relative bias proportional to $(\Delta\Gamma_s/\Gamma_s)^2$, as shown in Eq. (36). Including the constraint from the world-average flavour-specific B_s^0 lifetime, given in Eq. (37), leads to the results shown in the last column of Table 17. These world averages are displayed as the gray contours labelled ‘‘Combined’’ in the plots of Fig. 7. The average for the decay-width difference,

$$\Delta\Gamma_s = +0.095 \pm 0.014 \text{ ps}^{-1} \quad \text{and} \quad \Delta\Gamma_s/\Gamma_s = +0.144 \pm 0.021, \quad (63)$$

is in good agreement with the Standard Model prediction $\Delta\Gamma_s = 0.087 \pm 0.021 \text{ ps}^{-1}$ [91].

Independent estimates of $\Delta\Gamma_s/\Gamma_s$ obtained from measurements of the $B_s^0 \rightarrow D_s^{(*)+} D_s^{(*)-}$ branching fraction [104, 159–161] have not been used¹⁹, since they are based on the questionable [91] assumption that these decays account for all CP -even final states. The results of early lifetime analyses attempting to measure $\Delta\Gamma_s/\Gamma_s$ [62, 69, 96, 101] have not been used either.

The strength of B_s^0 mixing is known to be large since more than 20 years. Indeed the time-integrated measurements of $\bar{\chi}$ (see Sec. 3.1.3), when compared to our knowledge of χ_d and the b -hadron fractions, indicated that χ_s should be close to its maximal possible value of 1/2. Many searches of the time dependence of this mixing were performed by ALEPH [162], CDF (Run I) [163], DELPHI [96, 101, 131, 164], OPAL [165, 166] and SLD [167–169], but did not have enough statistical power and proper time resolution to resolve the small period of the B_s^0 oscillations.

B_s^0 oscillations have been observed for the first time in 2006 by the CDF collaboration [170], based on samples of flavour-tagged hadronic and semileptonic B_s^0 decays (in flavour-specific final states), partially or fully reconstructed in 1 fb^{-1} of data collected during Tevatron’s Run II. This was shortly followed by an independent evidence obtained by the D0 collaboration with 2.4 fb^{-1} of data [171]. Recently the LHCb collaboration obtained the most precise results using fully reconstructed $B_s^0 \rightarrow D_s^- \pi^+$ and $B_s^0 \rightarrow D_s^- \pi^+ \pi^- \pi^+$ decays at the LHC [172, 173]. The measurements of Δm_s are summarized in Table 18.

A simple average of the CDF and LHCb results²⁰, taking into account the correlated systematic uncertainties between the two LHCb measurements, yields

$$\Delta m_s = 17.719 \pm 0.036 \pm 0.023 \text{ ps}^{-1} = 17.719 \pm 0.043 \text{ ps}^{-1} \quad (64)$$

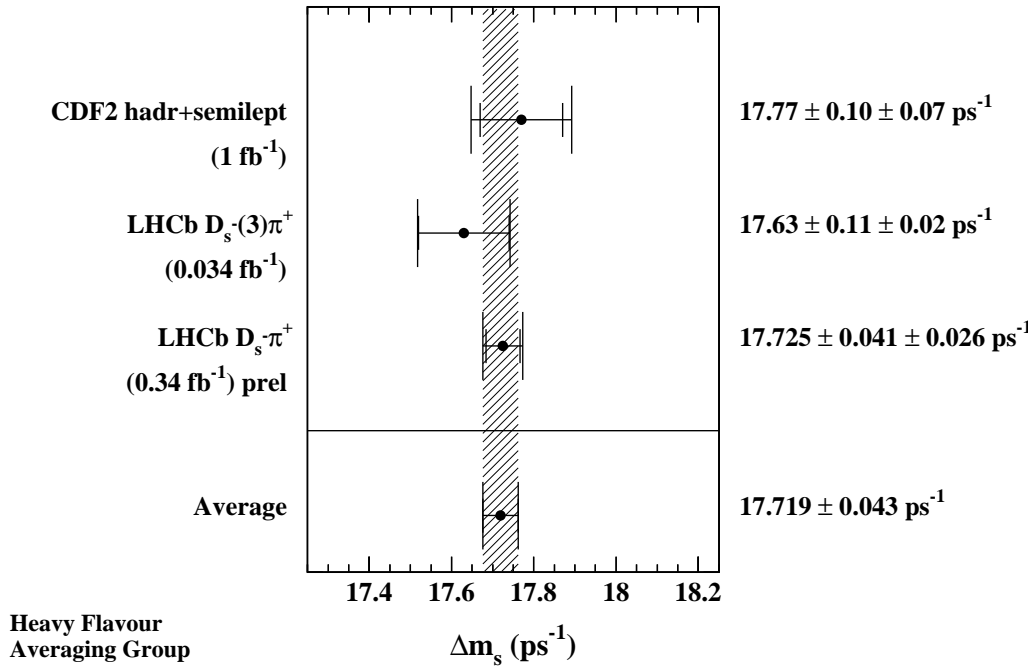
¹⁹ Our average is $\mathcal{B} = 0.044 \pm 0.014$, from which one would get $\Delta\Gamma_s/\Gamma_s \sim 2\mathcal{B}/(1 - \mathcal{B}) = +0.093 \pm 0.031$.

²⁰We do not include the old unpublished D0 [171] result in the average.

Table 18: Measurements of Δm_s .

Experiment	Method	Data set	Δm_s (ps ⁻¹)	Ref.
CDF2	$D_s^{(*)-} \ell^+ \nu, D_s^{(*)-} \pi^+, D_s^- \rho^+$	1 fb ⁻¹	$17.77 \pm 0.10 \pm 0.07$	[170]
D0	$D_s^- \ell^+ X, D_s^- \pi^+ X$	2.4 fb ⁻¹	$18.53 \pm 0.93 \pm 0.30$	[171] ^u
LHCb	$D_s^- \pi^+, D_s^- \pi^+ \pi^- \pi^+$	2010 0.034 fb ⁻¹	$17.63 \pm 0.11 \pm 0.02$	[172]
LHCb	$D_s^- \pi^+$	2011 0.34 fb ⁻¹	$17.725 \pm 0.041 \pm 0.026$	[173] ^p
Average of CDF and LHCb measurements			$17.719 \pm 0.036 \pm 0.023$	

^u Unpublished. ^p Preliminary.


 Figure 8: Published and recent preliminary measurements of Δm_s , together with their average.

and is illustrated in Figure 8. Multiplying this result with the mean B_s^0 lifetime of Eq. (44), $1/\Gamma_s = 1.509 \pm 0.012$ ps, yields

$$x_s = \frac{\Delta m_s}{\Gamma_s} = 26.74 \pm 0.22. \quad (65)$$

With $2y_s = \Delta\Gamma_s/\Gamma_s = +0.144 \pm 0.021$ (see Eq. (63)) and under the assumption of no CP violation in B_s^0 mixing, this corresponds to

$$\chi_s = \frac{x_s^2 + y_s^2}{2(x_s^2 + 1)} = 0.499305 \pm 0.000011. \quad (66)$$

The ratio of the B^0 and B_s^0 oscillation frequencies, obtained from Eqs. (56) and (64),

$$\frac{\Delta m_d}{\Delta m_s} = 0.02861 \pm 0.00026, \quad (67)$$

can be used to extract the following ratio of CKM matrix elements,

$$\left| \frac{V_{td}}{V_{ts}} \right| = \xi \sqrt{\frac{\Delta m_d m(B_s^0)}{\Delta m_s m(B^0)}} = 0.2110 \pm 0.0009 \pm 0.0055, \quad (68)$$

where the first quoted error is from experimental uncertainties (with the masses $m(B_s^0)$ and $m(B^0)$ taken from Ref. [18]), and where the second quoted error is from theoretical uncertainties in the estimation of the SU(3) flavour-symmetry breaking factor $\xi = 1.237 \pm 0.032$ obtained from lattice QCD calculations [174].

3.3.3 CP violation in B^0 and B_s^0 mixing

Evidence for CP violation in B^0 mixing has been searched for, both with flavour-specific and inclusive B^0 decays, in samples where the initial flavour state is tagged. In the case of semileptonic (or other flavour-specific) decays, where the final state tag is also available, the following asymmetry

$$\mathcal{A}_{\text{SL}}^d = \frac{N(\overline{B}^0(t) \rightarrow \ell^+ \nu_\ell X) - N(B^0(t) \rightarrow \ell^- \bar{\nu}_\ell X)}{N(\overline{B}^0(t) \rightarrow \ell^+ \nu_\ell X) + N(B^0(t) \rightarrow \ell^- \bar{\nu}_\ell X)} = \frac{|p/q|_d^2 - |q/p|_d^2}{|p/q|_d^2 + |q/p|_d^2} \quad (69)$$

has been measured, either in time-integrated analyses at CLEO [148, 149, 175], CDF [176, 177] and D0 [178], or in time-dependent analyses at OPAL [134], ALEPH [179], BABAR [150, 180, 181] and Belle [182]. In the inclusive case, also investigated and published at ALEPH [179] and OPAL [71], no final state tag is used, and the asymmetry [183]

$$\frac{N(B^0(t) \rightarrow \text{all}) - N(\overline{B}^0(t) \rightarrow \text{all})}{N(B^0(t) \rightarrow \text{all}) + N(\overline{B}^0(t) \rightarrow \text{all})} \simeq \mathcal{A}_{\text{SL}}^d \left[\frac{\Delta m_d}{2\Gamma_d} \sin(\Delta m_d t) - \sin^2 \left(\frac{\Delta m_d t}{2} \right) \right] \quad (70)$$

must be measured as a function of the proper time to extract information on CP violation. Table 19 summarized the different measurements: in all cases asymmetries compatible with zero have been found, with a precision limited by the available statistics.

A simple average of all measurements performed at B factories [149, 150, 175, 180, 182]¹⁸ yields

$$\mathcal{A}_{\text{SL}}^d = -0.0005 \pm 0.0056 \quad \iff \quad |q/p|_d = 1.0002 \pm 0.0028, \quad (71)$$

where the relation between $\mathcal{A}_{\text{SL}}^d$ and $|q/p|_d$ is given in Eq. (69). The latest dimuon D0 analysis [178] separates the B^0 and B_s^0 contributions by exploiting the dependence on the muon impact parameter cut; combining the $\mathcal{A}_{\text{SL}}^d$ result quoted by D0 with the above B factory average yields $\mathcal{A}_{\text{SL}}^d = -0.0009 \pm 0.0038$.

All the other analyses performed at high energy, either at LEP or at the Tevatron, did not separate the contributions from the B^0 and B_s^0 mesons. Under the assumption of no CP

¹⁸An old unpublished measurement by BABAR [181] is no longer included in our averages, nor in Table 19.

Table 19: Measurements^{18,19} of CP violation in B^0 mixing and their average in terms of both $\mathcal{A}_{\text{SL}}^d$ and $|q/p|_d$. The individual results are listed as quoted in the original publications, or converted²² to an $\mathcal{A}_{\text{SL}}^d$ value. When two errors are quoted, the first one is statistical and the second one systematic. The last group of results from OPAL and ALEPH assume no CP violation in B_s^0 mixing.

Exp. & Ref.	Method	Measured $\mathcal{A}_{\text{SL}}^d$	Measured $ q/p _d$
CLEO [149]	partial hadronic rec.	+0.017 ±0.070 ±0.014	
CLEO [175]	dileptons	+0.013 ±0.050 ±0.005	
CLEO [175]	average of above two	+0.014 ±0.041 ±0.006	
BABAR [150]	full hadronic rec.		1.029 ±0.013 ±0.011
BABAR [180]	dileptons		0.9992 ±0.0027±0.0019
Belle [182]	dileptons	-0.0011 ±0.0079±0.0085	1.0005 ±0.0040±0.0043
Average of above 6 B factory results		-0.0005 ± 0.0056 (tot)	1.0002 ± 0.0028 (tot)
D0 [178]	dimuons	-0.0012 ± 0.0052 (tot)	
Average of above 7 direct measurements		-0.0009 ± 0.0038 (tot)	1.0004 ± 0.0019 (tot)
OPAL [134]	leptons	+0.008 ±0.028 ±0.012	
OPAL [71]	inclusive (Eq. (70))	+0.005 ±0.055 ±0.013	
ALEPH [179]	leptons	-0.037 ±0.032 ±0.007	
ALEPH [179]	inclusive (Eq. (70))	+0.016 ±0.034 ±0.009	
ALEPH [179]	average of above two	-0.013 ± 0.026 (tot)	
Average of above 12 results		-0.0010 ± 0.0037 (tot)	1.0005 ± 0.0019 (tot)
Best fit value from 2D combination of $\mathcal{A}_{\text{SL}}^d$ and $\mathcal{A}_{\text{SL}}^s$ results (see Eq. (74))		-0.0033 ± 0.0033 (tot)	1.0017 ± 0.0017 (tot)

violation in B_s^0 mixing, a number of these analyses [44, 71, 134, 179] quote a measurement of $\mathcal{A}_{\text{SL}}^d$ or $|q/p|_d$ for the B^0 meson. Including also these results¹⁹ in the previous average leads to $\mathcal{A}_{\text{SL}}^d = -0.0010 \pm 0.0037$ under the assumption $\mathcal{A}_{\text{SL}}^s = 0$. The latter assumption makes sense within the Standard Model, since $\mathcal{A}_{\text{SL}}^s$ is predicted to be much smaller than $\mathcal{A}_{\text{SL}}^d$ [91], but may not be suitable in presence of New Physics.

The following constraints on a combination of $\mathcal{A}_{\text{SL}}^d$ and $\mathcal{A}_{\text{SL}}^s$ (or equivalently $|q/p|_d$ and $|q/p|_s$) have been obtained by the Tevatron experiments, using inclusive semileptonic decays of b hadrons:

$$\frac{1}{4} (f'_d \chi_d \mathcal{A}_{\text{SL}}^d + f'_s \chi_s \mathcal{A}_{\text{SL}}^s) = +0.0015 \pm 0.0038(\text{stat}) \pm 0.0020(\text{syst}) \quad \text{CDF1 [176]}, \quad (72)$$

$$\mathcal{A}_{\text{SL}}^b = \frac{f'_d Z_d \mathcal{A}_{\text{SL}}^d + f'_s Z_s \mathcal{A}_{\text{SL}}^s}{f'_d Z_d + f'_s Z_s} = -0.00787 \pm 0.00172(\text{stat}) \pm 0.00093(\text{syst}) \quad \text{D0 [178]}, \quad (73)$$

where²⁰ $Z_q = 1/(1 - y_q^2) - 1/(1 + x_q^2) = 2\chi_q/(1 - y_q^2)$, $q = d, s$. While the CDF measurement

¹⁹A low-statistics result published by CDF using the Run I data [176] and an unpublished result by CDF using Run II data [177] are not included in our averages, nor in Table 19.

²⁰In Ref. [184], the D0 result $\frac{1}{4} (\mathcal{A}_{\text{SL}}^d + \mathcal{A}_{\text{SL}}^s \frac{f'_s \chi_s}{f'_d \chi_d}) = -0.0023 \pm 0.0011(\text{stat}) \pm 0.0008(\text{syst})$ [44] (now superseded by that of Ref. [178]) was reinterpreted by replacing χ_s/χ_d with Z_s/Z_d . For simplicity, and since this has anyway

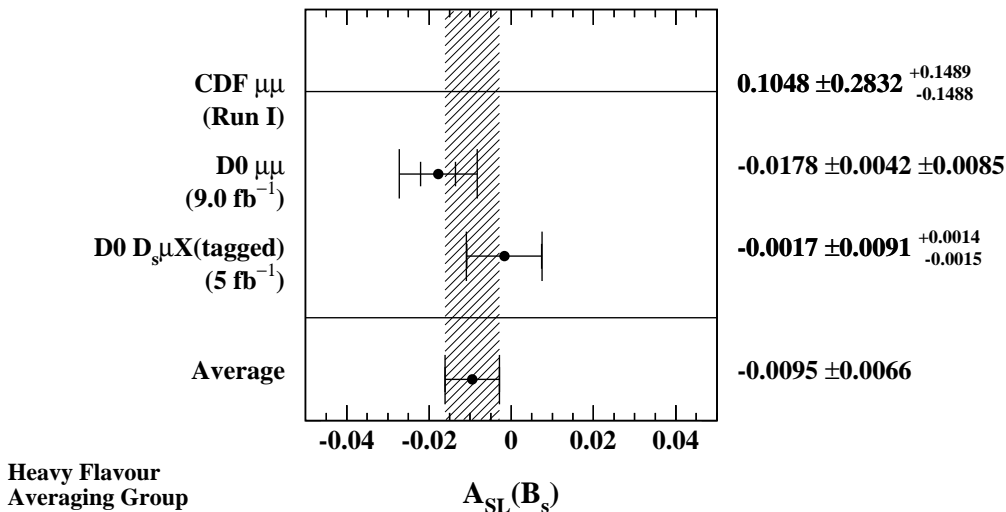


Figure 9: Measurements of $\mathcal{A}_{\text{SL}}^s$, derived from CDF [176]²⁰ and D0 [178, 185] analyses and adjusted to the B factory average of $\mathcal{A}_{\text{SL}}^d$, the Tevatron averages of the b -hadron fractions, and the latest averages of the mixing parameters. The combined value of $\mathcal{A}_{\text{SL}}^s$ is also shown.

is compatible with no CP violation²¹, the more precise D0 result of Eq. (73), obtained by measuring the charge asymmetry of like-sign dimuons, differs by 3.9 standard deviations from the Standard Model prediction of $\mathcal{A}_{\text{SL}}^b(\text{SM}) = (-2.8_{-0.6}^{+0.5}) \times 10^{-4}$ [91, 178].

Using the average $\mathcal{A}_{\text{SL}}^d = -0.0005 \pm 0.0056$ of Eq. (71), obtained from results at B factories, the averages of the Tevatron b -hadron fractions and their correlations listed in Table 5, and the averages of the mixing parameters presented in this chapter, the two results of Eqs. (72) and (73) are turned into the measurements of $\mathcal{A}_{\text{SL}}^s$ displayed in the top part of Fig. 9. Taking into account the uncertainties in f'_d, f'_s, Z_d , and Z_s , the value derived from the D0 result does not show evidence of CP violation in the B_s^0 system. In addition, the third line of Fig. 9 shows a direct determination of $\mathcal{A}_{\text{SL}}^s$ obtained by D0 by measuring the charge asymmetry of tagged $B_s^0 \rightarrow D_s \mu X$ decays [185]. The three results of Fig. 9 are combined to yield $\mathcal{A}_{\text{SL}}^s = -0.0095 \pm 0.0038(\text{stat}) \pm 0.0054(\text{syst}) = -0.0095 \pm 0.0066$ or, equivalently through Eq. (69), $|q/p|_s = 1.0048 \pm 0.0019(\text{stat}) \pm 0.0027(\text{syst}) = 1.0048 \pm 0.0033$. The quoted systematic errors include experimental systematics as well as the correlated dependence on external parameters.

In the latest update of the D0 like-sign dimuon analysis, the dependence of the charge asymmetry is investigated for the first time as a function of the muon impact parameters, allowing the separation of the B^0 and B_s^0 contributions to the result of Eq. (73). Using the mixing parameters and the LEP b -hadron fractions of Ref. [4], the D0 collaboration extracts [178] values for $\mathcal{A}_{\text{SL}}^d$ and $\mathcal{A}_{\text{SL}}^s$ and their correlation coefficient, as shown in the first line of Table 20.

a negligible numerical effect on our combined result of Fig. 9, we follow the same interpretation and set $\chi_q = Z_q/2$ in Eq. (72). We also set $f'_q = f_q$.

²¹A more precise result from CDF2, $\mathcal{A}_{\text{SL}}^b = +0.0080 \pm 0.0090(\text{stat}) \pm 0.0068(\text{syst})$ [177], is also compatible with no CP violation, but since it is unpublished since 2007 we no longer include it in our averages, nor in Fig. 9.

Table 20: Direct measurements of CP violation in B_s^0 and B^0 mixing, together with their two-dimensional average. Only total errors are quoted.

Exp. & Ref.	Method	Measured $\mathcal{A}_{\text{SL}}^s$	Measured $\mathcal{A}_{\text{SL}}^d$	$\rho(\mathcal{A}_{\text{SL}}^s, \mathcal{A}_{\text{SL}}^d)$
D0 [178]	dimuons	-0.0181 ± 0.0106	-0.0012 ± 0.0052	-0.799
D0 [185]	tagged $B_s^0 \rightarrow D_s \mu X$	-0.0017 ± 0.0092		
B factory average of Eq. (71)			-0.0005 ± 0.0056	
Average of all above		-0.0105 ± 0.0064	-0.0033 ± 0.0033	-0.574

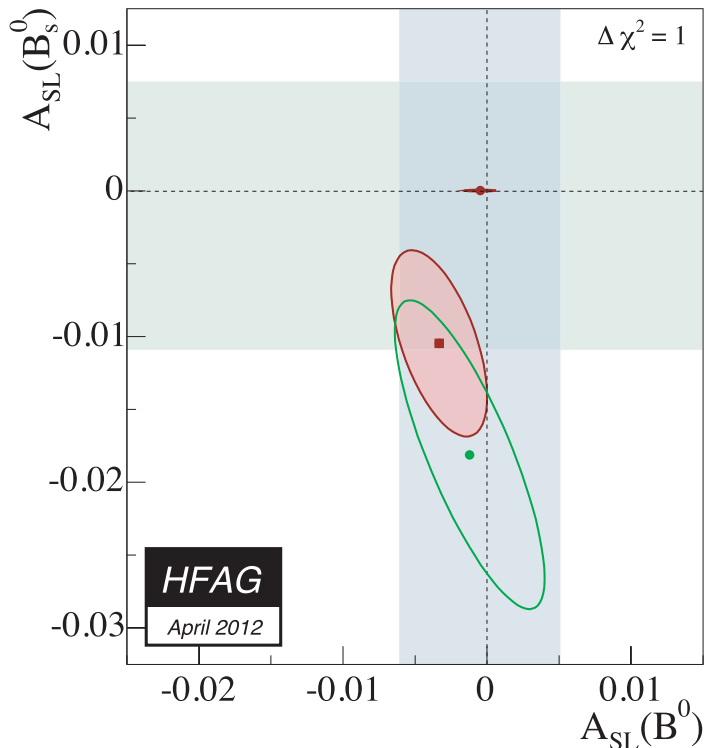


Figure 10: Direct measurements of $\mathcal{A}_{\text{SL}}^s$ and $\mathcal{A}_{\text{SL}}^d$ listed in Table 20 (B -factory average as the vertical blue shaded band, D0 measurements as the horizontal green shaded band and as the green ellipse), together with their two-dimensional average (red shaded ellipse). The red point close to $(0, 0)$ is the Standard Model prediction of Ref. [91] with error bars multiplied by 10.

However, the individual contributions to the total quoted errors from this analysis and from the external inputs are not given, so the adjustment of these results to different or more recent values of the external inputs cannot (easily) be done. Using a two-dimensional fit, these values are combined with the B factory average of Eq. (71) and with the result from the tagged $B_s^0 \rightarrow D_s \mu X$ analysis [185], assumed to be independent and also shown in Table 20. The result, shown graphically in Fig. 10, is

$$\mathcal{A}_{\text{SL}}^d = -0.0033 \pm 0.0033 \iff |q/p|_d = 1.0017 \pm 0.0017, \quad (74)$$

$$\mathcal{A}_{\text{SL}}^s = -0.0105 \pm 0.0064 \iff |q/p|_s = 1.0052 \pm 0.0032, \quad (75)$$

$$\rho(\mathcal{A}_{\text{SL}}^d, \mathcal{A}_{\text{SL}}^s) = -0.574. \quad (76)$$

The average of Fig. 9 ignores the impact parameter study of D0 and is adjusted to the b -hadron fractions at the Tevatron. The average of Eq. (75) ignores the CDF1 result (which has a very large uncertainty anyway) and is adjusted to the b -hadron fractions at LEP. We choose the results of Eqs. (74), (75), and (76) as our final averages²¹, since they better incorporate the available published data.

The above averages are compatible with no CP violation in B^0 and B_s^0 mixing. They are also compatible with the very small predictions of the Standard Model, $\mathcal{A}_{\text{SL}}^d{}^{\text{SM}} = -(4.1 \pm 0.6) \times 10^{-4}$ and $\mathcal{A}_{\text{SL}}^s{}^{\text{SM}} = +(1.9 \pm 0.3) \times 10^{-5}$ [91]. However, given the current size of the experimental uncertainties, there is still a large room for a possible New Physics contribution, especially in the B_s^0 system. In this respect, the deviation of the D0 dimuon asymmetry [178] from expectation has generated a lot of excitement, and new experimental data (in particular from LHCb) is awaited eagerly.

At the more fundamental level, CP violation in B_s^0 mixing²² is caused by the weak phase difference

$$\phi_{12} = \arg[-M_{12}/\Gamma_{12}], \quad (77)$$

where M_{12} and Γ_{12} are the off-diagonal elements of the mass and decay matrices of the $B_s^0 - \bar{B}_s^0$ system. This is related to the observed decay-width difference through the relation

$$\Delta\Gamma_s = 2|\Gamma_{12}| \cos \phi_{12} + \mathcal{O}\left(\left|\frac{\Gamma_{12}}{M_{12}}\right|^2\right), \quad (78)$$

where quadratic (or higher-order) terms in the small quantity $|\Gamma_{12}/M_{12}| \sim \mathcal{O}(m_b^2/m_t^2)$ can be neglected. The SM prediction for this phase is tiny, $\phi_{12}^{\text{SM}} = 0.0038 \pm 0.0010$ [91]; however, new physics in B_s^0 mixing could change this observed phase to

$$\phi_{12} = \phi_{12}^{\text{SM}} + \phi_{12}^{\text{NP}}. \quad (79)$$

The B_s^0 semileptonic asymmetry can be expressed as [186]

$$\mathcal{A}_{\text{SL}}^s = \text{Im}\left(\frac{\Gamma_{12}}{M_{12}}\right) + \mathcal{O}\left(\left|\frac{\Gamma_{12}}{M_{12}}\right|^2\right) = \frac{\Delta\Gamma_s}{\Delta m_s} \tan \phi_{12} + \mathcal{O}\left(\left|\frac{\Gamma_{12}}{M_{12}}\right|^2\right). \quad (80)$$

Using this relation, the current knowledge of $\mathcal{A}_{\text{SL}}^s$, $\Delta\Gamma_s$ and Δm_s , given in Eqs. (75), (63), and (64) respectively, yield a very first experimental determination of ϕ_{12} ,

$$\tan \phi_{12} = \mathcal{A}_{\text{SL}}^s \frac{\Delta m_s}{\Delta\Gamma_s} = -1.9 \pm 1.2, \quad (81)$$

which only represents a very weak constraint at present.

²¹Early analyses and (perhaps hence) the PDG use the complex parameter $\epsilon_B = (p - q)/(p + q)$; if CP violation in the mixing is small, $\mathcal{A}_{\text{SL}}^d \cong 4\text{Re}(\epsilon_B)/(1 + |\epsilon_B|^2)$ and the averages of Eqs. (71) and (74) correspond to $\text{Re}(\epsilon_B)/(1 + |\epsilon_B|^2) = -0.0001 \pm 0.0014$ and -0.0008 ± 0.0008 , respectively.

²²Of course, a similar formalism exists for the B^0 system; for simplicity we omit here the subscript s for ϕ_{12} , M_{12} and Γ_{12} .

Table 21: Direct experimental measurements of $\phi_s^{c\bar{c}s}$, $\Delta\Gamma_s$ and Γ_s using $B_s^0 \rightarrow J/\psi\phi$ and $B_s^0 \rightarrow J/\psi\pi\pi$ decays. Only the solution with $\Delta\Gamma_s > 0$ is shown, since the two-fold ambiguity has been resolved in Ref. [93]. The first error is due to statistics, the second one to systematics. The last line gives our average.

Exp.	Mode	Ref.	$\phi_s^{c\bar{c}s}$	$\Delta\Gamma_s$ (ps ⁻¹)	Γ_s (ps ⁻¹)
CDF	$J/\psi\phi$	[153] ^p	$[-0.60, 0.12]$, 68% CL	$0.068 \pm 0.026 \pm 0.007$	$0.654 \pm 0.008 \pm 0.004$
D0	$J/\psi\phi$	[155]	$-0.55^{+0.38}_{-0.36}$	$0.163^{+0.065}_{-0.064}$	$0.693^{+0.018}_{-0.017}$
LHCb	$J/\psi\phi$	[156] ^{a,p}	$-0.001 \pm 0.101 \pm 0.027$	$0.116 \pm 0.018 \pm 0.006$	$0.6580 \pm 0.0054 \pm 0.0066$
LHCb	$J/\psi\pi\pi$	[188] ^a	$-0.019^{+0.173+0.004}_{-0.174-0.003}$	—	—
Combined			$-0.044^{+0.090}_{-0.085}$	$+0.105 \pm 0.015$	0.6604 ± 0.0058

^a The combined LHCb result quoted in [156] is $\phi_s^{c\bar{c}s} = -0.002 \pm 0.083 \pm 0.027$.

^p Preliminary.

3.3.4 Mixing-induced CP violation in B_s^0 decays

CP violation induced by $B_s^0 - \bar{B}_s^0$ mixing has been a field of very active study and fast experimental progress in the past couple of years. Similarly to what has happened at the B factories a decade ago, when the B^0 mixing-induced phase 2β was measured, the Tevatron and LHC experiments are now obtaining point estimates of the B_s^0 mixing-induced phase $\phi_s^{c\bar{c}s}$. This CP -violating phase is defined as the weak phase difference between the $B_s^0 - \bar{B}_s^0$ mixing amplitude and the $b \rightarrow c\bar{c}s$ decay amplitude.

The golden mode for such studies is $B_s^0 \rightarrow J/\psi\phi$, followed by $J/\psi \rightarrow \mu^+\mu^-$ and $\phi \rightarrow K^+K^-$, for which a full angular analysis of the decay products is performed to separate statistically the CP -even and CP -odd contributions in the final state. As already mentioned in Sec. 3.3.2, CDF [153,154], D0 [155] and LHCb [156,157] have used both untagged and tagged $B_s^0 \rightarrow J/\psi\phi$ events for the measurement of $\phi_s^{c\bar{c}s}$. In addition, the newly observed CP -odd decay mode $B_s^0 \rightarrow J/\psi f_0(980)$, $f_0(980) \rightarrow \pi^+\pi^-$ has also been analyzed by LHCb [187], without the need for an angular analysis; this analysis was (superseded and) extended to the three-body decay mode $B_s^0 \rightarrow J/\psi\pi^+\pi^-$ [188], which has been shown to be almost CP pure with a CP -odd fraction larger than 0.977 at 95% CL [189].

All these analyses provide two mirror solutions related by the transformation $(\Delta\Gamma_s, \phi_s) \rightarrow (-\Delta\Gamma_s, \pi - \phi_s)$. However, a recent LHCb analysis of $B_s^0 \rightarrow J/\psi K^+K^-$ resolved this ambiguity and ruled out the solution with negative $\Delta\Gamma_s$ [93]. Therefore, in what follows we only consider the solution with $\Delta\Gamma_s > 0$.

We perform a combination of the CDF [153], D0 [155] and LHCb [156,188] results summarized in Table 21. This is done by adding the two-dimensional log profile-likelihood scans of $\Delta\Gamma_s$ and $\phi_s^{c\bar{c}s}$ from the three $B_s^0 \rightarrow J/\psi\phi$ analyses and a one-dimensional log profile-likelihood of $\phi_s^{c\bar{c}s}$ from the $B_s^0 \rightarrow J/\psi\pi^+\pi^-$ analysis, where in each case the $-\log$ -likelihood is minimized with respect to all other parameters, including Γ_s . Since the $B_s^0 \rightarrow J/\psi\phi$ two-dimensional scan provided by LHCb in Ref. [156] contains only statistical uncertainty, on each $(\Delta\Gamma_s, \phi_s^{c\bar{c}s})$ point, we decrease the log-likelihood by the quantity

$$\Delta \log \mathcal{L}^{\text{new}} - \Delta \log \mathcal{L}^{\text{old}} = \frac{(\phi_s^{c\bar{c}s} - \phi_{s-\text{min}}^{c\bar{c}s})^2 \sigma_{\phi-\text{syst}}^2}{2\sigma_{\phi-\text{stat}}^2 (\sigma_{\phi-\text{stat}}^2 + \sigma_{\phi-\text{syst}}^2)} + \frac{(\Delta\Gamma_s - \Delta\Gamma_{s-\text{min}})^2 \sigma_{\Delta\Gamma-\text{syst}}^2}{2\sigma_{\Delta\Gamma-\text{stat}}^2 (\sigma_{\Delta\Gamma-\text{stat}}^2 + \sigma_{\Delta\Gamma-\text{syst}}^2)}, \quad (82)$$

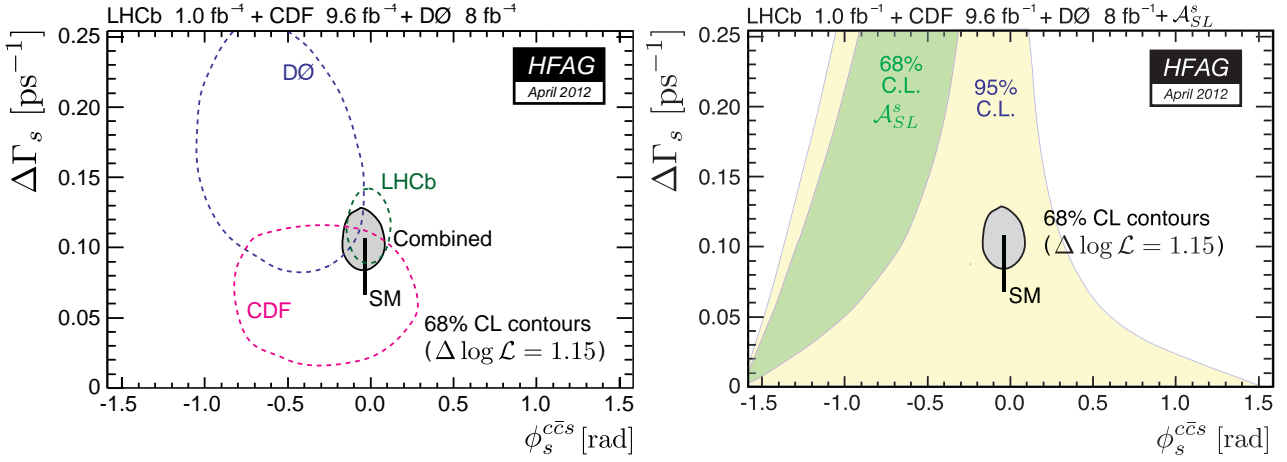


Figure 11: Left: 68% CL regions in B_s^0 width difference $\Delta\Gamma_s$ and weak phase $\phi_s^{c\bar{c}s}$ obtained from individual and combined CDF [153], D0 [155] and LHCb [156, 188] likelihoods of $B_s^0 \rightarrow J/\psi \phi$ and $B_s^0 \rightarrow J/\psi \pi\pi$ [188] samples. Right: same combined contour compared with the 68% CL (green) and 95% CL (yellow) regions allowed by the measurements of \mathcal{A}_{SL}^s and Δm_s . The expectation within the Standard Model [91, 152] is shown as the black rectangle.

where $\phi_{s-\min}$ and $\Delta\Gamma_{s-\min}$ are the values of $\phi_s^{c\bar{c}s}$ and $\Delta\Gamma_s$ at the minimum of the likelihood, and $\sigma_{\phi-\text{stat}}$ ($\sigma_{\Delta\Gamma-\text{stat}}$) and $\sigma_{\phi-\text{syst}}$ ($\sigma_{\Delta\Gamma-\text{syst}}$) the statistical and systematic uncertainties on $\phi_s^{c\bar{c}s}$ ($\Delta\Gamma_s$). This assumes that the systematic uncertainties are Gaussian and independent of $\Delta\Gamma_s$ and $\phi_s^{c\bar{c}s}$. Both the D0 and CDF log profile-likelihood scans are corrected for coverage and include systematic uncertainties. We obtain the individual and combined contours shown in Fig. 11 (left). Profiling the likelihood in each of the $\Delta\Gamma_s$ and ϕ_s dimensions, we find, as summarized in Table 21:

$$\Delta\Gamma_s = +0.105 \pm 0.015 \text{ ps}^{-1}, \quad (83)$$

$$\phi_s^{c\bar{c}s} = -0.044_{-0.085}^{+0.090}. \quad (84)$$

In the Standard Model and ignoring sub-leading penguin contributions, $\phi_s^{c\bar{c}s}$ is expected to be equal to $-2\beta_s$, where $\beta_s = \arg[-(V_{ts}V_{tb}^*)/(V_{cs}V_{cb}^*)]$ is a phase analogous to the angle β of the usual CKM unitarity triangle (aside from a sign change). An indirect determination via global fits to experimental data gives [152]

$$(\phi_s^{c\bar{c}s})^{\text{SM}} = -2\beta_s = -0.0363_{-0.0015}^{+0.0016}. \quad (85)$$

The average value of $\phi_s^{c\bar{c}s}$ from Eq. (84) is consistent with this Standard Model expectation.

New physics could contribute $\phi_s^{c\bar{c}s}$. Assuming that new physics only enters in M_{12} (rather than in Γ_{12}), one can write [91]

$$\phi_s^{c\bar{c}s} = -2\beta_s + \phi_{12}^{\text{NP}}, \quad (86)$$

where the new physics phase ϕ_{12}^{NP} is the same as that appearing in Eq. (79). In this case

$$\phi_{12} = \phi_{12}^{\text{SM}} + 2\beta_s + \phi_s^{c\bar{c}s} \quad (87)$$

and Eq. (80) then provides a relation between $\Delta\Gamma_s$ and $\phi_s^{c\bar{c}s}$, based on the measured values of \mathcal{A}_{SL}^s and Δm_s (Eqs. (75) and (64)) as well as the expectations for ϕ_{12}^{SM} and $-2\beta_s$. The

allowed region in the $(\Delta\Gamma_s, \phi_s^{c\bar{c}s})$ plane is shown in Fig. 11 (right), where it is compared both with the direct measurement of $\Delta\Gamma_s$ and $\phi_s^{c\bar{c}s}$, and with the Standard Model expectations. No inconsistency is observed between all these data.

4 Measurements related to Unitarity Triangle angles

The charge of the “ $CP(t)$ and Unitarity Triangle angles” group is to provide averages of measurements from time-dependent asymmetry analyses, and other quantities that are related to the angles of the Unitarity Triangle (UT). In cases where considerable theoretical input is required to extract the fundamental quantities, no attempt is made to do so at this stage. However, straightforward interpretations of the averages are given, where possible.

In Sec. 4.1 a brief introduction to the relevant phenomenology is given. In Sec. 4.2 an attempt is made to clarify the various different notations in use. In Sec. 4.3 the common inputs to which experimental results are rescaled in the averaging procedure are listed. We also briefly introduce the treatment of experimental errors. In the remainder of this section, the experimental results and their averages are given, divided into subsections based on the underlying quark-level decays.

4.1 Introduction

The Standard Model Cabibbo-Kobayashi-Maskawa (CKM) quark mixing matrix V must be unitary. A 3×3 unitary matrix has four free parameters,²³ and these are conventionally written by the product of three (complex) rotation matrices [190], where the rotations are characterised by the Euler angles θ_{12} , θ_{13} and θ_{23} , which are the mixing angles between the generations, and one overall phase δ ,

$$V = \begin{pmatrix} V_{ud} & V_{us} & V_{ub} \\ V_{cd} & V_{cs} & V_{cb} \\ V_{td} & V_{ts} & V_{tb} \end{pmatrix} = \begin{pmatrix} c_{12}c_{13} & s_{12}c_{13} & s_{13}e^{-i\delta} \\ -s_{12}c_{23} - c_{12}s_{23}s_{13}e^{i\delta} & c_{12}c_{23} - s_{12}s_{23}s_{13}e^{i\delta} & s_{23}c_{13} \\ s_{12}s_{23} - c_{12}c_{23}s_{13}e^{i\delta} & -c_{12}s_{23} - s_{12}c_{23}s_{13}e^{i\delta} & c_{23}c_{13} \end{pmatrix} \quad (88)$$

where $c_{ij} = \cos \theta_{ij}$, $s_{ij} = \sin \theta_{ij}$ for $i < j = 1, 2, 3$.

Following the observation of a hierarchy between the different matrix elements, the Wolfenstein parametrisation [191] is an expansion of V in terms of the four real parameters λ (the expansion parameter), A , ρ and η . Defining to all orders in λ [192]

$$\begin{aligned} s_{12} &\equiv \lambda, \\ s_{23} &\equiv A\lambda^2, \\ s_{13}e^{-i\delta} &\equiv A\lambda^3(\rho - i\eta), \end{aligned} \quad (89)$$

and inserting these into the representation of Eq. (88), unitarity of the CKM matrix is achieved to all orders. A Taylor expansion of V leads to the familiar approximation

$$V = \begin{pmatrix} 1 - \lambda^2/2 & \lambda & A\lambda^3(\rho - i\eta) \\ -\lambda & 1 - \lambda^2/2 & A\lambda^2 \\ A\lambda^3(1 - \rho - i\eta) & -A\lambda^2 & 1 \end{pmatrix} + \mathcal{O}(\lambda^4). \quad (90)$$

At order λ^5 , the obtained CKM matrix in this extended Wolfenstein parametrisation is:

$$V = \begin{pmatrix} 1 - \frac{1}{2}\lambda^2 - \frac{1}{8}\lambda^4 & \lambda & A\lambda^3(\rho - i\eta) \\ -\lambda + \frac{1}{2}A^2\lambda^5[1 - 2(\rho + i\eta)] & 1 - \frac{1}{2}\lambda^2 - \frac{1}{8}\lambda^4(1 + 4A^2) & A\lambda^2 \\ A\lambda^3[1 - (1 - \frac{1}{2}\lambda^2)(\rho + i\eta)] & -A\lambda^2 + \frac{1}{2}A\lambda^4[1 - 2(\rho + i\eta)] & 1 - \frac{1}{2}A^2\lambda^4 \end{pmatrix} + \mathcal{O}(\lambda^6). \quad (91)$$

²³ In the general case there are nine free parameters, but five of these are absorbed into unobservable quark phases.

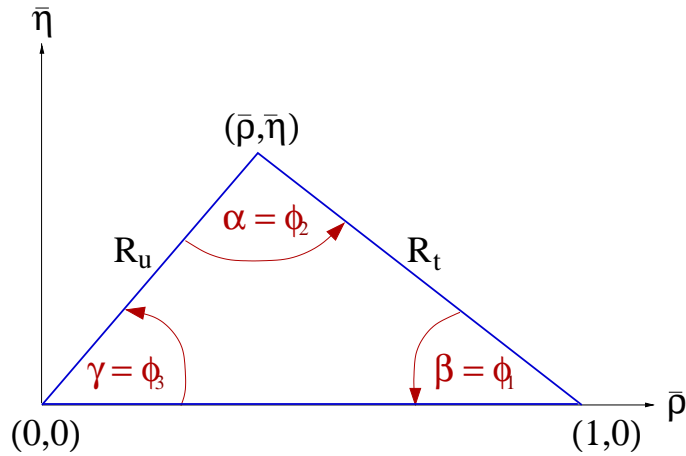


Figure 12: The Unitarity Triangle.

The non-zero imaginary part of the CKM matrix, which is the origin of CP violation in the Standard Model, is encapsulated in a non-zero value of η .

The unitarity relation $V^\dagger V = 1$ results in a total of nine expressions, that can be written as $\sum_{i=u,c,t} V_{ij}^* V_{ik} = \delta_{jk}$, where δ_{jk} is the Kronecker symbol. Of the off-diagonal expressions ($j \neq k$), three can be transformed into the other three leaving six relations, in which three complex numbers sum to zero, which therefore can be expressed as triangles in the complex plane. More details about unitarity triangles can be found in [193–198].

One of these relations,

$$V_{ud}V_{ub}^* + V_{cd}V_{cb}^* + V_{td}V_{tb}^* = 0, \quad (92)$$

is of particular importance to the B system, being specifically related to flavour changing neutral current $b \rightarrow d$ transitions. The three terms in Eq. (92) are of the same order ($\mathcal{O}(\lambda^3)$), and this relation is commonly known as the Unitarity Triangle. For presentational purposes, it is convenient to rescale the triangle by $(V_{cd}V_{cb}^*)^{-1}$, as shown in Fig. 12.

Two popular naming conventions for the UT angles exist in the literature:

$$\alpha \equiv \phi_2 = \arg \left[-\frac{V_{td}V_{tb}^*}{V_{ud}V_{ub}^*} \right], \quad \beta \equiv \phi_1 = \arg \left[-\frac{V_{cd}V_{cb}^*}{V_{td}V_{tb}^*} \right], \quad \gamma \equiv \phi_3 = \arg \left[-\frac{V_{ud}V_{ub}^*}{V_{cd}V_{cb}^*} \right]. \quad (93)$$

In this document the (α, β, γ) set is used.²⁴ The sides R_u and R_t of the Unitarity Triangle (the third side being normalised to unity) are given by

$$R_u = \left| \frac{V_{ud}V_{ub}^*}{V_{cd}V_{cb}^*} \right| = \sqrt{\bar{\rho}^2 + \bar{\eta}^2}, \quad R_t = \left| \frac{V_{td}V_{tb}^*}{V_{cd}V_{cb}^*} \right| = \sqrt{(1 - \bar{\rho})^2 + \bar{\eta}^2}. \quad (94)$$

where $\bar{\rho}$ and $\bar{\eta}$ define the apex of the Unitarity Triangle [192]

$$\bar{\rho} + i\bar{\eta} \equiv -\frac{V_{ud}V_{ub}^*}{V_{cd}V_{cb}^*} \equiv 1 + \frac{V_{td}V_{tb}^*}{V_{cd}V_{cb}^*} = \frac{\sqrt{1 - \lambda^2}(\rho + i\eta)}{\sqrt{1 - A^2\lambda^4} + \sqrt{1 - \lambda^2}A^2\lambda^4(\rho + i\eta)}. \quad (95)$$

²⁴ The relevant unitarity triangle for the B_s^0 system is obtained by replacing $d \leftrightarrow s$ in Eq. 92. Definitions of the set of angles $(\alpha_s, \beta_s, \gamma_s)$ can be obtained using equivalent relations to those of Eq. 93, for example $\beta_s = \arg[-(V_{cs}V_{cb}^*)/(V_{ts}V_{tb}^*)]$. This definition gives a value of β_s that is negative in the Standard Model, so that the sign is often flipped in the literature.

The exact relation between (ρ, η) and $(\bar{\rho}, \bar{\eta})$ is

$$\rho + i\eta = \frac{\sqrt{1 - A^2\lambda^4}(\bar{\rho} + i\bar{\eta})}{\sqrt{1 - \lambda^2}[1 - A^2\lambda^4(\bar{\rho} + i\bar{\eta})]}. \quad (96)$$

By expanding in powers of λ , several useful approximate expressions can be obtained, including

$$\bar{\rho} = \rho(1 - \frac{1}{2}\lambda^2) + \mathcal{O}(\lambda^4), \quad \bar{\eta} = \eta(1 - \frac{1}{2}\lambda^2) + \mathcal{O}(\lambda^4), \quad V_{td} = A\lambda^3(1 - \bar{\rho} - i\bar{\eta}) + \mathcal{O}(\lambda^6). \quad (97)$$

4.2 Notations

Several different notations for CP violation parameters are commonly used. This section reviews those found in the experimental literature, in the hope of reducing the potential for confusion, and to define the frame that is used for the averages.

In some cases, when B mesons decay into multibody final states via broad resonances (ρ , K^* , *etc.*), the experimental analyses ignore the effects of interference between the overlapping structures. This is referred to as the quasi-two-body (Q2B) approximation in the following.

4.2.1 CP asymmetries

The CP asymmetry is defined as the difference between the rate involving a b quark and that involving a \bar{b} quark, divided by the sum. For example, the partial rate (or charge) asymmetry for a charged B decay would be given as

$$\mathcal{A}_f \equiv \frac{\Gamma(B^- \rightarrow f) - \Gamma(B^+ \rightarrow \bar{f})}{\Gamma(B^- \rightarrow f) + \Gamma(B^+ \rightarrow \bar{f})}. \quad (98)$$

4.2.2 Time-dependent CP asymmetries in decays to CP eigenstates

If the amplitudes for B^0 and \bar{B}^0 to decay to a final state f , which is a CP eigenstate with eigenvalue η_f , are given by A_f and \bar{A}_f , respectively, then the decay distributions for neutral B mesons, with known flavour at time $\Delta t = 0$, are given by

$$\Gamma_{\bar{B}^0 \rightarrow f}(\Delta t) = \frac{e^{-|\Delta t|/\tau(B^0)}}{4\tau(B^0)} \left[1 + \frac{2 \operatorname{Im}(\lambda_f)}{1 + |\lambda_f|^2} \sin(\Delta m \Delta t) - \frac{1 - |\lambda_f|^2}{1 + |\lambda_f|^2} \cos(\Delta m \Delta t) \right], \quad (99)$$

$$\Gamma_{B^0 \rightarrow f}(\Delta t) = \frac{e^{-|\Delta t|/\tau(B^0)}}{4\tau(B^0)} \left[1 - \frac{2 \operatorname{Im}(\lambda_f)}{1 + |\lambda_f|^2} \sin(\Delta m \Delta t) + \frac{1 - |\lambda_f|^2}{1 + |\lambda_f|^2} \cos(\Delta m \Delta t) \right]. \quad (100)$$

Here $\lambda_f = \frac{q \bar{A}_f}{p A_f}$ contains terms related to B^0 - \bar{B}^0 mixing and to the decay amplitude (the eigenstates of the effective Hamiltonian in the $B^0\bar{B}^0$ system are $|B_{\pm}\rangle = p|B^0\rangle \pm q|\bar{B}^0\rangle$). This formulation assumes CPT invariance, and neglects possible lifetime differences (between the eigenstates of the effective Hamiltonian; see Section 3.3 where the mass difference Δm is also defined) in the neutral B meson system. The case where non-zero lifetime differences are taken into account is discussed in Section 4.2.3. Note that the notation and normalisation used here is that which is relevant for the e^+e^- B factory experiments. At hadron collider experiments,

the flavour tagging is done at production ($\Delta t = t = 0$), and therefore t is usually used in place of Δt . Moreover, since negative values of t are not allowed, the normalisation is such that $\int_0^{+\infty} (\Gamma_{\bar{B}^0 \rightarrow f}(t) + \Gamma_{B^0 \rightarrow f}(t)) dt = 1$, rather than $\int_{-\infty}^{+\infty} (\Gamma_{\bar{B}^0 \rightarrow f}(\Delta t) + \Gamma_{B^0 \rightarrow f}(\Delta t)) d(\Delta t) = 1$, as in Eqs. 99 and 100.

The time-dependent CP asymmetry, again defined as the difference between the rate involving a b quark and that involving a \bar{b} quark, is then given by

$$\mathcal{A}_f(\Delta t) \equiv \frac{\Gamma_{\bar{B}^0 \rightarrow f}(\Delta t) - \Gamma_{B^0 \rightarrow f}(\Delta t)}{\Gamma_{\bar{B}^0 \rightarrow f}(\Delta t) + \Gamma_{B^0 \rightarrow f}(\Delta t)} = \frac{2 \operatorname{Im}(\lambda_f)}{1 + |\lambda_f|^2} \sin(\Delta m \Delta t) - \frac{1 - |\lambda_f|^2}{1 + |\lambda_f|^2} \cos(\Delta m \Delta t). \quad (101)$$

While the coefficient of the $\sin(\Delta m \Delta t)$ term in Eq. (101) is everywhere²⁵ denoted S_f :

$$S_f \equiv \frac{2 \operatorname{Im}(\lambda_f)}{1 + |\lambda_f|^2}, \quad (102)$$

different notations are in use for the coefficient of the $\cos(\Delta m \Delta t)$ term:

$$C_f \equiv -A_f \equiv \frac{1 - |\lambda_f|^2}{1 + |\lambda_f|^2}. \quad (103)$$

The C notation is used by the *BABAR* collaboration (see *e.g.* [199]), and also in this document. The A notation is used by the Belle collaboration (see *e.g.* [200]).

Neglecting effects due to CP violation in mixing (by taking $|q/p| = 1$), if the decay amplitude contains terms with a single weak (*i.e.*, CP violating) phase then $|\lambda_f| = 1$ and one finds $S_f = -\eta_f \sin(\phi_{\text{mix}} + \phi_{\text{dec}})$, $C_f = 0$, where $\phi_{\text{mix}} = \arg(q/p)$ and $\phi_{\text{dec}} = \arg(\bar{A}_f/A_f)$. Note that the B^0 - \bar{B}^0 mixing phase $\phi_{\text{mix}} \approx 2\beta$ in the Standard Model (in the usual phase convention) [201,202].

If amplitudes with different weak phases contribute to the decay, no clean interpretation of S_f is possible without further input. If the decay amplitudes have in addition different CP conserving strong phases, then $|\lambda_f| \neq 1$ and additional input is required for interpretation. The coefficient of the cosine term becomes non-zero, indicating direct CP violation. The sign of A_f as defined above is consistent with that of \mathcal{A}_f in Eq. (98).

Due to the fact that $\sin(\Delta m \Delta t)$ and $\cos(\Delta m \Delta t)$ are respectively odd and even functions of Δt , only small correlations (that can be induced by backgrounds, for example) between S_f and C_f are expected at B factory experiments, where the range of Δt is $-\infty < \Delta t < +\infty$. The situation is different for measurements at hadron collider experiments, where the range of the time variable is $0 < \Delta t < +\infty$, so that more sizable correlations can be expected. We include the correlations in the averages where available.

Frequently, we are interested in combining measurements governed by similar or identical short-distance physics, but with different final states (*e.g.*, $B^0 \rightarrow J/\psi K_S^0$ and $B^0 \rightarrow J/\psi K_L^0$). In this case, we remove the dependence on the CP eigenvalue of the final state by quoting $-\eta S_f$. In cases where the final state is not a CP eigenstate but has an effective CP content (see below), the reported $-\eta S$ is corrected by the effective CP .

4.2.3 Time-dependent distributions with non-zero decay width difference

A complete analysis of the time-dependent decay rates of neutral B mesons must also take into account the lifetime difference between the eigenstates of the effective Hamiltonian, denoted by

²⁵ Occasionally one also finds Eq. (101) written as $\mathcal{A}_f(\Delta t) = \mathcal{A}_f^{\text{mix}} \sin(\Delta m \Delta t) + \mathcal{A}_f^{\text{dir}} \cos(\Delta m \Delta t)$, or similar.

$\Delta\Gamma$. This is particularly important in the B_s system, since non-negligible values of $\Delta\Gamma_s$ have now been established (see Section 3.3 for the latest experimental constraints). Neglecting CP violation in mixing, the relevant replacements for Eqs. 99 & 100 are [203]

$$\Gamma_{\bar{B}_s \rightarrow f}(\Delta t) = \mathcal{N} \frac{e^{-|\Delta t|/\tau(B_s^0)}}{4\tau(B_s^0)} \left[\cosh\left(\frac{\Delta\Gamma\Delta t}{2}\right) + \frac{2\text{Im}(\lambda_f)}{1+|\lambda_f|^2} \sin(\Delta m\Delta t) - \frac{1-|\lambda_f|^2}{1+|\lambda_f|^2} \cos(\Delta m\Delta t) - \frac{2\text{Re}(\lambda_f)}{1+|\lambda_f|^2} \sinh\left(\frac{\Delta\Gamma\Delta t}{2}\right) \right], \quad (104)$$

and

$$\Gamma_{B_s^0 \rightarrow f}(\Delta t) = \mathcal{N} \frac{e^{-|\Delta t|/\tau(B_s^0)}}{4\tau(B_s^0)} \left[\cosh\left(\frac{\Delta\Gamma\Delta t}{2}\right) - \frac{2\text{Im}(\lambda_f)}{1+|\lambda_f|^2} \sin(\Delta m\Delta t) + \frac{1-|\lambda_f|^2}{1+|\lambda_f|^2} \cos(\Delta m\Delta t) - \frac{2\text{Re}(\lambda_f)}{1+|\lambda_f|^2} \sinh\left(\frac{\Delta\Gamma\Delta t}{2}\right) \right]. \quad (105)$$

To be consistent with our earlier notation,²⁶ we write here the coefficient of the sinh term as

$$A_f^{\Delta\Gamma} = -\frac{2\text{Re}(\lambda_f)}{1+|\lambda_f|^2}. \quad (106)$$

A complete, tagged, time-dependent analysis of CP asymmetries in B_s decays to a CP eigenstate f can thus obtain the parameters S_f , C_f and $A_f^{\Delta\Gamma}$. Note that, by definition,

$$(S_f)^2 + (C_f)^2 + (A_f^{\Delta\Gamma})^2 = 1, \quad (107)$$

and this constraint can be imposed or not in the fits. Since these parameters have sensitivity to both $\text{Im}(\lambda_f)$ and $\text{Re}(\lambda_f)$, alternative choices of parametrisation, including those directly involving CP violating phases (such as β_s), are possible. These can also be adopted for vector-vector final states.

The *untagged* time-dependent decay rate is given by

$$\Gamma_{\bar{B}_s \rightarrow f}(\Delta t) + \Gamma_{B_s^0 \rightarrow f}(\Delta t) = \mathcal{N} \frac{e^{-|\Delta t|/\tau(B_s^0)}}{2\tau(B_s^0)} \left[\cosh\left(\frac{\Delta\Gamma\Delta t}{2}\right) - \frac{2\text{Re}(\lambda_f)}{1+|\lambda_f|^2} \sinh\left(\frac{\Delta\Gamma\Delta t}{2}\right) \right]. \quad (108)$$

With the requirement $\int_{-\infty}^{+\infty} \Gamma_{\bar{B}_s \rightarrow f}(\Delta t) + \Gamma_{B_s^0 \rightarrow f}(\Delta t) d(\Delta t) = 1$, the normalisation factor \mathcal{N} is fixed to $1 - (\frac{\Delta\Gamma}{2\Gamma})^2$. Note that an untagged time-dependent analysis can probe λ_f , through $\text{Re}(\lambda_f)$, when $\Delta\Gamma \neq 0$. This is equivalent to determining the “*effective lifetime*” [158], as discussed in Sec. 3.2.4. The tagged analysis is, of course, more sensitive.

Other expressions can be similarly modified to take into account non-zero lifetime differences. Note that when the final state contains a mixture of CP -even and CP -odd states (as, for example, for vector-vector or multibody self-conjugate states), that $\text{Re}(\lambda_f)$ contains terms proportional to both the sine and cosine of the weak phase difference, albeit with rather different sensitivities.

4.2.4 Time-dependent CP asymmetries in decays to vector-vector final states

Consider B decays to states consisting of two spin-1 particles, such as $J/\psi K^{*0} (\rightarrow K_s^0 \pi^0)$, $D^{*+} D^{*-}$ and $\rho^+ \rho^-$, which are eigenstates of charge conjugation but not of parity.²⁷ In fact, for

²⁶ As ever, alternative and conflicting notations appear in the literature. One popular alternative notation for this parameter is $\mathcal{A}_{\Delta\Gamma}$. Particular care must be taken over the signs.

²⁷ This is not true of all vector-vector final states, *e.g.*, $D^{*\pm} \rho^\mp$ is clearly not an eigenstate of charge conjugation.

such a system, there are three possible final states; in the helicity basis these can be written h_{-1}, h_0, h_{+1} . The h_0 state is an eigenstate of parity, and hence of CP ; however, CP transforms $h_{+1} \leftrightarrow h_{-1}$ (up to an unobservable phase). In the transversity basis, these states are transformed into $h_{\parallel} = (h_{+1} + h_{-1})/2$ and $h_{\perp} = (h_{+1} - h_{-1})/2$. In this basis all three states are CP eigenstates, and h_{\perp} has the opposite CP to the others.

The amplitudes to these states are usually given by $A_{0,\perp,\parallel}$ (here we use a normalisation such that $|A_0|^2 + |A_{\perp}|^2 + |A_{\parallel}|^2 = 1$). Then the effective CP of the vector-vector state is known if $|A_{\perp}|^2$ is measured. An alternative strategy is to measure just the longitudinally polarised component, $|A_0|^2$ (sometimes denoted by f_{long}), which allows a limit to be set on the effective CP since $|A_{\perp}|^2 \leq |A_{\perp}|^2 + |A_{\parallel}|^2 = 1 - |A_0|^2$. The most complete treatment for neutral B decays to vector-vector final states is time-dependent angular analysis (also known as time-dependent transversity analysis). In such an analysis, the interference between the CP -even and CP -odd states provides additional sensitivity to the weak and strong phases involved.

In most analyses of time-dependent CP asymmetries in decays to vector-vector final states carried out to date, an assumption has been made that each helicity (or transversity) amplitude has the same weak phase. This is a good approximation for decays that are dominated by amplitudes with a single weak phase, such as $B^0 \rightarrow J/\psi K^{*0}$, and is a reasonable approximation in any mode for which only very limited statistics are available. However, for modes that have contributions from amplitudes with different weak phases, the relative size of these contributions can be different for each helicity (or transversity) amplitude, and therefore the time-dependent CP asymmetry parameters can also differ. The most generic analysis, suitable for modes with sufficient statistics, would allow for this effect; an intermediate analysis can allow different parameters for the CP -even and CP -odd components. Such an analysis has been carried out by *BABAR* for the decay $B^0 \rightarrow D^{*+} D^{*-}$ [204].

4.2.5 Time-dependent asymmetries: self-conjugate multiparticle final states

Amplitudes for neutral B decays into self-conjugate multiparticle final states such as $\pi^+ \pi^- \pi^0$, $K^+ K^- K_s^0$, $\pi^+ \pi^- K_s^0$, $J/\psi \pi^+ \pi^-$ or $D\pi^0$ with $D \rightarrow K_s^0 \pi^+ \pi^-$ may be written in terms of CP -even and CP -odd amplitudes. As above, the interference between these terms provides additional sensitivity to the weak and strong phases involved in the decay, and the time-dependence depends on both the sine and cosine of the weak phase difference. In order to perform unbinned maximum likelihood fits, and thereby extract as much information as possible from the distributions, it is necessary to select a model for the multiparticle decay, and therefore the results acquire some model dependence (binned, model independent methods are also possible, though are not as statistically powerful). The number of observables depends on the final state (and on the model used); the key feature is that as long as there are regions where both CP -even and CP -odd amplitudes contribute, the interference terms will be sensitive to the cosine of the weak phase difference. Therefore, these measurements allow distinction between multiple solutions for, *e.g.*, the four values of β from the measurement of $\sin(2\beta)$.

We now consider the various notations which have been used in experimental studies of time-dependent asymmetries in decays to self-conjugate multiparticle final states.

$$B^0 \rightarrow D^{(*)} h^0 \text{ with } D \rightarrow K_s^0 \pi^+ \pi^-$$

The states $D\pi^0$, $D^* \pi^0$, $D\eta$, $D^* \eta$, $D\omega$ are collectively denoted $D^{(*)} h^0$. When the D decay model is fixed, fits to the time-dependent decay distributions can be performed to extract the

weak phase difference. However, it is experimentally advantageous to use the sine and cosine of this phase as fit parameters, since these behave as essentially independent parameters, with low correlations and (potentially) rather different uncertainties. A parameter representing direct CP violation in the B decay can also be floated. For consistency with other analyses, this could be chosen to be C_f , but could equally well be $|\lambda_f|$, or other possibilities.

Belle performed an analysis of these channels with $\sin(2\phi_1)$ and $\cos(2\phi_1)$ as free parameters [205]. *BABAR* have performed an analysis floating also $|\lambda_f|$ [206] (and, of course, replacing $\phi_1 \Leftrightarrow \beta$).

$B^0 \rightarrow D^{*+} D^{*-} K_S^0$

The hadronic structure of the $B^0 \rightarrow D^{*+} D^{*-} K_S^0$ decay is not sufficiently well understood to perform a full time-dependent Dalitz plot analysis. Instead, following Browder *et al.* [207], *BABAR* [208] divide the Dalitz plane in two: $m(D^{*+} K_S^0)^2 > m(D^{*-} K_S^0)^2$ ($\eta_y = +1$) and $m(D^{*+} K_S^0)^2 < m(D^{*-} K_S^0)^2$ ($\eta_y = -1$); and then fit to a decay time distribution with asymmetry given by

$$\mathcal{A}_f(\Delta t) = \eta_y \frac{J_c}{J_0} \cos(\Delta m \Delta t) - \left[\frac{2J_{s1}}{J_0} \sin(2\beta) + \eta_y \frac{2J_{s2}}{J_0} \cos(2\beta) \right] \sin(\Delta m \Delta t). \quad (109)$$

A similar analysis has also been carried out by Belle [209]. The measured values are $\frac{J_c}{J_0}$, $\frac{2J_{s1}}{J_0} \sin(2\beta)$ and $\frac{2J_{s2}}{J_0} \cos(2\beta)$, where the parameters J_0 , J_c , J_{s1} and J_{s2} are the integrals over the half Dalitz plane $m(D^{*+} K_S^0)^2 < m(D^{*-} K_S^0)^2$ of the functions $|a|^2 + |\bar{a}|^2$, $|a|^2 - |\bar{a}|^2$, $\text{Re}(\bar{a}a^*)$ and $\text{Im}(\bar{a}a^*)$ respectively, where a and \bar{a} are the decay amplitudes of $B^0 \rightarrow D^{*+} D^{*-} K_S^0$ and $\bar{B}^0 \rightarrow D^{*+} D^{*-} K_S^0$ respectively. The parameter J_{s2} (and hence J_{s2}/J_0) is predicted to be positive; with this assumption it is possible to determine the sign of $\cos(2\beta)$.

$B^0 \rightarrow K^+ K^- K^0$

Studies of $B^0 \rightarrow K^+ K^- K^0$ [210–212] and of the related decay $B^+ \rightarrow K^+ K^- K^+$ [212–214], show that the decay is dominated by a large nonresonant contribution with significant components from the intermediate $K^+ K^-$ resonances $\phi(1020)$, $f_0(980)$, and other higher resonances,²⁸ as well a contribution from χ_{c0} .

The full time-dependent Dalitz plot analysis allows the complex amplitudes of each contributing term to be determined from data, including CP violation effects (*i.e.* allowing the complex amplitude for the B^0 decay to be independent from that for \bar{B}^0 decay), although one amplitude must be fixed to give a reference point. There are several choices for parametrisation of the complex amplitudes (*e.g.* real and imaginary part, or magnitude and phase). Similarly, there are various approaches to include CP violation effects. Note that positive definite parameters such as magnitudes are disfavoured in certain circumstances (they inevitably lead to biases for small values). In order to compare results between analyses, it is useful for each experiment to present results in terms of the parameters that can be measured in a Q2B analysis (such as \mathcal{A}_f , S_f , C_f , $\sin(2\beta^{\text{eff}})$, $\cos(2\beta^{\text{eff}})$, *etc.*)

In the *BABAR* analysis of $B^0 \rightarrow K^+ K^- K^0$ [212], the complex amplitude for each resonant

²⁸ The broad structure that peaks near $m(K^+ K^-) \sim 1550$ MeV/ c^2 and was denoted $X_0(1550)$ is now believed to originate from interference effects.

contribution is written as

$$A_f = c_f(1 + b_f)e^{i(\phi_f + \delta_f)}, \quad \bar{A}_f = c_f(1 - b_f)e^{i(\phi_f - \delta_f)}, \quad (110)$$

where b_f and δ_f introduce CP violation in the magnitude and phase respectively. Belle [211] use the same parametrisation but with a different notation for the parameters.²⁹ [The weak phase in B^0 - \bar{B}^0 mixing (2β) also appears in the full formula for the time-dependent decay distribution.] The Q2B direct CP violation parameter is directly related to b_f

$$\mathcal{A}_f = \frac{-2b_f}{1 + b_f^2} \approx C_f, \quad (111)$$

and the mixing-induced CP violation parameter can be used to obtain $\sin(2\beta^{\text{eff}})$

$$-\eta_f S_f \approx \frac{1 - b_f^2}{1 + b_f^2} \sin(2\beta_f^{\text{eff}}), \quad (112)$$

where the approximations are exact in the case that $|q/p| = 1$.

Both *BABAR* [212] and Belle [211] present results for c_f and ϕ_f , for each resonant contribution, and in addition present results for \mathcal{A}_f and β_f^{eff} for $\phi(1020)K^0$, $f_0(980)K^0$ and for the remainder of the contributions to the $K^+K^-K^0$ Dalitz plot combined.³⁰ The models used to describe the resonant structure of the Dalitz plot differ, however. Both analyses suffer from multiple solutions, from which we select only one for averaging.

$B^0 \rightarrow \pi^+\pi^-K_s^0$

Studies of $B^0 \rightarrow \pi^+\pi^-K_s^0$ [215, 216] and of the related decay $B^+ \rightarrow \pi^+\pi^-K^+$ [213, 217–219] show that the decay is dominated by components from intermediate resonances in the $K\pi$ ($K^*(892)$, $K_0^*(1430)$) and $\pi\pi$ ($\rho(770)$, $f_0(980)$, $f_2(1270)$) spectra, together with a poorly understood scalar structure that peaks near $m(\pi\pi) \sim 1300$ MeV/ c^2 and is denoted $f_X(1300)$ (that could be identified as either the $f_0(1370)$ or $f_0(1500)$), and a large nonresonant component. There is also a contribution from the χ_{c0} state.

The full time-dependent Dalitz plot analysis allows the complex amplitudes of each contributing term to be determined from data, including CP violation effects. In the *BABAR* analysis [215], the magnitude and phase of each component (for both B^0 and \bar{B}^0 decays) are measured relative to $B^0 \rightarrow f_0(980)K_s^0$, using the following parametrisation

$$A_f = |A_f| e^{i \arg(A_f)}, \quad \bar{A}_f = |\bar{A}_f| e^{i \arg(\bar{A}_f)}. \quad (113)$$

In the Belle analysis [216], the $B^0 \rightarrow K^{*+}\pi^-$ amplitude is chosen as the reference, and the amplitudes are parametrised as

$$A_f = a_f(1 + c_f)e^{i(b_f + d_f)}, \quad \bar{A}_f = a_f(1 - c_f)e^{i(b_f - d_f)}. \quad (114)$$

In both cases, the results are translated into quasi-two-body parameters such as $2\beta_f^{\text{eff}}$, S_f , C_f for each CP eigenstate f , and direct CP asymmetries for each flavour-specific state. Relative phase differences between resonant terms are also extracted.

²⁹ $(c, b, \phi, \delta) \leftrightarrow (a, c, b, d)$.

³⁰ *BABAR* also present results for the Q2B parameter S_f for these channels.

$B^0 \rightarrow \pi^+\pi^-\pi^0$

The $B^0 \rightarrow \pi^+\pi^-\pi^0$ decay is dominated by intermediate ρ resonances. Though it is possible, as above, to determine directly the complex amplitudes for each component, an alternative approach [220, 221], has been used by both *BABAR* [222] and *Belle* [223, 224]. The amplitudes for B^0 and \bar{B}^0 to $\pi^+\pi^-\pi^0$ are written

$$A_{3\pi} = f_+ A_+ + f_- A_- + f_0 A_0, \quad \bar{A}_{3\pi} = f_+ \bar{A}_+ + f_- \bar{A}_- + f_0 \bar{A}_0 \quad (115)$$

respectively. A_+ , A_- and A_0 represent the complex decay amplitudes for $B^0 \rightarrow \rho^+\pi^-$, $B^0 \rightarrow \rho^-\pi^+$ and $B^0 \rightarrow \rho^0\pi^0$ while \bar{A}_+ , \bar{A}_- and \bar{A}_0 represent those for $\bar{B}^0 \rightarrow \rho^+\pi^-$, $\bar{B}^0 \rightarrow \rho^-\pi^+$ and $\bar{B}^0 \rightarrow \rho^0\pi^0$ respectively. f_+ , f_- and f_0 incorporate kinematic and dynamical factors and depend on the Dalitz plot coordinates. The full time-dependent decay distribution can then be written in terms of 27 free parameters, one for each coefficient of the form factor bilinears, as listed in Table 22. These parameters are often referred to as ‘‘the U s and I s’’, and can be expressed in terms of A_+ , A_- , A_0 , \bar{A}_+ , \bar{A}_- and \bar{A}_0 . If the full set of parameters is determined, together with their correlations, other parameters, such as weak and strong phases, direct CP violation parameters, *etc.*, can be subsequently extracted. Note that one of the parameters (typically U_+^+) is often fixed to unity to provide a reference point; this does not affect the analysis.

4.2.6 Time-dependent CP asymmetries in decays to non- CP eigenstates

Consider a non- CP eigenstate f , and its conjugate \bar{f} . For neutral B decays to these final states, there are four amplitudes to consider: those for B^0 to decay to f and \bar{f} (A_f and $A_{\bar{f}}$, respectively), and the equivalents for \bar{B}^0 (\bar{A}_f and $\bar{A}_{\bar{f}}$). If CP is conserved in the decay, then $A_f = \bar{A}_{\bar{f}}$ and $A_{\bar{f}} = \bar{A}_f$.

The time-dependent decay distributions can be written in many different ways. Here, we follow Sec. 4.2.2 and define $\lambda_f = \frac{q}{p} \frac{\bar{A}_f}{A_f}$ and $\lambda_{\bar{f}} = \frac{q}{p} \frac{\bar{A}_{\bar{f}}}{A_{\bar{f}}}$. The time-dependent CP asymmetries then follow Eq. (101):

$$\mathcal{A}_f(\Delta t) \equiv \frac{\Gamma_{\bar{B}^0 \rightarrow f}(\Delta t) - \Gamma_{B^0 \rightarrow f}(\Delta t)}{\Gamma_{\bar{B}^0 \rightarrow f}(\Delta t) + \Gamma_{B^0 \rightarrow f}(\Delta t)} = S_f \sin(\Delta m \Delta t) - C_f \cos(\Delta m \Delta t), \quad (116)$$

$$\mathcal{A}_{\bar{f}}(\Delta t) \equiv \frac{\Gamma_{\bar{B}^0 \rightarrow \bar{f}}(\Delta t) - \Gamma_{B^0 \rightarrow \bar{f}}(\Delta t)}{\Gamma_{\bar{B}^0 \rightarrow \bar{f}}(\Delta t) + \Gamma_{B^0 \rightarrow \bar{f}}(\Delta t)} = S_{\bar{f}} \sin(\Delta m \Delta t) - C_{\bar{f}} \cos(\Delta m \Delta t), \quad (117)$$

with the definitions of the parameters C_f , S_f , $C_{\bar{f}}$ and $S_{\bar{f}}$, following Eqs. (102) and (103).

The time-dependent decay rates are given by

$$\Gamma_{\bar{B}^0 \rightarrow f}(\Delta t) = \frac{e^{-|\Delta t|/\tau(B^0)}}{8\tau(B^0)} (1 + \langle \mathcal{A}_{f\bar{f}} \rangle) \{1 + S_f \sin(\Delta m \Delta t) - C_f \cos(\Delta m \Delta t)\}, \quad (118)$$

$$\Gamma_{B^0 \rightarrow f}(\Delta t) = \frac{e^{-|\Delta t|/\tau(B^0)}}{8\tau(B^0)} (1 + \langle \mathcal{A}_{f\bar{f}} \rangle) \{1 - S_f \sin(\Delta m \Delta t) + C_f \cos(\Delta m \Delta t)\}, \quad (119)$$

$$\Gamma_{\bar{B}^0 \rightarrow \bar{f}}(\Delta t) = \frac{e^{-|\Delta t|/\tau(B^0)}}{8\tau(B^0)} (1 - \langle \mathcal{A}_{f\bar{f}} \rangle) \{1 + S_{\bar{f}} \sin(\Delta m \Delta t) - C_{\bar{f}} \cos(\Delta m \Delta t)\}, \quad (120)$$

$$\Gamma_{B^0 \rightarrow \bar{f}}(\Delta t) = \frac{e^{-|\Delta t|/\tau(B^0)}}{8\tau(B^0)} (1 - \langle \mathcal{A}_{f\bar{f}} \rangle) \{1 - S_{\bar{f}} \sin(\Delta m \Delta t) + C_{\bar{f}} \cos(\Delta m \Delta t)\}, \quad (121)$$

Table 22: Definitions of the U and I coefficients. Modified from [222].

Parameter	Description
U_+^+	Coefficient of $ f_+ ^2$
U_0^+	Coefficient of $ f_0 ^2$
U_-^+	Coefficient of $ f_- ^2$
U_0^-	Coefficient of $ f_0 ^2 \cos(\Delta m \Delta t)$
U_-^-	Coefficient of $ f_- ^2 \cos(\Delta m \Delta t)$
U_+^-	Coefficient of $ f_+ ^2 \cos(\Delta m \Delta t)$
I_0	Coefficient of $ f_0 ^2 \sin(\Delta m \Delta t)$
I_-	Coefficient of $ f_- ^2 \sin(\Delta m \Delta t)$
I_+	Coefficient of $ f_+ ^2 \sin(\Delta m \Delta t)$
$U_{+-}^{+,Im}$	Coefficient of $\text{Im}[f_+ f_-^*]$
$U_{+-}^{+,Re}$	Coefficient of $\text{Re}[f_+ f_-^*]$
$U_{+-}^{-,Im}$	Coefficient of $\text{Im}[f_+ f_-^*] \cos(\Delta m \Delta t)$
$U_{+-}^{-,Re}$	Coefficient of $\text{Re}[f_+ f_-^*] \cos(\Delta m \Delta t)$
I_{+-}^{Im}	Coefficient of $\text{Im}[f_+ f_-^*] \sin(\Delta m \Delta t)$
I_{+-}^{Re}	Coefficient of $\text{Re}[f_+ f_-^*] \sin(\Delta m \Delta t)$
$U_{+0}^{+,Im}$	Coefficient of $\text{Im}[f_+ f_0^*]$
$U_{+0}^{+,Re}$	Coefficient of $\text{Re}[f_+ f_0^*]$
$U_{+0}^{-,Im}$	Coefficient of $\text{Im}[f_+ f_0^*] \cos(\Delta m \Delta t)$
$U_{+0}^{-,Re}$	Coefficient of $\text{Re}[f_+ f_0^*] \cos(\Delta m \Delta t)$
I_{+0}^{Im}	Coefficient of $\text{Im}[f_+ f_0^*] \sin(\Delta m \Delta t)$
I_{+0}^{Re}	Coefficient of $\text{Re}[f_+ f_0^*] \sin(\Delta m \Delta t)$
$U_{-0}^{+,Im}$	Coefficient of $\text{Im}[f_- f_0^*]$
$U_{-0}^{+,Re}$	Coefficient of $\text{Re}[f_- f_0^*]$
$U_{-0}^{-,Im}$	Coefficient of $\text{Im}[f_- f_0^*] \cos(\Delta m \Delta t)$
$U_{-0}^{-,Re}$	Coefficient of $\text{Re}[f_- f_0^*] \cos(\Delta m \Delta t)$
I_{-0}^{Im}	Coefficient of $\text{Im}[f_- f_0^*] \sin(\Delta m \Delta t)$
I_{-0}^{Re}	Coefficient of $\text{Re}[f_- f_0^*] \sin(\Delta m \Delta t)$

where the time-independent parameter $\langle \mathcal{A}_{f\bar{f}} \rangle$ represents an overall asymmetry in the production of the f and \bar{f} final states,³¹

$$\langle \mathcal{A}_{f\bar{f}} \rangle = \frac{\left(|A_f|^2 + |\bar{A}_f|^2 \right) - \left(|A_{\bar{f}}|^2 + |\bar{A}_{\bar{f}}|^2 \right)}{\left(|A_f|^2 + |\bar{A}_f|^2 \right) + \left(|A_{\bar{f}}|^2 + |\bar{A}_{\bar{f}}|^2 \right)}. \quad (122)$$

Assuming $|q/p| = 1$, the parameters C_f and $C_{\bar{f}}$ can also be written in terms of the decay

³¹ This parameter is often denoted \mathcal{A}_f (or \mathcal{A}_{CP}), but here we avoid this notation to prevent confusion with the time-dependent CP asymmetry.

amplitudes as follows:

$$C_f = \frac{|A_f|^2 - |\bar{A}_f|^2}{|A_f|^2 + |\bar{A}_f|^2} \quad \text{and} \quad C_{\bar{f}} = \frac{|A_{\bar{f}}|^2 - |\bar{A}_{\bar{f}}|^2}{|A_{\bar{f}}|^2 + |\bar{A}_{\bar{f}}|^2}, \quad (123)$$

giving asymmetries in the decay amplitudes of B^0 and \bar{B}^0 to the final states f and \bar{f} respectively. In this notation, the direct CP invariance conditions are $\langle \mathcal{A}_{f\bar{f}} \rangle = 0$ and $C_f = -C_{\bar{f}}$. Note that C_f and $C_{\bar{f}}$ are typically non-zero; *e.g.*, for a flavour-specific final state, $\bar{A}_f = A_{\bar{f}} = 0$ ($A_f = \bar{A}_{\bar{f}} = 0$), they take the values $C_f = -C_{\bar{f}} = 1$ ($C_f = -C_{\bar{f}} = -1$).

The coefficients of the sine terms contain information about the weak phase. In the case that each decay amplitude contains only a single weak phase (*i.e.*, no direct CP violation), these terms can be written

$$S_f = \frac{-2|A_f||\bar{A}_f|\sin(\phi_{\text{mix}} + \phi_{\text{dec}} - \delta_f)}{|A_f|^2 + |\bar{A}_f|^2} \quad \text{and} \quad S_{\bar{f}} = \frac{-2|A_{\bar{f}}||\bar{A}_{\bar{f}}|\sin(\phi_{\text{mix}} + \phi_{\text{dec}} + \delta_f)}{|A_{\bar{f}}|^2 + |\bar{A}_{\bar{f}}|^2}, \quad (124)$$

where δ_f is the strong phase difference between the decay amplitudes. If there is no CP violation, the condition $S_f = -S_{\bar{f}}$ holds. If decay amplitudes with different weak and strong phases contribute, no clean interpretation of S_f and $S_{\bar{f}}$ is possible.

Since two of the CP invariance conditions are $C_f = -C_{\bar{f}}$ and $S_f = -S_{\bar{f}}$, there is motivation for a rotation of the parameters:

$$S_{f\bar{f}} = \frac{S_f + S_{\bar{f}}}{2}, \quad \Delta S_{f\bar{f}} = \frac{S_f - S_{\bar{f}}}{2}, \quad C_{f\bar{f}} = \frac{C_f + C_{\bar{f}}}{2}, \quad \Delta C_{f\bar{f}} = \frac{C_f - C_{\bar{f}}}{2}. \quad (125)$$

With these parameters, the CP invariance conditions become $S_{f\bar{f}} = 0$ and $C_{f\bar{f}} = 0$. The parameter $\Delta C_{f\bar{f}}$ gives a measure of the ‘‘flavour-specificity’’ of the decay: $\Delta C_{f\bar{f}} = \pm 1$ corresponds to a completely flavour-specific decay, in which no interference between decays with and without mixing can occur, while $\Delta C_{f\bar{f}} = 0$ results in maximum sensitivity to mixing-induced CP violation. The parameter $\Delta S_{f\bar{f}}$ is related to the strong phase difference between the decay amplitudes of B^0 to f and to \bar{f} . We note that the observables of Eq. (125) exhibit experimental correlations (typically of $\sim 20\%$, depending on the tagging purity, and other effects) between $S_{f\bar{f}}$ and $\Delta S_{f\bar{f}}$, and between $C_{f\bar{f}}$ and $\Delta C_{f\bar{f}}$. On the other hand, the final state specific observables of Eq. (116) tend to have low correlations.

Alternatively, if we recall that the CP invariance conditions at the decay amplitude level are $A_f = \bar{A}_{\bar{f}}$ and $A_{\bar{f}} = \bar{A}_f$, we are led to consider the parameters [225]

$$\mathcal{A}_{f\bar{f}} = \frac{|\bar{A}_{\bar{f}}|^2 - |A_f|^2}{|\bar{A}_{\bar{f}}|^2 + |A_f|^2} \quad \text{and} \quad \mathcal{A}_{\bar{f}f} = \frac{|\bar{A}_f|^2 - |A_{\bar{f}}|^2}{|\bar{A}_f|^2 + |A_{\bar{f}}|^2}. \quad (126)$$

These are sometimes considered more physically intuitive parameters since they characterise direct CP violation in decays with particular topologies. For example, in the case of $B^0 \rightarrow \rho^\pm \pi^\mp$ (choosing $f = \rho^+ \pi^-$ and $\bar{f} = \rho^- \pi^+$), $\mathcal{A}_{f\bar{f}}$ (also denoted $\mathcal{A}_{\rho\pi}^{+-}$) parametrises direct CP violation in decays in which the produced ρ meson does not contain the spectator quark, while $\mathcal{A}_{\bar{f}f}$ (also denoted $\mathcal{A}_{\rho\pi}^{-+}$) parametrises direct CP violation in decays in which it does. Note that we have again followed the sign convention that the asymmetry is the difference between the rate

involving a b quark and that involving a \bar{b} quark, *cf.* Eq. (98). Of course, these parameters are not independent of the other sets of parameters given above, and can be written

$$\mathcal{A}_{f\bar{f}} = -\frac{\langle \mathcal{A}_{f\bar{f}} \rangle + C_{f\bar{f}} + \langle \mathcal{A}_{f\bar{f}} \rangle \Delta C_{f\bar{f}}}{1 + \Delta C_{f\bar{f}} + \langle \mathcal{A}_{f\bar{f}} \rangle C_{f\bar{f}}} \quad \text{and} \quad \mathcal{A}_{\bar{f}f} = \frac{-\langle \mathcal{A}_{f\bar{f}} \rangle + C_{f\bar{f}} + \langle \mathcal{A}_{f\bar{f}} \rangle \Delta C_{f\bar{f}}}{-1 + \Delta C_{f\bar{f}} + \langle \mathcal{A}_{f\bar{f}} \rangle C_{f\bar{f}}}. \quad (127)$$

They usually exhibit strong correlations.

We now consider the various notations which have been used in experimental studies of time-dependent CP asymmetries in decays to non- CP eigenstates.

$B^0 \rightarrow D^{*\pm} D^\mp$

The $(\langle \mathcal{A}_{f\bar{f}} \rangle, C_f, S_f, C_{\bar{f}}, S_{\bar{f}})$, set of parameters was used in early publications by both *BABAR* [226] and *Belle* [227] (albeit with slightly different notations) in the $D^{*\pm} D^\mp$ system ($f = D^{*+} D^-$, $\bar{f} = D^{*-} D^+$). In their most recent paper on this topic *Belle* [228] instead used the parametrisation $(A_{D^*D}, S_{D^*D}, \Delta S_{D^*D}, C_{D^*D}, \Delta C_{D^*D})$, while *BABAR* [204] give results in both sets of parameters. We therefore use the $(A_{D^*D}, S_{D^*D}, \Delta S_{D^*D}, C_{D^*D}, \Delta C_{D^*D})$ set.

$B^0 \rightarrow \rho^\pm \pi^\mp$

In the $\rho^\pm \pi^\mp$ system, the $(\langle \mathcal{A}_{f\bar{f}} \rangle, C_{f\bar{f}}, S_{f\bar{f}}, \Delta C_{f\bar{f}}, \Delta S_{f\bar{f}})$ set of parameters has been used originally by *BABAR* [229] and *Belle* [230], in the Q2B approximation; the exact names³² used in this case are $(\mathcal{A}_{CP}^{\rho\pi}, C_{\rho\pi}, S_{\rho\pi}, \Delta C_{\rho\pi}, \Delta S_{\rho\pi})$, and these names are also used in this document.

Since $\rho^\pm \pi^\mp$ is reconstructed in the final state $\pi^+ \pi^- \pi^0$, the interference between the ρ resonances can provide additional information about the phases (see Sec. 4.2.5). Both *BABAR* [222] and *Belle* [223, 224] have performed time-dependent Dalitz plot analyses, from which the weak phase α is directly extracted. In such an analysis, the measured Q2B parameters are also naturally corrected for interference effects. See Sec. 4.2.5.

$B^0 \rightarrow D^\pm \pi^\mp, D^{*\pm} \pi^\mp, D^\pm \rho^\mp$

Time-dependent CP analyses have also been performed for the final states $D^\pm \pi^\mp$, $D^{*\pm} \pi^\mp$ and $D^\pm \rho^\mp$. In these theoretically clean cases, no penguin contributions are possible, so there is no direct CP violation. Furthermore, due to the smallness of the ratio of the magnitudes of the suppressed ($b \rightarrow u$) and favoured ($b \rightarrow c$) amplitudes (denoted R_f), to a very good approximation, $C_f = -C_{\bar{f}} = 1$ (using $f = D^{(*)-} h^+$, $\bar{f} = D^{(*)+} h^-$, $h = \pi, \rho$), and the coefficients of the sine terms are given by

$$S_f = -2R_f \sin(\phi_{\text{mix}} + \phi_{\text{dec}} - \delta_f) \quad \text{and} \quad S_{\bar{f}} = -2R_f \sin(\phi_{\text{mix}} + \phi_{\text{dec}} + \delta_f). \quad (128)$$

Thus weak phase information can be cleanly obtained from measurements of S_f and $S_{\bar{f}}$, although external information on at least one of R_f or δ_f is necessary. (Note that $\phi_{\text{mix}} + \phi_{\text{dec}} = 2\beta + \gamma$ for all the decay modes in question, while R_f and δ_f depend on the decay mode.)

Again, different notations have been used in the literature. *BABAR* [231, 232] defines the time-dependent probability function by

$$f^\pm(\eta, \Delta t) = \frac{e^{-|\Delta t|/\tau}}{4\tau} [1 \mp S_\zeta \sin(\Delta m \Delta t) \mp \eta C_\zeta \cos(\Delta m \Delta t)], \quad (129)$$

³² *BABAR* has used the notations $A_{CP}^{\rho\pi}$ [229] and $\mathcal{A}_{\rho\pi}$ [222] in place of $\mathcal{A}_{CP}^{\rho\pi}$.

Table 23: Conversion between the various notations used for CP violation parameters in the $D^\pm\pi^\mp$, $D^{*\pm}\pi^\mp$ and $D^\pm\rho^\mp$ systems. The b_i terms used by *BABAR* have been neglected. Recall that $(\alpha, \beta, \gamma) = (\phi_2, \phi_1, \phi_3)$.

	<i>BABAR</i>	Belle partial rec.	Belle full rec.
$S_{D^+\pi^-}$	$-S_- = -(a + c_i)$	N/A	$2R_{D\pi} \sin(2\phi_1 + \phi_3 + \delta_{D\pi})$
$S_{D^-\pi^+}$	$-S_+ = -(a - c_i)$	N/A	$2R_{D\pi} \sin(2\phi_1 + \phi_3 - \delta_{D\pi})$
$S_{D^{*+}\pi^-}$	$-S_- = -(a + c_i)$	S^+	$-2R_{D^*\pi} \sin(2\phi_1 + \phi_3 + \delta_{D^*\pi})$
$S_{D^{*-}\pi^+}$	$-S_+ = -(a - c_i)$	S^-	$-2R_{D^*\pi} \sin(2\phi_1 + \phi_3 - \delta_{D^*\pi})$
$S_{D^+\rho^-}$	$-S_- = -(a + c_i)$	N/A	N/A
$S_{D^-\rho^+}$	$-S_+ = -(a - c_i)$	N/A	N/A

where the upper (lower) sign corresponds to the tagging meson being a B^0 (\bar{B}^0). [Note here that a tagging B^0 (\bar{B}^0) corresponds to $-S_\zeta$ ($+S_\zeta$).] The parameters η and ζ take the values $+1$ and -1 (-1 and -1) when the final state is, *e.g.*, $D^-\pi^+$ ($D^+\pi^-$). However, in the fit, the substitutions $C_\zeta = 1$ and $S_\zeta = a \mp \eta b_i - \eta c_i$ are made.³³ [Note that, neglecting b terms, $S_+ = a - c$ and $S_- = a + c$, so that $a = (S_+ + S_-)/2$, $c = (S_- - S_+)/2$, in analogy to the parameters of Eq. (125).] The subscript i denotes the tagging category. These are motivated by the possibility of CP violation on the tag side [233], which is absent for semileptonic B decays (mostly lepton tags). The parameter a is not affected by tag side CP violation. The parameter b only depends on tag side CP violation parameters and is not directly useful for determining UT angles. A clean interpretation of the c parameter is only possible for lepton-tagged events, so the *BABAR* measurements report c measured with those events only.

The parameters used by Belle in the analysis using partially reconstructed B decays [234], are similar to the S_ζ parameters defined above. However, in the Belle convention, a tagging B^0 corresponds to a $+$ sign in front of the sine coefficient; furthermore the correspondence between the super/subscript and the final state is opposite, so that S_\pm (*BABAR*) = $-S^\mp$ (Belle). In this analysis, only lepton tags are used, so there is no effect from tag side CP violation. In the Belle analysis using fully reconstructed B decays [235], this effect is measured and taken into account using $D^*l\nu$ decays; in neither Belle analysis are the a , b and c parameters used. In the latter case, the measured parameters are $2R_{D^{(*)}\pi} \sin(2\phi_1 + \phi_3 \pm \delta_{D^{(*)}\pi})$; the definition is such that S^\pm (Belle) = $-2R_{D^*\pi} \sin(2\phi_1 + \phi_3 \pm \delta_{D^*\pi})$. However, the definition includes an angular momentum factor $(-1)^L$ [236], and so for the results in the $D\pi$ system, there is an additional factor of -1 in the conversion.

Explicitly, the conversion then reads as given in Table 23, where we have neglected the b_i terms used by *BABAR* (which are zero in the absence of tag side CP violation). For the averages in this document, we use the a and c parameters, and give the explicit translations used in Table 24. It is to be fervently hoped that the experiments will converge on a common notation in future.

Time-dependent asymmetries in radiative B decays

As a special case of decays to non- CP eigenstates, let us consider radiative B decays. Here,

³³ The subscript i denotes tagging category.

Table 24: Translations used to convert the parameters measured by Belle to the parameters used for averaging in this document. The angular momentum factor L is -1 for $D^*\pi$ and $+1$ for $D\pi$. Recall that $(\alpha, \beta, \gamma) = (\phi_2, \phi_1, \phi_3)$.

$D^*\pi$ partial rec.		$D^{(*)}\pi$ full rec.
a	$-(S^+ + S^-)$	$\frac{1}{2}(-1)^{L+1} (2R_{D^{(*)}\pi} \sin(2\phi_1 + \phi_3 + \delta_{D^{(*)}\pi}) + 2R_{D^{(*)}\pi} \sin(2\phi_1 + \phi_3 - \delta_{D^{(*)}\pi}))$
c	$-(S^+ - S^-)$	$\frac{1}{2}(-1)^{L+1} (2R_{D^{(*)}\pi} \sin(2\phi_1 + \phi_3 + \delta_{D^{(*)}\pi}) - 2R_{D^{(*)}\pi} \sin(2\phi_1 + \phi_3 - \delta_{D^{(*)}\pi}))$

the emitted photon has a distinct helicity, which is in principle observable, but in practise is not usually measured. Thus the measured time-dependent decay rates are given by [237, 238]

$$\begin{aligned} \Gamma_{\bar{B}^0 \rightarrow X\gamma}(\Delta t) &= \Gamma_{\bar{B}^0 \rightarrow X\gamma_L}(\Delta t) + \Gamma_{\bar{B}^0 \rightarrow X\gamma_R}(\Delta t) \\ &= \frac{e^{-|\Delta t|/\tau(B^0)}}{4\tau(B^0)} \{1 + (S_L + S_R) \sin(\Delta m \Delta t) - (C_L + C_R) \cos(\Delta m \Delta t)\}, \end{aligned} \quad (130)$$

$$\begin{aligned} \Gamma_{B^0 \rightarrow X\gamma}(\Delta t) &= \Gamma_{B^0 \rightarrow X\gamma_L}(\Delta t) + \Gamma_{B^0 \rightarrow X\gamma_R}(\Delta t) \\ &= \frac{e^{-|\Delta t|/\tau(B^0)}}{4\tau(B^0)} \{1 - (S_L + S_R) \sin(\Delta m \Delta t) + (C_L + C_R) \cos(\Delta m \Delta t)\}, \end{aligned} \quad (131)$$

where in place of the subscripts f and \bar{f} we have used L and R to indicate the photon helicity. In order for interference between decays with and without B^0 - \bar{B}^0 mixing to occur, the X system must not be flavour-specific, *e.g.*, in case of $B^0 \rightarrow K^{*0}\gamma$, the final state must be $K_s^0\pi^0\gamma$. The sign of the sine term depends on the C eigenvalue of the X system. At leading order, the photons from $b \rightarrow q\gamma$ ($\bar{b} \rightarrow \bar{q}\gamma$) are predominantly left (right) polarised, with corrections of order m_q/m_b , thus interference effects are suppressed. Higher order effects can lead to corrections of order Λ_{QCD}/m_b [239, 240], though explicit calculations indicate such corrections are small for exclusive final states [241, 242]. The predicted smallness of the S terms in the Standard Model results in sensitivity to new physics contributions.

4.2.7 Asymmetries in $B \rightarrow D^{(*)}K^{(*)}$ decays

CP asymmetries in $B \rightarrow D^{(*)}K^{(*)}$ decays are sensitive to γ . The neutral $D^{(*)}$ meson produced is an admixture of $D^{(*)0}$ (produced by a $b \rightarrow c$ transition) and $\bar{D}^{(*)0}$ (produced by a colour-suppressed $b \rightarrow u$ transition) states. If the final state is chosen so that both $D^{(*)0}$ and $\bar{D}^{(*)0}$ can contribute, the two amplitudes interfere, and the resulting observables are sensitive to γ , the relative weak phase between the two B decay amplitudes [243]. Various methods have been proposed to exploit this interference, including those where the neutral D meson is reconstructed as a CP eigenstate (GLW) [244, 245], in a suppressed final state (ADS) [246, 247], or in a self-conjugate three-body final state, such as $K_s^0\pi^+\pi^-$ (Dalitz) [248, 249]. It should be emphasised that while each method differs in the choice of D decay, they are all sensitive to the same parameters of the B decay, and can be considered as variations of the same technique.

Consider the case of $B^\mp \rightarrow DK^\mp$, with D decaying to a final state f , which is accessible to both D^0 and \bar{D}^0 . We can write the decay rates for B^- and B^+ (Γ_{\mp}), the charge averaged rate

($\Gamma = (\Gamma_- + \Gamma_+)/2$) and the charge asymmetry ($\mathcal{A} = (\Gamma_- - \Gamma_+)/(\Gamma_- + \Gamma_+)$, see Eq. (98)) as

$$\Gamma_{\mp} \propto r_B^2 + r_D^2 + 2r_B r_D \cos(\delta_B + \delta_D \mp \gamma), \quad (132)$$

$$\Gamma \propto r_B^2 + r_D^2 + 2r_B r_D \cos(\delta_B + \delta_D) \cos(\gamma), \quad (133)$$

$$\mathcal{A} = \frac{2r_B r_D \sin(\delta_B + \delta_D) \sin(\gamma)}{r_B^2 + r_D^2 + 2r_B r_D \cos(\delta_B + \delta_D) \cos(\gamma)}, \quad (134)$$

where the ratio of B decay amplitudes³⁴ is usually defined to be less than one,

$$r_B = \frac{|A(B^- \rightarrow \bar{D}^0 K^-)|}{|A(B^- \rightarrow D^0 K^-)|}, \quad (135)$$

and the ratio of D decay amplitudes is correspondingly defined by

$$r_D = \frac{|A(D^0 \rightarrow f)|}{|A(\bar{D}^0 \rightarrow f)|}. \quad (136)$$

The strong phase differences between the B and D decay amplitudes are given by δ_B and δ_D , respectively. The values of r_D and δ_D depend on the final state f : for the GLW analysis, $r_D = 1$ and δ_D is trivial (either zero or π), in the Dalitz plot analysis r_D and δ_D vary across the Dalitz plot, and depend on the D decay model used, for the ADS analysis, the values of r_D and δ_D are not trivial.

Note that, for given values of r_B and r_D , the maximum size of \mathcal{A} (at $\sin(\delta_B + \delta_D) = 1$) is $2r_B r_D \sin(\gamma) / (r_B^2 + r_D^2)$. Thus even for D decay modes with small r_D , large asymmetries, and hence sensitivity to γ , may occur for B decay modes with similar values of r_B . For this reason, the ADS analysis of the decay $B^\mp \rightarrow D\pi^\mp$ is also of interest.

In the GLW analysis, the measured quantities are the partial rate asymmetry, and the charge averaged rate, which are measured both for CP -even and CP -odd D decays. The former is defined as

$$R_{CP} = \frac{2\Gamma(B^- \rightarrow D_{CP}K^-)}{\Gamma(B^- \rightarrow D^0K^-)}. \quad (137)$$

It is experimentally convenient to measure R_{CP} using a double ratio,

$$R_{CP} = \frac{\Gamma(B^- \rightarrow D_{CP}K^-) / \Gamma(B^- \rightarrow D^0K^-)}{\Gamma(B^- \rightarrow D_{CP}\pi^-) / \Gamma(B^- \rightarrow D^0\pi^-)} \quad (138)$$

that is normalised both to the rate for the favoured $D^0 \rightarrow K^-\pi^+$ decay, and to the equivalent quantities for $B^- \rightarrow D\pi^-$ decays (charge conjugate modes are implicitly included in Eq. (137) and (138)). In this way the constant of proportionality drops out of Eq. (133). Eq. (138) is exact in the limit that the contribution of the $b \rightarrow u$ decay amplitude to $B^- \rightarrow D\pi^-$ vanishes and when the flavour-specific rates $\Gamma(B^- \rightarrow D^0 h^-)$ ($h = \pi, K$) are determined using appropriately flavour-specific D decays. In reality, the decay $D \rightarrow K\pi$ is invariably used, leading to a small source of systematic uncertainty. The direct CP asymmetry is defined as

$$A_{CP} = \frac{\Gamma(B^- \rightarrow D_{CP}K^-) - \Gamma(B^+ \rightarrow D_{CP}K^+)}{\Gamma(B^- \rightarrow D_{CP}K^-) + \Gamma(B^+ \rightarrow D_{CP}K^+)}. \quad (139)$$

³⁴ Note that here we use the notation r_B to denote the ratio of B decay amplitudes, whereas in Sec. 4.2.6 we used, *e.g.*, $R_{D\pi}$, for a rather similar quantity. The reason is that here we need to be concerned also with D decay amplitudes, and so it is convenient to use the subscript to denote the decaying particle. Hopefully, using r in place of R will help reduce potential confusion.

For the ADS analysis, using a suppressed $D \rightarrow f$ decay, the measured quantities are again the partial rate asymmetry, and the charge averaged rate. In this case it is sufficient to measure the rate in a single ratio (normalised to the favoured $D \rightarrow \bar{f}$ decay) since detection systematics cancel naturally; the observed quantity is then

$$R_{\text{ADS}} = \frac{\Gamma(B^- \rightarrow [f]_D K^-)}{\Gamma(B^- \rightarrow [\bar{f}]_D K^-)}, \quad (140)$$

where inclusion of charge conjugate modes is implied. The direct CP asymmetry is defined as

$$A_{\text{ADS}} = \frac{\Gamma(B^- \rightarrow [f]_D K^-) - \Gamma(B^+ \rightarrow [f]_D K^+)}{\Gamma(B^- \rightarrow [f]_D K^-) + \Gamma(B^+ \rightarrow [f]_D K^+)}. \quad (141)$$

Since the uncertainty of A_{ADS} depends on the central value of R_{ADS} , for some statistical treatments it is preferable to use an alternative pair of parameters (as discussed in Refs. [250, 251])

$$R_- = \frac{\Gamma(B^- \rightarrow [f]_D K^-)}{\Gamma(B^- \rightarrow [\bar{f}]_D K^-)} \quad R_+ = \frac{\Gamma(B^+ \rightarrow [\bar{f}]_D K^+)}{\Gamma(B^+ \rightarrow [f]_D K^+)}, \quad (142)$$

where there is no inclusion of charge conjugated processes. We use the $(R_{\text{ADS}}, A_{\text{ADS}})$ set in our compilation.

In the ADS analysis, there are an additional two unknowns (r_D and δ_D) compared to the GLW case. However, the value of r_D can be measured using decays of D mesons of known flavour, and δ_D can be measured from interference effects in decays of quantum-correlated $D\bar{D}$ pairs produced at the $\psi(3770)$ resonance. In fact, the most precise information on both r_D and δ_D currently comes from global fits on charm mixing parameters, as discussed in Sec. 8.1.

In the Dalitz plot analysis, once a model is assumed for the D decay, which gives the values of r_D and δ_D across the Dalitz plot, it is possible to perform a simultaneous fit to the B^+ and B^- samples and directly extract γ , r_B and δ_B . However, the uncertainties on the phases depend approximately inversely on r_B . Furthermore, r_B is positive definite (and small), and therefore tends to be overestimated, which can lead to an underestimation of the uncertainty. Some statistical treatment is necessary to correct for this bias. An alternative approach is to extract from the data the ‘‘Cartesian’’ variables

$$(x_{\pm}, y_{\pm}) = (\text{Re}(r_B e^{i(\delta_B \pm \gamma)}), \text{Im}(r_B e^{i(\delta_B \pm \gamma)})) = (r_B \cos(\delta_B \pm \gamma), r_B \sin(\delta_B \pm \gamma)). \quad (143)$$

These are (a) approximately statistically uncorrelated and (b) almost Gaussian. The pairs of variables (x_{\pm}, y_{\pm}) can be extracted from independent fits of the B^{\pm} data samples. Use of these variables makes the combination of results much simpler.

However, if the Dalitz plot is effectively dominated by one CP state, there will be additional sensitivity to γ in the numbers of events in the B^{\pm} data samples. This can be taken into account in various ways. One possibility is to extract GLW-like variables in addition to the (x_{\pm}, y_{\pm}) parameters. An alternative proceeds by defining $z_{\pm} = x_{\pm} + iy_{\pm}$ and $x_0 = -\int \text{Re}[f(s_1, s_2)f^*(s_2, s_1)] ds_1 ds_2$, where s_1, s_2 are the coordinates of invariant mass squared that define the Dalitz plot and f is the complex amplitude for D decay as a function of the Dalitz plot coordinates.³⁵ The fitted parameters $(\rho^{\pm}, \theta^{\pm})$ are then defined by

$$\rho^{\pm} e^{i\theta^{\pm}} = z_{\pm} - x_0. \quad (144)$$

³⁵ The x_0 parameter is closely related to the c_i parameters of the model dependent Dalitz plot analysis [248, 252, 253], and the coherence factor of inclusive ADS-type analyses [254], integrated over the entire Dalitz plot.

Note that the yields of B^\pm decays are proportional to $1 + (\rho^\pm)^2 - (x_0)^2$. This choice of variables has been used by *BABAR* in the analysis of $B^\mp \rightarrow DK^\mp$ with $D \rightarrow \pi^+\pi^-\pi^0$ [255]; for this D decay, $x_0 = 0.850$.

The relations between the measured quantities and the underlying parameters are summarised in Table 25. Note carefully that the hadronic factors r_B and δ_B are different, in general, for each B decay mode.

Table 25: Summary of relations between measured and physical parameters in GLW, ADS and Dalitz analyses of $B \rightarrow D^{(*)}K^{(*)}$.

GLW analysis	
$R_{CP\pm}$	$1 + r_B^2 \pm 2r_B \cos(\delta_B) \cos(\gamma)$
$A_{CP\pm}$	$\pm 2r_B \sin(\delta_B) \sin(\gamma) / R_{CP\pm}$
ADS analysis	
R_{ADS}	$r_B^2 + r_D^2 + 2r_B r_D \cos(\delta_B + \delta_D) \cos(\gamma)$
A_{ADS}	$2r_B r_D \sin(\delta_B + \delta_D) \sin(\gamma) / R_{\text{ADS}}$
Dalitz analysis ($D \rightarrow K_S^0 \pi^+ \pi^-$)	
x_\pm	$r_B \cos(\delta_B \pm \gamma)$
y_\pm	$r_B \sin(\delta_B \pm \gamma)$
Dalitz analysis ($D \rightarrow \pi^+ \pi^- \pi^0$)	
ρ^\pm	$ z_\pm - x_0 $
θ^\pm	$\tan^{-1}(\text{Im}(z_\pm) / (\text{Re}(z_\pm) - x_0))$

Results from model-dependent Dalitz plot fits tend to suffer from significant uncertainties due to the choice of model to describe hadronic effects. This can be obviated by a model-independent analysis, in which the Dalitz plot is binned [248, 252, 253]. It is then necessary to gain information on effective parameters which describe the average strong phase difference between a certain bin and its conjugate (found by reflecting in the symmetry axis of the Dalitz plot³⁶). Such information can be obtained from interference effects in decays of quantum-correlated $D\bar{D}$ pairs produced at the $\psi(3770)$ resonance.

4.3 Common inputs and error treatment

The common inputs used for rescaling are listed in Table 26. The B^0 lifetime ($\tau(B^0)$), mixing parameter (Δm_d) and relative width difference ($\Delta\Gamma_d/\Gamma_d$) averages are provided by the HFAG Lifetimes and Oscillations subgroup (Sec. 3). The fraction of the perpendicularly polarised component ($|A_\perp|^2$) in $B \rightarrow J/\psi K^*(892)$ decays, which determines the CP composition in these decays, is averaged from results by *BABAR* [256], Belle [257], CDF [258], D0 [77] and LHCb [259]. See also HFAG B to Charm Decay Parameters subgroup (Sec. 6).

At present, we only rescale to a common set of input parameters for modes with reasonably small statistical errors ($b \rightarrow c\bar{c}s$ transitions). Correlated systematic errors are taken into account in these modes as well. For all other modes, the effect of such a procedure is currently negligible.

³⁶Here we restrict the discussion to three-body self conjugate final states such as $K_S^0 \pi^+ \pi^-$ and $K_S^0 K^+ K^-$, though it can be extended to other modes, including four-body final states.

Table 26: Common inputs used in calculating the averages.

$\tau(B^0)$ (ps)	1.519 ± 0.007
Δm_d (ps^{-1})	0.507 ± 0.004
$\Delta\Gamma_d/\Gamma_d$	0.015 ± 0.018
$ A_\perp ^2(J/\psi K^*)$	0.213 ± 0.008

As explained in Sec. 1, we do not apply a rescaling factor on the error of an average that has $\chi^2/\text{dof} > 1$ (unlike the procedure currently used by the PDG [5]). We provide a confidence level of the fit so that one can know the consistency of the measurements included in the average, and attach comments in case some care needs to be taken in the interpretation. Note that, in general, results obtained from data samples with low statistics will exhibit some non-Gaussian behaviour. We average measurements with asymmetric errors using the PDG [5] prescription. In cases where several measurements are correlated (*e.g.* S_f and C_f in measurements of time-dependent CP violation in B decays to a particular CP eigenstate) we take these into account in the averaging procedure if the uncertainties are sufficiently Gaussian. For measurements where one error is given, it represents the total error, where statistical and systematic uncertainties have been added in quadrature. If two errors are given, the first is statistical and the second systematic. If more than two errors are given, the origin of the additional uncertainty will be explained in the text.

4.4 Time-dependent asymmetries in $b \rightarrow c\bar{c}s$ transitions

4.4.1 Time-dependent CP asymmetries in $b \rightarrow c\bar{c}s$ decays to CP eigenstates

In the Standard Model, the time-dependent parameters for $b \rightarrow c\bar{c}s$ transitions are predicted to be: $S_{b \rightarrow c\bar{c}s} = -\eta \sin(2\beta)$, $C_{b \rightarrow c\bar{c}s} = 0$ to very good accuracy. The averages for $-\eta S_{b \rightarrow c\bar{c}s}$ and $C_{b \rightarrow c\bar{c}s}$ are provided in Table 27. The averages for $-\eta S_{b \rightarrow c\bar{c}s}$ are shown in Fig. 13.

Both *BABAR* and Belle have used the $\eta = -1$ modes $J/\psi K_S^0$, $\psi(2S)K_S^0$, $\chi_{c1}K_S^0$ and $\eta_c K_S^0$, as well as $J/\psi K_L^0$, which has $\eta = +1$ and $J/\psi K^{*0}(892)$, which is found to have η close to $+1$ based on the measurement of $|A_\perp|$ (see Sec. 4.3). The most recent Belle result does not use $\eta_c K_S^0$ or $J/\psi K^{*0}(892)$. ALEPH, OPAL, CDF and LHCb have used only the $J/\psi K_S^0$ final state. *BABAR* have also determined the CP -violation parameters of the $B^0 \rightarrow \chi_{c0} K_S^0$ decay from the time-dependent Dalitz plot analysis of $B^0 \rightarrow \pi^+ \pi^- K_S^0$ (see subsection 4.6.2). In addition, Belle have performed a measurement with data accumulated at the $\Upsilon(5S)$ resonance, using the $J/\psi K_S^0$ final state – this involves a different flavour tagging method compared to the measurements performed with data accumulated at the $\Upsilon(4S)$ resonance. A breakdown of results in each charmonium-kaon final state is given in Table 28.

Table 27: $S_{b \rightarrow c\bar{c}s}$ and $C_{b \rightarrow c\bar{c}s}$.

Experiment		Sample size	$-\eta S_{b \rightarrow c\bar{c}s}$	$C_{b \rightarrow c\bar{c}s}$
<i>BABAR</i>	[260]	$N(B\bar{B}) = 465\text{M}$	$0.687 \pm 0.028 \pm 0.012$	$0.024 \pm 0.020 \pm 0.016$
<i>BABAR</i> $\chi_{c0} K_S^0$	[215]	$N(B\bar{B}) = 383\text{M}$	$0.69 \pm 0.52 \pm 0.04 \pm 0.07$	$-0.29^{+0.53}_{-0.44} \pm 0.03 \pm 0.05$
<i>BABAR</i> $J/\psi K_S^0$ (*)	[261]	$N(B\bar{B}) = 88\text{M}$	$1.56 \pm 0.42 \pm 0.21$	–
Belle	[262]	$N(B\bar{B}) = 722\text{M}$	$0.667 \pm 0.023 \pm 0.012$	$-0.006 \pm 0.016 \pm 0.012$
B factory average			0.679 ± 0.020	0.005 ± 0.017
Confidence level			0.28	0.47
ALEPH	[263]	–	$0.84^{+0.82}_{-1.04} \pm 0.16$	–
OPAL	[264]	–	$3.2^{+1.8}_{-2.0} \pm 0.5$	–
CDF	[265]	–	$0.79^{+0.41}_{-0.44}$	–
LHCb	[266]	0.035 fb^{-1}	$0.53^{+0.28}_{-0.29} \pm 0.05$	–
Belle $\Upsilon(5S)$	[267]	121 fb^{-1}	$0.57 \pm 0.58 \pm 0.06$	–
Average			0.679 ± 0.020	0.005 ± 0.017

* This result uses "hadronic and previously unused muonic decays of the J/ψ ". We neglect a small possible correlation of this result with the main *BABAR* result [260] that could be caused by reprocessing of the data.

It should be noted that, while the uncertainty in the average for $-\eta S_{b \rightarrow c\bar{c}s}$ is still limited by statistics, that for $C_{b \rightarrow c\bar{c}s}$ is close to being dominated by systematics. This occurs due to the possible effect of tag side interference on the $C_{b \rightarrow c\bar{c}s}$ measurement, an effect which is correlated between the different experiments. Understanding of this effect may continue to improve in future, allowing the uncertainty to reduce.

From the average for $-\eta S_{b \rightarrow c\bar{c}s}$ above, we obtain the following solutions for β (in $[0, \pi]$):

$$\beta = (21.4 \pm 0.8)^\circ \quad \text{or} \quad \beta = (68.6 \pm 0.8)^\circ \quad (145)$$

In radians, these values are $\beta = (0.375 \pm 0.014)$, $\beta = (1.197 \pm 0.014)$.

Table 28: Breakdown of B factory results on $S_{b \rightarrow c\bar{c}s}$ and $C_{b \rightarrow c\bar{c}s}$.

Mode		$N(B\bar{B})$	$-\eta S_{b \rightarrow c\bar{c}s}$	$C_{b \rightarrow c\bar{c}s}$
<i>BABAR</i>				
$J/\psi K_S^0$	[260]	465M	$0.657 \pm 0.036 \pm 0.012$	$0.026 \pm 0.025 \pm 0.016$
$J/\psi K_L^0$	[260]	465M	$0.694 \pm 0.061 \pm 0.031$	$-0.033 \pm 0.050 \pm 0.027$
$J/\psi K^0$	[260]	465M	$0.666 \pm 0.031 \pm 0.013$	$0.016 \pm 0.023 \pm 0.018$
$\psi(2S)K_S^0$	[260]	465M	$0.897 \pm 0.100 \pm 0.036$	$0.089 \pm 0.076 \pm 0.020$
$\chi_{c1}K_S^0$	[260]	465M	$0.614 \pm 0.160 \pm 0.040$	$0.129 \pm 0.109 \pm 0.025$
$\eta_c K_S^0$	[260]	465M	$0.925 \pm 0.160 \pm 0.057$	$0.080 \pm 0.124 \pm 0.029$
$J/\psi K^{*0}(892)$	[260]	465M	$0.601 \pm 0.239 \pm 0.087$	$0.025 \pm 0.083 \pm 0.054$
All	[260]	465M	$0.687 \pm 0.028 \pm 0.012$	$0.024 \pm 0.020 \pm 0.016$
<i>Belle</i>				
$J/\psi K_S^0$	[262]	722M	$0.670 \pm 0.029 \pm 0.013$	$0.015 \pm 0.021^{+0.023}_{-0.045}$
$J/\psi K_L^0$	[262]	722M	$0.642 \pm 0.047 \pm 0.021$	$-0.019 \pm 0.026^{+0.041}_{-0.017}$
$\psi(2S)K_S^0$	[262]	722M	$0.738 \pm 0.079 \pm 0.036$	$-0.104 \pm 0.055^{+0.027}_{-0.047}$
$\chi_{c1}K_S^0$	[262]	722M	$0.640 \pm 0.117 \pm 0.040$	$0.017 \pm 0.083^{+0.026}_{-0.046}$
All	[262]	722M	$0.667 \pm 0.023 \pm 0.012$	$-0.006 \pm 0.016 \pm 0.012$
Averages				
$J/\psi K_S^0$			0.665 ± 0.024	0.024 ± 0.026
$J/\psi K_L^0$			0.663 ± 0.041	-0.023 ± 0.030
$\psi(2S)K_S^0$			0.807 ± 0.067	-0.009 ± 0.055
$\chi_{c1}K_S^0$			0.632 ± 0.099	0.066 ± 0.074

This result gives a precise constraint on the $(\bar{\rho}, \bar{\eta})$ plane, as shown in Fig. 13. The measurement is in remarkable agreement with other constraints from CP conserving quantities, and with CP violation in the kaon system, in the form of the parameter ϵ_K . Such comparisons have been performed by various phenomenological groups, such as CKMfitter [225] and UTFit [268].

4.4.2 Time-dependent transversity analysis of $B^0 \rightarrow J/\psi K^{*0}$

B meson decays to the vector-vector final state $J/\psi K^{*0}$ are also mediated by the $b \rightarrow c\bar{c}s$ transition. When a final state which is not flavour-specific ($K^{*0} \rightarrow K_S^0 \pi^0$) is used, a time-dependent transversity analysis can be performed allowing sensitivity to both $\sin(2\beta)$ and $\cos(2\beta)$ [269]. Such analyses have been performed by both B factory experiments. In principle, the strong phases between the transversity amplitudes are not uniquely determined by such an analysis, leading to a discrete ambiguity in the sign of $\cos(2\beta)$. The *BABAR* collaboration resolves this ambiguity using the known variation [270] of the P-wave phase (fast) relative to the S-wave phase (slow) with the invariant mass of the $K\pi$ system in the vicinity of the $K^*(892)$ resonance. The result is in agreement with the prediction from s quark helicity conservation, and corresponds to Solution II defined by Suzuki [271]. We use this phase convention for the averages given in Table 29.

At present the results are dominated by large and non-Gaussian statistical errors, and exhibit significant correlations. We perform uncorrelated averages, the interpretation of which has to be done with the greatest care. Nonetheless, it is clear that $\cos(2\beta) > 0$ is preferred by

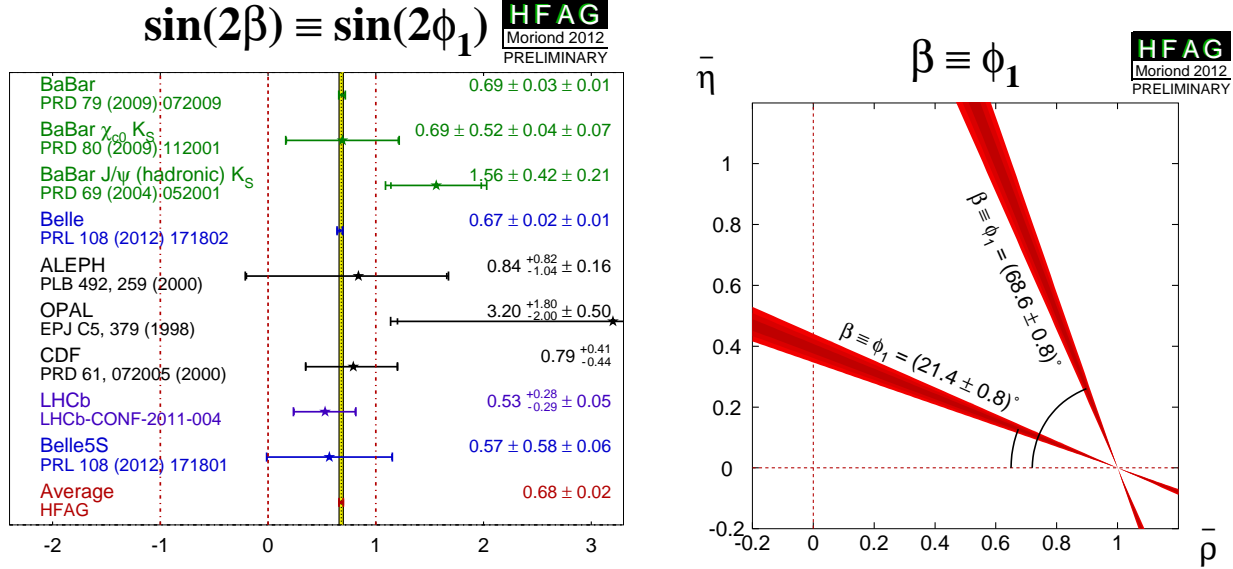


Figure 13: (Left) Average of measurements of $S_{b \rightarrow c\bar{c}s}$. (Right) Constraints on the $(\bar{\rho}, \bar{\eta})$ plane, obtained from the average of $-\eta S_{b \rightarrow c\bar{c}s}$ and Eq. 145.

Table 29: Averages from $B^0 \rightarrow J/\psi K^{*0}$ transversity analyses.

Experiment	$N(B\bar{B})$	$\sin 2\beta$	$\cos 2\beta$	Correlation
BABAR [272]	88M	$-0.10 \pm 0.57 \pm 0.14$	$3.32^{+0.76}_{-0.96} \pm 0.27$	-0.37
Belle [257]	275M	$0.24 \pm 0.31 \pm 0.05$	$0.56 \pm 0.79 \pm 0.11$	0.22
Average		0.16 ± 0.28	1.64 ± 0.62	uncorrelated averages
Confidence level		0.61 (0.5 σ)	0.03 (2.2 σ)	

the experimental data in $J/\psi K^*$. [BABAR [272] find a confidence level for $\cos(2\beta) > 0$ of 89%.]

4.4.3 Time-dependent CP asymmetries in $B^0 \rightarrow D^{*+} D^{*-} K_s^0$ decays

Both BABAR [208] and Belle [209] have performed time-dependent analyses of the $B^0 \rightarrow D^{*+} D^{*-} K_s^0$ decay, to obtain information on the sign of $\cos(2\beta)$. More information can be found in Sec. 4.2.5. The results are shown in Table 30, and Fig. 14.

From the above result and the assumption that $J_{s2} > 0$, BABAR infer that $\cos(2\beta) > 0$ at the 94% confidence level [208].

4.4.4 Time-dependent analysis of $B_s^0 \rightarrow J/\psi \phi$

As described in Sec. 4.2.3, time-dependent analysis of $B_s^0 \rightarrow J/\psi \phi$ probes the CP violating phase of $B_s^0 - \bar{B}_s$ oscillations, ϕ_s . Within the Standard Model, this parameter is predicted to be small.³⁷ The combination of results is performed by the HFAG Lifetimes and Oscillations

³⁷ We make the approximation $\phi_s = 2\beta_s$, where $\phi_s \equiv \arg[-M_{12}/\Gamma_{12}]$ and $2\beta_s \equiv 2 \arg[-(V_{ts}V_{tb}^*)/(V_{cs}V_{cb}^*)]$ (see Section 4.1). This is a reasonable approximation since, although the equality does not hold in the Standard

Table 30: Results from time-dependent analysis of $B^0 \rightarrow D^{*+}D^{*-}K_S^0$.

Experiment	$N(B\bar{B})$	$\frac{J_c}{J_0}$	$\frac{2J_{s1}}{J_0} \sin(2\beta)$	$\frac{2J_{s2}}{J_0} \cos(2\beta)$
BaBar [208]	230M	$0.76 \pm 0.18 \pm 0.07$	$0.10 \pm 0.24 \pm 0.06$	$0.38 \pm 0.24 \pm 0.05$
Belle [209]	449M	$0.60^{+0.25}_{-0.28} \pm 0.08$	$-0.17 \pm 0.42 \pm 0.09$	$-0.23^{+0.43}_{-0.41} \pm 0.13$
Average		0.71 ± 0.16	0.03 ± 0.21	0.24 ± 0.22
Confidence level		0.63 (0.5σ)	0.59 (0.5σ)	0.23 (1.2σ)

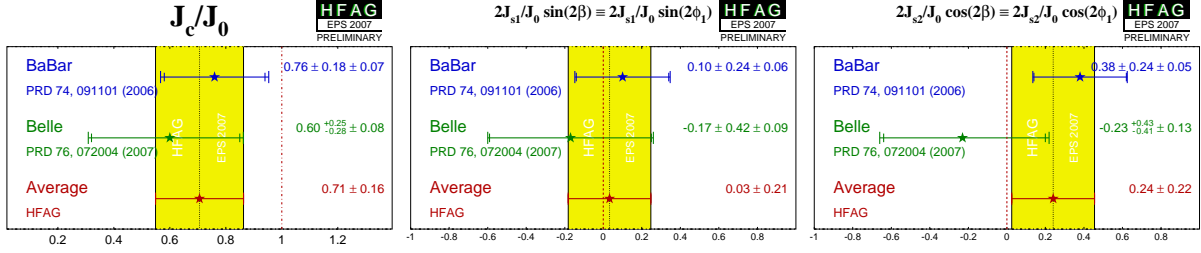


Figure 14: Averages of (left) (J_c/J_0) , (middle) $(2J_{s1}/J_0) \sin(2\beta)$ and (right) $(2J_{s2}/J_0) \cos(2\beta)$ from time-dependent analyses of $B^0 \rightarrow D^{*+}D^{*-}K_S^0$ decays.

group, see Sec. 3.

Model [91], both are much smaller than the current experimental resolution, whereas new physics contributions add a phase ϕ_{NP} to ϕ_s and subtract the same phase from $2\beta_s$, so that the approximation remains valid.

4.5 Time-dependent CP asymmetries in colour-suppressed $b \rightarrow c\bar{u}d$ transitions

Decays of B mesons to final states such as $D\pi^0$ are governed by $b \rightarrow c\bar{u}d$ transitions. If the final state is a CP eigenstate, *e.g.* $D_{CP}\pi^0$, the usual time-dependence formulae are recovered, with the sine coefficient sensitive to $\sin(2\beta)$. Since there is no penguin contribution to these decays, there is even less associated theoretical uncertainty than for $b \rightarrow c\bar{c}s$ decays like $B \rightarrow J/\psi K_s^0$. Such measurements therefore allow to test the Standard Model prediction that the CP violation parameters in $b \rightarrow c\bar{u}d$ transitions are the same as those in $b \rightarrow c\bar{c}s$ [273].

Note that there is an additional contribution from CKM suppressed $b \rightarrow u\bar{c}d$ decays. The effect of this contribution is small, and can be taken into account in the analysis [274, 275].

Results of such an analysis are available from *BABAR* [276]. The decays $B^0 \rightarrow D\pi^0$, $B^0 \rightarrow D\eta$, $B^0 \rightarrow D\omega$, $B^0 \rightarrow D^*\pi^0$ and $B^0 \rightarrow D^*\eta$ are used. The daughter decay $D^* \rightarrow D\pi^0$ is used. The CP -even D decay to K^+K^- is used for all decay modes, with the CP -odd D decay to $K_s^0\omega$ also used in $B^0 \rightarrow D^{(*)}\pi^0$ and the additional CP -odd D decay to $K_s^0\pi^0$ also used in $B^0 \rightarrow D\omega$. Results are presented separately for CP -even and CP -odd $D^{(*)}$ decays (denoted $D_+^{(*)}h^0$ and $D_-^{(*)}h^0$ respectively), and for both combined, with the different CP factors accounted for (denoted $D_{CP}^{(*)}h^0$). The results are summarised in Table 31.

Table 31: Results from analyses of $B^0 \rightarrow D^{(*)}h^0$, $D \rightarrow CP$ eigenstates decays.

Experiment	$N(B\bar{B})$	S_{CP}	C_{CP}	Correlation	
		$D_+^{(*)}h^0$			
<i>BABAR</i>	[276]	383M	$-0.65 \pm 0.26 \pm 0.06$	$-0.33 \pm 0.19 \pm 0.04$	0.04
		$D_-^{(*)}h^0$			
<i>BABAR</i>	[276]	383M	$-0.46 \pm 0.46 \pm 0.13$	$-0.03 \pm 0.28 \pm 0.07$	-0.14
		$D_{CP}^{(*)}h^0$			
<i>BABAR</i>	[276]	383M	$-0.56 \pm 0.23 \pm 0.05$	$-0.23 \pm 0.16 \pm 0.04$	-0.02

When multibody D decays, such as $D \rightarrow K_s^0\pi^+\pi^-$ are used, a time-dependent analysis of the Dalitz plot of the neutral D decay allows a direct determination of the weak phase: 2β . (Equivalently, both $\sin(2\beta)$ and $\cos(2\beta)$ can be measured.) This information allows to resolve the ambiguity in the measurement of 2β from $\sin(2\beta)$ [277].

Results of such analyses are available from both Belle [205] and *BABAR* [206]. The decays $B \rightarrow D\pi^0$, $B \rightarrow D\eta$, $B \rightarrow D\omega$, $B \rightarrow D^*\pi^0$ and $B \rightarrow D^*\eta$ are used. [This collection of states is denoted by $D^{(*)}h^0$.] The daughter decays are $D^* \rightarrow D\pi^0$ and $D \rightarrow K_s^0\pi^+\pi^-$. The results are shown in Table 32, and Fig. 15. Note that *BABAR* quote uncertainties due to the D decay model separately from other systematic errors, while Belle do not.

Again, it is clear that the data prefer $\cos(2\beta) > 0$. Indeed, Belle [205] determine the sign of $\cos(2\phi_1)$ to be positive at 98.3% confidence level, while *BABAR* [206] favour the solution of β with $\cos(2\beta) > 0$ at 87% confidence level. Note, however, that the Belle measurement has strongly non-Gaussian behaviour. Therefore, we perform uncorrelated averages, from which any interpretation has to be done with the greatest care.

Table 32: Averages from $B^0 \rightarrow D^{(*)}h^0$, $D \rightarrow K_S\pi^+\pi^-$ analyses.

Experiment	$N(B\bar{B})$	$\sin 2\beta$	$\cos 2\beta$	$ \lambda $
BABAR [206]	383M	$0.29 \pm 0.34 \pm 0.03 \pm 0.05$	$0.42 \pm 0.49 \pm 0.09 \pm 0.13$	$1.01 \pm 0.08 \pm 0.02$
Belle [205]	386M	$0.78 \pm 0.44 \pm 0.22$	$1.87^{+0.40+0.22}_{-0.53-0.32}$	–
Average		0.45 ± 0.28	1.01 ± 0.40	1.01 ± 0.08
Confidence level		0.59 (0.5σ)	0.12 (1.6σ)	–

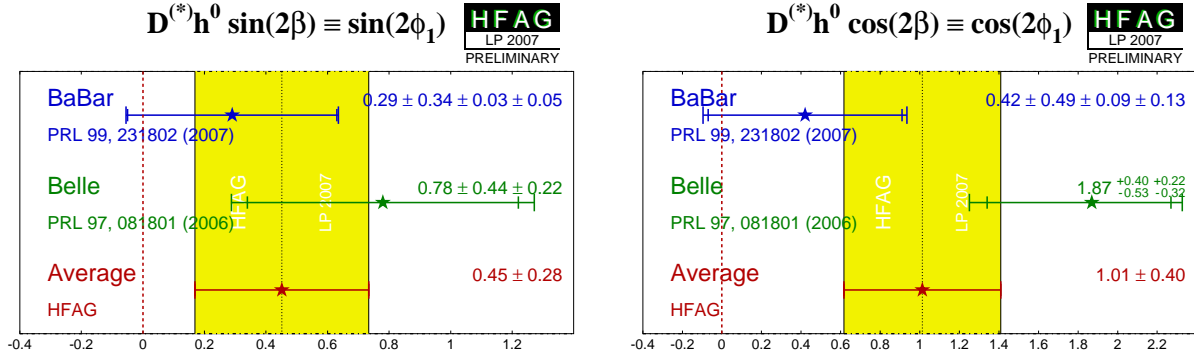


Figure 15: Averages of (left) $\sin(2\beta)$ and (right) $\cos(2\beta)$ measured in colour-suppressed $b \rightarrow c\bar{u}d$ transitions.

4.6 Time-dependent CP asymmetries in charmless $b \rightarrow q\bar{q}s$ transitions

The flavour changing neutral current $b \rightarrow s$ penguin can be mediated by any up-type quark in the loop, and hence the amplitude can be written as

$$\begin{aligned} A_{b \rightarrow s} &= F_u V_{ub} V_{us}^* + F_c V_{cb} V_{cs}^* + F_t V_{tb} V_{ts}^* \\ &= (F_u - F_c) V_{ub} V_{us}^* + (F_t - F_c) V_{tb} V_{ts}^* \\ &= \mathcal{O}(\lambda^4) + \mathcal{O}(\lambda^2) \end{aligned} \quad (146)$$

using the unitarity of the CKM matrix. Therefore, in the Standard Model, this amplitude is dominated by $V_{tb} V_{ts}^*$, and to within a few degrees ($\delta\beta \lesssim 2^\circ$ for $\beta \approx 20^\circ$) the time-dependent parameters can be written³⁸ $S_{b \rightarrow q\bar{q}s} \approx -\eta \sin(2\beta)$, $C_{b \rightarrow q\bar{q}s} \approx 0$, assuming $b \rightarrow s$ penguin contributions only ($q = u, d, s$).

Due to the large virtual mass scales occurring in the penguin loops, additional diagrams from physics beyond the Standard Model, with heavy particles in the loops, may contribute. In general, these contributions will affect the values of $S_{b \rightarrow q\bar{q}s}$ and $C_{b \rightarrow q\bar{q}s}$. A discrepancy between the values of $S_{b \rightarrow c\bar{c}s}$ and $S_{b \rightarrow q\bar{q}s}$ can therefore provide a clean indication of new physics [273, 278–280].

However, there is an additional consideration to take into account. The above argument assumes only the $b \rightarrow s$ penguin contributes to the $b \rightarrow q\bar{q}s$ transition. For $q = s$ this is a good assumption, which neglects only rescattering effects. However, for $q = u$ there is a colour-suppressed $b \rightarrow u$ tree diagram (of order $\mathcal{O}(\lambda^4)$), which has a different weak (and possibly strong) phase. In the case $q = d$, any light neutral meson that is formed from $d\bar{d}$ also has a $u\bar{u}$ component, and so again there is “tree pollution”. The B^0 decays to $\pi^0 K_s^0$, $\rho^0 K_s^0$ and ωK_s^0 belong to this category. The mesons ϕ , f_0 and η' are expected to have predominant $s\bar{s}$ parts, which reduces the relative size of the possible tree pollution. If the inclusive decay $B^0 \rightarrow K^+ K^- K^0$ (excluding ϕK^0) is dominated by a nonresonant three-body transition, an OZI-rule suppressed tree-level diagram can occur through insertion of an $s\bar{s}$ pair. The corresponding penguin-type transition proceeds via insertion of a $u\bar{u}$ pair, which is expected to be favoured over the $s\bar{s}$ insertion by fragmentation models. Neglecting rescattering, the final state $K^0 \bar{K}^0 K^0$ (reconstructed as $K_s^0 K_s^0 K_s^0$) has no tree pollution [281]. Various estimates, using different theoretical approaches, of the values of $\Delta S = S_{b \rightarrow q\bar{q}s} - S_{b \rightarrow c\bar{c}s}$ exist in the literature [282–295]. In general, there is agreement that the modes ϕK^0 , $\eta' K^0$ and $K^0 \bar{K}^0 K^0$ are the cleanest, with values of $|\Delta S|$ at or below the few percent level (ΔS is usually positive).

4.6.1 Time-dependent CP asymmetries: $b \rightarrow q\bar{q}s$ decays to CP eigenstates

The averages for $-\eta S_{b \rightarrow q\bar{q}s}$ and $C_{b \rightarrow q\bar{q}s}$ can be found in Table 33, and are shown in Figs. 16, 17 and 18. Results from both *BABAR* and *Belle* are averaged for the modes $\eta' K^0$ (K^0 indicates that both K_s^0 and K_L^0 are used) $K_s^0 K_s^0 K_s^0$, $\pi^0 K_s^{039}$ and ωK_s^0 . Results on ϕK_s^0 and $K^+ K^- K_s^0$ (implicitly excluding ϕK_s^0 and $f_0 K_s^0$) are taken from time-dependent Dalitz plot analyses of

³⁸ The presence of a small ($\mathcal{O}(\lambda^2)$) weak phase in the dominant amplitude of the s penguin decays introduces a phase shift given by $S_{b \rightarrow q\bar{q}s} = -\eta \sin(2\beta) \cdot (1 + \Delta)$. Using the CKMfitter results for the Wolfenstein parameters [225], one finds: $\Delta \simeq 0.033$, which corresponds to a shift of 2β of $+2.1$ degrees. Nonperturbative contributions can alter this result.

³⁹ *Belle* [296] include the $\pi^0 K_L^0$ final state in order to improve the constraint on the direct CP violation parameter; these events cannot be used for time-dependent analysis.

$K^+K^-K_s^0$, results on $\rho^0 K_s^0$, $f_2K_s^0$, $f_XK_s^0$ and $\pi^+\pi^-K_s^0$ nonresonant are taken from time-dependent Dalitz plot analyses of $\pi^+\pi^-K_s^0$ (see subsection 4.6.2). The results on $f_0K_s^0$ are from combinations of both Dalitz plot analyses. *BABAR* also has presented results with the final states $\pi^0\pi^0K_s^0$,⁴⁰ and $\phi K_s^0\pi^0$.

Of these final states, ϕK_s^0 , $\eta'K_s^0$, $\pi^0K_s^0$, $\rho^0K_s^0$, ωK_s^0 and $f_0K_s^0$ have CP eigenvalue $\eta = -1$, while ϕK_L^0 , $\eta'K_L^0$, $K_s^0K_s^0K_s^0$, $f_0K_s^0$, $f_2K_s^0$, $f_XK_s^0$,⁴¹ $\pi^0\pi^0K_s^0$ and $\pi^+\pi^-K_s^0$ nonresonant have $\eta = +1$. The final state $K^+K^-K_s^0$ (with ϕK_s^0 and $f_0K_s^0$ implicitly excluded) is not a CP eigenstate, but the CP -content can be absorbed in the amplitude analysis to allow the determination of a single effective S parameter. (In earlier analyses of the $K^+K^-K^0$ final state, its CP composition was determined using an isospin argument [298] and a moments analysis [299].)

The final state $\phi K_s^0\pi^0$ is also not a CP -eigenstate but its CP -composition can be determined from an angular analysis. Since the angular parameters are common to the $B^0 \rightarrow \phi K_s^0\pi^0$ and $B^0 \rightarrow \phi K^+\pi^-$ decays (because only $K\pi$ resonance contribute), *BABAR* perform a simultaneous analysis of the two final states [304] (see subsection 4.6.3).

It must be noted that Q2B parameters extracted from Dalitz plot analyses are constrained to lie within the physical boundary ($S_{CP}^2 + C_{CP}^2 < 1$) and consequently the obtained errors are highly non-Gaussian when the central value is close to the boundary. This is particularly evident in the *BABAR* results for $B^0 \rightarrow f_0K^0$ with $f_0 \rightarrow \pi^+\pi^-$ [215]. These results must be treated with extreme caution.

As explained above, each of the modes listed in Table 33 has different uncertainties within the Standard Model, and so each may have a different value of $-\eta S_{b \rightarrow q\bar{q}s}$. Therefore, there is no strong motivation to make a combined average over the different modes. We refer to such an average as a “naïve s -penguin average.” It is naïve not only because of the neglect of the theoretical uncertainty, but also since possible correlations of systematic effects between different modes are neglected. In spite of these caveats, there remains substantial interest in the value of this quantity, and therefore it is given here: $\langle -\eta S_{b \rightarrow q\bar{q}s} \rangle = 0.64 \pm 0.03$, with confidence level 0.74 (0.3σ). This value is in agreement with the average $-\eta S_{b \rightarrow c\bar{c}s}$ given in Sec. 4.4.1. (The average for $C_{b \rightarrow q\bar{q}s}$ is $\langle C_{b \rightarrow q\bar{q}s} \rangle = -0.01 \pm 0.03$ with confidence level 0.74 (0.3σ).) We emphasise again that we do not advocate the use of these averages, and that the values should be treated with *extreme caution*, if at all.

From Table 33 it may be noted that the averages for $-\eta S_{b \rightarrow q\bar{q}s}$ in ϕK_s^0 , $\eta'K^0$, $f_0K_s^0$ and $K^+K^-K_s^0$ are all now more than 5σ away from zero, so that CP violation in these modes can be considered well established. There is no evidence (above 2σ) for direct CP violation in any $b \rightarrow q\bar{q}s$ mode.

4.6.2 Time-dependent Dalitz plot analyses: $B^0 \rightarrow K^+K^-K^0$ and $B^0 \rightarrow \pi^+\pi^-K_s^0$

As mentioned in Sec. 4.2.5 and above, both *BABAR* and Belle have performed time-dependent Dalitz plot analysis of $B^0 \rightarrow K^+K^-K^0$ and $B^0 \rightarrow \pi^+\pi^-K_s^0$ decays. The results are summarised in Tabs. 35 and 36. Averages for the $B^0 \rightarrow f_0K_s^0$ decay, which contributes to both Dalitz plots, are shown in Fig. 19. Results are presented in terms of the effective weak phase (from mixing and decay) difference β^{eff} and the direct CP violation parameter \mathcal{A} ($\mathcal{A} = -C$) for each of the resonant contributions. Note that Dalitz plot analyses, including all those included in these

⁴⁰ We do not include a preliminary result from Belle [297], which remains unpublished after more than two years.

⁴¹ The f_X is assumed to be spin even.

Table 33: Averages of $-\eta S_{b \rightarrow q\bar{q}s}$ and $C_{b \rightarrow q\bar{q}s}$.

Experiment	$N(B\bar{B})$	$-\eta S_{b \rightarrow q\bar{q}s}$	$C_{b \rightarrow q\bar{q}s}$	Correlation
ϕK^0				
BABAR	[212] 470M	$0.66 \pm 0.17 \pm 0.07$	$0.05 \pm 0.18 \pm 0.05$	–
Belle	[211] 657M	$0.90^{+0.09}_{-0.19}$	$-0.04 \pm 0.20 \pm 0.10 \pm 0.02$	–
Average		$0.74^{+0.11}_{-0.13}$	0.01 ± 0.14	uncorrelated averages
$\eta' K^0$				
BABAR	[300] 467M	$0.57 \pm 0.08 \pm 0.02$	$-0.08 \pm 0.06 \pm 0.02$	0.03
Belle	[301] 535M	$0.64 \pm 0.10 \pm 0.04$	$0.01 \pm 0.07 \pm 0.05$	0.09
Average		0.59 ± 0.07	-0.05 ± 0.05	0.04
Confidence level		$0.63 (0.5\sigma)$		
$K_s^0 K_s^0 K_s^0$				
BABAR	[302] 468M	$0.94^{+0.21}_{-0.24} \pm 0.06$	$-0.17 \pm 0.18 \pm 0.04$	0.16
Belle	[301] 535M	$0.30 \pm 0.32 \pm 0.08$	$-0.31 \pm 0.20 \pm 0.07$	–
Average		0.72 ± 0.19	-0.24 ± 0.14	0.09
Confidence level		$0.26 (1.1\sigma)$		
$\pi^0 K^0$				
BABAR	[300] 467M	$0.55 \pm 0.20 \pm 0.03$	$0.13 \pm 0.13 \pm 0.03$	0.06
Belle	[296] 657M	$0.67 \pm 0.31 \pm 0.08$	$-0.14 \pm 0.13 \pm 0.06$	–0.04
Average		0.57 ± 0.17	0.01 ± 0.10	0.02
Confidence level		$0.37 (0.9\sigma)$		
$\rho^0 K_s^0$				
BABAR	[215] 383M	$0.35^{+0.26}_{-0.31} \pm 0.06 \pm 0.03$	$-0.05 \pm 0.26 \pm 0.10 \pm 0.03$	–
Belle	[216] 657M	$0.64^{+0.19}_{-0.25} \pm 0.09 \pm 0.10$	$-0.03^{+0.24}_{-0.23} \pm 0.11 \pm 0.10$	–
Average		$0.54^{+0.18}_{-0.21}$	-0.06 ± 0.20	uncorrelated averages
ωK_s^0				
BABAR	[300] 467M	$0.55^{+0.26}_{-0.29} \pm 0.02$	$-0.52^{+0.22}_{-0.20} \pm 0.03$	0.03
Belle	[298] 535M	$0.11 \pm 0.46 \pm 0.07$	$0.09 \pm 0.29 \pm 0.06$	–0.04
Average		0.45 ± 0.24	-0.32 ± 0.17	0.01
Confidence level		$0.18 (1.3\sigma)$		
$f_0 K^0$				
BABAR	[212, 215]	$0.74^{+0.12}_{-0.15}$	0.15 ± 0.16	–
Belle	[211, 216]	$0.63^{+0.16}_{-0.19}$	0.13 ± 0.17	–
Average		$0.69^{+0.10}_{-0.12}$	0.14 ± 0.12	uncorrelated averages
$f_2 K_s^0$				
BABAR	[215] 383M	$0.48 \pm 0.52 \pm 0.06 \pm 0.10$	$0.28^{+0.35}_{-0.40} \pm 0.08 \pm 0.07$	–
$f_X K_s^0$				
BABAR	[215] 383M	$0.20 \pm 0.52 \pm 0.07 \pm 0.07$	$0.13^{+0.33}_{-0.35} \pm 0.04 \pm 0.09$	–

averages, often suffer from ambiguous solutions – we quote the results corresponding to those presented as solution 1 in all cases. Results on flavour specific amplitudes that may contribute to these Dalitz plots (such as $K^{*+}\pi^-$) are averaged by the HFAG Rare Decays subgroup (Sec. 7).

Table 34: Averages of $-\eta S_{b \rightarrow q\bar{q}s}$ and $C_{b \rightarrow q\bar{q}s}$ (continued).

Experiment	$N(B\bar{B})$	$-\eta S_{b \rightarrow q\bar{q}s}$	$C_{b \rightarrow q\bar{q}s}$	Correlation
			$\pi^0 \pi^0 K_s^0$	
BABAR [303]	227M	$-0.72 \pm 0.71 \pm 0.08$	$0.23 \pm 0.52 \pm 0.13$	-0.02
			$\phi K_s^0 \pi^0$	
BABAR [304]	465M	$0.97^{+0.03}_{-0.52}$	$-0.20 \pm 0.14 \pm 0.06$	-
			$\pi^+ \pi^- K_s^0$ nonresonant	
BABAR [215]	383M	$0.01 \pm 0.31 \pm 0.05 \pm 0.09$	$0.01 \pm 0.25 \pm 0.06 \pm 0.05$	-
			$K^+ K^- K^0$	
BABAR [212]	470M	$0.65 \pm 0.12 \pm 0.03$	$0.02 \pm 0.09 \pm 0.03$	-
Belle [211]	657M	$0.76^{+0.14}_{-0.18}$	$0.14 \pm 0.11 \pm 0.08 \pm 0.03$	-
Average		$0.68^{+0.09}_{-0.10}$	0.06 ± 0.08	uncorrelated averages

4.6.3 Time-dependent analyses of $B^0 \rightarrow \phi K_s^0 \pi^0$

The final state in the decay $B^0 \rightarrow \phi K_s^0 \pi^0$ is a mixture of CP -even and CP -odd amplitudes. However, since only ϕK^{*0} resonant states contribute (in particular, $\phi K^{*0}(892)$, $\phi K_0^{*0}(1430)$ and $\phi K_2^{*0}(1430)$ are seen), the composition can be determined from the analysis of $B \rightarrow \phi K^+ \pi^-$, assuming only that the ratio of branching fractions $\mathcal{B}(K^{*0} \rightarrow K_s^0 \pi^0)/\mathcal{B}(K^{*0} \rightarrow K^+ \pi^-)$ is the same for each excited kaon state.

BABAR [304] have performed a simultaneous analysis of $B^0 \rightarrow \phi K_s^0 \pi^0$ and $B^0 \rightarrow \phi K^+ \pi^-$ that is time-dependent for the former mode and time-integrated for the latter. Such an analysis allows, in principle, all parameters of the $B^0 \rightarrow \phi K^{*0}$ system to be determined, including mixing-induced CP violation effects. The latter is determined to be $\Delta\phi_{00} = 0.28 \pm 0.42 \pm 0.04$, where $\Delta\phi_{00}$ is half the weak phase difference between B^0 and \bar{B}^0 decays to $\phi K_0^{*0}(1430)$. As discussed above, this can also be presented in terms of the quasi-two-body parameter $\sin(2\beta_{00}^{\text{eff}}) = \sin(2\beta + 2\Delta\phi_{00}) = 0.97^{+0.03}_{-0.52}$. The highly asymmetric uncertainty arises due to the conversion from the phase to the sine of the phase, and the proximity of the physical boundary.

Similar $\sin(2\beta^{\text{eff}})$ parameters can be defined for each of the helicity amplitudes for both $\phi K^{*0}(892)$ and $\phi K_2^{*0}(1430)$. However, the relative phases between these decays are constrained due to the nature of the simultaneous analysis of $B^0 \rightarrow \phi K_s^0 \pi^0$ and $B^0 \rightarrow \phi K^+ \pi^-$, and therefore these measurements are highly correlated. Instead of quoting all these results, BABAR provide an illustration of their measurements with the following differences:

$$\sin(2\beta - 2\Delta\delta_{01}) - \sin(2\beta) = -0.42^{+0.26}_{-0.34} \quad (147)$$

$$\sin(2\beta - 2\Delta\phi_{\parallel 1}) - \sin(2\beta) = -0.32^{+0.22}_{-0.30} \quad (148)$$

$$\sin(2\beta - 2\Delta\phi_{\perp 1}) - \sin(2\beta) = -0.30^{+0.23}_{-0.32} \quad (149)$$

$$\sin(2\beta - 2\Delta\phi_{\perp 1}) - \sin(2\beta - 2\Delta\phi_{\parallel 1}) = 0.02 \pm 0.23 \quad (150)$$

$$\sin(2\beta - 2\Delta\delta_{02}) - \sin(2\beta) = -0.10^{+0.18}_{-0.29} \quad (151)$$

where the first subscript indicates the helicity amplitude and the second indicates the spin of the kaon resonance. For the complete definitions of the $\Delta\delta$ and $\Delta\phi$ parameters, please refer to the BABAR paper [304].

Table 35: Results from time-dependent Dalitz plot analysis of the $B^0 \rightarrow K^+K^-K^0$ decay. Correlations (not shown) are taken into account in the average.

Experiment	$N(B\bar{B})$	ϕK_s^0		$f_0 K_s^0$		$K^+K^-K_s^0$	
		$\beta^{\text{eff}} (^\circ)$	\mathcal{A}	$\beta^{\text{eff}} (^\circ)$	\mathcal{A}	$\beta^{\text{eff}} (^\circ)$	\mathcal{A}
BABAR [212]	470M	$21 \pm 6 \pm 2$	$-0.05 \pm 0.18 \pm 0.05$	$18 \pm 6 \pm 4$	$-0.28 \pm 0.24 \pm 0.09$	$20.3 \pm 4.3 \pm 1.2$	$-0.02 \pm 0.09 \pm 0.03$
Belle [211]	657M	$32.2 \pm 9.0 \pm 2.6 \pm 1.4$	$0.04 \pm 0.20 \pm 0.10 \pm 0.02$	$31.3 \pm 9.0 \pm 3.4 \pm 4.0$	$-0.30 \pm 0.29 \pm 0.11 \pm 0.09$	$24.9 \pm 6.4 \pm 2.1 \pm 2.5$	$-0.14 \pm 0.11 \pm 0.08 \pm 0.03$
Average		24 ± 5	-0.01 ± 0.14	22 ± 6	-0.29 ± 0.20	21.6 ± 3.7	-0.06 ± 0.08
Confidence level				0.93 (0.1 σ)			

Table 36: Results from time-dependent Dalitz plot analysis of the $B^0 \rightarrow \pi^+\pi^-K_s^0$ decay. Correlations (not shown) are taken into account in the average.

Experiment	$N(B\bar{B})$	β^{eff}	$\rho^0 K_s^0$	\mathcal{A}	β^{eff}	$f_0 K_s^0$	\mathcal{A}
BABAR [215]	383M	$(10.2 \pm 8.9 \pm 3.0 \pm 1.9)^\circ$	$0.05 \pm 0.26 \pm 0.10 \pm 0.03$		$(36.0 \pm 9.8 \pm 2.1 \pm 2.1)^\circ$	$-0.08 \pm 0.19 \pm 0.03 \pm 0.04$	
Belle [216]	657M	$(20.0^{+8.6}_{-8.5} \pm 3.2 \pm 3.5)^\circ$	$0.03^{+0.23}_{-0.24} \pm 0.11 \pm 0.10$		$(12.7^{+6.9}_{-6.5} \pm 2.8 \pm 3.3)^\circ$	$-0.06 \pm 0.17 \pm 0.07 \pm 0.09$	
Average		16.4 ± 6.8		0.06 ± 0.20		20.6 ± 6.2	-0.07 ± 0.14
Confidence level		$0.39 (0.9\sigma)$					

Experiment	$N(B\bar{B})$	β^{eff}	$f_2 K_s^0$	\mathcal{A}	β^{eff}	$f_X K_s^0$	\mathcal{A}
BABAR [215]	383M	$(14.9 \pm 17.9 \pm 3.1 \pm 5.2)^\circ$	$-0.28^{+0.40}_{-0.35} \pm 0.08 \pm 0.07$		$(5.8 \pm 15.2 \pm 2.2 \pm 2.3)^\circ$	$-0.13^{+0.35}_{-0.33} \pm 0.04 \pm 0.09$	

Experiment	$N(B\bar{B})$	β^{eff}	$B^0 \rightarrow \pi^+\pi^-K_s^0$ nonresonant	\mathcal{A}	β^{eff}	$\chi_{c0} K_s^0$	\mathcal{A}
BABAR [215]	383M	$(0.4 \pm 8.8 \pm 1.9 \pm 3.8)^\circ$	$-0.01 \pm 0.25 \pm 0.06 \pm 0.05$		$(23.2 \pm 22.4 \pm 2.3 \pm 4.2)^\circ$	$0.29^{+0.44}_{-0.53} \pm 0.03 \pm 0.05$	

Direct CP violation parameters for each of the contributing helicity amplitudes can also be measured. Again, these are determined from a simultaneous fit of $B^0 \rightarrow \phi K_s^0 \pi^0$ and $B^0 \rightarrow \phi K^+ \pi^-$, with the precision being dominated by the statistics of the latter mode. Direct CP violation measurements are tabulated by HFAG - Rare Decays (Sec. 7).

4.6.4 Time-dependent CP asymmetries in $B_s^0 \rightarrow K^+ K^-$

The decay $B_s^0 \rightarrow K^+ K^-$ involves a $b \rightarrow u\bar{u}s$ transition, and hence has both penguin and tree contributions. Both mixing-induced and direct CP violation effects may arise, and additional input is needed to disentangle the contributions and determine γ and β_s^{eff} . For example, the observables in $B^0 \rightarrow \pi^+ \pi^-$ can be related using U-spin, as proposed by Fleischer [305].

The observables are $A_{\text{mix}} = S_{CP}$, $A_{\text{dir}} = -C_{CP}$, and $A_{\Delta\Gamma}$. They can all be treated as free parameters, but are physically constrained to satisfy $A_{\text{mix}}^2 + A_{\text{dir}}^2 + A_{\Delta\Gamma}^2 = 1$. Note that the untagged decay distribution, from which an “effective lifetime” can be measured, retains sensitivity to $A_{\Delta\Gamma}$. Averages of effective lifetimes are performed by the HFAG Lifetimes and Oscillations group, see Sec. 3.

The observables in $B_s^0 \rightarrow K^+ K^-$ have been measured by LHCb, who impose the constraint mentioned above to eliminate $A_{\Delta\Gamma}$.

Table 37: Results from time-dependent analysis of the $B_s^0 \rightarrow K^+ K^-$ decay.

Experiment	Sample size	A_{mix}	A_{dir}	Correlation
LHCb [306]	0.7 fb^{-1}	$0.17 \pm 0.18 \pm 0.05$	$0.02 \pm 0.18 \pm 0.04$	-0.10

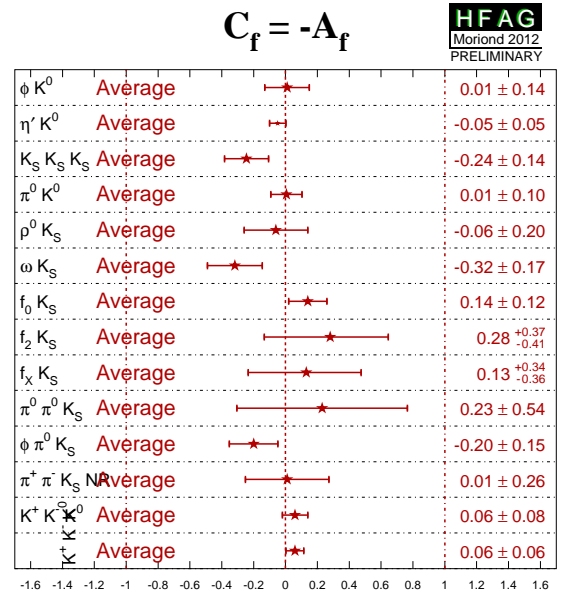
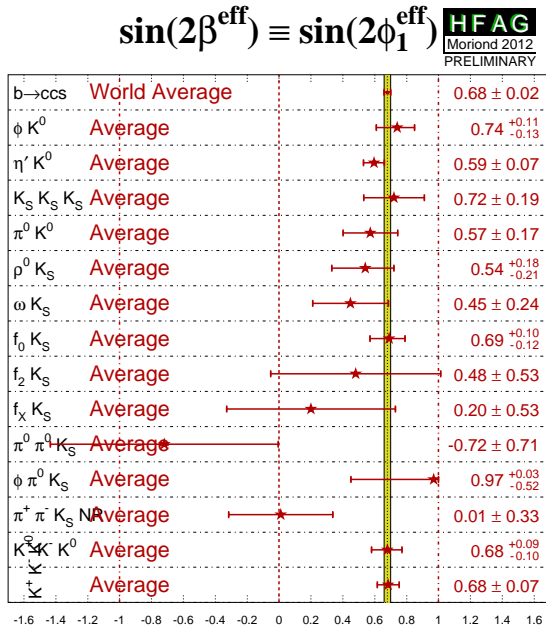
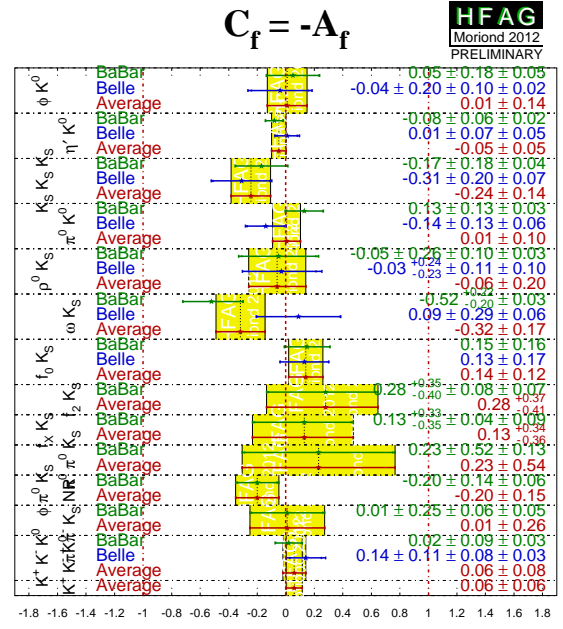
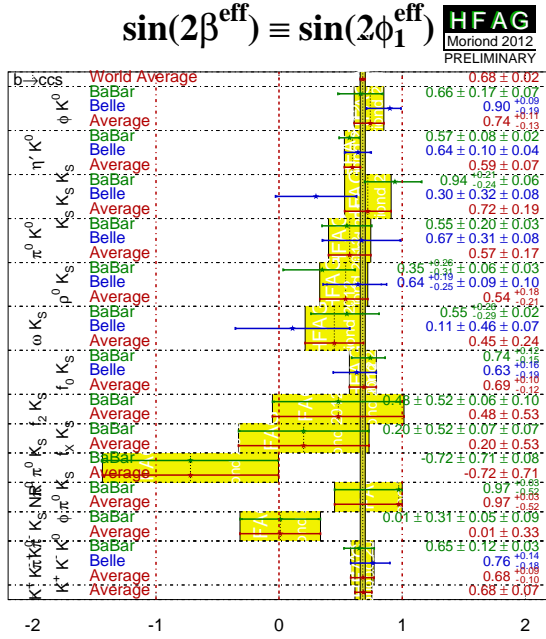


Figure 16: (Top) Averages of (left) $-\eta S_{b \rightarrow q\bar{q}s}$ and (right) $C_{b \rightarrow q\bar{q}s}$. The $-\eta S_{b \rightarrow q\bar{q}s}$ figure compares the results to the world average for $-\eta S_{b \rightarrow c\bar{c}s}$ (see Section 4.4.1). (Bottom) Same, but only averages for each mode are shown. More figures are available from the HFAG web pages.

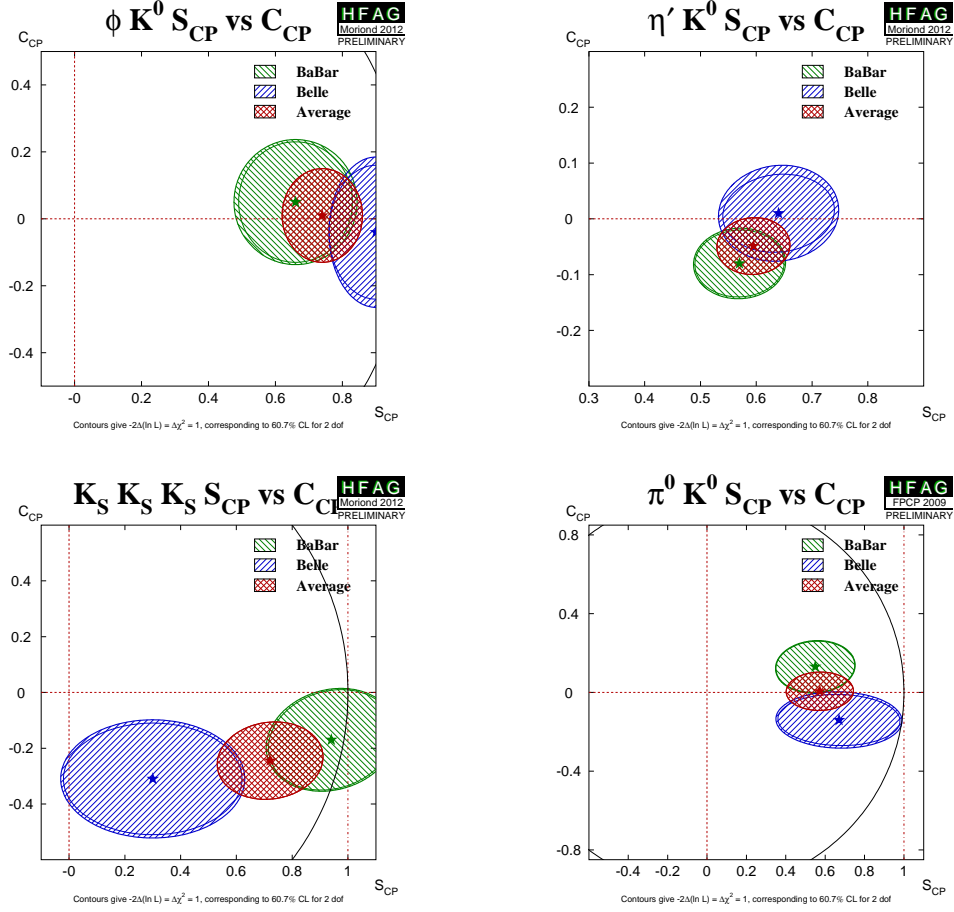


Figure 17: Averages of four $b \rightarrow q\bar{q}s$ dominated channels, for which correlated averages are performed, in the S_{CP} vs. C_{CP} plane, where S_{CP} has been corrected by the CP eigenvalue to give $\sin(2\beta^{\text{eff}})$. (Top left) $B^0 \rightarrow \phi K^0$, (top right) $B^0 \rightarrow \eta' K^0$, (bottom left) $B^0 \rightarrow K_S^0 K_S^0 K_S^0$, (bottom right) $B^0 \rightarrow \pi^0 K_S^0$. More figures are available from the HFAG web pages.

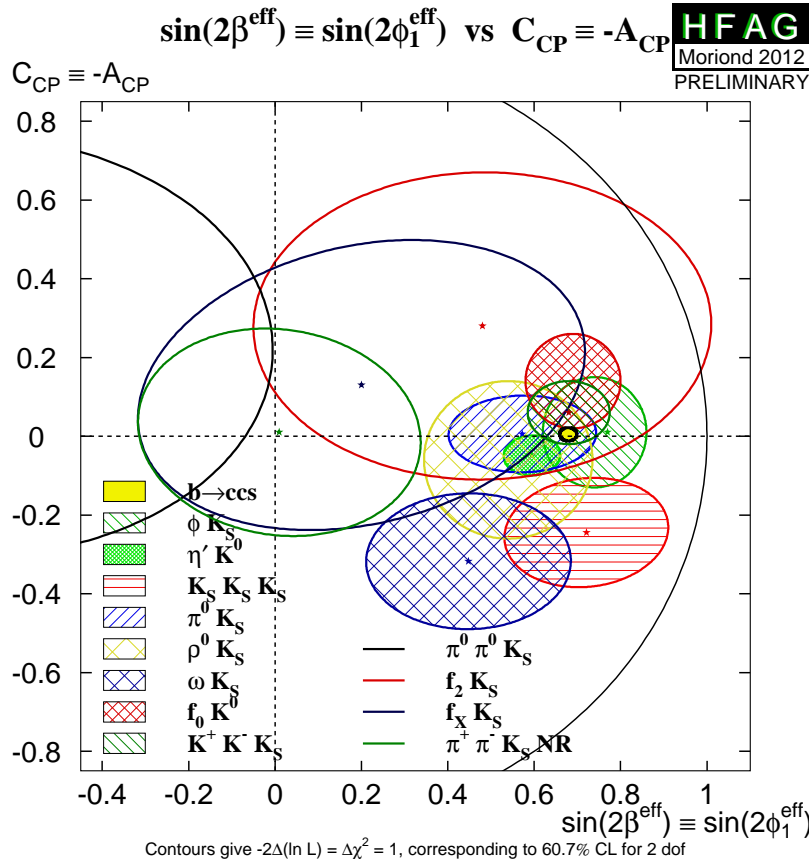


Figure 18: Compilation of constraints in the $-\eta S_{b \rightarrow q\bar{q}s}$ vs. $C_{b \rightarrow q\bar{q}s}$ plane.

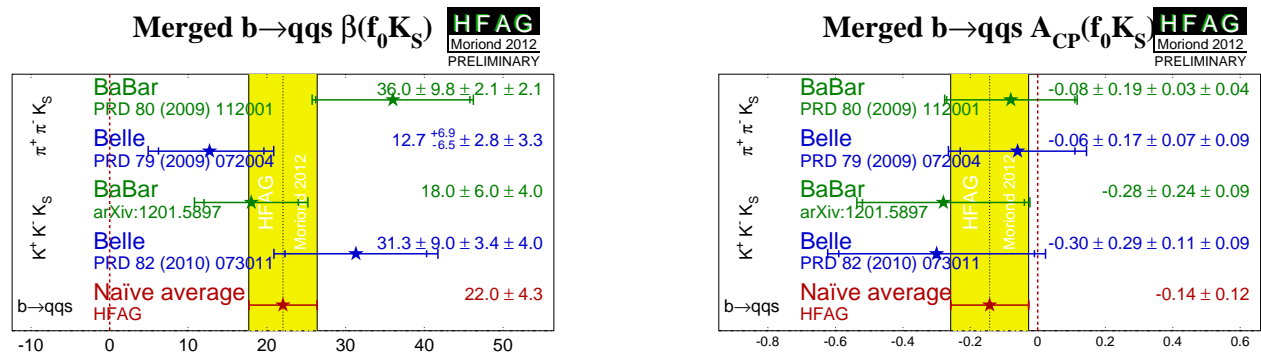


Figure 19: (Top) Averages of (left) $\beta^{\text{eff}} \equiv \phi_1^{\text{eff}}$ and (right) A_{CP} for the $B^0 \rightarrow f_0 K_S^0$ decay including measurements from Dalitz plot analyses of both $B^0 \rightarrow K^+ K^- K_S^0$ and $B^0 \rightarrow \pi^+ \pi^- K_S^0$.

4.7 Time-dependent CP asymmetries in $b \rightarrow c\bar{c}d$ transitions

The transition $b \rightarrow c\bar{c}d$ can occur via either a $b \rightarrow c$ tree or a $b \rightarrow d$ penguin amplitude. Similarly to Eq. (146), the amplitude for the $b \rightarrow d$ penguin can be written

$$\begin{aligned} A_{b \rightarrow d} &= F_u V_{ub} V_{ud}^* + F_c V_{cb} V_{cd}^* + F_t V_{tb} V_{td}^* \\ &= (F_u - F_c) V_{ub} V_{ud}^* + (F_t - F_c) V_{tb} V_{td}^* \\ &= \mathcal{O}(\lambda^3) + \mathcal{O}(\lambda^3). \end{aligned} \quad (152)$$

From this it can be seen that the $b \rightarrow d$ penguin amplitude contains terms with different weak phases at the same order of CKM suppression.

In the above, we have followed Eq. (146) by eliminating the F_c term using unitarity. However, we could equally well write

$$\begin{aligned} A_{b \rightarrow d} &= (F_u - F_t) V_{ub} V_{ud}^* + (F_c - F_t) V_{cb} V_{cd}^*, \\ &= (F_c - F_u) V_{cb} V_{cd}^* + (F_t - F_u) V_{tb} V_{td}^*. \end{aligned} \quad (153)$$

Since the $b \rightarrow c\bar{c}d$ tree amplitude has the weak phase of $V_{cb} V_{cd}^*$, either of the above expressions allow the penguin to be decomposed into parts with weak phases the same and different to the tree amplitude (the relative weak phase can be chosen to be either β or γ). However, if the tree amplitude dominates, there is little sensitivity to any phase other than that from $B^0 - \bar{B}^0$ mixing.

The $b \rightarrow c\bar{c}d$ transitions can be investigated with studies of various different final states. Results are available from both *BABAR* and Belle using the final states $J/\psi \pi^0$, $D^+ D^-$, $D^{*+} D^{*-}$ and $D^{*\pm} D^\mp$, the averages of these results are given in Tables 38 and 39. The results using the CP eigenstate ($\eta = +1$) modes $J/\psi \pi^0$ and $D^+ D^-$ are shown in Fig. 20 and Fig. 21 respectively, with two-dimensional constraints shown in Fig. 22.

The vector-vector mode $D^{*+} D^{*-}$ is found to be dominated by the CP -even longitudinally polarised component; *BABAR* measures a CP -odd fraction of $0.158 \pm 0.028 \pm 0.006$ [204] while Belle measures a CP -odd fraction of $0.125 \pm 0.043 \pm 0.023$ [307]. These values, listed as R_\perp , are included in the averages which ensures the correlations to be taken into account.⁴² *BABAR* have also performed an additional fit in which the CP -even and CP -odd components are allowed to have different CP violation parameters S and C . These results are included in Table 39. Results using $D^{*+} D^{*-}$ are shown in Fig. 23.

As discussed in Sec. 4.2.6, the most recent papers on the non- CP eigenstate mode $D^{*\pm} D^\mp$ use the $(A, S, \Delta S, C, \Delta C)$ set of parameters, and we therefore perform the averages with this choice.

In the absence of the penguin contribution (tree dominance), the time-dependent parameters would be given by $S_{b \rightarrow c\bar{c}d} = -\eta \sin(2\beta)$, $C_{b \rightarrow c\bar{c}d} = 0$, $S_{+-} = \sin(2\beta + \delta)$, $S_{-+} = \sin(2\beta - \delta)$, $C_{+-} = -C_{-+}$ and $\mathcal{A} = 0$, where δ is the strong phase difference between the $D^{*+} D^-$ and $D^{*-} D^+$ decay amplitudes. In the presence of the penguin contribution, there is no clean interpretation in terms of CKM parameters, however direct CP violation may be observed as any of $C_{b \rightarrow c\bar{c}d} \neq 0$, $C_{+-} \neq -C_{-+}$ or $A_{+-} \neq 0$.

The averages for the $b \rightarrow c\bar{c}d$ modes are shown in Figs. 24 and 25. Results are consistent with tree dominance, and with the Standard Model, though the Belle results in $B^0 \rightarrow D^+ D^-$ [311]

⁴² Note that the *BABAR* value given in Table 39 differs from that given above, since that in the table is not corrected for efficiency.

Table 38: Averages for the $b \rightarrow c\bar{c}d$ modes, $B^0 \rightarrow J/\psi\pi^0$ and D^+D^- .

Experiment	$N(B\bar{B})$	S_{CP}	C_{CP}	Correlation
$J/\psi\pi^0$				
BABAR [308]	466M	$-1.23 \pm 0.21 \pm 0.04$	$-0.20 \pm 0.19 \pm 0.03$	0.20
Belle [309]	535M	$-0.65 \pm 0.21 \pm 0.05$	$-0.08 \pm 0.16 \pm 0.05$	-0.10
Average		-0.93 ± 0.15	-0.10 ± 0.13	0.04
Confidence level		0.15 (1.4 σ)		
D^+D^-				
BABAR [204]	467M	$-0.65 \pm 0.36 \pm 0.05$	$-0.07 \pm 0.23 \pm 0.03$	-0.01
Belle [228]	772M	$-1.06^{+0.21}_{-0.14} \pm 0.08$	$-0.43 \pm 0.16 \pm 0.05$	-0.12
Average		-0.98 ± 0.17	-0.31 ± 0.14	-0.08
Confidence level		0.26 (1.1 σ)		

show an indication of direct CP violation, and hence a non-zero penguin contribution. The average of $S_{b \rightarrow c\bar{c}d}$ in both $J/\psi\pi^0$ and $D^{*+}D^{*-}$ final states is more than 5σ from zero, corresponding to observations of CP violation in these decay channels. That in the D^+D^- final state is more than 3σ from zero; however, due to the large uncertainty and possible non-Gaussian effects, any strong conclusion should be deferred.

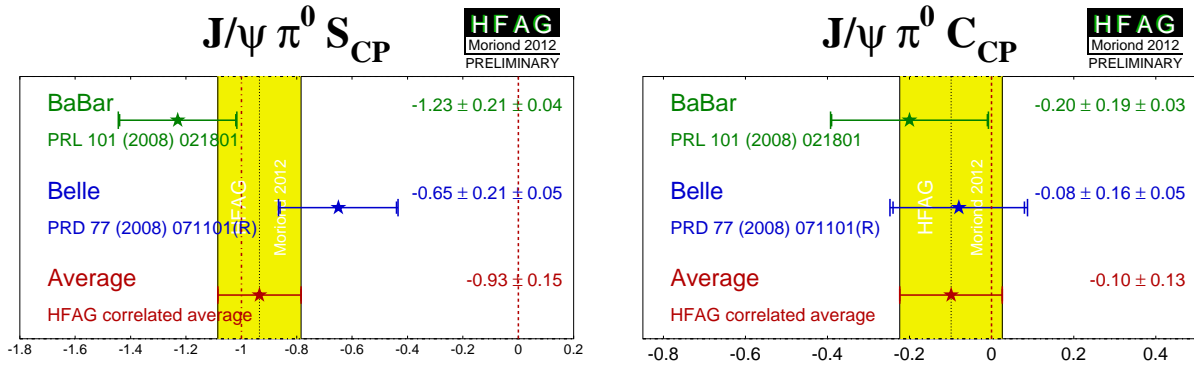


Figure 20: Averages of (left) $S_{b \rightarrow c\bar{c}d}$ and (right) $C_{b \rightarrow c\bar{c}d}$ for the mode $B^0 \rightarrow J/\psi\pi^0$.

Table 39: Averages for the $b \rightarrow c\bar{c}d$ modes, $D^{*+}D^{*-}$ and $D^{*\pm}D^{\mp}$.

Experiment		$N(B\bar{B})$	S_{CP}	C_{CP}	R_{\perp}
$D^{*+}D^{*-}$					
BABAR	[204]	467M	$-0.71 \pm 0.16 \pm 0.03$	$0.05 \pm 0.09 \pm 0.02$	0.17 ± 0.03
Belle	[310]	772M	$-0.79 \pm 0.13 \pm 0.03$	$-0.15 \pm 0.08 \pm 0.02$	$0.14 \pm 0.02 \pm 0.01$
Average			-0.77 ± 0.10	-0.06 ± 0.06	0.15 ± 0.02
Confidence level				$0.31 (1.0\sigma)$	

Experiment	$N(B\bar{B})$	S_{CP+}	C_{CP+}	S_{CP-}	C_{CP-}	R_{\perp}	
$D^{*+}D^{*-}$							
BABAR	[204]	467M	$-0.76 \pm 0.16 \pm 0.04$	$0.02 \pm 0.12 \pm 0.02$	$-1.81 \pm 0.71 \pm 0.16$	$0.41 \pm 0.50 \pm 0.08$	0.15 ± 0.03

Experiment	$N(B\bar{B})$	S	C	ΔS	ΔC	\mathcal{A}	
$D^{*\pm}D^{\mp}$							
BABAR	[204]	467M	$-0.68 \pm 0.15 \pm 0.04$	$0.04 \pm 0.12 \pm 0.03$	$0.05 \pm 0.15 \pm 0.02$	$0.04 \pm 0.12 \pm 0.03$	$0.01 \pm 0.05 \pm 0.01$
Belle	[228]	772M	$-0.78 \pm 0.15 \pm 0.05$	$-0.01 \pm 0.11 \pm 0.04$	$-0.13 \pm 0.15 \pm 0.04$	$0.12 \pm 0.11 \pm 0.03$	$0.06 \pm 0.05 \pm 0.02$
Average			-0.73 ± 0.11	0.01 ± 0.09	-0.04 ± 0.11	0.08 ± 0.08	0.03 ± 0.04
Confidence level			$0.65 (0.5\sigma)$	$0.77 (0.3\sigma)$	$0.41 (0.8\sigma)$	$0.63 (0.5\sigma)$	$0.48 (0.7\sigma)$

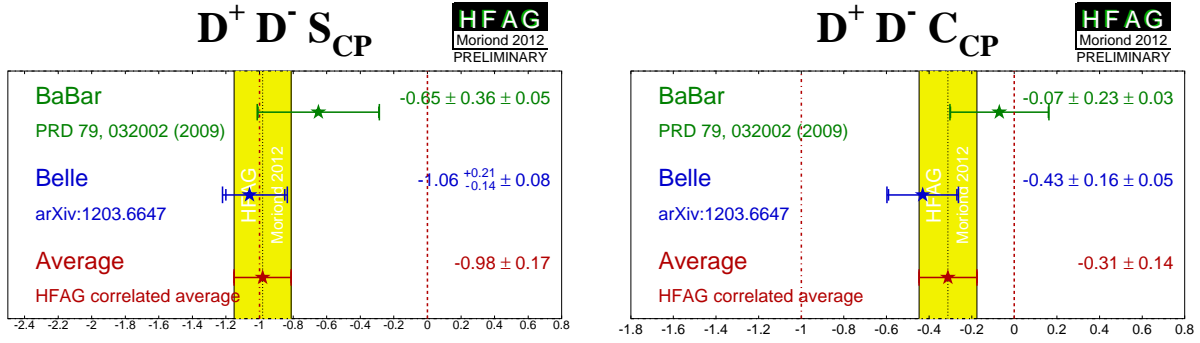


Figure 21: Averages of (left) $S_{b \rightarrow c\bar{c}d}$ and (right) $C_{b \rightarrow c\bar{c}d}$ for the mode $B^0 \rightarrow D^+ D^-$.

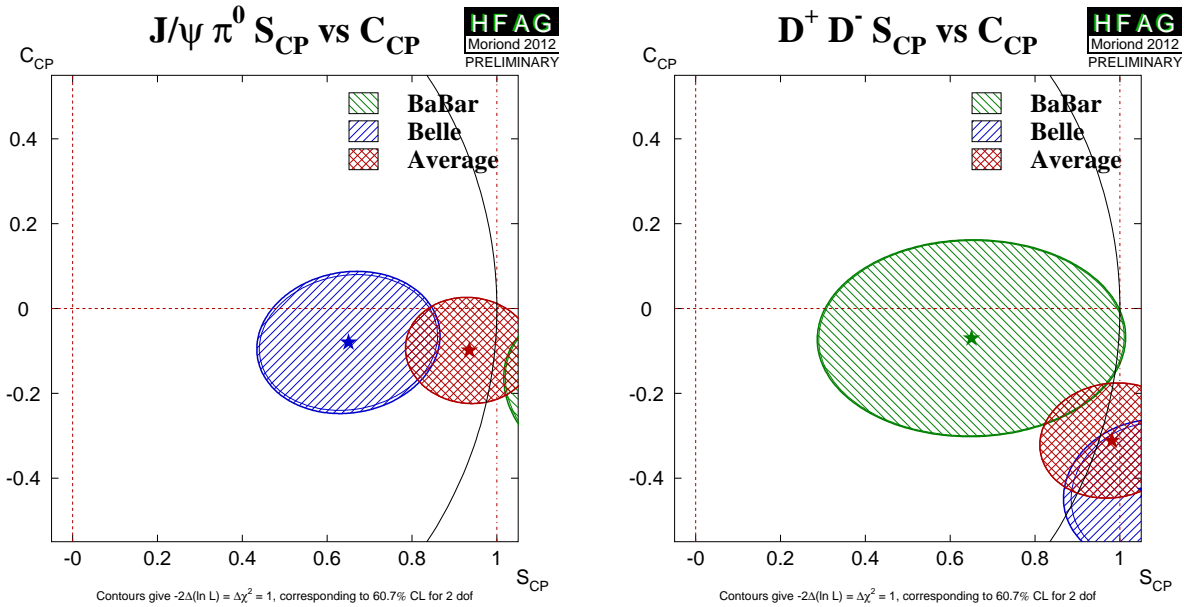


Figure 22: Averages of two $b \rightarrow c\bar{c}d$ dominated channels, for which correlated averages are performed, in the S_{CP} vs. C_{CP} plane. (Left) $B^0 \rightarrow J/\psi\pi^0$ and (right) $B^0 \rightarrow D^+ D^-$.

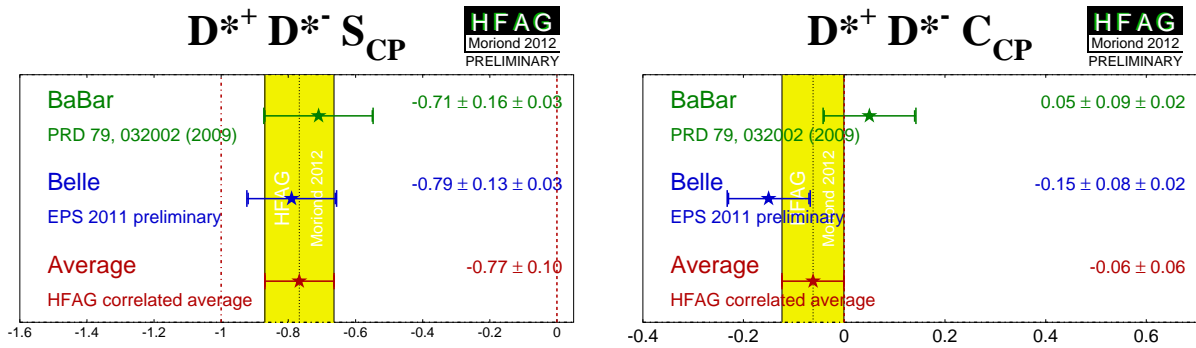


Figure 23: Averages of (left) $S_{b \rightarrow c\bar{c}d}$ and (right) $C_{b \rightarrow c\bar{c}d}$ for the mode $B^0 \rightarrow D^{*+} D^{*-}$.

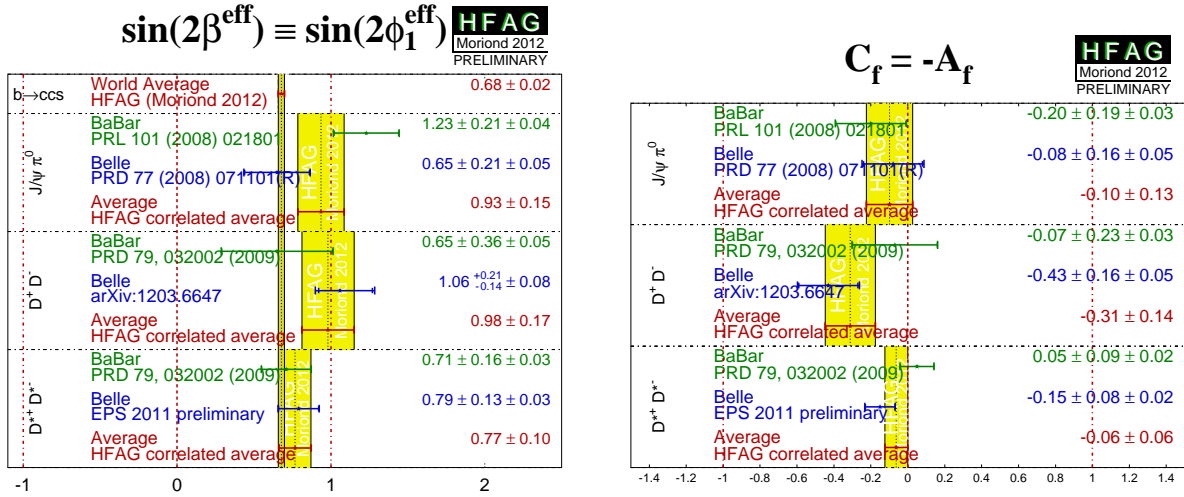


Figure 24: Averages of (left) $-\eta S_{b \rightarrow c\bar{c}d}$ and (right) $C_{b \rightarrow c\bar{c}d}$. The $-\eta S_{b \rightarrow q\bar{q}s}$ figure compares the results to the world average for $-\eta S_{b \rightarrow c\bar{c}s}$ (see Section 4.4.1).

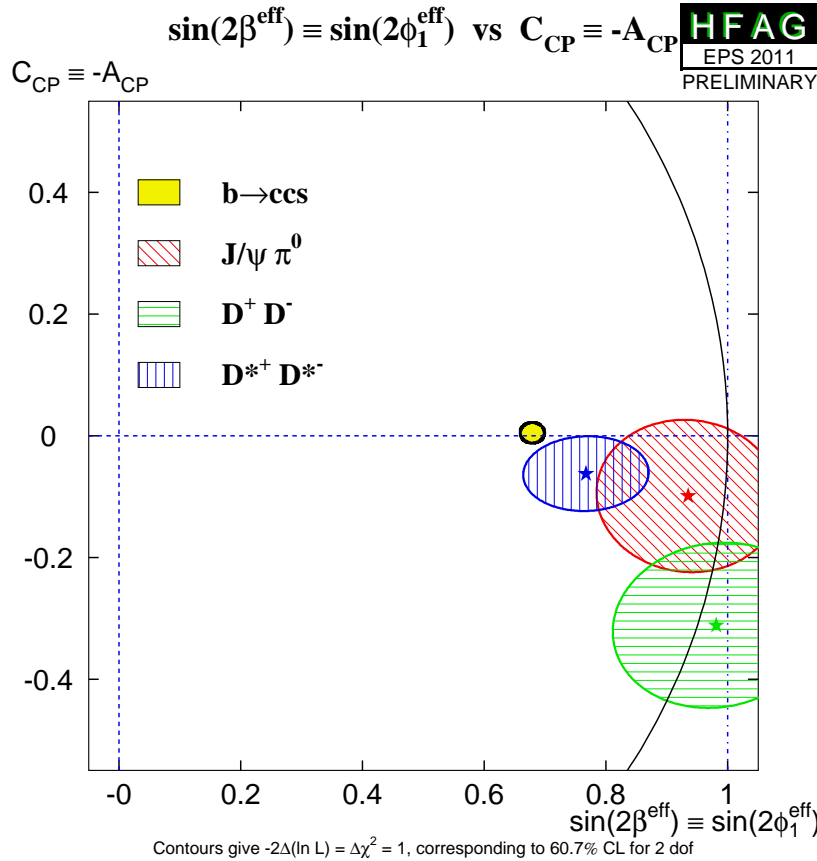


Figure 25: Compilation of constraints in the $-\eta S_{b \rightarrow c\bar{c}d}$ vs. $C_{b \rightarrow c\bar{c}d}$ plane.

4.8 Time-dependent CP asymmetries in $b \rightarrow q\bar{q}d$ transitions

Decays such as $B^0 \rightarrow K_S^0 K_S^0$ are pure $b \rightarrow q\bar{q}d$ penguin transitions. As shown in Eq. 152, this diagram has different contributing weak phases, and therefore the observables are sensitive to the difference (which can be chosen to be either β or γ). Note that if the contribution with the top quark in the loop dominates, the weak phase from the decay amplitudes should cancel that from mixing, so that no CP violation (neither mixing-induced nor direct) occurs. Non-zero contributions from loops with intermediate up and charm quarks can result in both types of effect (as usual, a strong phase difference is required for direct CP violation to occur).

Both *BABAR* [312] and Belle [313] have performed time-dependent analyses of $B^0 \rightarrow K_S^0 K_S^0$. The results are shown in Table 40 and Fig. 26.

Table 40: Results for $B^0 \rightarrow K_S^0 K_S^0$.

Experiment	$N(B\bar{B})$	S_{CP}	C_{CP}	Correlation
<i>BABAR</i> [312]	350M	$-1.28^{+0.80+0.11}_{-0.73-0.16}$	$-0.40 \pm 0.41 \pm 0.06$	-0.32
Belle [313]	657M	$-0.38^{+0.69}_{-0.77} \pm 0.09$	$0.38 \pm 0.38 \pm 0.05$	0.48
Average		-1.08 ± 0.49	-0.06 ± 0.26	0.14
Confidence level		0.29 (1.1 σ)		

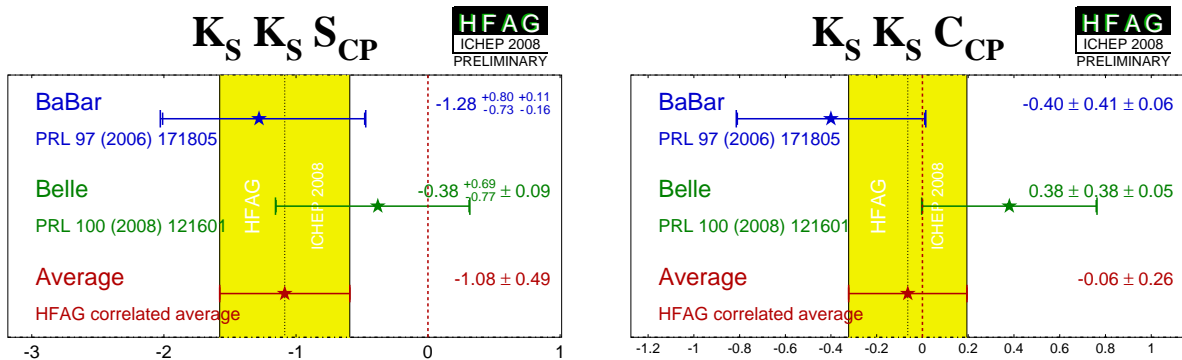


Figure 26: Averages of (left) $S_{b \rightarrow q\bar{q}d}$ and (right) $C_{b \rightarrow q\bar{q}d}$ for the mode $B^0 \rightarrow K_S^0 K_S^0$.

4.9 Time-dependent asymmetries in $b \rightarrow s\gamma$ transitions

The radiative decays $b \rightarrow s\gamma$ produce photons which are highly polarised in the Standard Model. The decays $B^0 \rightarrow F\gamma$ and $\bar{B}^0 \rightarrow F\gamma$ produce photons with opposite helicities, and since the polarisation is, in principle, observable, these final states cannot interfere. The finite mass of the s quark introduces small corrections to the limit of maximum polarisation, but any large mixing induced CP violation would be a signal for new physics. Since a single weak phase dominates the $b \rightarrow s\gamma$ transition in the Standard Model, the cosine term is also expected to be small.

Atwood *et al.* [238] have shown that an inclusive analysis with respect to $K_s^0\pi^0\gamma$ can be performed, since the properties of the decay amplitudes are independent of the angular momentum of the $K_s^0\pi^0$ system. However, if non-dipole operators contribute significantly to the amplitudes, then the Standard Model mixing-induced CP violation could be larger than the naïve expectation $S \simeq -2(m_s/m_b)\sin(2\beta)$ [239,240]. In this case, the CP parameters may vary over the $K_s^0\pi^0\gamma$ Dalitz plot, for example as a function of the $K_s^0\pi^0$ invariant mass. Explicit calculations indicate such corrections are small for exclusive final states [241,242].

With the above in mind, we quote two averages: one for $K^*(892)$ candidates only, and the other one for the inclusive $K_s^0\pi^0\gamma$ decay (including the $K^*(892)$). If the Standard Model dipole operator is dominant, both should give the same quantities (the latter naturally with smaller statistical error). If not, care needs to be taken in interpretation of the inclusive parameters, while the results on the $K^*(892)$ resonance remain relatively clean. Results from *BABAR* [314] and *Belle* [315] are used for both averages; both experiments use the invariant mass range $0.60 \text{ GeV}/c^2 < M_{K_s^0\pi^0} < 1.80 \text{ GeV}/c^2$ in the inclusive analysis. In addition to the $K_s^0\pi^0\gamma$ decay, *BABAR* have presented results using $K_s^0\eta\gamma$ [316], and *Belle* have presented results using $K_s^0\rho\gamma$ [317] and $K_s^0\phi\gamma$ [318].

Table 41: Averages for $b \rightarrow s\gamma$ modes.

Experiment	$N(B\bar{B})$	$S_{CP}(b \rightarrow s\gamma)$	$C_{CP}(b \rightarrow s\gamma)$	Correlation
$K^*(892)\gamma$				
<i>BABAR</i> [314]	467M	$-0.03 \pm 0.29 \pm 0.03$	$-0.14 \pm 0.16 \pm 0.03$	0.05
<i>Belle</i> [315]	535M	$-0.32_{-0.33}^{+0.36} \pm 0.05$	$0.20 \pm 0.24 \pm 0.05$	0.08
Average		-0.16 ± 0.22	-0.04 ± 0.14	0.06
Confidence level 0.40 (0.9 σ)				
$K_s^0\pi^0\gamma$ (including $K^*(892)\gamma$)				
<i>BABAR</i> [314]	467M	$-0.17 \pm 0.26 \pm 0.03$	$-0.19 \pm 0.14 \pm 0.03$	0.04
<i>Belle</i> [315]	535M	$-0.10 \pm 0.31 \pm 0.07$	$0.20 \pm 0.20 \pm 0.06$	0.08
Average		-0.15 ± 0.20	-0.07 ± 0.12	0.05
Confidence level 0.30 (1.0 σ)				
$K_s^0\eta\gamma$				
<i>BABAR</i> [316]	465M	$-0.18_{-0.46}^{+0.49} \pm 0.12$	$-0.32_{-0.39}^{+0.40} \pm 0.07$	-0.17
$K_s^0\rho^0\gamma$				
<i>Belle</i> [317]	657M	$0.11 \pm 0.33_{-0.09}^{+0.05}$	$-0.05 \pm 0.18 \pm 0.06$	0.04
$K_s^0\phi\gamma$				
<i>Belle</i> [318]	772M	$0.74_{-1.05}^{+0.72} \pm 0.10_{-0.24}$	$-0.35 \pm 0.58_{-0.23}^{+0.10}$	-

The results are shown in Table 41, and in Figs. 27 and 28. No significant CP violation results are seen; the results are consistent with the Standard Model and with other measurements in the $b \rightarrow s\gamma$ system (see Sec. 7).

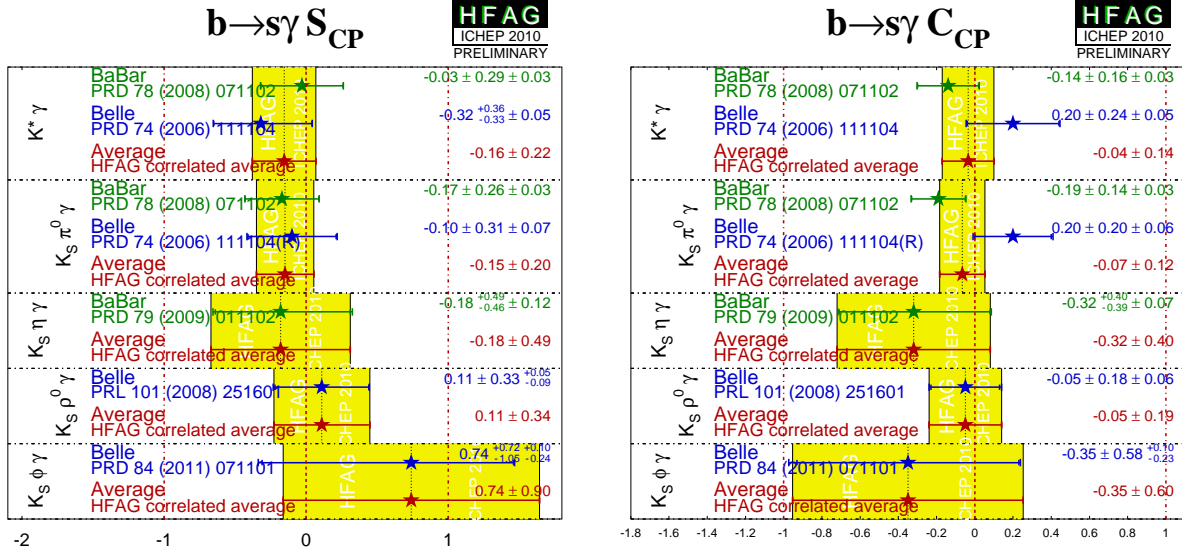


Figure 27: Averages of (left) $S_{b \rightarrow s\gamma}$ and (right) $C_{b \rightarrow s\gamma}$. Recall that the data for $K^*\gamma$ is a subset of that for $K_S^0\pi^0\gamma$.

4.10 Time-dependent asymmetries in $b \rightarrow d\gamma$ transitions

The formalism for the radiative decays $b \rightarrow d\gamma$ is much the same as that for $b \rightarrow s\gamma$ discussed above. Assuming dominance of the top quark in the loop, the weak phase in decay should cancel with that from mixing, so that the mixing-induced CP violation parameter S_{CP} should be very small. Corrections due to the finite light quark mass are smaller compared to $b \rightarrow s\gamma$, since $m_d < m_s$, and although QCD corrections may still play a role, they cannot significantly affect the prediction $S_{b \rightarrow d\gamma} \simeq 0$. Large direct CP violation effects could, however, be seen through a non-zero value of $C_{b \rightarrow d\gamma}$, since the top loop is not the only contribution.

Results using the mode $B^0 \rightarrow \rho^0\gamma$ are available from Belle and are shown in Table 42.

Table 42: Averages for $B^0 \rightarrow \rho^0\gamma$.

Experiment	$N(B\bar{B})$	S_{CP}	C_{CP}	Correlation
Belle [319]	657M	$-0.83 \pm 0.65 \pm 0.18$	$0.44 \pm 0.49 \pm 0.14$	-0.08

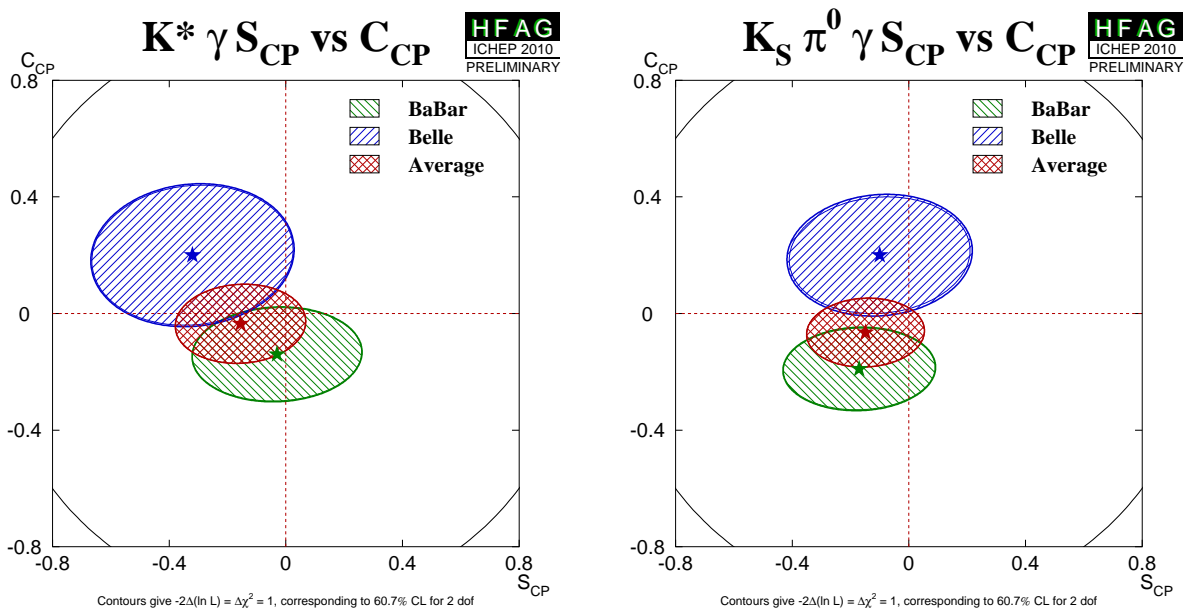


Figure 28: Averages of $b \rightarrow s\gamma$ dominated channels, for which correlated averages are performed, in the S_{CP} vs. C_{CP} plane. (Left) $B^0 \rightarrow K^*\gamma$ and (right) $B^0 \rightarrow K_S^0\pi^0\gamma$ (including $K^*\gamma$).

4.11 Time-dependent CP asymmetries in $b \rightarrow u\bar{u}d$ transitions

The $b \rightarrow u\bar{u}d$ transition can be mediated by either a $b \rightarrow u$ tree amplitude or a $b \rightarrow d$ penguin amplitude. These transitions can be investigated using the time dependence of B^0 decays to final states containing light mesons. Results are available from both *BABAR* and Belle for the CP eigenstate ($\eta = +1$) $\pi^+\pi^-$ final state and for the vector-vector final state $\rho^+\rho^-$, which is found to be dominated by the CP -even longitudinally polarised component (*BABAR* measure $f_{\text{long}} = 0.992 \pm 0.024^{+0.026}_{-0.013}$ [320] while Belle measure $f_{\text{long}} = 0.941^{+0.034}_{-0.040} \pm 0.030$ [321]). *BABAR* have also performed a time-dependent analysis of the vector-vector final state $\rho^0\rho^0$ [322], in which they measure $f_{\text{long}} = 0.70 \pm 0.14 \pm 0.05$; Belle measures a smaller branching fraction than *BABAR* for $B^0 \rightarrow \rho^0\rho^0$ [323] with corresponding signal yields too small to perform time-dependent or angular analyses. *BABAR* have furthermore performed a time-dependent analysis of the $B^0 \rightarrow a_1^\pm\pi^\mp$ decay [324]; further experimental input for the extraction of α from this channel is reported in a later publication [325].

Results, and averages, of time-dependent CP -violation parameters in $b \rightarrow u\bar{u}d$ transitions are listed in Table 43. The averages for $\pi^+\pi^-$ are shown in Fig. 29, and those for $\rho^+\rho^-$ are shown in Fig. 30, with the averages in the S_{CP} vs. C_{CP} plane shown in Fig. 31.

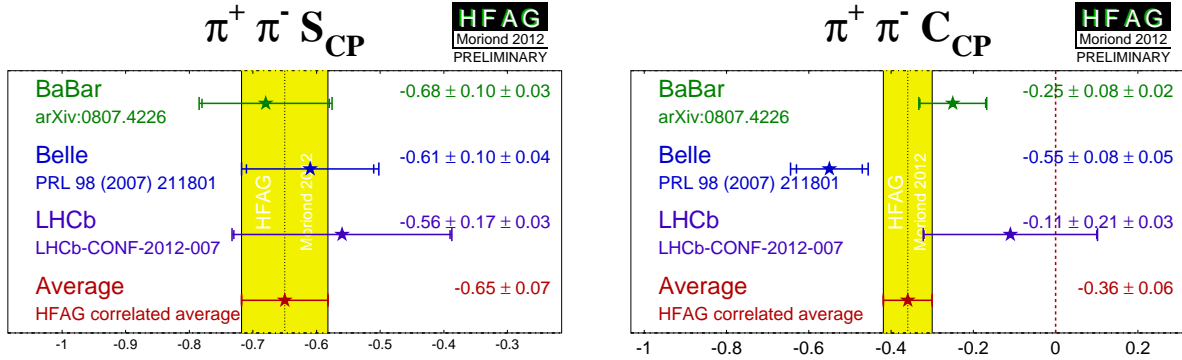


Figure 29: Averages of (left) $S_{b \rightarrow u\bar{u}d}$ and (right) $C_{b \rightarrow u\bar{u}d}$ for the mode $B^0 \rightarrow \pi^+\pi^-$.

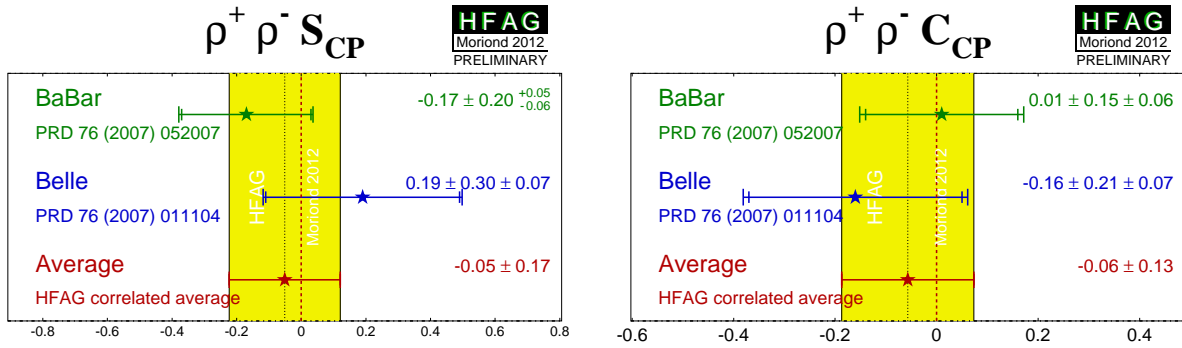


Figure 30: Averages of (left) $S_{b \rightarrow u\bar{u}d}$ and (right) $C_{b \rightarrow u\bar{u}d}$ for the mode $B^0 \rightarrow \rho^+\rho^-$.

Table 43: Averages for $b \rightarrow u\bar{u}d$ modes.

Experiment	Sample size	S_{CP}	C_{CP}	Correlation		
		$\pi^+\pi^-$				
BABAR [326]	$N(B\bar{B}) = 467\text{M}$	$-0.68 \pm 0.10 \pm 0.03$	$-0.25 \pm 0.08 \pm 0.02$	-0.06		
Belle [327]	$N(B\bar{B}) = 535\text{M}$	$-0.61 \pm 0.10 \pm 0.04$	$-0.55 \pm 0.08 \pm 0.05$	-0.15		
LHCb [306]	0.7 fb^{-1}	$-0.56 \pm 0.17 \pm 0.03$	$-0.11 \pm 0.21 \pm 0.03$	0.34		
Average		-0.65 ± 0.07	-0.36 ± 0.06	-0.03		
Confidence level			$0.12 (1.6\sigma)$			
		$\rho^+\rho^-$				
BABAR [320]	$N(B\bar{B}) = 387\text{M}$	$-0.17 \pm 0.20^{+0.05}_{-0.06}$	$0.01 \pm 0.15 \pm 0.06$	-0.04		
Belle [328]	$N(B\bar{B}) = 535\text{M}$	$0.19 \pm 0.30 \pm 0.07$	$-0.16 \pm 0.21 \pm 0.07$	0.10		
Average		-0.05 ± 0.17	-0.06 ± 0.13	0.01		
Confidence level			$0.50 (0.7\sigma)$			
		$\rho^0\rho^0$				
BABAR [322]	$N(B\bar{B}) = 465\text{M}$	$0.3 \pm 0.7 \pm 0.2$	$0.2 \pm 0.8 \pm 0.3$	-0.04		
Experiment	$N(B\bar{B})$	A_{CP}	C	S	ΔC	ΔS
			$a_1^\pm\pi^\mp$			
BABAR [324]	384M	$-0.07 \pm 0.07 \pm 0.02$	$-0.10 \pm 0.15 \pm 0.09$	$0.37 \pm 0.21 \pm 0.07$	$0.26 \pm 0.15 \pm 0.07$	$-0.14 \pm 0.21 \pm 0.06$

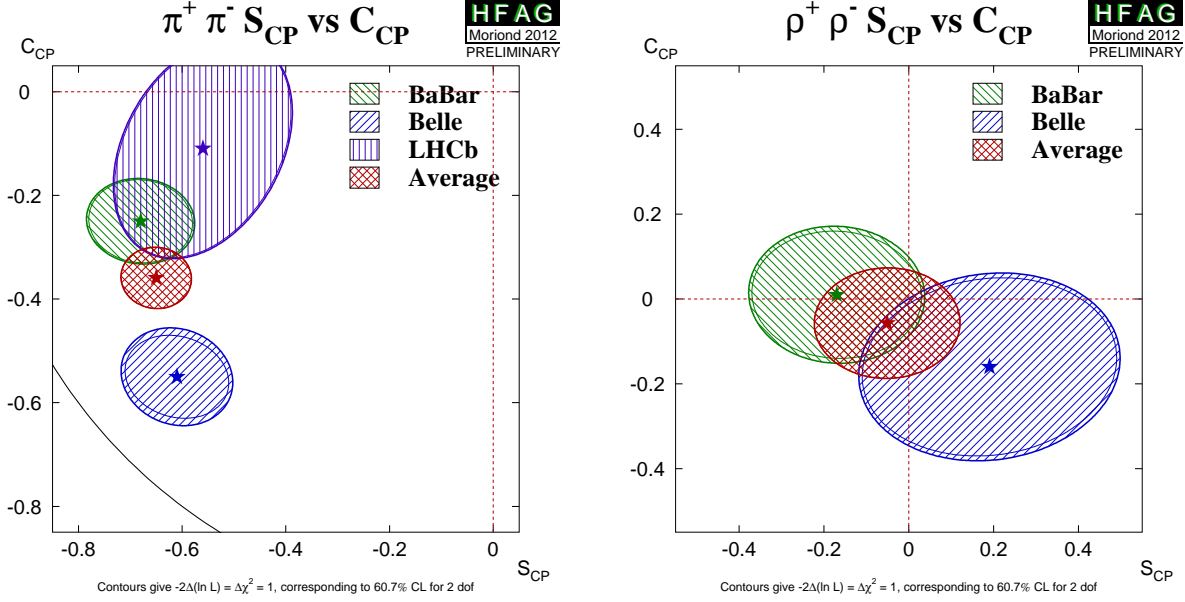


Figure 31: Averages of $b \rightarrow u\bar{u}d$ dominated channels, for which correlated averages are performed, in the S_{CP} vs. C_{CP} plane. (Left) $B^0 \rightarrow \pi^+\pi^-$ and (right) $B^0 \rightarrow \rho^+\rho^-$.

If the penguin contribution is negligible, the time-dependent parameters for $B^0 \rightarrow \pi^+\pi^-$ and $B^0 \rightarrow \rho^+\rho^-$ are given by $S_{b \rightarrow u\bar{u}d} = \eta \sin(2\alpha)$ and $C_{b \rightarrow u\bar{u}d} = 0$. In the presence of the penguin contribution, direct CP violation may arise, and there is no straightforward interpretation of $S_{b \rightarrow u\bar{u}d}$ and $C_{b \rightarrow u\bar{u}d}$. An isospin analysis [329] can be used to disentangle the contributions and extract α .

For the non- CP eigenstate $\rho^\pm\pi^\mp$, both *BABAR* [222] and *Belle* [223, 224] have performed time-dependent Dalitz plot (DP) analyses of the $\pi^+\pi^-\pi^0$ final state [220]; such analyses allow direct measurements of the phases. Both experiments have measured the U and I parameters discussed in Sec. 4.2.5 and defined in Table 22. We have performed a full correlated average of these parameters, the results of which are summarised in Fig. 32.

Both experiments have also extracted the Q2B parameters. We have performed a full correlated average of these parameters, which is equivalent to determining the values from the averaged U and I parameters. The results are shown in Table. 44. Averages of the $B^0 \rightarrow \rho^0\pi^0$ Q2B parameters are shown in Figs. 33 and 34.

With the notation described in Sec. 4.2 (Eq. (125)), the time-dependent parameters for the Q2B $B^0 \rightarrow \rho^\pm\pi^\mp$ analysis are, neglecting penguin contributions, given by

$$S_{\rho\pi} = \sqrt{1 - \left(\frac{\Delta C}{2}\right)^2} \sin(2\alpha) \cos(\delta), \quad \Delta S_{\rho\pi} = \sqrt{1 - \left(\frac{\Delta C}{2}\right)^2} \cos(2\alpha) \sin(\delta) \quad (154)$$

and $C_{\rho\pi} = \mathcal{A}_{CP}^{\rho\pi} = 0$, where $\delta = \arg(A_{-+}A_{+-}^*)$ is the strong phase difference between the $\rho^-\pi^+$ and $\rho^+\pi^-$ decay amplitudes. In the presence of the penguin contribution, there is no straightforward interpretation of the Q2B observables in the $B^0 \rightarrow \rho^\pm\pi^\mp$ system in terms of CKM parameters. However direct CP violation may arise, resulting in either or both of $C_{\rho\pi} \neq 0$ and $\mathcal{A}_{CP}^{\rho\pi} \neq 0$. Equivalently, direct CP violation may be seen by either of the decay-type-specific observables $\mathcal{A}_{\rho\pi}^{+-}$ and $\mathcal{A}_{\rho\pi}^{-+}$, defined in Eq. (126), deviating from zero. Results and averages for

Table 44: Averages of quasi-two-body parameters extracted from time-dependent Dalitz plot analysis of $B^0 \rightarrow \pi^+ \pi^- \pi^0$.

Experiment	$N(B\bar{B})$	$\mathcal{A}_{CP}^{\rho\pi}$	$C_{\rho\pi}$	$S_{\rho\pi}$	$\Delta C_{\rho\pi}$	$\Delta S_{\rho\pi}$
BABAR [222]	375M	$-0.14 \pm 0.05 \pm 0.02$	$0.15 \pm 0.09 \pm 0.05$	$-0.03 \pm 0.11 \pm 0.04$	$0.39 \pm 0.09 \pm 0.09$	$-0.01 \pm 0.14 \pm 0.06$
Belle [223, 224]	449M	$-0.12 \pm 0.05 \pm 0.04$	$-0.13 \pm 0.09 \pm 0.05$	$0.06 \pm 0.13 \pm 0.05$	$0.36 \pm 0.10 \pm 0.05$	$-0.08 \pm 0.13 \pm 0.05$
Average		-0.13 ± 0.04	0.01 ± 0.07	0.01 ± 0.09	0.37 ± 0.08	-0.04 ± 0.10
Confidence level				$0.52 (0.6\sigma)$		

Experiment	$N(B\bar{B})$	$\mathcal{A}_{\rho\pi}^{-+}$	$\mathcal{A}_{\rho\pi}^{+-}$	Correlation
BABAR [222]	375M	$-0.37^{+0.16}_{-0.10} \pm 0.09$	$0.03 \pm 0.07 \pm 0.04$	0.62
Belle [223, 224]	449M	$0.08 \pm 0.16 \pm 0.11$	$0.21 \pm 0.08 \pm 0.04$	0.47
Average		-0.18 ± 0.12	0.11 ± 0.06	0.40
Confidence level			$0.14 (1.5\sigma)$	

Experiment	$N(B\bar{B})$	$C_{\rho^0\pi^0}$	$S_{\rho^0\pi^0}$	Correlation
BABAR [222]	375M	$-0.10 \pm 0.40 \pm 0.53$	$0.04 \pm 0.44 \pm 0.18$	0.35
Belle [223, 224]	449M	$0.49 \pm 0.36 \pm 0.28$	$0.17 \pm 0.57 \pm 0.35$	0.08
Average		0.30 ± 0.38	0.12 ± 0.38	0.12
Confidence level			$0.76 (0.3\sigma)$	

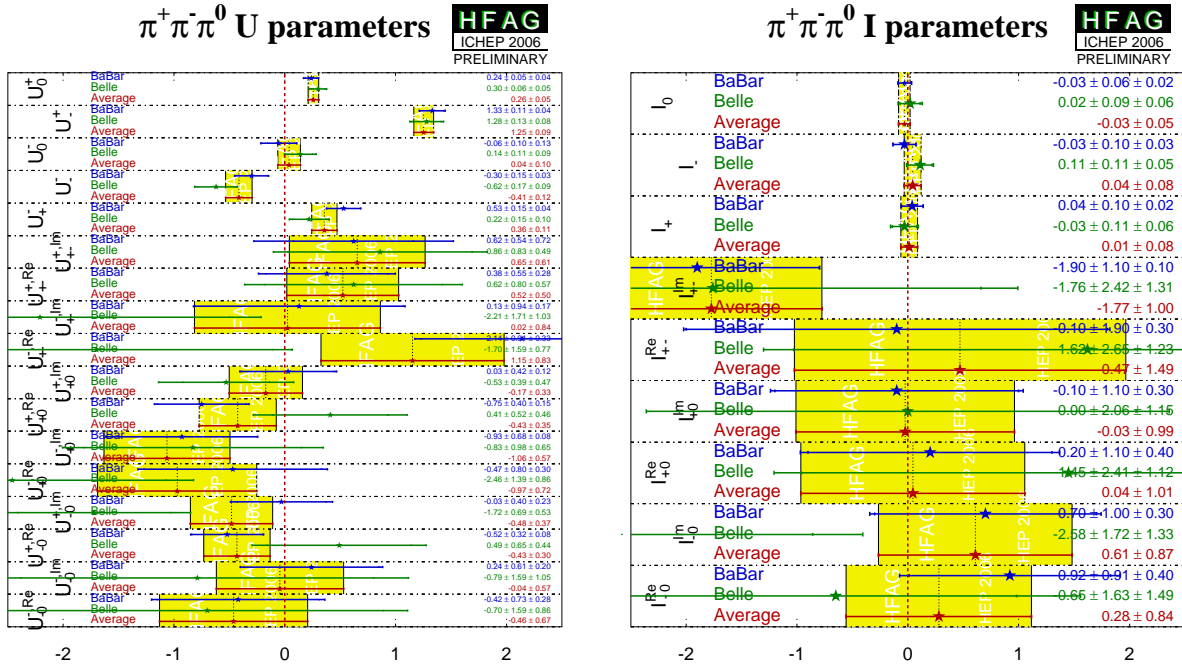


Figure 32: Summary of the U and I parameters measured in the time-dependent $B^0 \rightarrow \pi^+\pi^-\pi^0$ Dalitz plot analysis.

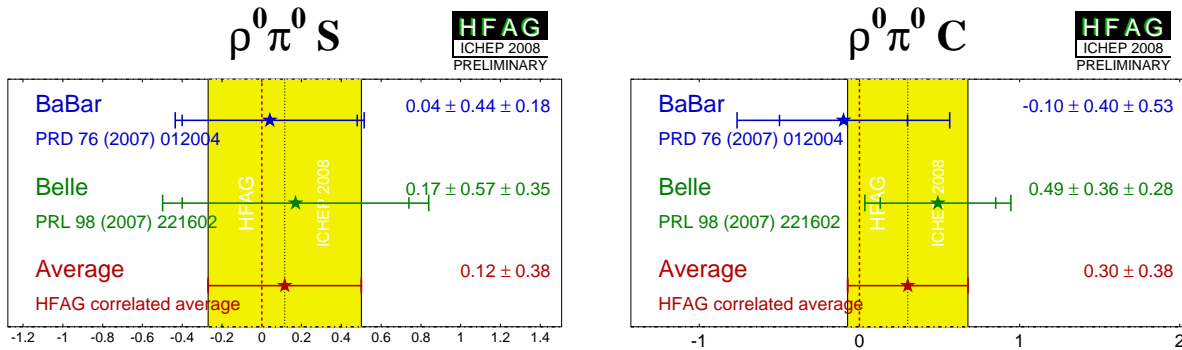


Figure 33: Averages of (left) $S_{b \rightarrow u\bar{d}}$ and (right) $C_{b \rightarrow u\bar{d}}$ for the mode $B^0 \rightarrow \rho^0\pi^0$.

these parameters are also given in Table 44. Averages of the direct CP violation effect in $B^0 \rightarrow \rho^\pm\pi^\mp$ are shown in Fig. 35, both in $\mathcal{A}_{CP}^{\rho\pi}$ vs. $C_{\rho\pi}$ space and in $\mathcal{A}_{\rho\pi}^-$ vs. $\mathcal{A}_{\rho\pi}^+$ space.

Some difference is seen between the *BABAR* and *Belle* measurements in the $\pi^+\pi^-$ system. The confidence level of the average is 0.034, which corresponds to a 2.1σ discrepancy. Since there is no evidence of systematic problems in either analysis, we do not rescale the errors of the averages. The averages for $S_{b \rightarrow u\bar{d}}$ and $C_{b \rightarrow u\bar{d}}$ in $B^0 \rightarrow \pi^+\pi^-$ are both more than 5σ away from zero, suggesting that both mixing-induced and direct CP violation are well-established in this channel. Nonetheless, due to the possible discrepancy mentioned above, a slightly cautious interpretation should be made with regard to the significance of direct CP violation.

In $B^0 \rightarrow \rho^\pm\pi^\mp$, however, both experiments see an indication of direct CP violation in the

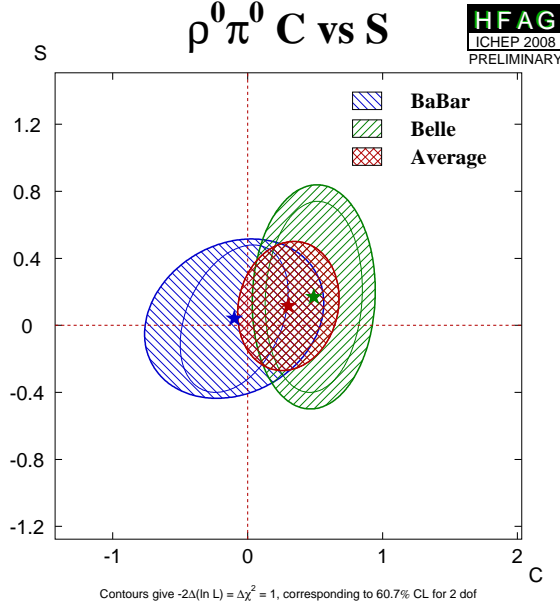


Figure 34: Averages of $b \rightarrow u\bar{u}d$ dominated channels, for the mode $B^0 \rightarrow \rho^0\pi^0$ in the S_{CP} vs. C_{CP} plane.

$\mathcal{A}_{CP}^{\rho\pi}$ parameter (as seen in Fig. 35). The average is more than 3σ from zero, providing evidence of direct CP violation in this channel.

Constraints on α

The precision of the measured CP violation parameters in $b \rightarrow u\bar{u}d$ transitions allows constraints to be set on the UT angle α . Constraints have been obtained with various methods:

- Both *BABAR* [330] and Belle [327] have performed isospin analyses in the $\pi\pi$ system. Belle exclude $9^\circ < \phi_2 < 81^\circ$ at the 95.4% C.L. while *BABAR* give a confidence level interpretation for α , exclude the range $23^\circ < \alpha < 67^\circ$ at the 90% C.L. In both cases, only solutions in 0° – 180° are considered.
- Both experiments have also performed isospin analyses in the $\rho\rho$ system. The most recent result from *BABAR* is given in an update of the measurements of the $B^+ \rightarrow \rho^+\rho^0$ decay [331], and sets the constraint $\alpha = (92.4_{-6.5}^{+6.0})^\circ$. The most recent result from Belle is given in an update of the search for the $B^0 \rightarrow \rho^0\rho^0$ decay and sets the constraint $\phi_2 = (91.7 \pm 14.9)^\circ$ [323].
- The time-dependent Dalitz plot analysis of the $B^0 \rightarrow \pi^+\pi^-\pi^0$ decay allows a determination of α without input from any other channels. *BABAR* [222] obtain the constraint $75^\circ < \alpha < 152^\circ$ at 68% C.L. Belle [223, 224] have performed a similar analysis, and in addition have included information from the SU(2) partners of $B \rightarrow \rho\pi$, which can be used to constrain α via an isospin pentagon relation [332]. With this analysis, Belle obtain the tighter constraint $\phi_2 = (83_{-23}^{+12})^\circ$ (where the errors correspond to 1σ , *i.e.* 68.3% confidence level).
- The results from *BABAR* on $B^0 \rightarrow a_1^\pm\pi^\mp$ [324] can be combined with results from modes related by isospin [333] leading to the following constraint: $\alpha = (79 \pm 7 \pm 11)^\circ$ [325].

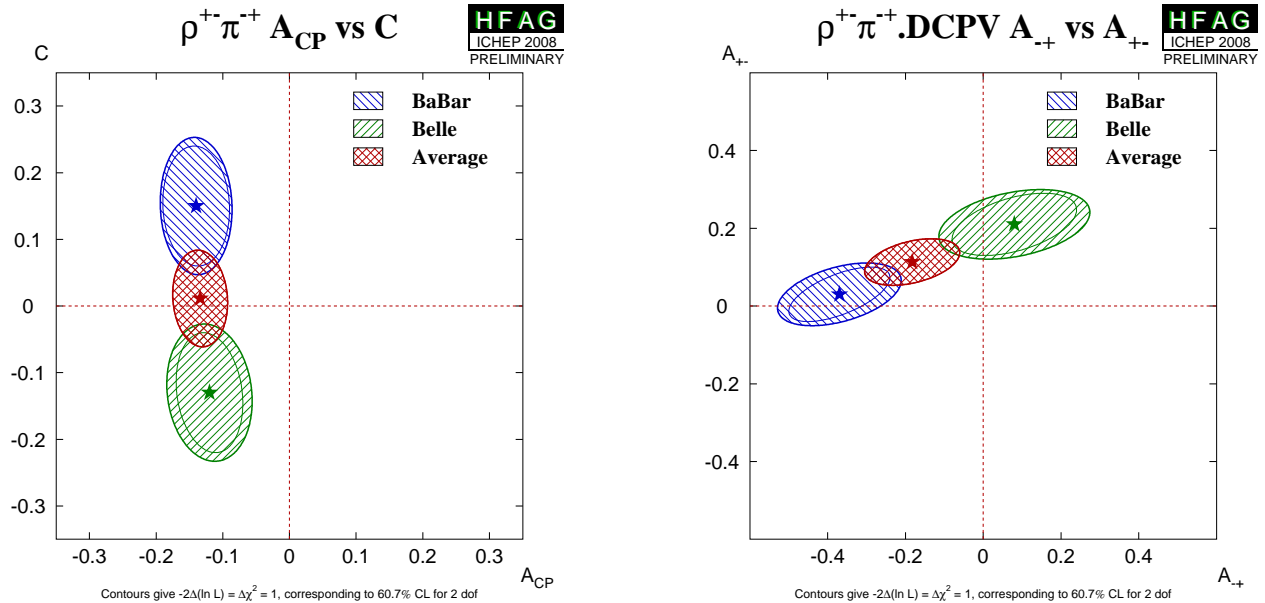


Figure 35: Direct CP violation in $B^0 \rightarrow \rho^\pm \pi^\mp$. (Left) $\mathcal{A}_{CP}^{\rho\pi}$ vs. $C_{\rho\pi}$ space, (right) $\mathcal{A}_{\rho\pi}^{-+}$ vs. $\mathcal{A}_{\rho\pi}^{+-}$ space.

- Each experiment has obtained a value of α from combining its results in the different $b \rightarrow u\bar{u}d$ modes (with some input also from HFAG). These values have appeared in talks, but not in publications, and are not listed here.
- The CKMfitter [225] and UTfit [268] groups use the measurements from Belle and *BABAR* given above with other branching fractions and CP asymmetries in $B \rightarrow \pi\pi$, $\rho\pi$ and $\rho\rho$ modes, to perform isospin analyses for each system, and to make combined constraints on α .

Note that methods based on isospin symmetry make extensive use of measurements of branching fractions and direct CP asymmetries, as averaged by the HFAG Rare Decays subgroup (Sec. 7). Note also that each method suffers from discrete ambiguities in the solutions. The model assumption in the $B^0 \rightarrow \pi^+\pi^-\pi^0$ analysis allows to resolve some of the multiple solutions, and results in a single preferred value for α in $[0, \pi]$. All the above measurements correspond to the choice that is in agreement with the global CKM fit.

At present we make no attempt to provide an HFAG average for α . More details on procedures to calculate a best fit value for α can be found in Refs. [225, 268].

4.12 Time-dependent CP asymmetries in $b \rightarrow c\bar{u}d/u\bar{c}d$ transitions

Non- CP eigenstates such as $D^\pm\pi^\mp$, $D^{*\pm}\pi^\mp$ and $D^\pm\rho^\mp$ can be produced in decays of B^0 mesons either via Cabibbo favoured ($b \rightarrow c$) or doubly Cabibbo suppressed ($b \rightarrow u$) tree amplitudes. Since no penguin contribution is possible, these modes are theoretically clean. The ratio of the magnitudes of the suppressed and favoured amplitudes, R , is sufficiently small (predicted to be about 0.02), that terms of $\mathcal{O}(R^2)$ can be neglected, and the sine terms give sensitivity to the combination of UT angles $2\beta + \gamma$.

As described in Sec. 4.2.6, the averages are given in terms of parameters a and c . CP violation would appear as $a \neq 0$. Results are available from both *BABAR* and Belle in the modes $D^\pm\pi^\mp$ and $D^{*\pm}\pi^\mp$; for the latter mode both experiments have used both full and partial reconstruction techniques. Results are also available from *BABAR* using $D^\pm\rho^\mp$. These results, and their averages, are listed in Table 45, and are shown in Fig. 36. The constraints in c vs. a space for the $D\pi$ and $D^*\pi$ modes are shown in Fig. 37. It is notable that the average value of a from $D^*\pi$ is more than 3σ from zero, providing evidence of CP violation in this channel.

Table 45: Averages for $b \rightarrow c\bar{u}d/u\bar{c}d$ modes.

Experiment		$N(B\bar{B})$	a	c
$D^\pm\pi^\mp$				
<i>BABAR</i> (full rec.)	[231]	232M	$-0.010 \pm 0.023 \pm 0.007$	$-0.033 \pm 0.042 \pm 0.012$
Belle (full rec.)	[235]	386M	$-0.050 \pm 0.021 \pm 0.012$	$-0.019 \pm 0.021 \pm 0.012$
Average			-0.030 ± 0.017	-0.022 ± 0.021
Confidence level			0.24 (1.2 σ)	0.78 (0.3 σ)
$D^{*\pm}\pi^\mp$				
<i>BABAR</i> (full rec.)	[231]	232M	$-0.040 \pm 0.023 \pm 0.010$	$0.049 \pm 0.042 \pm 0.015$
<i>BABAR</i> (partial rec.)	[232]	232M	$-0.034 \pm 0.014 \pm 0.009$	$-0.019 \pm 0.022 \pm 0.013$
Belle (full rec.)	[235]	386M	$-0.039 \pm 0.020 \pm 0.013$	$-0.011 \pm 0.020 \pm 0.013$
Belle (partial rec.)	[234]	657M	$-0.046 \pm 0.013 \pm 0.015$	$-0.015 \pm 0.013 \pm 0.015$
Average			-0.039 ± 0.013	-0.017 ± 0.016
Confidence level			0.97 (0.03 σ)	0.59 (0.6 σ)
$D^\pm\rho^\mp$				
<i>BABAR</i> (full rec.)	[231]	232M	$-0.024 \pm 0.031 \pm 0.009$	$-0.098 \pm 0.055 \pm 0.018$

For each of $D\pi$, $D^*\pi$ and $D\rho$, there are two measurements (a and c , or S^+ and S^-) which depend on three unknowns (R , δ and $2\beta + \gamma$), of which two are different for each decay mode. Therefore, there is not enough information to solve directly for $2\beta + \gamma$. However, for each choice of R and $2\beta + \gamma$, one can find the value of δ that allows a and c to be closest to their measured values, and calculate the distance in terms of numbers of standard deviations. (We currently neglect experimental correlations in this analysis.) These values of $N(\sigma)_{\min}$ can then be plotted as a function of R and $2\beta + \gamma$ (and can trivially be converted to confidence levels). These plots are given for the $D\pi$ and $D^*\pi$ modes in Figure 37; the uncertainties in the $D\rho$ mode are currently too large to give any meaningful constraint.

The constraints can be tightened if one is willing to use theoretical input on the values of R and/or δ . One popular choice is the use of SU(3) symmetry to obtain R by relating

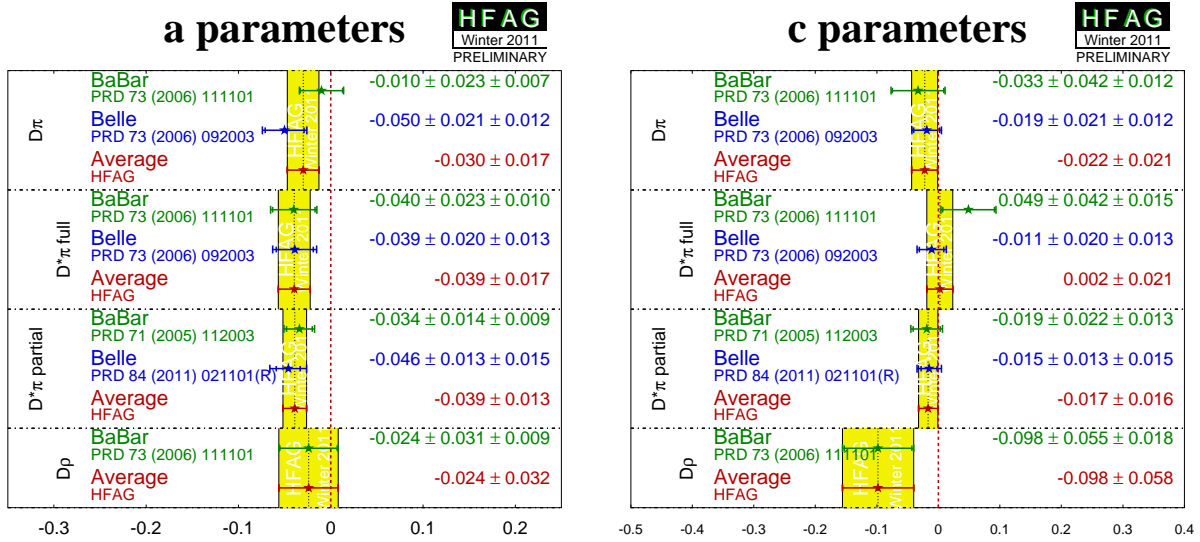


Figure 36: Averages for $b \rightarrow \bar{c}u\bar{d}/u\bar{c}d$ modes.

the suppressed decay mode to B decays involving D_s mesons. More details can be found in Refs. [225, 268].

4.13 Time-dependent CP asymmetries in $b \rightarrow \bar{c}u\bar{s}/u\bar{c}s$ transitions

Time-dependent analyses of transitions such as $B^0 \rightarrow D^\pm K_s^0 \pi^\mp$ can be used to probe $\sin(2\beta + \gamma)$ in a similar way to that discussed above (Sec. 4.12). Since the final state contains three particles, a Dalitz plot analysis is necessary to maximise the sensitivity. *BABAR* [334] have carried out such an analysis. They obtain $2\beta + \gamma = (83 \pm 53 \pm 20)^\circ$ (with an ambiguity $2\beta + \gamma \leftrightarrow 2\beta + \gamma + \pi$) assuming the ratio of the $b \rightarrow u$ and $b \rightarrow c$ amplitude to be constant across the Dalitz plot at 0.3.

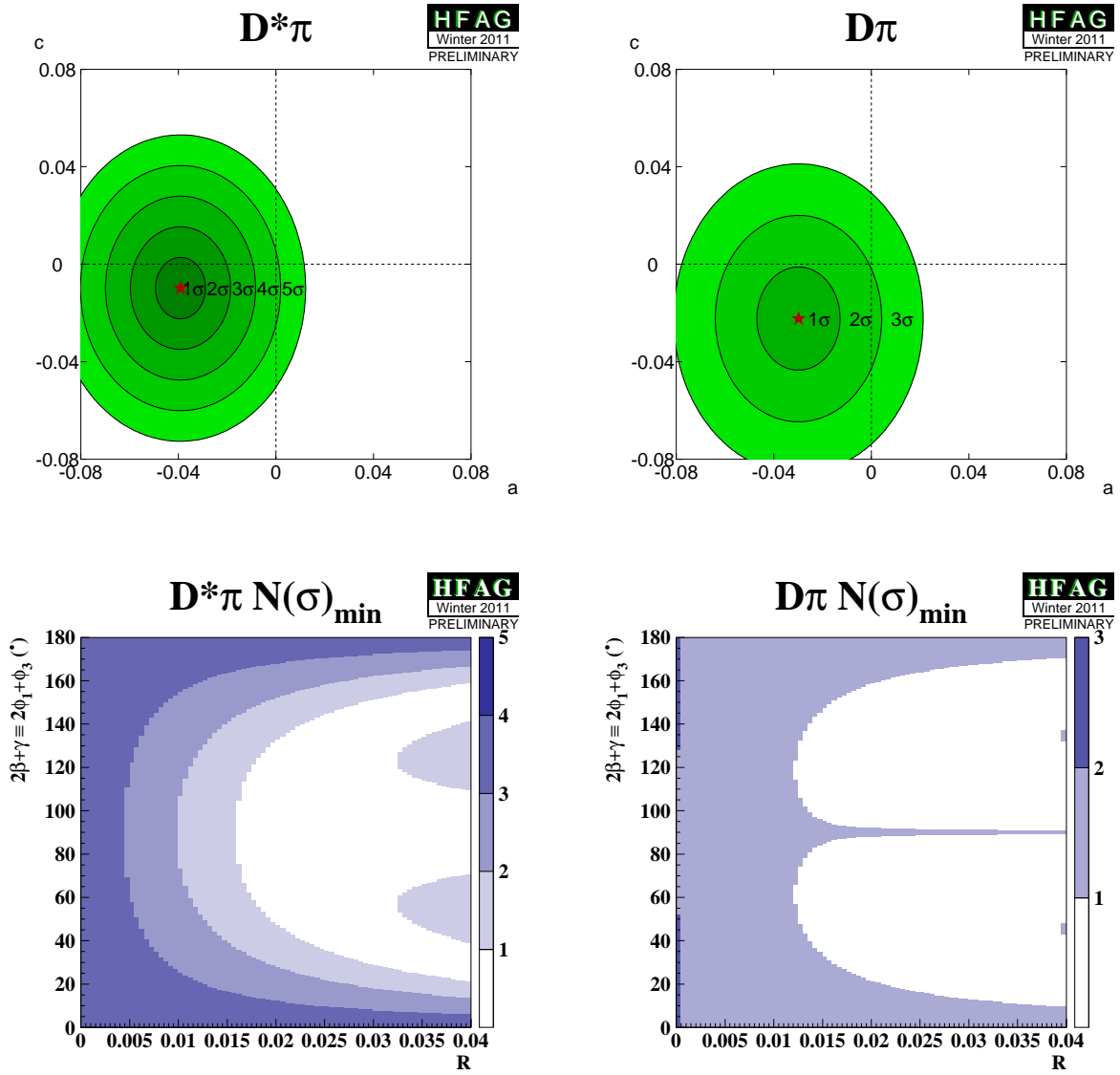


Figure 37: Results from $b \rightarrow \bar{c}u\bar{d}/u\bar{c}d$ modes. (Top) Constraints in c vs. a space. (Bottom) Constraints in $2\beta + \gamma$ vs. R space. (Left) $D^*\pi$ and (right) $D\pi$ modes.

4.14 Rates and asymmetries in $B^\mp \rightarrow D^{(*)}K^{(*)\mp}$ decays

As explained in Sec. 4.2.7, rates and asymmetries in $B^\mp \rightarrow D^{(*)}K^{(*)\mp}$ decays are sensitive to γ . Various methods using different $D^{(*)}$ final states exist.

4.14.1 D decays to CP eigenstates

Results are available from both *BABAR* and Belle on GLW analyses in the decay modes $B^\mp \rightarrow DK^\mp$, $B^\mp \rightarrow D^*K^\mp$ and $B^\mp \rightarrow DK^{*\mp}$.⁴³ Both experiments use the CP -even D decay final states K^+K^- and $\pi^+\pi^-$ in all three modes; both experiments generally use the CP -odd decay modes $K_S^0\pi^0$, $K_S^0\omega$ and $K_S^0\phi$, though care is taken to avoid statistical overlap with the $K_S^0K^+K^-$ sample used for Dalitz plot analysis (see Sec. 4.14.3), and asymmetric systematic errors are assigned due to CP -even pollution under the $K_S^0\omega$ and $K_S^0\phi$ signals. Both experiments also use the $D^* \rightarrow D\pi^0$ decay, which gives $CP(D^*) = CP(D)$; *BABAR* in addition use the $D^* \rightarrow D\gamma$ decays, which gives $CP(D^*) = -CP(D)$. In addition, results from CDF and LHCb are available in the decay mode $B^\mp \rightarrow DK^\mp$, for CP -even final states (K^+K^- and $\pi^+\pi^-$) only. The results and averages are given in Table 46 and shown in Fig. 38.

Table 46: Averages from GLW analyses of $b \rightarrow c\bar{u}s/u\bar{c}s$ modes.

Experiment	Sample size	A_{CP+}	A_{CP-}	R_{CP+}	R_{CP-}
$D_{CP}K^-$					
<i>BABAR</i> [336]	$N(B\bar{B}) = 467\text{M}$	$0.25 \pm 0.06 \pm 0.02$	$-0.09 \pm 0.07 \pm 0.02$	$1.18 \pm 0.09 \pm 0.05$	$1.07 \pm 0.08 \pm 0.04$
Belle [337]	$N(B\bar{B}) = 772\text{M}$	$0.29 \pm 0.06 \pm 0.02$	$-0.12 \pm 0.06 \pm 0.01$	$1.03 \pm 0.07 \pm 0.03$	$1.13 \pm 0.09 \pm 0.05$
CDF [338]	1 fb^{-1}	$0.39 \pm 0.17 \pm 0.04$	–	$1.30 \pm 0.24 \pm 0.12$	–
LHCb [339]	1 fb^{-1}	$0.14 \pm 0.03 \pm 0.01$	–	$1.01 \pm 0.04 \pm 0.01$	–
Average		0.19 ± 0.03	-0.11 ± 0.05	1.03 ± 0.03	1.10 ± 0.07
Confidence level		$0.09 (1.7\sigma)$	$0.75 (0.3\sigma)$	$0.33 (1.0\sigma)$	$0.66 (0.4\sigma)$
$D_{CP}^*K^-$					
<i>BABAR</i> [340]	$N(B\bar{B}) = 383\text{M}$	$-0.11 \pm 0.09 \pm 0.01$	$0.06 \pm 0.10 \pm 0.02$	$1.31 \pm 0.13 \pm 0.03$	$1.09 \pm 0.12 \pm 0.04$
Belle [341]	$N(B\bar{B}) = 275\text{M}$	$-0.20 \pm 0.22 \pm 0.04$	$0.13 \pm 0.30 \pm 0.08$	$1.41 \pm 0.25 \pm 0.06$	$1.15 \pm 0.31 \pm 0.12$
Average		-0.12 ± 0.08	0.07 ± 0.10	1.33 ± 0.12	1.10 ± 0.12
Confidence level		$0.71 (0.4\sigma)$	$0.83 (0.2\sigma)$	$0.73 (0.4\sigma)$	$0.87 (0.2\sigma)$
$D_{CP}K^{*-}$					
<i>BABAR</i> [342]	$N(B\bar{B}) = 379\text{M}$	$0.09 \pm 0.13 \pm 0.06$	$-0.23 \pm 0.21 \pm 0.07$	$2.17 \pm 0.35 \pm 0.09$	$1.03 \pm 0.27 \pm 0.13$

4.14.2 D decays to suppressed final states

For ADS analysis, both *BABAR* and Belle have studied the modes $B^\mp \rightarrow DK^\mp$ and $B^\mp \rightarrow D\pi^\mp$. *BABAR* has also analysed the $B^\mp \rightarrow D^*K^\mp$ and $B^\mp \rightarrow DK^{*\mp}$ modes. There is an effective shift of π in the strong phase difference between the cases that the D^* is reconstructed as $D\pi^0$ and $D\gamma$ [250], therefore these modes are studied separately. $K^{*\mp}$ is reconstructed as $K_S^0\pi^\mp$. In all cases the suppressed decay $D \rightarrow K^+\pi^-$ has been used. *BABAR* also has results using $B^\mp \rightarrow DK^\mp$ with $D \rightarrow K^+\pi^-\pi^0$. The results and averages are given in Table 47 and shown in Figs. 39 and 40.

⁴³ We do not include a preliminary result from Belle [335], which remains unpublished after more than two years.

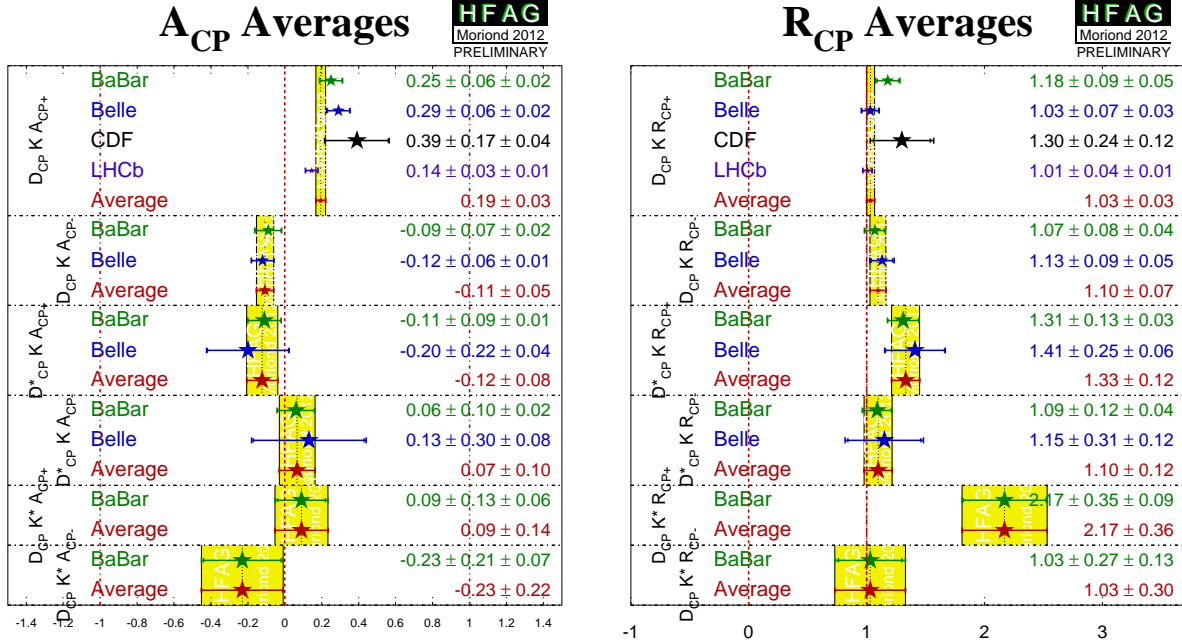


Figure 38: Averages of A_{CP} and R_{CP} from GLW analyses.

BABAR [347] have also presented results on a similar analysis with self-tagging neutral B decays: $B^0 \rightarrow DK^{*0}$ with $D \rightarrow K^-\pi^+$, $D \rightarrow K^-\pi^+\pi^0$ and $D \rightarrow K^-\pi^+\pi^+\pi^-$ (all with $K^{*0} \rightarrow K^+\pi^-$). Effects due to the natural width of the K^{*0} are handled using the parametrisation suggested by Gronau [348].

The following 95% C.L. limits are set:

$$R_{ADS}(K\pi) < 0.244 \quad R_{ADS}(K\pi\pi^0) < 0.181 \quad R_{ADS}(K\pi\pi\pi) < 0.391. \quad (155)$$

Combining the results and using additional input from CLEOc [349,350] a limit on the ratio between the $b \rightarrow u$ and $b \rightarrow c$ amplitudes of $r_s \in [0.07, 0.41]$ at 95% C.L. limit is set.

Belle [351] have obtained the constraint

$$R_{ADS}(K\pi) < 0.16. \quad (156)$$

4.14.3 D decays to multiparticle self-conjugate final states

For the Dalitz plot analysis, both *BABAR* [352] and Belle [353, 354] have studied the modes $B^\mp \rightarrow DK^\mp$, $B^\mp \rightarrow D^*K^\mp$ and $B^\mp \rightarrow DK^{*\mp}$. For $B^\mp \rightarrow D^*K^\mp$, both experiments have used both D^* decay modes, $D^* \rightarrow D\pi^0$ and $D^* \rightarrow D\gamma$, taking the effective shift in the strong phase difference into account. In all cases the decay $D \rightarrow K_s^0\pi^+\pi^-$ has been used. *BABAR* also used the decay $D \rightarrow K_s^0K^+K^-$. *BABAR* has also performed an analysis of $B^\mp \rightarrow DK^\mp$ with $D \rightarrow \pi^+\pi^-\pi^0$ [255]. Results and averages are given in Table 48. The third error on each measurement is due to D decay model uncertainty.

The parameters measured in the analyses are explained in Sec. 4.2.7. Both *BABAR* and Belle have measured the ‘‘Cartesian’’ (x_\pm, y_\pm) variables, and perform frequentist statistical

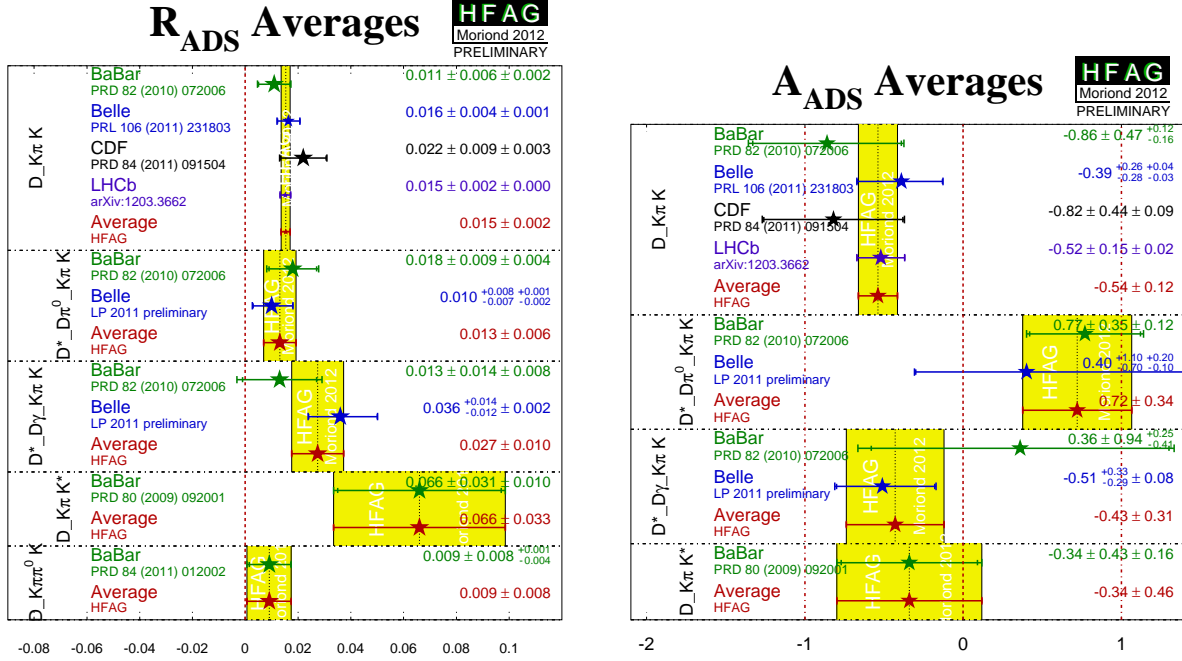


Figure 39: Averages of R_{ADS} and A_{ADS} for $B \rightarrow D^{(*)}K^{(*)}$ decays.

procedures, to convert these into measurements of γ , r_B and δ_B . In the $B^\mp \rightarrow DK^\mp$ with $D \rightarrow \pi^+\pi^-\pi^0$ analysis, the parameters (ρ^\pm, θ^\pm) are used instead.

Both experiments reconstruct $K^{*\mp}$ as $K_s^0\pi^\mp$, but the treatment of possible nonresonant $K_s^0\pi^\mp$ differs: Belle assign an additional model uncertainty, while BABAR use a parametrisation suggested by Gronau [348]. The parameters r_B and δ_B are replaced with effective parameters κr_s and δ_s ; no attempt is made to extract the true hadronic parameters of the $B^\mp \rightarrow DK^{*\mp}$ decay.

We perform averages using the following procedure, which is based on a set of (more or less) reasonable, though imperfect, assumptions.

- It is assumed that effects due to the different D decay models used by the two experiments are negligible. Therefore, we do not rescale the results to a common model.
- It is further assumed that the model uncertainty is 100% correlated between experiments, and therefore this source of error is not used in the averaging procedure. (This approximation is significantly less valid now that the BABAR results include $D \rightarrow K_s^0 K^+ K^-$ decays in addition to $D \rightarrow K_s^0 \pi^+ \pi^-$.)
- We include in the average the effect of correlations within each experiments set of measurements.
- At present it is unclear how to assign an average model uncertainty. We have not attempted to do so. Our average includes only statistical and systematic error. An unknown amount of model uncertainty should be added to the final error.
- We follow the suggestion of Gronau [348] in making the DK^* averages. Explicitly, we assume that the selection of $K^{*\pm} \rightarrow K_s^0 \pi^\pm$ is the same in both experiments (so that κ ,

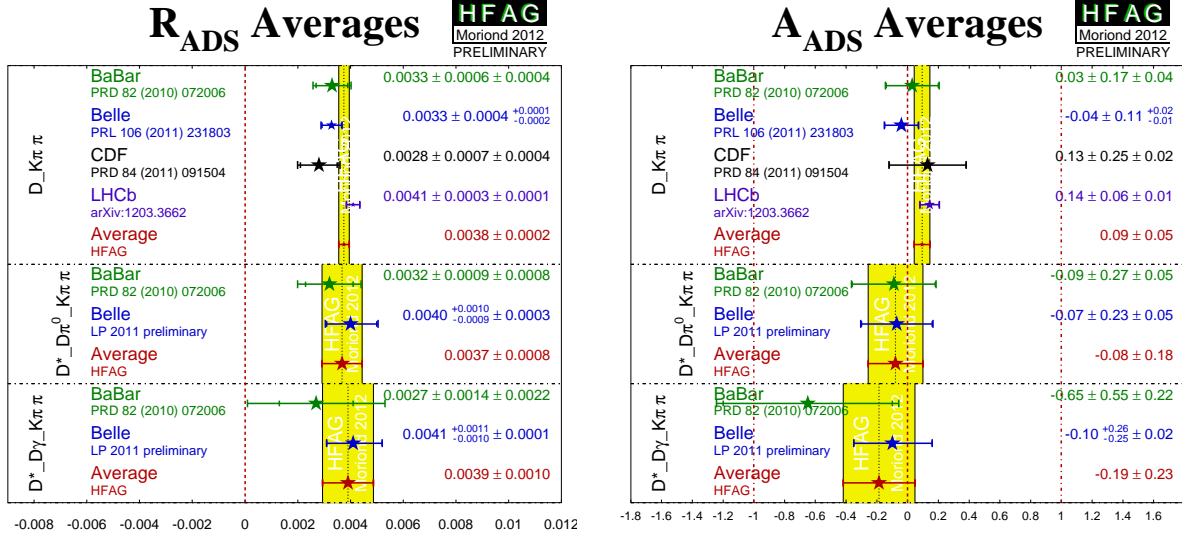


Figure 40: Averages of R_{ADS} and A_{ADS} for $B \rightarrow D^{(*)}\pi$ decays.

r_s and δ_s are the same), and drop the additional source of model uncertainty assigned by Belle due to possible nonresonant decays.

- We do not consider common systematic errors, other than the D decay model.

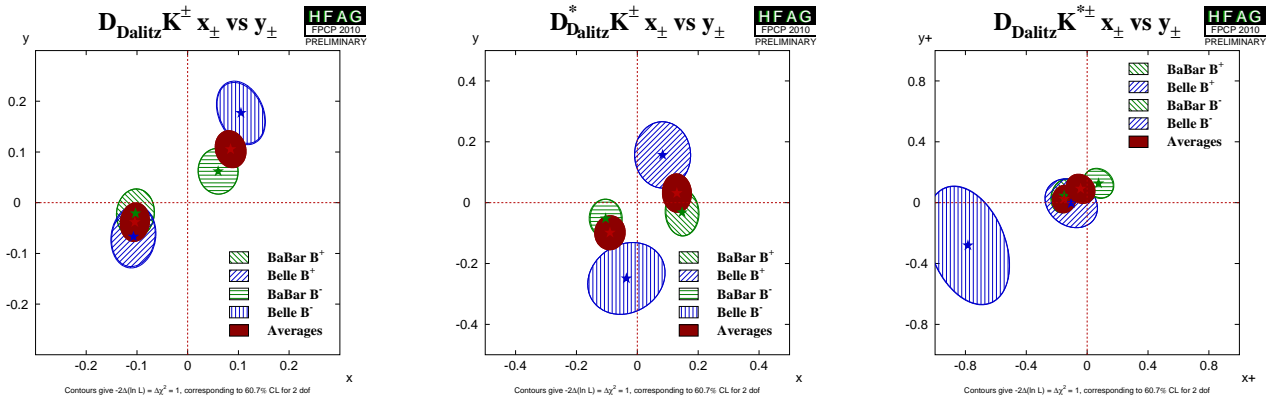


Figure 41: Contours in the (x_{\pm}, y_{\pm}) from $B^{\mp} \rightarrow D^{(*)}K^{(*)\pm}$. (Left) $B^{\mp} \rightarrow DK^{\mp}$, (middle) $B^{\mp} \rightarrow D^*K^{\mp}$, (right) $B^{\mp} \rightarrow DK^{*\mp}$. Note that the uncertainties assigned to the averages given in these plots do not include model errors.

Constraints on γ

The measurements of (x_{\pm}, y_{\pm}) can be used to obtain constraints on γ , as well as the hadronic parameters r_B and δ_B . Both *BABAR* [355] and Belle [353, 354] have done so using a frequentist procedure (there are some differences in the details of the techniques used).

- *BABAR* obtain $\gamma = (68_{-14}^{+15} \pm 4 \pm 3)^{\circ}$ from DK^{\pm} , D^*K^{\pm} and $DK^{*\pm}$

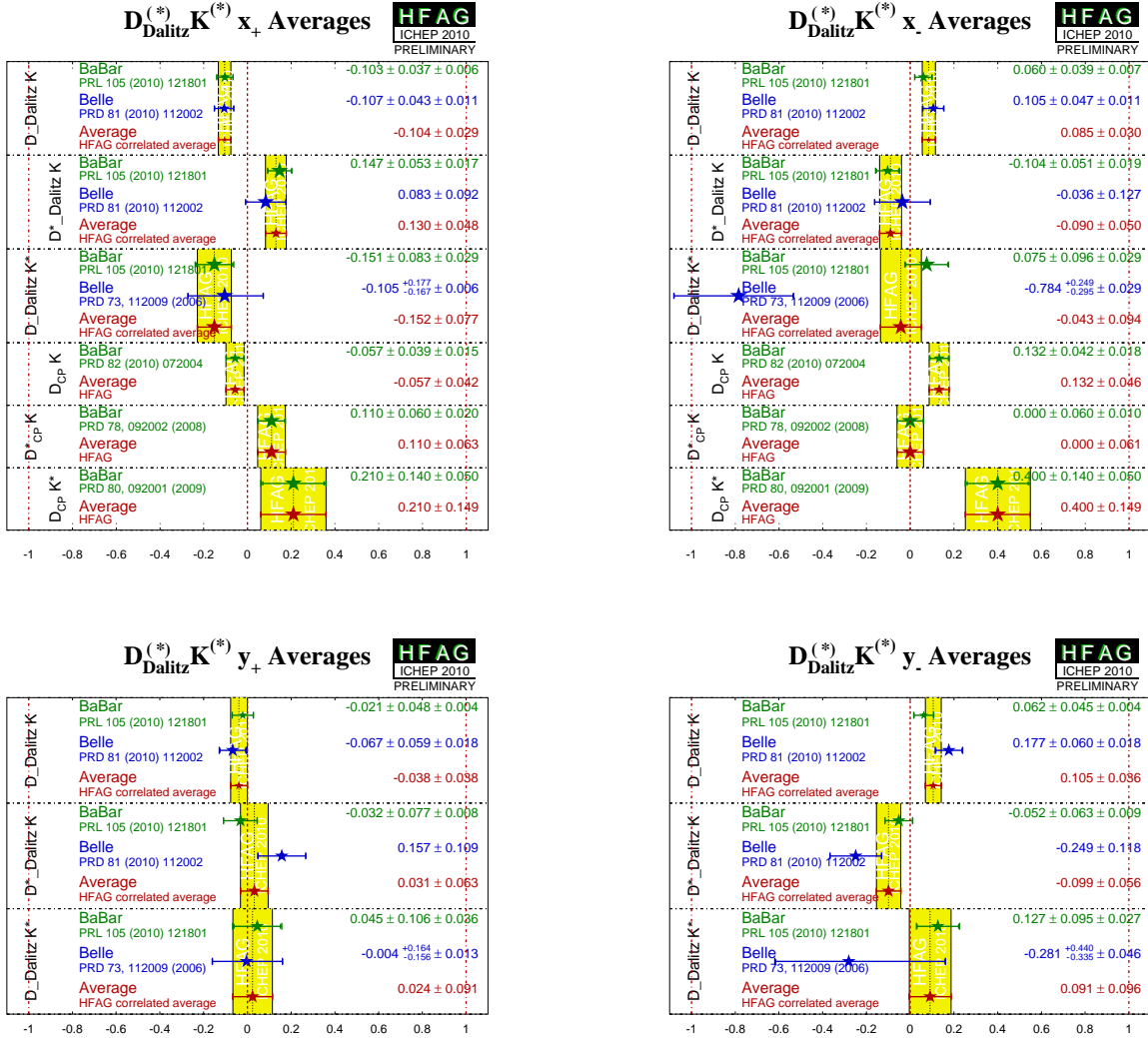


Figure 42: Averages of (x_{\pm}, y_{\pm}) from $B^{\pm} \rightarrow D^{(*)}K^{(*)\pm}$. (Top left) x_+ , (top right) x_- , (bottom left) y_+ , (bottom right) y_- . The top plots include constraints on x_{\pm} obtained from GLW analyses (see Sec. 4.14.1). Note that the uncertainties assigned to the averages given in these plots do not include model errors.

- Belle obtain $\phi_3 = (78_{-12}^{+11} \pm 4 \pm 9)^\circ$ from DK^{\pm} and D^*K^{\pm}
- The experiments also obtain values for the hadronic parameters as detailed in Tab. 49.
- Improved constraints can be achieved combining the information from $B^{\pm} \rightarrow DK^{\pm}$ analysis with different D decay modes. The experiments have not yet published such results, and none are listed here.
- The CKMfitter [225] and UTfit [268] groups use the measurements from Belle and BABAR given above to make combined constraints on γ .
- In the BABAR analysis of $B^{\mp} \rightarrow DK^{\mp}$ with $D \rightarrow \pi^+\pi^-\pi^0$ [255], a constraint of $-30^\circ < \gamma < 76^\circ$ is obtained at the 68% confidence level.

At present we make no attempt to provide an HFAG average for γ , nor indeed for the hadronic parameters. More details on procedures to calculate a best fit value for γ can be found in Refs. [225, 268].

BABAR [356] have also performed a similar Dalitz plot analysis to that described above using the self-tagging neutral B decay $B^0 \rightarrow DK^{*0}$ (with $K^{*0} \rightarrow K^+\pi^-$). Effects due to the natural width of the K^{*0} are handled using the parametrisation suggested by Gronau [348].

BABAR extract the three-dimensional likelihood for the parameters (γ, δ_S, r_S) and, combining with a separately measured PDF for r_S (using a Bayesian technique), obtain bounds on each of the three parameters.

$$\gamma = (162 \pm 56)^\circ \quad \delta_S = (62 \pm 57)^\circ \quad r_S < 0.55, \quad (157)$$

where the limit on r_S is at 95% probability. Note that there is an ambiguity in the solutions $(\gamma, \delta_S \leftrightarrow \gamma + \pi, \delta_S + \pi)$.

Table 47: Averages from ADS analyses of $b \rightarrow c\bar{u}s/u\bar{c}s$ and $b \rightarrow c\bar{u}d/u\bar{c}d$ modes.

Experiment	Sample size	A_{ADS}	R_{ADS}
$DK^-, D \rightarrow K^+\pi^-$			
BABAR [343]	$N(B\bar{B}) = 467\text{M}$	$-0.86 \pm 0.47^{+0.12}_{-0.16}$	$0.011 \pm 0.006 \pm 0.002$
Belle [344]	$N(B\bar{B}) = 772\text{M}$	$-0.39^{+0.26+0.04}_{-0.28-0.03}$	$0.0163^{+0.0044+0.0007}_{-0.0041-0.0013}$
CDF [345]	7 fb^{-1}	$-0.82 \pm 0.44 \pm 0.09$	$0.0220 \pm 0.0086 \pm 0.0026$
LHCb [339]	1 fb^{-1}	$-0.52 \pm 0.15 \pm 0.02$	$0.0152 \pm 0.0020 \pm 0.0004$
Average		-0.54 ± 0.12	0.0153 ± 0.0017
Confidence level		$0.77 (0.3\sigma)$	$0.78 (0.3\sigma)$
Experiment	$N(B\bar{B})$	A_{ADS}	R_{ADS}
$D^*K^-, D^* \rightarrow D\pi^0, D \rightarrow K^+\pi^-$			
BABAR [343]	467M	$0.77 \pm 0.35 \pm 0.12$	$0.018 \pm 0.009 \pm 0.004$
Belle [337]	772M	$0.4^{+1.1+0.2}_{-0.7-0.1}$	$0.010^{+0.008+0.001}_{-0.007-0.002}$
Average		0.72 ± 0.34	0.013 ± 0.006
Confidence level		$0.71 (0.4\sigma)$	$0.52 (0.6\sigma)$
$D^*K^-, D^* \rightarrow D\gamma, D \rightarrow K^+\pi^-$			
BABAR [343]	467M	$0.36 \pm 0.94^{+0.25}_{-0.41}$	$0.013 \pm 0.014 \pm 0.008$
Belle [337]	772M	$-0.51^{+0.33}_{-0.29} \pm 0.08$	$0.036^{+0.014}_{-0.012} \pm 0.002$
Average		-0.43 ± 0.31	0.027 ± 0.010
Confidence level		$0.42 (0.8\sigma)$	$0.26 (1.1\sigma)$
$DK^{*-}, D \rightarrow K^+\pi^-, K^{*-} \rightarrow K_S^0\pi^-$			
BABAR [342]	379M	$-0.34 \pm 0.43 \pm 0.16$	$0.066 \pm 0.031 \pm 0.010$
$DK^-, D \rightarrow K^+\pi^-\pi^0$			
BABAR [346]	474M	$0.0091^{+0.0082+0.0014}_{-0.0076-0.0037}$	
Experiment	Sample size	R_{ADS}	Correlation
$D\pi^-, D \rightarrow K^+\pi^-$			
BABAR [343]	$N(B\bar{B}) = 467\text{M}$	$0.03 \pm 0.17 \pm 0.04$	$0.0033 \pm 0.0006 \pm 0.0004$
Belle [344]	$N(B\bar{B}) = 772\text{M}$	$-0.04 \pm 0.11^{+0.02}_{-0.01}$	$0.00328^{+0.00038+0.00012}_{-0.00036-0.00018}$
CDF [345]	7 fb^{-1}	$0.13 \pm 0.25 \pm 0.02$	$0.00280 \pm 0.00070 \pm 0.00040$
LHCb [339]	1 fb^{-1}	$0.14300 \pm 0.06200 \pm 0.01100$	$0.00410 \pm 0.00025 \pm 0.00005$
Average		0.09 ± 0.05	0.00375 ± 0.00020
Confidence level		$0.53 (0.6\sigma)$	$0.17 (1.4\sigma)$
Experiment	$N(B\bar{B})$	R_{ADS}	Correlation
$D^*\pi^-, D^* \rightarrow D\pi^0, D \rightarrow K^+\pi^-$			
BABAR [343]	467M	$-0.09 \pm 0.27 \pm 0.05$	$0.0032 \pm 0.0009 \pm 0.0008$
Belle [337]	772M	$-0.07 \pm 0.23 \pm 0.05$	$0.0040^{+0.0010}_{-0.0009} \pm 0.0003$
Average		-0.08 ± 0.18	0.0037 ± 0.0008
Confidence level		$0.96 (0.1\sigma)$	$0.61 (0.5\sigma)$
$D^*\pi^-, D^* \rightarrow D\gamma, D \rightarrow K^+\pi^-$			
BABAR [343]	467M	$-0.65 \pm 0.55 \pm 0.22$	$0.0027 \pm 0.0014 \pm 0.0022$
Belle [337]	772M	$-0.10^{+0.26}_{-0.25} \pm 0.02$	$0.0041^{+0.0011}_{-0.0010} \pm 0.0001$
Average		-0.19 ± 0.23	0.0039 ± 0.0010
Confidence level		$0.39 (0.9\sigma)$	$0.62 (0.5\sigma)$

Table 48: Averages from Dalitz plot analyses of $b \rightarrow c\bar{u}s/u\bar{c}s$ modes. Note that the uncertainties assigned to the averages do not include model errors.

Experiment	$N(B\bar{B})$	x_+	y_+	x_-	y_-
$DK^-, D \rightarrow K_s^0 \pi^+ \pi^-$					
BABAR [355]	468M	$-0.103 \pm 0.037 \pm 0.006 \pm 0.007$	$-0.021 \pm 0.048 \pm 0.004 \pm 0.009$	$0.060 \pm 0.039 \pm 0.007 \pm 0.006$	$0.062 \pm 0.045 \pm 0.004 \pm 0.006$
Belle [353]	657M	$-0.107 \pm 0.043 \pm 0.011 \pm 0.055$	$-0.067 \pm 0.059 \pm 0.018 \pm 0.063$	$0.105 \pm 0.047 \pm 0.011 \pm 0.064$	$0.177 \pm 0.060 \pm 0.018 \pm 0.054$
Average		-0.104 ± 0.029	-0.038 ± 0.038	0.085 ± 0.030	0.105 ± 0.036
Confidence level				$0.47 (0.7\sigma)$	
$D^*K^-, D^* \rightarrow D\pi^0 \text{ or } D\gamma, D \rightarrow K_s^0 \pi^+ \pi^-$					
BABAR [355]	468M	$0.147 \pm 0.053 \pm 0.017 \pm 0.003$	$-0.032 \pm 0.077 \pm 0.008 \pm 0.006$	$-0.104 \pm 0.051 \pm 0.019 \pm 0.002$	$-0.052 \pm 0.063 \pm 0.009 \pm 0.007$
Belle [353]	657M	$0.083 \pm 0.092 \pm 0.081$	$0.157 \pm 0.109 \pm 0.063$	$-0.036 \pm 0.127 \pm 0.090$	$-0.249 \pm 0.118 \pm 0.049$
Average		0.130 ± 0.048	0.031 ± 0.063	-0.090 ± 0.050	-0.099 ± 0.056
Confidence level				$0.29 (1.1\sigma)$	
$DK^{*-}, D \rightarrow K_s^0 \pi^+ \pi^-$					
BABAR [355]	468M	$-0.151 \pm 0.083 \pm 0.029 \pm 0.006$	$0.045 \pm 0.106 \pm 0.036 \pm 0.008$	$0.075 \pm 0.096 \pm 0.029 \pm 0.007$	$0.127 \pm 0.095 \pm 0.027 \pm 0.006$
Belle [354]	386M	$-0.105^{+0.177}_{-0.167} \pm 0.006 \pm 0.088$	$-0.004^{+0.164}_{-0.156} \pm 0.013 \pm 0.095$	$-0.784^{+0.249}_{-0.295} \pm 0.029 \pm 0.097$	$-0.281^{+0.440}_{-0.335} \pm 0.046 \pm 0.086$
Average		-0.152 ± 0.077	0.024 ± 0.091	-0.043 ± 0.094	0.091 ± 0.096
Confidence level				$0.011 (2.5\sigma)$	
$DK^-, D \rightarrow \pi^+ \pi^- \pi^0$					
Experiment	$N(B\bar{B})$	ρ^+	θ^+	ρ^-	θ^-
BABAR [255]	324M	$0.75 \pm 0.11 \pm 0.04$	$147 \pm 23 \pm 1$	$0.72 \pm 0.11 \pm 0.04$	$173 \pm 42 \pm 2$

Table 49: Summary of constraints on hadronic parameters in $B^\pm \rightarrow D^{(*)}K^{(*)\pm}$ decays. Note the alternative parametrisation of the hadronic parameters used by *BABAR* in the $DK^{*\pm}$ mode.

	r_B	δ_B
$\text{In } DK^\pm$		
<i>BABAR</i>	$0.096 \pm 0.029 \pm 0.005 \pm 0.004$	$\delta_B(DK^\pm) = (119_{-20}^{+19} \pm 3 \pm 3)^\circ$
<i>Belle</i>	$0.160_{-0.038}^{+0.040} \pm 0.011_{-0.010}^{+0.05}$	$(138_{-16}^{+13} \pm 4 \pm 23)^\circ$
$\text{In } D^*K^\pm$		
<i>BABAR</i>	$0.133_{-0.039}^{+0.042} \pm 0.014 \pm 0.003$	$(-82 \pm 21 \pm 5 \pm 3)^\circ$
<i>Belle</i>	$0.196_{-0.069}^{+0.072} \pm 0.012_{-0.012}^{+0.062}$	$(342_{-21}^{+19} \pm 3 \pm 23)^\circ$
$\text{In } DK^{*\pm}$		
<i>BABAR</i>	$\kappa r_S = 0.149_{-0.062}^{+0.066} \pm 0.026 \pm 0.006$	$\delta_S = (111 \pm 32 \pm 11 \pm 3)^\circ$
<i>Belle</i>	$0.56_{-0.16}^{+0.22} \pm 0.04 \pm 0.08$	$(243_{-23}^{+20} \pm 3 \pm 50)^\circ$

5 Semileptonic B decays

Measurements of semileptonic B -meson decays are an important tool to study the magnitude of the CKM matrix elements $|V_{cb}|$ and $|V_{ub}|$, the Heavy Quark parameters (e.g. b and c -quark masses), QCD form factors, QCD dynamics, new physics, etc.

In the following, we provide averages of exclusive and inclusive branching fractions, the product of $|V_{cb}|$ and the form factor normalization $\mathcal{F}(1)$ and $\mathcal{G}(1)$ for $\overline{B} \rightarrow D^* \ell^- \overline{\nu}_\ell$ and $\overline{B} \rightarrow D \ell^- \overline{\nu}_\ell$ decays, respectively, and $|V_{ub}|$ as determined from inclusive and exclusive measurements of $B \rightarrow X_u \ell \nu_\ell$ decays. We will compute Heavy Quark parameters and extract QCD form factors for $\overline{B} \rightarrow D^* \ell^- \overline{\nu}_\ell$ decays. Throughout this section, charge conjugate states are implicitly included, unless otherwise indicated.

Brief descriptions of all parameters and analyses (published or preliminary) relevant for the determination of the combined results are given. The descriptions are based on the information available on the web page at

<http://www.slac.stanford.edu/xorg/hfag/semi/EndOfYear11>

A description of the technique employed for calculating averages was presented in the previous update [357]. Asymmetric errors have been introduced in the current averages for $\overline{B} \rightarrow X_u \ell \overline{\nu}$ decays to take into account theoretical asymmetric errors.

5.1 Exclusive CKM-favored decays

This section contains the measurements of $\overline{B} \rightarrow D^* \ell^- \overline{\nu}_\ell$ and $\overline{B} \rightarrow D \ell^- \overline{\nu}_\ell$, relevant for the determination of $|V_{cb}|$ from exclusive decays. We then provide averages for the inclusive branching fractions $\mathcal{B}(\overline{B} \rightarrow D^{(*)} \pi \ell^- \overline{\nu}_\ell)$ and for B semileptonic decays into orbitally-excited P -wave charm mesons (D^{**}). As the D^{**} branching fraction is poorly known, we report the averages for the products $\mathcal{B}(B^- \rightarrow D^{**} (D^{(*)} \pi) \ell^- \overline{\nu}_\ell) \times \mathcal{B}(D^{**} \rightarrow D^{(*)} \pi)$.

5.1.1 $\overline{B} \rightarrow D^* \ell^- \overline{\nu}_\ell$

In the parameterization of Caprini, Lellouch and Neubert (CLN), the shape and normalization of the form factor $\mathcal{F}(w)$, which describes the decay $\overline{B} \rightarrow D^* \ell^- \overline{\nu}_\ell$, can be described by four quantities: $\mathcal{F}(1)|V_{cb}|$, ρ^2 , $R_1(1)$ and $R_2(1)$ [358]. Our average and the determination of $|V_{cb}|$ are based on this parameterization.

We use the measurements of these form factor parameters shown in Table 50 and rescale them to the latest values of the input parameters (mainly branching fractions of charmed mesons) [359]. Most of the measurements in Table 50 are based exclusively on the decay $\overline{B}^0 \rightarrow D^{*+} \ell^- \overline{\nu}_\ell$. Some measurements [360, 361] are sensitive also to $B^- \rightarrow D^{*0} \ell^- \overline{\nu}_\ell$ and one measurement [362] is based exclusively on the decay $B^- \rightarrow D^{*0} \ell^- \overline{\nu}_\ell$. Our analysis thus assumes isospin symmetry.

In the next step, we perform a four-dimensional fit of the parameters $\mathcal{F}(1)|V_{cb}|$, ρ^2 , $R_1(1)$ and $R_2(1)$ using the rescaled measurements and taking into account correlated systematic uncertainties. Only two measurements constrain all four parameters [367, 368], the remaining measurements constrain only the normalization $\mathcal{F}(1)|V_{cb}|$ and the slope ρ^2 . The result of the

Table 50: Measurements of $\overline{B} \rightarrow D^* \ell^- \overline{\nu}_\ell$ in the parameterization of Caprini, Lellouch and Neubert (CLN) [358]. The average is the result of a 4-dimensional fit to the rescaled measurements of $\mathcal{F}(1)|V_{cb}|$, ρ^2 , $R_1(1)$ and $R_2(1)$. The χ^2 value of the combination is 29.7 for 23 degrees of freedom (CL=15.7%). The total correlation between the average $\mathcal{F}(1)|V_{cb}|$ and ρ^2 is 0.32.

Experiment	$\mathcal{F}(1) V_{cb} [10^{-3}]$ (rescaled) $\mathcal{F}(1) V_{cb} [10^{-3}]$ (published)	ρ^2 (rescaled) ρ^2 (published)
ALEPH [363]	$31.34 \pm 1.80_{\text{stat}} \pm 1.26_{\text{syst}}$ $31.9 \pm 1.8_{\text{stat}} \pm 1.9_{\text{syst}}$	$0.490 \pm 0.227_{\text{stat}} \pm 0.146_{\text{syst}}$ $0.37 \pm 0.26_{\text{stat}} \pm 0.14_{\text{syst}}$
CLEO [360]	$40.00 \pm 1.24_{\text{stat}} \pm 1.62_{\text{syst}}$ $43.1 \pm 1.3_{\text{stat}} \pm 1.8_{\text{syst}}$	$1.366 \pm 0.085_{\text{stat}} \pm 0.088_{\text{syst}}$ $1.61 \pm 0.09_{\text{stat}} \pm 0.21_{\text{syst}}$
OPAL excl [364]	$36.57 \pm 1.60_{\text{stat}} \pm 1.48_{\text{syst}}$ $36.8 \pm 1.6_{\text{stat}} \pm 2.0_{\text{syst}}$	$1.234 \pm 0.212_{\text{stat}} \pm 0.145_{\text{syst}}$ $1.31 \pm 0.21_{\text{stat}} \pm 0.16_{\text{syst}}$
OPAL partial reco [364]	$37.20 \pm 1.19_{\text{stat}} \pm 2.35_{\text{syst}}$ $37.5 \pm 1.2_{\text{stat}} \pm 2.5_{\text{syst}}$	$1.149 \pm 0.145_{\text{stat}} \pm 0.295_{\text{syst}}$ $1.12 \pm 0.14_{\text{stat}} \pm 0.29_{\text{syst}}$
DELPHI partial reco [365]	$35.38 \pm 1.40_{\text{stat}} \pm 2.34_{\text{syst}}$ $35.5 \pm 1.4_{\text{stat}} \begin{smallmatrix} +2.3 \\ -2.4 \end{smallmatrix}_{\text{syst}}$	$1.174 \pm 0.126_{\text{stat}} \pm 0.376_{\text{syst}}$ $1.34 \pm 0.14_{\text{stat}} \begin{smallmatrix} +0.24 \\ -0.22 \end{smallmatrix}_{\text{syst}}$
DELPHI excl [366]	$36.19 \pm 1.70_{\text{stat}} \pm 1.98_{\text{syst}}$ $39.2 \pm 1.8_{\text{stat}} \pm 2.3_{\text{syst}}$	$1.082 \pm 0.142_{\text{stat}} \pm 0.154_{\text{syst}}$ $1.32 \pm 0.15_{\text{stat}} \pm 0.33_{\text{syst}}$
Belle [367]	$34.73 \pm 0.17_{\text{stat}} \pm 1.02_{\text{syst}}$ $34.6 \pm 0.2_{\text{stat}} \pm 1.0_{\text{syst}}$	$1.214 \pm 0.034_{\text{stat}} \pm 0.008_{\text{syst}}$ $1.214 \pm 0.034_{\text{stat}} \pm 0.009_{\text{syst}}$
BABAR excl [368]	$34.09 \pm 0.30_{\text{stat}} \pm 1.00_{\text{syst}}$ $34.7 \pm 0.3_{\text{stat}} \pm 1.1_{\text{syst}}$	$1.184 \pm 0.048_{\text{stat}} \pm 0.029_{\text{syst}}$ $1.18 \pm 0.05_{\text{stat}} \pm 0.03_{\text{syst}}$
BABAR D^{*0} [362]	$35.14 \pm 0.59_{\text{stat}} \pm 1.33_{\text{syst}}$ $35.9 \pm 0.6_{\text{stat}} \pm 1.4_{\text{syst}}$	$1.126 \pm 0.058_{\text{stat}} \pm 0.055_{\text{syst}}$ $1.16 \pm 0.06_{\text{stat}} \pm 0.08_{\text{syst}}$
BABAR global fit [361]	$35.83 \pm 0.20_{\text{stat}} \pm 1.10_{\text{syst}}$ $35.7 \pm 0.2_{\text{stat}} \pm 1.2_{\text{syst}}$	$1.194 \pm 0.020_{\text{stat}} \pm 0.061_{\text{syst}}$ $1.21 \pm 0.02_{\text{stat}} \pm 0.07_{\text{syst}}$
Average	$35.90 \pm 0.11_{\text{stat}} \pm 0.44_{\text{syst}}$	$1.207 \pm 0.015_{\text{stat}} \pm 0.021_{\text{syst}}$

fit is

$$\mathcal{F}(1)|V_{cb}| = (35.90 \pm 0.45) \times 10^{-3} , \quad (158)$$

$$\rho^2 = 1.207 \pm 0.026 , \quad (159)$$

$$R_1(1) = 1.403 \pm 0.033 , \quad (160)$$

$$R_2(1) = 0.854 \pm 0.020 , \quad (161)$$

and the correlation coefficients are

$$\rho_{\mathcal{F}(1)|V_{cb}|,\rho^2} = 0.324 , \quad (162)$$

$$\rho_{\mathcal{F}(1)|V_{cb}|,R_1(1)} = -0.109 , \quad (163)$$

$$\rho_{\mathcal{F}(1)|V_{cb}|,R_2(1)} = -0.063 , \quad (164)$$

$$\rho_{\rho^2,R_1(1)} = 0.566 , \quad (165)$$

$$\rho_{\rho^2,R_2(1)} = -0.807 , \quad (166)$$

$$\rho_{R_1(1),R_2(1)} = -0.759 . \quad (167)$$

$$(168)$$

The uncertainties and correlations quoted here include both statistical and systematic contributions. The χ^2 of the fit is 29.7 for 23 degrees of freedom, which corresponds to a confidence level of 15.7%. An illustration of this fit result is given in Fig. 43.

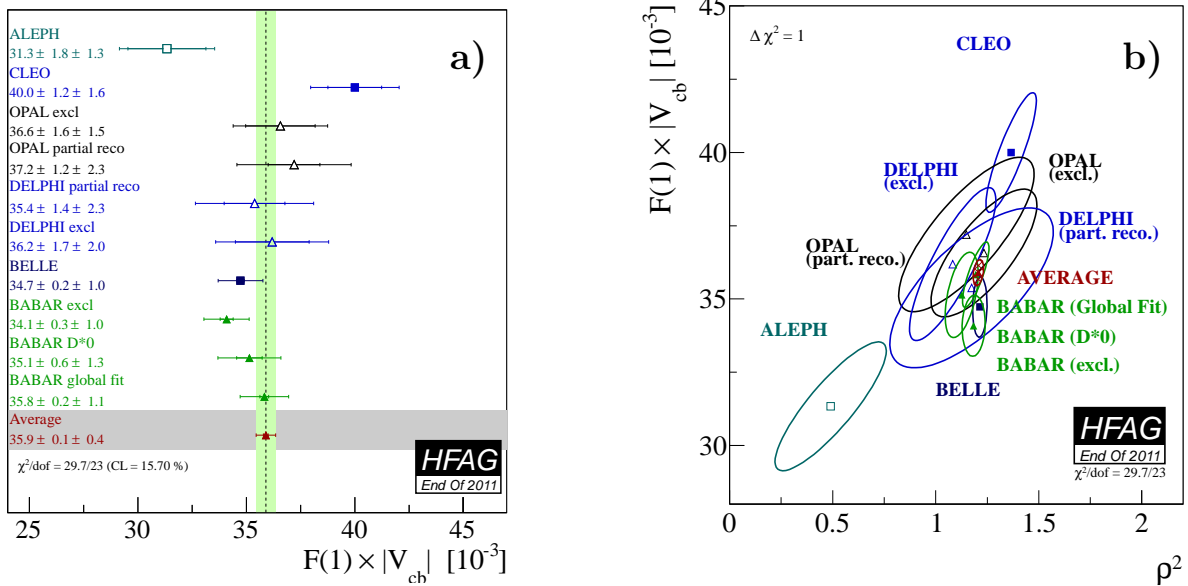


Figure 43: (a) Illustration of the $\mathcal{F}(1)|V_{cb}|$ average. (b) Illustration of the $\mathcal{F}(1)|V_{cb}|$ vs. ρ^2 average. The error ellipses correspond to $\Delta\chi^2 = 1$ (CL=39%).

Using the form factor normalization $\mathcal{F}(1)$ of the latest LQCD calculation [369],

$$\mathcal{F}(1) = 0.908 \pm 0.017 , \quad (169)$$

we obtain the following determination of $|V_{cb}|$ from Eq. 158,

$$|V_{cb}| = (39.54 \pm 0.50_{\text{exp}} \pm 0.74_{\text{th}}) \times 10^{-3} , \quad (170)$$

where the first uncertainty is experimental and the second stems from the LQCD calculation.

From each rescaled measurement in Table 50, we calculate the $\bar{B} \rightarrow D^* \ell^- \bar{\nu}_\ell$ form factor $\mathcal{F}(w)$ and, by numerical integration, the branching ratio of the decay $\bar{B}^0 \rightarrow D^{*+} \ell^- \bar{\nu}_\ell$. For measurements which do not determine the parameters $R_1(1)$ and $R_2(1)$ we assume the average

values Eqs. 160 and 161. The results are quoted in Table 51. The branching ratio found for the average values of $\mathcal{F}(1)|V_{cb}|$, ρ^2 , $R_1(1)$ and $R_2(1)$ is

$$\mathcal{B}(\bar{B}^0 \rightarrow D^{*+}\ell^{-}\bar{\nu}) = (4.95 \pm 0.11)\% . \quad (171)$$

Again, this analysis assumes isospin symmetry although most of the measurements included are sensitive only to $\bar{B}^0 \rightarrow D^{*+}\ell^{-}\bar{\nu}$. For an independent analysis of the decay $B^- \rightarrow D^{*0}\ell^{-}\bar{\nu}_\ell$, we have performed a simple 1-dimensional average of measurements sensitive to the decay $B^- \rightarrow D^{*0}\ell^{-}\bar{\nu}_\ell$ only, which is shown in Table 52. Fig. 44 illustrates these two averages of $\bar{B} \rightarrow D^*\ell^{-}\bar{\nu}_\ell$.

Table 51: $\bar{B}^0 \rightarrow D^{*+}\ell^{-}\bar{\nu}$ branching fractions calculated from the rescaled measurements in Table 50, assuming the CLN parameterization of the form factor [358]. The branching ratios published in Refs. [361, 362] have been rescaled by the factor $\tau(B^0)/\tau(B^+)$. While the fit assumes isospin symmetry, most measurements included here use only the decay $\bar{B}^0 \rightarrow D^{*+}\ell^{-}\bar{\nu}$.

Experiment	$\mathcal{B}(\bar{B}^0 \rightarrow D^{*+}\ell^{-}\bar{\nu})$ [%] (calculated)	$\mathcal{B}(\bar{B}^0 \rightarrow D^{*+}\ell^{-}\bar{\nu})$ [%] (published)
ALEPH [363]	$5.38 \pm 0.25_{\text{stat}} \pm 0.30_{\text{syst}}$	$5.53 \pm 0.26_{\text{stat}} \pm 0.52_{\text{syst}}$
CLEO [360]	$5.64 \pm 0.18_{\text{stat}} \pm 0.26_{\text{syst}}$	$6.09 \pm 0.19_{\text{stat}} \pm 0.40_{\text{syst}}$
OPAL excl [364]	$5.06 \pm 0.19_{\text{stat}} \pm 0.42_{\text{syst}}$	$5.11 \pm 0.19_{\text{stat}} \pm 0.49_{\text{syst}}$
OPAL partial reco [364]	$5.48 \pm 0.25_{\text{stat}} \pm 0.53_{\text{syst}}$	$5.92 \pm 0.27_{\text{stat}} \pm 0.68_{\text{syst}}$
DELPHI partial reco [365]	$4.89 \pm 0.14_{\text{stat}} \pm 0.72_{\text{syst}}$	$4.70 \pm 0.13_{\text{stat}} \pm 0.36_{\text{syst}}$
DELPHI excl [366]	$5.37 \pm 0.20_{\text{stat}} \pm 0.38_{\text{syst}}$	$5.90 \pm 0.22_{\text{stat}} \pm 0.50_{\text{syst}}$
Belle [367]	$4.59 \pm 0.03_{\text{stat}} \pm 0.26_{\text{syst}}$	$4.58 \pm 0.03_{\text{stat}} \pm 0.26_{\text{syst}}$
BABAR excl [368]	$4.58 \pm 0.04_{\text{stat}} \pm 0.25_{\text{syst}}$	$4.69 \pm 0.04_{\text{stat}} \pm 0.34_{\text{syst}}$
BABAR D^{*0} [362]	$4.95 \pm 0.07_{\text{stat}} \pm 0.34_{\text{syst}}$	$5.15 \pm 0.07_{\text{stat}} \pm 0.38_{\text{syst}}$
BABAR global fit [361]	$4.96 \pm 0.02_{\text{stat}} \pm 0.20_{\text{syst}}$	$5.00 \pm 0.02_{\text{stat}} \pm 0.19_{\text{syst}}$
Average	$4.95 \pm 0.01_{\text{stat}} \pm 0.11_{\text{syst}}$	$\chi^2/\text{dof} = 29.7/23$ (CL=15.7%)

Table 52: Average of the $B^- \rightarrow D^{*0}\ell^{-}\bar{\nu}_\ell$ branching fraction measurements. This fit uses only measurements of $B^- \rightarrow D^{*0}\ell^{-}\bar{\nu}_\ell$.

Experiment	$\mathcal{B}(B^- \rightarrow D^{*0}\ell^{-}\bar{\nu}_\ell)$ [%] (rescaled)	$\mathcal{B}(B^- \rightarrow D^{*0}\ell^{-}\bar{\nu}_\ell)$ [%] (published)
CLEO [360]	$6.61 \pm 0.20_{\text{stat}} \pm 0.39_{\text{syst}}$	$6.50 \pm 0.20_{\text{stat}} \pm 0.43_{\text{syst}}$
BABAR tagged [370]	$5.72 \pm 0.15_{\text{stat}} \pm 0.30_{\text{syst}}$	$5.83 \pm 0.15_{\text{stat}} \pm 0.30_{\text{syst}}$
BABAR [362]	$5.35 \pm 0.08_{\text{stat}} \pm 0.40_{\text{syst}}$	$5.56 \pm 0.08_{\text{stat}} \pm 0.41_{\text{syst}}$
BABAR [361]	$5.43 \pm 0.02_{\text{stat}} \pm 0.21_{\text{syst}}$	$5.40 \pm 0.02_{\text{stat}} \pm 0.21_{\text{syst}}$
Average	$5.70 \pm 0.02_{\text{stat}} \pm 0.19_{\text{syst}}$	$\chi^2/\text{dof} = 9.1/3$ (CL=2.8%)

5.1.2 $\bar{B} \rightarrow D\ell^{-}\bar{\nu}_\ell$

Similarly, the average of $\bar{B} \rightarrow D\ell^{-}\bar{\nu}_\ell$ is also based on the CLN parameterization [358]. The form factor $\mathcal{G}(w)$ of the decay is described by only two parameters: the normalization $\mathcal{G}(1)|V_{cb}|$ and the slope ρ^2 .

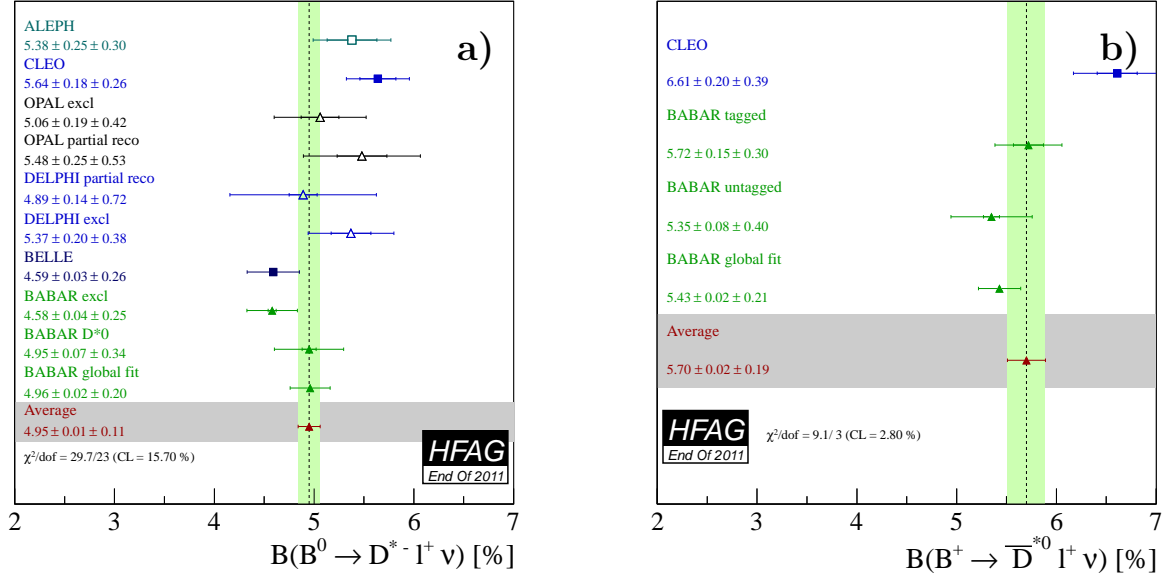


Figure 44: (a) Average branching fractions of exclusive semileptonic B decays $\bar{B} \rightarrow D^* \ell^- \bar{\nu}_\ell$: (a) $\bar{B}^0 \rightarrow D^{*+} \ell^- \bar{\nu}$ (Table 51) and (b) $B^- \rightarrow D^{*0} \ell^- \bar{\nu}_\ell$ (Table 52).

We use the measurements of these two form factor parameters shown in Table 53 and correct them to match the latest values of the input parameters [359]. These measurements are sensitive to both isospin states ($\bar{B}^0 \rightarrow D^+ \ell^- \bar{\nu}$ and $B^- \rightarrow D^0 \ell^- \bar{\nu}_\ell$). So, isospin symmetry is assumed in this analysis.

Table 53: Measurements of $\bar{B} \rightarrow D \ell^- \bar{\nu}_\ell$ in the parameterization of Caprini, Lellouch and Neubert (CLN) [358]. The average is the result of a 2-dimensional fit to the rescaled measurements of $\mathcal{G}(1)|V_{cb}|$ and ρ^2 . The χ^2 value of the combination is 0.5 for 8 degrees of freedom (CL=100.0%). The total correlation between the average $\mathcal{G}(1)|V_{cb}|$ and ρ^2 is 0.83.

Experiment	$\mathcal{G}(1) V_{cb} $ [10^{-3}] (rescaled) $\mathcal{G}(1) V_{cb} $ [10^{-3}] (published)	ρ^2 (rescaled) ρ^2 (published)
ALEPH [363]	$38.89 \pm 11.80_{\text{stat}} \pm 6.09_{\text{syst}}$ $31.1 \pm 9.9_{\text{stat}} \pm 8.6_{\text{syst}}$	$0.951 \pm 0.980_{\text{stat}} \pm 0.357_{\text{syst}}$ $0.70 \pm 0.98_{\text{stat}} \pm 0.50_{\text{syst}}$
CLEO [371]	$44.90 \pm 5.97_{\text{stat}} \pm 3.30_{\text{syst}}$ $44.8 \pm 6.1_{\text{stat}} \pm 3.7_{\text{syst}}$	$1.270 \pm 0.250_{\text{stat}} \pm 0.140_{\text{syst}}$ $1.30 \pm 0.27_{\text{stat}} \pm 0.14_{\text{syst}}$
Belle [372]	$40.84 \pm 4.37_{\text{stat}} \pm 5.17_{\text{syst}}$ $41.1 \pm 4.4_{\text{stat}} \pm 5.1_{\text{syst}}$	$1.120 \pm 0.220_{\text{stat}} \pm 0.140_{\text{syst}}$ $1.12 \pm 0.22_{\text{stat}} \pm 0.14_{\text{syst}}$
BABAR global fit [361]	$43.42 \pm 0.81_{\text{stat}} \pm 2.08_{\text{syst}}$ $43.1 \pm 0.8_{\text{stat}} \pm 2.3_{\text{syst}}$	$1.204 \pm 0.040_{\text{stat}} \pm 0.057_{\text{syst}}$ $1.20 \pm 0.04_{\text{stat}} \pm 0.07_{\text{syst}}$
BABAR tagged [373]	$42.45 \pm 1.88_{\text{stat}} \pm 1.05_{\text{syst}}$ $42.3 \pm 1.9_{\text{stat}} \pm 1.0_{\text{syst}}$	$1.180 \pm 0.089_{\text{stat}} \pm 0.051_{\text{syst}}$ $1.20 \pm 0.09_{\text{stat}} \pm 0.04_{\text{syst}}$
Average	$42.64 \pm 0.72_{\text{stat}} \pm 1.35_{\text{syst}}$	$1.186 \pm 0.036_{\text{stat}} \pm 0.041_{\text{syst}}$

The form factor parameters are extracted by a two-dimensional fit to the rescaled measurements of $\mathcal{G}(1)|V_{cb}|$ and ρ^2 taking into account correlated systematic uncertainties. The result of the fit reads

$$\mathcal{G}(1)|V_{cb}| = (42.64 \pm 1.53) \times 10^{-3}, \quad (172)$$

$$\rho^2 = 1.186 \pm 0.054, \quad (173)$$

with a correlation of

$$\rho_{\mathcal{G}(1)|V_{cb}|, \rho^2} = 0.829. \quad (174)$$

The uncertainties and the correlation coefficient include both statistical and systematic contributions. The χ^2 of the fit is 0.5 for 8 degrees of freedom, which corresponds to a confidence level of 100.0%. An illustration of this fit result is given in Fig. 45.

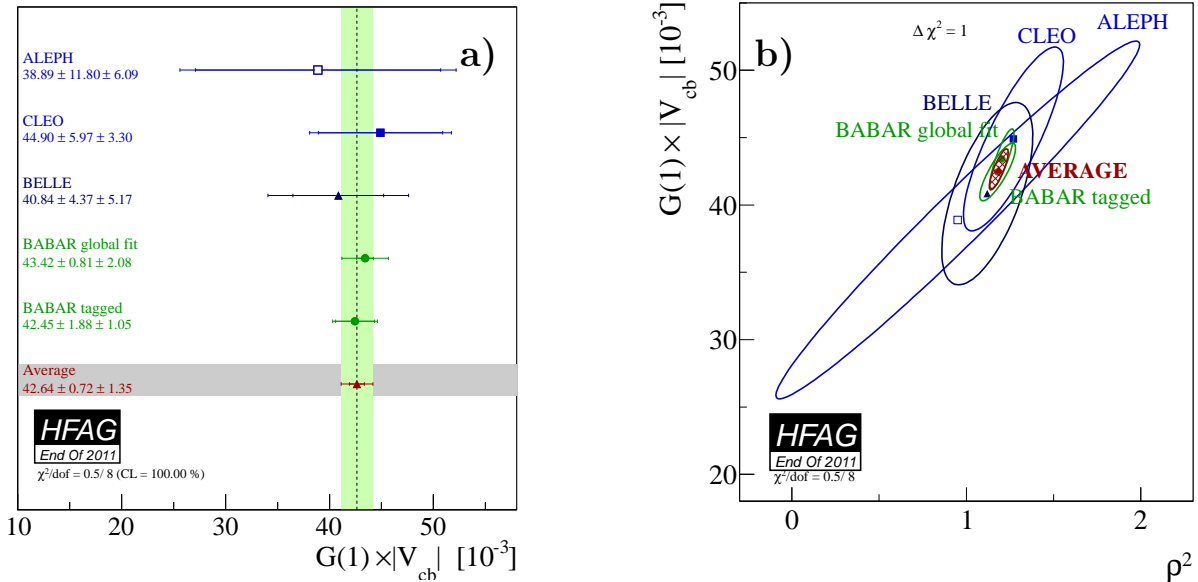


Figure 45: (a) Illustration of the $\mathcal{G}(1)|V_{cb}|$ average. (b) Illustration of the $\mathcal{G}(1)|V_{cb}|$ vs. ρ^2 average. The error ellipses correspond to $\Delta\chi^2 = 1$ (CL=39%).

The most recent result obtained for the form factor normalization $\mathcal{G}(1)$ in LQCD is [374]

$$\mathcal{G}(1) = 1.074 \pm 0.024, \quad (175)$$

which can be used to turn Eq. 172 into a determination of $|V_{cb}|$,

$$|V_{cb}| = (39.70 \pm 1.42_{\text{exp}} \pm 0.89_{\text{th}}) \times 10^{-3}, \quad (176)$$

where the first error is experimental and the second theoretical. This number is in excellent agreement with $|V_{cb}|$ obtained from decays $\bar{B} \rightarrow D^* \ell^- \bar{\nu}_\ell$, Eq. 170.

From each rescaled measurement in Table 53, we have calculated the $\bar{B} \rightarrow D \ell^- \bar{\nu}_\ell$ form factor $\mathcal{G}(w)$ and, by numerical integration, the branching ratio of the decay $\bar{B}^0 \rightarrow D^+ \ell^- \bar{\nu}$. The results are quoted in Table 54 and illustrated in Fig. 46. The branching ratio found for the average values of $\mathcal{G}(1)|V_{cb}|$ and ρ^2 is

$$\mathcal{B}(\bar{B}^0 \rightarrow D^+ \ell^- \bar{\nu}) = (2.13 \pm 0.09)\%. \quad (177)$$

Table 54: $\overline{B}^0 \rightarrow D^+\ell^-\overline{\nu}_\ell$ branching fractions calculated from the rescaled measurements in Table 53, assuming the CLN parameterization of the form factor [358]. The fit assumes isospin symmetry.

Experiment	$\mathcal{B}(\overline{B}^0 \rightarrow D^+\ell^-\overline{\nu}_\ell)$ [%] (calculated)	$\mathcal{B}(\overline{B}^0 \rightarrow D^+\ell^-\overline{\nu}_\ell)$ [%] (published)
ALEPH [363]	$2.16 \pm 0.18_{\text{stat}} \pm 0.46_{\text{syst}}$	$2.35 \pm 0.20_{\text{stat}} \pm 0.44_{\text{syst}}$
CLEO [371]	$2.19 \pm 0.16_{\text{stat}} \pm 0.35_{\text{syst}}$	$2.20 \pm 0.16_{\text{stat}} \pm 0.19_{\text{syst}}$
Belle [372]	$2.07 \pm 0.12_{\text{stat}} \pm 0.52_{\text{syst}}$	$2.13 \pm 0.12_{\text{stat}} \pm 0.39_{\text{syst}}$
BABAR global fit [361]	$2.18 \pm 0.03_{\text{stat}} \pm 0.13_{\text{syst}}$	$2.34 \pm 0.03_{\text{stat}} \pm 0.13_{\text{syst}}$
BABAR tagged [373]	$2.12 \pm 0.10_{\text{stat}} \pm 0.06_{\text{syst}}$	$2.23 \pm 0.11_{\text{stat}} \pm 0.11_{\text{syst}}$
Average	$2.13 \pm 0.03_{\text{stat}} \pm 0.09_{\text{syst}}$	$\chi^2/\text{dof} = 0.5/8$ (CL=100.0%)

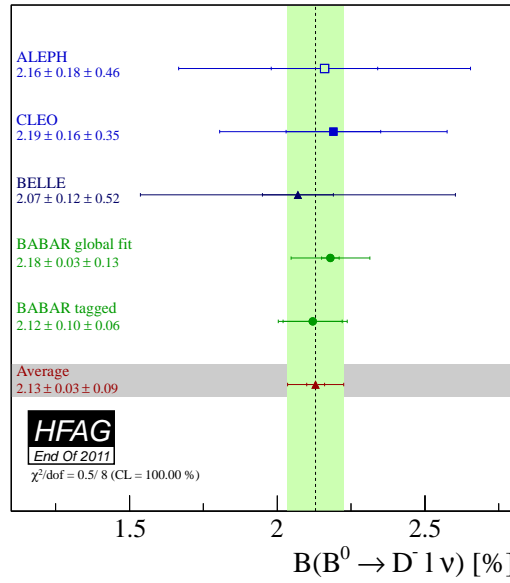


Figure 46: Average branching fraction of exclusive semileptonic B decays $\overline{B}^0 \rightarrow D^+\ell^-\overline{\nu}_\ell$ (Table 54). The fit assumes isospin conservation.

This analysis assumes isospin symmetry.

We have also performed simple 1-dimensional averages of measurements of $\overline{B}^0 \rightarrow D^+\ell^-\overline{\nu}_\ell$ and $B^- \rightarrow D^0\ell^-\overline{\nu}_\ell$. These fits are shown Tables 55 and 56.

5.1.3 $\overline{B} \rightarrow D^{(*)}\pi\ell^-\overline{\nu}_\ell$

The average inclusive branching fractions for $\overline{B} \rightarrow D^{(*)}\pi\ell^-\overline{\nu}_\ell$ decays, where no constrain is applied to the hadronic $D^{(*)}\pi$ system, are determined by the combination of the results provided in Table 57 for $\overline{B}^0 \rightarrow D^0\pi^+\ell^-\overline{\nu}_\ell$, $\overline{B}^0 \rightarrow D^{*0}\pi^+\ell^-\overline{\nu}_\ell$, $B^- \rightarrow D^+\pi^-\ell^-\overline{\nu}_\ell$, and $B^- \rightarrow D^{*+}\pi^-\ell^-\overline{\nu}_\ell$. The measurements included in the average are scaled to a consistent set of input parameters and their errors [359].

For both the *BABAR* and *Belle* results, the B semileptonic signal yields are extracted from

Table 55: Average of the $\overline{B}^0 \rightarrow D^+ \ell^- \overline{\nu}$ branching fraction measurements. This fit uses only measurements of $\overline{B}^0 \rightarrow D^+ \ell^- \overline{\nu}$.

Experiment	$\mathcal{B}(\overline{B}^0 \rightarrow D^+ \ell^- \overline{\nu})$ [%] (rescaled)	$\mathcal{B}(\overline{B}^0 \rightarrow D^+ \ell^- \overline{\nu})$ [%] (published)
ALEPH [363]	$2.29 \pm 0.18_{\text{stat}} \pm 0.35_{\text{syst}}$	$2.35 \pm 0.20_{\text{stat}} \pm 0.44_{\text{syst}}$
CLEO [371]	$2.13 \pm 0.13_{\text{stat}} \pm 0.15_{\text{syst}}$	$2.20 \pm 0.16_{\text{stat}} \pm 0.19_{\text{syst}}$
Belle [372]	$2.10 \pm 0.12_{\text{stat}} \pm 0.39_{\text{syst}}$	$2.13 \pm 0.12_{\text{stat}} \pm 0.39_{\text{syst}}$
BABAR [370]	$2.21 \pm 0.11_{\text{stat}} \pm 0.12_{\text{syst}}$	$2.21 \pm 0.11_{\text{stat}} \pm 0.12_{\text{syst}}$
Average	$2.18 \pm 0.06_{\text{stat}} \pm 0.10_{\text{syst}}$	$\chi^2/\text{dof} = 0.2/3$ (CL=97.4%)

Table 56: Average of the $B^- \rightarrow D^0 \ell^- \overline{\nu}_\ell$ branching fraction measurements. This fit uses only measurements of $B^- \rightarrow D^0 \ell^- \overline{\nu}_\ell$.

Experiment	$\mathcal{B}(B^- \rightarrow D^0 \ell^- \overline{\nu}_\ell)$ [%] (rescaled)	$\mathcal{B}(B^- \rightarrow D^0 \ell^- \overline{\nu}_\ell)$ [%] (published)
CLEO [371]	$2.21 \pm 0.13_{\text{stat}} \pm 0.17_{\text{syst}}$	$2.32 \pm 0.17_{\text{stat}} \pm 0.20_{\text{syst}}$
BABAR [370]	$2.28 \pm 0.09_{\text{stat}} \pm 0.09_{\text{syst}}$	$2.33 \pm 0.09_{\text{stat}} \pm 0.09_{\text{syst}}$
Average	$2.26 \pm 0.07_{\text{stat}} \pm 0.08_{\text{syst}}$	$\chi^2/\text{dof} = 0.1/1$ (CL=76.0%)

a fit to the missing mass squared in a sample of fully reconstructed $B\overline{B}$ events.

Figure 47 illustrates the measurements and the resulting average.

Table 57: Average of the branching fraction $B \rightarrow D^{(*)} \pi^- \ell^- \overline{\nu}_\ell$ and individual results.

Experiment	$\mathcal{B}(B^- \rightarrow D^+ \pi^- \ell^- \overline{\nu}_\ell)$ [%] (rescaled)	
Belle [375]	$0.42 \pm 0.04_{\text{stat}} \pm 0.05_{\text{syst}}$	
BABAR [370]	$0.42 \pm 0.06_{\text{stat}} \pm 0.03_{\text{syst}}$	
Average	0.42 ± 0.05	$\chi^2/\text{dof} = 0.001$ (CL=97%)
Experiment	$\mathcal{B}(B^- \rightarrow D^{*+} \pi^- \ell^- \overline{\nu}_\ell)$ [%] (rescaled)	
Belle [375]	$0.67 \pm 0.08_{\text{stat}} \pm 0.07_{\text{syst}}$	
BABAR [370]	$0.59 \pm 0.05_{\text{stat}} \pm 0.04_{\text{syst}}$	
Average	0.61 ± 0.05	$\chi^2/\text{dof} = 0.15$ (CL=69%)
Experiment	$\mathcal{B}(\overline{B}^0 \rightarrow D^0 \pi^+ \ell^- \overline{\nu}_\ell)$ [%] (rescaled)	
Belle [375]	$0.43 \pm 0.07_{\text{stat}} \pm 0.05_{\text{syst}}$	
BABAR [370]	$0.43 \pm 0.08_{\text{stat}} \pm 0.03_{\text{syst}}$	
Average	0.43 ± 0.06	$\chi^2/\text{dof} = 0.002$ (CL=97%)
Experiment	$\mathcal{B}(\overline{B}^0 \rightarrow D^{*0} \pi^+ \ell^- \overline{\nu}_\ell)$ [%] (rescaled)	
Belle [375]	$0.57 \pm 0.21_{\text{stat}} \pm 0.07_{\text{syst}}$	
BABAR [370]	$0.48 \pm 0.08_{\text{stat}} \pm 0.04_{\text{syst}}$	
Average	0.49 ± 0.08	$\chi^2/\text{dof} = 0.15$ (CL=69%)

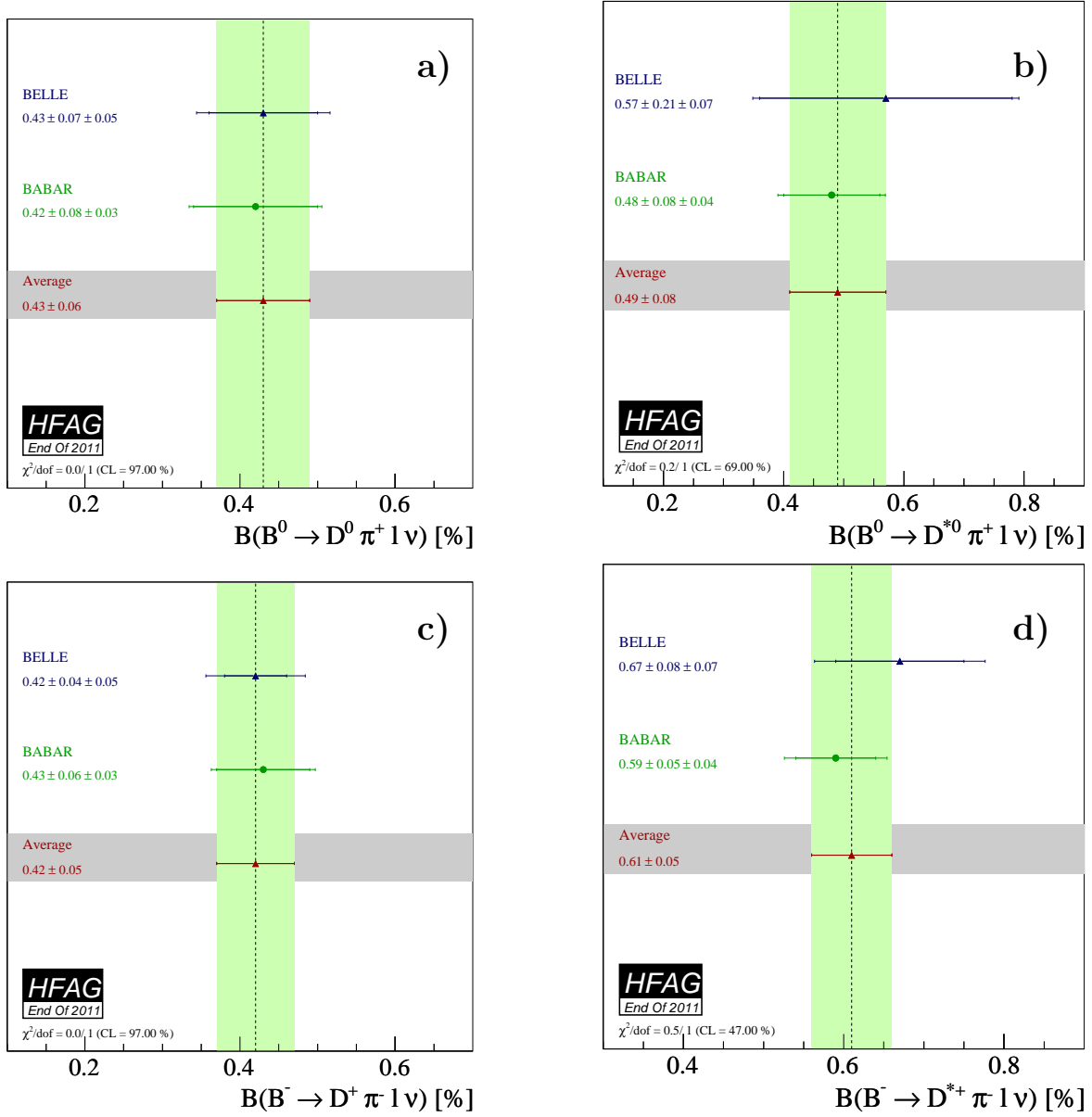


Figure 47: Average branching fraction of exclusive semileptonic B decays (a) $\bar{B}^0 \rightarrow D^0 \pi^+ \ell^- \bar{\nu}_\ell$, (b) $\bar{B}^0 \rightarrow D^{*0} \pi^+ \ell^- \bar{\nu}_\ell$, (c) $B^- \rightarrow D^+ \pi^- \ell^- \bar{\nu}_\ell$, and (d) $B^- \rightarrow D^{*+} \pi^- \ell^- \bar{\nu}_\ell$. The corresponding individual results are also shown.

5.1.4 $\bar{B} \rightarrow D^{**} \ell^- \bar{\nu}_\ell$

The D^{**} mesons contain one charm quark and one light quark with relative angular momentum $L = 1$. According to Heavy Quark Symmetry (HQS) [376], they form one doublet of states with angular momentum $j \equiv s_q + L = 3/2$ [$D_1(2420), D_2^*(2460)$] and another doublet with $j = 1/2$ [$D_0^*(2400), D_1'(2430)$], where s_q is the light quark spin. Parity and angular momentum conservation constrain the decays allowed for each state. The D_1 and D_2^* states decay through a D-wave to $D^* \pi$ and $D^{(*)} \pi$, respectively, and have small decay widths, while the D_0^* and D_1'

states decay through an S-wave to $D\pi$ and $D^*\pi$ and are very broad. For the narrow states, the average are determined by the combination of the results provided in Table 58 and 59 for $\mathcal{B}(B^- \rightarrow D_1^0(D^{*+}\pi^-)\ell^-\bar{\nu}_\ell) \times \mathcal{B}(D_1^0 \rightarrow D^{*+}\pi^-)$ and $\mathcal{B}(B^- \rightarrow D_2^0(D^{*+}\pi^-)\ell^-\bar{\nu}_\ell) \times \mathcal{B}(D_2^0 \rightarrow D^{*+}\pi^-)$. For the broad states, the average are determined by the combination of the results provided in Table 60 and 61 for $\mathcal{B}(B^- \rightarrow D_1^{*0}(D^{*+}\pi^-)\ell^-\bar{\nu}_\ell) \times \mathcal{B}(D_1^{*0} \rightarrow D^{*+}\pi^-)$ and $\mathcal{B}(B^- \rightarrow D_0^{*0}(D^+\pi^-)\ell^-\bar{\nu}_\ell) \times \mathcal{B}(D_0^{*0} \rightarrow D^+\pi^-)$. The measurements included in the average are scaled to a consistent set of input parameters and their errors [359].

For both the B-factory and the LEP and Tevatron results, the B semileptonic signal yields are extracted from a fit to the invariant mass distribution of the $D^{(*)+}\pi^-$ system. Apart for the CLEO and Belle results, the other measurements are for the final state $\bar{B} \rightarrow D_2(D^{*+}\pi^-)X\ell^-\bar{\nu}_\ell$. We assume that no particle is left in the X system. Figure 48 and 49 illustrate the measurements and the resulting average.

Table 58: Average of the branching fraction $\mathcal{B}(B^- \rightarrow D_1^0(D^{*+}\pi^-)\ell^-\bar{\nu}_\ell) \times \mathcal{B}(D_1^0 \rightarrow D^{*+}\pi^-)$ and individual results.

Experiment		$\mathcal{B}(B^- \rightarrow D_1^0(D^{*+}\pi^-)\ell^-\bar{\nu}_\ell)[\%]$ (rescaled)	$\mathcal{B}(B^- \rightarrow D_1^0(D^{*+}\pi^-)\ell^-\bar{\nu}_\ell)[\%]$ (published)
ALEPH	[377]	$0.45 \pm 0.10_{\text{stat}} \pm 0.07_{\text{syst}}$	$0.47 \pm 0.098_{\text{stat}} \pm 0.074_{\text{syst}}$
OPAL	[378]	$0.59 \pm 0.21_{\text{stat}} \pm 0.10_{\text{syst}}$	$0.698 \pm 0.21_{\text{stat}} \pm 0.10_{\text{syst}}$
CLEO	[379]	$0.35 \pm 0.09_{\text{stat}} \pm 0.06_{\text{syst}}$	$0.373 \pm 0.085_{\text{stat}} \pm 0.057_{\text{syst}}$
D0	[380]	$0.22 \pm 0.02_{\text{stat}} \pm 0.04_{\text{syst}}$	$0.219 \pm 0.018_{\text{stat}} \pm 0.035_{\text{syst}}$
Belle Tagged B^-	[375]	$0.44 \pm 0.07_{\text{stat}} \pm 0.06_{\text{syst}}$	$0.42 \pm 0.07_{\text{stat}} \pm 0.07_{\text{syst}}$
Belle Tagged B^0	[375]	$0.60 \pm 0.20_{\text{stat}} \pm 0.08_{\text{syst}}$	$0.42 \pm 0.07_{\text{stat}} \pm 0.07_{\text{syst}}$
BABAR Tagged	[381]	$0.28 \pm 0.03_{\text{stat}} \pm 0.03_{\text{syst}}$	$0.29 \pm 0.03_{\text{stat}} \pm 0.03_{\text{syst}}$
BABAR Untagged B^-	[382]	$0.29 \pm 0.02_{\text{stat}} \pm 0.02_{\text{syst}}$	$0.30 \pm 0.02_{\text{stat}} \pm 0.02_{\text{syst}}$
BABAR Untagged B^0	[382]	$0.30 \pm 0.03_{\text{stat}} \pm 0.03_{\text{syst}}$	$0.30 \pm 0.02_{\text{stat}} \pm 0.02_{\text{syst}}$
Average		0.285 ± 0.018	$\chi^2/\text{dof} = 11.0/8$ (CL=13.3%)

Table 59: Average of the branching fraction $\mathcal{B}(B^- \rightarrow D_2^0(D^{*+}\pi^-)\ell^-\bar{\nu}_\ell) \times \mathcal{B}(D_2^0 \rightarrow D^{*+}\pi^-)$ and individual results.

Experiment		$\mathcal{B}(B^- \rightarrow D_2^0(D^{*+}\pi^-)\ell^-\bar{\nu}_\ell)[\%]$ (rescaled)	$\mathcal{B}(B^- \rightarrow D_2^0(D^{*+}\pi^-)\ell^-\bar{\nu}_\ell)[\%]$ (published)
CLEO	[379]	$0.055 \pm 0.07_{\text{stat}} \pm 0.01_{\text{syst}}$	$0.059 \pm 0.066_{\text{stat}} \pm 0.011_{\text{syst}}$
D0	[380]	$0.088 \pm 0.018_{\text{stat}} \pm 0.020_{\text{syst}}$	$0.088 \pm 0.018_{\text{stat}} \pm 0.020_{\text{syst}}$
Belle	[375]	$0.187 \pm 0.060_{\text{stat}} \pm 0.025_{\text{syst}}$	$0.18 \pm 0.06_{\text{stat}} \pm 0.03_{\text{syst}}$
BABAR Tagged	[381]	$0.068 \pm 0.009_{\text{stat}} \pm 0.016_{\text{syst}}$	$0.068 \pm 0.009_{\text{stat}} \pm 0.016_{\text{syst}}$
BABAR Untagged B^-	[382]	$0.089 \pm 0.009_{\text{stat}} \pm 0.007_{\text{syst}}$	$0.087 \pm 0.013_{\text{stat}} \pm 0.007_{\text{syst}}$
BABAR Untagged B^0	[382]	$0.066 \pm 0.010_{\text{stat}} \pm 0.006_{\text{syst}}$	$0.087 \pm 0.013_{\text{stat}} \pm 0.007_{\text{syst}}$
Average		0.074 ± 0.007	$\chi^2/\text{dof} = 7.3/5$ (CL=20%)

Table 60: Average of the branching fraction $\mathcal{B}(B^- \rightarrow D_1^0(D^{*+}\pi^-)\ell^-\bar{\nu}_\ell) \times \mathcal{B}(D_1^0 \rightarrow D^{*+}\pi^-)$ and individual results.

Experiment	$\mathcal{B}(B^- \rightarrow D_1^0(D^{*+}\pi^-)\ell^-\bar{\nu}_\ell)[\%]$ (rescaled)	$\mathcal{B}(B^- \rightarrow D_1^0(D^{*+}\pi^-)\ell^-\bar{\nu}_\ell)[\%]$ (published)
DELPHI [383]	$0.74 \pm 0.17_{\text{stat}} \pm 0.18_{\text{syst}}$	$0.83 \pm 0.17_{\text{stat}} \pm 0.18_{\text{syst}}$
Belle [375]	$-0.03 \pm 0.06_{\text{stat}} \pm 0.07_{\text{syst}}$	$-0.03 \pm 0.06_{\text{stat}} \pm 0.07_{\text{syst}}$
BABAR [381]	$0.27 \pm 0.04_{\text{stat}} \pm 0.04_{\text{syst}}$	$0.27 \pm 0.04_{\text{stat}} \pm 0.05_{\text{syst}}$
Average	0.13 ± 0.04	$\chi^2/\text{dof} = 18./2$ (CL=0.001%)

Table 61: Average of the branching fraction $\mathcal{B}(B^- \rightarrow D_0^{*0}(D^+\pi^-)\ell^-\bar{\nu}_\ell) \times \mathcal{B}(D_0^{*0} \rightarrow D^+\pi^-)$ and individual results.

Experiment	$\mathcal{B}(B^- \rightarrow D_0^{*0}(D^+\pi^-)\ell^-\bar{\nu}_\ell)[\%]$ (rescaled)	$\mathcal{B}(B^- \rightarrow D_0^{*0}(D^+\pi^-)\ell^-\bar{\nu}_\ell)[\%]$ (published)
Belle Tagged B^- [375]	$0.25 \pm 0.04_{\text{stat}} \pm 0.06_{\text{syst}}$	$0.24 \pm 0.04_{\text{stat}} \pm 0.06_{\text{syst}}$
Belle Tagged B^0 [375]	$0.23 \pm 0.08_{\text{stat}} \pm 0.06_{\text{syst}}$	$0.24 \pm 0.04_{\text{stat}} \pm 0.06_{\text{syst}}$
BABAR Tagged [381]	$0.32 \pm 0.04_{\text{stat}} \pm 0.05_{\text{syst}}$	$0.26 \pm 0.05_{\text{stat}} \pm 0.04_{\text{syst}}$
Average	0.29 ± 0.05	$\chi^2/\text{dof} = 0.83/2$ (CL=66%)

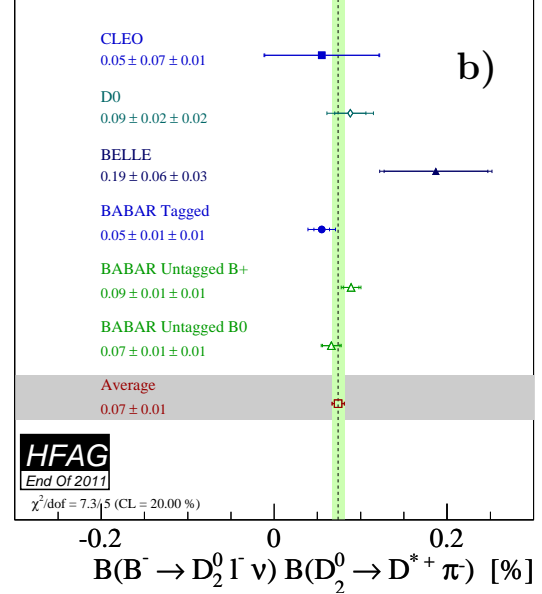
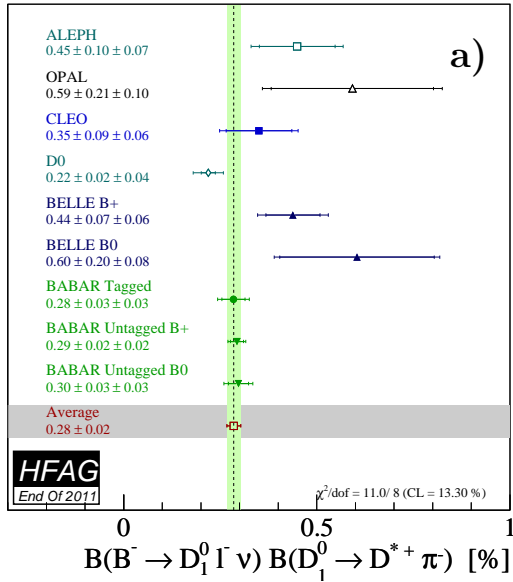


Figure 48: Average of the product of branching fraction (a) $\mathcal{B}(B^- \rightarrow D_1^0(D^{*+}\pi^-)\ell^-\bar{\nu}_\ell) \times \mathcal{B}(D_1^0 \rightarrow D^{*+}\pi^-)$ and (b) $\mathcal{B}(B^- \rightarrow D_2^0(D^{*+}\pi^-)\ell^-\bar{\nu}_\ell) \times \mathcal{B}(D_2^0 \rightarrow D^{*+}\pi^-)$. The corresponding individual results are also shown.

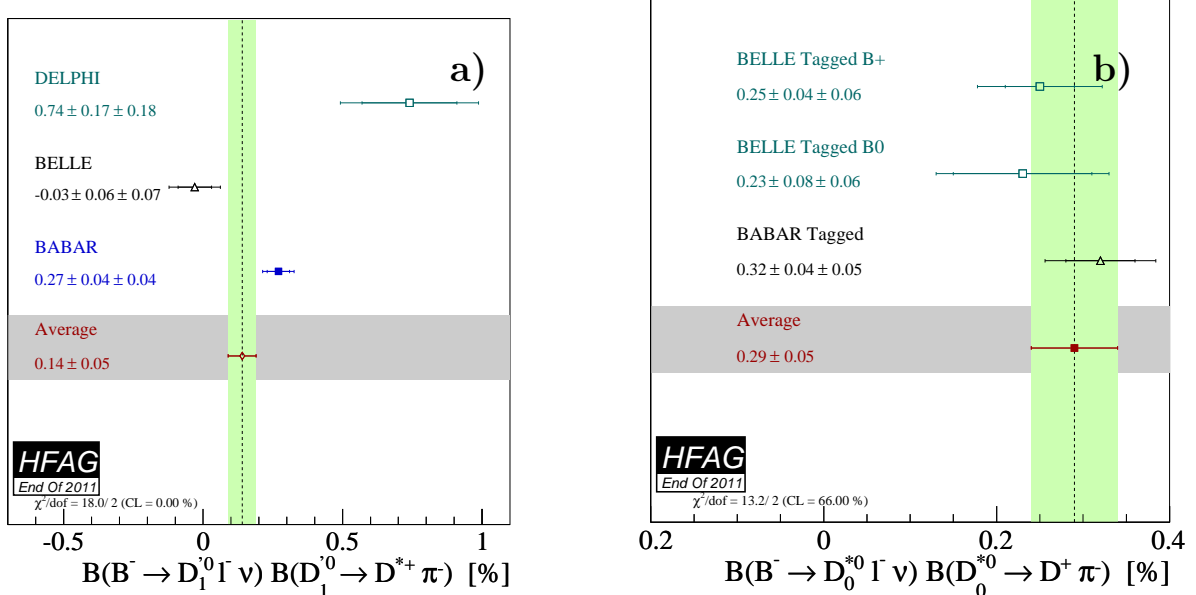


Figure 49: Average of the product of branching fraction (a) $\mathcal{B}(B^- \rightarrow D_1^0(D^{*+}\pi^-)\ell^- \bar{\nu}_\ell) \times \mathcal{B}(D_1^0 \rightarrow D^{*+}\pi^-)$ and (b) $\mathcal{B}(B^- \rightarrow D_0^{*0}(D^{*+}\pi^-)\ell^- \bar{\nu}_\ell) \times \mathcal{B}(D_0^{*0} \rightarrow D^+\pi^-)$. The corresponding individual results are also shown.

5.2 Inclusive CKM-favored decays

5.2.1 Global analysis of $\bar{B} \rightarrow X_c \ell^- \bar{\nu}_\ell$

The semileptonic width $\Gamma(\bar{B} \rightarrow X_c \ell^- \bar{\nu}_\ell)$ has been calculated in the framework of the Operator Product Expansion. The result is a double-expansion in Λ_{QCD}/m_b and α_s , which depends on a number of non-perturbative parameters. These parameters can be measured using other observables in $\bar{B} \rightarrow X_c \ell^- \bar{\nu}_\ell$ decays, such as the moments of the lepton energy and the hadronic mass spectrum.

Two independent sets of theoretical expressions, referred to as kinetic [384–386] and 1S schemes [387] are available for this kind of analysis. The non-perturbative parameters in the kinetic scheme are: the quark masses m_b and m_c , μ_π^2 and μ_G^2 at $O(1/m_b^2)$, and ρ_D^3 and ρ_{LS}^3 at $O(1/m_b^3)$. In the 1S scheme, the parameters are: m_b , λ_1 at $O(1/m_b^2)$, and ρ_1 , τ_1 , τ_2 and τ_3 at $O(1/m_b^3)$. Note that due to the different definitions, the results for the quark masses cannot be compared directly between the two schemes.

Our analysis uses all available measurements of moments in $\bar{B} \rightarrow X_c \ell^- \bar{\nu}_\ell$, excluding only points with too high correlation to avoid numerical issues. The list of included measurements is given in Table 62. The only external input is the average lifetime τ_B of neutral and charged B mesons, taken to be (1.582 ± 0.007) ps (Sect. 3).

Both in the kinetic and 1S scheme, the moments in $\bar{B} \rightarrow X_c \ell^- \bar{\nu}_\ell$ are not sufficient to constrain the b -quark mass precisely, which limits the precision of the determination of $|V_{cb}|$. This limitation can be overcome:

- by including the photon energy moments in $B \rightarrow X_s \gamma$ into the fit, or
- by applying a precise constraint on the c -quark mass.

Table 62: Experimental inputs used in the global analysis of $\overline{B} \rightarrow X_c \ell^- \overline{\nu}_\ell$. n is the order of the moment, c is the threshold value in GeV. In total, there are 29 measurements from *BABAR*, 25 measurements from Belle and 12 from other experiments.

Experiment	Hadron moments $\langle M_X^n \rangle$	Lepton moments $\langle E_\ell^n \rangle$	Photons moment $\langle E_\gamma^n \rangle$
<i>BABAR</i>	$n = 2, c = 0.9, 1.1, 1.3, 1.5$ $n = 4, c = 0.8, 1.0, 1.2, 1.4$ $n = 6, c = 0.9, 1.3$ [390]	$n = 0, c = 0.6, 1.2, 1.5$ $n = 1, c = 0.6, 0.8, 1.0, 1.2, 1.5$ $n = 2, c = 0.6, 1.0, 1.5$ $n = 3, c = 0.8, 1.2$ [390, 391]	$n = 1, c = 1.9, 2.0$ $n = 2, c = 1.9$ [388, 389]
Belle	$n = 2, c = 0.7, 1.1, 1.3, 1.5$ $n = 4, c = 0.7, 0.9, 1.3$ [392]	$n = 0, c = 0.6, 1.0, 1.4$ $n = 1, c = 0.6, 0.8, 1.0, 1.2, 1.4$ $n = 2, c = 0.6, 1.0, 1.4$ $n = 3, c = 0.8, 1.0, 1.2$ [394]	$n = 1, c = 1.8, 1.9$ $n = 2, c = 1.8, 2.0$ [393]
CDF	$n = 2, c = 0.7$ $n = 4, c = 0.7$ [395]		
CLEO	$n = 2, c = 1.0, 1.5$ $n = 4, c = 1.0, 1.5$ [397]		$n = 1, c = 2.0$ [396]
DELPHI	$n = 2, c = 0.0$ $n = 4, c = 0.0$ [383]	$n = 1, c = 0.0$ $n = 2, c = 0.0$ $n = 3, c = 0.0$ [383]	

For the former, calculations of the $B \rightarrow X_s \gamma$ moments are available both in the kinetic [398] and the 1S scheme [387]. For the latter, we use the c -quark mass calculated in Ref. [399] in the kinetic scheme analysis,

$$m_c^{\overline{\text{MS}}}(3 \text{ GeV}) = (0.998 \pm 0.029) \text{ GeV} . \quad (178)$$

5.2.2 Analysis in the kinetic scheme

The fit relies on the calculations of the spectral moments in $\overline{B} \rightarrow X_c \ell^- \overline{\nu}_\ell$ decays described in Ref. [386]. The photon energy moments are calculated in Ref. [398]. The theoretical uncertainties and correlations are estimated as explained in Ref. [400]. Namely, we assume 100% correlation between calculations of the same moment at different threshold values and no theory correlation between different moments. The fit determines $|V_{cb}|$ and the 6 non-perturbative parameters mentioned above.

The result of the fit using the c -quark mass constraint is

$$|V_{cb}| = (41.88 \pm 0.73) \times 10^{-3} , \quad (179)$$

$$m_b^{\text{kin}} = 4.560 \pm 0.023 \text{ GeV} , \quad (180)$$

$$\mu_\pi^2 = 0.453 \pm 0.036 \text{ GeV}^2 , \quad (181)$$

with a χ^2 of 33.4 for 55 – 7 degrees of freedom. The detailed result of the fit is given in Table 63. This result is also consistent with the fit using the $B \rightarrow X_s \gamma$ constraint (Table 64). An illustration of the fit is given in Fig. 50.

The fit using the c -quark mass constraint yields a $\overline{B} \rightarrow X_c \ell^- \overline{\nu}_\ell$ branching fraction of

$$\mathcal{B}(\overline{B} \rightarrow X_c \ell^- \overline{\nu}_\ell) = (10.51 \pm 0.13)\% . \quad (182)$$

Table 63: Fit result in the kinetic scheme, using a precise c -quark mass constraint. The error matrix of the fit (σ_{fit}) contains experimental and theoretical contributions. The expression for calculating $|V_{cb}|$ has an additional uncertainty of 1.4% (σ_{th}). In the lower part of the table, the correlation matrix of the parameters is given.

	$ V_{cb} [10^{-3}]$	$m_b^{\text{kin}} [\text{GeV}]$	$m_c^{\text{MS}} [\text{GeV}]$	$\mu_\pi^2 [\text{GeV}^2]$	$\rho_D^3 [\text{GeV}^3]$	$\mu_G^2 [\text{GeV}^2]$	$\rho_{LS}^3 [\text{GeV}^3]$
value	41.88	4.560	1.010	0.453	0.164	0.229	-0.140
σ_{fit}	0.44	0.023	0.027	0.036	0.020	0.043	0.086
σ_{th}	0.59						
$ V_{cb} $	1.000	-0.164	0.137	0.089	0.328	-0.324	0.146
m_b^{kin}		1.000	0.745	-0.117	-0.177	0.128	-0.179
m_c^{MS}			1.000	-0.199	-0.006	-0.433	0.258
μ_π^2				1.000	0.335	-0.109	-0.078
ρ_D^3					1.000	-0.308	-0.238
μ_G^2						1.000	-0.323
ρ_{LS}^3							1.000

Table 64: Fit result in the kinetic scheme for different constraints. Refer to the text for more details.

Constraint	$ V_{cb} [10^{-3}]$	$m_b^{\text{kin}} [\text{GeV}]$	$\mu_\pi^2 [\text{GeV}^2]$	$\chi^2/\text{d.o.f.}$
$B \rightarrow X_s \gamma$	$41.94 \pm 0.43_{\text{fit}} \pm 0.59_{\text{th}}$	4.574 ± 0.032	0.459 ± 0.037	$27.0/(66 - 7)$
$m_c^{\text{MS}}(3 \text{ GeV})$	$41.88 \pm 0.44_{\text{fit}} \pm 0.59_{\text{th}}$	4.560 ± 0.023	0.453 ± 0.036	$33.4/(55 - 7)$

Correcting for charmless semileptonic decays (Sect. 5.4), $\mathcal{B}(\overline{B} \rightarrow X_u \ell^- \overline{\nu}_\ell) = (2.08 \pm 0.30) \times 10^{-3}$, we obtain the semileptonic branching fraction,

$$\mathcal{B}(\overline{B} \rightarrow X \ell^- \overline{\nu}_\ell) = (10.72 \pm 0.13)\% . \quad (183)$$

5.2.3 Analysis in the 1S scheme

The fit relies on the calculations of the spectral moments described in Ref. [387]. The theoretical uncertainties are estimated as explained in Ref. [400]. Only trivial theory correlations, *i.e.*, between the same moment at the same threshold are included in the analysis. The fit determines $|V_{cb}|$ and the 6 non-perturbative parameters mentioned above.

The result of the fit using the $B \rightarrow X_s \gamma$ constraint is

$$|V_{cb}| = (41.96 \pm 0.45) \times 10^{-3} , \quad (184)$$

$$m_b^{1S} = 4.691 \pm 0.037 \text{ GeV} , \quad (185)$$

$$\lambda_1 = -0.362 \pm 0.067 \text{ GeV}^2 , \quad (186)$$

with a χ^2 of 23.0 for 66-7 degrees of freedom. The detailed result of the fit is given in Table 65. This result is consistent with the fit using the $\overline{B} \rightarrow X_c \ell^- \overline{\nu}_\ell$ data only (Table 66).

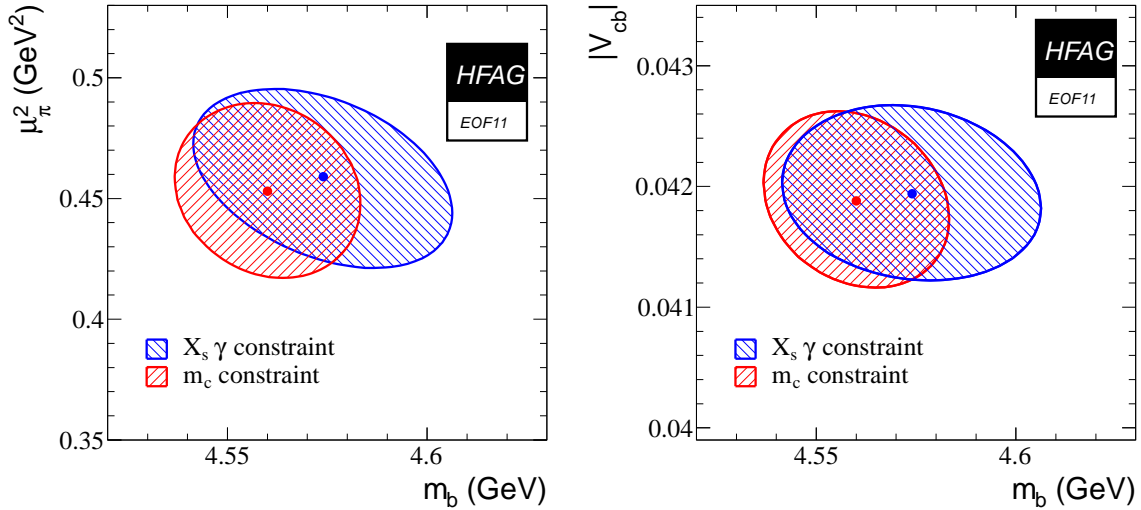


Figure 50: $\Delta\chi^2 = 1$ contours of the fit result in the kinetic mass scheme.

Table 65: Fit result in the 1S scheme, using $B \rightarrow X_s\gamma$ moments as a constraint. In the lower part of the table, the correlation matrix of the parameters is given.

	m_b^{1S} [GeV]	λ_1 [GeV ²]	ρ_1 [GeV ³]	τ_1 [GeV ³]	τ_2 [GeV ³]	τ_3 [GeV ³]	$ V_{cb} $ [10^{-3}]
value	4.691	-0.362	0.043	0.161	-0.017	0.213	41.96
error	0.037	0.067	0.048	0.122	0.062	0.102	0.45
m_b^{1S}	1.000	0.434	0.213	-0.058	-0.629	-0.019	-0.215
λ_1		1.000	-0.467	-0.602	-0.239	-0.547	-0.403
ρ_1			1.000	0.129	-0.624	0.494	0.286
τ_1				1.000	0.062	-0.148	0.194
τ_2					1.000	-0.009	-0.145
τ_3						1.000	0.376
$ V_{cb} $							1.000

Table 66: Fit result in the 1S scheme for different data sets.

Data	$ V_{cb} $ [10^{-3}]	m_b^{1S} [GeV]	λ_1 [GeV ²]	$\chi^2/\text{d.o.f.}$
$X_c\ell\nu$ and $X_s\gamma$	41.96 ± 0.45	4.691 ± 0.037	-0.362 ± 0.067	23.0/(66 - 7)
$X_c\ell\nu$ only	42.37 ± 0.65	4.622 ± 0.085	-0.412 ± 0.084	13.7/(55 - 7)

5.3 Exclusive CKM-suppressed decays

In this section, we list results on exclusive charmless semileptonic branching fractions and determinations of $|V_{ub}|$ based on $\bar{B} \rightarrow \pi\ell\bar{\nu}$ decays. The measurements are based on two different event selections: tagged events, in which case the second B meson in the event is fully recon-

structured in either a hadronic decay (“ B_{reco} ”) or in a CKM-favored semileptonic decay (“SL”); and untagged events, in which case the selection infers the momentum of the undetected neutrino based on measurements of the total momentum sum of detected particles and knowledge of the initial state. We present averages for $\bar{B} \rightarrow \rho \ell \bar{\nu}$ and $\bar{B} \rightarrow \omega \ell \bar{\nu}$. Moreover, the average for the branching fraction $\bar{B} \rightarrow \eta \ell \bar{\nu}$ is presented for the first time.

The results for the full and partial branching fraction for $\bar{B} \rightarrow \pi \ell \bar{\nu}$ are given in Table 67 and shown in Figure 51 (a).

When averaging these results, systematic uncertainties due to external inputs, e.g., form factor shapes and background estimates from the modeling of $\bar{B} \rightarrow X_c \ell \bar{\nu}$ and $\bar{B} \rightarrow X_u \ell \bar{\nu}$ decays, are treated as fully correlated (in the sense of Eq. 10). Uncertainties due to experimental reconstruction effects are treated as fully correlated among measurements from a given experiment. Varying the assumed dependence of the quoted errors on the measured value for error sources where the dependence was not obvious had no significant impact.

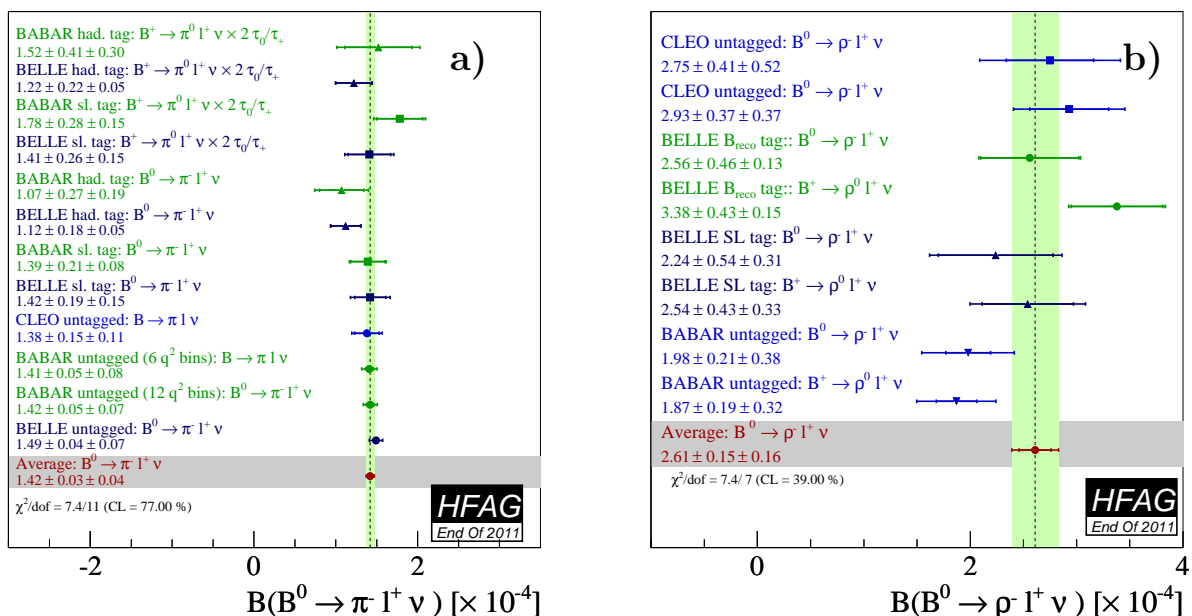


Figure 51: (a) Summary of exclusive determinations of $\mathcal{B}(\bar{B} \rightarrow \pi \ell \bar{\nu})$ and their average. Measured branching fractions for $B \rightarrow \pi^0 l \nu$ have been multiplied by $2 \times \tau_{B^0} / \tau_{B^+}$ in accordance with isospin symmetry. The labels “ B_{reco} ” and “SL” refer to type of B decay tag used in a measurement. “untagged” refers to an untagged measurement. (b) Summary of exclusive determinations of $\mathcal{B}(\bar{B} \rightarrow \rho \ell \bar{\nu})$ and their average.

The determination of $|V_{ub}|$ from $\bar{B} \rightarrow \pi \ell \bar{\nu}$ decays is shown in Table 68, and uses our averages for the partial branching fractions given in Table 67. Two theoretical approaches are used: unquenched Lattice QCD and QCD light-cone sum rules. Lattice calculations of the form factors are limited to small hadron momenta, i.e. large q^2 , while calculations based on light-cone sum rules are restricted to small q^2 .

An alternative method to determine $|V_{ub}|$ from $\bar{B} \rightarrow \pi \ell \bar{\nu}$ decays that makes use of the measurement over the full q^2 range is based on a simultaneous fit of the BCL (Bourrely, Caprini, Lellouch) form factor parameterization to the data and the LQCD predictions. The result of the simultaneous fit to the three untagged measurements from BABAR and Belle and the

FNAL/MILC LQCD calculations is shown in Figure 52. A value of $|V_{ub}| = (3.23 \pm 0.30) \times 10^{-3}$ is obtained.

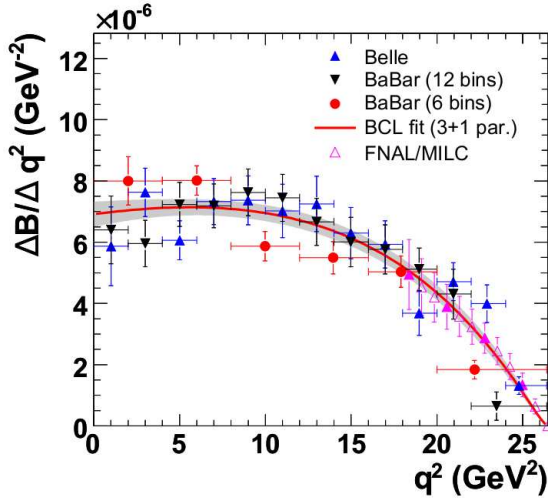


Figure 52: Simultaneous fit of the untagged $\bar{B} \rightarrow \pi \ell \bar{\nu}$ measurements from *BABAR* and Belle and the FNAL/MILC LQCD calculations. This fit yields $|V_{ub}| = (3.23 \pm 0.30) \times 10^{-3}$.

The branching fractions for $\bar{B} \rightarrow \rho \ell \bar{\nu}$ decays is computed based on the measurements in Table 69 and is shown in Figure 51 (b). The determination of $|V_{ub}|$ from these other channels looks less promising than for $\bar{B} \rightarrow \pi \ell \bar{\nu}$ and at the moment it is not extracted.

We also report the branching fraction average for $\bar{B} \rightarrow \omega \ell \bar{\nu}$, $\bar{B} \rightarrow \eta \ell \bar{\nu}$ and $\bar{B} \rightarrow \eta' \ell \bar{\nu}$. The measurements for $\bar{B} \rightarrow \omega \ell \bar{\nu}$ are reported in Table 70 and shown in Figure 53, while the ones for $\bar{B} \rightarrow \eta \ell \bar{\nu}$ and $\bar{B} \rightarrow \eta' \ell \bar{\nu}$ are reported in Table 71 and 72, and are shown in Figure 54.

5.4 Inclusive CKM-suppressed decays

The large background from $B \rightarrow X_c \ell^+ \nu_\ell$ decays is the chief experimental limitation in determinations of $|V_{ub}|$. Cuts designed to reject this background limit the acceptance for $B \rightarrow X_u \ell^+ \nu_\ell$ decays. The calculation of partial rates for these restricted acceptances is more complicated and requires substantial theoretical machinery. In this update, we use several theoretical calculations to extract $|V_{ub}|$. We do not advocate the use of one method over another. The authors for the different calculations have provided codes to compute the partial rates in limited regions of phase space covered by the measurements. Latest results by Belle [416] and *BABAR* [417] explore bigger and bigger portions of phase space, with a consequent reduction of the theoretical uncertainties.

For the averages we performed, the systematic errors associated with the modeling of $B \rightarrow X_c \ell^+ \nu_\ell$ and $B \rightarrow X_u \ell^+ \nu_\ell$ decays and the theoretical uncertainties are taken as fully correlated among all measurements. Reconstruction-related uncertainties are taken as fully correlated within a given experiment. We use all results published by *BABAR* in [417], since the statistical correlations are given. To make use of the theoretical calculations of Ref. [418], we restrict the

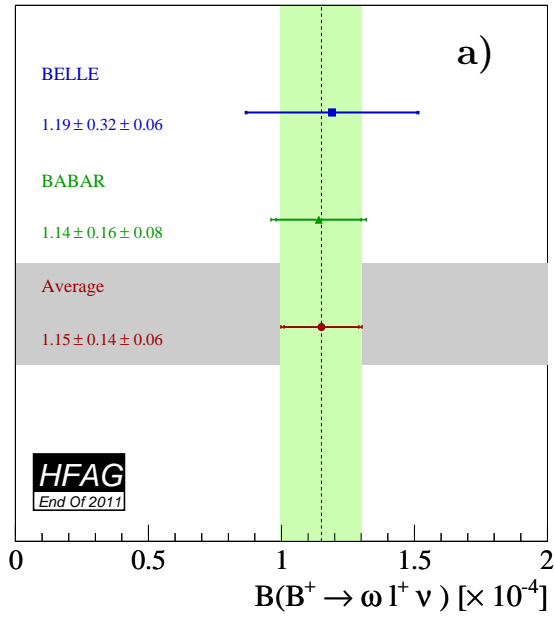


Figure 53: (a) Summary of exclusive determinations of $\mathcal{B}(\bar{B} \rightarrow \omega \ell \bar{\nu})$ and their average.

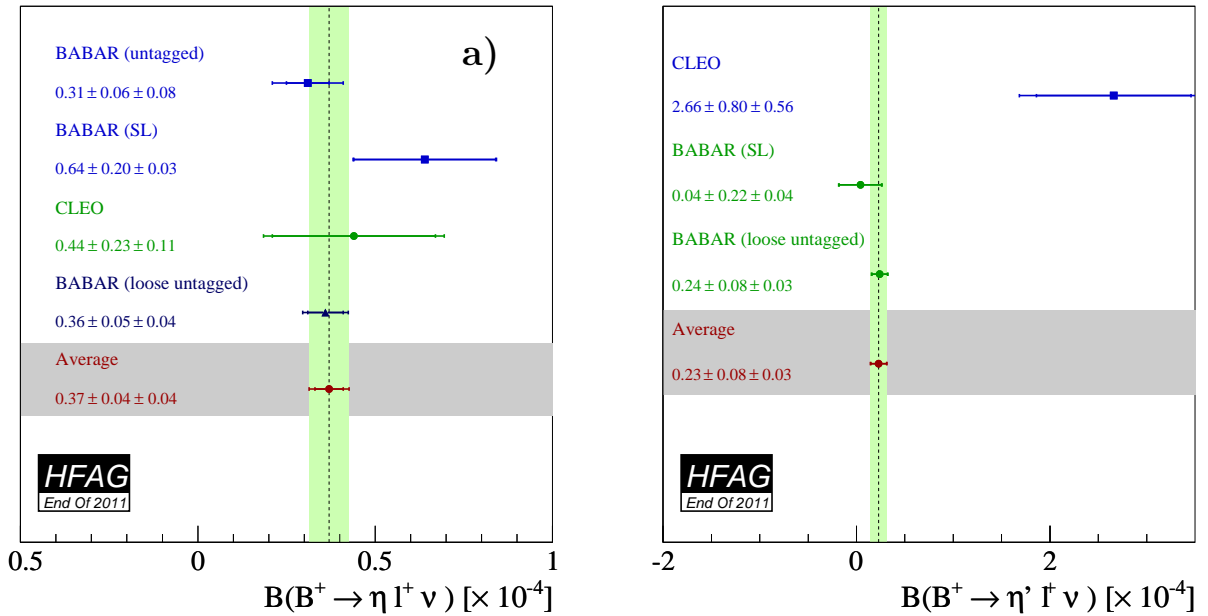


Figure 54: (a) Summary of exclusive determinations of $\mathcal{B}(\bar{B} \rightarrow \eta \ell \bar{\nu})$ and their average. (b) Summary of exclusive determinations of $\mathcal{B}(\bar{B} \rightarrow \eta' \ell \bar{\nu})$ and their average.

kinematic range in M_X and q^2 , thereby reducing the size of the data sample significantly, but also the theoretical uncertainty, as stated by the authors [418]. The dependence of the quoted error on the measured value for each source of error is taken into account in the calculation of the averages. Measurements of partial branching fractions for $B \rightarrow X_u \ell^+ \nu_\ell$ transitions from $\Upsilon(4S)$ decays, together with the corresponding accepted region, are given in Table 73. The signal yields for all the measurements shown in Table 73 are not rescaled to common input

values of the B meson lifetime (see Sect. 3) and the semileptonic width [419].

It has been first suggested by Neubert [420] and later detailed by Leibovich, Low, and Rothstein (LLR) [421] and Lange, Neubert and Paz (LNP) [422], that the uncertainty of the leading shape functions can be eliminated by comparing inclusive rates for $B \rightarrow X_u \ell^+ \nu_\ell$ decays with the inclusive photon spectrum in $B \rightarrow X_s \gamma$, based on the assumption that the shape functions for transitions to light quarks, u or s , are the same to first order. However, shape function uncertainties are only eliminated at the leading order and they still enter via the signal models used for the determination of efficiency. For completeness, we provide a comparison of the results using calculations with reduced dependence on the shape function, as just introduced, with our averages using different theoretical approaches. Results are presented by *BABAR* in Ref. [423] using the LLR prescription. In another work (Ref. [424]), $|V_{ub}|$ was extracted from the endpoint spectrum of $B \rightarrow X_u \ell^+ \nu_\ell$ from *BABAR* [425], using several theoretical approaches with reduced dependence on the shape function. In both cases, the photon energy spectrum in the rest frame of the B -meson by *BABAR* [388] has been used.

5.4.1 BLNP

Bosch, Lange, Neubert and Paz (BLNP) [432–435] provide theoretical expressions for the triple differential decay rate for $B \rightarrow X_u \ell^+ \nu_\ell$ events, incorporating all known contributions, whilst smoothly interpolating between the “shape-function region” of large hadronic energy and small invariant mass, and the “OPE region” in which all hadronic kinematical variables scale with the b -quark mass. BLNP assign uncertainties to the b -quark mass which enters through the leading shape function, to sub-leading shape function forms, to possible weak annihilation contribution, and to matching scales. The BLNP calculation uses the shape function renormalization scheme; the heavy quark parameters determined from the global fit in the kinetic scheme, described in 5.2.2, were therefore translated into the shape function scheme by using a prescription by Neubert [436, 437]. The resulting parameters are $m_b(SF) = (4.588 \pm 0.023 \pm 0.011)$ GeV, $\mu_\pi^2(SF) = (0.189 \pm 0.041_{-0.040}^{+0.020})$ GeV², where the second uncertainty is due to the scheme translation. The extracted values of $|V_{ub}|$ for each measurement along with their average are given in Table 74 and illustrated in Figure 55. The total uncertainty is ${}_{-5.9}^{+5.6}\%$ and is due to: statistics (${}_{-2.1}^{+2.1}\%$), detector (${}_{-1.8}^{+1.7}\%$), $B \rightarrow X_c \ell^+ \nu_\ell$ model (${}_{-1.2}^{+1.2}\%$), $B \rightarrow X_u \ell^+ \nu_\ell$ model (${}_{-1.6}^{+1.7}\%$), heavy quark parameters (${}_{-2.4}^{+2.3}\%$), SF functional form (${}_{-0.3}^{+0.3}\%$), sub-leading shape functions (${}_{-0.7}^{+0.5}\%$), BLNP theory: matching scales μ, μ_i, μ_h (${}_{-3.7}^{+3.7}\%$), and weak annihilation (${}_{-1.7}^{+0.0}\%$). The error on the HQE parameters (b -quark mass and μ_π^2) is the source of the largest uncertainty, while the uncertainty assigned for the matching scales is a close second. The uncertainty due to weak annihilation has been assumed to be asymmetric, i.e. it only tends to decrease $|V_{ub}|$.

5.4.2 DGE

J.R. Andersen and E. Gardi (Dressed Gluon Exponentiation, DGE) [438] provide a framework where the on-shell b -quark calculation, converted into hadronic variables, is directly used as an approximation to the meson decay spectrum without the use of a leading-power non-perturbative function (or, in other words, a shape function). The on-shell mass of the b -quark within the B -meson (m_b) is required as input. The DGE calculation uses the \overline{MS} renormalization scheme; the heavy quark parameters determined from the global fit in the kinetic scheme, described in 5.2.2, were therefore translated into the \overline{MS} scheme by using a calculation by

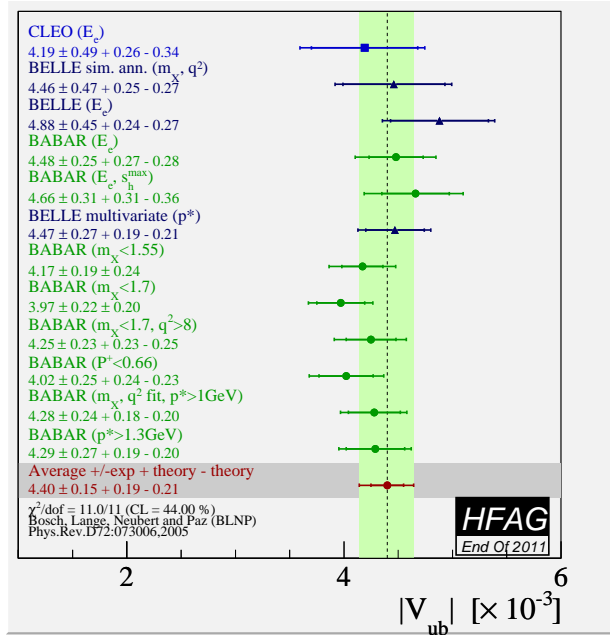


Figure 55: Measurements of $|V_{ub}|$ from inclusive semileptonic decays and their average based on the BLNP prescription. “ E_e ”, “ M_X ”, “ (M_X, q^2) ”, “ P^+ ”, “ p^* ” and “ (E_e, s_h^{max}) ” indicate the distributions and cuts used for the measurement of the partial decay rates.

Gardi, giving $m_b(\overline{MS}) = (4.194 \pm 0.043)$ GeV. The extracted values of $|V_{ub}|$ for each measurement along with their average are given in Table 74 and illustrated in Figure 56. The total error is $+4.8\%$, whose breakdown is: statistics ($+2.0\%$), detector ($+1.7\%$), $B \rightarrow X_c \ell^+ \nu_\ell$ model ($+1.3\%$), $B \rightarrow X_u \ell^+ \nu_\ell$ model ($+2.0\%$), strong coupling α_s ($+0.5\%$), m_b ($+3.1\%$), weak annihilation ($+0.0\%$), DGE theory: matching scales ($+0.6\%$). The largest contribution to the total error is due to the effect of the uncertainty on m_b . The uncertainty due to weak annihilation has been assumed to be asymmetric, i.e. it only tends to decrease $|V_{ub}|$.

5.4.3 GGOU

Gambino, Giordano, Ossola and Uraltsev (GGOU) [439] compute the triple differential decay rates of $B \rightarrow X_u \ell^+ \nu_\ell$, including all perturbative and non-perturbative effects through $O(\alpha_s^2 \beta_0)$ and $O(1/m_b^3)$. The Fermi motion is parameterized in terms of a single light-cone function for each structure function and for any value of q^2 , accounting for all subleading effects. The calculations are performed in the kinetic scheme, a framework characterized by a Wilsonian treatment with a hard cutoff $\mu \sim 1$ GeV. GGOU have not included calculations for the “ (E_e, s_h^{max}) ” analysis. The heavy quark parameters determined from the global fit in the kinetic scheme, described in 5.2.2, are used as inputs: $m_b(kin) = (4.560 \pm 0.023)$ GeV, $\mu_\pi^2(kin) = (0.453 \pm 0.036)$ GeV². The extracted values of $|V_{ub}|$ for each measurement along with their average are given in Table 74 and illustrated in Figure 57. The total error is $+4.4\%$ whose breakdown is: statistics ($+2.0\%$), detector ($+1.7\%$), $B \rightarrow X_c \ell^+ \nu_\ell$ model ($+1.3\%$), $B \rightarrow X_u \ell^+ \nu_\ell$ model ($+1.9\%$), α_s , m_b and other non-perturbative parameters ($+1.9\%$), higher order perturbative and non-perturbative corrections ($+1.4\%$), modelling of the q^2 tail and choice of the scale q^{2*} ($+1.3\%$), weak annihilations matrix element ($+0.0\%$), functional form of the distribution functions ($+0.2\%$). The leading

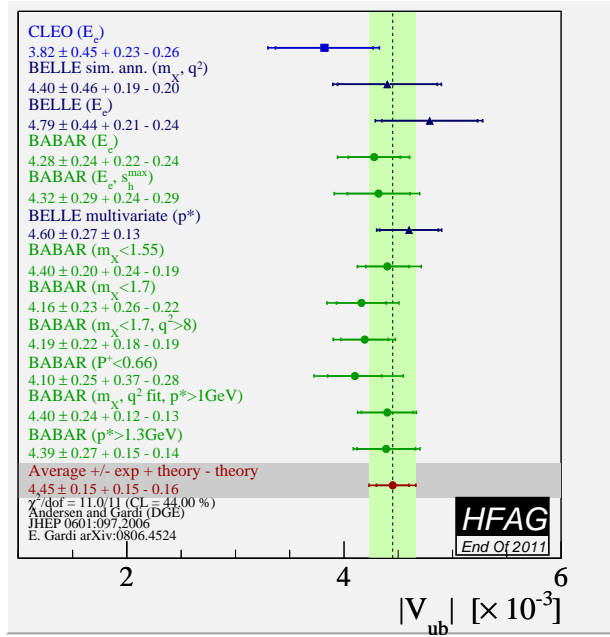


Figure 56: Measurements of $|V_{ub}|$ from inclusive semileptonic decays and their average based on the DGE prescription. “ E_e ”, “ M_X ”, “ (M_X, q^2) ”, “ P^+ ”, “ p^* ” and “ (E_e, s_h^{max}) ” indicate the analysis type and applied cut.

uncertainties on $|V_{ub}|$ are both from theory, and are due to perturbative and non-perturbative parameters and the modelling of the q^2 tail and choice of the scale q^{2*} . The uncertainty due to weak annihilation has been assumed to be asymmetric, i.e. it only tends to decrease $|V_{ub}|$.

5.4.4 ADFR

Aglietti, Di Lodovico, Ferrera and Ricciardi (ADFR) [440] use an approach to extract $|V_{ub}|$, which makes use of the ratio of the $B \rightarrow X_c \ell^+ \nu_\ell$ and $B \rightarrow X_u \ell^+ \nu_\ell$ widths. The normalized triple differential decay rate for $B \rightarrow X_u \ell^+ \nu_\ell$ [441–444] is calculated with a model based on (i) soft-gluon resummation to next-to-next-leading order and (ii) an effective QCD coupling without Landau pole. This coupling is constructed by means of an extrapolation to low energy of the high-energy behaviour of the standard coupling. More technically, an analyticity principle is used. The lower cut on the electron energy for the endpoint analyses is 2.3 GeV [441]. The ADFR calculation uses the \overline{MS} renormalization scheme; the heavy quark parameters determined from the global fit in the kinetic scheme, described in 5.2.2, were therefore translated into the \overline{MS} scheme by using a calculation by Gardi, giving $m_b(\overline{MS}) = (4.194 \pm 0.043)$ GeV. The extracted values of $|V_{ub}|$ for each measurement along with their average are given in Table 74 and illustrated in Figure 58. The total error is $^{+5.4\%}_{-5.5\%}$ whose breakdown is: statistics ($^{+1.9\%}_{-1.9\%}$), detector ($^{+1.8\%}_{-1.8\%}$), $B \rightarrow X_c \ell^+ \nu_\ell$ model ($^{+1.3\%}_{-1.3\%}$), $B \rightarrow X_u \ell^+ \nu_\ell$ model ($^{+1.2\%}_{-1.4\%}$), α_s ($^{+0.8\%}_{-1.2\%}$), $|V_{cb}|$ ($^{+1.7\%}_{-1.7\%}$), m_b ($^{+0.7\%}_{-0.7\%}$), m_c ($^{+1.3\%}_{-1.3\%}$), semileptonic branching fraction ($^{+0.7\%}_{-0.7\%}$), theory model ($^{+3.6\%}_{-3.6\%}$). The leading uncertainties, both from theory, are due to the m_c mass and the theory model.

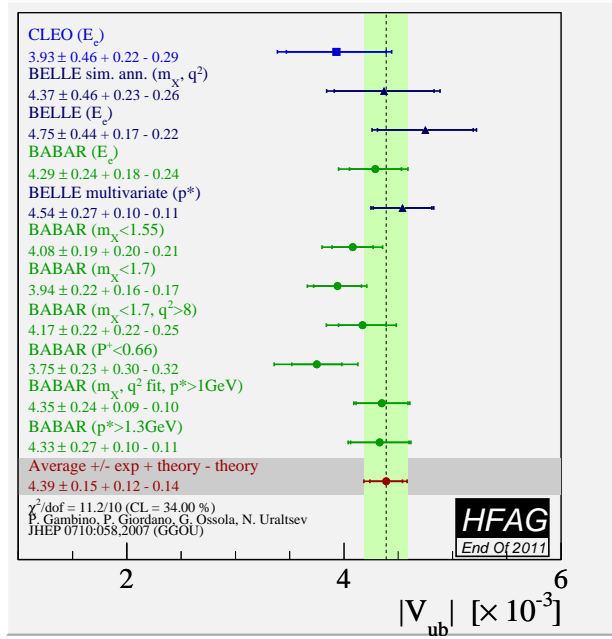


Figure 57: Measurements of $|V_{ub}|$ from inclusive semileptonic decays and their average based on the GGOU prescription. “ E_e ”, “ M_X ”, “ (M_X, q^2) ”, “ P^+ ”, “ p^* ” and “ (E_e, s_h^{max}) ” indicate the analysis type and applied cut.

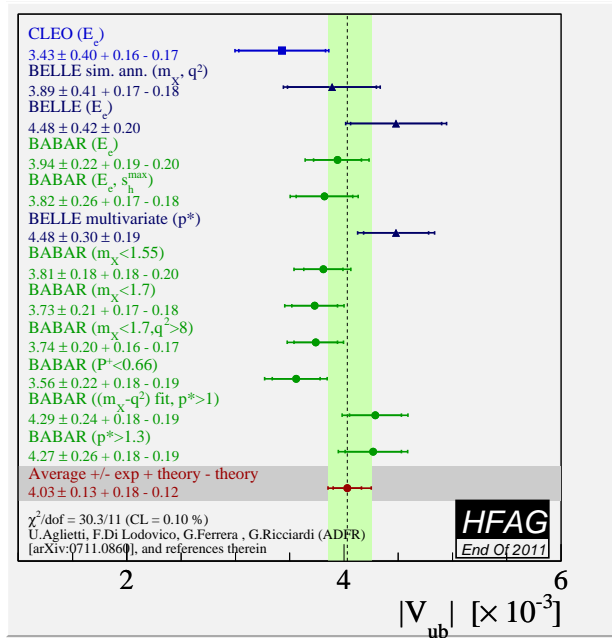


Figure 58: Measurements of $|V_{ub}|$ from inclusive semileptonic decays and their average based on the ADFR prescription. “ E_e ”, “ M_X ”, “ (M_X, q^2) ”, “ P^+ ”, “ p^* ” and “ (E_e, s_h^{max}) ” indicate the analysis type and applied cut.

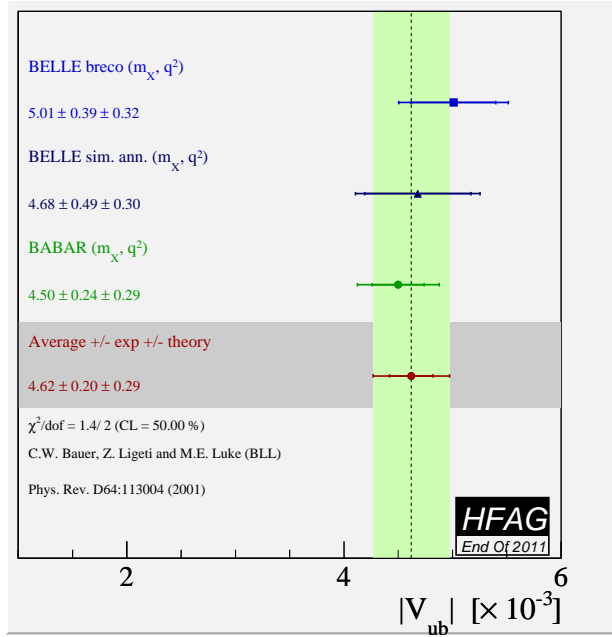


Figure 59: Measurements of $|V_{ub}|$ from inclusive semileptonic decays and their average in the BLL prescription. “(M_X, q^2)” indicates the analysis type.

5.4.5 BLL

Bauer, Ligeti, and Luke (BLL) [418] give a HQET-based prescription that advocates combined cuts on the dilepton invariant mass, q^2 , and hadronic mass, m_X , to minimise the overall uncertainty on $|V_{ub}|$. In their reckoning a cut on m_X only, although most efficient at preserving phase space ($\sim 80\%$), makes the calculation of the partial rate untenable due to uncalculable corrections to the b -quark distribution function or shape function. These corrections are suppressed if events in the low q^2 region are removed. The cut combination used in measurements is $M_x < 1.7 \text{ GeV}/c^2$ and $q^2 > 8 \text{ GeV}^2/c^2$. The extracted values of $|V_{ub}|$ for each measurement along with their average are given in Table 74 and illustrated in Figure 59. The total error is $^{+7.7\%}_{-7.7\%}$ whose breakdown is: statistics ($^{+3.3\%}_{-3.3\%}$), detector ($^{+3.0\%}_{-3.0\%}$), $B \rightarrow X_c \ell^+ \nu_\ell$ model ($^{+1.6\%}_{-1.6\%}$), $B \rightarrow X_u \ell^+ \nu_\ell$ model ($^{+1.1\%}_{-1.1\%}$), spectral fraction (m_b) ($^{+3.0\%}_{-3.0\%}$), perturbative : strong coupling α_s ($^{+3.0\%}_{-3.0\%}$), residual shape function ($^{+2.5\%}_{-2.5\%}$), third order terms in the OPE ($^{+4.0\%}_{-4.0\%}$). The leading uncertainties, both from theory, are due to residual shape function effects and third order terms in the OPE expansion. The leading experimental uncertainty is due to statistics.

5.4.6 Summary

A summary of the averages presented in several different frameworks and results by V.B. Golubev, V.G. Luth and Yu.I. Skovpen [424], based on prescriptions by LLR [421] and LNP [422] to reduce the leading shape function uncertainties are presented in Table 75. A value judgement based on a direct comparison should be avoided at the moment, experimental and theoretical uncertainties play out differently between the schemes and the theoretical assumptions for the theory calculations are different.

Table 67: Summary of exclusive determinations of $\mathcal{B}(\bar{B} \rightarrow \pi \ell \bar{\nu})$. The errors quoted correspond to statistical and systematic uncertainties, respectively. Measured branching fractions for $B \rightarrow \pi^0 l \nu$ have been multiplied by $2 \times \tau_{B^0} / \tau_{B^+}$ in accordance with isospin symmetry. The labels “ B_{reco} ” and “SL” tags refer to the type of B decay tag used in a measurement, and “untagged” refers to an untagged measurement.

	$\mathcal{B}[10^{-4}]$	$\mathcal{B}(q^2 < 12 \text{ GeV}^2/c^2)[10^{-4}]$	$\mathcal{B}(q^2 < 16 \text{ GeV}^2/c^2)[10^{-4}]$	$\mathcal{B}(q^2 > 16 \text{ GeV}^2/c^2)[10^{-4}]$
CLEO π^+, π^0 [401]	$1.38 \pm 0.15 \pm 0.11$	$0.70 \pm 0.12 \pm 0.07$	$0.97 \pm 0.13 \pm 0.09$	$0.41 \pm 0.08 \pm 0.04$
BABAR π^+, π^0 [402]	$1.41 \pm 0.05 \pm 0.08$	$0.88 \pm 0.04 \pm 0.05$	$1.10 \pm 0.04 \pm 0.06$	$0.32 \pm 0.02 \pm 0.03$
BABAR π^+ [403]	$1.42 \pm 0.05 \pm 0.07$	$0.83 \pm 0.03 \pm 0.04$	$1.09 \pm 0.04 \pm 0.05$	$0.33 \pm 0.03 \pm 0.03$
Belle π^+ [404]	$1.49 \pm 0.04 \pm 0.07$	$0.83 \pm 0.03 \pm 0.04$	$1.10 \pm 0.03 \pm 0.05$	$0.40 \pm 0.02 \pm 0.02$
Belle SL π^+ [405]	$1.42 \pm 0.19 \pm 0.15$	$0.80 \pm 0.14 \pm 0.08$	$1.04 \pm 0.16 \pm 0.11$	$0.37 \pm 0.10 \pm 0.04$
Belle SL π^0 [405]	$1.41 \pm 0.26 \pm 0.15$	$0.71 \pm 0.17 \pm 0.08$	$1.04 \pm 0.22 \pm 0.12$	$0.36 \pm 0.15 \pm 0.04$
BABAR SL π^+ [406]	$1.39 \pm 0.21 \pm 0.08$	$0.77 \pm 0.14 \pm 0.05$	$0.92 \pm 0.16 \pm 0.05$	$0.46 \pm 0.13 \pm 0.03$
BABAR SL π^0 [406]	$1.78 \pm 0.28 \pm 0.15$	$1.07 \pm 0.20 \pm 0.09$	$1.34 \pm 0.22 \pm 0.11$	$0.44 \pm 0.17 \pm 0.06$
BABAR $B_{reco} \pi^+$ [407]	$1.07 \pm 0.27 \pm 0.19$	$0.26 \pm 0.15 \pm 0.04$	$0.42 \pm 0.18 \pm 0.06$	$0.65 \pm 0.20 \pm 0.13$
BABAR $B_{reco} \pi^0$ [407]	$1.52 \pm 0.41 \pm 0.30$	$0.67 \pm 0.30 \pm 0.12$	$1.04 \pm 0.35 \pm 0.18$	$0.48 \pm 0.22 \pm 0.12$
Belle $B_{reco} \pi^+$ [408]	$1.12 \pm 0.18 \pm 0.05$	$0.65 \pm 0.14 \pm 0.03$	$0.85 \pm 0.16 \pm 0.04$	$0.26 \pm 0.08 \pm 0.01$
Belle $B_{reco} \pi^0$ [408]	$1.22 \pm 0.22 \pm 0.05$	$0.65 \pm 0.19 \pm 0.03$	$0.80 \pm 0.19 \pm 0.03$	$0.41 \pm 0.11 \pm 0.02$
Average	$1.42 \pm 0.03 \pm 0.04$	$0.81 \pm 0.02 \pm 0.03$	$1.05 \pm 0.02 \pm 0.03$	$0.37 \pm 0.01 \pm 0.02$

Table 68: Determinations of $|V_{ub}|$ based on the average partial $\bar{B} \rightarrow \pi \ell \bar{\nu}$ decay branching fractions stated in Table 67. The first uncertainty is experimental and the second is from theory. The full or partial branching fractions are used as indicated. Acronyms for the calculations refer to either the method (LCSR) or the collaboration working on it (HPQCD, FNAL/MILC).

Method	$ V_{ub} [10^{-3}]$
LCSR 1, $q^2 < 12 \text{ GeV}^2/c^2$ [409]	$3.40 \pm 0.07^{+0.37}_{-0.32}$
LCSR 2, $q^2 < 16 \text{ GeV}^2/c^2$ [410]	$3.57 \pm 0.06^{+0.59}_{-0.39}$
HPQCD, $q^2 > 16 \text{ GeV}^2/c^2$ [411]	$3.45 \pm 0.09^{+0.60}_{-0.39}$
FNAL/MILC, $q^2 > 16 \text{ GeV}^2/c^2$ [412]	$3.30 \pm 0.09^{+0.37}_{-0.30}$

Table 69: Summary of exclusive determinations of $\mathcal{B}(\bar{B} \rightarrow \rho \ell \bar{\nu})$. The errors quoted correspond to statistical and systematic uncertainties, respectively.

$\mathcal{B}[10^{-4}]$	
CLEO ρ^+ [413]	$2.75 \pm 0.41 \pm 0.52$
CLEO ρ^+ [401]	$2.93 \pm 0.37 \pm 0.37$
Belle ρ^+ [408]	$2.56 \pm 0.46 \pm 0.13$
Belle ρ^0 [408]	$3.38 \pm 0.43 \pm 0.15$
Belle ρ^+ [405]	$2.24 \pm 0.54 \pm 0.31$
Belle ρ^0 [405]	$2.54 \pm 0.43 \pm 0.33$
BABAR ρ^+ [402]	$1.98 \pm 0.21 \pm 0.38$
BABAR ρ^0 [402]	$1.87 \pm 0.19 \pm 0.32$
Average	$2.61 \pm 0.15 \pm 0.16$

Table 70: Summary of exclusive determinations of $\mathcal{B}(\bar{B} \rightarrow \omega \ell \bar{\nu})$. The errors quoted correspond to statistical and systematic uncertainties, respectively.

$\mathcal{B}[10^{-4}]$	
Belle ω [408]	$1.19 \pm 0.32 \pm 0.06$
BABAR ω [414]	$1.14 \pm 0.16 \pm 0.08$
Average	$1.15 \pm 0.14 \pm 0.06$

Table 71: Summary of exclusive determinations of $\mathcal{B}(\bar{B} \rightarrow \eta \ell \bar{\nu})$. The errors quoted correspond to statistical and systematic uncertainties, respectively.

$\mathcal{B}[10^{-4}]$	
CLEO η [415]	$0.44 \pm 0.23 \pm 0.11$
BABAR η [414]	$0.31 \pm 0.06 \pm 0.08$
BABAR η [406]	$0.64 \pm 0.20 \pm 0.03$
BABAR η [403]	$0.36 \pm 0.05 \pm 0.04$
Average	$0.37 \pm 0.04 \pm 0.04$

Table 72: Summary of exclusive determinations of $\mathcal{B}(\bar{B} \rightarrow \eta' \ell \bar{\nu})$. The errors quoted correspond to statistical and systematic uncertainties, respectively.

$\mathcal{B}[10^{-4}]$	
CLEO η' [415]	$2.66 \pm 0.80 \pm 0.56$
BABAR η' [406]	$0.04 \pm 0.22 \pm 0.04$
BABAR η' [403]	$0.24 \pm 0.08 \pm 0.03$
Average	$0.23 \pm 0.08 \pm 0.03$

Table 73: Summary of inclusive determinations of partial branching fractions for $B \rightarrow X_u \ell^+ \nu_\ell$ decays. The errors quoted on $\Delta\mathcal{B}$ correspond to statistical and systematic uncertainties. The s_h^{\max} variable is described in Refs. [426, 427].

Measurement	Accepted region	$\Delta\mathcal{B}[10^{-4}]$	Notes
CLEO [428]	$E_e > 2.1 \text{ GeV}$	$3.3 \pm 0.2 \pm 0.7$	
BABAR [427]	$E_e > 2.0 \text{ GeV}, s_h^{\max} < 3.5 \text{ GeV}^2$	$4.4 \pm 0.4 \pm 0.4$	
BABAR [425]	$E_e > 2.0 \text{ GeV}$	$5.7 \pm 0.4 \pm 0.5$	
Belle [429]	$E_e > 1.9 \text{ GeV}$	$8.5 \pm 0.4 \pm 1.5$	
BABAR [417]	$M_X < 1.7 \text{ GeV}/c^2, q^2 > 8 \text{ GeV}^2/c^2$	$6.8 \pm 0.6 \pm 0.4$	
Belle [430]	$M_X < 1.7 \text{ GeV}/c^2, q^2 > 8 \text{ GeV}^2/c^2$	$7.4 \pm 0.9 \pm 1.3$	
Belle [431]	$M_X < 1.7 \text{ GeV}/c^2, q^2 > 8 \text{ GeV}^2/c^2$	$8.4 \pm 0.8 \pm 1.0$	used only in BLL average
BABAR [417]	$P_+ < 0.66 \text{ GeV}$	$9.8 \pm 0.9 \pm 0.8$	
BABAR [417]	$M_X < 1.7 \text{ GeV}/c^2$	$11.5 \pm 1.0 \pm 0.8$	
BABAR [417]	$M_X < 1.55 \text{ GeV}/c^2$	$10.8 \pm 0.8 \pm 0.6$	
Belle [416]	$p_\ell^* > 1 \text{ GeV}/c$	$19.6 \pm 1.7 \pm 1.6$	
BABAR [417]	(M_X, q^2) fit, $p_\ell^* > 1 \text{ GeV}/c$	$18.0 \pm 1.3 \pm 1.5$	
BABAR [417]	$p_\ell^* > 1.3 \text{ GeV}/c$	$15.3 \pm 1.3 \pm 1.4$	

Table 74: Summary of input parameters used by the different theory calculations, corresponding inclusive determinations of $|V_{ub}|$ and their average. The errors quoted on $|V_{ub}|$ correspond to experimental and theoretical uncertainties, respectively.

	BLNP	DGE	GGOU	ADFR	BLL
Input parameters					
scheme	SF	\overline{MS}	kinetic	\overline{MS}	1S
Ref.	[436, 437]	Ref. [5]	see Sect. 5.2.2	Ref. [5]	Ref. [357]
m_b (GeV)	4.588 ± 0.025	4.194 ± 0.043	4.560 ± 0.023	4.194 ± 0.043	4.704 ± 0.029
μ_π^2 (GeV ²)	$0.189^{+0.046}_{-0.057}$	-	0.453 ± 0.036	-	-
Ref.	$ V_{ub} $ values				
E_e [428]	$4.19 \pm 0.49^{+0.26}_{-0.34}$	$3.82 \pm 0.45^{+0.23}_{-0.26}$	$3.93 \pm 0.46^{+0.22}_{-0.29}$	$3.43 \pm 0.40^{+0.16}_{-0.17}$	-
M_X, q^2 [430]	$4.46 \pm 0.47^{+0.25}_{-0.27}$	$4.40 \pm 0.46^{+0.19}_{-0.20}$	$4.37 \pm 0.46^{+0.23}_{-0.26}$	$3.89 \pm 0.41^{+0.17}_{-0.18}$	$4.68 \pm 0.49^{+0.30}_{-0.30}$
E_e [429]	$4.88 \pm 0.45^{+0.24}_{-0.27}$	$4.79 \pm 0.44^{+0.21}_{-0.24}$	$4.75 \pm 0.44^{+0.17}_{-0.22}$	$4.48 \pm 0.42^{+0.20}_{-0.20}$	-
E_e [425]	$4.48 \pm 0.25^{+0.27}_{-0.28}$	$4.28 \pm 0.24^{+0.22}_{-0.24}$	$4.29 \pm 0.24^{+0.18}_{-0.24}$	$3.94 \pm 0.22^{+0.19}_{-0.20}$	-
E_e, s_h^{\max} [427]	$4.66 \pm 0.31^{+0.31}_{-0.36}$	$4.32 \pm 0.29^{+0.24}_{-0.29}$	-	$3.82 \pm 0.26^{+0.17}_{-0.18}$	-
p_ℓ^* [416]	$4.47 \pm 0.27^{+0.19}_{-0.21}$	$4.60 \pm 0.27^{+0.11}_{-0.13}$	$4.54 \pm 0.27^{+0.10}_{-0.11}$	$4.48 \pm 0.30^{+0.19}_{-0.19}$	-
M_X [417]	$4.17 \pm 0.19^{+0.24}_{-0.24}$	$4.40 \pm 0.20^{+0.24}_{-0.19}$	$4.08 \pm 0.19^{+0.20}_{-0.21}$	$3.81 \pm 0.18^{+0.18}_{-0.20}$	-
M_X [417]	$3.97 \pm 0.22^{+0.20}_{-0.20}$	$4.16 \pm 0.23^{+0.26}_{-0.22}$	$3.94 \pm 0.22^{+0.16}_{-0.17}$	$3.73 \pm 0.21^{+0.17}_{-0.18}$	-
M_X, q^2 [417]	$4.25 \pm 0.23^{+0.23}_{-0.25}$	$4.19 \pm 0.22^{+0.18}_{-0.19}$	$4.17 \pm 0.22^{+0.22}_{-0.25}$	$3.74 \pm 0.20^{+0.16}_{-0.17}$	$4.50 \pm 0.24^{+0.29}_{-0.29}$
P_+ [417]	$4.02 \pm 0.25^{+0.24}_{-0.23}$	$4.10 \pm 0.25^{+0.37}_{-0.28}$	$3.75 \pm 0.23^{+0.30}_{-0.32}$	$3.56 \pm 0.22^{+0.18}_{-0.19}$	-
$p_\ell^*, (M_X, q^2)$ fit [417]	$4.28 \pm 0.24^{+0.18}_{-0.20}$	$4.40 \pm 0.24^{+0.12}_{-0.13}$	$4.35 \pm 0.24^{+0.09}_{-0.10}$	$4.29 \pm 0.24^{+0.18}_{-0.19}$	-
p_ℓ^* [417]	$4.29 \pm 0.27^{+0.19}_{-0.20}$	$4.39 \pm 0.27^{+0.15}_{-0.14}$	$4.33 \pm 0.27^{+0.10}_{-0.11}$	$4.27 \pm 0.26^{+0.18}_{-0.19}$	-
M_X, q^2 [431]	-	-	-	-	$5.01 \pm 0.39^{+0.32}_{-0.32}$
Average	$4.40 \pm 0.15^{+0.19}_{-0.21}$	$4.45 \pm 0.15^{+0.15}_{-0.16}$	$4.39 \pm 0.15^{+0.12}_{-0.14}$	$4.03 \pm 0.13^{+0.18}_{-0.12}$	$4.62 \pm 0.20^{+0.29}_{-0.29}$

Table 75: Summary of inclusive determinations of $|V_{ub}|$. The errors quoted on $|V_{ub}|$ correspond to experimental and theoretical uncertainties, except for the last two measurements where the errors are due to the *BABAR* endpoint analysis, the *BABAR* $b \rightarrow s\gamma$ analysis [423], the theoretical errors and V_{ts} for the last averages.

Framework	$ V_{ub} [10^{-3}]$
BLNP	$4.40 \pm 0.15^{+0.19}_{-0.21}$
DGE	$4.45 \pm 0.15^{+0.15}_{-0.16}$
GGOU	$4.39 \pm 0.15^{+0.12}_{-0.20}$
ADFR	$4.03 \pm 0.13^{+0.18}_{-0.12}$
BLL (m_X/q^2 only)	$4.62 \pm 0.20 \pm 0.29$
LLR (<i>BABAR</i>) [423]	$4.43 \pm 0.45 \pm 0.29$
LLR (<i>BABAR</i>) [424]	$4.28 \pm 0.29 \pm 0.29 \pm 0.26 \pm 0.28$
LNP (<i>BABAR</i>) [424]	$4.40 \pm 0.30 \pm 0.41 \pm 0.23$

6 B decays to charmed hadrons

This section reports the updated contribution to the HFAG report from the “ $B \rightarrow$ charm” group⁴⁴. The mandate of the group is to compile measurements and perform averages of all available quantities related to B decays to charmed particles, excluding CP related quantities. To date the group has analyzed a total of 651 measurements reported in 233 papers, principally branching fractions. The group aims to organize and present the copious information on b -hadron decays to charmed particles obtained from a combined sample of about two billion B -meson from the BABAR, Belle Collaborations and data collected in hadronic colliders by the CDF, D0 and LHCb Experiments.

These huge samples of b -hadrons allow to measure decays to states with open or hidden charm content with unprecedented precision. Branching fractions for rare b -hadron decays or decay chains of a few 10^{-7} are being measured with statistical uncertainties typically below 30%, and new decay chains can be accessed with branching fractions down to 10^{-8} . Results for more common decay chains, with branching fractions around 10^{-4} , are becoming precision measurements, with uncertainties typically at the 3% level.

The measurements are classified according to the decaying particle: B^+ , B^0 , B_s^0 , B_c^+ , A_b and Others ; the decay products and the type of quantity: branching fraction, product of branching fractions, ratio of branching fractions or other quantities. For the decay product classification the below precedence order is used to ensure that each measurement appears in only one category.

- new particles
- strange D mesons
- baryons
- J/ψ
- charmonium other than J/ψ
- multiple D , D^* or D^{**} mesons
- a single D^* or D^{**} meson
- a single D meson
- other particles

Within each table the measurements are color coded according to the publication status and age. Table 76 provides a key to the color scheme and categories used. When viewing the tables with most pdf viewers every number, label and average provides hyperlinks to the corresponding reference and individual quantity web pages on the HFAG/BtoCharm group website <http://hfag.phys.ntu.edu.tw>. The links provided in the captions of the table lead to the corresponding compilation pages. Both the individual and compilation webpages provide a graphical view of the results, in a variety of formats.

Tables 77 to 129 provide either limits at 90% confidence level or measurements with statistical and systematic uncertainties and in some cases a third error corresponding to correlated systematics. For details on the meanings of the uncertainties and access to the references click

⁴⁴The HFAG/BtoCharm group was formed in the spring of 2005; it performs its work using an XML database backed web application.

on the numbers to visit the corresponding web pages. Where there are multiple determinations of the same quantity by one experiment the table footnotes act to distinguish the methods or datasets used; such cases are visually highlighted in the table by presenting the measurements on the lines beneath the quantity label. Where both limits and measured values of a quantity are available the limits are presented in the tables but are not used in the determination of the average. Where only limits are available the most stringent is presented in the Average column of the tables. Where available the PDG 2010 result is also presented.

Table 76: Key to the colors used to classify the results presented in tables 77 to 129. When viewing these tables in a pdf viewer each number, label and average provides a hyperlink to the corresponding online version provided by the charm subgroup website <http://hfag.phys.ntu.edu.tw/b2charm/>. Where an experiment has multiple determinations of a single quantity they are distinguished by the table footnotes.

Class	Definition
waiting	Results without a preprint available
pubhot	Results published during or after 2011
prehot	Preprint released during or after 2011
pub	Results published during or after 2008 but before 2011
pre	Preprint released during or after 2008 but before 2011
pubold	Results published before 2008
preold	Preprint released before 2008
error	Incomplete information to classify
superceeded	Results superceeded by more recent measurements from the same experiment
inactive	Results in the process of being entered into the database
noquo	Results without quotes

Table 77: Branching fractions of charged B modes producing new particles in units of 10^{-3} , upper limits are at 90% CL. The latest version is available at: <http://hfag.phys.ntu.edu.tw/b2charm/00101.html>

Mode	PDG 2010	Belle	BABAR	CDF	D0	LHCb	Average
$X(3872)K^-$	< 0.32		< 0.32				< 0.32
$D_{sJ}^-(2460)D^0$	3.10 ± 1.00		$4.3 \pm 1.6 \pm 1.3$				4.3 ± 2.1
$D_{sJ}^-(2460)D^{*0}(2007)$	12.0 ± 3.0		$11.2 \pm 2.6 \pm 2.0$				11.2 ± 3.3

Table 78: Product branching fractions of charged B modes producing new particles in units of 10^{-4} , upper limits are at 90% CL. The latest version is available at: <http://hfag.phys.ntu.edu.tw/b2charm/00101.html>

Mode	PDG 2010	Belle	BABAR	CDF	D0	LHCb	Average
$K^- X(3872)[J/\psi(1S)\gamma]$	0.028 ± 0.008		$0.0280 \pm 0.0080 \pm 0.0010$				0.020 ± 0.003
$K^{*-}(892)X(3872)[J/\psi(1S)\gamma]$	< 0.048		< 0.048				< 0.048
$K^- X(3872)[J/\psi(1S)\omega(782)]$			$0.06 \pm 0.02 \pm 0.01$				0.06 ± 0.02
$K^- X(3872)[J/\psi(1S)\eta]$	< 0.077		< 0.077				< 0.077
$K^- X(3872)[\psi(2S)\gamma]$	0.09 ± 0.03	< 0.034	$0.095 \pm 0.027 \pm 0.006$				0.09 ± 0.03
$K^- X(3872)[\pi^+\pi^- J/\psi(1S)]$	0.10 ± 0.02	$0.13 \pm 0.02 \pm 0.01$	$0.084 \pm 0.015 \pm 0.007$				0.10 ± 0.01
$\bar{K}^0 Z^-(4430)[J/\psi(1S)\pi^-]$	< 0.150		< 0.130				< 0.130
$K^- Y(3940)[J/\psi(1S)\gamma]$	< 0.140		< 0.140				< 0.140
$K^- Y(4260)[J/\psi(1S)\pi^+\pi^-]$	< 0.29		$0.20 \pm 0.07 \pm 0.02$				0.20 ± 0.07
$\bar{K}^0 X^-(3872)[J/\psi(1S)\pi^-\pi^0]$	< 0.22		< 0.22				< 0.22
$K^{*-}(892)X(3872)[\psi(2S)\gamma]$	< 0.28		< 0.28				< 0.28
$K^- Y(3940)[J/\psi(1S)\omega(782)]$			$0.30 \pm 0.07 \pm 0.03$				0.30 ± 0.08
$K^- X(3872)[D^+ D^-]$	< 0.40	< 0.40					< 0.40
$\bar{K}^0 Z^-(4430)[\psi(2S)\pi^-]$	< 0.47		< 0.43				< 0.43
$K^- X(3872)[D^0 \bar{D}^0 \pi^0]$	1.00 ± 0.40	< 0.60					< 0.60
$K^- X(3872)[D^0 \bar{D}^0]$	< 0.60	< 0.60					< 0.60
$K^- X(3872)[\bar{D}^{*0}(2007)D^0]$	0.85 ± 0.26		$1.67 \pm 0.36 \pm 0.47$				1.67 ± 0.59
$D^0 D_{sJ}^-(2460)[D_s^- \pi^+ \pi^-]$	< 2.2	< 2.2					< 2.2
$D^0 D_{sJ}^-(2460)[D_s^- \pi^0]$	< 2.7	< 2.7					< 2.7
$D^0 D_{sJ}^-(2460)[D_s^- \gamma]$	4.6 ± 1.2	$5.6 \pm 1.6 \pm 1.7$	$6.00 \pm 2.00 \pm 1.00 \pm 2.00$				5.8 ± 1.7
$D^0 D_{sJ}^*(2317)^-[D_s^{*-} \gamma]$	< 7.6	< 7.6					< 7.6
$D^{*0}(2007)D_{sJ}^*(2317)^-[D_s^- \pi^0]$	9.0 ± 7.0		$9.0 \pm 6.0 \pm 2.0 \pm 3.0$				9.0 ± 7.0
$D^0 D_{sJ}^*(2317)^-[D_s^- \pi^0]$	7.3 ± 2.0	$8.1 \pm 3.0 \pm 2.4$	$10.00 \pm 3.00 \pm 1.00 \pm 4.00$				8.9 ± 3.2
$D^0 D_{sJ}^-(2460)[D_s^{*-} \gamma]$	< 9.8	< 9.8					< 9.8
$D^{*0}(2007)D_{sJ}^-(2460)[D_s^- \gamma]$	14.0 ± 7.0		$14.0 \pm 4.0 \pm 3.0 \pm 5.0$				14.0 ± 7.1
$D^0 D_{sJ}^-(2460)[D_s^{*-} \pi^0]$		$11.9 \pm 6.1 \pm 3.6$	$27.0 \pm 7.0 \pm 5.0 \pm 9.0$				15.0 ± 5.8
$D^{*0}(2007)D_{sJ}^-(2460)[D_s^{*-} \pi^0]$			$76 \pm 17 \pm 18 \pm 26$				76 ± 29

¹ Observation of $X(3872) \rightarrow J/\psi\gamma$ and search for $X(3872) \rightarrow \psi'\gamma$ in B decays (772M $B\bar{B}$ pairs)

² Observation of $X(3872) \rightarrow \gamma J/\psi$ and evidence for the sub-threshold decay $X(3872) \rightarrow \omega J/\psi$

Table 79: Branching fractions of charged B modes producing strange D mesons in units of 10^{-4} , upper limits are at 90% CL. The latest version is available at: <http://hfag.phys.ntu.edu.tw/b2charm/00102.html>

Mode	PDG 2010	Belle	BABAR	CDF	D0	LHCb	Average
$D_s^- \phi(1020)$	< 0.019		< 0.019				< 0.019
$D_s^+ K^- K^-$	0.11 ± 0.04		$0.110 \pm 0.040 \pm 0.020 \pm 0.003$				0.11 ± 0.04
$D_s^{*-} \phi(1020)$	< 0.120		< 0.120				< 0.120
$D_s^{*+} K^- K^-$	< 0.150		< 0.150				< 0.150
$D_s^- \pi^0$	0.16 ± 0.05		$0.15 \pm_{0.04}^{0.05} \pm 0.01 \pm 0.02$				0.15 ± 0.05
$D_s^{*+} K^- \pi^-$	1.45 ± 0.24	$1.47 \pm_{0.14}^{0.15} \pm_{0.19}^{0.19} \pm 0.13$	$1.67 \pm 0.16 \pm 0.35 \pm 0.05$				1.54 ± 0.22
$D_s^{*+} K^- \pi^-$	1.80 ± 0.22		$2.02 \pm 0.13 \pm 0.38 \pm 0.06$				1.90 ± 0.18
		$1.94 \pm_{0.08}^{0.09} \pm_{0.20}^{0.20} \pm 0.17$ ¹					
		$1.77 \pm 0.12 \pm 0.16 \pm 0.23$ ²					
$D_s^- D^0$	100 ± 17	$85.2 \pm_{3.8}^{3.9}$	$133 \pm 18 \pm 32$				$85.7 \pm_{3.9}^{3.8}$
$D_s^{*-} D^0$	76 ± 16		$93 \pm 18 \pm 19$				93 ± 26
$D_s^- D^{*0}(2007)$	82 ± 17		$121 \pm 23 \pm 20$				121 ± 30
$D_s^{*-} D^{*0}(2007)$	171 ± 24		$170 \pm 26 \pm 24$				170 ± 35

¹ Measurement of $B \rightarrow D_s^{(*)} K \pi$ branching fractions (657M $B\bar{B}$ pairs)

² Measurement of B - Ds K pi branching ratios (520M $B\bar{B}$ pairs)

Table 80: Product branching fractions of charged B modes producing strange D mesons in units of 10^{-4} , upper limits are at 90% CL. The latest version is available at: <http://hfag.phys.ntu.edu.tw/b2charm/00102.html>

Mode	PDG 2010	Belle	BABAR	CDF	D0	LHCb	Average
$D^0 D_{s1}^- (2536) [\overline{D}^{*0} (2007) K^-]$	2.20 ± 0.70		$2.16 \pm 0.52 \pm 0.45$				2.16 ± 0.69
$D^0 D_{s1}^- (2536) [D^{*-} (2010) \overline{K}^0]$	2.3 ± 1.1		$2.30 \pm 0.98 \pm 0.43$				2.3 ± 1.1
$D^{*0} (2007) D_s^- [\phi(1020) \pi^-]$			$2.95 \pm 0.65 \pm 0.36$				2.95 ± 0.74
$D_s^{*-} D^0 [D_s^- \rightarrow \phi(1020) \pi^-]$			$3.13 \pm 1.19 \pm 0.58$				3.1 ± 1.3
$\overline{D}_s^0 D_{s1}^+ (2536) [D^{*0} (2007) K^+ + D^{*+} (2010) K^0]$		$3.97 \pm 0.85 \pm 0.56$					4.0 ± 1.0
$D^0 D_s^- [\phi(1020) \pi^-]$			$4.00 \pm 0.61 \pm 0.61$				4.00 ± 0.86
$\overline{D}^{*0} (2007) D_{s1}^- (2536) [\overline{D}^{*0} (2007) K^-]$	5.5 ± 1.6		$5.5 \pm 1.2 \pm 1.0$				5.5 ± 1.6
$D_s^{*-} D^{*0} (2007) [D_s^- \rightarrow \phi(1020) \pi^-]$			$8.6 \pm 1.5 \pm 1.1$				8.6 ± 1.9
$D^{*0} (2007) D_{s1}^- (2536) [D^{*-} (2010) \overline{K}^0]$	3.9 ± 2.6		< 10.7				< 10.7

Table 81: Branching fractions of charged B modes producing baryons in units of 10^{-4} , upper limits are at 90% CL. The latest version is available at: <http://hfag.phys.ntu.edu.tw/b2charm/00103.html>

Mode	PDG 2010	Belle	BABAR	CDF	D0	LHCb	Average
$J/\psi(1S)\Sigma^0\bar{p}$	< 0.110	< 0.110					< 0.110
$J/\psi(1S)\Lambda\bar{p}$	0.12 ± 0.03	$0.12 \pm 0.03 \pm_{0.02}^{0.02}$	$0.12 \pm_{0.05}^{0.07} \pm_{0.02}^{0.04}$				0.12 ± 0.03
$\bar{p}\Lambda D^0$		$0.14 \pm_{0.02}^{0.03} \pm_{0.02}^{0.02}$					0.14 ± 0.03
$D^{*-}(2010)p\bar{p}$	< 0.150	< 0.150					< 0.150
$D^-p\bar{p}$	< 0.150	< 0.150					< 0.150
$\Sigma_c^{*0}\bar{p}$		< 0.46					< 0.46
$\bar{p}\Lambda D^{*0}(2007)$		> 0.48					> 0.48
$\Sigma_c^0\bar{p}$	0.35 ± 0.10	< 0.93					< 0.93
$D^+p\bar{p}\pi^-\pi^-$			$1.66 \pm 0.13 \pm 0.27$				1.66 ± 0.30
$D^{*+}(2010)p\bar{p}\pi^-\pi^-$			$1.86 \pm 0.16 \pm 0.19$				1.86 ± 0.25
$\Lambda_c^+\bar{p}\pi^-$	2.80 ± 0.80	$1.87 \pm_{0.40}^{0.43} \pm 0.28 \pm 0.49$	$3.38 \pm 0.12 \pm 0.12 \pm 0.88$				2.44 ± 0.55
$D^0p\bar{p}\pi^-$			$3.72 \pm 0.11 \pm 0.25$				3.72 ± 0.27
$D^{*0}(2007)p\bar{p}\pi^-$			$3.73 \pm 0.17 \pm 0.27$				3.73 ± 0.32
$\Lambda_c^+\Lambda_c^-K^-$	8.7 ± 3.5	$6.50 \pm_{0.90}^{1.00} \pm 1.10 \pm 3.40$	$11.4 \pm 1.5 \pm 1.7 \pm 6.0$				7.7 ± 3.2

Table 82: Product branching fractions of charged B modes producing baryons in units of 10^{-5} , upper limits are at 90% CL. The latest version is available at: <http://hfag.phys.ntu.edu.tw/b2charm/00103.html>

Mode	PDG 2010	Belle	BABAR	CDF	D0	LHCb	Average
$K^- \eta_c(1S)[\Lambda\bar{\Lambda}]$		$0.095 \pm_{0.022}^{0.025} \pm_{0.011}^{0.008}$					0.10 ± 0.03
$K^- \eta_c(1S)[p\bar{p}]$		$0.14 \pm 0.01 \pm_{0.02}^{0.02}$	$0.18 \pm_{0.02}^{0.03} \pm 0.02$				0.15 ± 0.02
$K^- J/\psi(1S)[\Lambda\bar{\Lambda}]$		$0.20 \pm_{0.03}^{0.03} \pm 0.03$					0.20 ± 0.05
$K^- J/\psi(1S)[p\bar{p}]$		$0.22 \pm 0.01 \pm 0.01$	$0.22 \pm 0.02 \pm 0.01$				0.22 ± 0.01
$\Lambda_c^- \Xi_c^0[\Xi^- \pi^+]$	3.0 ± 1.1	$4.80 \pm_{0.90}^{1.00} \pm 1.10 \pm 1.20$	$2.08 \pm 0.65 \pm 0.29 \pm 0.54$				2.57 ± 0.81

Table 83: Ratios of branching fractions of charged B modes producing baryons in units of 10^{-1} , upper limits are at 90% CL. The latest version is available at: <http://hfag.phys.ntu.edu.tw/b2charm/00103.html>

Mode	PDG 2010	Belle	BABAR	CDF	D0	LHCb	Average
$\frac{\mathcal{B}(B^- \rightarrow \Sigma_c^0(2800)\bar{p})}{\mathcal{B}(B^- \rightarrow \Lambda_c^+ \bar{p}\pi^-)}$			$1.17 \pm 0.23 \pm 0.24$				1.17 ± 0.33
$\frac{\mathcal{B}(B^- \rightarrow \Sigma_c^0(2455)\bar{p})}{\mathcal{B}(B^- \rightarrow \Lambda_c^+ \bar{p}\pi^-)}$			$1.23 \pm 0.12 \pm 0.08$				1.23 ± 0.14
$\frac{\mathcal{B}(B^- \rightarrow \eta_c(1S)K^-) \times \mathcal{B}(\eta_c(1S) \rightarrow p\bar{p})}{\mathcal{B}(B^- \rightarrow J/\psi(1S)K^-) \times \mathcal{B}(J/\psi(1S) \rightarrow p\bar{p})}$						$7.10 \pm 2.00 \pm 0.70$	7.1 ± 2.1
$\frac{\mathcal{B}(B^- \rightarrow \Lambda_c^+ \bar{p}\pi^-)}{\mathcal{B}(B^0 \rightarrow \Lambda_c^+ \bar{p})}$			$154.0 \pm 18.0 \pm 3.0$				154 ± 18

Table 84: Branching fractions of charged B modes producing $J/\psi(1S)$ in units of 10^{-4} , upper limits are at 90% CL. The latest version is available at: <http://hfag.phys.ntu.edu.tw/b2charm/00104.html>

Mode	PDG 2010	Belle	BABAR	CDF	D0	LHCb	Average
$\pi^- \pi^0 J/\psi(1S)$	< 0.073		< 0.073				< 0.073
$J/\psi(1S)D^0\pi^-$	< 0.25	< 0.25	< 0.52				< 0.25
$J/\psi(1S)\phi(1020)K^-$	0.52 ± 0.17		$0.44 \pm 0.14 \pm 0.05 \pm 0.01$				0.44 ± 0.15
$J/\psi(1S)\pi^-$	0.49 ± 0.04	$0.38 \pm 0.06 \pm 0.03$	$0.54 \pm 0.04 \pm 0.02$				0.48 ± 0.04
$\rho^-(770)J/\psi(1S)$	0.50 ± 0.08		$0.50 \pm 0.07 \pm 0.03$				0.50 ± 0.08
$J/\psi(1S)\eta K^-$	1.08 ± 0.33		$1.08 \pm 0.23 \pm 0.24 \pm 0.03$				1.08 ± 0.33
$J/\psi(1S)D^-$	< 1.20		< 1.20				< 1.20
$J/\psi(1S)\omega(782)K^-$	3.50 ± 0.40		$3.20 \pm 0.10 \pm 0.60$				3.20 ± 0.61
$J/\psi(1S)K^-\pi^+\pi^-$	10.7 ± 1.9	$7.16 \pm 0.10 \pm 0.60$	$11.60 \pm 0.70 \pm 0.90$	$6.9 \pm 1.8 \pm 1.2$			8.07 ± 0.52
$J/\psi(1S)K^-$	10.14 ± 0.34						10.26 ± 0.37
		$10.10 \pm 0.20 \pm 0.70 \pm 0.20$	$10.10 \pm 0.90 \pm 0.60$ ¹				
			$8.10 \pm 1.30 \pm 0.70$ ²				
			$10.61 \pm 0.15 \pm 0.44 \pm 0.18$ ³				
$J/\psi(1S)K^{*-}(892)$	14.30 ± 0.80	$12.80 \pm 0.70 \pm 1.40 \pm 0.20$	$14.54 \pm 0.47 \pm 0.94 \pm 0.25$	$15.8 \pm 4.7 \pm 2.7$			14.03 ± 0.88
$J/\psi(1S)K_1^-(1270)$	18.0 ± 5.2	$18.0 \pm 3.4 \pm 3.0 \pm 2.5$					18.0 ± 5.2

¹ MEASUREMENT OF THE $B^+ \rightarrow p\bar{p}K^+$ BRANCHING FRACTION AND STUDY OF THE DECAY DYNAMICS (232M $B\bar{B}$ pairs) ; $B^- \rightarrow J/\psi K^-$ with $J/\psi \rightarrow p\bar{p}$

² Measurements of the absolute branching fractions of $B^\pm \rightarrow K^\pm X_{c\bar{c}}$ (231.8M $B\bar{B}$ pairs) ; $B^- \rightarrow J/\psi K^-$ (inclusive)

³ MEASUREMENT OF BRANCHING FRACTIONS AND CHARGE ASYMMETRIES FOR EXCLUSIVE B DECAYS TO CHARMONIUM (124M $B\bar{B}$ pairs) ; $B^- \rightarrow J/\psi K^-$ with J/ψ to leptons

Table 85: Product branching fractions of charged B modes producing $J/\psi(1S)$ in units of 10^{-4} , upper limits are at 90% CL. The latest version is available at: <http://hfag.phys.ntu.edu.tw/b2charm/00104.html>

Mode	PDG 2010	Belle	BABAR	CDF	D0	LHCb	Average
$K^- h_c(1P)[J/\psi(1S)\pi^+\pi^-]$	< 0.034		< 0.034				< 0.034

Table 86: Ratios of branching fractions of charged B modes producing $J/\psi(1S)$ in units of 10^{-1} , upper limits are at 90% CL. The latest version is available at: <http://hfag.phys.ntu.edu.tw/b2charm/00104.html>

Mode	PDG 2010	Belle	BABAR	CDF	D0	LHCb	Average
$\frac{\mathcal{B}(B^- \rightarrow J/\psi(1S)\pi^-)}{\mathcal{B}(B^- \rightarrow J/\psi(1S)K^-)}$	0.49 ± 0.04		$0.54 \pm 0.04 \pm 0.01$	$0.500 \pm_{0.170}^{0.190} \pm 0.010$ ¹ $0.49 \pm 0.08 \pm 0.01$ ²		$0.39 \pm 0.04 \pm 0.02$	0.46 ± 0.03
$\frac{\mathcal{B}(B^- \rightarrow X(4140)[J/\psi(1S)\phi(1020)]K^-)}{\mathcal{B}(B^- \rightarrow J/\psi(1S)\phi(1020)K^-)}$				$1.49 \pm 0.39 \pm 0.24$		< 0.70	1.49 ± 0.46
$\frac{\mathcal{B}(B^- \rightarrow J/\psi(1S)K_1^-(1400))}{\mathcal{B}(B^- \rightarrow J/\psi(1S)K_1^-(1270))}$	< 3.0	< 3.0					< 3.0
$\frac{\mathcal{B}(B^- \rightarrow \chi_{c1}(1P)\bar{K}^0\pi^-)}{\mathcal{B}(B^- \rightarrow J/\psi(1S)\bar{K}^0\pi^-)}$			$5.01 \pm 0.24 \pm 0.55$				5.01 ± 0.60
$\frac{\mathcal{B}(B^- \rightarrow \chi_{c0}(1P)K^-)}{\mathcal{B}(B^- \rightarrow J/\psi(1S)K^-)}$	6.0 ± 2.0	$6.00 \pm_{1.80}^{2.10} \pm 0.50 \pm 0.80$					$6.0 \pm_{2.0}^{2.3}$
$\frac{\mathcal{B}(B_s^0 \rightarrow J/\psi(1S)K^-)}{\mathcal{B}(B^- \rightarrow \psi(2S)K^-)}$					$6.50 \pm 0.40 \pm 0.30 \pm 0.70$		6.50 ± 0.86
$\frac{\mathcal{B}(B^- \rightarrow \eta_c(1S)K^-)}{\mathcal{B}(B^- \rightarrow J/\psi(1S)K^-)}$	13.3 ± 4.4						11.2 ± 2.0
$\frac{\mathcal{B}(B^- \rightarrow J/\psi(1S)K^{*-}(892))}{\mathcal{B}(B^- \rightarrow J/\psi(1S)K^-)}$	13.90 ± 0.90		$10.60 \pm 2.30 \pm 0.40$ ³ $12.80 \pm 1.00 \pm 3.80$ ⁴		$19.2 \pm 6.0 \pm 1.7$		13.82 ± 0.93
$\frac{\mathcal{B}(B^- \rightarrow J/\psi(1S)K_1^-(1270))}{\mathcal{B}(B^- \rightarrow J/\psi(1S)K^-)}$		$18.0 \pm 3.4 \pm 3.4$					18.0 ± 4.8

¹ Measurement of the Branching Fraction $B(B^+ \rightarrow J/\psi\pi^+)$ and Search for $B^{c+} \rightarrow J/\psi\pi^+$

¹ Measurement of the Branching Fraction $B(B^+ \rightarrow J/\psi\pi^+)$ and Search for $B^{c+} \rightarrow J/\psi\pi^+$

² Measurement of the Ratio of Branching Fractions $\mathcal{B}(B^+ \rightarrow J/\psi\pi^+)/\mathcal{B}(B^+ \rightarrow J/\psi K^+)$; $\text{Br}(B \rightarrow J/\psi\pi)/\text{Br}(B \rightarrow J/\psi K)$

³ Measurements of the absolute branching fractions of $B^\pm \rightarrow K^\pm X_{cE}$ (231.8M $B\bar{B}$ pairs) ; Ratio $B^- \rightarrow \eta_c K^-$ to $B^- \rightarrow J/\psi K^-$ (inclusive analysis)

⁴ Branching Fraction Measurements of $B \rightarrow \eta_c K$ Decays (86.1M $B\bar{B}$ pairs) ; Ratio $B^- \rightarrow \eta_c K^-$ to $B^- \rightarrow J/\psi K^-$ with $\eta_c \rightarrow K\bar{K}\pi$

Table 87: Branching fractions of charged B modes producing charmonium other than $J/\psi(1S)$ in units of 10^{-4} , upper limits are at 90% CL. The latest version is available at: <http://hfag.phys.ntu.edu.tw/b2charm/00105.html>

Mode	PDG 2010	Belle	BABAR	CDF	D0	LHCb	Average
$h_c(1P)K^-$	< 0.38	< 0.038					< 0.038
$\chi_{c2}(1P)K^-$	< 0.180	$0.111 \pm_{0.034}^{0.036} \pm 0.009$	< 0.180				0.11 ± 0.04
$\chi_{c1}(1P)\pi^-$	0.20 ± 0.04	$0.22 \pm 0.04 \pm 0.03$					0.22 ± 0.05
$\chi_{c0}(1P)\pi^-$			< 0.61				< 0.61
$\chi_{c2}(1P)K^{*-}(892)$	< 0.120		< 1.20				< 1.20
$\chi_{c0}(1P)K^-$	1.33 ± 0.19	$6.00 \pm_{1.80}^{2.10} \pm 0.70 \pm 0.90$	2.70 ± 0.70 ²				1.88 ± 0.30
			$1.84 \pm 0.32 \pm 0.14 \pm 0.28$ ³				
			$1.34 \pm 0.45 \pm 0.15 \pm 0.14$ ¹				
			< 1.80 ^{5b}				
$\chi_{c1}(1P)K^{*-}(892)$	3.00 ± 0.60	$4.10 \pm 0.60 \pm 0.90$	$2.60 \pm 0.50 \pm 0.40$				2.99 ± 0.55
$\eta_c(2S)K^-$	3.4 ± 1.8		$3.40 \pm 1.80 \pm 0.30$				3.4 ± 1.8
$\chi_{c1}(1P)K^0$		$3.78 \pm_{0.16}^{0.17} \pm 0.33$					3.78 ± 0.37
$\psi(2S)K^-\pi^+\pi^-$	19 ± 12	$4.31 \pm 0.20 \pm 0.50$					4.31 ± 0.54
$\psi(3770)K^-$	4.9 ± 1.3	$4.80 \pm 1.10 \pm 0.70$	$3.50 \pm 2.50 \pm 0.30$				4.5 ± 1.2
$\chi_{c1}(1P)K^-$	4.60 ± 0.40	$4.94 \pm 0.11 \pm 0.33$	$8.00 \pm 1.40 \pm 0.70$ ^{5c}	$15.5 \pm 5.4 \pm 2.0$			4.79 ± 0.23
			$4.50 \pm 0.10 \pm 0.30$ ⁴				5.52 ± 0.66
			$5.52 \pm 0.26 \pm 0.61$				6.32 ± 0.37
$\chi_{c1}(1P)\bar{K}^0\pi^-$		6.90 ± 0.60	$4.90 \pm 1.60 \pm 0.40$ ^{5a}	$5.50 \pm 1.00 \pm 0.60$			
$\psi(2S)K^-$	6.46 ± 0.33		$6.17 \pm 0.32 \pm 0.38 \pm 0.23$ ⁶				
			$5.92 \pm 0.85 \pm 0.86 \pm 0.22$				7.07 ± 0.85
$\psi(2S)K^{*-}(892)$	6.2 ± 1.2	$8.13 \pm 0.77 \pm 0.89$	$13.8 \pm_{1.5}^{2.3} \pm 1.5 \pm 4.2$ ⁷				9.8 ± 1.3
$\eta_c(1S)K^-$	9.1 ± 1.3	$12.50 \pm 1.40 \pm_{1.20}^{1.00} \pm 3.80$	8.7 ± 1.5 ^{5d}				
			$12.90 \pm 0.90 \pm 1.30 \pm 3.60$ ⁸				
			$12.1 \pm_{3.5}^{4.3} \pm_{2.8}^{3.4} \pm_{2.8}^{5.4}$				$12.1 \pm_{5.3}^{7.7}$
$\eta_c(1S)K^{*-}(892)$	12.0 ± 7.0						< 2.1
$\chi_{c0}(1P)K^{*-}(892)$	< 2.1		< 2.1 ⁹				< 2.1
			< 29 ¹⁰				

¹ Dalitz-plot analysis of the decays $B^\pm \rightarrow K^\pm\pi^\mp\pi^\pm$ (226M $B\bar{B}$ pairs) ; $B^- \rightarrow \chi_{c0}K^-$ with $\chi_{c0} \rightarrow \pi^+\pi^-$ (Dalitz analysis)

² MEASUREMENT OF THE BRANCHING FRACTION FOR $B^\pm \rightarrow \chi_{c0}K^\pm$. (88.9M $B\bar{B}$ pairs) ; $B^- \rightarrow \chi_{c0}K^-$ with $\chi_{c0} \rightarrow K^+K^-, \pi^+\pi^-$

³ Dalitz plot analysis of the decay $B^\pm \rightarrow K^\pm K^\pm K^\mp$ (226M $B\bar{B}$ pairs) ; $B^\pm \rightarrow K^\pm\chi_{c0}$, with $\chi_{c0} \rightarrow K^+K^-$ (Dalitz analysis)

⁴ Search for $X(3872) \rightarrow \psi(2S)\gamma$ in $B^\pm \rightarrow X(3872)K^\pm$ decays, and a study of $B \rightarrow \bar{c}c\gamma K$

⁴ Search for $X(3872) \rightarrow \psi(2S)\gamma$ in $B^\pm \rightarrow X(3872)K^\pm$ decays, and a study of $B \rightarrow \bar{c}c\gamma K$

⁵ Measurements of the absolute branching fractions of $B^\pm \rightarrow K^\pm\chi_{c\bar{c}}$ (231.8M $B\bar{B}$ pairs) ; ^{5a} $B^- \rightarrow \psi(2S)K^-$ (inclusive) ; ^{5b} $B^- \rightarrow \chi_{c0}K^-$ (inclusive) ; ^{5c} $B^- \rightarrow \chi_{c1}K^-$ (inclusive) ; ^{5d} $B^- \rightarrow \eta_c K^-$ (inclusive)

⁶ MEASUREMENT OF BRANCHING FRACTIONS AND CHARGE ASYMMETRIES FOR EXCLUSIVE B DECAYS TO CHARMONIUM (124M $B\bar{B}$ pairs) ; $B^- \rightarrow \psi(2S)K^-$ with $\psi(2S)$ to leptons

⁷ MEASUREMENT OF THE $B^+ \rightarrow p\bar{p}K^+$ BRANCHING FRACTION AND STUDY OF THE DECAY DYNAMICS (232M $B\bar{B}$ pairs) ; $B^- \rightarrow \eta_c K^-$ with $\eta_c \rightarrow p\bar{p}$

⁸ Branching Fraction Measurements of $B \rightarrow \eta_c K$ Decays (86.1M $B\bar{B}$ pairs) ; $B^- \rightarrow \eta_c K^-$ with $\eta_c \rightarrow K\bar{K}\pi$

⁹ Observation of $B^0 \rightarrow \chi_{c0}K^{*0}$ and Evidence for $B^+ \rightarrow \chi_{c0}K^{*+}$

¹⁰ SEARCH FOR FACTORIZATION-SUPPRESSED $B \rightarrow \chi_c K^{(*)}$ DECAYS (124M $B\bar{B}$ pairs)

Table 88: Product branching fractions of charged B modes producing charmonium other than $J/\psi(1S)$ in units of 10^{-5} , upper limits are at 90% CL. The latest version is available at: <http://hfag.phys.ntu.edu.tw/b2charm/00105.html>

Mode	PDG 2010	Belle	BABAR	CDF	D0	LHCb	Average
$K^-\eta_c(2S)[K^0K^-\pi^+]$		$0.0034 \pm_{0.0015}^{0.0022} \pm_{0.0004}^{0.0005}$					0.003 ± 0.002
$K^-\eta_c(1S)[K^0K^+\pi^+]$		$0.027 \pm 0.001 \pm_{0.003}^{0.003} \pm_{0.005}^{0.005}$					0.027 ± 0.006
$K^-h_c(1P)[\eta_c(1S)\gamma]$			< 4.8				< 4.8
$K^-\psi(3770)[D^+D^-]$	9.4 ± 3.5		$8.4 \pm 3.2 \pm 2.1$				8.4 ± 3.8
$K^-\psi(3770)[D^0\bar{D}^0]$	16.0 ± 4.0		$14.1 \pm 3.0 \pm 2.2$				14.1 ± 3.7

Table 89: Ratios of branching fractions of charged B modes producing charmonium other than $J/\psi(1S)$ in units of 10^{-1} , upper limits are at 90% CL. The latest version is available at: <http://hfag.phys.ntu.edu.tw/b2charm/00105.html>

Mode	PDG 2010	Belle	BABAR	CDF	D0	LHCb	Average
$\frac{\mathcal{B}(B^-\rightarrow\chi_{c1}(1P)\pi^-)}{\mathcal{B}(B^-\rightarrow\chi_{c1}(1P)K^-)}$	0.43 ± 0.09	$0.43 \pm 0.08 \pm 0.03$					0.43 ± 0.09
$\frac{\mathcal{B}(B^-\rightarrow h_c(1P)K^-) \times \mathcal{B}(h_c(1P) \rightarrow \eta_c(1S)\gamma)}{\mathcal{B}(B^-\rightarrow \eta_c(1S)K^-)}$			< 0.58				< 0.58
$\frac{\mathcal{B}(B^-\rightarrow\chi_{c1}(1P)K^{*-}(892))}{\mathcal{B}(B^-\rightarrow\chi_{c1}(1P)K^-)}$	5.1 ± 2.3		$5.1 \pm 1.7 \pm 1.6$				5.1 ± 2.3
$\frac{\mathcal{B}(B^-\rightarrow\psi(2S)K^{*-}(892))}{\mathcal{B}(B^-\rightarrow\psi(2S)K^-)}$	9.6 ± 1.7		$9.60 \pm 1.50 \pm 0.90$				9.6 ± 1.7

Table 90: Branching fractions of charged B modes producing multiple D , D^* or D^{**} mesons in units of 10^{-3} , upper limits are at 90% CL. The latest version is available at: <http://hfag.phys.ntu.edu.tw/b2charm/00106.html>

Mode	PDG 2010	Belle	BABAR	CDF	D0	LHCb	Average
$D^0\bar{D}^0\pi^0K^-$		$0.11 \pm 0.03 \pm_{0.03}^{0.02}$					0.11 ± 0.04
$D^+D^-K^-$	0.22 ± 0.07	< 0.90	$0.22 \pm 0.05 \pm 0.05$				0.22 ± 0.07
$D^0D^{*-}(2010)$	0.39 ± 0.05	$0.46 \pm 0.07 \pm 0.06$	$0.36 \pm 0.05 \pm 0.04$				0.39 ± 0.05
D^0D^-	0.38 ± 0.04						0.41 ± 0.04
		$0.56 \pm 0.08 \pm 0.06$ ¹	$0.38 \pm 0.06 \pm 0.04 \pm 0.03$				
		$0.38 \pm 0.03 \pm 0.04$ ²					
$D^{*+}(2010)D^-K^-$	0.60 ± 0.07		$0.60 \pm 0.10 \pm 0.08$				0.60 ± 0.13
$D^+D^{*-}(2010)K^-$	0.63 ± 0.11		$0.63 \pm 0.09 \pm 0.06$				0.63 ± 0.11
$D^{*0}(2007)D^-$			$0.63 \pm 0.14 \pm 0.08 \pm 0.06$				0.63 ± 0.17
$D^{*0}(2007)D^{*-}(2010)$	0.81 ± 0.17		$0.81 \pm 0.12 \pm 0.11 \pm 0.06$				0.81 ± 0.17
$D^0\bar{D}^0K^-$	1.45 ± 0.33	$1.17 \pm 0.21 \pm 0.15$	$1.31 \pm 0.07 \pm 0.12$				1.28 ± 0.12
$D^{*-}(2010)D^{*+}(2010)K^-$	1.32 ± 0.18		$1.32 \pm 0.13 \pm 0.12$				1.32 ± 0.18
$D^0D^-\bar{K}^0$	1.55 ± 0.21		$1.55 \pm 0.17 \pm 0.13$				1.55 ± 0.21
$D^{*0}(2007)D^-\bar{K}^0$	2.10 ± 0.50		$2.06 \pm 0.38 \pm 0.30$				2.06 ± 0.48
$D^{*0}(2007)\bar{D}^0K^-$	2.26 ± 0.23		$2.26 \pm 0.16 \pm 0.17$				2.26 ± 0.23
$D^0D^{*-}(2010)\bar{K}^0$	3.80 ± 0.40		$3.81 \pm 0.31 \pm 0.23$				3.81 ± 0.39
$D^0\bar{D}^{*0}(2007)K^-$			$6.32 \pm 0.19 \pm 0.45$				6.32 ± 0.49
$D^{*0}(2007)D^{*-}(2010)\bar{K}^0$	9.2 ± 1.2		$9.17 \pm 0.83 \pm 0.90$				9.2 ± 1.2
$\bar{D}^{*0}(2007)D^{*0}(2007)K^-$			$11.23 \pm 0.36 \pm 1.26$				11.2 ± 1.3

¹ Observation of $B^0 \rightarrow D^+D^-$, $B^- \rightarrow D^0D^-$ and $B^- \rightarrow D^0D^{*-}$ decays (152M $B\bar{B}$ pairs)

² Measurement of $B^+ - D^+ D^0\bar{D}^0$ branching fraction and charge asymmetry and search for $B^0 - D^0 D^0\bar{D}^0$ (656.7M $B\bar{B}$ pairs)

Table 91: Product branching fractions of charged B modes producing multiple D , D^* or D^{**} mesons in units of 10^{-4} , upper limits are at 90% CL. The latest version is available at: <http://hfag.phys.ntu.edu.tw/b2charm/00106.html>

Mode	PDG 2010	Belle	BABAR	CDF	D0	LHCb	Average
$\pi^- D_1^0(2420)[D^{*0}(2007)\pi^-\pi^+]$	< 0.060	< 0.060					< 0.060
$\pi^- D_2^{*0}(2460)[D^{*0}(2007)\pi^-\pi^+]$	< 0.22	< 0.22					< 0.22
$\pi^- D_2^{*0}(2460)[D^{*+}(2010)\pi^-]$	1.80 ± 0.50	$1.80 \pm 0.30 \pm 0.30 \pm 0.20$	$1.80 \pm 0.30 \pm 0.50$				1.80 ± 0.36
$\pi^- D_1^0(2420)[D^0\pi^-\pi^+]$	1.80 ± 0.60	$1.85 \pm 0.29 \pm 0.35 \pm_{0.46}^{0.90}$					$1.85 \pm_{0.65}^{0.45}$
$\pi^- D_2^{*0}(2460)[D^+\pi^-]$	3.50 ± 0.40	$3.40 \pm 0.30 \pm 0.60 \pm 0.40$	$3.50 \pm 0.20 \pm 0.20 \pm 0.40$				3.47 ± 0.42
$\pi^- D_1^0(H)[D^{*+}(2010)\pi^-]$		$5.00 \pm 0.40 \pm 1.00 \pm 0.40$					5.0 ± 1.1
$\pi^- D_1^0(2420)[D^{*+}(2010)\pi^-]$		$6.80 \pm 0.70 \pm 1.30 \pm 0.30$	$5.90 \pm 0.30 \pm 1.10$				6.23 ± 0.91
$\pi^- D_0^{*0}[D^+\pi^-]$	6.40 ± 0.40	$6.10 \pm 0.60 \pm 0.90 \pm 1.60$	$6.80 \pm 0.30 \pm 0.40 \pm 2.00$				6.4 ± 1.4

Table 92: Ratios of branching fractions of charged B modes producing multiple D , D^* or D^{**} mesons in units of 10^{-1} , upper limits are at 90% CL. The latest version is available at: <http://hfag.phys.ntu.edu.tw/b2charm/00106.html>

Mode	PDG 2010	Belle	BABAR	CDF	D0	LHCb	Average
$\frac{\mathcal{B}(B^- \rightarrow D_2^{*+}(2460)\pi^-) \times (D_2^{*+}(2460) \rightarrow D^0 \pi^-)}$						< 0.30	< 0.30
$\frac{\mathcal{B}(B^- \rightarrow D_2^{*0}(2460)\pi^-) \times (\overline{D}_2^{*0}(2460) \rightarrow D^{*+}(2010)\pi^-)}$						$0.39 \pm 0.12 \pm 0.04$	0.39 ± 0.13
$\frac{\mathcal{B}(B^- \rightarrow D_2^{*0}(2460)\pi^-) \times (\overline{D}_2^{*0}(2460) \rightarrow D^0 \pi^- \pi^+ \pi^-)}$						$0.40 \pm 0.10 \pm 0.04$	0.40 ± 0.11
$\frac{\mathcal{B}(B^- \rightarrow D_1^0(2420)\pi^-) \times (D_1^0(2420) \rightarrow D^0 \pi^- \pi^+ \pi^-)}$						$0.40 \pm 0.07 \pm 0.05$	0.40 ± 0.09
$\frac{\mathcal{B}(B^- \rightarrow D^0 K^-)}{\mathcal{B}(B^- \rightarrow D^0 \pi^-)}$							0.72 ± 0.02
		$0.77 \pm 0.05 \pm 0.06$ ¹ $0.68 \pm 0.02 \pm 0.03$ ²	$0.83 \pm 0.03 \pm 0.02$	$0.65 \pm 0.07 \pm 0.04$		$0.63 \pm 0.04 \pm 0.04$	
$\frac{\mathcal{B}(B^- \rightarrow D^{*0}(2007)K^-)}{\mathcal{B}(B^- \rightarrow D^{*0}(2007)\pi^-)}$							0.81 ± 0.05
$\frac{\mathcal{B}(B^- \rightarrow D_1^0(H)\pi^-) \times (D_1^0(H) \rightarrow D^{*+}(2010)\pi^-)}$		$0.78 \pm 0.19 \pm 0.09$	$0.81 \pm 0.04 \pm 0.04$ _{0.03}				
$\frac{\mathcal{B}(B^- \rightarrow D^0 K^- \pi^+ \pi^-)}{\mathcal{B}(B^- \rightarrow D^0 \pi^- \pi^+ \pi^-)}$						$0.93 \pm 0.16 \pm 0.09$	0.93 ± 0.18
$\frac{\mathcal{B}(B^- \rightarrow D^0(H)\pi^-) \times (D^0(H) \rightarrow D^0 \pi^- \pi^+ \pi^-)}$						$0.96 \pm 0.15 \pm 0.08$	0.96 ± 0.17
$\frac{\mathcal{B}(B^- \rightarrow D^0 K^- \pi^+ \pi^-)}{\mathcal{B}(B^- \rightarrow D^0 \pi^- \pi^+ \pi^-)}$						$1.03 \pm 0.15 \pm 0.09$	1.03 ± 0.17
$\frac{\mathcal{B}(B^- \rightarrow \overline{D}^0 K^-)}{\mathcal{B}(B^- \rightarrow D^0 K^-)}$		< 1.90					< 1.90
$\frac{\mathcal{B}(B^- \rightarrow D_2^{*0}(2460)\pi^-)}{\mathcal{B}(B^- \rightarrow D_1^0(2420)\pi^-)}$							8.0 ± 1.7
$\frac{\mathcal{B}(B^- \rightarrow D^{*0}(2007)\pi^-)}{\mathcal{B}(B^- \rightarrow D^0 \pi^-)}$							11.40 ± 0.81
$\frac{\mathcal{B}(B^- \rightarrow D^{*0}\pi^-)}{\mathcal{B}(B^- \rightarrow D^0 \pi^- \pi^+ \pi^-)}$							12.2 ± 2.6
$\frac{\mathcal{B}(B^- \rightarrow D^0 \pi^-)}{\mathcal{B}(B^- \rightarrow D^0 \pi^-)}$						$12.70 \pm 0.60 \pm 1.10$	12.7 ± 1.3
$\frac{\mathcal{B}(B^- \rightarrow D^0 \pi^-)}{\mathcal{B}(\overline{B}^0 \rightarrow D^+ \pi^-)}$					$19.70 \pm 1.00 \pm 2.10$		19.7 ± 2.3

¹ MEASUREMENT OF BRANCHING FRACTION RATIOS AND CP ASYMMETRIES IN $B^{+-} \rightarrow D(\text{CP}) K^{+-}$. (85.4M $B\overline{B}$ pairs)

² Study of the suppressed B meson decay $B^- \rightarrow D^- K^-$, $D^- K^+ \pi^-$ (657M $B\overline{B}$ pairs)

Table 93: Branching fractions of charged B modes producing a single D^* or D^{**} meson in units of 10^{-4} , upper limits are at 90% CL. The latest version is available at: <http://hfag.phys.ntu.edu.tw/b2charm/00107.html>

Mode	PDG 2010	Belle	BABAR	CDF	D0	LHCb	Average
$D^{*-}(2010)\bar{K}^0$	< 0.090		< 0.090				< 0.090
$D^{*-}(2010)\pi^0$	< 0.036						< 0.030
		< 0.030 ¹ < 0.36 ²					
$D^{*0}(2007)K^-$	4.21 ± 0.35	$3.59 \pm 0.87 \pm 0.41 \pm 0.31$					3.6 ± 1.0
$D^{*0}(2007)K^{*-}(892)$	8.1 ± 1.4		$8.30 \pm 1.10 \pm 0.96 \pm 0.27$				8.3 ± 1.5
$D^{*0}(2007)K^-K^0$	< 10.6	< 10.6					< 10.6
$D^{*+}(2010)\pi^-\pi^-$	13.5 ± 2.2	$12.50 \pm 0.80 \pm 2.20$	$12.20 \pm 0.50 \pm 1.80$				12.3 ± 1.5
$D^{*0}(2007)K^-K^{*0}(892)$	15.0 ± 4.0	$15.3 \pm 3.1 \pm 2.9$					15.3 ± 4.2
$D^{*+}(2010)\pi^-\pi^+\pi^-\pi^-$	26.0 ± 4.0	$25.6 \pm 2.6 \pm 3.3$					25.6 ± 4.2
$D^{*0}(2007)\pi^-$	51.9 ± 2.6						52.8 ± 2.8
			$55.20 \pm 1.70 \pm 4.20 \pm 0.20$ ³				
			$51.3 \pm 2.2 \pm 2.8$ ⁴				
$D^{**0}\pi^-$	59 ± 13		$55.0 \pm 5.2 \pm 10.4$				55 ± 12
$D^{*0}(2007)\pi^-\pi^+\pi^-\pi^+\pi^-$	57 ± 12	$56.7 \pm 9.1 \pm 8.5$					57 ± 12
$D^{*0}(2007)\pi^-\pi^+\pi^-$	103 ± 12	$105.5 \pm 4.7 \pm 12.9$					106 ± 14

¹ Study of $B^+ \rightarrow D^{(*)+}\pi^0$ decay and the ratio of suppressed and favoured amplitudes in $B \rightarrow D^{(*)}\pi$ decays. (657M $B\bar{B}$ pairs)

² Search for $B^+ \rightarrow D^{*+}\pi^0$ decay (657M $B\bar{B}$ pairs)

³ Branching fraction measurements and isospin analyses for $\bar{B} \rightarrow D^{(*)}\pi^-$ decays (65M $B\bar{B}$ pairs) ; $B^- \rightarrow D^{*0}\pi^-$

⁴ Measurement of the Absolute Branching Fractions $B \rightarrow D^{(**)}\pi$ with a Missing Mass method (231M $B\bar{B}$ pairs) ; $B^- \rightarrow D^{*0}\pi^-$

Table 94: Branching fractions of charged B modes producing a single D meson in units of 10^{-4} , upper limits are at 90% CL. The latest version is available at: <http://hfag.phys.ntu.edu.tw/b2charm/00108.html>

Mode	PDG 2010	Belle	BABAR	CDF	D0	LHCb	Average
$D^- \mu^+ \mu^+$		> 0.010					> 0.010
$D^- e^+ \mu^+$		> 0.018					> 0.018
$D^- e^+ e^+$		> 0.026					> 0.026
$D^- \bar{K}^0$	< 0.029		< 0.029				< 0.029
$D^- \bar{K}^{*0}(892)$	< 0.030		< 0.030				< 0.030
$D^0 K^-$	3.68 ± 0.33	$3.83 \pm 0.25 \pm 0.30 \pm 0.22$					3.83 ± 0.45
$D^0 K^{*-}(892)$			$5.29 \pm 0.30 \pm 0.34$				5.29 ± 0.45
$D^0 K^- K^0$	5.5 ± 1.6	$5.50 \pm 1.40 \pm 0.80$					5.5 ± 1.6
$D^0 K^- K^{*0}(892)$	7.5 ± 1.7	$7.5 \pm 1.3 \pm 1.1$					7.5 ± 1.7
$D^+ \pi^- \pi^-$	10.70 ± 0.50	$10.20 \pm 0.40 \pm 1.50$	$10.80 \pm 0.30 \pm 0.50$				10.73 ± 0.55
$D^0 \pi^-$	48.4 ± 1.5						47.5 ± 1.9
			$49.00 \pm 0.70 \pm 2.20 \pm 0.06$ ¹				
			$44.9 \pm 2.1 \pm 2.3$ ²				

¹ Branching fraction measurements and isospin analyses for $\bar{B} \rightarrow D^{(*)} \pi^-$ decays (65M $B\bar{B}$ pairs) ; $B^- \rightarrow D^0 \pi^-$

² Measurement of the Absolute Branching Fractions $B \rightarrow D^{(*,**)} \pi$ with a Missing Mass method (231M $B\bar{B}$ pairs) ; $B^- \rightarrow D^0 \pi^-$

Table 95: Branching fractions of neutral B modes producing new particles in units of 10^{-4} , upper limits are at 90% CL. The latest version is available at: <http://hfag.phys.ntu.edu.tw/b2charm/00201.html>

Mode	PDG 2010	Belle	BABAR	CDF	D0	LHCb	Average
$D_{sJ}^*(2317)^+ K^-$		$0.53 \pm_{0.14}^{0.13} \pm 0.07 \pm 0.02$					0.53 ± 0.15
$X^+(3872) K^-$	< 5.0		< 5.0				< 5.0
$D_{sJ}^-(2460) D^+$	35 ± 11		$26.0 \pm 15.0 \pm 7.0$				26 ± 17
$D_{sJ}^-(2460) D^{*+}(2010)$	93 ± 22		$88 \pm 20 \pm 14$				88 ± 24

Table 96: Product branching fractions of neutral B modes producing new particles in units of 10^{-4} , upper limits are at 90% CL. The latest version is available at: <http://hfag.phys.ntu.edu.tw/b2charm/00201.html>

Mode	PDG 2010	Belle	BABAR	CDF	D0	LHCb	Average
$K^0 X(3872)[J/\psi(1S)\gamma]$		> 0.024					> 0.024
$\bar{K}^{*0}(892)X(3872)[J/\psi(1S)\gamma]$	< 0.028		< 0.028				< 0.028
$K^- Z^+(4430)[J/\psi(1S)\pi^+]$			< 0.030				< 0.030
$\pi^+ D_{sJ}^-(2460)[D_s^- \gamma]$	< 0.040	< 0.040					< 0.040
$\bar{K}^{*0}(892)X(3872)[\psi(2S)\gamma]$	< 0.044		< 0.044				< 0.044
$\bar{K}^0 X(3872)[J/\psi(1S)\gamma]$	< 0.049		< 0.049				< 0.049
$K^- X^+(3872)[J/\psi(1S)\pi^+ \pi^0]$	< 0.054		< 0.054				< 0.054
$\bar{K}^0 X(3872)[J/\psi(1S)\pi^+ \pi^-]$	< 0.060		< 0.060				< 0.060
$\bar{K}^0 X(3872)[J/\psi(1S)\omega(782)]$			$0.06 \pm 0.03 \pm 0.01$				0.06 ± 0.03
$K^0 X(3872)[\psi(2S)\gamma]$		> 0.066					> 0.066
$K^- D_{sJ}^+(2460)[D_s^+ \gamma]$		< 0.086					< 0.086
$\bar{K}^0 X(3872)[\psi(2S)\gamma]$	< 0.190		< 0.190				< 0.190
$\bar{K}^0 Y(3940)[J/\psi(1S)\omega(782)]$			$0.21 \pm 0.09 \pm 0.03$				0.21 ± 0.09
$\pi^+ D_{sJ}^*(2317)^- [D_s^- \pi^0]$	< 0.25	< 0.25					< 0.25
$K^- Z1(4050)[\chi_{c1}(1P)\pi^+]$		$0.30 \pm_{-0.08}^{+0.15} \pm_{-0.16}^{+0.37}$	< 0.180				$0.30 \pm_{-0.18}^{+0.40}$
$K^- Z^+(4430)[\psi(2S)\pi^+]$		$0.32 \pm_{-0.09}^{+0.18} \pm_{-0.16}^{+0.53}$	< 0.29				$0.32 \pm_{-0.18}^{+0.56}$
$K^- Z2(4250)[\pi^+ \psi(2S)]$		$0.40 \pm_{-0.09}^{+0.23} \pm_{-0.05}^{+1.97}$					$0.4 \pm_{-0.1}^{+2.0}$
$K^- D_{sJ}^*(2317)^+ [D_s^+ \pi^0]$	0.42 ± 0.14	$0.44 \pm 0.08 \pm 0.06 \pm 0.11$					0.44 ± 0.15
$K^- Z2(4250)[\chi_{c1}(1P)\pi^+]$			< 0.47				< 0.47
$D^+ D_{sJ}^-(2460)[D_s^- \pi^+ \pi^-]$	< 2.00	< 2.00					< 2.00
$D^+ D_{sJ}^-(2460)[D_s^- \pi^0]$	< 3.6	< 3.6					< 3.6
$\bar{K}^0 X(3872)[\bar{D}^{*0}(2007)D^0]$	1.20 ± 0.40		< 4.4				< 4.4
$D^+ D_{sJ}^-(2460)[D_s^- \gamma]$	< 6.0	< 6.0					< 6.0
$D^+ D_{sJ}^-(2460)[D_s^- \gamma]$	6.5 ± 1.6	$8.2 \pm_{-1.9}^{+2.2} \pm 2.5$	$8.00 \pm 2.00 \pm 1.00 \pm_{-2.00}^{+3.00}$				$8.1 \pm_{-2.5}^{+2.2}$
$D^+ D_{sJ}^*(2317)^- [D_s^{*-} \gamma]$	< 9.5	< 9.5					< 9.5
$D^+ D_{sJ}^*(2317)^- [D_s^- \pi^0]$	9.7 ± 3.7	$8.6 \pm_{-2.6}^{+3.3} \pm 2.6$	$18.0 \pm 4.0 \pm 3.0 \pm_{-4.0}^{+6.0}$				$10.4 \pm_{-3.5}^{+3.2}$
$D^{*+}(2010)D_{sJ}^*(2317)^- [D_s^- \pi^0]$	15.0 ± 6.0		$15.0 \pm 4.0 \pm 2.0 \pm_{-3.0}^{+5.0}$				$15.0 \pm_{-6.7}^{+5.4}$
$D^{*+}(2010)D_{sJ}^-(2460)[D_s^- \gamma]$	23.0 ± 8.0		$23.0 \pm 3.0 \pm 3.0 \pm_{-5.0}^{+8.0}$				$23.0 \pm_{-6.6}^{+9.4}$
$D^+ D_{sJ}^-(2460)[D_s^- \pi^0]$		$22.7 \pm_{-6.2}^{+7.3} \pm 6.8$	$28.0 \pm 8.0 \pm 5.0 \pm_{-6.0}^{+10.0}$				$24.6 \pm_{-8.2}^{+7.2}$
$D^{*+}(2010)D_{sJ}^-(2460)[D_s^{*-} \pi^0]$			$55.0 \pm 12.0 \pm 10.0 \pm_{-12.0}^{+19.0}$				$55 \pm_{20}^{+25}$

Table 97: Ratios of branching fractions of neutral B modes producing new particles in units of 10^0 , upper limits are at 90% CL. The latest version is available at: <http://hfag.phys.ntu.edu.tw/b2charm/00201.html>

Mode	PDG 2010	Belle	BABAR	CDF	D0	LHCb	Average
$\frac{\mathcal{B}(\bar{B}^0 \rightarrow X(3872)\bar{K}^0)}{\mathcal{B}(B^- \rightarrow X(3872)K^-)}$			$0.41 \pm 0.24 \pm 0.05$ ¹				0.46 ± 0.23
			$1.00 \pm_{0.60}^{0.80} \pm_{0.20}^{0.10}$ ²				
$\frac{\mathcal{B}(\bar{B}^0 \rightarrow Y(3940)\bar{K}^0)}{\mathcal{B}(B^- \rightarrow Y(3940)K^-)}$			$0.70 \pm_{0.30}^{0.40} \pm 0.10$				$0.70 \pm_{0.32}^{0.41}$

¹ Study of $B \rightarrow X(3872)K$, with $X(3872) \rightarrow J/\psi\pi^+\pi^-$

² Evidence for the decay $X(3872) \rightarrow J/\psi\omega$

Table 98: Branching fractions of neutral B modes producing strange D mesons in units of 10^{-3} , upper limits are at 90% CL. The latest version is available at: <http://hfag.phys.ntu.edu.tw/b2charm/00202.html>

Mode	PDG 2010	Belle	BABAR	CDF	D0	LHCb	Average
$D_s^- a_0^+ (980)$	< 0.019		< 0.019				< 0.019
$D_s^- \pi^+$	0.021 ± 0.004	$0.018 \pm 0.003 \pm 0.002 \pm 0.001$	$0.026 \pm_{0.004}^{0.005} \pm 0.001 \pm 0.001$				0.020 ± 0.003
$D_s^- \pi^+$	0.024 ± 0.004	$0.024 \pm_{0.008}^{0.010} \pm 0.004 \pm 0.006$ ¹ $0.020 \pm 0.003 \pm 0.002$ ^{2b}	$0.025 \pm 0.004 \pm 0.001 \pm 0.001$				0.022 ± 0.003
$D_s^{*+} K^-$	0.022 ± 0.003	$0.020 \pm 0.003 \pm 0.002 \pm 0.001$	$0.024 \pm 0.004 \pm 0.001 \pm 0.001$				0.022 ± 0.003
$D_s^+ K^-$	0.030 ± 0.004	$0.046 \pm_{0.011}^{0.012} \pm 0.006 \pm 0.012$ ¹ $0.019 \pm 0.002 \pm 0.002$ ²	$0.029 \pm 0.004 \pm 0.001 \pm 0.002$				0.023 ± 0.002
$D_s^- \rho^+ (770)$	< 0.024		< 0.024				< 0.019
$D_s^+ \Lambda \bar{p}$	0.028 ± 0.009	$0.036 \pm 0.009 \pm 0.006 \pm 0.009$ ³ $0.029 \pm 0.007 \pm 0.005 \pm 0.004$ ⁴					0.031 ± 0.008
$D_s^{*+} K^{*-} (892)$	0.03 ± 0.01		$0.032 \pm_{0.012}^{0.014} \pm 0.004 \pm 0.002$				0.03 ± 0.01
$D_s^+ K^{*-} (892)$	0.035 ± 0.010		$0.035 \pm_{0.009}^{0.010} \pm 0.003 \pm 0.002$				0.04 ± 0.01
$D_s^- a_0^+ (980)$	< 0.036		< 0.036				< 0.036
$D_s^- \rho^+ (770)$	0.04 ± 0.01		$0.041 \pm_{0.012}^{0.013} \pm 0.003 \pm 0.002$				0.04 ± 0.01
$D_s^+ K_S^0 \pi^-$	0.06 ± 0.02		$0.055 \pm 0.013 \pm 0.010 \pm 0.002$				0.06 ± 0.02
$D_s^{*+} K^0 \pi^-$	< 0.110		< 0.055				< 0.055
$D_s^+ D_s^-$	< 0.036	< 0.036 ⁶ < 0.200 ⁵	< 0.100				< 0.036
$D_s^- D_s^{*+}$	< 0.130		< 0.130				< 0.130
$D_s^- a_2^+ (1320)$	< 0.190		< 0.190				< 0.190
$D_s^- a_2^+ (1320)$	< 0.200		< 0.200				< 0.200
$D_s^{*+} D_s^{*-}$	< 0.24		< 0.24				< 0.24
$D_s^{*-} D_s^+$	7.4 ± 1.6		$6.7 \pm 2.0 \pm 1.1$				6.7 ± 2.3
$D_s^- D^+$	7.20 ± 0.80	$7.50 \pm 0.20 \pm 0.80 \pm 0.80$ ⁶ $7.42 \pm 0.23 \pm 1.36$ ⁵	$9.0 \pm 1.8 \pm 1.4$				7.67 ± 0.82
$D_s^- D^{*+} (2010)$	8.0 ± 1.1		$10.3 \pm 1.4 \pm 1.3 \pm 2.6$ ^{7a} $5.70 \pm 1.60 \pm 0.90$ ^{8a}				6.8 ± 1.6
$D_s^{*-} D^{*+} (2010)$	17.7 ± 1.4		$18.80 \pm 0.90 \pm 1.60 \pm 0.60$ ⁹ $19.7 \pm 1.5 \pm 3.0 \pm 4.9$ ^{7b} $16.5 \pm 2.3 \pm 1.9$ ^{8b}				18.2 ± 1.6
$D_{s1}^- (2536) D^{*+} (2010)$			$92.00 \pm 24.00 \pm 1.00$				92 ± 24

¹ OBSERVATION OF D+(S) K- AND EVIDENCE FOR D+(S) PI- FINAL STATES IN NEUTRAL B DECAYS (85M $B\bar{B}$ pairs)

² Measurements of branching fractions for $B^0 \rightarrow D_s^+ \pi^-$ and $B^0 \rightarrow D_s^+ K^-$ (657M $B\bar{B}$ pairs) ; ^{2b} Measurements of branching fractions for $B^0 \rightarrow D_s^+ \pi^-$ and $B^0 \rightarrow D_s^+ K^-$

³ Observation of B0bar to Ds+ Lambda pbar (447M $B\bar{B}$ pairs)

⁴ Observation of B0bar - Ds+ Lambda pbar decay (449M $B\bar{B}$ pairs)

⁵ Improved measurement of $\bar{B}^0 \rightarrow D_s^- D^+$ and search for $\bar{B}^0 \rightarrow D_s^+ D_s^-$ at Belle

⁶ Improved measurement of B0bar - Ds-D+ and search for B0bar - Ds+Ds- (449M $B\bar{B}$ pairs)

⁷ Measurement of $\bar{B}^0 \rightarrow D_s^{(*)} D^*$ Branching Fractions and $D_s^* D^*$ Polarization with a Partial Reconstruction technique (22.7M $B\bar{B}$ pairs) ; ^{7a} $\bar{B}^0 \rightarrow D_s^- D^{*+}$; ^{7b} $\bar{B}^0 \rightarrow D_s^{*-} D^{*+}$

⁸ Study of $\bar{B} \rightarrow D^{(*)+} X^-$ and $\bar{B} \rightarrow D_s^{(*)-} X^{+,0}$ decays and measurement of D_s^- and $D_{sJ}^- (2460)$ absolute branching fractions (230M $B\bar{B}$ pairs) ; ^{8a} $\bar{B}^0 \rightarrow D_s^- D^{*+}$; ^{8b} $\bar{B}^0 \rightarrow D_s^{*-} D^{*+}$

⁹ Measurement of the $\bar{B}^0 \rightarrow D_s^{*-} D^+$ and $D_s^+ \rightarrow \phi \pi^+$ branching fractions (123M $B\bar{B}$ pairs) ; $\bar{B}^0 \rightarrow D_s^{*-} D^{*+}$

Table 99: Product branching fractions of neutral B modes producing strange D mesons in units of 10^{-4} , upper limits are at 90% CL. The latest version is available at: <http://hfag.phys.ntu.edu.tw/b2charm/00202.html>

Mode	PDG 2010	Belle	BABAR	CDF	D0	LHCb	Average
$D^+ D_s^- [\pi^- \phi(1020) [K^+ K^-]]$		$1.47 \pm 0.05 \pm 0.21$					1.47 ± 0.22
$D^+ D_{s1}^- (2536) [K^- \bar{D}^{*0} (2007)]$	1.70 ± 0.60		$1.71 \pm 0.48 \pm 0.32$				1.71 ± 0.58
$D^+ D_{s1}^- (2536) [D^{*-} (2010) \bar{K}^0]$	2.6 ± 1.1		$2.61 \pm 1.03 \pm 0.31$				2.6 ± 1.1
$D^+ D_s^- [\phi(1020) \pi^-]$			$2.67 \pm 0.61 \pm 0.47$				2.67 ± 0.77
$D^- D_{s1}^+ (2536) [D^{*0} (2007) K^+ + D^{*+} (2010) K^0]$		$2.75 \pm 0.62 \pm 0.36$					2.75 ± 0.72
$D^{*+} (2010) D_{s1}^- (2536) [\bar{D}^{*0} (2007) K^+]$	3.3 ± 1.1		$3.32 \pm 0.88 \pm 0.66$				3.3 ± 1.1
$D_s^- D^+ [D_s^- \rightarrow \phi(1020) \pi^-]$			$4.14 \pm 1.19 \pm 0.94$				4.1 ± 1.5
$D^{*+} (2010) D_{s1}^- (2536) [D^{*-} (2010) \bar{K}^0]$	5.0 ± 1.7		$5.00 \pm 1.51 \pm 0.67$				5.0 ± 1.7
$D^{*-} (2010) D_{s1}^+ (2536) [D^{*0} (2007) K^+ + D^{*+} (2010) K^0]$		$5.01 \pm 1.21 \pm 0.70$					5.0 ± 1.4
$D^{*+} (2010) D_s^- [\phi(1020) \pi^-]$			$5.11 \pm 0.94 \pm 0.72$				5.1 ± 1.2
$D^{*-} (2010) D_{s1}^+ (2536) [D^{*+} (2010) K_S^0]$	2.50 ± 0.90	< 6.0					< 6.0
$D_s^- D^{*+} (2010) [D_s^- \rightarrow \phi(1020) \pi^-]$			$12.2 \pm 2.2 \pm 2.2$				12.2 ± 3.1

Table 100: Ratios of branching fractions of neutral B modes producing strange D mesons in units of 10^0 , upper limits are at 90% CL. The latest version is available at: <http://hfag.phys.ntu.edu.tw/b2charm/00202.html>

Mode	PDG 2010	Belle	BABAR	CDF	D0	LHCb	Average
$\frac{\mathcal{B}(\bar{B}^0 \rightarrow D_s^{*-} D^+)}{\mathcal{B}(\bar{B}^0 \rightarrow D_s^- D^+)}$				$0.90 \pm 0.20 \pm 0.10$			0.90 ± 0.22
$\frac{\mathcal{B}(\bar{B}^0 \rightarrow D_s^- D^{*+} (2010))}{\mathcal{B}(\bar{B}^0 \rightarrow D_s^- D^+)}$				$1.50 \pm 0.40 \pm 0.10$			1.50 ± 0.41
$\frac{\mathcal{B}(\bar{B}^0 \rightarrow D^+ \pi^+ \pi^- \pi^-)}{\mathcal{B}(\bar{B}^0 \rightarrow D_s^- D^+)}$				$1.99 \pm 0.13 \pm 0.11 \pm 0.45$			1.99 ± 0.48
$\frac{\mathcal{B}(\bar{B}^0 \rightarrow D_s^{*-} D^{*+} (2010))}{\mathcal{B}(\bar{B}^0 \rightarrow D_s^- D^+)}$				$2.60 \pm 0.50 \pm 0.20$			2.60 ± 0.54

Table 101: Branching fractions of neutral B modes producing baryons in units of 10^{-5} , upper limits are at 90% CL. The latest version is available at: <http://hfag.phys.ntu.edu.tw/b2charm/00203.html>

Mode	PDG 2010	Belle	BABAR	CDF	D0	LHCb	Average
$J/\psi(1S)\bar{p}p$	< 0.083	< 0.083	< 0.190				< 0.083
$\Sigma_c^{++}\bar{p}K^-$			$1.11 \pm 0.30 \pm 0.09 \pm 0.29$				1.11 ± 0.43
$\Lambda_c^+\bar{p}$	2.00 ± 0.40	$2.19 \pm_{0.49}^{0.56} \pm 0.32 \pm 0.57$	$1.89 \pm 0.21 \pm 0.06 \pm 0.49$				1.98 ± 0.45
$\Lambda_c^+\bar{p}K^{*0}(892)$	< 2.4		< 2.4				< 2.4
$\Lambda_c^+\bar{\Lambda}K^-$			$3.80 \pm 0.80 \pm 0.20 \pm 1.00$				3.8 ± 1.3
$\Lambda_c^+\bar{p}K^-\pi^+$	4.3 ± 1.4		$4.33 \pm 0.82 \pm 0.33 \pm 1.13$				4.3 ± 1.4
$\Lambda_c^+\Lambda_c^-$	< 6.2	< 5.7					< 5.7
$\Sigma_c^{*0}\bar{p}\pi^+$	< 3.8						< 3.3
		< 12.1 ¹					
		< 3.3 ²					
$D^{*0}(2007)p\bar{p}$	10.3 ± 1.3	$12.0 \pm_{2.3}^{3.3} \pm 2.1$	$9.70 \pm 0.70 \pm 0.90$				9.9 ± 1.1
$D^0p\bar{p}$	11.40 ± 0.90	$11.8 \pm 1.5 \pm 1.6$	$10.20 \pm 0.40 \pm 0.60$				10.36 ± 0.69
$\Sigma_c^{*++}\bar{p}\pi^-$							$12.9 \pm_{3.4}^{3.3}$
		$16.3 \pm_{5.1}^{5.7} \pm 2.8 \pm 4.2$ ¹					
		$12.0 \pm 1.0 \pm 2.0 \pm 3.0$ ²					
$\Sigma_c^0\bar{p}\pi^+$	15.0 ± 5.0						14.0 ± 4.9
		$14.0 \pm 2.0 \pm 2.0 \pm 4.0$ ²					
		< 15.9 ¹					
$D^{*0}(2007)p\bar{p}\pi^-\pi^+$			$19.1 \pm 3.6 \pm 2.9$				19.1 ± 4.6
$\Lambda_c^+\bar{p}\pi^0$	< 59		$19.4 \pm 1.7 \pm 1.4 \pm 5.0$				19.4 ± 5.5
$\Sigma_c^{*++}\bar{p}\pi^-$	22.0 ± 7.0						$21.8 \pm_{5.2}^{5.1}$
		$23.8 \pm_{5.5}^{6.3} \pm 4.1 \pm 6.2$ ¹					
		$21.0 \pm 2.0 \pm 3.0 \pm 5.0$ ^{2a}					
$D^0p\bar{p}\pi^-\pi^+$			$29.9 \pm 2.1 \pm 4.5$				29.9 ± 5.0
$D^+p\bar{p}\pi^-$	33.8 ± 3.2		$33.2 \pm 1.0 \pm 2.9$				33.2 ± 3.1
$D^{*+}(2010)p\bar{p}\pi^-$	50.0 ± 5.0		$45.5 \pm 1.6 \pm 3.9$				45.5 ± 4.2
$\Lambda_c^+\Lambda_c^-\bar{K}^0$	54 ± 32	$79 \pm_{23}^{39} \pm 12 \pm 41$	< 150				$79 \pm_{49}^{52}$
$\Lambda_c^+\bar{p}\pi^+\pi^-$	130 ± 40	$110 \pm_{12}^{12} \pm 19 \pm 29$					110 ± 37

¹ STUDY OF EXCLUSIVE B DECAYS TO CHARMED BARYONS AT BELLE. (31.7M $B\bar{B}$ pairs)

² Study of the charmed baryonic decays $\bar{B}^0 \rightarrow \Sigma_c^{++}\bar{p}\pi^-$ and $\bar{B}^0 \rightarrow \Sigma_c^0\bar{p}\pi^+$ (386M $B\bar{B}$ pairs) ; ^{2a} B0bar to Sigmac(2455)++ pbar pi

Table 102: Product branching fractions of neutral B modes producing baryons in units of 10^{-5} , upper limits are at 90% CL. The latest version is available at: <http://hfag.phys.ntu.edu.tw/b2charm/00203.html>

Mode	PDG 2010	Belle	BABAR	CDF	D0	LHCb	Average
$\Sigma_c^+ \bar{p}[\Lambda_c^+ \rightarrow pK^- \pi^+]$			< 0.150				$< \mathbf{0.150}$
$\Lambda_c^- \Xi_c^+[\Xi_c^- \pi^+ \pi^+]$	2.2 ± 2.3	$9.3 \pm_{2.8}^{3.7} \pm 1.9 \pm 2.4$	< 5.6				$9.3 \pm_{4.1}^{4.8}$

Table 103: Branching fractions of neutral B modes producing $J/\psi(1S)$ in units of 10^{-5} , upper limits are at 90% CL. The latest version is available at: <http://hfag.phys.ntu.edu.tw/b2charm/00204.html>

Mode	PDG 2010	Belle	BABAR	CDF	D0	LHCb	Average
$J/\psi(1S)\phi(1020)$	< 0.094	< 0.094					< 0.094
$J/\psi(1S)\gamma$	< 0.160		< 0.160				< 0.160
$J/\psi(1S)\phi(1020)$	< 0.094		< 0.90				< 0.90
$J/\psi(1S)f_2(1270)$	< 0.46						0.98 ± 0.44
		$0.98 \pm 0.39 \pm 0.20$ ⁴	< 0.46				
		< 0.49 ³					
$J/\psi(1S)\eta$	0.95 ± 0.19						1.08 ± 0.13
		$0.96 \pm 0.17 \pm 0.07$ ¹	< 2.7				
		$1.22 \pm 0.17 \pm 0.09$ ²					
$J/\psi(1S)D^0$	< 1.30	< 2.0	< 1.30				< 1.30
$J/\psi(1S)\pi^0$	1.76 ± 0.16	$2.30 \pm 0.50 \pm 0.20$	$1.69 \pm 0.14 \pm 0.07$				1.74 ± 0.15
$J/\psi(1S)\pi^+\pi^-$	4.60 ± 0.90						2.20 ± 0.36
		$2.20 \pm 0.30 \pm 0.20$ ³	< 1.20				
		< 1.00 ⁴					
$J/\psi(1S)\rho^0(770)$	2.70 ± 0.40						2.33 ± 0.20
		$2.80 \pm 0.30 \pm 0.30$ ⁴	$2.70 \pm 0.30 \pm 0.20$				
		$1.90 \pm 0.20 \pm 0.20$ ³					
		> 1.10	< 6.3				> 1.10
$J/\psi(1S)\eta'(958)$	< 6.3						
$J/\psi(1S)\eta K_S^0$	8.0 ± 4.0		$8.40 \pm 2.60 \pm 2.70 \pm 0.20$				8.4 ± 3.8
$J/\psi(1S)\phi(1020)\bar{K}^0$	9.4 ± 2.6		$10.20 \pm 3.80 \pm 1.00 \pm 0.20$				10.2 ± 3.9
$J/\psi(1S)\omega(782)\bar{K}^0$			$23.0 \pm 3.0 \pm 3.0$				23.0 ± 4.2
$J/\psi(1S)\bar{K}^0\rho^0(770)$	54 ± 30			$54.0 \pm 29.0 \pm 9.0$			54 ± 30
$J/\psi(1S)\bar{K}^{*0}(892)\pi^+\pi^-$	66 ± 22			66 ± 19 ± 11			66 ± 22
$J/\psi(1S)K^{*-}(892)\pi^+$	80 ± 40			77 ± 41 ± 13			77 ± 43
$J/\psi(1S)\bar{K}^0$	87.1 ± 3.2	$79.0 \pm 4.0 \pm 9.0 \pm 1.0$	$86.9 \pm 2.2 \pm 2.6 \pm 1.5$	115 ± 23 ± 17			86.3 ± 3.5
$J/\psi(1S)\bar{K}^0\pi^+\pi^-$	120 ± 40			103 ± 33 ± 15			103 ± 36
$J/\psi(1S)\bar{K}_1^0(1270)$	130 ± 50	$130 \pm 34 \pm 25 \pm 18$					130 ± 46
$J/\psi(1S)\bar{K}^{*0}(892)$	133.0 ± 6.0	$129.0 \pm 5.0 \pm 13.0 \pm 2.0$	$130.9 \pm 2.6 \pm 7.4 \pm 2.2$	$174 \pm 20 \pm 18$			133.2 ± 6.8

¹ Observation of the decay $B^0 \rightarrow J/\psi\eta$ (447M $B\bar{B}$ pairs)

² Measurement of $B^0 \rightarrow J/\psi\eta^{(\prime)}$ and determination of the $\eta - \eta'$ mixing angle (772M $B\bar{B}$ pairs)

³ Study of $B^0 \rightarrow J/\psi\pi^+\pi^-$ decays with 449 million $B\bar{B}$ pairs at Belle (449M $B\bar{B}$ pairs)

⁴ MEASUREMENT OF BRANCHING FRACTIONS IN $B^0 \rightarrow J/\psi\pi^+\pi^-$ DECAY. (152M $B\bar{B}$ pairs)

Table 104: Ratios of branching fractions of neutral B modes producing $J/\psi(1S)$ in units of 10^0 , upper limits are at 90% CL. The latest version is available at: <http://hfag.phys.ntu.edu.tw/b2charm/00204.html>

Mode	PDG 2010	Belle	BABAR	CDF	D0	LHCb	Average
$\frac{\mathcal{B}(\overline{B}^0 \rightarrow \chi_{c1}(1P)K^- \pi^+)}{\mathcal{B}(\overline{B}^0 \rightarrow J/\psi(1S)K^- \pi^+)}$			$0.47 \pm 0.01 \pm 0.05$				0.47 ± 0.06
$\frac{\mathcal{B}(\overline{B}^0 \rightarrow J/\psi(1S)\omega(782)\overline{K}^0)}{\mathcal{B}(B^- \rightarrow J/\psi(1S)\omega(782)K^-)}$			$0.70 \pm 0.10 \pm 0.10$				0.70 ± 0.14
$\frac{\mathcal{B}(\overline{B}^0 \rightarrow J/\psi(1S)\overline{K}^*(1270))}{\mathcal{B}(B^- \rightarrow J/\psi(1S)K^-)}$		$1.30 \pm 0.34 \pm 0.28$					1.30 ± 0.44
$\frac{\mathcal{B}(\overline{B}^0 \rightarrow \eta_c(1S)\overline{K}^0)}{\mathcal{B}(\overline{B}^0 \rightarrow J/\psi(1S)\overline{K}^0)}$	1.39 ± 0.49		$1.34 \pm 0.19 \pm 0.13 \pm 0.38$				1.34 ± 0.44
$\frac{\mathcal{B}(\overline{B}^0 \rightarrow J/\psi(1S)\overline{K}^{*0}(892))}{\mathcal{B}(\overline{B}^0 \rightarrow J/\psi(1S)\overline{K}^0)}$	1.50 ± 0.09		$1.51 \pm 0.05 \pm 0.08$	$1.39 \pm 0.36 \pm 0.10$			1.50 ± 0.09

Table 105: Miscellaneous quantities of neutral B modes producing $J/\psi(1S)$ in units of 10^0 , upper limits are at 90% CL. The latest version is available at: <http://hfag.phys.ntu.edu.tw/b2charm/00204.html>

Mode	PDG 2010	Belle	BABAR	CDF	D0	LHCb	Average
$ \mathcal{A}_0 ^2(\overline{B}^0 \rightarrow J/\psi(1S)\overline{K}^{*0}(892))$			< 0.26				< 0.26
$ \mathcal{A}_0 ^2(B^0 \rightarrow J/\psi(1S)K^{*0}(892))$			< 0.32				< 0.32

Table 106: Branching fractions of neutral B modes producing charmonium other than $J/\psi(1S)$ in units of 10^{-4} , upper limits are at 90% CL. The latest version is available at: <http://hfag.phys.ntu.edu.tw/b2charm/00205.html>

Mode	PDG 2010	Belle	BABAR	CDF	D0	LHCb	Average
$\chi_{c1}(1P)\pi^0$	0.11 ± 0.03	$0.11 \pm 0.02 \pm 0.01$					0.11 ± 0.03
$\chi_{c2}(1P)K^0$		> 0.150					> 0.150
$\chi_{c2}(1P)\bar{K}^0$	< 0.26		< 0.28				< 0.28
$\chi_{c2}(1P)\bar{K}^{*0}(892)$	0.66 ± 0.19		$0.66 \pm 0.18 \pm 0.05$				0.66 ± 0.19
$\chi_{c0}(1P)\bar{K}^{*0}(892)$	1.70 ± 0.40		$1.70 \pm 0.30 \pm 0.20$ ²				1.70 ± 0.36
			< 7.7 ¹				
$\chi_{c1}(1P)\bar{K}^{*0}(892)$	2.20 ± 0.40	$3.10 \pm 0.30 \pm 0.70$	$2.50 \pm 0.20 \pm 0.20$				2.57 ± 0.26
$\eta_c(2S)\bar{K}^{*0}(892)$	6.10 ± 1.00		< 3.9				< 3.9
$\chi_{c1}(1P)\bar{K}^0$	3.90 ± 0.33		$4.20 \pm 0.30 \pm 0.30$				4.20 ± 0.42
$\chi_{c1}(1P)K^-\pi^+$	3.80 ± 0.40		$5.11 \pm 0.14 \pm 0.58$				5.11 ± 0.60
$K^{*0}(892)\psi(2S)$	6.10 ± 0.50	$5.52 \pm_{-0.32}^{+0.35} \pm_{0.58}$					$5.52 \pm_{-0.66}^{+0.64}$
$\eta_c(1S)\bar{K}^{*0}(892)$	6.10 ± 1.00						$6.1 \pm_{-1.1}^{+1.0}$
		$16.2 \pm 3.2 \pm_{-3.4}^{+2.4} \pm 5.0$	$8.0 \pm_{-1.9}^{+2.1} \pm_{-1.9}^{+1.3} \pm_{-1.9}^{+3.5}$ ⁴				
			$5.70 \pm 0.60 \pm 0.40 \pm 0.80$ ³				
$\psi(2S)\bar{K}^0$	6.20 ± 0.60	6.7 ± 1.1	$6.46 \pm 0.65 \pm 0.44 \pm 0.25$				6.55 ± 0.66
$\psi(2S)\bar{K}^{*0}(892)$	6.10 ± 0.50	$7.20 \pm 0.43 \pm 0.65$	$6.49 \pm 0.59 \pm 0.94 \pm 0.25$	$9.00 \pm 2.20 \pm 0.90$			7.11 ± 0.62
$\eta_c(1S)\bar{K}^0$	8.9 ± 1.6						8.7 ± 1.9
		$12.3 \pm 2.3 \pm_{-1.6}^{+1.2} \pm 3.8$	$6.40 \pm_{-2.00}^{+2.20} \pm_{-1.50}^{+0.40} \pm_{-1.50}^{+2.80}$ ⁴				
			$11.4 \pm 1.5 \pm 1.2 \pm 3.2$ ⁵				
$\chi_{c0}(1P)\bar{K}^0$	1.40 ± 0.60		< 12.4				< 12.4

¹ SEARCH FOR FACTORIZATION-SUPPRESSED $B \rightarrow \chi_c K^{(*)}$ DECAYS (124M $B\bar{B}$ pairs)

² Observation of $B^0 \rightarrow \chi_{c0}K^{*0}$ and Evidence for $B^+ \rightarrow \chi_{c0}K^{*+}$

³ Study of B-meson decays to etac $K^{(*)}$, etac(2S) $K^{(*)}$ and etac gamma $K^{(*)}$

⁴ Evidence for the $B^0 \rightarrow p\bar{p}K^{*0}$ and $B^+ \rightarrow \eta_c K^{*+}$ decays and Study of the Decay Dynamics of B Meson Decays into $p\bar{p}h$ Final States. (232M $B\bar{B}$ pairs)

⁵ Branching Fraction Measurements of $B \rightarrow \eta_c K$ Decays (86.1M $B\bar{B}$ pairs)

Table 107: Product branching fractions of neutral B modes producing charmonium other than $J/\psi(1S)$ in units of 10^{-4} , upper limits are at 90% CL. The latest version is available at: <http://hfag.phys.ntu.edu.tw/b2charm/00205.html>

Mode	PDG 2010	Belle	BABAR	CDF	D0	LHCb	Average
$\overline{K}^0\psi(3770)[D^0\overline{D}^0]$	< 1.23		< 1.23				< 1.23
$\overline{K}^0\psi(3770)[D^+D^-]$	< 1.88		< 1.88				< 1.88
$\overline{K}^{*0}(892)h_c(1P)[\eta_c(1S)\gamma]$			< 2.2				< 2.2

Table 108: Ratios of branching fractions of neutral B modes producing charmonium other than $J/\psi(1S)$ in units of 10^0 , upper limits are at 90% CL. The latest version is available at: <http://hfag.phys.ntu.edu.tw/b2charm/00205.html>

Mode	PDG 2010	Belle	BABAR	CDF	D0	LHCb	Average
$\frac{\mathcal{B}(\overline{B}^0 \rightarrow h_c(1P)\overline{K}^{*0}(892)) \times \mathcal{B}(h_c(1P) \rightarrow \eta_c(1S)\gamma)}{\mathcal{B}(B^- \rightarrow \eta_c(1S)K^-)}$			< 0.26				< 0.26
$\frac{\mathcal{B}(\overline{B}^0 \rightarrow h_c(1P)\overline{K}^{*0}(892)) \times \mathcal{B}(h_c(1P) \rightarrow \eta_c(1S)\gamma)}{\mathcal{B}(\overline{B}^0 \rightarrow \eta_c(1S)\overline{K}^{*0}(892))}$			< 0.39				< 0.39
$\frac{\mathcal{B}(\overline{B}^0 \rightarrow \eta_c(1S)\overline{K}^{*0}(892))}{\mathcal{B}(B^- \rightarrow \eta_c(1S)K^-)}$			$0.67 \pm 0.09 \pm 0.07$				0.67 ± 0.11
$\frac{\mathcal{B}(\overline{B}^0 \rightarrow \chi_{c1}(1P)\overline{K}^{*0}(892))}{\mathcal{B}(\overline{B}^0 \rightarrow \eta_c(1S)\overline{K}^0)}$	0.72 ± 0.16		$0.72 \pm 0.11 \pm 0.12$				0.72 ± 0.16
$\frac{\mathcal{B}(B^- \rightarrow \eta_c(1S)K^-)}{\mathcal{B}(\overline{B}^0 \rightarrow \psi(2S)\overline{K}^{*0}(892))}$			$0.87 \pm 0.13 \pm 0.07$				0.87 ± 0.15
$\frac{\mathcal{B}(\overline{B}^0 \rightarrow \psi(2S)\overline{K}^{*0}(892))}{\mathcal{B}(\overline{B}^0 \rightarrow \eta_c(1S)\overline{K}^0)}$	0.99 ± 0.10		$1.00 \pm 0.14 \pm 0.09$				1.00 ± 0.17
$\frac{\mathcal{B}(\overline{B}^0 \rightarrow \eta_c(1S)\overline{K}^{*0}(892))}{\mathcal{B}(\overline{B}^0 \rightarrow \eta_c(1S)\overline{K}^0)}$	1.30 ± 0.40	$1.33 \pm 0.36 \pm_{0.33}^{0.24}$					$1.33 \pm_{0.49}^{0.43}$

Table 109: Branching fractions of neutral B modes producing multiple D , D^* or D^{**} mesons in units of 10^{-3} , upper limits are at 90% CL. The latest version is available at: <http://hfag.phys.ntu.edu.tw/b2charm/00206.html>

Mode	PDG 2010	Belle	BABAR	CDF	D0	LHCb	Average
$D^0\bar{D}^0$	< 0.043	< 0.042	< 0.060				< 0.042
$D^{*0}(2007)\bar{D}^{*0}(2007)$	< 0.090		< 0.090				< 0.090
$D^0\bar{D}^0\pi^0\bar{K}^0$		$0.17 \pm 0.07 \pm_{0.05}^{0.03}$					0.17 ± 0.08
D^-D^+	0.21 ± 0.03						0.21 ± 0.01
		$0.32 \pm 0.06 \pm 0.05$ ¹	$0.28 \pm 0.04 \pm 0.03 \pm 0.04$				
		$0.209 \pm 0.015 \pm 0.007$ ²					
		$0.20 \pm 0.02 \pm 0.02$ ³					
$D^0\bar{D}^0\bar{K}^0$			$0.27 \pm 0.10 \pm 0.05$				0.27 ± 0.11
$D^0\bar{D}^{*0}(2007)$	< 0.29		< 0.29				< 0.29
$D^{*-}(2010)D^+$		$1.17 \pm 0.26 \pm_{0.24}^{0.20} \pm 0.08$	$0.57 \pm 0.07 \pm 0.06 \pm 0.04$				0.62 ± 0.09
$D^+D^-\bar{K}^0$	0.75 ± 0.17		$0.75 \pm 0.12 \pm 0.12$				0.75 ± 0.17
$D^{*-}(2010)D^{*+}(2010)$	0.82 ± 0.09						0.79 ± 0.06
		$0.81 \pm 0.08 \pm 0.11$ ⁴	$0.81 \pm 0.06 \pm 0.09 \pm 0.05$				
		$0.78 \pm 0.04 \pm 0.06$ ⁵					
$D^+\bar{D}^0K^-$	1.07 ± 0.11		$1.07 \pm 0.07 \pm 0.09$				1.07 ± 0.11
$D^0\bar{D}^{*0}(2007)\bar{K}^0$	1.10 ± 0.50		$1.08 \pm 0.32 \pm 0.36$				1.08 ± 0.48
$D^{*0}(2007)\bar{D}^{*0}(2007)\bar{K}^0$	2.40 ± 0.90		$2.40 \pm 0.55 \pm 0.67$				2.40 ± 0.87
$D^{*+}(2010)\bar{D}^0K^-$	2.47 ± 0.21		$2.47 \pm 0.10 \pm 0.18$				2.47 ± 0.21
$D^+\bar{D}^{*0}(2007)K^-$	3.50 ± 0.40		$3.46 \pm 0.18 \pm 0.37$				3.46 ± 0.41
$D^{*-}(2010)D^{*+}(2010)K_S^0$		$3.40 \pm 0.40 \pm 0.70$	$4.40 \pm 0.40 \pm 0.70 \pm 0.04$				3.90 ± 0.57
$D^{*+}(2010)D^-\bar{K}^0$	6.40 ± 0.50		$6.41 \pm 0.36 \pm 0.39$				6.41 ± 0.53
$D^{*-}(2010)D^{*+}(2010)\bar{K}^0$	8.10 ± 0.70		$8.26 \pm 0.43 \pm 0.67$				8.26 ± 0.80
$D^{*+}(2010)\bar{D}^{*0}(2007)K^-$	10.60 ± 0.90		$10.60 \pm 0.33 \pm 0.86$				10.60 ± 0.92

¹ Observation of $B^0 \rightarrow D^+D^-$, $B^- \rightarrow D^0D^-$ and $B^- \rightarrow D^0D^{*-}$ decays (152M $B\bar{B}$ pairs)

² $B \rightarrow D^+D^-$ (772M $B\bar{B}$ pairs)

³ Evidence for CP Violation in $B^0 - D+D^-$ Decays (535M $B\bar{B}$ pairs)

⁴ Branching Fraction, Polarization and CP -Violating Asymmetries in $B^0 \rightarrow D^{*+}D^{*-}$ Decays (152M $B\bar{B}$ pairs)

⁵ $B^- \rightarrow D^{*+}D^{*-}$

Table 110: Product branching fractions of neutral B modes producing multiple D , D^* or D^{**} mesons in units of 10^{-4} , upper limits are at 90% CL. The latest version is available at: <http://hfag.phys.ntu.edu.tw/b2charm/00206.html>

Mode	PDG 2010	Belle	BABAR	CDF	D0	LHCb	Average
$K^- D_2^{*+}(2460)[D^0 \pi^+]$	0.18 ± 0.05		$0.18 \pm 0.04 \pm 0.03$				0.18 ± 0.05
$\pi^- D_2^{*+}(2460)[D^{*+}(2010)\pi^- \pi^+]$	< 0.24	< 0.24					< 0.24
$\pi^- D_1^+(2420)[D^{*+}(2010)\pi^- \pi^+]$	< 0.33	< 0.33					< 0.33
$\pi^- D_1^+(H)[D^{*0}(2007)\pi^+]$		< 0.70					< 0.70
$\pi^- D_1^+(2420)[D^+ \pi^- \pi^+]$	0.89 ± 0.29	$0.89 \pm 0.15 \pm 0.17 \pm_{-0.26}^{0.00}$					$0.89 \pm_{-0.34}^{0.23}$
$\pi^- D_0^{*+}[D^0 \pi^+]$	0.60 ± 0.30	< 1.20					< 1.20
$\pi^- D_2^{*+}(2460)[D^{*0}(2007)\pi^+]$		$2.45 \pm 0.42 \pm_{-0.45}^{0.35} \pm_{-0.17}^{0.39}$					$2.45 \pm_{-0.64}^{0.67}$
$\pi^- D_2^{*+}(2460)[D^0 \pi^+]$	2.15 ± 0.35	$3.08 \pm 0.33 \pm 0.09 \pm_{-0.02}^{0.15}$					$3.08 \pm_{-0.34}^{0.37}$
$\pi^- D_1^+(2420)[D^{*0}(2007)\pi^+]$		$3.68 \pm 0.60 \pm_{-0.40}^{0.71} \pm_{-0.30}^{0.65}$					$3.68 \pm_{-0.78}^{1.13}$
$\omega(782)D_1^0(H)[D^{*+}(2010)\pi^-]$	4.1 ± 1.6		$4.10 \pm 1.20 \pm 1.00 \pm 0.40$				4.1 ± 1.6

Table 111: Ratios of branching fractions of neutral B modes producing multiple D , D^* or D^{**} mesons in units of 10^{-1} , upper limits are at 90% CL. The latest version is available at: <http://hfag.phys.ntu.edu.tw/b2charm/00206.html>

Mode	PDG 2010	Belle	BABAR	CDF	D0	LHCb	Average
$\frac{\mathcal{B}(\overline{B}^0 \rightarrow D_1^+(2420)\pi^-) \times (D_1^+(2420) \rightarrow D^+\pi^-\pi^+) }{\mathcal{B}(\overline{B}^0 \rightarrow D^+\pi^-\pi^+\pi^-)}$						$0.21 \pm 0.05 \pm_{0.05}^{0.03}$	0.21 ± 0.06
$\frac{\mathcal{B}(\overline{B}^0 \rightarrow D^+K^-\pi^+\pi^-)}{\mathcal{B}(\overline{B}^0 \rightarrow D^+\pi^-\pi^+\pi^-)}$						$0.52 \pm 0.09 \pm 0.05$	0.52 ± 0.10
$\frac{\mathcal{B}(\overline{B}^0 \rightarrow D^+K^-)}{\mathcal{B}(\overline{B}^0 \rightarrow D^+\pi^-)}$		$0.68 \pm 0.15 \pm 0.07$					0.68 ± 0.17
$\frac{\mathcal{B}(\overline{B}^0 \rightarrow D^{*+}(2010)K^-)}{\mathcal{B}(\overline{B}^0 \rightarrow D^{*+}(2010)\pi^-)}$		$0.74 \pm 0.15 \pm 0.06$	$0.78 \pm 0.03 \pm 0.03$				0.77 ± 0.04
$\frac{\mathcal{B}(\overline{B}^0 \rightarrow D^{*+}\pi^-)}{\mathcal{B}(\overline{B}^0 \rightarrow D^+\pi^-)}$			$7.7 \pm 2.2 \pm 2.9$				7.7 ± 3.6
$\frac{\mathcal{B}(\overline{B}^0 \rightarrow D^{*+}(2010)\pi^-)}{\mathcal{B}(\overline{B}^0 \rightarrow D^+\pi^-)}$			$9.90 \pm 1.10 \pm 0.80$				9.9 ± 1.4
$\frac{\mathcal{B}(\overline{B}^0 \rightarrow D^0\rho^0(770))}{\mathcal{B}(\overline{B}^0 \rightarrow D^+\pi^-\pi^+\pi^-)}$		16.0 ± 8.0					16.0 ± 8.0
$\frac{\mathcal{B}(\overline{B}^0 \rightarrow D^+\pi^-\pi^+\pi^-)}{\mathcal{B}(\overline{B}^0 \rightarrow D^+\pi^-)}$						$23.8 \pm 1.1 \pm 2.1$	23.8 ± 2.4
$\frac{\mathcal{B}(\overline{B}^0 \rightarrow D^+\mu^-\overline{\nu}_\mu)}{\mathcal{B}(\overline{B}^0 \rightarrow D^+\pi^-)}$					$99.0 \pm 10.0 \pm 6.0 \pm 4.0$		99 ± 12
$\frac{\mathcal{B}(\overline{B}^0 \rightarrow D^{*+}(2010)\mu^-\overline{\nu}_\mu)}{\mathcal{B}(\overline{B}^0 \rightarrow D^{*+}(2010)\pi^-)}$					$165.0 \pm 23.0 \pm 6.0 \pm 5.0$		165 ± 24

Table 112: Branching fractions of neutral B modes producing a single D^* or D^{**} meson in units of 10^{-4} , upper limits are at 90% CL. The latest version is available at: <http://hfag.phys.ntu.edu.tw/b2charm/00207.html>

Mode	PDG 2010	Belle	BABAR	CDF	D0	LHCb	Average
$D^{*0}(2007)\bar{K}^0$	0.36 ± 0.12	< 0.66	$0.36 \pm 0.12 \pm 0.03$				0.36 ± 0.12
$\bar{D}^{*0}(2007)\bar{K}^{*0}(892)$		< 0.40					< 0.40
$D^{*0}(2007)\bar{K}^{*0}(892)$	< 0.69	< 0.69					< 0.69
$D^{*0}(2007)\eta'(958)$	1.23 ± 0.35	$1.21 \pm 0.34 \pm 0.22$	$1.48 \pm 0.22 \pm 0.13$				1.40 ± 0.22
$f_2(1270)D^{*0}(2007)$		$1.86 \pm 0.65 \pm 0.60 \pm_{0.52}^{0.80}$					$1.9 \pm_{1.0}^{1.2}$
$D^{*+}(2010)K^-$	2.14 ± 0.16	$2.04 \pm 0.41 \pm 0.17 \pm 0.16$					2.04 ± 0.47
$D^{*0}(2007)\pi^0$	1.70 ± 0.40	$1.39 \pm 0.18 \pm 0.26$	$3.05 \pm 0.14 \pm 0.28$				2.23 ± 0.22
$D^{*0}(2007)\eta$	2.00 ± 0.50	$1.40 \pm 0.28 \pm 0.26$	$2.69 \pm 0.14 \pm 0.23$				2.26 ± 0.22
$D^{*+}(2010)K^0\pi^-$	3.00 ± 0.80		$3.00 \pm 0.70 \pm 0.22 \pm 0.20$				3.00 ± 0.76
$D^{*+}(2010)K^{*-}(892)$	3.30 ± 0.60		$3.20 \pm 0.60 \pm 0.27 \pm 0.12$				3.20 ± 0.67
$D^{*0}(2007)\omega(782)$	3.30 ± 0.70	$2.29 \pm 0.39 \pm 0.40$	$4.55 \pm 0.24 \pm 0.39$				3.64 ± 0.35
$\rho^0(770)D^{*0}(2007)$	< 5.1	$3.73 \pm 0.87 \pm 0.46 \pm_{0.08}^{0.18}$ ¹					3.73 ± 0.99
		< 5.1 ²					
$D^{*+}(2010)K^-K^0$	< 4.7	< 4.7					< 4.7
$D^{*0}(2007)\pi^+\pi^-$	6.2 ± 2.2	$10.90 \pm 0.80 \pm 1.60$ ¹					9.0 ± 1.4
		$6.2 \pm 1.2 \pm 1.8$ ²					
$D^{*+}(2010)K^-K^{*0}(892)$		$12.9 \pm 2.2 \pm 2.5$					12.9 ± 3.3
$D^{*+}\pi^-$	21.0 ± 10.0		$23.4 \pm 6.5 \pm 8.8$				23 ± 11
$D^{*0}(2007)\pi^-\pi^+\pi^-\pi^+$	27.0 ± 5.0	$26.0 \pm 4.7 \pm 3.7$					26.0 ± 6.0
$D^{*+}(2010)\pi^-$		$23.00 \pm 0.60 \pm 1.90$	$27.90 \pm 0.80 \pm 1.70 \pm 0.05$ ³				26.2 ± 1.3
			$29.9 \pm 2.3 \pm 2.4$ ⁴				
$D^{*+}(2010)\omega(782)\pi^-$	28.9 ± 3.0		$28.8 \pm 2.1 \pm 2.8 \pm 1.4$				28.8 ± 3.8
$D^{*+}(2010)\pi^-\pi^+\pi^-\pi^+\pi^-$	47.0 ± 9.0	$47.2 \pm 5.9 \pm 7.1$					47.2 ± 9.2
$D^{*+}(2010)\pi^-\pi^+\pi^-$	70.0 ± 8.0	$68.1 \pm 2.3 \pm 7.2$					68.1 ± 7.6

¹ Study of $\bar{B}^0 \rightarrow D^{(*)0}\pi^+\pi^-$ decays ; Dalitz fit analysis (152M $B\bar{B}$ pairs)

² Study of $\bar{B}^0 \rightarrow D^{(*)0}\pi^+\pi^-$ Decays (31.3M $B\bar{B}$ pairs)

³ Branching fraction measurements and isospin analyses for $\bar{B} \rightarrow D^{(*)}\pi^-$ decays (65M $B\bar{B}$ pairs) ; $\bar{B}^0 \rightarrow D^{*+}\pi^-$

⁴ Measurement of the Absolute Branching Fractions $B \rightarrow D^{(*,**)}\pi$ with a Missing Mass method (231M $B\bar{B}$ pairs) ; $\bar{B}^0 \rightarrow D^{*+}\pi^-$

Table 113: Branching fractions of neutral B modes producing a single D meson in units of 10^{-4} , upper limits are at 90% CL. The latest version is available at: <http://hfag.phys.ntu.edu.tw/b2charm/00208.html>

Mode	PDG 2010	Belle	BABAR	CDF	D0	LHCb	Average
$\overline{D}^0 \overline{K}^{*0}(892)$	< 0.110	< 0.180	< 0.110				< 0.110
$\overline{D}^0 K^- \pi^+$	0.06 ± 0.04		< 0.190				< 0.190
$D^0 \overline{K}^{*0}(892)$	0.42 ± 0.06	$0.48 \pm_{0.10}^{0.11} \pm 0.05$	$0.40 \pm 0.07 \pm 0.03$				0.42 ± 0.06
$D^0 \overline{K}^0$	0.52 ± 0.07	$0.50 \pm_{0.12}^{0.13} \pm 0.06$	$0.53 \pm 0.07 \pm 0.03$				0.52 ± 0.07
$D^0 K^- \pi^+$	0.88 ± 0.17		$0.88 \pm 0.15 \pm 0.09$				0.88 ± 0.17
$D^0 \eta'(958)$	1.25 ± 0.23	$1.14 \pm 0.20 \pm_{0.13}^{0.10}$	$1.48 \pm 0.13 \pm 0.07$				1.39 ± 0.13
$f_2(1270)D^0$	1.20 ± 0.40	$1.95 \pm 0.34 \pm 0.38 \pm_{-0.02}^{0.32}$					$1.95 \pm_{0.51}^{0.60}$
$D^+ K^-$	2.00 ± 0.60	$2.04 \pm 0.45 \pm 0.21 \pm 0.27$				$2.01 \pm 0.18 \pm 0.14$	2.01 ± 0.21
$D^0 \eta$	2.02 ± 0.35	$1.77 \pm 0.16 \pm 0.21$	$2.53 \pm 0.09 \pm 0.11$				2.36 ± 0.13
$D^0 \omega(782)$	2.59 ± 0.30	$2.37 \pm 0.23 \pm 0.28$	$2.57 \pm 0.11 \pm 0.14$				2.53 ± 0.16
$D^0 \pi^0$	2.61 ± 0.24	$2.25 \pm 0.14 \pm 0.35$	$2.69 \pm 0.09 \pm 0.13$				2.62 ± 0.15
$\rho^0(770)D^0$		$2.91 \pm 0.28 \pm 0.33 \pm_{0.34}^{0.98}$ ¹					$2.91 \pm_{0.40}^{0.58}$
		$2.90 \pm 1.00 \pm 0.40$ ²					
$D^+ K^- K^0$	< 3.1	< 3.1					< 3.1
$D^+ K^{*-}(892)$	4.50 ± 0.70		$4.60 \pm 0.60 \pm 0.47 \pm 0.16$				4.60 ± 0.78
$D^+ K^0 \pi^-$	4.90 ± 0.90		$4.90 \pm 0.70 \pm 0.38 \pm 0.32$				4.90 ± 0.86
$D^+ K^- K^{*0}(892)$		$8.8 \pm 1.1 \pm 1.5$					8.8 ± 1.9
$D^0 \pi^+ \pi^-$		$10.70 \pm 0.60 \pm 1.00$ ¹					9.78 ± 0.95
		$8.00 \pm 0.60 \pm 1.50$ ²					
$D^+ \pi^-$	26.8 ± 1.3						26.5 ± 1.5
			$25.50 \pm 0.50 \pm 1.60 \pm 0.10$ ³				
			$30.3 \pm 2.3 \pm 2.3$ ⁴				

¹ Study of $\overline{B}^0 \rightarrow D^{(*)0} \pi^+ \pi^-$ decays ; Dalitz fit analysis (152M $B\overline{B}$ pairs)

² Study of $\overline{B}^0 \rightarrow D^{(*)0} \pi^+ \pi^-$ Decays (31.3M $B\overline{B}$ pairs)

³ Branching fraction measurements and isospin analyses for $\overline{B} \rightarrow D^{(*)} \pi^-$ decays (65M $B\overline{B}$ pairs) ; $\overline{B}^0 \rightarrow D^+ \pi^-$

⁴ Measurement of the Absolute Branching Fractions $B \rightarrow D^{(**)} \pi$ with a Missing Mass method (231M $B\overline{B}$ pairs) ; $\overline{B}^0 \rightarrow D^+ \pi^-$

Table 114: Product branching fractions of neutral B modes producing a single D meson in units of 10^{-5} , upper limits are at 90% CL. The latest version is available at: <http://hfag.phys.ntu.edu.tw/b2charm/00208.html>

Mode	PDG 2010	Belle	BABAR	CDF	D0	LHCb	Average
$D^0 \bar{K}^{*0}(892)[K^- \pi^+]$			$3.80 \pm 0.60 \pm 0.40$				3.80 ± 0.72

Table 115: Branching fractions of strange B modes producing strange D mesons in units of 10^{-2} , upper limits are at 90% CL. The latest version is available at: <http://hfag.phys.ntu.edu.tw/b2charm/00402.html>

Mode	PDG 2010	Belle	BABAR	CDF	D0	LHCb	Average
$D_s^+ K^-$		$0.024 \pm_{0.010}^{0.012} \pm 0.003 \pm 0.003$				$0.0197 \pm 0.0018 \pm_{0.0020}^{0.0019} \pm_{0.0010}^{0.0011}$	0.020 ± 0.003
$D_s^{*+} \pi^-$		$0.24 \pm_{0.04}^{0.05} \pm 0.03 \pm 0.03$					0.24 ± 0.06
$D_s^+ \pi^-$		$0.37 \pm_{0.03}^{0.04} \pm 0.04 \pm 0.05$				$0.30 \pm 0.02 \pm 0.02 \pm_{0.02}^{0.02}$	0.32 ± 0.03
$D_s^+ \rho^-(770)$		$0.85 \pm_{0.13}^{0.12} \pm 0.11 \pm 0.13$					0.85 ± 0.21
$D_s^+ D_s^-$		$1.00 \pm_{0.30}^{0.40} \pm 0.30$					$1.00 \pm_{0.36}^{0.50}$
$D_s^{*-} \rho^-(770)$		$1.18 \pm_{0.20}^{0.22} \pm 0.17 \pm 0.18$					1.18 ± 0.32
$D_s^+ D_s^{*-}$		$2.80 \pm_{0.70}^{0.80} \pm 0.70$					$2.8 \pm_{1.0}^{1.1}$
$D_s^{*+} D_s^{*-}$		$3.10 \pm_{1.00}^{1.20} \pm 0.80$			$3.50 \pm 1.00 \pm 1.10$		$3.28 \pm_{1.02}^{0.96}$

Table 116: Ratios of branching fractions of strange B modes producing strange D mesons in units of 10^{-1} , upper limits are at 90% CL. The latest version is available at: <http://hfag.phys.ntu.edu.tw/b2charm/00402.html>

Mode	PDG 2010	Belle	BABAR	CDF	D0	LHCb	Average
$\frac{\mathcal{B}(\overline{B}_s^0 \rightarrow D_s^{*+} (2573) \mu^- \overline{\nu}_\mu X)}{\mathcal{B}(\overline{B}_s^0 \rightarrow \mu^- \overline{\nu}_\mu)}$						$0.33 \pm 0.11 \pm 0.04$	0.33 ± 0.12
$\frac{\mathcal{B}(\overline{B}_s^0 \rightarrow D_s^{*+} (2536) \mu^- \nu_\mu X)}{\mathcal{B}(\overline{B}_s^0 \rightarrow \mu^- \nu_\mu)}$						$0.54 \pm 0.12 \pm 0.05$	0.54 ± 0.13
$\frac{\mathcal{B}(\overline{B}_s^0 \rightarrow D_s^{*+} K^-)}{\mathcal{B}(\overline{B}_s^0 \rightarrow D_s^{*+} \pi^-)}$				$0.97 \pm 0.18 \pm 0.09$			0.97 ± 0.20
$\frac{\mathcal{B}(\overline{B}_s^0 \rightarrow D_s^+ D_s^+)}{\mathcal{B}(\overline{B}_s^0 \rightarrow D_s^- D^+)}$							7.4 ± 1.3
$\frac{\mathcal{B}(\overline{B}_s^0 \rightarrow D_s^+ \pi^+ \pi^- \pi^-)}{\mathcal{B}(\overline{B}_s^0 \rightarrow D^+ \pi^+ \pi^- \pi^-)}$				$14.40 \pm 3.80 \pm 0.80 \pm 2.10$ ¹			
$\frac{\mathcal{B}(\overline{B}_s^0 \rightarrow D_s^+ \pi^-)}{\mathcal{B}(\overline{B}_s^0 \rightarrow D^+ \pi^-)}$				$6.80 \pm 0.78 \pm 0.63 \pm 0.84$ ²			
$\frac{\mathcal{B}(\overline{B}_s^0 \rightarrow D_s^+ \pi^-)}{\mathcal{B}(\overline{B}_s^0 \rightarrow D^+ \pi^-)}$				$11.30 \pm 0.80 \pm 0.50 \pm 1.50$			11.3 ± 1.8
$\frac{\mathcal{B}(\overline{B}_s^0 \rightarrow D_s^- D_s^+)}{\mathcal{B}(\overline{B}_s^0 \rightarrow D_s^- D^+)}$							15.7 ± 2.9
$\frac{\mathcal{B}(\overline{B}_s^0 \rightarrow D_s^+ \pi^- \pi^+ \pi^-)}{\mathcal{B}(\overline{B}_s^0 \rightarrow D_s^+ \pi^-)}$						$20.1 \pm 3.7 \pm 2.0$	20.1 ± 4.2
$\frac{\mathcal{B}(\overline{B}_s^0 \rightarrow D_s^* - D_s^{*+})}{\mathcal{B}(\overline{B}_s^0 \rightarrow D_s^- D^+)}$							24.3 ± 4.7
$\frac{\mathcal{B}(\overline{B}_s^0 \rightarrow D_s^* - D_s^{*+})}{\mathcal{B}(\overline{B}_s^0 \rightarrow D_s^- D^+)}$							24.3 ± 4.7

¹ First Observation of the Decay $B_s^0 - D_s D_s^+$ and Measurement of Its Branching Ratio

² Measurement of $B_s - D_s^*(*) + D_s^*(*) -$ Branching Ratios

Table 117: Branching fractions of strange B modes producing baryons in units of 10^{-4} , upper limits are at 90% CL. The latest version is available at: <http://hfag.phys.ntu.edu.tw/b2charm/00403.html>

Mode	PDG 2010	Belle	BABAR	CDF	D0	LHCb	Average
$\Lambda_c^+ \pi^- \bar{\Lambda}$		$4.80 \pm 1.40 \pm 0.90 \pm 1.30$					4.8 ± 2.1

Table 118: Branching fractions of strange B modes producing $J/\psi(1S)$ in units of 10^{-4} , upper limits are at 90% CL. The latest version is available at: <http://hfag.phys.ntu.edu.tw/b2charm/00404.html>

Mode	PDG 2010	Belle	BABAR	CDF	D0	LHCb	Average
$J/\psi(1S)\bar{K}^0$				$0.35 \pm 0.06 \pm 0.04 \pm 0.04$		$0.33 \pm 0.05 \pm 0.02 \pm 0.03$	0.34 ± 0.05
$J/\psi(1S)K^{*0}(892)$						$0.35 \pm_{0.10}^{0.11} \pm 0.09$	0.35 ± 0.14
$J/\psi(1S)K^+\pi^-$						$0.39 \pm_{0.06}^{0.07} \pm 0.07$	0.39 ± 0.09
$J/\psi(1S)\bar{K}^{*0}(892)$				$0.83 \pm_{0.14} \pm 0.34 \pm 0.10$			$0.83 \pm_{0.35}^{0.38}$
$J/\psi(1S)\eta$		$5.11 \pm 0.50 \pm 0.35 \pm 0.68$					5.11 ± 0.91
$J/\psi(1S)\phi(1020)$				$9.3 \pm 2.8 \pm 1.7$			9.3 ± 3.3

Table 119: Product branching fractions of strange B modes producing $J/\psi(1S)$ in units of 10^{-4} , upper limits are at 90% CL. The latest version is available at: <http://hfag.phys.ntu.edu.tw/b2charm/00404.html>

Mode	PDG 2010	Belle	BABAR	CDF	D0	LHCb	Average
$J/\psi(1S)f_0(1370)[\pi^+\pi^-]$							0.34 ± 0.14
$J/\psi(1S)f_0(980)[\pi^+\pi^-]$							$1.16 \pm_{0.32}^{0.43}$

Table 120: Ratios of branching fractions of strange B modes producing $J/\psi(1S)$ in units of 10^{-1} , upper limits are at 90% CL. The latest version is available at: <http://hfag.phys.ntu.edu.tw/b2charm/00404.html>

Mode	PDG 2010	Belle	BABAR	CDF	D0	LHCb	Average
$\frac{\mathcal{B}(\overline{B}_s^0 \rightarrow J/\psi(1S)K_S^0)}{\mathcal{B}(\overline{B}_s^0 \rightarrow J/\psi(1S)K_S^0)}$						$0.38 \pm 0.06 \pm 0.02 \pm 0.03$	0.38 ± 0.07
$\frac{\mathcal{B}(\overline{B}_s^0 \rightarrow J/\psi(1S)\pi^+\pi^-)}{\mathcal{B}(\overline{B}_s^0 \rightarrow J/\psi(1S)\phi(1020))}$						$1.62 \pm 0.22 \pm 0.16$	1.62 ± 0.27
$\frac{\mathcal{B}(\overline{B}_s^0 \rightarrow J/\psi(1S)f_2'(1525))}{\mathcal{B}(\overline{B}_s^0 \rightarrow J/\psi(1S)\phi(1020))}$					$1.90 \pm 0.50 \pm 0.40$	$2.64 \pm 0.27 \pm 0.24$	2.46 ± 0.32
$\frac{\mathcal{B}(\overline{B}_s^0 \rightarrow J/\psi(1S)f_0(980))}{\mathcal{B}(\overline{B}_s^0 \rightarrow J/\psi(1S)\phi(1020))}$						$2.52 \pm_{0.32}^{0.46} \pm_{0.33}^{0.27}$	$2.53 \pm_{0.43}^{0.39}$
$\frac{\mathcal{B}(\overline{B}_s^0 \rightarrow J/\psi(1S)f_0(980)) \times \mathcal{B}(f_0(980) \rightarrow \pi^+\pi^-)}{\mathcal{B}(\overline{B}_s^0 \rightarrow J/\psi(1S)\phi(1020)) \times \mathcal{B}(\phi(1020) \rightarrow K^+K^-)}$				$2.57 \pm 0.20 \pm 0.14$			2.57 ± 0.24
$\frac{\mathcal{B}(\overline{B}_s^0 \rightarrow \psi(2S)\phi(1020))}{\mathcal{B}(\overline{B}_s^0 \rightarrow J/\psi(1S)\phi(1020))}$				$5.20 \pm 1.30 \pm 0.70$	$5.50 \pm 1.10 \pm 0.70 \pm 0.60$	$6.80 \pm 1.00 \pm 0.90 \pm 0.70$	5.81 ± 0.85
$\frac{\mathcal{B}(\overline{B}_s^0 \rightarrow J/\psi(1S)\phi(1020))}{\mathcal{B}(\overline{B}_s^0 \rightarrow J/\psi(1S)\phi(1020))}$				$8.90 \pm 0.10 \pm 0.70 \pm 1.10$			8.9 ± 1.3
$\frac{\mathcal{B}(\overline{B}^0 \rightarrow J/\psi(1S)\overline{K}^{*0}(892))}{\mathcal{B}(\overline{B}^0 \rightarrow J/\psi(1S)\overline{K}^{*0}(892))}$							

Table 121: Ratios of branching fractions of strange B modes producing multiple D , D^* or D^{**} mesons in units of 10^0 , upper limits are at 90% CL. The latest version is available at: <http://hfag.phys.ntu.edu.tw/b2charm/00406.html>

Mode	PDG 2010	Belle	BABAR	CDF	D0	LHCb	Average
$\frac{\mathcal{B}(\overline{B}_s^0 \rightarrow D^0 K^{*0}(892))}{\mathcal{B}(B^- \rightarrow D^0 \rho^0(770))}$						$1.48 \pm 0.34 \pm 0.15 \pm 0.12$	1.48 ± 0.39

Table 122: Branching fractions of strange B modes producing a single D meson in units of 10^{-4} , upper limits are at 90% CL. The latest version is available at: <http://hfag.phys.ntu.edu.tw/b2charm/00408.html>

Mode	PDG 2010	Belle	BABAR	CDF	D0	LHCb	Average
$D^0\bar{K}^{*0}$ (892)						$4.72 \pm 1.07 \pm 0.48 \pm 0.37$	4.7 ± 1.2

Table 123: Ratios of branching fractions of charmed B modes producing $J/\psi(1S)$ in units of 10^{-1} , upper limits are at 90% CL. The latest version is available at: <http://hfag.phys.ntu.edu.tw/b2charm/00504.html>

Mode	PDG 2010	Belle	BABAR	CDF	D0	LHCb	Average
$\frac{\sigma(B_c^+) \times \mathcal{B}(B_c^+ \rightarrow J/\psi(1S)\pi^+)}{\sigma(B^+) \times \mathcal{B}(B^+ \rightarrow J/\psi(1S)K^+)}$						$0.22 \pm 0.08 \pm 0.02$	0.22 ± 0.08
$\frac{\mathcal{B}(B_c^+ \rightarrow J/\psi(1S)\pi^+\pi^-\pi^+)}{\mathcal{B}(B_c^+ \rightarrow J/\psi(1S)\pi^+)}$						$30.0 \pm 6.0 \pm 4.0$	30.0 ± 7.2

Table 124: Branching fractions of lambda b modes producing baryons in units of 10^{-3} , upper limits are at 90% CL. The latest version is available at: <http://hfag.phys.ntu.edu.tw/b2charm/00603.html>

Mode	PDG 2010	Belle	BABAR	CDF	D0	LHCb	Average
$J/\psi(1S)\bar{\Lambda}$				$0.47 \pm 0.21 \pm 0.19$			0.47 ± 0.28
$\Lambda_c^+ \pi^- \pi^+ \pi^-$				$26.8 \pm 2.9 \pm_{4.9}^{6.2} \pm 9.7$			$27 \pm_{11}^{12}$

Table 125: Ratios of branching fractions of lambda b modes producing baryons in units of 10^{-1} , upper limits are at 90% CL. The latest version is available at: <http://hfag.phys.ntu.edu.tw/b2charm/00603.html>

Mode	PDG 2010	Belle	BABAR	CDF	D0	LHCb	Average
$\frac{\mathcal{B}(\Lambda_b^0 \rightarrow \Sigma_c^{++} \pi^- \pi^+) \times (\Sigma_c^{++} \rightarrow \Lambda_c^+ \pi^-)}{\mathcal{B}(\Lambda_b^0 \rightarrow \Lambda_c^+ \pi^- \pi^+ \pi^-)}$						$0.42 \pm 0.18 \pm 0.07$	0.42 ± 0.19
$\frac{\mathcal{B}(\Lambda_b^0 \rightarrow \Lambda_c^+ (2625) \pi^-) \times (\Lambda_c^+ (2625) \rightarrow \Lambda_c^+ \pi^- \pi^+)}{\mathcal{B}(\Lambda_b^0 \rightarrow \Lambda_c^+ \pi^- \pi^+ \pi^-)}$						$0.43 \pm 0.15 \pm 0.04$	0.43 ± 0.16
$\frac{\mathcal{B}(\Lambda_b^0 \rightarrow \Lambda_c^+ (2595) \pi^-) \times (\Lambda_c^+ (2595) \rightarrow \Lambda_c^+ \pi^- \pi^+)}{\mathcal{B}(\Lambda_b^0 \rightarrow \Lambda_c^+ \pi^- \pi^+ \pi^-)}$						$0.44 \pm 0.17 \pm_{0.04}^{0.06}$	0.44 ± 0.18
$\frac{\mathcal{B}(\Lambda_b^0 \rightarrow \Sigma_c^0 \pi^+ \pi^-) \times (\Sigma_c^0 \rightarrow \Lambda_c^+ \pi^-)}{\mathcal{B}(\Lambda_b^0 \rightarrow \Lambda_c^+ \pi^- \pi^+ \pi^-)}$						$0.74 \pm 0.24 \pm 0.12$	0.74 ± 0.27
$\frac{\mathcal{B}(\Lambda_b^0 \rightarrow \Sigma_c^0 \pi^+ \mu^- \bar{\nu}_\mu + \Sigma_c^{++} \pi^- \mu^- \bar{\nu}_\mu)}{\mathcal{B}(\Lambda_b^0 \rightarrow \Lambda_c^+ \mu^- \bar{\nu}_\mu)}$				$1.08 \pm 0.44 \pm_{0.36}^{0.42}$			$1.08 \pm_{0.57}^{0.61}$
$\frac{\mathcal{B}(\Lambda_b^0 \rightarrow D^0 p K^-)}{\mathcal{B}(\Lambda_b^0 \rightarrow D^0 p \pi^-)}$						$1.12 \pm 0.19 \pm_{0.14}^{0.11}$	1.12 ± 0.23
$\frac{\mathcal{B}(\Lambda_b^0 \rightarrow \Lambda_c^+ (2595) \mu^- \bar{\nu}_\mu)}{\mathcal{B}(\Lambda_b^0 \rightarrow \Lambda_c^+ \mu^- \bar{\nu}_\mu)}$				$1.26 \pm 0.33 \pm_{0.38}^{0.47}$			$1.26 \pm_{0.50}^{0.57}$
$\frac{\mathcal{B}(\Lambda_b^0 \rightarrow \Lambda_c^+ (2625) \mu^- \bar{\nu}_\mu)}{\mathcal{B}(\Lambda_b^0 \rightarrow \Lambda_c^+ \mu^- \bar{\nu}_\mu)}$				$2.10 \pm 0.42 \pm_{0.50}^{0.71}$			$2.10 \pm_{0.65}^{0.82}$
$\frac{\mathcal{B}(\Lambda_b^0 \rightarrow \Lambda_c^+ \pi^- \pi^+ \pi^-)}{\mathcal{B}(\Lambda_b^0 \rightarrow \Lambda_c^+ \pi^-)}$						$14.3 \pm 1.6 \pm 1.3$	14.3 ± 2.1
$\frac{\mathcal{B}(\Lambda_b^0 \rightarrow \Lambda_c^+ \pi^+ \pi^- \pi^+)}{\mathcal{B}(\Lambda_b^0 \rightarrow \Lambda_c^+ \pi^-)}$				$30.4 \pm 3.3 \pm_{5.5}^{7.0}$			$30.4 \pm_{6.4}^{7.7}$
$\frac{\mathcal{B}(\Lambda_b^0 \rightarrow \Lambda_c^- \pi^+)}{\mathcal{B}(\bar{B}^0 \rightarrow D^+ \pi^-)}$				$33.0 \pm 3.0 \pm 4.0 \pm 11.0$			33 ± 12
$\frac{\mathcal{B}(\Lambda_b^0 \rightarrow \Lambda_c^- \mu^+ \nu_\mu)}{\mathcal{B}(\bar{B}^0 \rightarrow \Lambda_c^- \pi^+)}$				$166.0 \pm 30.0 \pm 10.0 \pm_{34.0}^{26.0}$			$166 \pm_{46}^{41}$

Table 126: Branching fractions of miscellaneous modes producing charmed particles in units of 10^{-4} , upper limits are at 90% CL. The latest version is available at: <http://hfag.phys.ntu.edu.tw/b2charm/00300.html>

Mode	PDG 2010	Belle	BABAR	CDF	D0	LHCb	Average
$\mathcal{B}(B \rightarrow D^0 \bar{D}^0 \pi^0 K)$		$1.27 \pm 0.31 \pm_{0.39}^{0.22}$					$1.27 \pm_{0.50}^{0.38}$

Table 127: Product branching fractions of miscellaneous modes producing charmed particles in units of 10^{-4} , upper limits are at 90% CL. The latest version is available at: <http://hfag.phys.ntu.edu.tw/b2charm/00300.html>

Mode	PDG 2010	Belle	BABAR	CDF	D0	LHCb	Average
$\mathcal{B}(b \rightarrow A_b^0) \times \mathcal{B}(A_b^0 \rightarrow J/\psi(1S)\Lambda)$					$0.60 \pm 0.06 \pm 0.06 \pm 0.03$		0.60 ± 0.09
$\mathcal{B}(B \rightarrow Y(3940)K) \times \mathcal{B}(Y(3940) \rightarrow D^{*0}(2007)\bar{D}^0)$		< 0.67					< 0.67
$\mathcal{B}(B \rightarrow KY(3940)[\omega(782)J/\psi(1S)])$		$0.71 \pm 0.13 \pm 0.31$					0.71 ± 0.34
$\mathcal{B}(B \rightarrow X(3872)K) \times \mathcal{B}(X(3872) \rightarrow D^{*0}(2007)\bar{D}^0)$		$0.80 \pm 0.20 \pm 0.10$					0.80 ± 0.22

Table 128: Ratios of branching fractions of miscellaneous modes producing charmed particles in units of 10^0 , upper limits are at 90% CL. The latest version is available at: <http://hfag.phys.ntu.edu.tw/b2charm/00300.html>

Mode	PDG 2010	Belle	BABAR	CDF	D0	LHCb	Average
$\frac{\sigma(\Omega_b^-) \times \mathcal{B}(\Omega_b^- \rightarrow J/\psi(1S)\Omega^-)}{\sigma(\Lambda_b^0) \times \mathcal{B}(\Lambda_b^0 \rightarrow J/\psi(1S)\Lambda)}$				$0.045 \pm 0.017 \pm 0.004$			0.04 ± 0.02
$\frac{\sigma(\Xi_b^-) \times \mathcal{B}(\Xi_b^- \rightarrow J/\psi(1S)\Xi^-)}{\sigma(\Lambda_b^0) \times \mathcal{B}(\Lambda_b^0 \rightarrow J/\psi(1S)\Lambda)}$				$0.17 \pm 0.04 \pm 0.01$			0.17 ± 0.03

Table 129: Miscellaneous quantities of miscellaneous modes producing charmed particles in units of 10^0 , upper limits are at 90% CL. The latest version is available at: <http://hfag.phys.ntu.edu.tw/b2charm/00300.html>

Mode	PDG 2010	Belle	BABAR	CDF	D0	LHCb	Average
$\delta_{\parallel}(B \rightarrow J/\psi(1S)K^*)$		$-2.887 \pm 0.090 \pm 0.008$	$-2.93 \pm 0.08 \pm 0.04$				-2.91 ± 0.06
$\delta_{\parallel}(B \rightarrow \psi(2S)K^*)$			$-2.80 \pm 0.40 \pm 0.10$				-2.80 ± 0.41
$\delta_{\parallel}(B \rightarrow \chi_{c1}(1P)K^*)$			$0.00 \pm 0.30 \pm 0.10$				0.00 ± 0.32
$ \mathcal{A}_{\perp} ^2(B \rightarrow \chi_{c1}(1P)K^*)$			$0.03 \pm 0.04 \pm 0.02$				0.03 ± 0.04
$ \mathcal{A}_{\parallel} ^2(B \rightarrow \chi_{c1}(1P)K^*)$			$0.20 \pm 0.07 \pm 0.04$				0.20 ± 0.08
$ \mathcal{A}_{\perp} ^2(B \rightarrow J/\psi(1S)K^*)$		$0.195 \pm 0.012 \pm 0.008$	$0.233 \pm 0.010 \pm 0.005$				0.219 ± 0.009
$ \mathcal{A}_{\parallel} ^2(B \rightarrow J/\psi(1S)K^*)$		$0.231 \pm 0.012 \pm 0.008$	$0.211 \pm 0.010 \pm 0.006$				0.219 ± 0.009
$ \mathcal{A}_{\parallel} ^2(B \rightarrow \psi(2S)K^*)$			$0.22 \pm 0.06 \pm 0.02$				0.22 ± 0.06
$ \mathcal{A}_{\perp} ^2(B \rightarrow \psi(2S)K^*)$			$0.30 \pm 0.06 \pm 0.02$				0.30 ± 0.06
$ \mathcal{A}_0 ^2(B \rightarrow \psi(2S)K^*)$			$0.48 \pm 0.05 \pm 0.02$				0.48 ± 0.05
$ \mathcal{A}_0 ^2(B \rightarrow J/\psi(1S)K^*)$		$0.574 \pm 0.012 \pm 0.009$	$0.556 \pm 0.009 \pm 0.010$				0.56 ± 0.01
$ \mathcal{A}_0 ^2(B \rightarrow \chi_{c1}(1P)K^*)$			$0.77 \pm 0.07 \pm 0.04$				0.77 ± 0.08
$\delta_{\perp}(B \rightarrow \psi(2S)K^*)$			$2.80 \pm 0.30 \pm 0.10$				2.80 ± 0.32
$\delta_{\perp}(B \rightarrow J/\psi(1S)K^*)$		$2.938 \pm 0.064 \pm 0.010$	$2.91 \pm 0.05 \pm 0.03$				2.92 ± 0.04

7 B decays to charmless final states

The aim of this section is to provide the branching fractions, polarization fractions, and the partial rate asymmetries (A_{CP}) of charmless B decays. The asymmetry is defined as $A_{CP} = \frac{N_{\bar{B}} - N_B}{N_{\bar{B}} + N_B}$, where $N_{\bar{B}}$ and N_B are respectively number of \bar{B}^0/B^- and B^0/B^+ decaying into a specific final state. Four different B decay categories are considered: charmless mesonic, baryonic, radiative and leptonic. We also include measurements of B_s decays. Measurements supported with written documents are accepted in the averages; written documents include journal papers, conference contributed papers, preprints or conference proceedings. Results from A_{CP} measurements obtained from time dependent analyses are listed and described in Sec. 4.

So far all branching fractions from *BABAR* and Belle assume equal production of charged and neutral B pairs. The best measurements to date show that this is still a reasonable approximation (see Sec. 3). For branching fractions, we provide either averages or the most stringent 90% confidence level upper limits. If one or more experiments have measurements with $>4\sigma$ for a decay channel, all available central values for that channel are used in the averaging. We also give central values and errors for cases where the significance of the average value is at least 3σ , even if no single measurement is above 4σ . Since a few decay modes are sensitive to the contribution of new physics and the current experimental upper limits are not far from the Standard Model expectation, we provide the combined upper limits or averages in these cases. Their upper limits can be estimated assuming that the errors are Gaussian. For A_{CP} we provide averages in all cases.

Our averaging is performed by maximizing the likelihood, $\mathcal{L} = \prod_i \mathcal{P}_i(x)$, where \mathcal{P}_i is the probability density function (PDF) of the i th measurement, and x is the branching fraction or A_{CP} . The PDF is modeled by an asymmetric Gaussian function with the measured central value as its mean and the quadratic sum of the statistical and systematic errors as the standard deviations. The experimental uncertainties are considered to be uncorrelated with each other when the averaging is performed. No error scaling is applied when the fit χ^2 is greater than 1 since we believe that tends to overestimate the errors except in cases of extreme disagreement (we have no such cases). One exception to consider the correlated systematic errors is the inclusive $B \rightarrow X_s \gamma$ mode, which is sensitive to physics beyond the Standard Model. In this update, we have included new measurements from both Belle and *BABAR* to perform the average. The detail is described in Sec. 7.3.

At present, we have measurements of more than 400 decay modes, reported in about 300 papers. Because the number of references is so large, we do not include them with the tables shown here but the full set of references is available quickly from active gifs at the “2011” link on the rare web page: <http://www.slac.stanford.edu/xorg/hfag/rare/index.html>. The largest improvement since the last report has been inclusion of a variety of new measurements from the LHC, especially LHCb. The measurements of B_s decays are particularly noteworthy.

7.1 Mesonic charmless decays

Table 130: Branching fractions (BF) of charmless mesonic B^+ decays with kaons (in units of $\times 10^6$). Upper limits are at 90% CL. Values in red (blue) are new published (preliminary) results since PDG2010 [as of March 12, 2012].

RPP#	Mode	PDG2010 Avg.	BABAR	Belle	CLEO	CDF	New avg.
220	$K^0\pi^+$	23.1 ± 1.0	$23.9 \pm 1.1 \pm 1.0$	$23.97^{+0.53}_{-0.52} \pm 0.69$	$18.8^{+3.7+2.1}_{-3.3-1.8}$		23.80 ± 0.74
221	$K^+\pi^0$	12.9 ± 0.6	$13.6 \pm 0.6 \pm 0.7$	$12.62 \pm 0.31 \pm 0.56$	$12.9^{+2.4+1.2}_{-2.2-1.1}$		$12.94^{+0.52}_{-0.51}$
222	$\eta'K^+$	70.6 ± 2.5	$71.5 \pm 1.3 \pm 3.2$	$69.2 \pm 2.2 \pm 3.7$	$80^{+10}_{-9} \pm 7$		71.1 ± 2.6
223	$\eta'K^{*+}$	$4.9^{+2.1}_{-1.9}$	$4.8^{+1.6}_{-1.4} \pm 0.8$	< 2.9	$11.1^{+12.7}_{-8.0}$		$5.0^{+1.8}_{-1.6}$
–	$\eta'K_0^*(1430)^+$	New	$5.2 \pm 1.9 \pm 1.0$				5.2 ± 2.1
–	$\eta'K_2^*(1430)^+$	New	$28.0^{+4.6}_{-4.3} \pm 2.6$				$28.0^{+5.3}_{-5.0}$
224	ηK^+	$2.33^{+0.33}_{-0.29}$	$2.94^{+0.39}_{-0.34} \pm 0.21$	$2.12 \pm 0.23 \pm 0.11$	$2.2^{+2.8}_{-2.2}$		$2.36^{+0.22}_{-0.21}$
225	ηK^{*+}	19.3 ± 1.6	$18.9 \pm 1.8 \pm 1.3$	$19.3^{+2.0}_{-1.9} \pm 1.5$	$26.4^{+9.6}_{-8.2} \pm 3.3$		19.3 ± 1.6
226	$\eta K_0^*(1430)^+$	15.8 ± 3.1	$15.8 \pm 2.2 \pm 2.2$				15.8 ± 3.1
227	$\eta K_2^*(1430)^+$	9.1 ± 3.0	$9.1 \pm 2.7 \pm 1.4$				9.1 ± 3.0
228	$\eta(1295)K^+\dagger$	$2.9^{+0.8}_{-0.7}$	< 4.0				< 4.0
230	$\eta(1405)K^+\dagger$	< 1.2	< 1.2				< 1.2
231	$\eta(1475)K^+\dagger$	$13.8^{+2.1}_{-1.8}$	$13.8^{+1.8+1.0}_{-1.7-0.6}$				$13.8^{+2.1}_{-1.8}$
232	$f_1(1285)K^+$	< 2.0	< 2.0				< 2.0
233	$f_1(1420)K^+\dagger$	< 2.9	< 2.9				< 2.9
235	$\phi(1680)K^+\dagger$	< 3.4	< 3.4				< 3.4
236	ωK^+	6.7 ± 0.8	$6.3 \pm 0.5 \pm 0.3$	$8.1 \pm 0.6 \pm 0.6$	$3.2^{+2.4}_{-1.9} \pm 0.8$		6.7 ± 0.5
237	ωK^{*+}	< 7.4	< 7.4		< 87		< 7.4
239	$\omega K_0^*(1430)^+$	24.0 ± 5.1	$24.0 \pm 2.6 \pm 4.4$				24.0 ± 5.1
240	$\omega K_2^*(1430)^+$	21.5 ± 4.3	$21.5 \pm 3.6 \pm 2.4$				21.5 ± 4.3
240	$a_0(980)^0 K^+\dagger$	< 2.5	< 2.5				< 2.5
241	$a_0(980)^+ K^0\dagger$	< 3.9	< 3.9				< 3.9
243	$K^{*0}\pi^+$	10.1 ± 0.9	$10.8 \pm 0.6^{+1.2}_{-1.4}$	$9.7 \pm 0.6^{+0.8}_{-0.9}$	$7.6^{+3.5}_{-3.0} \pm 1.6$		$9.9^{+0.8}_{-0.9}$
244	$K^{*+}\pi^0$	6.9 ± 2.4	$8.2 \pm 1.5 \pm 1.1$		$7.1^{+11.4}_{-7.1} \pm 1.0$		8.2 ± 1.8
245	$K^+\pi^+\pi^-$	51 ± 2.9	$54.4 \pm 1.1 \pm 4.6$	$48.8 \pm 1.1 \pm 3.6$			51.0 ± 3.0
246	$K^+\pi^+\pi^-(NR)$	$16.3^{+2.1}_{-1.5}$	$9.3 \pm 1.0^{+6.9}_{-1.7}$	$16.9 \pm 1.3^{+1.7}_{-1.6}$	< 28		16.3 ± 2.0
–	$K^+\pi^0\pi^0$	New	$16.2 \pm 1.2 \pm 1.5$				16.2 ± 1.9
248	$f_0(980)K^+\dagger$	$9.4^{+1.0}_{-1.2}$	$10.3 \pm 0.5^{+2.0}_{-1.4}$	$8.8 \pm 0.8^{+0.9}_{-1.8}$			$9.4^{+0.9}_{-1.0}$
249	$f_2(1270)^0 K^+$	1.07 ± 0.27	$0.88 \pm 0.26^{+0.26}_{-0.21}$	$1.33 \pm 0.30^{+0.23}_{-0.34}$			$1.06^{+0.28}_{-0.29}$
250	$f_0(1370)^0 K^+\dagger$	< 10.7	< 10.7				< 10.7
251	$\rho^0(1450)K^+$	< 11.7	< 11.7				< 11.7
253	$f_0(1500)K^+\dagger$	0.73 ± 0.52	$0.73 \pm 0.21 \pm 0.47$				0.73 ± 0.52
254	$f_2'(1525)K^+\dagger$	< 3.4	< 3.4	< 4.9			< 3.4
255	$\rho^0 K^+$	3.7 ± 0.5	$3.56 \pm 0.45^{+0.57}_{-0.46}$	$3.89 \pm 0.47^{+0.43}_{-0.41}$	$8.4^{+4.0}_{-3.4} \pm 1.8$		$3.81^{+0.48}_{-0.46}$
256	$K_0^*(1430)^0\pi^+$	45^{+9}_{-7}	$32.0 \pm 1.2^{+10.8}_{-6.0}$	$51.6 \pm 1.7^{+7.0}_{-7.5}$			45.1 ± 6.3
257	$K_2^*(1430)^0\pi^+$	$5.6^{+2.2}_{-1.5}$	$5.6 \pm 1.2^{+1.8}_{-0.8}$	< 6.9			$5.6^{+2.2}_{-1.4}$
258	$K^*(1410)^0\pi^+$	< 45	< 45	< 45			< 45
259	$K^*(1680)^0\pi^+$	< 12	< 15	< 12			< 12
260	$K^-\pi^+\pi^+$	< 0.95	< 0.95	< 4.5			< 0.95
262	$K_1(1270)^0\pi^+$	< 40	< 40				< 40
263	$K_1(1400)^0\pi^+$	< 39	< 39				< 39
264	$K^0\pi^+\pi^0$	< 66			< 66		< 66
265	$\rho^+ K^0$	8.0 ± 1.5	$8.0^{+1.4}_{-1.3} \pm 0.6$		< 48		$8.0^{+1.5}_{-1.4}$
266	$K^{*+}\pi^+\pi^-$	75 ± 10	$75.3 \pm 6.0 \pm 8.1$				75.3 ± 10.1
267	$K^{*+}\rho^0$	< 6.1	$4.6 \pm 1.0 \pm 0.4$		< 74		4.6 ± 1.1
268	$f_0(980)K^{*+}\dagger$	5.2 ± 1.3	$4.2 \pm 0.6 \pm 0.3$				4.2 ± 0.7

†Product BF - daughter BF taken to be 100%

Table 131: Branching Fractions (BF) of charmless mesonic B^+ decays with kaons - part 2 (in units of 10^{-6}). Upper limits are at 90% CL. Values in red (blue) are new published (preliminary) results since PDG2010 [as of March 12, 2012].

RPP#	Mode	PDG2010 Avg.	BABAR	Belle	CLEO	CDF	New avg.
269	$a_1^+ K^0$	35 ± 7	$34.9 \pm 5.0 \pm 4.4$				34.9 ± 6.7
270	$b_1^+ K^0 \dagger$	9.6 ± 1.9	$9.6 \pm 1.7 \pm 0.9$				9.6 ± 1.9
271	$K^{*0} \rho^+$	9.2 ± 1.5	$9.6 \pm 1.7 \pm 1.5$	$8.9 \pm 1.7 \pm 1.2$			9.2 ± 1.5
274	$b_1^0 K^+ \dagger$	9.1 ± 2.0	$9.1 \pm 1.7 \pm 1.0$				9.1 ± 2.0
275	$b_1^+ K^{*0} \dagger$	< 5.9	< 5.9				< 5.9
276	$b_1^0 K^{*+} \dagger$	< 6.7	< 6.7				< 6.7
277	$K^+ \bar{K}^0$	1.36 ± 0.27	$1.61 \pm 0.44 \pm 0.09$	$1.11^{+0.19}_{-0.18} \pm 0.05$	< 3.3		1.19 ± 0.18
278	$\bar{K}^0 K^+ \pi^0$	< 24			< 24		< 24
279	$K^+ K_S K_S$	11.5 ± 1.3	$10.7 \pm 1.2 \pm 1.0$	$13.4 \pm 1.9 \pm 1.5$			11.5 ± 1.3
280	$K_S K_S \pi^+$	< 0.51	< 0.51	< 3.2			< 0.51
281	$K^+ K^- \pi^+$	5.0 ± 0.7	$5.0 \pm 0.5 \pm 0.5$	< 13			5.0 ± 0.7
283	$\bar{K}^{*0} K^+$	< 1.1	< 1.1		< 5.3		< 1.1
284	$\bar{K}_0^*(1430)^0 K^+$	< 2.2	< 2.2				< 2.2
–	$\bar{K}_2^*(1430)^0 K^+$	New					< 1.1
285	$K^+ K^+ \pi^-$	< 0.16	< 0.16	< 2.4			< 0.16
288	$K^{*+} \pi^+ K^-$	< 11.8	< 11.8				< 11.8
289	$K^{*+} \bar{K}^{*0}$	1.2 ± 0.5	$1.2 \pm 0.5 \pm 0.1$		< 71		1.2 ± 0.5
290	$K^{*+} K^+ \pi^-$	< 6.1	< 6.1				< 6.1
291	$K^+ K^- K^+$	33.7 ± 2.2	$33.5 \pm 0.9 \pm 1.6$	$30.6 \pm 1.2 \pm 2.3$			32.5 ± 1.5
292	ϕK^+	8.3 ± 0.7	$8.4 \pm 0.7 \pm 0.7$	$9.60 \pm 0.92^{+1.05}_{-0.84}$	$5.5^{+2.1}_{-1.8} \pm 0.6$	$7.6 \pm 1.3 \pm 0.6$	8.30 ± 0.65
294	$a_2(1320) K^+ \dagger$	< 1.1		< 1.1			< 1.1
297	$\phi(1680) K^+ \dagger$	< 0.8		< 0.8			< 0.8
300	$K^{*+} K^+ K^-$	36 ± 5	$36.2 \pm 3.3 \pm 3.6$				36.2 ± 4.9
301	ϕK^{*+}	10.0 ± 2.0	$11.2 \pm 1.0 \pm 0.9$	$6.7^{+2.1+0.7}_{-1.9-1.0}$	$10.6^{+6.4+1.8}_{-4.9-1.6}$		10.0 ± 1.1
303	$\phi K_1(1270)^+$	6.1 ± 1.9	$6.1 \pm 1.6 \pm 1.1$				6.1 ± 1.9
304	$\phi K_1(1400)^+$	< 3.2	< 3.2				< 3.2
305	$\phi K^*(1410)^+$	< 4.3	< 4.3				< 4.3
306	$\phi K_0^*(1430)^+$	7.0 ± 1.6	$7.0 \pm 1.3 \pm 0.9$				7.0 ± 1.6
307	$\phi K_2^*(1430)^+$	8.4 ± 2.1	$8.4 \pm 1.8 \pm 1.0$				8.4 ± 2.1
308	$\phi K_2(1770)^+$	< 15	< 15				< 15
309	$\phi K_2(1820)^+$	< 16	< 16				< 16
–	$a_1^+ K^{*0}$	New	< 3.6				< 3.6
310	$\phi \phi K^+ \S$	$4.9^{+2.4}_{-2.2}$	$5.6 \pm 0.5 \pm 0.3$	$3.2^{+0.6}_{-0.5} \pm 0.3$			4.6 ± 0.4
311	$\eta' \eta' K^+$	< 25	< 25				< 25
312	$K^+ \omega \phi$	< 1.9		< 1.9			< 1.9
313	$K^+ X(1812) \dagger$	< 0.32		< 0.32			< 0.32

\dagger Product BF - daughter BF taken to be 100%; $\S M_{\phi\phi} < 2.85 \text{ GeV}/c^2$

Table 132: Branching Fractions (BF) of charmless mesonic B^+ decays without kaons (in units of 10^{-6}). Upper limits are at 90% CL. Values in red (blue) are new published (preliminary) results since PDG2010 [as of March 12, 2012].

RPP#	Mode	PDG2010 Avg.	BABAR	Belle	CLEO	CDF	New avg.
330	$\pi^+\pi^0$	5.7 ± 0.5	$5.02 \pm 0.46 \pm 0.29$	$5.86 \pm 0.26 \pm 0.38$	$4.6^{+1.8+0.6}_{-1.6-0.7}$		$5.48^{+0.35}_{-0.34}$
331	$\pi^+\pi^+\pi^-$	15.2 ± 1.5	$15.2 \pm 0.6 \pm 1.3$				15.2 ± 1.4
332	$\rho^0\pi^+$	8.3 ± 1.2	$8.1 \pm 0.7^{+1.3}_{-1.6}$	$8.0^{+2.3}_{-2.0} \pm 0.7$	$10.4^{+3.3}_{-3.4} \pm 2.1$		$8.3^{+1.2}_{-1.3}$
333	$f_0(980)\pi^+ \dagger$	< 1.5	< 1.5				< 1.5
334	$f_2(1270)\pi^+$	$1.57^{+0.69}_{-0.49}$	$1.57 \pm 0.42^{+0.55}_{-0.25}$				$1.57^{+0.69}_{-0.49}$
335	$\rho(1450)^0\pi^+ \dagger$	$1.4^{+0.6}_{-0.9}$	$1.4 \pm 0.4^{+0.5}_{-0.8}$				$1.4^{+0.6}_{-0.9}$
336	$f_0(1370)\pi^+ \dagger$	< 4.0	< 4.0				< 4.0
338	$\pi^+\pi^-\pi^+(NR)$	$5.3^{+1.5}_{-1.1}$	$5.3 \pm 0.7^{+1.3}_{-0.8}$				$5.3^{+1.5}_{-1.1}$
340	$\rho^+\pi^0$	10.9 ± 1.4	$10.2 \pm 1.4 \pm 0.9$	$13.2 \pm 2.3^{+1.4}_{-1.9}$	< 43		$10.9^{+1.5}_{-1.4}$
342	$\rho^+\rho^0$	24.0 ± 1.9	$23.7 \pm 1.4 \pm 1.4$	$31.7 \pm 7.1^{+3.8}_{-6.7}$			$24.0^{+1.9}_{-2.0}$
343	$f_0(980)\rho^+ \dagger$	< 2.0	< 2.0				< 2.0
344	$a_1^+\pi^0$	26 ± 7	$26.4 \pm 5.4 \pm 4.1$				26.4 ± 6.8
345	$a_1^0\pi^+$	20 ± 6	$20.4 \pm 4.7 \pm 3.4$				20.4 ± 5.8
346	$\omega\pi^+$	6.9 ± 0.5	$6.7 \pm 0.5 \pm 0.4$	$6.9 \pm 0.6 \pm 0.5$	$11.3^{+3.3}_{-2.9} \pm 1.4$		6.9 ± 0.5
347	$\omega\rho^+$	15.9 ± 2.1	$15.9 \pm 1.6 \pm 1.4$		< 61		15.9 ± 2.1
348	$\eta\pi^+$	4.07 ± 0.32	$4.00 \pm 0.40 \pm 0.24$	$4.07 \pm 0.26 \pm 0.21$	$1.2^{+2.8}_{-1.2}$		4.02 ± 0.27
349	$\eta\rho^+$	7.0 ± 2.9	$9.9 \pm 1.2 \pm 0.8$	$4.1^{+1.4}_{-1.3} \pm 0.4$	$4.8^{+5.2}_{-3.8}$		6.9 ± 1.0
350	$\eta'\pi^+$	2.7 ± 0.9	$3.5 \pm 0.6 \pm 0.2$	$1.8^{+0.7}_{-0.6} \pm 0.1$	$1.0^{+5.8}_{-1.0}$		$2.7^{+0.5}_{-0.4}$
351	$\eta'\rho^+$	$8.7^{+3.9}_{-3.1}$	$9.7^{+1.9}_{-1.8} \pm 1.1$	< 5.8	$11.2^{+11.9}_{-7.0}$		$9.8^{+2.1}_{-2.0}$
352	$\phi\pi^+$	< 0.24	< 0.24		< 5		< 0.24
353	$\phi\rho^+$	< 3.0	< 3.0		< 16		< 3.0
354	$a_0(980)^0\pi^+ \dagger$	< 5.8	< 5.8				< 5.8
355	$a_0(980)^+\pi^0 \dagger$	< 1.4	< 1.4				< 1.4
359	$b_1^0\pi^+ \dagger$	6.7 ± 2.0	$6.7 \pm 1.7 \pm 1.0$				6.7 ± 2.0
360	$b_1^+\pi^0 \dagger$	< 3.3	< 3.3				< 3.3
362	$b_1^+\rho^0 \dagger$	< 5.2	< 5.2				< 5.2
364	$b_1^0\rho^+ \dagger$	< 3.3	< 3.3				< 3.3

†Product BF - daughter BF taken to be 100%;

Table 133: Branching fractions of charmless mesonic B^0 decays with kaons (in units of 10^{-6}). Upper limits are at 90% CL. Values in red (blue) are new published (preliminary) results since PDG2010 [as of March 12, 2012].

RPP#	Mode	PDG2010 Avg.	BABAR	Belle	CLEO	CDF	New avg.
210	$K^+\pi^-$	19.4 ± 0.6	$19.1 \pm 0.6 \pm 0.6$	$20.0 \pm 0.34 \pm 0.63$	$18.0^{+2.3+1.2}_{-2.1-0.9}$		$19.55^{+0.54}_{-0.53}$
211	$K^0\pi^0$	9.5 ± 0.8	$10.1 \pm 0.6 \pm 0.4$	$9.66 \pm 0.46 \pm 0.49$	$12.8^{+4.0+1.7}_{-3.3-1.4}$		$9.92^{+0.49}_{-0.48}$
212	$\eta'K^0$	66 ± 4	$68.5 \pm 2.2 \pm 3.1$	$58.9^{+3.6}_{-3.5} \pm 4.3$	$89^{+18}_{-16} \pm 9$		66.1 ± 3.1
213	$\eta'K^{*0}$	$3.8 \pm 1.1 \pm 0.5$	$3.1^{+0.9}_{-0.8} \pm 0.3$	< 2.6	$7.8^{+7.7}_{-5.7}$		3.1 ± 0.9
–	$\eta'K_0^*(1430)^0$	New	$6.3 \pm 1.3 \pm 0.9$				6.3 ± 1.6
–	$\eta'K_2^*(1430)^0$	New	$13.7^{+3.0}_{-1.9} \pm 1.2$				$13.7^{+3.2}_{-2.2}$
214	ηK^0	$1.15^{+0.43}_{-0.38} \pm 0.09$	$1.15^{+0.43}_{-0.38} \pm 0.09$	$1.27^{+0.33}_{-0.29} \pm 0.08$	$0.0^{+3.0}_{-0.0}$		$1.23^{+0.27}_{-0.24}$
215	ηK^{*0}	15.9 ± 1.0	$16.5 \pm 1.1 \pm 0.8$	$15.2 \pm 1.2 \pm 1.0$	$13.8^{+5.5}_{-4.6} \pm 1.6$		15.9 ± 1.0
216	$\eta K_0^*(1430)^0$	9.6 ± 1.9	$9.6 \pm 1.4 \pm 1.3$				9.6 ± 1.9
217	$\eta K_2^*(1430)^0$	9.6 ± 2.1	$9.6 \pm 1.8 \pm 1.1$				9.6 ± 2.1
218	ωK^0	5.0 ± 0.6	$5.4 \pm 0.8 \pm 0.3$	$4.4^{+0.8}_{-0.7} \pm 0.4$	$10.0^{+5.4}_{-4.2} \pm 1.4$		5.0 ± 0.6
219	$a_0(980)^0 K^0 \ddagger$	< 7.8	< 7.8				< 7.8
220	$b_1^0 K^0 \ddagger$	< 7.8	< 7.8				< 7.8
221	$a_0(980)^- K^+ \ddagger$	< 1.9	< 1.9				< 1.9
222	$b_1^- K^+ \ddagger$	7.4 ± 1.4	$7.4 \pm 1.0 \pm 1.0$				7.4 ± 1.4
223	$b_1^0 K^{*0} \ddagger$	< 8.0	< 8.0				< 8.0
224	$b_1^- K^{*+} \ddagger$	< 5.0	< 5.0				< 5.0
225	$a_0(1450)^- K^+ \ddagger$	< 3.1	< 3.1				< 3.1
227	ωK^{*0}	2.0 ± 0.5	$2.2 \pm 0.6 \pm 0.2$	$1.8 \pm 0.7^{+0.3}_{-0.2}$	< 23		2.0 ± 0.5
229	$\omega K^*(1430)^0$	16.0 ± 3.4	$16.0 \pm 1.6 \pm 3.0$				16.0 ± 3.4
230	$\omega K_2^*(1430)^0$	10.1 ± 2.3	$10.1 \pm 2.0 \pm 1.1$				10.1 ± 2.3
231	$\omega K^+\pi^- (NR)^1$	5.1 ± 1.0		$5.1 \pm 0.7 \pm 0.7$			5.1 ± 1.0
232	$K^+\pi^-\pi^0$	$35.9^{+2.8}_{-2.4}$	$38.5 \pm 1.0 \pm 3.9$	$36.6^{+4.2}_{-4.3} \pm 3.0$	< 40		37.8 ± 3.2
233	$\rho^- K^+$	$8.4^{+1.6}_{-2.2}$	$6.6 \pm 0.5 \pm 0.8$	$15.1^{+3.4+2.4}_{-3.3-2.6}$	$16^{+8}_{-6} \pm 3$		7.2 ± 0.9
234	$\rho(1450)^- K^+$	< 2.1	$2.4 \pm 1.0 \pm 0.6$				2.4 ± 1.2
235	$\rho(1700)^- K^+$	< 1.1	$0.6 \pm 0.6 \pm 0.4$				0.6 ± 0.7
236	$K^+\pi^-\pi^0 (NR)$	4.4 ± 1.0	$2.8 \pm 0.5 \pm 0.4$	< 9.4			2.8 ± 0.6
239	$K_2^*(1430)^0 \pi^0$	< 4.0	< 4.0				< 4.0
240	$K^*(1680)^0 \pi^0$	< 7.5	< 7.5				< 7.5
242	$K^0 \pi^+ \pi^-$	49.6 ± 2.0	$50.2 \pm 1.5 \pm 1.8$	$47.5 \pm 2.4 \pm 3.7$	$50^{+10}_{-9} \pm 7$		49.6 ± 2.0
243	$K^0 \pi^+ \pi^- (NR)$	$14.7^{+4.0}_{-2.6}$	$11.1^{+2.5}_{-1.0} \pm 0.9$	$19.9 \pm 2.5^{+1.7}_{-2.0}$			14.7 ± 2.0
244	$\rho^0 K^0$	4.7 ± 0.6	$4.4 \pm 0.7 \pm 0.3$	$6.1 \pm 1.0^{+1.1}_{-1.2}$	< 39		4.7 ± 0.7
245	$K^{*+} \pi^-$	$9.4^{+1.3}_{-1.2}$	$8.3^{+0.9}_{-0.8} \pm 0.8$	$8.4 \pm 1.1^{+1.0}_{-0.9}$	$16^{+6}_{-5} \pm 2$		8.6 ± 0.9
246	$K_0^*(1430)^+ \pi^-$	33 ± 7	$29.9^{+2.3}_{-1.7} \pm 3.6$	$49.7 \pm 3.8^{+6.8}_{-8.2}$			$33.5^{+3.9}_{-3.8}$
248	$K^*(1410)^+ \pi^- \ddagger$	< 86		< 86			< 86
249	$f_0(980)K^0 \ddagger$	7.0 ± 0.9	$6.9 \pm 0.8 \pm 0.6$	$7.6 \pm 1.7^{+0.9}_{-1.3}$			7.0 ± 0.9
250	$f_2(1270)^0 K^0$	$2.7^{+1.0}_{-0.8} \pm 0.9$	$2.7^{+1.0}_{-0.8} \pm 0.9$	$< 2.5 \ddagger$			$2.7^{+1.3}_{-1.2}$

\ddagger Product BF - daughter BF taken to be 100%, \ddagger Relative BF converted to absolute BF $^1 0.755 < M(K\pi) < 1.250 \text{ GeV}/c^2$. 2 Excludes $M(K_S K_S)$ regions [3.400,3.429] and [3.540,3.585] and $M(K_S K_L) < 1.049 \text{ GeV}/c^2$ 3 Includes $K\pi$ S-wave contribution and uncorrected for $K^*(1430)$ branching fraction

Table 134: Branching fractions of charmless mesonic B^0 decays with kaons - Part 2 (in units of 10^{-6}). Upper limits are at 90% CL. Values in red (blue) are new published (preliminary) results since PDG2010 [as of March 12, 2012].

RPP#	Mode	PDG2010 Avg.	BABAR	Belle	CLEO	CDF	New avg.
252	$K^{*0}\pi^0$	$3.6 \pm 0.7 \pm 0.4$	$3.3 \pm 0.5 \pm 0.4$	$0.4^{+1.9}_{-1.7} \pm 0.1$	$0.0^{+1.3+0.5}_{-0.0-0.0}$		2.5 ± 0.6
253	$K_2^*(1430)^+\pi^-$	< 6.3	< 16.2	< 6.3			< 6.3
254	$K_2^*(1680)^+\pi^-$	< 10	< 25	< 10.1			< 10.1
256	$\rho^0 K^+\pi^-$	$2.8 \pm 0.5 \pm 0.5$		$2.8 \pm 0.5 \pm 0.5$ ²			2.8 ± 0.7
257	$f_0(980)K^+\pi^-$	$1.4 \pm 0.4^{+0.3}_{-0.4}$		$1.4 \pm 0.4^{+0.3}_{-0.4}$ ²			$1.4^{+0.5}_{-0.6}$
258	$K^+\pi^-\pi^+\pi^-$	< 2.1		< 2.1			< 2.1
259	$K^{*0}\pi^+\pi^-$	54 ± 5	$54.5 \pm 2.9 \pm 4.3$	$4.5^{+1.1+0.9}_{-1.0-1.6}$ ¹			54.5 ± 5.2
260	$K^{*0}\rho^0$	$3.4^{+1.7}_{-1.3}$	$5.1 \pm 0.6^{+0.6}_{-0.8}$	$2.1^{+0.8+0.9}_{-0.7-0.5}$	< 34		3.9 ± 0.8
261	$f_0(980)K^{*0}\dagger$	< 2.2	$5.7 \pm 0.6 \pm 0.3$	< 2.2			5.7 ± 0.7
—	$f_0(980)K_2^*(1430)^0\dagger$	New	$8.6 \pm 1.7 \pm 1.0$				8.6 ± 2.0
262	$K_1(1270)^+\pi^-$	< 30	17^{+8}_{-11}				17^{+8}_{-11}
263	$K_1(1400)^+\pi^-$	< 27	17^{+7}_{-9}				17^{+7}_{-9}
264	$a_1^- K^+$	16 ± 4	$16.3 \pm 2.9 \pm 2.3$				16.3 ± 3.7
265	$K^{*+}\rho^-$	< 12	$10.3 \pm 2.3 \pm 1.3$				10.3 ± 2.6
267	K^+K^-	< 0.41	$0.04 \pm 0.15 \pm 0.08$	$0.09^{+0.18}_{-0.13} \pm 0.01$	< 0.8	$0.23 \pm 0.10 \pm 0.10\dagger$	$0.13^{+0.10}_{-0.09}$
268	$K^0\bar{K}^0$	$0.96^{+0.20}_{-0.18}$	$1.08 \pm 0.28 \pm 0.11$	$1.26^{+0.19}_{-0.18} \pm 0.06$	< 3.3		1.21 ± 0.16
269	$K^0 K^-\pi^+$	< 18	$6.4 \pm 1.0 \pm 0.6$	< 18	< 21		6.4 ± 1.2
270	$K^{*0}\bar{K}^0$	< 1.9	< 1.9				< 1.9
271	$K^+K^-\pi^0$	< 19			< 19		< 19
272	$K_S K_S \pi^0$	< 0.9	< 0.9				< 0.9
273	$K_S K_S \eta$	< 1.0	< 1.0				< 1.0
274	$K_S K_S \eta'$	< 2.0	< 2.0				< 2.0
275	$K^+K^-K^0$	24.7 ± 2.3	$23.8 \pm 2.0 \pm 1.6$	$28.3 \pm 3.3 \pm 4.0$			24.7 ± 2.3
276	ϕK^0	$8.6^{+1.3}_{-1.1}$	$8.4^{+1.5}_{-1.3} \pm 0.5$	$9.0^{+2.2}_{-1.8} \pm 0.7$	$5.4^{+3.7}_{-2.7} \pm 0.7$		$8.3^{+1.2}_{-1.0}$
277	$K_S K_S K_S$	$6.2^{+1.2}_{-1.1}$	$6.19 \pm 0.48 \pm 0.19$	$4.2^{+1.6}_{-1.3} \pm 0.8$			6.04 ± 0.50
—	$f_0(1710)K_S\dagger$	New	$0.50^{+0.46}_{-0.24} \pm 0.11\dagger$				$0.50^{+0.47}_{-0.26}$
—	$f_0(2010)K_S\dagger$	New	$0.54^{+0.21}_{-0.20} \pm 0.52\dagger$				0.54 ± 0.56
278	$K_S K_S K_L$	< 16	$< 16^2$				$< 16^2$
279	$K^{*0}K^+K^-$	27.5 ± 2.6	$27.5 \pm 1.3 \pm 2.2$				27.5 ± 2.6
280	ϕK^{*0}	9.8 ± 0.6	$9.7 \pm 0.5 \pm 0.6$	$10.0^{+1.6+0.7}_{-1.5-0.8}$	$11.5^{+4.5+1.8}_{-3.7-1.7}$		9.8 ± 0.7
281	$K^{*0}\pi^+K^-$	4.6 ± 1.4	$4.6 \pm 1.1 \pm 0.8$	< 13.9 ³			4.6 ± 1.4
282	$K^{*0}\bar{K}^{*0}$	$1.28^{+0.35}_{-0.30} \pm 0.11$	$1.28^{+0.35}_{-0.30} \pm 0.11$	$0.26^{+0.33+0.10}_{-0.29-0.08}$	< 22		0.81 ± 0.23
—	$K_0^*(1430)^0\bar{K}_0^*(1430)^0$	New		< 8.4			< 8.4
—	$K_0^*(1430)^0\bar{K}^{*0}$	New		< 3.3			< 3.3
—	$K_0^*(1430)^0\pi^+K^-$	New		< 31.8 ³			< 31.8 ³
—	$K^+\pi^-\pi^+K^-$	New		< 72 ³			< 72 ³
283	$K^{*0}K^+\pi^-$	< 2.2	< 2.2	< 7.6 ³			< 2.2
284	$K^{*0}K^0$	< 0.41	< 0.41	< 0.2	< 37		< 0.2
—	$K_0^*(1430)^0 K_0^*(1430)^0$	New		< 4.7			< 4.7
—	$K_0^*(1430)^0 K^{*0}$	New		< 1.7			< 1.7
—	$K^+\pi^-K^+\pi^-$	New		< 6.0 ³			< 6.0 ³
285	$K^{*+}K^{*-}$	< 2.0	< 2.0		< 141		< 2.0
289	$\phi K_0^*(1430)^0$	$3.9 \pm 0.5 \pm 0.6$	$3.9 \pm 0.5 \pm 0.6$				3.9 ± 0.8
290	$\phi K^*(1680)^0$	< 3.5	< 3.5				< 3.5
291	$\phi K_3^*(1780)^0$	< 2.7	< 2.7				< 2.7
292	$\phi K_4^*(2045)^0$	< 15.3	< 15.3				< 15.3
294	$\phi K_2^*(1430)^0$	7.5 ± 1.0	$7.5 \pm 0.9 \pm 0.5$				7.5 ± 1.0
295	$\phi\phi K^0 \S$	$4.1^{+1.7}_{-1.4} \pm 0.4$	$4.5 \pm 0.8 \pm 0.3$	$2.3^{+1.0}_{-0.7} \pm 0.2$			3.6 ± 0.7
296	$\eta'\eta'K^0$	< 31	< 31				< 31

\dagger Product BF - daughter BF taken to be 100%, $\S M_{\phi\phi} < 2.85 \text{ GeV}/c^2$ $\ddagger 0.55 < M(\pi\pi) < 1.42 \text{ GeV}/c^2$ and $0.75 < M(K\pi) < 1.20 \text{ GeV}/c^2$; ${}^1 0.55 < M(\pi\pi) < 1.42 \text{ GeV}/c^2$; ${}^2 0.75 < M(K\pi) < 1.20 \text{ GeV}/c^2$

Table 135: Branching fractions of charmless mesonic B^0 decays without kaons (in units of 10^{-6}). Upper limits are at 90% CL. Values in red (blue) are new published (preliminary) results since PDG2010 [as of March 12, 2012].

RPP#	Mode	PDG2010 Avg.	BABAR	Belle	CLEO	CDF	New avg.
315	$\pi^+\pi^-$	5.13 ± 0.24	$5.5 \pm 0.4 \pm 0.3$	$5.04 \pm 0.21 \pm 0.19$	$4.5^{+1.4+0.5}_{-1.2-0.4}$	$5.02 \pm 0.33 \pm 0.35\dagger$	5.11 ± 0.22
316	$\pi^0\pi^0$	1.62 ± 0.31	$1.83 \pm 0.21 \pm 0.13$	$2.3^{+0.4+0.2}_{-0.5-0.3}$	< 4.4		$1.91^{+0.22}_{-0.23}$
317	$\eta\pi^0$	< 1.5	< 1.5	< 2.5	< 2.9		< 1.5
318	$\eta\eta$	< 1.0	< 1.0	< 2.0	< 18		< 1.0
319	$\eta'\pi^0$	1.2 ± 0.6	$0.9 \pm 0.4 \pm 0.1$	$2.8 \pm 1.0 \pm 0.3$	$0.0^{+1.8}_{-0.0}$		1.2 ± 0.4
320	$\eta'\eta'$	< 1.7	< 1.7	< 6.5	< 47		< 1.7
321	$\eta'\eta$	< 1.2	< 1.2	< 4.5	< 27		< 1.2
322	$\eta'\rho^0$	< 1.3	< 2.8	< 1.3	< 12		< 1.3
323	$f_0(980)\eta'\dagger$	< 1.5	< 0.9				< 0.9
324	$\eta\rho^0$	< 1.5	< 1.5	< 1.9	< 10		< 1.5
325	$f_0(980)\eta\dagger$	< 0.4	< 0.4				< 0.4
326	$\omega\eta$	$0.94^{+0.35}_{-0.30} \pm 0.09$	< 1.4		< 12		< 1.4
327	$\omega\eta'$	$1.01^{+0.46}_{-0.38} \pm 0.09$	< 1.8	< 2.2	< 60		< 1.8
328	$\omega\rho^0$	< 1.6	< 1.6		< 11		< 1.6
329	$f_0(980)\omega\dagger$	< 1.5	< 1.5				< 1.5
330	$\omega\omega$	< 4.0	< 4.0		< 19		< 4.0
331	$\phi\pi^0$	< 0.28	< 0.28		< 5		< 0.28
332	$\phi\eta$	< 0.5	< 0.5		< 9		< 0.5
333	$\phi\eta'$	< 0.5	< 1.1	< 0.5	< 31		< 0.5
334	$\phi\rho^0$	< 0.33	< 0.33		< 13		< 0.33
335	$f_0(980)\phi\dagger$	< 0.38	< 0.38				< 0.38
336	$\omega\phi$	< 1.2	< 1.2		< 21		< 1.2
337	$\phi\phi$	< 0.2	< 0.2		< 12		< 0.2
338	$a_0^{\mp}(980)\pi^{\pm}\dagger$	< 3.1	< 3.1				< 3.1
339	$a_0^{\mp}(1450)\pi^{\pm}\dagger$	< 2.3	< 2.3				< 2.3
341	$\rho^0\pi^0$	2.0 ± 0.5	$1.4 \pm 0.6 \pm 0.3$	$3.0 \pm 0.5 \pm 0.7$	$1.6^{+2.0}_{-1.4} \pm 0.8$		2.0 ± 0.5
342	$\rho^{\mp}\pi^{\pm}$	23.0 ± 2.3	$22.6 \pm 1.8 \pm 2.2$	$22.6 \pm 1.1 \pm 4.4$	$27.6^{+8.4}_{-7.4} \pm 4.2$		23.0 ± 2.3
343	$\pi^+\pi^-\pi^+\pi^-$	< 19.3	< 23.1	< 19.3			< 19.3
344	$\rho^0\pi^+\pi^-(NR)$	< 8.8	< 8.8	< 12			< 8.8
345	$\rho^0\rho^0$	0.73 ± 0.28	$0.92 \pm 0.32 \pm 0.14$	$0.4 \pm 0.4^{+0.2}_{-0.3}$	< 18		$0.73^{+0.27}_{-0.28}$
346	$f_0(980)\pi^+\pi^-(NR)$	< 3.8		< 3.8			< 3.8
347	$f_0(980)\rho^0\dagger$	< 0.3	< 0.40	< 0.3			< 0.3
348	$f_0(980)f_0(980)\dagger$	< 0.1	< 0.19	< 0.1			< 0.1
350	$a_1^{\mp}\pi^{\pm}$	33 ± 5	$33.2 \pm 3.8 \pm 3.0$				33.2 ± 4.8
353	$\rho^+\rho^-$	24.2 ± 3.1	$25.5 \pm 2.1^{+3.6}_{-3.9}$	$22.8 \pm 3.8^{+2.3}_{-2.6}$			$24.2^{+3.1}_{-3.2}$
355	$\omega\pi^0$	< 0.5	< 0.5	< 2.0	< 5.5		< 0.5
357	$a_1^{\pm}\rho^{\mp}$	< 61	< 61				< 61
359	$b_1^{\mp}\pi^{\pm}\dagger$	10.9 ± 1.5	$10.9 \pm 1.2 \pm 0.9$				10.9 ± 1.5
360	$b_1^0\pi^0\dagger$	< 1.9	< 1.9				< 1.9
361	$b_1^{\pm}\rho^{\mp}\dagger$	< 1.4	< 1.4				< 1.4
362	$b_1^0\rho^0\dagger$	< 3.4	< 3.4				< 3.4
364	$a_1^{\pm}a_1^{\mp}$	$47.3 \pm 10.5 \pm 6.3$	$47.3 \pm 10.5 \pm 6.3$				47.3 ± 12.2

\dagger Product BF - daughter BF taken to be 100%, \ddagger Relative BF converted to absolute BF

Table 136: Relative branching fractions of $B^0 \rightarrow K^+K^-, K^+\pi^-, \pi^+\pi^-$. Values in red (blue) are new **published** (**preliminary**) result since PDG2010 [as of March 12, 2012].

RPP#	Mode	PDG2010 Avg.	CDF	DØ	New avg.
267	$\mathcal{B}(B^0 \rightarrow K^+K^-)/\mathcal{B}(B^0 \rightarrow K^+\pi^-)$		0.020 ± 0.008 ± 0.006		0.020 ± 0.010
315	$\mathcal{B}(B^0 \rightarrow \pi^+\pi^-)/\mathcal{B}(B^0 \rightarrow K^+\pi^-)$		0.259 ± 0.017 ± 0.016		0.259 ± 0.023

7.2 Radiative and leptonic decays

Table 137: Branching fractions of semileptonic and radiative B^+ decays (in units of 10^{-6}). Upper limits are at 90% CL. Values in red (blue) are new published (preliminary) results since PDG2010 [as of March 12, 2012].

RPP#	Mode	PDG2010 Avg.	BABAR	Belle	CLEO	CDF	New Avg.
314	$K^{*+}\gamma$	42.1 ± 1.8	$42.2 \pm 1.4 \pm 1.6$	$42.5 \pm 3.1 \pm 2.4$	$37.6_{-8.3}^{+8.9} \pm 2.8$		42.1 ± 1.8
315	$K_1^+(1270)\gamma$	43 ± 13		$43 \pm 9 \pm 9$			43 ± 12
316	$K^+\eta\gamma$	7.9 ± 0.9	$7.7 \pm 1.0 \pm 0.4$	$8.4_{-1.2}^{+1.5} \pm 0.9$			7.9 ± 0.9
317	$K^+\eta'\gamma$	< 4.2	$1.9_{-1.2}^{+1.5} \pm 0.1$	$3.6 \pm 1.2 \pm 0.4$			$2.9_{-0.9}^{+1.0}$
318	$K^+\phi\gamma$	3.5 ± 0.6	$3.5 \pm 0.6 \pm 0.4$	$2.48 \pm 0.30 \pm 0.24$			2.71 ± 0.34
319	$K^+\pi^-\pi^+\gamma$	27.6 ± 2.2	$29.5 \pm 1.3 \pm 2.0 \dagger$	$25.0 \pm 1.8 \pm 2.2 \ddagger$			27.6 ± 1.8
320	$K^{*0}\pi^+\gamma \S$	20_{-6}^{+7}		$20_{-6}^{+7} \pm 2$			20_{-6}^{+7}
321	$K^+\rho^0\gamma \S$	< 20		< 20			< 20
322	$K^+\pi^-\pi^+\gamma$ (N.R.) \S	< 9.2		< 9.2			< 9.2
323	$K^0\pi^+\pi^0\gamma$	46 ± 5	$45.6 \pm 4.2 \pm 3.1 \dagger$				45.6 ± 5.2
324	$K_1^+(1400)\gamma$	< 15		< 15			< 15
325	$K_2^*(1430)^+\gamma$	14 ± 4	$14.5 \pm 4.0 \pm 1.5$				14.5 ± 4.3
327	$K_3^*(1780)^+\gamma$	< 39		< 39			< 39
329	$\rho^+\gamma$	0.98 ± 0.25	$1.20_{-0.37}^{+0.42} \pm 0.20$	$0.87_{-0.27-0.11}^{+0.29+0.09}$	< 13		$0.98_{-0.24}^{+0.25}$
379	$p\bar{A}\gamma$	$2.5_{-0.4}^{+0.5}$		$2.45_{-0.38}^{+0.44} \pm 0.22$			$2.45_{-0.44}^{+0.49}$
383	$p\Sigma^0\gamma$	< 4.6		< 4.6			< 4.6
412	$\pi^+\ell^+\ell^-$	< 0.049	< 0.12	< 0.049			< 0.049
413	$\pi^+e^+e^-$	< 0.080	< 0.18	< 0.080			< 0.080
414	$\pi^+\mu^+\mu^-$	< 0.069	< 0.28	< 0.069			< 0.069
415	$\pi^+\nu\bar{\nu}$	< 100	< 100	< 170			< 100
416	$K^+\ell^+\ell^-$	0.51 ± 0.05	$0.48 \pm 0.09 \pm 0.02$	$0.53_{-0.05}^{+0.06} \pm 0.03$			0.51 ± 0.05
417	$K^+e^+e^-$	0.55 ± 0.07	$0.51_{-0.11}^{+0.12} \pm 0.02$	$0.57_{-0.08}^{+0.09} \pm 0.03$	< 2.4		0.55 ± 0.07
418	$K^+\mu^+\mu^-$	0.52 ± 0.07	$0.41_{-0.15}^{+0.16} \pm 0.02$	$0.53 \pm 0.08_{-0.03}^{+0.07}$	< 3.68	$0.46 \pm 0.04 \pm 0.02$	0.47 ± 0.04
419	$K^+\nu\bar{\nu}$	< 14	< 13	< 14	< 240		< 13
420	$\rho^+\nu\bar{\nu}$	< 150		< 150			< 150
421	$K^{*+}\ell^+\ell^-$	1.29 ± 0.21	$1.40_{-0.37}^{+0.40} \pm 0.09$	$1.24_{-0.21}^{+0.23} \pm 0.13$			$1.29_{-0.21}^{+0.22}$
422	$K^{*+}e^+e^-$	$1.55_{-0.31}^{+0.40}$	$1.38_{-0.42}^{+0.47} \pm 0.08$	$1.73_{-0.42}^{+0.50} \pm 0.20$			$1.55_{-0.32}^{+0.35}$
423	$K^{*+}\mu^+\mu^-$	$1.16_{-0.27}^{+0.31}$	$1.46_{-0.75}^{+0.79} \pm 0.12$	$1.11_{-0.27}^{+0.32} \pm 0.10$		$0.95 \pm 0.32 \pm 0.08$	$1.07_{-0.20}^{+0.22}$
424	$K^{*+}\nu\bar{\nu}$	< 80	< 80	< 140			< 80
427	$\pi^+e^\pm\mu^\mp$	< 0.17	< 0.17				< 0.17
428	$K^+e^\pm\mu^\mp$	< 0.091	< 0.091				< 0.091
429	$K^+e^-\mu^+$	< 0.13	< 0.13				< 0.13
431	$K^+\tau^\pm\mu^\mp$	< 77	< 77				< 77
434	$K^{*+}e^\pm\mu^\mp$	< 1.4	< 1.4				< 1.4
435	$\pi^-e^+e^+$	< 1.6			< 1.6		< 1.6
436	$\pi^-\mu^+\mu^+$	< 1.4			< 1.4		< 1.4
437	$\pi^-e^+\mu^+$	< 1.3			< 1.3		< 1.3
438	$\rho^-e^+e^+$	< 2.6			< 2.6		< 2.6
439	$\rho^-\mu^+\mu^+$	< 5.0			< 5.0		< 5.0
443	$\rho^-e^+\mu^+$	< 3.3			< 3.3		< 3.3
441	$K^-e^+e^+$	< 1.0			< 1.0		< 1.0
442	$K^-\mu^+\mu^+$	< 1.8			< 1.8		< 1.8
443	$K^-e^+\mu^+$	< 2.0			< 2.0		< 2.0
444	$K^{*-}e^+e^+$	< 2.8			< 2.8		< 2.8
445	$K^{*-}\mu^+\mu^+$	< 8.3			< 8.3		< 8.3
446	$K^{*-}e^+\mu^+$	< 4.4			< 4.4		< 4.4

$\dagger M_{K\pi\pi} < 1.8 \text{ GeV}/c^2$; $\ddagger 1.0 < M_{K\pi\pi} < 2.0 \text{ GeV}/c^2$; $\S M_{K\pi\pi} < 2.4 \text{ GeV}/c^2$

Table 138: Branching fractions of semileptonic and radiative B^0 decays (in units of 10^{-6}). Upper limits are at 90% CL. Values in red (blue) are new published (preliminary) results since PDG2010 [as of March 12, 2012].

RPP#	Mode	PDG2010 Avg.	BABAR	Belle	CLEO	CDF	New Avg.
297	$K^0 \eta \gamma$	7.6 ± 1.8	$7.1^{+2.1}_{-2.0} \pm 0.4$	$8.7^{+3.1+1.9}_{-2.7-1.6}$			$7.6^{+1.8}_{-1.7}$
298	$K^0 \eta' \gamma$	< 6.6	< 6.6	< 6.4			< 6.4
299	$K^0 \phi \gamma$	< 2.7	< 2.7	$2.74 \pm 0.60 \pm 0.32$			2.74 ± 0.68
300	$K^+ \pi^- \gamma$ §	4.6 ± 1.4		$4.6^{+1.3+0.5}_{-1.2-0.7}$			4.6 ± 1.4
301	$K^{*0} \gamma$	43.3 ± 1.5	$44.7 \pm 1.0 \pm 1.6$	$40.1 \pm 2.1 \pm 1.7$	$45.5^{+7.2}_{-6.8} \pm 3.4$		43.3 ± 1.5
302	$K^*(1410)^0 \gamma$	< 130		< 130			< 130
303	$K^+ \pi^- \gamma$ (N.R.) §	< 2.6		< 2.6			< 2.6
304	$K^0 \pi^+ \pi^- \gamma$	19.5 ± 2.2	$18.5 \pm 2.1 \pm 1.2$ †	$24 \pm 4 \pm 3$ ‡			19.5 ± 2.2
305	$K^+ \pi^- \pi^0 \gamma$	41 ± 4	$40.7 \pm 2.2 \pm 3.1$ †				40.7 ± 3.8
306	$K_1^0(1270) \gamma$	< 58		< 58			< 58
307	$K_1^0(1400) \gamma$	< 15		< 15			< 15
308	$K_2^*(1430)^0 \gamma$	12.4 ± 2.4	$12.2 \pm 2.5 \pm 1.0$	$13 \pm 5 \pm 1$			12.4 ± 2.4
310	$K_3^*(1780)^0 \gamma$	< 83		< 83			< 83
312	$\rho^0 \gamma$	0.86 ± 0.15	$0.97^{+0.24}_{-0.22} \pm 0.06$	$0.78^{+0.17+0.09}_{-0.16-0.10}$	< 17		$0.86^{+0.15}_{-0.14}$
313	$\omega \gamma$	$0.44^{+0.18}_{-0.16}$	$0.50^{+0.27}_{-0.23} \pm 0.09$	$0.40^{+0.19}_{-0.17} \pm 0.13$	< 9.2		$0.44^{+0.18}_{-0.16}$
314	$\phi \gamma$	< 0.85	< 0.85		< 3.3		< 0.85
418	$\pi^0 \ell^+ \ell^-$	< 0.12	< 0.12	< 0.154			< 0.12
419	$\pi^0 e^+ e^-$	< 0.14	< 0.14	< 0.227			< 0.14
420	$\pi^0 \mu^+ \mu^-$	< 1.8	< 0.51	< 0.184			< 0.184
421	$\pi^0 \nu \bar{\nu}$	< 220		< 220			< 220
422	$K^0 \ell^+ \ell^-$	$0.31^{+0.08}_{-0.07}$	$0.21^{+0.15}_{-0.13} \pm 0.02$	$0.34^{+0.09}_{-0.08} \pm 0.02$			$0.31^{+0.08}_{-0.07}$
423	$K^0 e^+ e^-$	$0.16^{+0.10}_{-0.08}$	$0.08^{+0.15}_{-0.12} \pm 0.01$	$0.20^{+0.14}_{-0.10} \pm 0.01$	< 8.45		$0.16^{+0.10}_{-0.08}$
424	$K^0 \mu^+ \mu^-$	$0.45^{+0.12}_{-0.10}$	$0.49^{+0.29}_{-0.25} \pm 0.03$	$0.44^{+0.13}_{-0.10} \pm 0.03$	< 6.64	$0.32 \pm 0.10 \pm 0.02$	0.38 ± 0.07
425	$K^0 \nu \bar{\nu}$	< 160	< 56	< 160			< 56
426	$\rho^0 \nu \bar{\nu}$	< 440		< 440			< 440
427	$K^{*0} \ell^+ \ell^-$	$0.99^{+0.12}_{-0.11}$	$1.03^{+0.22}_{-0.21} \pm 0.07$	$0.97^{+0.13}_{-0.11} \pm 0.07$			$0.99^{+0.13}_{-0.11}$
428	$K^{*0} e^+ e^-$	$1.03^{+0.19}_{-0.17}$	$0.86^{+0.26}_{-0.24} \pm 0.05$	$1.18^{+0.27}_{-0.27} \pm 0.09$			$1.03^{+0.19}_{-0.17}$
429	$K^{*0} \mu^+ \mu^-$	$1.05^{+0.16}_{-0.13}$	$1.35^{+0.40}_{-0.37} \pm 0.10$	$1.06^{+0.19}_{-0.14} \pm 0.07$		$1.02 \pm 0.10 \pm 0.06$	$1.05^{+0.16}_{-0.09}$
430	$K^{*0} \nu \bar{\nu}$	< 120	< 120	< 340			< 120
431	$\phi \nu \bar{\nu}$	< 58		< 58			< 58
433	$\pi^0 e^\pm \mu^\mp$	< 0.14	< 0.14				< 0.14
434	$K^0 e^\pm \mu^\mp$	< 0.27	< 0.27				< 0.27
437	$K^{*0} e^\pm \mu^\mp$	< 5.8	< 0.58				< 0.58

† $M_{K\pi\pi} < 1.8 \text{ GeV}/c^2$; ‡ $1.0 < M_{K\pi\pi} < 2.0 \text{ GeV}/c^2$; § $1.25 \text{ GeV}/c^2 < M_{K\pi} < 1.6 \text{ GeV}/c^2$

Table 139: Branching fractions of semileptonic and radiative B decays (in units of 10^{-6}). Upper limits are at 90% CL. Values in red (blue) are new published (preliminary) results since PDG2010 [as of March 12, 2012].

RPP#	Mode	PDG2010 Avg.	BA \overline{B}	Belle	CLEO	New Avg.
66	$K\eta\gamma$	$8.5^{+1.8}_{-1.6}$		$8.5^{+1.3}_{-1.2} \pm 0.9$		$8.5^{+1.6}_{-1.5}$
68	$K_2^*(1430)\gamma$	$1.7^{+0.6}_{-0.5}$			$1.7 \pm 0.6 \pm 0.1$	1.7 ± 0.6
70	$K_3^*(1780)\gamma$	< 37		< 2.8		< 2.8
77	$s\gamma$	360 ± 23	$327 \pm 18^{+55}_{-41}$	$345 \pm 15 \pm 40$	$321 \pm 43^{+32}_{-29}$	$355 \pm 24 \pm 9$
78	$d\gamma$	12 ± 6	$9.2 \pm 2.0 \pm 2.3$			9.2 ± 3.0
82	$\rho\gamma$	1.39 ± 0.25	$1.73^{+0.34}_{-0.32} \pm 0.17$	$1.21^{+0.24}_{-0.22} \pm 0.12$	< 14	$1.39^{+0.22}_{-0.21}$
83	$\rho/\omega\gamma$	1.39 ± 0.23	$1.63^{+0.30}_{-0.28} \pm 0.16$	$1.14 \pm 0.20^{+0.10}_{-0.12}$	< 14	$1.30^{+0.18}_{-0.19}$
113	$se^+e^- \ddagger$	4.7 ± 1.3	$6.0 \pm 1.7 \pm 1.3$	$4.56 \pm 1.15^{+0.33}_{-0.40}$	< 57	$4.91^{+1.04}_{-1.06}$
114	$s\mu^+\mu^-$	4.3 ± 1.2	$5.0 \pm 2.8 \pm 1.2$	$1.91 \pm 1.02^{+0.16}_{-0.18}$	< 58	$2.23^{+0.97}_{-0.98}$
115	$sl^+\ell^- \ddagger$	4.5 ± 1.0	$5.6 \pm 1.5 \pm 1.3$	$3.33 \pm 0.80^{+0.19}_{-0.24}$	< 42	$3.66^{+0.76}_{-0.77}$
116	$\pi\ell^+\ell^-$	< 0.062	< 0.091	< 0.062		< 0.062
117	Ke^+e^-	0.44 ± 0.06	$0.39^{+0.09}_{-0.08} \pm 0.02$	$0.48^{+0.08}_{-0.07} \pm 0.03$		0.44 ± 0.06
118	$K^*e^+e^-$	1.19 ± 0.20	$0.99^{+0.23}_{-0.21} \pm 0.06$	$1.39^{+0.23}_{-0.20} \pm 0.12$		$1.19^{+0.17}_{-0.16}$
119	$K\mu^+\mu^-$	0.48 ± 0.06	$0.41^{+0.13}_{-0.12} \pm 0.02$	$0.50 \pm 0.06 \pm 0.03$		0.48 ± 0.06
120	$K^*\mu^+\mu^-$	1.15 ± 0.15	$1.35^{+0.35}_{-0.33} \pm 0.10$	$1.10^{+0.16}_{-0.14} \pm 0.08$		$1.15^{+0.16}_{-0.15}$
121	$K\ell^+\ell^-$	0.45 ± 0.04	$0.39 \pm 0.07 \pm 0.02$	$0.48^{+0.05}_{-0.04} \pm 0.03$	< 1.7	0.45 ± 0.04
122	$K^*\ell^+\ell^-$	1.08 ± 0.11	$1.11^{+0.19}_{-0.18} \pm 0.07$	$1.07^{+0.11}_{-0.10} \pm 0.09$	< 3.3	$1.08^{+0.12}_{-0.11}$
–	$K\nu\overline{\nu}$	New	< 14			< 14
123	$K^*\nu\overline{\nu}$	< 80	< 80			< 80
125	$\pi e^\pm\mu^\mp$	< 0.092	< 0.092		< 1.6	< 0.092
126	$\rho e^\pm\mu^\mp$	< 3.2			< 3.2	< 3.2
127	$Ke^\pm\mu^\mp$	< 0.038	< 0.038		< 1.6	< 0.038
128	$K^*e^\pm\mu^\mp$	< 0.51	< 0.51		< 6.2	< 0.51
–	$s\gamma$ with baryons	New			$< 38 \ddagger$	$< 38 \ddagger$

$\ddagger E_\gamma > 2.0$ GeV; $\ddagger M(\ell^+\ell^-) > 0.2$ GeV/ c^2

Table 140: Isospin symmetry for various B decays. Values in red (blue) are new published (preliminary) results since PDG2010 [as of March 12, 2012].

RPP#	Parameter	PDG2010 Avg.	<i>BABAR</i>	Belle	New Avg.
65	$\Delta_0-(K^*\gamma)$	0.066 ± 0.030	$0.066 \pm 0.021 \pm 0.022$	$0.012 \pm 0.044 \pm 0.026$	0.052 ± 0.026
77	$\Delta_0-(X_s\gamma)$	-0.01 ± 0.06	-0.01 ± 0.06		-0.01 ± 0.06
82	$\Delta_{\rho\gamma}$	-0.46 ± 0.17	$-0.43^{+0.25}_{-0.22} \pm 0.10$	$-0.48^{+0.21+0.08}_{-0.19-0.09}$	$-0.46^{+0.17}_{-0.16}$
121	$\Delta_0-(K\ell\ell)^\dagger$	$-0.40^{+0.34}_{-0.30}$	$-1.43^{+0.56}_{-0.85} \pm 0.05$	$-0.31^{+0.17}_{-0.14} \pm 0.08$	$-0.40^{+0.16}_{-0.15}$
122	$\Delta_0-(K^*\ell\ell)^\dagger$	-0.44 ± 0.13	$-0.56^{+0.17}_{-0.15} \pm 0.03$	$-0.29 \pm 0.16 \pm 0.09$	$-0.44^{+0.13}_{-0.12}$
	$\Delta_0-(K^{(*)}\ell\ell)^\dagger$	-0.45 ± 0.17	$-0.64^{+0.15}_{-0.14} \pm 0.03$	$-0.30^{+0.12}_{-0.11} \pm 0.08$	-0.45 ± 0.10

$^\dagger m_{\ell\ell} < m_{J/\psi}$

Table 141: Partial branching fractions for various B decays. Values in red (blue) are new published (preliminary) results since PDG2010 [as of March 12, 2012].

RPP#	Mode	q^2 [(GeV/c ²) ²] †	PDG2010 Avg.	<i>BABAR</i>	Belle	CDF ‡	LHCb ‡	New Avg.
121	$K\ell^+\ell^-$	< 2.0		$0.81^{+0.18}_{-0.16} \pm 0.05$	$0.33 \pm 0.10 \pm 0.02$			0.46 ± 0.09
	$K\ell^+\ell^-$	[2.0, 4.3]		$0.46^{+0.14}_{-0.12} \pm 0.03$	$0.77 \pm 0.14 \pm 0.05$			0.61 ± 0.10
	$K\ell^+\ell^-$	[4.3, 8.68]		$1.00^{+0.19}_{-0.18} \pm 0.06$	$1.05 \pm 0.17 \pm 0.07$			$1.03^{+0.14}_{-0.13}$
	$K\ell^+\ell^-$	[10.09, 12.86]		$0.55^{+0.16}_{-0.14} \pm 0.03$	$0.48 \pm 0.10 \pm 0.03$			$0.50^{+0.09}_{-0.08}$
	$K\ell^+\ell^-$	[14.18, 16.00]		$0.38^{+0.19}_{-0.12} \pm 0.02$	$0.52 \pm 0.09 \pm 0.03$			$0.49^{+0.09}_{-0.08}$
	$K\ell^+\ell^-$	> 16.00		$0.98^{+0.20}_{-0.18} \pm 0.06$	$0.38 \pm 0.09 \pm 0.02$			0.49 ± 0.08
122	$K^*\ell^+\ell^-$	< 2.0		$1.46^{+0.40}_{-0.31} \pm 0.11$	$1.73 \pm 0.33 \pm 0.10$	$0.56 \pm 0.11 \pm 0.03$		0.74 ± 0.10
	$K^*\ell^+\ell^-$	[2.0, 4.3]		$0.86^{+0.31}_{-0.27} \pm 0.07$	$0.82 \pm 0.26 \pm 0.06$	$0.28 \pm 0.08 \pm 0.02$		0.37 ± 0.08
	$K^*\ell^+\ell^-$	[4.3, 8.68]		$1.37^{+0.47}_{-0.42} \pm 0.39$	$1.72 \pm 0.41 \pm 0.14$	$0.55 \pm 0.07 \pm 0.03$		0.60 ± 0.07
	$K^*\ell^+\ell^-$	[10.09, 12.86]		$2.24^{+0.44}_{-0.40} \pm 0.19$	$1.77 \pm 0.34 \pm 0.11$	$0.53 \pm 0.09 \pm 0.03$		0.68 ± 0.09
	$K^*\ell^+\ell^-$	[14.18, 16.00]		$1.05^{+0.29}_{-0.26} \pm 0.08$	$1.21 \pm 0.24 \pm 0.07$	$0.59 \pm 0.10 \pm 0.03$		0.72 ± 0.09
	$K^*\ell^+\ell^-$	> 16.00		$2.04^{+0.27}_{-0.24} \pm 0.16$	$0.88 \pm 0.22 \pm 0.05$	$0.48 \pm 0.08 \pm 0.03$		0.64 ± 0.08

† see the original paper for the exact q^2 selection. ‡ muon mode only ($\ell = \mu$).

7.3 $B \rightarrow X_s\gamma$

The decay $b \rightarrow s\gamma$ proceeds through a process of flavor changing neutral current. Since the charged Higgs or SUSY particles may contribute in the penguin loop, the branching fraction is sensitive to physics beyond the Standard Model. Experimentally, the branching fraction is measured using either a semi-inclusive or an inclusive approach. A minimum photon energy requirement is applied in the analysis and the branching fraction is corrected based on the theoretical model for the photon energy spectrum (shape function). Where there are multiple experimental results from an experiment, we use only the ones that are independent for *BABAR* and Belle to avoid dealing with correlated errors. Furthermore, the model uncertainties from the shape function should be highly correlated but no proper action was made in our older averages. To perform the average with better precision and good accuracy, it is important to use as many experimental results as possible and to handle the shape function issue in a proper way. In this note, we report the updated average of $b \rightarrow s\gamma$ branching fraction by implementing a common shape function.

Several shape function schemes are commonly used. Usually one is chosen to obtain the extrapolation factor, defined as the ratio of the $b \rightarrow s\gamma$ branching fractions with minimum photon energies above and at 1.6 GeV, and the difference between various schemes are treated as the model uncertainty. O. Buchmüller and H. Flächer have calculated the extrapolation factors [445]. Table 146 lists the extrapolation factors with various photon energy cuts for

Table 142: Forward-backward asymmetry for various B decays. Values in red (blue) are new published (preliminary) results since PDG2010 [as of March 12, 2012].

RPP#	Mode	q^2 [(GeV/c ²) ²] †	PDG2010 Avg.	Belle	CDF ‡	LHCb ‡	New Avg.
121	$K\ell^+\ell^-$	< 2.0	$0.06^{+0.32}_{-0.35} \pm 0.02$	$0.06^{+0.32}_{-0.35} \pm 0.02$	$0.13^{+0.42}_{-0.43} \pm 0.07$		$0.08^{+0.20}_{-0.22}$
	$K\ell^+\ell^-$	[2.0, 4.3]	$-0.43^{+0.38}_{-0.40} \pm 0.09$	$-0.43^{+0.38}_{-0.40} \pm 0.09$	$0.32^{+0.15}_{-0.16} \pm 0.05$		0.12 ± 0.14
	$K\ell^+\ell^-$	[4.3, 8.68]	$-0.20^{+0.12}_{-0.14} \pm 0.03$	$-0.20^{+0.12}_{-0.14} \pm 0.03$	$0.01^{+0.13}_{-0.10} \pm 0.01$		$-0.11^{+0.06}_{-0.07}$
	$K\ell^+\ell^-$	[10.09, 12.86]		$-0.21^{+0.17}_{-0.15} \pm 0.06$	$-0.03^{+0.11}_{-0.10} \pm 0.04$		$-0.08^{+0.10}_{-0.09}$
	$K\ell^+\ell^-$	[14.18, 16.00]		$0.04^{+0.32}_{-0.26} \pm 0.05$	$-0.05^{+0.09}_{-0.11} \pm 0.03$		$-0.04^{+0.09}_{-0.09}$
	$K\ell^+\ell^-$	> 16.00		$0.02^{+0.11}_{-0.08} \pm 0.02$	$0.09^{+0.17}_{-0.13} \pm 0.03$		$0.04^{+0.09}_{-0.07}$
122	$K^*\ell^+\ell^-$	< 2.0	$0.47^{+0.26}_{-0.32} \pm 0.03$	$0.47^{+0.26}_{-0.32} \pm 0.03$	$-0.35^{+0.26}_{-0.23} \pm 0.10$	$-0.17^{+0.22}_{-0.23} \pm 0.06$	0.03 ± 0.14
	$K^*\ell^+\ell^-$	[2.0, 4.3]	$0.11^{+0.31}_{-0.36} \pm 0.07$	$0.11^{+0.31}_{-0.36} \pm 0.07$	$0.29^{+0.32}_{-0.35} \pm 0.15$	$-0.04^{+0.19}_{-0.15} \pm 0.06$	$0.05^{+0.15}_{-0.14}$
	$K^*\ell^+\ell^-$	[4.3, 8.68]	$0.45^{+0.15}_{-0.21} \pm 0.15$	$0.45^{+0.15}_{-0.21} \pm 0.15$	$0.01^{+0.20}_{-0.20} \pm 0.09$	$0.28^{+0.06}_{-0.08} \pm 0.02$	$0.28^{+0.06}_{-0.07}$
	$K^*\ell^+\ell^-$	[10.09, 12.86]		$0.43^{+0.18}_{-0.20} \pm 0.03$	$0.38^{+0.16}_{-0.19} \pm 0.09$	$0.27^{+0.11}_{-0.13} \pm 0.03$	$0.33^{+0.09}_{-0.10}$
	$K^*\ell^+\ell^-$	[14.18, 16.00]		$0.70^{+0.16}_{-0.22} \pm 0.10$	$0.44^{+0.18}_{-0.21} \pm 0.10$	$0.50^{+0.06}_{-0.09} \pm 0.03$	$0.51^{+0.06}_{-0.08}$
	$K^*\ell^+\ell^-$	> 16.00		$0.66^{+0.11}_{-0.16} \pm 0.04$	$0.65^{+0.17}_{-0.18} \pm 0.16$	$0.10^{+0.13}_{-0.13} \pm 0.06$	0.39 ± 0.10

† see the original paper for the exact q^2 selection. ‡ muon mode only ($\ell = \mu$).

Table 143: Fraction of the longitudinal polarization (F_L) for various B decays. Values in red (blue) are new published (preliminary) results since PDG2010 [as of March 12, 2012].

RPP#	Mode	q^2 [(GeV/c ²) ²] †	PDG2010 Avg.	Belle	CDF ‡	LHCb ‡	New Avg.
122	$K^*\ell^+\ell^-$	< 2.0	$0.29^{+0.21}_{-0.18} \pm 0.02$	$0.29^{+0.21}_{-0.18} \pm 0.02$	$0.30^{+0.16}_{-0.16} \pm 0.02$	$0.03^{+0.15}_{-0.03} \pm 0.06$	$0.22^{+0.09}_{-0.08}$
	$K^*\ell^+\ell^-$	[2.0, 4.3]	$0.71 \pm 0.24 \pm 0.05$	$0.71 \pm 0.24 \pm 0.05$	$0.37^{+0.25}_{-0.24} \pm 0.10$	$0.84^{+0.15}_{-0.13} \pm 0.06$	0.73 ± 0.10
	$K^*\ell^+\ell^-$	[4.3, 8.68]	$0.64^{+0.23}_{-0.24} \pm 0.07$	$0.64^{+0.23}_{-0.24} \pm 0.07$	$0.68^{+0.15}_{-0.17} \pm 0.09$	$0.60 \pm 0.07 \pm 0.01$	0.61 ± 0.06
	$K^*\ell^+\ell^-$	[10.09, 12.86]		$0.17^{+0.17}_{-0.15} \pm 0.03$	$0.47^{+0.14}_{-0.14} \pm 0.03$	$0.44^{+0.12}_{-0.11} \pm 0.02$	0.39 ± 0.08
	$K^*\ell^+\ell^-$	[14.18, 16.00]		$-0.15^{+0.27}_{-0.23} \pm 0.07$	$0.29^{+0.14}_{-0.13} \pm 0.05$	$0.33^{+0.11}_{-0.08} \pm 0.04$	$0.28^{+0.08}_{-0.07}$
	$K^*\ell^+\ell^-$	> 16.00		$0.12^{+0.15}_{-0.13} \pm 0.02$	$0.20^{+0.19}_{-0.17} \pm 0.05$	$0.28^{+0.10}_{-0.09} \pm 0.04$	$0.22^{+0.08}_{-0.07}$

† see the original paper for the exact q^2 selection. ‡ muon mode only ($\ell = \mu$).

three different schemes and the average. The appropriate approach to average the experimental results is to first convert them according to the average extrapolation factors and then perform the average, assuming that the errors of the extrapolation factors are 100% correlated.

After surveying all available experimental results, the six shown in Table 147 are selected for the average. They have provided in their papers either the $b \rightarrow s\gamma$ branching fraction at a certain photon energy cut or the extrapolation factor used. Therefore we are able to convert them to the values at $E_{\min} = 1.6$ GeV using the information in Table 146. In the inclusive and full hadronic tag analysis, a possible $B \rightarrow X_d\gamma$ contamination has been considered according to the expectation $(4.5 \pm 0.3)\%$. Compared to the other systematic uncertainties, the error that arises from the $B \rightarrow X_d\gamma$ fraction is too small to be considered. We perform the average assuming that the systematic errors of the shape function and the $d\gamma$ fraction are correlated, and the other systematic errors and the statistical errors are Gaussian and uncorrelated. The obtained average is $\mathcal{B}(B \rightarrow X_s\gamma) = (355 \pm 24 \pm 9) \times 10^{-6}$ with a $\chi^2/\text{DOF} = 0.85/5$, where the errors are combined statistical and systematic, and systematic due to the shape function. The second error is estimated to be the difference of the average after simultaneously varying the central value of each experimental result by $\pm 1\sigma$. Although a small fraction of events was used in multiple analyses in the same experiment, we neglect their statistical correlations. Some other correlated systematic errors, such as photon detection and the background suppression, are not considered in our new average.

Table 144: Branching fractions of inclusive B decays (in units of 10^{-6}). Values in red (blue) are new published (preliminary) results since PDG2010 [as of March 12, 2012].

RPP#	Mode	PDG2010 Avg.	BABAR	Belle	CLEO	New Avg.
–	K^+X	New	$< 187^\dagger$			$< 187^\dagger$
–	K^0X	New	$195^{+51}_{-45} \pm 50^\dagger$			195^{+71}_{-67}
–	π^+X	New	$372^{+50}_{-47} \pm 59^\dagger$			372^{+77}_{-75}
80	$s\eta$	< 440		$261 \pm 30^{+44}_{-74} \S$	< 440	261^{+53}_{-79}
81	$s\eta'$	420 ± 90	$390 \pm 80 \pm 90^\ddagger$		$460 \pm 110 \pm 60^\ddagger$	423 ± 86

$^\dagger p^* > 2.34$ GeV; $\S 0.4 < M_{X_s} < 2.6$ GeV; $^\ddagger 2.0 < p^* < 2.7$ GeV

Table 145: Branching fractions of leptonic B decays (in units of 10^{-6}). Upper limits are at 90% CL. Values in red (blue) are new published (preliminary) results since PDG2010 [as of March 12, 2012].

RPP#	Mode	PDG2010 Avg.	BABAR	Belle	CLEO	CDF	D0	LHCb	CMS	New Avg.
24	$e^+\nu$	< 1.9	< 1.9	< 1.0	< 15					< 1.0
25	$\mu^+\nu$	< 1.0	< 1.0	< 1.7	< 21					< 1.0
26	$\tau^+\nu$	180 ± 50	176 ± 49	$162^{+31+25}_{-30-26}^\dagger$	< 840					167 ± 30
27	$\ell^+\nu_\ell\gamma$	< 15.6	< 15.6							< 15.6
28	$e^+\nu_e\gamma$	< 17	< 17		< 200					< 17
29	$\mu^+\nu_\mu\gamma$	< 24	< 26		< 52					< 26
412	$\gamma\gamma$	< 0.62	< 0.32	< 0.62						< 0.32
413	e^+e^-	< 0.083	< 0.113	< 0.19	< 0.83	< 0.083				< 0.083
414	$e^+e^-\gamma$	< 0.12	< 0.12							< 0.12
415	$\mu^+\mu^-$	< 0.015	< 0.052	< 0.16	< 0.61	< 0.0050		< 0.0026	< 0.0037	< 0.0026
416	$\mu^+\mu^-\gamma$	< 0.16	< 0.16							< 0.16
417	$\tau^+\tau^-$	< 4100	< 4100							< 4100
432	$e^\pm\mu^\mp$	< 0.064	< 0.092	< 0.17	< 1.5	< 0.064				< 0.064
438	$e^\pm\tau^\mp$	< 28	< 28		< 110					< 28
439	$\mu^\pm\tau^\mp$	< 22	< 22		< 38					< 22
440	$\nu\bar{\nu}$	< 220	< 220	< 130						< 130
441	$\nu\bar{\nu}\gamma$	< 47	< 47							< 47

† This result has been averaged with the earlier PRL 97, 251802 (2006).

Table 146: Extrapolation factor in various scheme with various minimum photon energy requirement (in GeV).

Scheme	$E_\gamma < 1.7$	$E_\gamma < 1.8$	$E_\gamma < 1.9$	$E_\gamma < 2.0$	$E_\gamma < 2.242$
Kinetic	0.986 ± 0.001	0.968 ± 0.002	0.939 ± 0.005	0.903 ± 0.009	0.656 ± 0.031
Neubert SF	0.982 ± 0.002	0.962 ± 0.004	0.930 ± 0.008	0.888 ± 0.014	0.665 ± 0.035
Kagan-Neubert	0.988 ± 0.002	0.970 ± 0.005	0.940 ± 0.009	0.892 ± 0.014	0.643 ± 0.033
Average	0.985 ± 0.004	0.967 ± 0.006	0.936 ± 0.010	0.894 ± 0.016	0.655 ± 0.037

7.4 Baryonic decays

Table 147: Reported branching fraction, minimum photon energy, branching fraction at minimum photon energy and converted branching fraction \mathcal{B}^{cnv} for the decay $b \rightarrow s\gamma$. All the branching fractions are in units of 10^{-6} . The errors are, in order, statistical, systematic and theoretical (if exists) for \mathcal{B} , and statistical, systematic and shape-function systematic for \mathcal{B}^{cnv} . Theoretical errors in $\mathcal{B}(\mathcal{E}_\gamma > \mathcal{E}_{\text{min}})$ are merged into the systematic error of \mathcal{B}^{cnv} during conversion. The CLEO measurement on the branching fraction at E_{min} includes $B \rightarrow X_d\gamma$ events.

Mode	Reported \mathcal{B}	E_{min}	\mathcal{B} at E_{min}	Modified \mathcal{B} ($E_{\text{min}} = 1.6$)
CLEO Inc. [396]	$321 \pm 43 \pm 27^{+18}_{-10}$	2.0	$306 \pm 41 \pm 26$	$327 \pm 44 \pm 28 \pm 6$
Belle Semi. [446]	$336 \pm 53 \pm 42^{+50}_{-54}$	2.24	—	$369 \pm 58 \pm 46^{+56}_{-60}$
BABAR Semi. [388]	$335 \pm 19^{+56+4}_{-41-9}$	1.9	$327 \pm 18^{+55+4}_{-40-9}$	$349 \pm 20^{+59+4}_{-46-3}$
BABAR Inc. [389]	—	1.9	$367 \pm 29 \pm 34 \pm 29$	$390 \pm 31 \pm 47 \pm 4$
BABAR Full [447]	$391 \pm 91 \pm 64$	1.9	$366 \pm 85 \pm 60$	$389 \pm 91 \pm 64 \pm 4$
Belle Inc. [393]	—	1.7	$345 \pm 15 \pm 40$	$347 \pm 15 \pm 40 \pm 1$
Average				$355 \pm 24 \pm 9$

Table 148: Branching fractions of baryonic B^+ decays (in units of 10^{-6}). Upper limits are at 90% CL. values in red (blue) are new published (preliminary) results since PDG2010 [as of March 12, 2012].

RPP#	Mode	PDG2010 Avg.	BABAR	Belle	CLEO	New Avg.
368	$p\bar{p}\pi^+$	1.62 ± 0.20	$1.69 \pm 0.29 \pm 0.26$ †	$1.57^{+0.17}_{-0.15} \pm 0.12$ §	< 160	$1.60^{+0.18}_{-0.17}$
371	$p\bar{p}K^+$	5.9 ± 0.5	$6.7 \pm 0.5 \pm 0.4$ †	$5.00^{+0.24}_{-0.22} \pm 0.32$ §		5.48 ± 0.34
372	$\Theta^{++}\bar{p}$ ¹	< 0.091	< 0.09	< 0.091		< 0.09
373	$f_J(2221)K^{+2}$	< 0.41		< 0.41		< 0.41
374	$p\bar{\Lambda}(1520)$	< 1.5	< 1.5			< 1.5
376	$p\bar{p}K^{*+}$	$3.6^{+0.8}_{-0.7}$	$5.3 \pm 1.5 \pm 1.3$ †	$3.38^{+0.73}_{-0.60} \pm 0.39$ ‡		$3.64^{+0.79}_{-0.70}$
377	$f_J(2221)K^{*+2}$	< 0.77	< 0.77			< 0.77
378	$p\bar{\Lambda}$	< 0.32		< 0.32	< 1.5	< 0.32
380	$p\bar{\Lambda}\pi^0$	$3.00^{+0.7}_{-0.6}$		$3.00^{+0.61}_{-0.53} \pm 0.33$		$3.00^{+0.69}_{-0.62}$
381	$p\bar{\Sigma}(1385)^0$	< 0.47		< 0.47		< 0.47
382	$\Delta^+\bar{\Lambda}$	< 0.82		< 0.82		< 0.82
384	$p\bar{\Lambda}\pi^+\pi^-$ (NR)	5.9 ± 1.1		$5.92^{+0.88}_{-0.84} \pm 0.69$		$5.92^{+1.12}_{-1.09}$
385	$p\bar{\Lambda}\rho^0$	4.8 ± 0.9		$4.78^{+0.67}_{-0.64} \pm 0.60$		$4.78^{+0.90}_{-0.88}$
386	$p\bar{\Lambda}f_2(1270)$	2.0 ± 0.8		$2.03^{+0.77}_{-0.72} \pm 0.27$		$2.03^{+0.82}_{-0.77}$
387	$\Lambda\bar{\Lambda}\pi^+$	< 0.94		< 0.94 §		< 0.94 §
388	$\Lambda\bar{\Lambda}K^+$	3.4 ± 0.6		$3.38^{+0.41}_{-0.36} \pm 0.41$ ‡		$3.38^{+0.58}_{-0.55}$
389	$\Lambda\bar{\Lambda}K^{*+}$	$2.2^{+1.2}_{-0.9}$		$2.19^{+1.13}_{-0.88} \pm 0.33$ §		$2.19^{+1.18}_{-0.94}$
390	$\bar{\Delta}^0 p$	< 1.38		< 1.38 §	< 380	< 1.38 §
391	$\Delta^{++}\bar{p}$	< 0.14		< 0.14 §	< 150	< 0.14 §

§Di-baryon mass is less than $2.85 \text{ GeV}/c^2$; † Charmonium decays to $p\bar{p}$ have been statistically subtracted;

‡ The charmonium mass region has been vetoed; ¹ $\Theta(1540)^{++} \rightarrow K^+p$ (pentaquark candidate);

² Product BF — daughter BF taken to be 100%

Table 149: Branching fractions of baryonic B^+ decays (in units of 10^{-6}). Upper limits are at 90% CL. values in red (blue) are new published (preliminary) results since PDG2010 [as of March 12, 2012].

RPP#	Mode	PDG2010 Avg.	BABAR	Belle	CLEO	New Avg.
366	$p\bar{p}$	< 0.11	< 0.27	< 0.11	< 1.4	< 0.11
368	$p\bar{p}K^0$	2.66 ± 0.32	$3.0 \pm 0.5 \pm 0.3$ †	$2.51^{+0.35}_{-0.29} \pm 0.21$ ‡		$2.66^{+0.34}_{-0.32}$
369	$\Theta^+\bar{p}$ ¹	< 0.05	< 0.05	< 0.23		< 0.05
370	$f_J(2221)K^0$ ²	< 0.45	< 0.45			< 0.45
371	$p\bar{p}K^{*0}$	$1.24^{+0.28}_{-0.25}$	$1.47 \pm 0.45 \pm 0.40$ †	$1.18^{+0.29}_{-0.25} \pm 0.11$ ‡		$1.24^{+0.28}_{-0.25}$
372	$f_J(2221)K^{*0}$ ²	< 0.15	< 0.15			< 0.15
373	$p\bar{\Lambda}\pi^-$	3.14 ± 0.29	$3.07 \pm 0.31 \pm 0.23$	$3.23^{+0.33}_{-0.29} \pm 0.29$	< 13	$3.14^{+0.29}_{-0.28}$
374	$p\bar{\Sigma}(1385)^-$	< 0.26		< 0.26		< 0.26
375	$\Delta^0\bar{\Lambda}$	< 0.93		< 0.93		< 0.93
376	$p\bar{\Lambda}K^-$	< 0.82		< 0.82		< 0.82
377	$p\bar{\Sigma}^0\pi^-$	< 3.8		< 3.8		< 3.8
340	$\bar{\Lambda}\Lambda$	< 0.32		< 0.32	< 1.2	< 0.32
379	$\bar{\Lambda}\Lambda K^0$	$4.8^{+1.0}_{-0.9}$		$4.76^{+0.84}_{-0.68} \pm 0.61$ ‡		$4.76^{+1.04}_{-0.91}$
380	$\Lambda\bar{\Lambda}K^{*0}$	$2.5^{+0.9}_{-0.8}$		$2.46^{+0.87}_{-0.72} \pm 0.34$ ‡		$2.46^{+0.93}_{-0.80}$

† Charmonium decays to $p\bar{p}$ have been statistically subtracted; ‡ The charmonium mass region has been vetoed;

¹ $\Theta(1540)^+ \rightarrow pK^0$ (pentaquark candidate); ² Product BF — daughter BF taken to be 100%.

7.5 B_s decays

Table 150: B_s branching fractions (in units of 10^{-6}). Upper limits are at 90% CL. Values in red (blue) are new published (preliminary) results since PDG2010 [as of March 12, 2012].

RPP#	Mode	PDG2010 Avg.	Belle	CDF	D0	LHCb	CMS	New Avg.
15	$\pi^+\pi^-$	< 1.2	< 12	$0.57 \pm 0.15 \pm 0.10^\dagger$		$0.98^{+0.23}_{-0.19} \pm 0.11$		0.73 ± 0.14
21	$\phi\phi$	14 ± 8		$23.2 \pm 1.8 \pm 8.2^\dagger$				23.2 ± 8.4
22	π^+K^-	4.9 ± 1.0	< 26	$5.0 \pm 0.7 \pm 0.8^\dagger$				5.0 ± 1.1
23	K^+K^-	33 ± 9	$38^{+10}_{-9} \pm 7$	$23.9 \pm 1.4 \pm 3.6^\dagger$				25.4 ± 3.7
—	$K^0\bar{K}^0$	New	< 66					< 66
25	$K^*0\bar{K}^{*0}$	New				$28.1 \pm 4.6 \pm 4.6$		28.1 ± 6.5
28	$\gamma\gamma$	< 8.7	< 8.7					< 8.7
29	$\phi\gamma$	57^{+18+12}_{-15-11}	57^{+18+12}_{-15-11}					57^{+21}_{-18}
30	$\mu^+\mu^-$	< 0.047		$< 0.035^\dagger$	$< 0.042^\dagger$	$< 0.012^\dagger$	$< 0.016^\dagger$	$< 0.012^\dagger$
31	e^+e^-	< 0.28		$< 0.28^\dagger$				$< 0.28^\dagger$
32	$e^\pm\mu^\mp$	< 0.20		$< 0.20^\dagger$				$< 0.20^\dagger$
33	$\phi\mu^+\mu^-$	< 3.2		$1.47 \pm 0.24 \pm 0.46^\dagger$	$< 3.2^\dagger$			1.47 ± 0.52

† Relative BF converted to absolute BF

Table 151: B_s rare relative branching fractions. Values in red (blue) are new published (preliminary) results since PDG2010 [as of March 12, 2012].

RPP#	Mode	PDG2010 Avg.	CDF	D0	New Avg.
13	$f_s\mathcal{B}(B_s^0 \rightarrow \pi^+\pi^-)/f_d\mathcal{B}(B^0 \rightarrow K^+\pi^-)$		$0.008 \pm 0.002 \pm 0.001$		0.008 ± 0.002
19	$\mathcal{B}(B_s^0 \rightarrow \phi\phi)/\mathcal{B}(B_s^0 \rightarrow J/\psi\phi)$		$(1.78 \pm 0.14 \pm 0.20) \times 10^{-2}$		1.78 ± 0.24
20	$f_s\mathcal{B}(B_s^0 \rightarrow K^+\pi^-)/f_d\mathcal{B}(B_d^0 \rightarrow K^+\pi^-)$		$0.071 \pm 0.010 \pm 0.007$		0.071 ± 0.012
21	$f_s\mathcal{B}(B_s^0 \rightarrow K^+K^-)/f_d\mathcal{B}(B_d^0 \rightarrow K^+\pi^-)$		$0.347 \pm 0.020 \pm 0.021$		0.347 ± 0.029
31	$\mathcal{B}(B_s^0 \rightarrow \phi\mu^+\mu^-)/\mathcal{B}(B_s^0 \rightarrow J/\psi\phi)$		$(1.11 \pm 0.25 \pm 0.09) \times 10^{-3}$	$< 3.5 \times 10^{-3}$	1.11 ± 0.27

7.6 Charge asymmetries

Table 152: CP asymmetries for charmless hadronic charged B decays (part I). Values in red (blue) are new published (preliminary) results since PDG2010 [as of March 12, 2012].

RPP#	Mode	PDG2010 Avg.	BABAR	Belle	CLEO	CDF	New Avg.
220	$K^0\pi^+$	0.009 ± 0.029	$-0.029 \pm 0.039 \pm 0.010$	$-0.014 \pm 0.012 \pm 0.006$	$0.18 \pm 0.24 \pm 0.02$		-0.015 ± 0.012
221	$K^+\pi^0$	0.051 ± 0.025	$0.030 \pm 0.039 \pm 0.010$	$0.043 \pm 0.024 \pm 0.002$	$-0.29 \pm 0.23 \pm 0.02$		0.037 ± 0.021
222	$\eta'K^+$	0.013 ± 0.017	$0.008^{+0.017}_{-0.018} \pm 0.009$	$0.028 \pm 0.028 \pm 0.021$	$0.03 \pm 0.12 \pm 0.02$		$0.013^{+0.016}_{-0.017}$
223	$\eta'K^{*+}$	$-0.30^{+0.33}_{-0.37} \pm 0.02$	$-0.26 \pm 0.27 \pm 0.02$				-0.26 ± 0.27
–	$\eta'K_0^*(1430)^+$	New	$0.06 \pm 0.20 \pm 0.02$				0.06 ± 0.20
–	$\eta'K_2^*(1430)^+$	New	$0.15 \pm 0.13 \pm 0.02$				0.15 ± 0.13
224	ηK^+	-0.37 ± 0.09	$-0.36 \pm 0.11 \pm 0.03$	$-0.38 \pm 0.11 \pm 0.01$			-0.37 ± 0.08
225	ηK^{*+}	0.02 ± 0.06	$0.01 \pm 0.08 \pm 0.02$	$0.03 \pm 0.10 \pm 0.01$			0.02 ± 0.06
226	$\eta K_0^*(1430)^+$	$0.05 \pm 0.13 \pm 0.02$	$0.05 \pm 0.13 \pm 0.02$				0.05 ± 0.13
227	$\eta K_2^*(1430)^+$	$-0.45 \pm 0.30 \pm 0.02$	$-0.45 \pm 0.30 \pm 0.02$				-0.45 ± 0.30
236	ωK^+	0.02 ± 0.05	$-0.01 \pm 0.07 \pm 0.01$	$0.05^{+0.08}_{-0.07} \pm 0.01$			0.02 ± 0.05
237	ωK^{*+}	0.29 ± 0.35	$0.29 \pm 0.35 \pm 0.02$				0.29 ± 0.35
239	$\omega K_0^*(1430)^+$	-0.10 ± 0.09	$-0.10 \pm 0.09 \pm 0.02$				-0.10 ± 0.09
240	$\omega K_2^*(1430)^+$	0.14 ± 0.15	$0.14 \pm 0.15 \pm 0.02$				0.14 ± 0.15
243	$K^{*0}\pi^+$	-0.04 ± 0.09	$0.032 \pm 0.052^{+0.016}_{-0.013}$	$-0.149 \pm 0.064 \pm 0.022$			-0.038 ± 0.042
244	$K^{*+}\pi^0$	$0.04 \pm 0.29 \pm 0.05$	$-0.06 \pm 0.24 \pm 0.04$				-0.06 ± 0.24
245	$K^+\pi^+\pi^-$	0.038 ± 0.022	$0.028 \pm 0.020 \pm 0.023$	$0.049 \pm 0.026 \pm 0.020$			0.038 ± 0.022
–	$K^+\pi^0\pi^0$	New	$-0.006 \pm 0.006 \pm 0.004$				-0.006 ± 0.007
248	$f_0(980)K^+$	$-0.10^{+0.05}_{-0.04}$	$-0.106 \pm 0.050^{+0.036}_{-0.015}$	$-0.077 \pm 0.065^{+0.046}_{-0.026}$			$-0.095^{+0.049}_{-0.042}$
249	$f_2(1270)K^+$	$-0.68^{+0.19}_{-0.017}$	$-0.85 \pm 0.22^{+0.26}_{-0.13}$	$-0.59 \pm 0.22 \pm 0.04$			$-0.68^{+0.20}_{-0.18}$
253	$f_0(1500)K^+ \dagger$	$0.28 \pm 0.26^{+0.15}_{-0.14}$	$0.28 \pm 0.26^{+0.15}_{-0.14}$				$0.28^{+0.30}_{-0.29}$
255	$\rho^0 K^+$	0.37 ± 0.10	$0.44 \pm 0.10^{+0.06}_{-0.14}$	$0.30 \pm 0.11^{+0.11}_{-0.05}$			0.37 ± 0.11
256	$K_0^*(1430)^0\pi^+$	0.55 ± 0.33	$0.032 \pm 0.035^{+0.034}_{-0.028}$	$0.076 \pm 0.038^{+0.028}_{-0.022}$			$0.055^{+0.034}_{-0.032}$
257	$K_2^*(1430)^0\pi^+$	$0.05 \pm 0.23^{+0.18}_{-0.08}$	$0.05 \pm 0.23^{+0.18}_{-0.08}$				$0.05^{+0.29}_{-0.24}$
265	$\rho^+ K^0$	$-0.12 \pm 0.17 \pm 0.02$	$-0.12 \pm 0.17 \pm 0.02$				-0.12 ± 0.17
266	$K^{*+}\pi^+\pi^-$	$0.07 \pm 0.07 \pm 0.04$	$0.07 \pm 0.07 \pm 0.04$				0.07 ± 0.08
267	$K^{*+}\rho^0$	$0.20^{+0.32}_{-0.29} \pm 0.04$	$0.31 \pm 0.13 \pm 0.03$				0.31 ± 0.13
268	$f_0(980)K^{*+}$	$-0.34 \pm 0.21 \pm 0.03$	$-0.15 \pm 0.12 \pm 0.03$				-0.15 ± 0.12
269	$a_1^+ K^0$	$0.12 \pm 0.11 \pm 0.02$	$0.12 \pm 0.11 \pm 0.02$				0.12 ± 0.11
270	$b_1^+ K^0$	-0.03 ± 0.15	$-0.03 \pm 0.15 \pm 0.02$				-0.03 ± 0.15
271	$K^{*0}\rho^+$	$-0.01 \pm 0.16 \pm 0.02$	$-0.01 \pm 0.16 \pm 0.02$				-0.01 ± 0.16
274	$b_1^0 K^+$	$-0.46 \pm 0.20 \pm 0.02$	$-0.46 \pm 0.20 \pm 0.02$				-0.46 ± 0.20
277	$K^+\bar{K}^0$	0.12 ± 0.18	$0.10 \pm 0.26 \pm 0.03$	$0.017 \pm 0.168 \pm 0.002$			0.041 ± 0.141
279	$K^+K_S K_S$	-0.04 ± 0.11	$-0.04 \pm 0.11 \pm 0.02$				-0.04 ± 0.11
281	$K^+K^-\pi^+$	$0.00 \pm 0.10 \pm 0.03$	$0.00 \pm 0.10 \pm 0.03$				0.00 ± 0.10
291	$K^+K^-K^+$	$-0.017 \pm 0.026 \pm 0.015$	$-0.02 \pm 0.03 \pm 0.02$				-0.02 ± 0.04
292	ϕK^+	-0.01 ± 0.06	$0.00 \pm 0.08 \pm 0.02$	$0.01 \pm 0.12 \pm 0.05$		$-0.07 \pm 0.17^{+0.03}_{-0.02}$	-0.01 ± 0.06
300	$K^{*+}K^+K^-$	$0.11 \pm 0.08 \pm 0.03$	$0.11 \pm 0.08 \pm 0.03$				0.11 ± 0.09
301	ϕK^{*+}	-0.01 ± 0.08	$0.00 \pm 0.09 \pm 0.04$	$-0.02 \pm 0.14 \pm 0.03$			-0.01 ± 0.08
303	$\phi K_1(1270)^+$	0.15 ± 0.20	$0.15 \pm 0.19 \pm 0.05$				0.15 ± 0.20
306	$\phi K_0^*(1430)^+$	0.04 ± 0.15	$0.04 \pm 0.15 \pm 0.04$				0.04 ± 0.15
307	$\phi K_2^*(1430)^+$	-0.23 ± 0.20	$-0.23 \pm 0.19 \pm 0.06$				-0.23 ± 0.20
310	$\phi\phi K^+$	New	$-0.10 \pm 0.08 \pm 0.02$	$0.01^{+0.19}_{-0.16} \pm 0.02$			-0.08 ± 0.07
314	$K^{*+}\gamma$	0.18 ± 0.29	$0.18 \pm 0.28 \pm 0.07$				0.18 ± 0.29
316	$K^+\eta\gamma$	-0.12 ± 0.07	$-0.09 \pm 0.10 \pm 0.01$	$-0.16 \pm 0.09 \pm 0.06$			-0.12 ± 0.07
318	$K^+\phi\gamma$	$-0.26 \pm 0.14 \pm 0.05$	$-0.26 \pm 0.14 \pm 0.05$	$-0.03 \pm 0.11 \pm 0.08$			-0.13 ± 0.10

Table 153: CP asymmetries for charmless hadronic charged B decays (part II). Values in red (blue) are new published (preliminary) results since PDG2010 [as of March 12, 2012].

RPP#	Mode	PDG2010 Avg.	BABAR	Belle	CLEO	CDF	New Avg.
329	$\rho^+\gamma$	-0.11 ± 0.33		$-0.11 \pm 0.32 \pm 0.09$			-0.11 ± 0.33
330	$\pi^+\pi^0$	0.06 ± 0.05	$0.03 \pm 0.08 \pm 0.01$	$0.025 \pm 0.043 \pm 0.007$			0.026 ± 0.039
331	$\pi^+\pi^-\pi^+$	$0.032^{+0.059}_{-0.057}$	$0.032 \pm 0.044^{+0.040}_{-0.037}$				$0.032^{+0.059}_{-0.057}$
332	$\rho^0\pi^+$	$0.18^{+0.09}_{-0.17}$	$0.18 \pm 0.07^{+0.05}_{-0.15}$				$0.18^{+0.09}_{-0.17}$
334	$f_2(1270)\pi^+$	$0.41^{+0.31}_{-0.29}$	$0.41 \pm 0.25^{+0.18}_{-0.15}$				$0.41^{+0.31}_{-0.29}$
335	$\rho(1450)^0\pi^+$	$-0.06^{+0.36}_{-0.42}$	$-0.06 \pm 0.28^{+0.23}_{-0.32}$				$-0.06^{+0.36}_{-0.42}$
338	$\pi^+\pi^-\pi^+(NR)$	$-0.14^{+0.23}_{-0.16}$	$-0.14 \pm 0.14^{+0.18}_{-0.08}$				$-0.14^{+0.23}_{-0.16}$
340	$\rho^+\pi^0$	0.02 ± 0.11	$-0.01 \pm 0.13 \pm 0.02$	$0.06 \pm 0.17^{+0.04}_{-0.05}$			0.02 ± 0.11
342	$\rho^+\rho^0$	-0.05 ± 0.05	$-0.054 \pm 0.055 \pm 0.010$	$0.00 \pm 0.22 \pm 0.03$			-0.051 ± 0.054
346	$\omega\pi^+$	-0.04 ± 0.06	$-0.02 \pm 0.08 \pm 0.01$	$-0.02 \pm 0.09 \pm 0.01$	$-0.34 \pm 0.25 \pm 0.02$		-0.04 ± 0.06
347	$\omega\rho^+$	-0.20 ± 0.09	$-0.20 \pm 0.09 \pm 0.02$				-0.20 ± 0.09
348	$\eta\pi^+$	-0.13 ± 0.10	$-0.03 \pm 0.09 \pm 0.03$	$-0.19 \pm 0.06 \pm 0.01$			-0.14 ± 0.05
349	$\eta\rho^+$	0.11 ± 0.11	$0.13 \pm 0.11 \pm 0.02$	$-0.04^{+0.34}_{-0.32} \pm 0.01$			0.11 ± 0.11
350	$\eta'\pi^+$	0.06 ± 0.16	$0.03 \pm 0.17 \pm 0.02$	$0.20^{+0.37}_{-0.36} \pm 0.04$			0.06 ± 0.15
351	$\eta'\rho^+$	$0.04 \pm 0.28 \pm 0.02$	$0.26 \pm 0.17 \pm 0.02$				0.26 ± 0.17
359	$b_1^0\pi^+$	$0.05 \pm 0.16 \pm 0.02$	$0.05 \pm 0.16 \pm 0.02$				0.05 ± 0.16
368	$p\bar{p}\pi^+$	0.00 ± 0.04	$0.04 \pm 0.07 \pm 0.04$	$-0.17 \pm 0.10 \pm 0.02$			-0.04 ± 0.06
371	$p\bar{p}K^+$	-0.16 ± 0.07	$-0.16 \pm 0.08 \pm 0.04$	$-0.02 \pm 0.05 \pm 0.02$			-0.06 ± 0.05
376	$p\bar{p}K^{*+}$	0.21 ± 0.16	$0.32 \pm 0.13 \pm 0.05$	$-0.01 \pm 0.19 \pm 0.02$			0.21 ± 0.11
379	$p\bar{\Lambda}\gamma$	$0.17 \pm 0.16 \pm 0.05$		$0.17 \pm 0.16 \pm 0.05$			0.17 ± 0.17
380	$p\bar{\Lambda}\pi^0$	$0.01 \pm 0.17 \pm 0.04$		$0.01 \pm 0.17 \pm 0.04$			0.01 ± 0.17
416	$K^+\ell\ell$	-0.01 ± 0.09	$-0.18 \pm 0.19 \pm 0.01$	$0.04 \pm 0.10 \pm 0.02$			-0.01 ± 0.09
417	$K^+e^+e^-$	0.14 ± 0.14		$0.14 \pm 0.14 \pm 0.03$			0.14 ± 0.14
418	$K^+\mu^+\mu^-$	-0.05 ± 0.13		$-0.05 \pm 0.13 \pm 0.03$			-0.05 ± 0.13
421	$K^{*+}\ell\ell$	-0.09 ± 0.14	$0.01^{+0.26}_{-0.24} \pm 0.02$	$-0.13^{+0.17}_{-0.16} \pm 0.01$			$-0.09^{+0.14}_{-0.13}$
422	$K^{*+}e^+e^-$	$-0.14^{+0.23}_{-0.22}$		$-0.14^{+0.23}_{-0.22} \pm 0.02$			$-0.14^{+0.23}_{-0.22}$
423	$K^{*+}\mu^+\mu^-$	-0.12 ± 0.24		$-0.12 \pm 0.24 \pm 0.02$			-0.12 ± 0.24

Table 154: CP asymmetries for charmless hadronic neutral B decays. Values in red (blue) are new published (preliminary) results since PDG2010 [as of March 12, 2012].

RPP#	Mode	PDG2010 Avg.	BABAR	Belle	CDF	LHCb	New Avg.
210	$K^+\pi^-$	-0.098 ± 0.013	$-0.107 \pm 0.016^{+0.006}_{-0.004}$	$-0.069 \pm 0.014 \pm 0.007$	$-0.086 \pm 0.023 \pm 0.009$	$-0.088 \pm 0.011 \pm 0.008$	-0.087 ± 0.008
213	$\eta' K^{*0}$	$0.08 \pm 0.25 \pm 0.02$	$0.02 \pm 0.23 \pm 0.02$				0.02 ± 0.23
–	$\eta' K_0^*(1430)^0$	New	$-0.19 \pm 0.17 \pm 0.02$				-0.19 ± 0.17
–	$\eta' K_2^*(1430)^0$	New	$0.14 \pm 0.18 \pm 0.02$				0.14 ± 0.18
215	ηK^{*0}	0.19 ± 0.05		$0.17 \pm 0.08 \pm 0.01$			0.19 ± 0.05
216	$\eta K_0^*(1430)^0$	$0.06 \pm 0.13 \pm 0.02$	$0.06 \pm 0.13 \pm 0.02$				0.06 ± 0.13
217	$\eta K_2^*(1430)^0$	$-0.07 \pm 0.19 \pm 0.02$	$-0.07 \pm 0.19 \pm 0.02$				-0.07 ± 0.19
222	$b_1^- K^+$	$0.07 \pm 0.12 \pm 0.02$	$0.07 \pm 0.12 \pm 0.02$				0.07 ± 0.12
227	ωK^{*0}	0.45 ± 0.25	$0.45 \pm 0.25 \pm 0.02$				0.45 ± 0.25
229	$\omega K_0^*(1430)^0$	-0.07 ± 0.09	$-0.07 \pm 0.09 \pm 0.02$				-0.07 ± 0.09
230	$\omega K_2^*(1430)^0$	0.37 ± 0.17	$0.37 \pm 0.17 \pm 0.02$				0.37 ± 0.17
232	$K^+\pi^-\pi^0$	0.00 ± 0.06	$-0.030^{+0.045}_{-0.051} \pm 0.055$	$0.07 \pm 0.11 \pm 0.01$			$0.000^{+0.059}_{-0.061}$
233	$\rho^- K^+$	0.15 ± 0.13	$0.20 \pm 0.09 \pm 0.08$	$0.22^{+0.22+0.06}_{-0.23-0.02}$			0.20 ± 0.11
236	$K^+\pi^-\pi^0(NR)$	$0.23^{+0.22}_{-0.28}$	$0.10 \pm 0.16 \pm 0.08$				0.10 ± 0.18
238	$K_0^*(1430)^0\pi^0$	-0.22 ± 0.32	$-0.15 \pm 0.10 \pm 0.04$				-0.15 ± 0.11
242	$K^0\pi^+\pi^-$	-0.01 ± 0.05	$-0.01 \pm 0.05 \pm 0.01$				-0.01 ± 0.05
245	$K^{*+}\pi^-$	-0.19 ± 0.07	$-0.24 \pm 0.07 \pm 0.02$	$-0.21 \pm 0.11 \pm 0.07$			-0.23 ± 0.06
246	$K_0^*(1430)^+\pi^-$	0.10 ± 0.07	$0.07 \pm 0.14 \pm 0.01$				0.07 ± 0.14
252	$K^{*0}\pi^0$	$-0.09^{+0.23}_{-0.26}$	$-0.15 \pm 0.12 \pm 0.04$				-0.15 ± 0.13
259	$K^{*0}\pi^+\pi^-$	$0.07 \pm 0.04 \pm 0.03$	$0.07 \pm 0.04 \pm 0.03$				0.07 ± 0.05
260	$K^{*0}\rho^0$	$0.09 \pm 0.19 \pm 0.02$	$-0.06 \pm 0.09 \pm 0.02$				-0.06 ± 0.09
265	$K^{*+}\rho^-$	New	$0.21 \pm 0.15 \pm 0.02$				0.21 ± 0.15
261	$f_0(980)K^{*0}$	-0.17 ± 0.28	$0.07 \pm 0.10 \pm 0.02$				0.07 ± 0.10
264	$a_1^- K^+$	$-0.16 \pm 0.12 \pm 0.01$	$-0.16 \pm 0.12 \pm 0.01$				-0.16 ± 0.12
279	$K^{*0}K^+K^-$	$0.01 \pm 0.05 \pm 0.02$	$0.01 \pm 0.05 \pm 0.02$				0.01 ± 0.05
280	ϕK^{*0}	0.01 ± 0.05	$0.01 \pm 0.06 \pm 0.03$	$0.02 \pm 0.09 \pm 0.02$			0.01 ± 0.05
281	$K^{*0}\pi^+K^-$	$0.22 \pm 0.33 \pm 0.20$	$0.22 \pm 0.33 \pm 0.20$				0.22 ± 0.39
289	$\phi K_0^*(1430)^0$	0.20 ± 0.15	$0.20 \pm 0.14 \pm 0.06$				0.20 ± 0.15
294	$\phi K_2^*(1430)^0$	-0.08 ± 0.13	$-0.08 \pm 0.12 \pm 0.05$				-0.08 ± 0.13
301	$K^{*0}\gamma$	-0.16 ± 0.23	$-0.16 \pm 0.22 \pm 0.07$				-0.16 ± 0.23
316	$\pi^0\pi^0$		$0.43 \pm 0.26 \pm 0.05$	$0.44^{+0.53}_{-0.52} \pm 0.17$			0.43 ± 0.24
359	$b_1^\mp\pi^\pm$	$-0.05 \pm 0.10 \pm 0.02$	$-0.05 \pm 0.10 \pm 0.02$				-0.05 ± 0.10
371	$p\bar{p}K^{*0}$	0.05 ± 0.12	$0.11 \pm 0.13 \pm 0.06$	$-0.08 \pm 0.20 \pm 0.02$			0.05 ± 0.12
373	$p\bar{A}\pi^-$	0.04 ± 0.07	$-0.10 \pm 0.10 \pm 0.02$	$-0.02 \pm 0.10 \pm 0.03$			-0.06 ± 0.07
427	$K^{*0}\ell\ell$	-0.05 ± 0.10	$0.02 \pm 0.20 \pm 0.02$	$-0.08 \pm 0.12 \pm 0.02$			-0.05 ± 0.10
428	$K^{*0}e^+e^-$	-0.21 ± 0.19		$-0.21 \pm 0.19 \pm 0.02$			-0.21 ± 0.19
429	$K^{*0}\mu^+\mu^-$	0.00 ± 0.15		$0.00 \pm 0.15 \pm 0.03$			0.00 ± 0.15

† Measurements of time-dependent CP asymmetries are listed in the section of the Unitarity Triangle.

Table 155: Charmless hadronic CP asymmetries for B^\pm/B^0 admixtures. Values in red (blue) are new published (preliminary) results since PDG2010 [as of March 12, 2012].

RPP#	Mode	PDG2010 Avg.	BABAR	Belle	CLEO	New Avg.
65	$K^*\gamma$	-0.003 ± 0.017	$-0.003 \pm 0.017 \pm 0.007$	$-0.015 \pm 0.044 \pm 0.012$	$0.08 \pm 0.13 \pm 0.03$	-0.003 ± 0.017
7	$s\gamma$	0.014 ± 0.028	$-0.011 \pm 0.030 \pm 0.014$	$0.002 \pm 0.050 \pm 0.030$	$-0.079 \pm 0.108 \pm 0.022$	-0.012 ± 0.028
–	$(s+d)\gamma$	$-0.110 \pm 0.115 \pm 0.017$	$-0.11 \pm 0.12 \pm 0.02$			-0.11 ± 0.12
–	K^+X	New	$0.17 \pm 0.24 \pm 0.05^\dagger$			0.17 ± 0.24
–	π^+X	New	$0.10 \pm 0.16 \pm 0.05^\dagger$			0.10 ± 0.17
80	$s\eta$	New		$0.13 \pm 0.04^{+0.02}_{-0.03}^\S$		$0.13^{+0.04}_{-0.05}$
115	$s\ell\ell$	-0.22 ± 0.26	$-0.22 \pm 0.26 \pm 0.02$			-0.22 ± 0.26
118	$K^*e^+e^-$	-0.18 ± 0.15		$-0.18 \pm 0.15 \pm 0.01$		-0.18 ± 0.15
120	$K^*\mu^+\mu^-$	-0.03 ± 0.13		$-0.03 \pm 0.13 \pm 0.02$		-0.03 ± 0.13
122	$K^*\ell\ell$	-0.07 ± 0.08	$0.01^{+0.16}_{-0.15} \pm 0.01$	$-0.10 \pm 0.10 \pm 0.01$		-0.07 ± 0.08

$^\dagger p^* > 2.34$ GeV; $^\S 0.4 < M_{X_s} < 2.6$ GeV;

Table 156: CP asymmetries for charmless hadronic B_s decays. Values in red (blue) are new published (preliminary) results since PDG2010 [as of March 12, 2012].

RPP#	Mode	PDG2010 Avg.	Belle	CDF	LHCb	New Avg.
22	$K^+\pi^-$	New		$0.39 \pm 0.15 \pm 0.08$	$0.27 \pm 0.08 \pm 0.02$	0.29 ± 0.07

7.7 Polarization measurements

Table 157: Longitudinal polarization fraction f_L for B^+ decays. Values in red (blue) are new published (preliminary) results since PDG2010 [as of March 12, 2012].

RPP#	Mode	PDG2010 Avg.	BABAR	Belle	New Avg.
237	ωK^{*+}	$0.41 \pm 0.18 \pm 0.05$	$0.41 \pm 0.18 \pm 0.05$		0.41 ± 0.19
240	$\omega K_2^*(1430)^+$	$0.56 \pm 0.10 \pm 0.04$	$0.56 \pm 0.10 \pm 0.04$		0.56 ± 0.11
267	$K^{*+} \rho^0$		$0.78 \pm 0.12 \pm 0.03$		0.78 ± 0.12
271	$K^{*0} \rho^+$	0.48 ± 0.08	$0.52 \pm 0.10 \pm 0.04$	$0.43 \pm 0.11^{+0.05}_{-0.02}$	0.48 ± 0.08
289	$K^{*+} \bar{K}^{*0}$	$0.75^{+0.16}_{-0.26} \pm 0.03$	$0.75^{+0.16}_{-0.26} \pm 0.03$		$0.75^{+0.16}_{-0.26}$
301	ϕK^{*+}	0.50 ± 0.05	$0.49 \pm 0.05 \pm 0.03$	$0.52 \pm 0.08 \pm 0.03$	0.50 ± 0.05
303	$\phi K_1(1270)^+$	$0.46^{+0.12+0.06}_{-0.13-0.07}$	$0.46^{+0.12+0.06}_{-0.13-0.07}$		$0.46^{+0.13}_{-0.15}$
307	$\phi K_2^*(1430)^+$	$0.80^{+0.09}_{-0.10} \pm 0.03$	$0.80^{+0.09}_{-0.10} \pm 0.03$		0.80 ± 0.10
342	$\rho^+ \rho^0$	0.950 ± 0.016	$0.950 \pm 0.015 \pm 0.006$	$0.95 \pm 0.11 \pm 0.02$	0.950 ± 0.016
347	$\omega \rho^+$	$0.90 \pm 0.05 \pm 0.03$	$0.90 \pm 0.05 \pm 0.03$		0.90 ± 0.06

Table 158: Full angular analysis of $B^+ \rightarrow \phi K^{*+}$. Values in red (blue) are new published (preliminary) results since PDG2010 [as of March 12, 2012].

Parameter	PDG2010 Avg.	BABAR	Belle	New Avg.
$f_{\perp} = A_{\perp\perp}$	0.20 ± 0.05	$0.21 \pm 0.05 \pm 0.02$	$0.19 \pm 0.08 \pm 0.02$	0.20 ± 0.05
ϕ_{\parallel}	2.34 ± 0.18	$2.47 \pm 0.20 \pm 0.07$	$2.10 \pm 0.28 \pm 0.04$	2.34 ± 0.17
ϕ_{\perp}	2.58 ± 0.17	$2.69 \pm 0.20 \pm 0.03$	$2.31 \pm 0.30 \pm 0.07$	2.58 ± 0.17
δ_0	$3.07 \pm 0.18 \pm 0.06$	$3.07 \pm 0.18 \pm 0.06$		3.07 ± 0.19
A_{CP}^0	$0.17 \pm 0.11 \pm 0.02$	$0.17 \pm 0.11 \pm 0.02$		0.17 ± 0.11
A_{CP}^{\perp}	$0.22 \pm 0.24 \pm 0.08$	$0.22 \pm 0.24 \pm 0.08$		0.22 ± 0.25
$\Delta\phi_{\parallel}$	$0.07 \pm 0.20 \pm 0.05$	$0.07 \pm 0.20 \pm 0.05$		0.07 ± 0.21
$\Delta\phi_{\perp}$	$0.19 \pm 0.20 \pm 0.07$	$0.19 \pm 0.20 \pm 0.07$		0.19 ± 0.21
$\Delta\delta_0$	$0.20 \pm 0.18 \pm 0.03$	$0.20 \pm 0.18 \pm 0.03$		0.20 ± 0.18

BR, f_L and A_{CP} are tabulated separately.

Table 159: Longitudinal polarization fraction f_L for B^0 decays. Values in red (blue) are new published (preliminary) results since PDG2010 [as of March 12, 2012].

RPP#	Mode	PDG2010 Avg.	BABAR	Belle	New Avg.
227	ωK^{*0}	0.69 ± 0.13	$0.72 \pm 0.14 \pm 0.02$	$0.56 \pm 0.29^{+0.18}_{-0.08}$	0.70 ± 0.13
230	$\omega K_2^*(1430)^0$	$0.45 \pm 0.12 \pm 0.02$	$0.45 \pm 0.12 \pm 0.02$		0.45 ± 0.12
260	$K^{*0} \rho^0$	$0.57 \pm 0.09 \pm 0.08$	$0.40 \pm 0.08 \pm 0.11$		0.40 ± 0.14
265	$K^{*+} \rho^-$	New	$0.38 \pm 0.13 \pm 0.03$		0.38 ± 0.13
280	ϕK^{*0}	0.480 ± 0.0030	$0.494 \pm 0.034 \pm 0.013$	$0.45 \pm 0.05 \pm 0.02$	0.480 ± 0.030
282	$K^{*0} \overline{K}^{*0}$	$0.80^{+0.10}_{-0.12} \pm 0.06$	$0.80^{+0.10}_{-0.12} \pm 0.06$		$0.80^{+0.12}_{-0.13}$
294	$\phi K_2^*(1430)^0$	$0.901^{+0.046}_{-0.058} \pm 0.037$	$0.901^{+0.046}_{-0.058} \pm 0.037$		$0.901^{+0.059}_{-0.069}$
345	$\rho^0 \rho^0$	$0.75^{+0.11}_{-0.14} \pm 0.04$	$0.75^{+0.11}_{-0.14} \pm 0.04$		$0.75^{+0.12}_{-0.15}$
353	$\rho^+ \rho^-$	$0.977^{+0.028}_{-0.024}$	$0.992 \pm 0.024^{+0.026}_{-0.013}$	$0.941^{+0.034}_{-0.040} \pm 0.030$	$0.978^{+0.025}_{-0.022}$
364	$a_1^\pm a_1^\mp$	$0.31 \pm 0.22 \pm 0.10$	$0.31 \pm 0.22 \pm 0.10$		0.31 ± 0.24

Table 160: Full angular analysis of $B^0 \rightarrow \phi K^{*0}$. Values in red (blue) are new published (preliminary) results since PDG2010 [as of March 12, 2012].

Parameter	PDG2010 Avg.	BABAR	Belle	New Avg.
$f_\perp = A_{\perp\perp}$	0.24 ± 0.05	$0.212 \pm 0.032 \pm 0.013$	$0.31^{+0.06}_{-0.05} \pm 0.02$	0.241 ± 0.029
ϕ_\parallel	2.40 ± 0.13	$2.40 \pm 0.13 \pm 0.08$	$2.40^{+0.28}_{-0.24} \pm 0.07$	$2.40^{+0.14}_{-0.13}$
ϕ_\perp	2.39 ± 0.13	$2.35 \pm 0.13 \pm 0.09$	$2.51 \pm 0.25 \pm 0.06$	2.39 ± 0.13
δ_0	$2.82 \pm 0.15 \pm 0.09$	$2.82 \pm 0.15 \pm 0.09$		2.82 ± 0.17
A_{CP}^0	0.04 ± 0.06	$0.01 \pm 0.07 \pm 0.02$	$0.13 \pm 0.12 \pm 0.04$	0.04 ± 0.06
A_{CP}^\perp	-0.11 ± 0.12	$-0.04 \pm 0.15 \pm 0.06$	$-0.20 \pm 0.18 \pm 0.04$	-0.11 ± 0.12
$\Delta\phi_\parallel$	0.11 ± 0.22	$0.22 \pm 0.12 \pm 0.08$	$-0.32 \pm 0.27 \pm 0.07$	0.11 ± 0.13
$\Delta\phi_\perp$	0.08 ± 0.22	$0.21 \pm 0.13 \pm 0.08$	$-0.30 \pm 0.25 \pm 0.06$	0.08 ± 0.13
$\Delta\delta_0$	$0.27 \pm 0.14 \pm 0.08$	$0.27 \pm 0.14 \pm 0.08$		0.27 ± 0.16

BR, f_L and A_{CP} are tabulated separately.

Table 161: Full angular analysis of $B^0 \rightarrow \phi K_2^*(1430)^0$. Values in red (blue) are new published (preliminary) results since PDG2010 [as of March 12, 2012].

Parameter	PDG2010 Avg.	BABAR	Belle	New Avg.
$f_{\perp} = A_{\perp\perp}$	$0.002^{+0.018}_{-0.002} \pm 0.031$	$0.002^{+0.018}_{-0.002} \pm 0.031$		$0.002^{+0.036}_{-0.031}$
ϕ_{\parallel}	$3.96 \pm 0.38 \pm 0.06$	$3.96 \pm 0.38 \pm 0.06$		3.96 ± 0.39
δ_0	$3.41 \pm 0.13 \pm 0.13$	$3.41 \pm 0.13 \pm 0.13$		3.41 ± 0.18
A_{CP}^0	$-0.05 \pm 0.06 \pm 0.01$	$-0.05 \pm 0.06 \pm 0.01$		-0.05 ± 0.06
$\Delta\phi_{\parallel}$	$-1.00 \pm 0.38 \pm 0.09$	$-1.00 \pm 0.38 \pm 0.09$		-1.00 ± 0.39
$\Delta\delta_0$	$0.11 \pm 0.13 \pm 0.06$	$0.11 \pm 0.13 \pm 0.06$		0.11 ± 0.14

BR, f_L and A_{CP} are tabulated separately.

Table 162: Longitudinal polarization fraction f_L for B_s decays. Values in red (blue) are new published (preliminary) results since PDG2010 [as of March 12, 2012].

RPP#	Mode	PDG2010 Avg.	CDF	LHCB	New Avg.
21	$\phi\phi$	New	$0.348 \pm 0.041 \pm 0.021$		0.348 ± 0.046
25	$K^{*0}\overline{K}^{*0}$	New		$0.38 \pm 0.11 \pm 0.04$	0.38 ± 0.12

8 D decays

8.1 D^0 - \bar{D}^0 mixing and CP violation

8.1.1 Introduction

In 2007 Belle [448] and *BABAR* [449] obtained the first evidence for D^0 - \bar{D}^0 mixing, which had been searched for for more than two decades. These results were later confirmed by CDF [450]. There are now numerous measurements of D^0 - \bar{D}^0 mixing with various levels of sensitivity. All the results are input into a global fit to determine world averages of mixing parameters, CP -violation (CPV) parameters, and strong phases.

Our notation is as follows. The mass eigenstates are denoted $D_1 = p|D^0\rangle - q|\bar{D}^0\rangle$ and $D_2 = p|D^0\rangle + q|\bar{D}^0\rangle$, where we use the convention $CP|D^0\rangle = -|\bar{D}^0\rangle$ and $CP|\bar{D}^0\rangle = -|D^0\rangle$. Thus in the absence of CP violation, D_1 is CP -even and D_2 is CP -odd. The weak phase $\phi \equiv \text{Arg}(q/p)$. The mixing parameters are defined as $x \equiv (m_1 - m_2)/\Gamma$ and $y \equiv (\Gamma_1 - \Gamma_2)/(2\Gamma)$, where m_1, m_2 and Γ_1, Γ_2 are the masses and decay widths for the mass eigenstates, and $\Gamma \equiv (\Gamma_1 + \Gamma_2)/2$.

The global fit determines central values and errors for ten underlying parameters. These consist of mixing parameters x and y ; a parameter describing the ratio of decay rates $R_D \equiv |\mathcal{A}(D^0 \rightarrow K^+\pi^-)/\mathcal{A}(\bar{D}^0 \rightarrow K^+\pi^-)|^2$; CPV parameters $|q/p|$, ϕ , and $A_D \equiv (R_D^+ - R_D^-)/(R_D^+ + R_D^-)$, where the $+$ ($-$) superscript corresponds to D^0 (\bar{D}^0) decays; *direct* CPV parameters A_{KK} and $A_{\pi\pi}$ (discussed below); the strong phase difference δ between $\bar{D}^0 \rightarrow K^-\pi^+$ and $D^0 \rightarrow K^-\pi^+$ amplitudes; and the strong phase difference $\delta_{K\rho\pi}$ between $\bar{D}^0 \rightarrow K^-\rho^+$ and $D^0 \rightarrow K^-\rho^+$ amplitudes.

The fit uses 38 observables taken from measurements of $D^0 \rightarrow K^+\ell^-\nu$, $D^0 \rightarrow K^+K^-$ and $D^0 \rightarrow \pi^+\pi^-$, $D^0 \rightarrow K^+\pi^-$, $D^0 \rightarrow K^+\pi^-\pi^0$, $D^0 \rightarrow K_S^0\pi^+\pi^-$, and $D^0 \rightarrow K_S^0K^+K^-$ decays,⁴⁵ and from double-tagged branching fractions measured at the $\psi(3770)$ resonance. Correlations among observables are accounted for by using covariance matrices provided by the experimental collaborations. Errors are assumed to be Gaussian, and systematic errors among different experiments are assumed uncorrelated unless specific correlations have been identified. We have checked this method with a second method that adds together three-dimensional log-likelihood functions for x , y , and δ obtained from several analyses; this combination accounts for non-Gaussian errors. When both methods are applied to the same set of measurements, equivalent results are obtained.

Mixing in heavy flavor systems such as those of B^0 and B_s^0 is governed by a short-distance box diagram. In the D^0 system, however, this diagram is doubly-Cabibbo-suppressed relative to amplitudes dominating the decay width, and it is also GIM-suppressed. Thus the short-distance mixing rate is tiny, and D^0 - \bar{D}^0 mixing is expected to be dominated by long-distance processes. These are difficult to calculate reliably, and theoretical estimates for x and y range over two-three orders of magnitude [451–454].

With the exception of $\psi(3770) \rightarrow DD$ measurements, all methods identify the flavor of the D^0 or \bar{D}^0 when produced by reconstructing the decay $D^{*+} \rightarrow D^0\pi^+$ or $D^{*-} \rightarrow \bar{D}^0\pi^-$. The charge of the pion, which has low momentum and is usually referred to as the “soft” pion π_s , identifies the D flavor. For signal decays, $M_{D^{*+}} - M_{D^0} - M_{\pi^+} \equiv Q \approx 6$ MeV, which is close to the threshold; thus analyses typically require that the reconstructed Q be small to suppress backgrounds. For time-dependent measurements, the D^0 decay time is calculated as $(d/p) \times M_{D^0}$, where d is the

⁴⁵Charge-conjugate modes are implicitly included.

distance between the D^* and D^0 decay vertices and p is the D^0 momentum. The D^* vertex position is taken to be at the primary vertex for $\bar{p}p$ collider experiments [450], and at the intersection of the D^0 momentum vector with the beamspot profile for e^+e^- experiments.

8.1.2 Input observables

The global fit determines central values and errors for the underlying parameters using a χ^2 statistic. The fitted parameters are x , y , R_D , A_D , $|q/p|$, ϕ , δ , $\delta_{K\pi\pi}$, A_{KK} and $A_{\pi\pi}$. The parameter $\delta_{K\pi\pi}$ is the strong phase difference between the amplitudes $\mathcal{A}(\bar{D}^0 \rightarrow K^+\rho^-)$ and $\mathcal{A}(D^0 \rightarrow K^+\rho^-)$. In the $D \rightarrow K^+\pi^-\pi^0$ Dalitz plot analysis that provides sensitivity to x and y , the $\bar{D}^0 \rightarrow K^+\pi^-\pi^0$ isobar phases are determined relative to that for $\mathcal{A}(\bar{D}^0 \rightarrow K^+\rho^-)$, and the $D^0 \rightarrow K^+\pi^-\pi^0$ isobar phases are determined relative to that for $\mathcal{A}(D^0 \rightarrow K^+\rho^-)$. As the \bar{D}^0 and D^0 Dalitz plots are fit independently, the phase difference $\delta_{K\pi\pi}$ between the two “normalizing” amplitudes cannot be determined from these fits.

All input measurements are listed in Tables 163-165. The observable $R_M = (x^2 + y^2)/2$ is calculated from $D^0 \rightarrow K^+\ell^-\nu$ decays [455–458] and is the world average (WA) value calculated by HFAG [459]. The inputs used for these averages are plotted in Fig. 60. The observables y_{CP} and A_Γ are also HFAG WA values [459]; the inputs used for these averages are plotted in Figs. 61 and 62. The $D^0 \rightarrow K^+\pi^-$ observables used are from Belle [460], *BABAR* [449], and CDF [450]; earlier measurements have much less precision and are not used. The observables from $D^0 \rightarrow K_S^0\pi^+\pi^-$ decays for no- CPV are from Belle [461] and *BABAR* [462], but for the CPV -allowed case only Belle measurements [461] are available. The $D^0 \rightarrow K^+\pi^-\pi^0$ results are from *BABAR* [463], and the $\psi(3770) \rightarrow \bar{D}D$ results are from CLEOc [464].

The relationships between the observables and the fitted parameters are listed in Table 166. For each set of correlated observables we construct a difference vector \vec{V} ; e.g., for $D^0 \rightarrow K_S^0\pi^+\pi^-$ decays, $\vec{V} = (\Delta x, \Delta y, \Delta|q/p|, \Delta\phi)$ where Δ represents the difference between the measured value and the fitted value. The contribution of a set of observables to the χ^2 is calculated as $\vec{V} \cdot (M^{-1}) \cdot \vec{V}^T$, where M^{-1} is the inverse of the covariance matrix for the measurement. Covariance matrices are constructed from the correlation coefficients among the measured observables. These coefficients (where applicable) are also listed in Tables 163-165.

8.1.3 Fit results

The global fit uses MINUIT with the MIGRAD minimizer, and all errors are obtained from MINOS [476]. Four separate fits are performed: (a) assuming CP conservation, i.e., fixing $A_D = 0$, $A_K = 0$, $A_\pi = 0$, $\phi = 0$, and $|q/p| = 1$; (b) assuming no direct CPV and fitting for parameters x , y , and ϕ ; (c) assuming no direct CPV and fitting for parameters $x_{12} = 2|M_{12}|/\Gamma$, $y_{12} = \Gamma_{12}/\Gamma$, and $\phi_{12} = \text{Arg}(M_{12}/\Gamma_{12})$, where M_{12} and Γ_{12} are the off-diagonal elements of the D^0 - \bar{D}^0 mass and decay matrices, respectively; and (d) allowing full CPV , i.e., floating all parameters.

For the no-direct- CPV fits, we set direct- CPV parameters $A_D = 0$, $A_K = 0$, and $A_\pi = 0$. In addition, for the first fit (b) we impose the relation [477, 478] $\tan\phi = (1 - |q/p|^2)/(1 + |q/p|^2) \times (x/y)$; this reduces four independent parameters to three.⁴⁶ We impose this relationship in two ways: first we float parameters x , y , and ϕ and from them derive $|q/p|$; then we repeat the fit floating x , y , and $|q/p|$ and from them derive ϕ . The central values returned by the two fits

⁴⁶One can also use Eq. (15) of Ref. [479] to reduce four parameters to three.

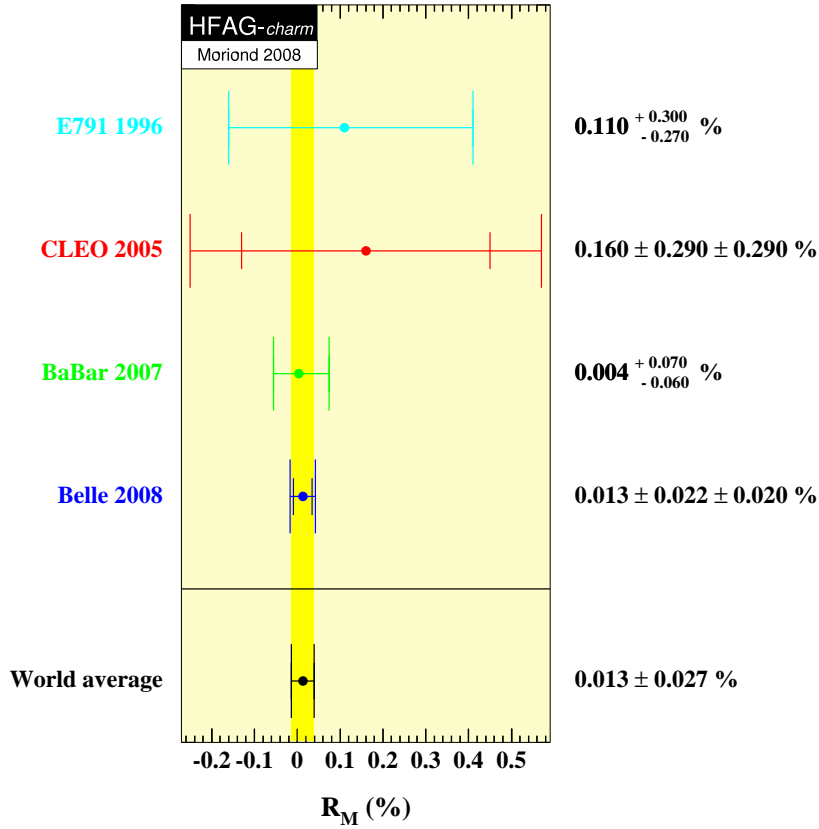


Figure 60: World average value of R_M from Ref. [459], as calculated from $D^0 \rightarrow K^+ \ell^- \nu$ measurements [455–458].

are identical, but the first fit yields MINOS errors for ϕ , while the second fit yields MINOS errors for $|q/p|$. For no-direct- CPV fit (c), we fit for the underlying parameters x_{12} , y_{12} , and ϕ_{12} , from which parameters x , y , $|q/p|$, and ϕ are derived.

All fit results are listed in Table 167. For the CPV -allowed fit, individual contributions to the χ^2 are listed in Table 168. The total χ^2 is 35.6 for $37 - 10 = 27$ degrees of freedom; this corresponds to a confidence level of 0.124, which is satisfactory.

Confidence contours in the two dimensions (x, y) or in $(|q/p|, \phi)$ are obtained by letting, for any point in the two-dimensional plane, all other fitted parameters take their preferred values. The resulting 1σ - 5σ contours are shown in Fig. 63 for the CP -conserving case, in Fig. 64 for the no-direct- CPV case, and in Fig. 65 for the CPV -allowed case. The contours are determined from the increase of the χ^2 above the minimum value. One observes that the (x, y) contours for the no- CPV fit are very similar to those for the CPV -allowed fit. In the latter fit, the χ^2 at the no-mixing point $(x, y) = (0, 0)$ is 110 units above the minimum value; for two degrees of freedom this has a confidence level corresponding to 10.2σ . Thus, no mixing is excluded at this high level. In the $(|q/p|, \phi)$ plot, the point $(1, 0)$ is within the 1σ contour; thus the data is consistent with CP conservation.

One-dimensional confidence curves for individual parameters are obtained by letting, for any value of the parameter, all other fitted parameters take their preferred values. The resulting functions $\Delta\chi^2 = \chi^2 - \chi^2_{\min}$ (χ^2_{\min} is the minimum value) are shown in Fig. 66. The points where $\Delta\chi^2 = 3.84$ determine 95% C.L. intervals for the parameters; these intervals are listed

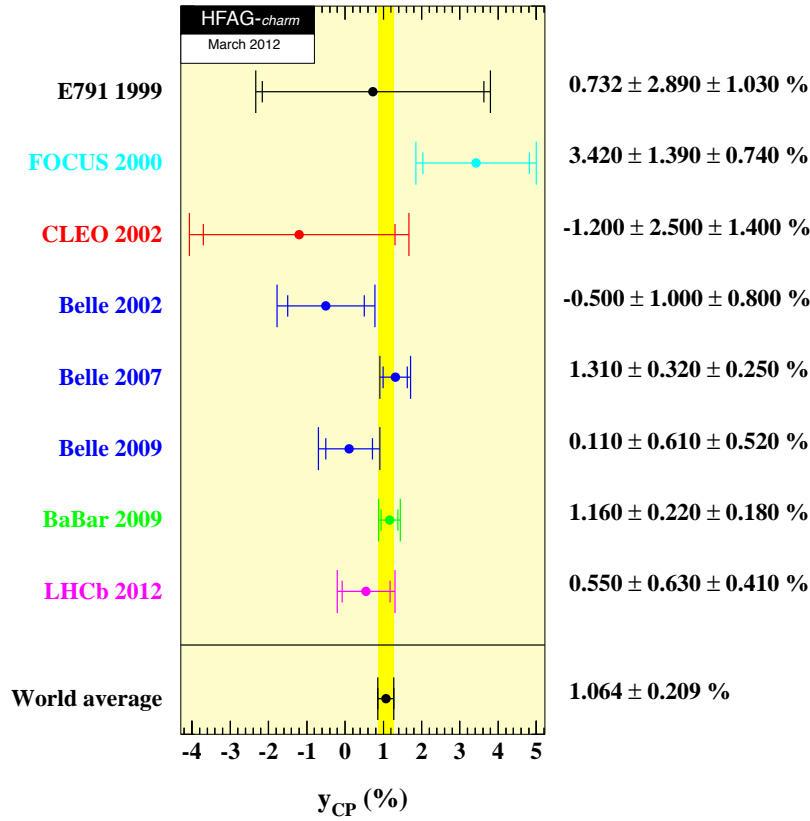


Figure 61: World average value of y_{CP} from Ref. [459], as calculated from $D^0 \rightarrow K^+K^- / \pi^+\pi^-$ measurements [448, 465–470].

in Table 167.

8.1.4 Conclusions

From the fit results listed in Table 167 and shown in Figs. 65 and 66, we conclude the following:

- the experimental data consistently indicate that D^0 mesons undergo mixing. The no-mixing point $x = y = 0$ is excluded at 10.2σ . The parameter x differs from zero by 2.7σ , and y differs from zero by 6.0σ . This mixing is presumably dominated by long-distance processes, which are difficult to calculate. Unless it turns out that $|x| \gg |y|$ [451], which is not indicated, it will probably be difficult to identify new physics from (x, y) alone.
- Since y_{CP} is positive, the CP -even state is shorter-lived as in the $K^0-\bar{K}^0$ system. However, since x also appears to be positive, the CP -even state is heavier, unlike in the $K^0-\bar{K}^0$ system.
- The LHCb and CDF experiments have obtained first evidence for *direct CPV* in D^0 decays. Higher statistics measurements should be able to clarify this effect. There is no evidence for CPV arising from $D^0-\bar{D}^0$ mixing ($|q/p| \neq 1$) or from a phase difference between the mixing amplitude and a direct decay amplitude ($\phi \neq 0$).

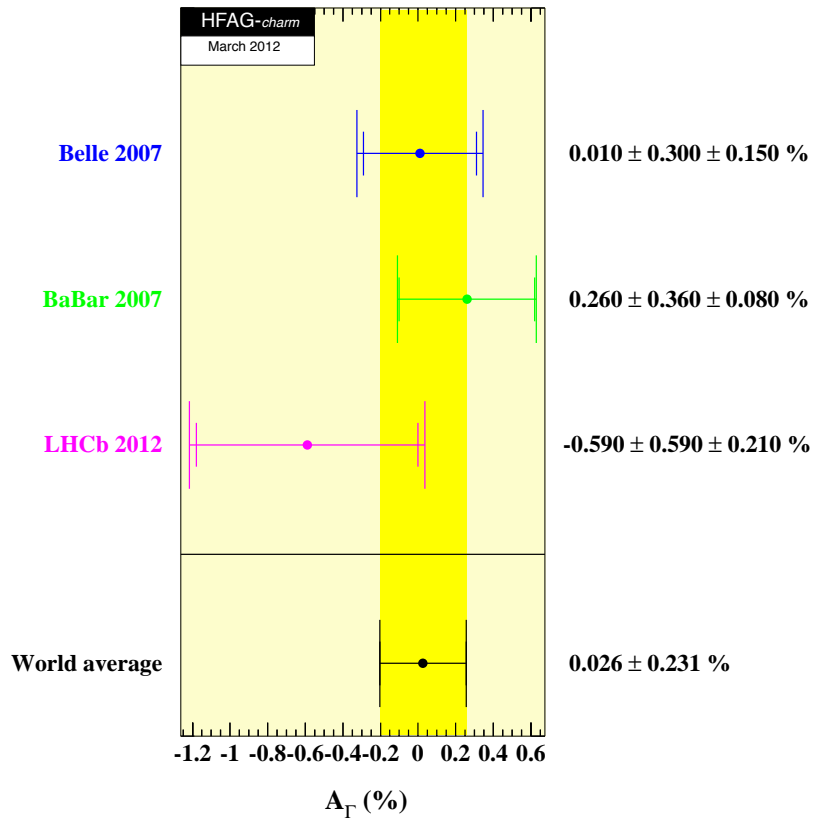


Figure 62: World average value of A_Γ from Ref. [459], as calculated from $D^0 \rightarrow K^+K^-/\pi^+\pi^-$ measurements [448, 468, 470].

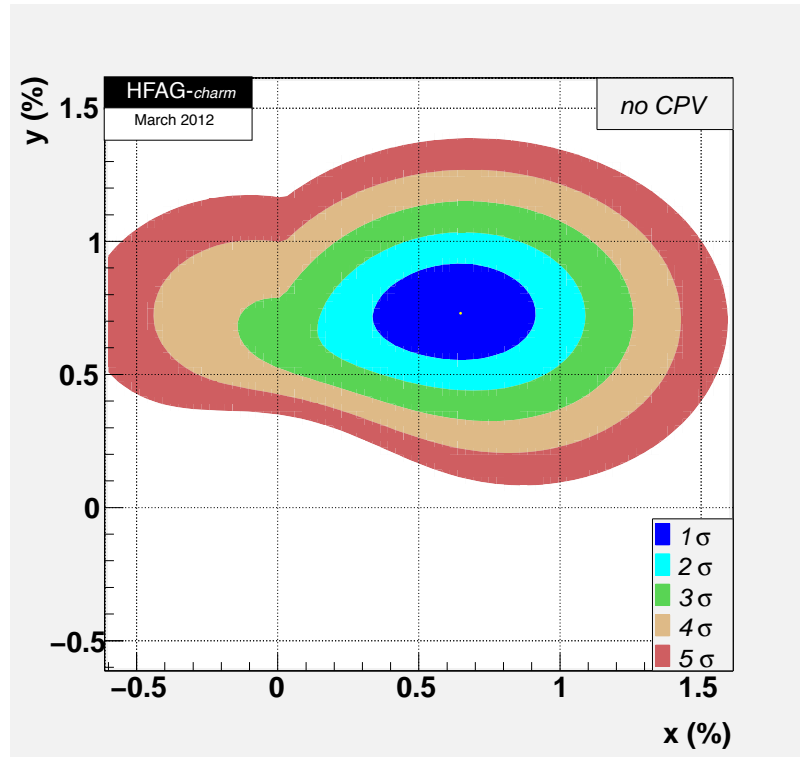


Figure 63: Two-dimensional contours for mixing parameters (x, y) , for no CPV .

Table 163: All observables used in the global fit except those from $D^0 \rightarrow K^+ \pi^-$ and those used for measuring direct CPV , from Refs. [448, 455–458, 461–468].

Mode	Observable	Values	Correlation coefficients
$D^0 \rightarrow K^+ K^- / \pi^+ \pi^-$, ϕK_S^0 [459]	y_{CP}	$(1.064 \pm 0.209)\%$	
	A_Γ	$(0.026 \pm 0.231)\%$	
$D^0 \rightarrow K_S^0 \pi^+ \pi^-$ [459] (Belle+CLEO WA: no CPV or no direct CPV)	x	$(0.811 \pm 0.334)\%$	
	y	$(0.309 \pm 0.281)\%$	
	$ q/p $	$0.95 \pm 0.22^{+0.10}_{-0.09}$	
	ϕ	$(-0.035 \pm 0.19 \pm 0.09)$ rad	
$D^0 \rightarrow K_S^0 \pi^+ \pi^-$ [461] (Belle: CPV -allowed)	x	$(0.81 \pm 0.30^{+0.13}_{-0.17})\%$	$\left\{ \begin{array}{cccc} 1 & -0.007 & -0.255\alpha & 0.216 \\ -0.007 & 1 & -0.019\alpha & -0.280 \\ -0.255\alpha & -0.019\alpha & 1 & -0.128\alpha \\ 0.216 & -0.280 & -0.128\alpha & 1 \end{array} \right\}$ $(\alpha = (q/p + 1)^2/2$ is a transformation factor)
	y	$(0.37 \pm 0.25^{+0.10}_{-0.15})\%$	
	$ q/p $	$0.86 \pm 0.30^{+0.10}_{-0.09}$	
	ϕ	$(-0.244 \pm 0.31 \pm 0.09)$ rad	
$D^0 \rightarrow K_S^0 \pi^+ \pi^-$ [462] $K_S^0 K^+ K^-$ (BABAR: no CPV)	x	$(0.16 \pm 0.23 \pm 0.12 \pm 0.08)\%$	0.0615
	y	$(0.57 \pm 0.20 \pm 0.13 \pm 0.07)\%$	
$D^0 \rightarrow K^+ \ell^- \nu$ [459]	R_M	$(0.0130 \pm 0.0269)\%$	
$D^0 \rightarrow K^+ \pi^- \pi^0$	x''	$(2.61^{+0.57}_{-0.68} \pm 0.39)\%$	-0.75
	y''	$(-0.06^{+0.55}_{-0.64} \pm 0.34)\%$	
$\psi(3770) \rightarrow \bar{D}D$ (CLEOc)	x^2	$(0.1549 \pm 0.2223)\%$	$\left\{ \begin{array}{ccccc} 1 & -0.6217 & -0.00224 & 0.3698 & 0.01567 \\ & 1 & 0.00414 & -0.5756 & -0.0243 \\ & & 1 & 0.0035 & 0.00978 \\ & & & 1 & 0.0471 \\ & & & & 1 \end{array} \right\}$
	y	$(2.997 \pm 2.293)\%$	
	R_D	$(0.4118 \pm 0.0948)\%$	
	$2\sqrt{R_D} \cos \delta$	$(12.64 \pm 2.86)\%$	
	$2\sqrt{R_D} \sin \delta$	$(-0.5242 \pm 6.426)\%$	

Table 164: $D^0 \rightarrow K^+ \pi^-$ observables used for the global fit, from Refs. [449, 450, 460].

Mode	Observable	Values	Correlation coefficients
$D^0 \rightarrow K^+ \pi^-$ (BABAR)	R_D	$(0.303 \pm 0.0189)\%$	$\begin{Bmatrix} 1 & 0.77 & -0.87 \\ 0.77 & 1 & -0.94 \\ -0.87 & -0.94 & 1 \end{Bmatrix}$
	x'^{2+}	$(-0.024 \pm 0.052)\%$	
	y'^+	$(0.98 \pm 0.78)\%$	
$\bar{D}^0 \rightarrow K^- \pi^+$ (BABAR)	A_D	$(-2.1 \pm 5.4)\%$	same as above
	x'^{2-}	$(-0.020 \pm 0.050)\%$	
	y'^-	$(0.96 \pm 0.75)\%$	
$D^0 \rightarrow K^+ \pi^-$ (Belle)	R_D	$(0.364 \pm 0.018)\%$	$\begin{Bmatrix} 1 & 0.655 & -0.834 \\ 0.655 & 1 & -0.909 \\ -0.834 & -0.909 & 1 \end{Bmatrix}$
	x'^{2+}	$(0.032 \pm 0.037)\%$	
	y'^+	$(-0.12 \pm 0.58)\%$	
$\bar{D}^0 \rightarrow K^- \pi^+$ (Belle)	A_D	$(2.3 \pm 4.7)\%$	same as above
	x'^{2-}	$(0.006 \pm 0.034)\%$	
	y'^-	$(0.20 \pm 0.54)\%$	
$D^0 \rightarrow K^+ \pi^-$ + c.c. (CDF)	R_D	$(0.304 \pm 0.055)\%$	$\begin{Bmatrix} 1 & 0.923 & -0.971 \\ 0.923 & 1 & -0.984 \\ -0.971 & -0.984 & 1 \end{Bmatrix}$
	x'^2	$(-0.012 \pm 0.035)\%$	
	y'	$(0.85 \pm 0.76)\%$	

Table 165: Measurements of direct CPV , from Refs. [471–475]. The parameter $A_{CP}(f)$ is defined as $[\Gamma(D^0 \rightarrow f) - \Gamma(\bar{D}^0 \rightarrow f)]/[\Gamma(D^0 \rightarrow f) + \Gamma(\bar{D}^0 \rightarrow f)]$.

Mode	Observable	Values	$\Delta\langle t \rangle/\tau$
$D^0 \rightarrow K^+ K^- / \pi^+ \pi^-$ (BABAR)	$A_{CP}(K^+ K^-)$	$(0.00 \pm 0.34 \pm 0.13)\%$	0
	$A_{CP}(\pi^+ \pi^-)$	$(-0.24 \pm 0.52 \pm 0.22)\%$	
$D^0 \rightarrow K^+ K^- / \pi^+ \pi^-$ (Belle)	$A_{CP}(K^+ K^-)$	$(-0.43 \pm 0.30 \pm 0.11)\%$	0
	$A_{CP}(\pi^+ \pi^-)$	$(0.43 \pm 0.52 \pm 0.12)\%$	
$D^0 \rightarrow K^+ K^- / \pi^+ \pi^-$ (LHCb 37 pb ⁻¹)	$A_{CP}(K^+ K^-) - A_{CP}(\pi^+ \pi^-)$	$(-0.82 \pm 0.21 \pm 0.11)\%$	0.0983 ± 0.00291
$D^0 \rightarrow K^+ K^- / \pi^+ \pi^-$ (CDF 9.7 fb ⁻¹ prelim.)	$A_{CP}(K^+ K^-) - A_{CP}(\pi^+ \pi^-)$	$(-0.62 \pm 0.21 \pm 0.10)\%$	0.26 ± 0.01
(CDF 5.9 fb ⁻¹ not used)	$A_{CP}(K^+ K^-)$	$(-0.24 \pm 0.22 \pm 0.09)\%$	2.65 ± 0.03
	$A_{CP}(\pi^+ \pi^-)$	$(0.22 \pm 0.24 \pm 0.11)\%$	2.40 ± 0.03

Table 166: Left: decay modes used to determine fitted parameters x , y , δ , $\delta_{K\pi\pi}$, R_D , A_D , $|q/p|$, and ϕ . Middle: the observables measured for each decay mode. Right: the relationships between the observables measured and the fitted parameters.

Decay Mode	Observables	Relationship
$D^0 \rightarrow K^+K^-/\pi^+\pi^-$	y_{CP} A_Γ	$2y_{CP} = (q/p + p/q) y \cos \phi -$ $(q/p - p/q) x \sin \phi$ $2A_\Gamma = (q/p - p/q) y \cos \phi -$ $(q/p + p/q) x \sin \phi$
$D^0 \rightarrow K_S^0 \pi^+ \pi^-$	x y $ q/p $ ϕ	
$D^0 \rightarrow K^+ \ell^- \nu$	R_M	$R_M = (x^2 + y^2)/2$
$D^0 \rightarrow K^+ \pi^- \pi^0$ (Dalitz plot analysis)	x'' y''	$x'' = x \cos \delta_{K\pi\pi} + y \sin \delta_{K\pi\pi}$ $y'' = y \cos \delta_{K\pi\pi} - x \sin \delta_{K\pi\pi}$
“Double-tagged” branching fractions measured in $\psi(3770) \rightarrow DD$ decays	R_M y R_D $\sqrt{R_D} \cos \delta$	$R_M = (x^2 + y^2)/2$
$D^0 \rightarrow K^+ \pi^-$	x'^2, y' x'^{2+}, x'^{2-} y'^+, y'^-	$x' = x \cos \delta + y \sin \delta$ $y' = y \cos \delta - x \sin \delta$ $A_M \equiv (q/p ^4 - 1)/(q/p ^4 + 1)$ $x'^{\pm} = [(1 \pm A_M)/(1 \mp A_M)]^{1/4} \times$ $(x' \cos \phi \pm y' \sin \phi)$ $y'^{\pm} = [(1 \pm A_M)/(1 \mp A_M)]^{1/4} \times$ $(y' \cos \phi \mp x' \sin \phi)$
$D^0 \rightarrow K^+ \pi^- / K^- \pi^+$ (time-integrated)	$\frac{\Gamma(D^0 \rightarrow K^+ \pi^-) + \Gamma(\bar{D}^0 \rightarrow K^- \pi^+)}{\Gamma(D^0 \rightarrow K^- \pi^+) + \Gamma(\bar{D}^0 \rightarrow K^+ \pi^-)}$ $\frac{\Gamma(D^0 \rightarrow K^+ \pi^-) - \Gamma(\bar{D}^0 \rightarrow K^- \pi^+)}{\Gamma(D^0 \rightarrow K^+ \pi^-) + \Gamma(\bar{D}^0 \rightarrow K^- \pi^+)}$	R_D A_D
$D^0 \rightarrow K^+ K^- / \pi^+ \pi^-$ (time-integrated)	$\frac{\Gamma(D^0 \rightarrow K^+ K^-) - \Gamma(\bar{D}^0 \rightarrow K^+ K^-)}{\Gamma(D^0 \rightarrow K^+ K^-) + \Gamma(\bar{D}^0 \rightarrow K^+ K^-)}$ $\frac{\Gamma(D^0 \rightarrow \pi^+ \pi^-) - \Gamma(\bar{D}^0 \rightarrow \pi^+ \pi^-)}{\Gamma(D^0 \rightarrow \pi^+ \pi^-) + \Gamma(\bar{D}^0 \rightarrow \pi^+ \pi^-)}$	$A_K + \frac{\langle t \rangle}{\tau_D} \mathcal{A}_{CP}^{\text{indirect}} \quad (\mathcal{A}_{CP}^{\text{indirect}} \approx -A_\Gamma)$ $A_\pi + \frac{\langle t \rangle}{\tau_D} \mathcal{A}_{CP}^{\text{indirect}} \quad (\mathcal{A}_{CP}^{\text{indirect}} \approx -A_\Gamma)$

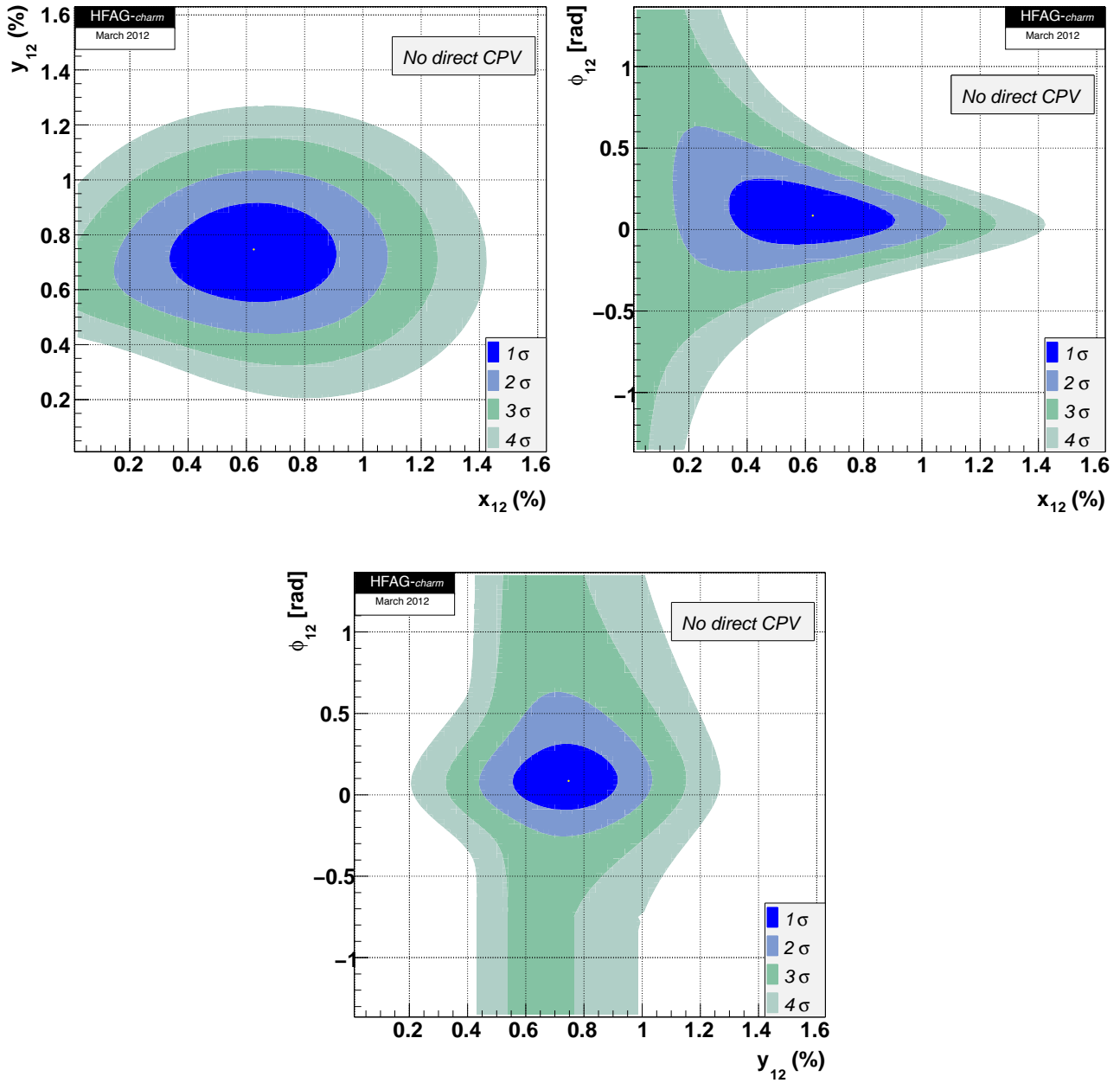


Figure 64: Two-dimensional contours for theoretical parameters (x_{12}, y_{12}) (top left), (x_{12}, ϕ_{12}) (top right), and (y_{12}, ϕ_{12}) (bottom), for no direct CPV .

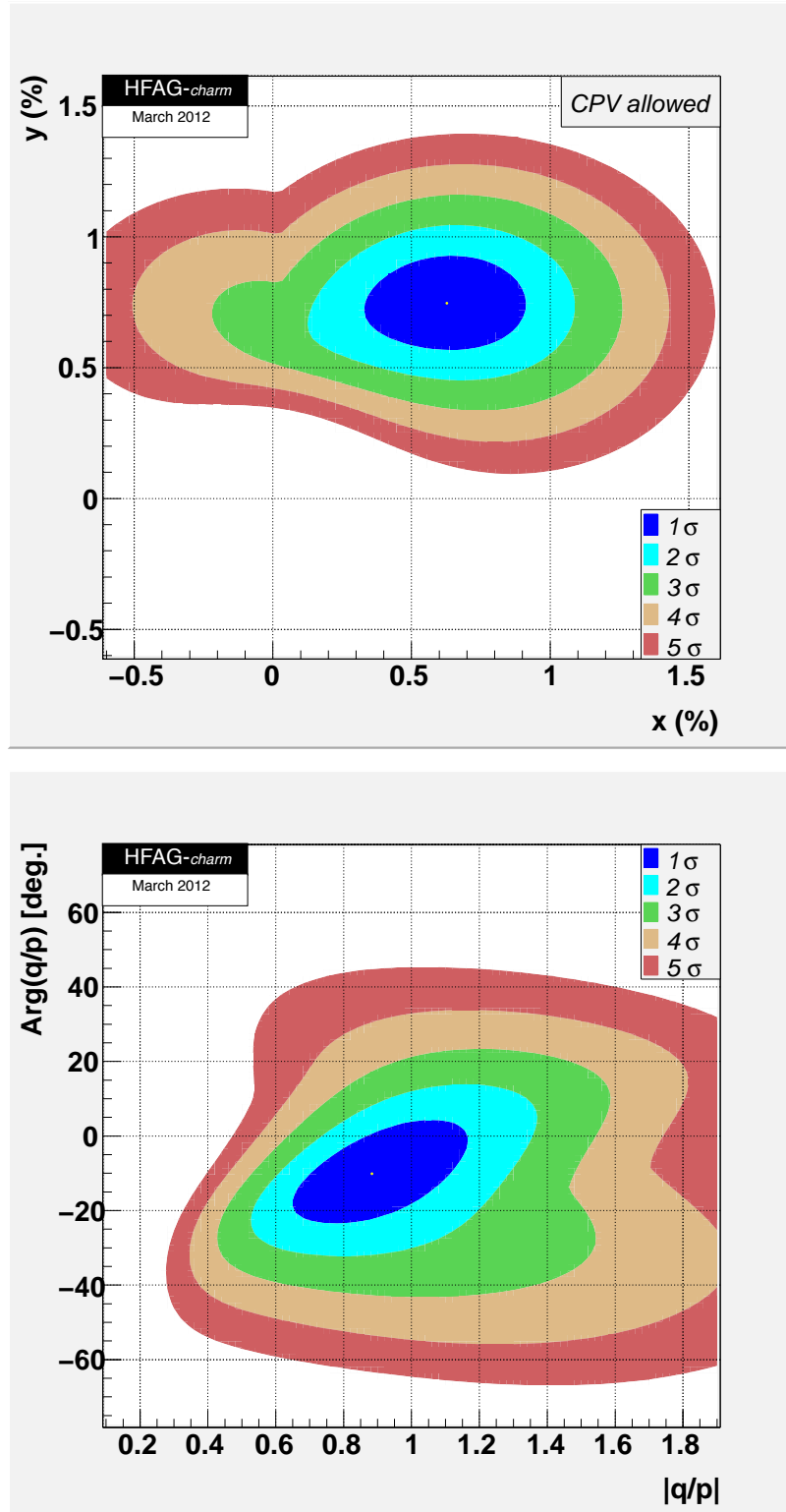


Figure 65: Two-dimensional contours for parameters (x, y) (top) and $(|q/p|, \phi)$ (bottom), allowing for CPV .

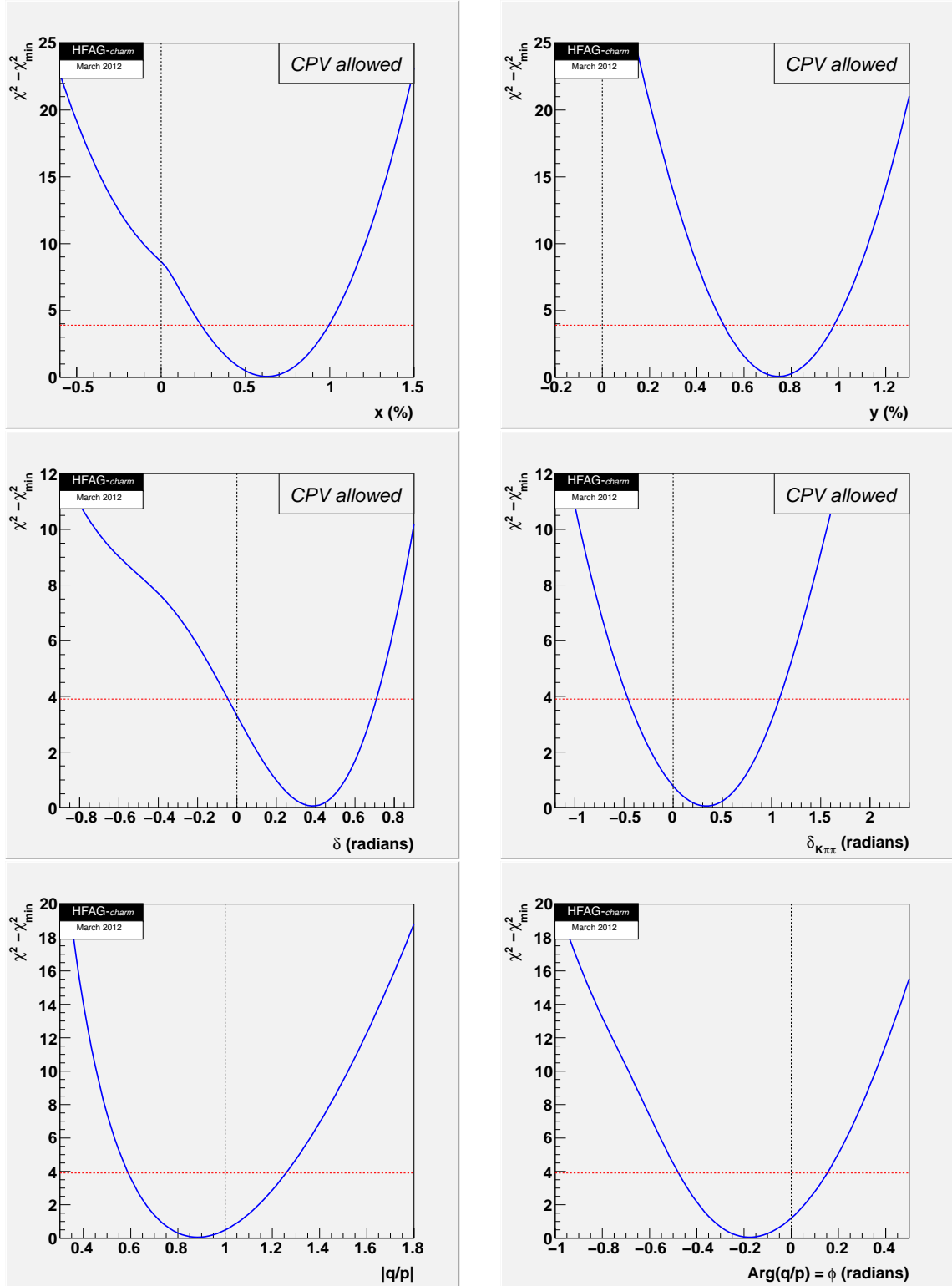


Figure 66: The function $\Delta\chi^2 = \chi^2 - \chi_{\min}^2$ for fitted parameters x , y , δ , $\delta_{K\pi\pi}$, $|q/p|$, and ϕ . The points where $\Delta\chi^2 = 3.84$ (denoted by dashed horizontal lines) determine 95% C.L. intervals.

Table 167: Results of the global fit for different assumptions concerning CPV .

Parameter	No CPV	No direct CPV	CPV -allowed	CPV -allowed 95% C.L.
x (%)	$0.65^{+0.18}_{-0.19}$	0.62 ± 0.19	$0.63^{+0.19}_{-0.20}$	[0.24, 0.99]
y (%)	0.73 ± 0.12	0.75 ± 0.12	0.75 ± 0.12	[0.51, 0.98]
δ ($^\circ$)	$21.0^{+9.8}_{-11.0}$	$22.2^{+9.9}_{-11.2}$	$22.1^{+9.7}_{-11.1}$	[-2.6, 40.6]
R_D (%)	0.3307 ± 0.0080	0.3305 ± 0.0080	0.3311 ± 0.0081	[0.315, 0.347]
A_D (%)	—	—	-1.7 ± 2.4	[-6.4, 3.0]
$ q/p $	—	$1.04^{+0.07}_{-0.06}$	$0.88^{+0.18}_{-0.16}$	[0.59, 1.26]
ϕ ($^\circ$)	—	$-2.02^{+2.67}_{-2.74}$	$-10.1^{+9.5}_{-8.9}$	[-27.4, 8.7]
$\delta_{K\pi\pi}$ ($^\circ$)	$17.8^{+21.7}_{-22.8}$	$19.4^{+21.8}_{-22.9}$	$19.3^{+21.8}_{-22.9}$	[-26.3, 61.8]
A_π	—	—	0.36 ± 0.25	[-0.13, 0.86]
A_K	—	—	-0.31 ± 0.24	[-0.78, 0.15]
x_{12} (%)	—	0.62 ± 0.19	—	[0.25, 0.99]
y_{12} (%)	—	0.75 ± 0.12	—	[0.51, 0.98]
ϕ_{12} ($^\circ$)	—	$4.9^{+7.7}_{-6.5}$	—	[-8.4, 24.6]

Table 168: Individual contributions to the χ^2 for the CPV -allowed fit.

Observable	χ^2	$\sum \chi^2$
y_{CP}	2.61	2.61
A_Γ	0.00	2.61
$x_{K^0\pi^+\pi^-}$ Belle	0.28	2.88
$y_{K^0\pi^+\pi^-}$ Belle	1.65	4.54
$ q/p _{K^0\pi^+\pi^-}$ Belle	0.01	4.54
$\phi_{K^0\pi^+\pi^-}$ Belle	0.51	5.05
$x_{K^0h^+h^-}$ BABAR	2.97	8.02
$y_{K^0h^+h^-}$ BABAR	0.37	8.38
$R_M(K^+\ell^-\nu)$	0.09	8.48
$x_{K^+\pi^-\pi^0}$ BABAR	5.71	14.19
$y_{K^+\pi^-\pi^0}$ BABAR	2.22	16.40
CLEOc		
$(x/y/R_D/\sqrt{R_D} \cos \delta/\sqrt{R_D} \sin \delta)$	7.28	23.68
$R_D^+/x'^{2+}/y'^+$ BABAR	2.34	26.02
$R_D^-/x'^{2-}/y'^-$ BABAR	1.30	27.31
$R_D^+/x'^{2+}/y'^+$ Belle	4.12	31.44
$R_D^-/x'^{2-}/y'^-$ Belle	1.35	32.79
$R_D/x'^2/y'$ CDF	0.39	33.17
$A_{KK}/A_{\pi\pi}$ BABAR	1.89	35.06
$A_{KK}/A_{\pi\pi}$ Belle	0.12	35.18
$A_{KK}/A_{\pi\pi}$ CDF	0.06	35.25
$A_{KK} - A_{\pi\pi}$ LHCb	0.37	35.62

8.2 Semileptonic decays

8.2.1 Introduction

Semileptonic decays of D mesons involve the interaction of a leptonic current with a hadronic current. The latter is nonperturbative and cannot be calculated from first principles; thus it is usually parameterized in terms of form factors. The transition matrix element is written

$$\mathcal{M} = -i \frac{G_F}{\sqrt{2}} V_{cq} L^\mu H_\mu, \quad (187)$$

where G_F is the Fermi constant and V_{cq} is a CKM matrix element. The leptonic current L_μ is evaluated directly from the lepton spinors and has a simple structure; this allows one to extract information about the form factors (in H_μ) from data on semileptonic decays [480]. Conversely, because there are no final-state interactions between the leptonic and hadronic systems, semileptonic decays for which the form factors can be calculated allow one to determine V_{cq} [2].

8.2.2 $D \rightarrow P\bar{\ell}\nu_\ell$ decays

When the final state hadron is a pseudoscalar, the hadronic current is given by

$$H_\mu = \langle P(p) | \bar{q} \gamma^\mu c | D(p') \rangle = f_+(q^2) \left[(p' + p)^\mu - \frac{m_D^2 - m_P^2}{q^2} q^\mu \right] + f_0(q^2) \frac{m_D^2 - m_P^2}{q^2} q^\mu, \quad (188)$$

where m_D and p' are the mass and four momentum of the parent D meson, m_P and p are those of the daughter meson, $f_+(q^2)$ and $f_0(q^2)$ are form factors, and $q = p' - p$. Kinematics require that $f_+(0) = f_0(0)$. The contraction $q^\mu L_\mu$ results in terms proportional to m_ℓ [481], and thus for $\ell = e$ the last two terms in Eq. (188) are negligible. Considering that, only the $f_+(q^2)$ form factor is relevant, the differential partial width is

$$\frac{d\Gamma(D \rightarrow P\bar{\ell}\nu_\ell)}{dq^2 d \cos \theta_\ell} = \frac{G_F^2 |V_{cq}|^2}{32\pi^3} p^{*3} |f_+(q^2)|^2 \sin^2 \theta_\ell, \quad (189)$$

where p^* is the magnitude of the momentum of the final state hadron in the D rest frame.

8.2.3 Form factor parameterizations

The form factor is traditionally parametrized with an explicit pole and a sum of effective poles:

$$f_+(q^2) = \frac{f_+(0)}{1 - \alpha} \left(\frac{1}{1 - q^2/m_{\text{pole}}^2} \right) + \sum_{k=1}^N \frac{\rho_k}{1 - q^2/(\gamma_k m_{\text{pole}}^2)}, \quad (190)$$

where ρ_k and γ_k are expansion parameters. The parameter m_{pole} is the mass of the lowest-lying $c\bar{q}$ resonance with the appropriate quantum numbers; this is expected to provide the largest contribution to the form factor for the $c \rightarrow q$ transition. For example, for $D \rightarrow \pi$ transitions the dominant resonance is expected to be D^* , and thus $m_{\text{pole}} = m_{D^*}$.

Simple pole

Equation (190) can be simplified by neglecting the sum over effective poles, leaving only the explicit vector meson pole. This approximation is referred to as “nearest pole dominance” or “vector-meson dominance.” The resulting parameterization is

$$f_+(q^2) = \frac{f_+(0)}{(1 - q^2/m_{\text{pole}}^2)}. \quad (191)$$

However, values of m_{pole} that give a good fit to the data do not agree with the expected vector meson masses [482]. To address this problem, the “modified pole” or Becirevic-Kaidalov (BK) parameterization [483] was introduced. $m_{\text{pole}}/\sqrt{\alpha_{\text{BK}}}$ is interpreted as the mass of an effective pole, higher than m_{pole} , thus it is expected that $\alpha_{\text{BK}} < 1$.

The parameterization takes the form

$$f_+(q^2) = \frac{f_+(0)}{(1 - q^2/m_{\text{pole}}^2)} \frac{1}{\left(1 - \alpha_{\text{BK}} \frac{q^2}{m_{\text{pole}}^2}\right)}. \quad (192)$$

This parameterization has been used by several experiments to determine form factor parameters. Measured values of m_{pole} and α_{BK} are listed Tables 169 and 170 for $D \rightarrow K\ell\nu_\ell$ and $D \rightarrow \pi\ell\nu_\ell$ decays, respectively.

z expansion

Several groups have advocated an alternative series expansion around some value $q^2 = t_0$ to parameterize f_+ [480, 484–486]. This expansion is given in terms of a complex parameter z , which is the analytic continuation of q^2 into the complex plane:

$$z(q^2, t_0) = \frac{\sqrt{t_+ - q^2} - \sqrt{t_+ - t_0}}{\sqrt{t_+ - q^2} + \sqrt{t_+ - t_0}}, \quad (193)$$

where $t_\pm \equiv (m_D \pm m_P)^2$ and t_0 is the (arbitrary) q^2 value corresponding to $z = 0$. The physical region corresponds to $|z| < 1$.

The form factor is expressed as

$$f_+(q^2) = \frac{1}{P(q^2)\phi(q^2, t_0)} \sum_{k=0}^{\infty} a_k(t_0)[z(q^2, t_0)]^k, \quad (194)$$

where the $P(q^2)$ factor accommodates sub-threshold resonances via

$$P(q^2) \equiv \begin{cases} 1 & (D \rightarrow \pi) \\ z(q^2, M_{D_s^*}^2) & (D \rightarrow K). \end{cases} \quad (195)$$

The “outer” function $\phi(t, t_0)$ can be any analytic function, but a preferred choice (see, *e.g.* Refs. [484, 485, 487]) obtained from the Operator Product Expansion (OPE) is

$$\phi(q^2, t_0) = \alpha \left(\sqrt{t_+ - q^2} + \sqrt{t_+ - t_0} \right) \times \frac{t_+ - q^2}{(t_+ - t_0)^{1/4}} \frac{(\sqrt{t_+ - q^2} + \sqrt{t_+ - t_0})^{3/2}}{(\sqrt{t_+ - q^2} + \sqrt{t_+})^5}, \quad (196)$$

with $\alpha = \sqrt{\pi m_c^2/3}$. The OPE analysis provides a constraint upon the expansion coefficients, $\sum_{k=0}^N a_k^2 \leq 1$. These coefficients receive $1/M_D$ corrections, and thus the constraint is only approximate. However, the expansion is expected to converge rapidly since $|z| < 0.051$ (0.17) for $D \rightarrow K$ ($D \rightarrow \pi$) over the entire physical q^2 range, and Eq. (194) remains a useful parameterization.

8.2.4 Experimental techniques and results

Different techniques by several experiments have been used to measure D meson semileptonic decays with a pseudoscalar particle in the final state. The most recent results are provided by the Belle [488], *BABAR* [489] and CLEO-c [490], [491] collaborations. The BES III experiment has also reported preliminary results at the CHARM 2012 conference with 923 pb^{-1} [492]. The Belle experiment fully reconstructs the D events from the continuum under the $\Upsilon(4S)$ resonance, achieving a very good q^2 resolution ($\Delta q^2 = 15 \text{ MeV}^2$) and low background level, but having a low efficiency. Using 282 fb^{-1} , about 1300 and 115 signal semileptonic decays are isolated for each lepton flavour (e and μ). The *BABAR* experiment uses a partial reconstruction technique where the semileptonic decays are tagged through the $D^{*+} \rightarrow D^0 \pi^+$ decay. The D direction and neutrino energy is obtained using information of the rest of the event. With 75 fb^{-1} 74000 signal events in the $D^0 \rightarrow K^- e^+ \nu$ mode are obtained. The measurement of the Cabibbo suppressed mode has not been published yet. This technique provides larger statistics but higher background level and poorer q^2 resolution (Δq^2 ranges from 66 to 219 MeV^2). In this case the measurement of the branching fraction is obtained by normalizing to the $D^0 \rightarrow K^- \pi^+$ decay channel and can benefit from future improvements in the determination of this reference channel. The CLEO-c experiment uses two different methods to measure charm semileptonic decays. Tagged analyses [490] rely on the full reconstruction of $\Psi(3770) \rightarrow D\bar{D}$ events. One of the D mesons is reconstructed in a hadronic decay mode, the other in the semileptonic channel. The only missing particle is the neutrino so the q^2 resolution is very good and the background level very low. With the entire CLEO-c data sample, 818 pb^{-1} , 14123 and 1374 signal events are reconstructed for the $D^0 \rightarrow K^- e^+ \nu$ and $D^0 \rightarrow \pi^- e^+ \nu$ channels, respectively, and 8467 and 838 for the $D^+ \rightarrow \bar{K}^0 e^+ \nu$ and $D^+ \rightarrow \pi^0 e^+ \nu$ decays. Another technique without tagging the D meson in a hadronic mode (“untagged” in the following) has been also used by CLEO-c [491]. This method rests upon the association of the missing energy and momentum in an event with the neutrino four momentum, with the penalty of larger background as compared to the tagged method.

Previous measurements were also performed by CLEO III and FOCUS experiments. Events registered at the $\Upsilon(4S)$ energy corresponding to an integrated luminosity of 7 fb^{-1} were analyzed by CLEO III [493]. In the FOCUS fixed target photo-production experiment D^0 semileptonic events were obtained from the decay of a D^{*+} , and the kaon or pion was reconstructed in the muon channel.

Results of the hadronic form factor parameters by the different groups are given in Tables 169 and 170 for m_{pole} and α_{BK} .

The z -expansion formalism has been used by *BABAR* [489] and CLEOc [490], [491]. BES III has also shown preliminary results [492]. Their fits used the first three terms of the expansion, and the results for the ratios $r_1 \equiv a_1/a_0$ and $r_2 \equiv a_2/a_0$ are listed in Tables 171 and 172. The CLEO III [493] and FOCUS [494] results listed are obtained by refitting their data using the full covariance matrix. The *BABAR* correlation coefficient listed is obtained by refitting their

Table 169: Results for m_{pole} and α_{BK} from various experiments for $D^0 \rightarrow K^- \ell^+ \nu$ and $D^+ \rightarrow K_S \ell^+ \nu$ decays. The last entry is a lattice QCD prediction (errors have been increased as compared to the publication to take into account remaining systematic uncertainties in Lattice calculations, as advised by the authors).

$D \rightarrow K \ell \nu_\ell$ Expt.	Ref.	m_{pole} (GeV/ c^2)	α_{BK}
CLEO III	[493]	$1.89 \pm 0.05^{+0.04}_{-0.03}$	$0.36 \pm 0.10^{+0.03}_{-0.07}$
FOCUS	[494]	$1.93 \pm 0.05 \pm 0.03$	$0.28 \pm 0.08 \pm 0.07$
Belle	[488]	$1.82 \pm 0.04 \pm 0.03$	$0.52 \pm 0.08 \pm 0.06$
<i>BABAR</i>	[489]	$1.889 \pm 0.012 \pm 0.015$	$0.366 \pm 0.023 \pm 0.029$
CLEO-c (tagged)	[490]	$1.93 \pm 0.02 \pm 0.01$	$0.30 \pm 0.03 \pm 0.01$
CLEO-c (untagged, D^0)	[491]	$1.97 \pm 0.03 \pm 0.01$	$0.21 \pm 0.05 \pm 0.03$
CLEO-c (untagged, D^+)	[491]	$1.96 \pm 0.04 \pm 0.02$	$0.22 \pm 0.08 \pm 0.03$
BESIII (prel)	[492]	$1.943 \pm 0.025 \pm 0.003$	$0.265 \pm 0.045 \pm 0.006$
Fermilab lattice/MILC/HPQCD	[495]	–	$0.50 \pm 0.04 \pm 0.07$

Table 170: Results for m_{pole} and α_{BK} from various experiments for $D^0 \rightarrow \pi^- \ell^+ \nu$ and $D^+ \rightarrow \pi^0 \ell^+ \nu$ decays. The last entry is a lattice QCD prediction (errors have been increased as compared to the publication to take into account remaining systematic uncertainties in Lattice calculations, as advised by the authors).

$D \rightarrow \pi \ell \nu_\ell$ Expt.	Ref.	m_{pole} (GeV/ c^2)	α_{BK}
CLEO III	[493]	$1.86^{+0.10+0.07}_{-0.06-0.03}$	$0.37^{+0.20}_{-0.31} \pm 0.15$
FOCUS	[494]	$1.91^{+0.30}_{-0.15} \pm 0.07$	–
Belle	[488]	$1.97 \pm 0.08 \pm 0.04$	$0.10 \pm 0.21 \pm 0.10$
CLEO-c (tagged)	[490]	$1.91 \pm 0.02 \pm 0.01$	$0.21 \pm 0.07 \pm 0.02$
CLEO-c (untagged, D^0)	[491]	$1.87 \pm 0.03 \pm 0.01$	$0.21 \pm 0.05 \pm 0.03$
CLEO-c (untagged, D^+)	[491]	$1.97 \pm 0.07 \pm 0.02$	$0.22 \pm 0.08 \pm 0.03$
BESIII (prel)	[492]	$1.876 \pm 0.023 \pm 0.004$	$0.315 \pm 0.071 \pm 0.012$
Fermilab lattice/MILC/HPQCD	[495]	–	$0.44 \pm 0.04 \pm 0.07$

published branching fraction using their published covariance matrix.

These measurements correspond to using the standard outer function $\phi(q^2, t_0)$ of Eq. (196) and $t_0 = t_+ \left(1 - \sqrt{1 - t_-/t_+}\right)$. This choice of t_0 constrains $|z|$ to vary between $\pm z_{\text{max}}$.

Tables 171 and 172 also list average values for r_1 and r_2 obtained from a 3D fit, taking the full correlations between $|V_{cq}|f_+(0)$, r_1 and r_2 into account, to CLEO III, FOCUS, *BABAR*, CLEO-c, and BES III data. Only the D^0 channels are entering in the fit. The fit is constrained by the branching fractions measured at Belle [488].

In the values quoted in Tables 169 and 171 the effect of radiative events has been taken into account slightly modifying the values from *BABAR* by correcting the numbers given in Tab. III

Table 171: Results for r_1 and r_2 from various experiments, for $D \rightarrow K\ell\nu_\ell$. The correlation coefficient listed is for the total uncertainties (statistical \oplus systematic) on r_1 and r_2 .

Expt. $D \rightarrow K\ell\nu_\ell$	mode	Ref.	r_1	r_2	ρ
CLEO III		[493]	$0.2^{+3.6}_{-3.0}$	-89^{+104}_{-120}	-0.99
FOCUS		[494]	-2.54 ± 0.75	7 ± 13	-0.97
<i>BABAR</i>		[489]	$-2.5 \pm 0.2 \pm 0.2$	$2.5 \pm 6.0 \pm 5.0$	-0.64
CLEO-c (tagged)	$D^0 \rightarrow K^-$	[490]	$-2.65 \pm 0.34 \pm 0.08$	$13 \pm 9 \pm 1$	-0.82
CLEO-c (tagged)	$D^+ \rightarrow \bar{K}^0$	[490]	$-1.66 \pm 0.44 \pm 0.10$	$-14 \pm 11 \pm 1$	-0.82
CLEO-c (untagged)	$D^0 \rightarrow K^-$	[491]	$-2.4 \pm 0.4 \pm 0.1$	$21 \pm 11 \pm 2$	-0.81
CLEO-c (untagged)	$D^+ \rightarrow \bar{K}^0$	[491]	$-2.8 \pm 6 \pm 2$	$32 \pm 18 \pm 4$	-0.84
BES III		[492]	$-2.18 \pm 0.36 \pm 0.05$	$5 \pm 9 \pm 1$	
Combined			-2.39 ± 0.17	6.2 ± 3.8	-0.82

Table 172: Results for r_1 and r_2 from various experiments, for $D \rightarrow \pi\ell\nu_\ell$. The correlation coefficient listed is for the total uncertainties (statistical \oplus systematic) on r_1 and r_2 .

Expt. $D \rightarrow \pi\ell\nu_\ell$	mode	Ref.	r_1	r_2	ρ
CLEO-c (tagged)	$D^0 \rightarrow \pi^+$	[490]	$-2.80 \pm 0.49 \pm 0.04$	$6 \pm 3 \pm 0$	-0.94
CLEO-c (tagged)	$D^+ \rightarrow \pi^0$	[490]	$-1.37 \pm 0.88 \pm 0.24$	$-4 \pm 5 \pm 1$	-0.96
CLEO-c (untagged)	$D^0 \rightarrow \pi^+$	[491]	$-2.1 \pm 0.7 \pm 0.3$	$-1.2 \pm 4.8 \pm 1.7$	-0.96
CLEO-c (untagged)	$D^+ \rightarrow \pi^0$	[491]	$-0.2 \pm 1.5 \pm 0.4$	$-9.8 \pm 9.1 \pm 2.1$	-0.97
BES III		[492]	$-2.73 \pm 0.48 \pm 0.08$	$4 \pm 3 \pm 1$	
Combined			-2.69 ± 0.32	4.18 ± 2.16	-0.95

of Ref. [489] by the shifts quoted in the last column of Tab. IV given in Ref. [489].

The $\chi^2/d.o.f$ of the combined fits are 16/22 and 6.2/10 for $D^0 \rightarrow K^-\ell^+\nu_\ell$ and $D^0 \rightarrow \pi^-\ell^+\nu_\ell$, respectively. The correlation matrices are given in Tables 173 and 174.

8.2.5 $D \rightarrow V\bar{\ell}\nu_\ell$ decays

When the final state hadron is a vector meson, the decay can proceed through both vector and axial vector currents, and four form factors are needed. The hadronic current is $H_\mu = V_\mu + A_\mu$,

Table 173: Correlation matrix for the combined fit for the $D^0 \rightarrow \pi^- \ell^+ \nu_\ell$ channel

	$ V_{cd} f_+^\pi(0)$	r_1	r_2
$ V_{cd} f_+^\pi(0)$	1.000	-0.446	0.672
r_1	-0.446	1.000	-0.946
r_2	0.672	-0.946	1.000

Table 174: Correlation matrix for the combined fit for the $D^0 \rightarrow K^- \ell^+ \nu_\ell$ channel

	$ V_{cs} f_+^K(0)$	r_1	r_2
$ V_{cs} f_+^K(0)$	1.000	-0.088	0.433
r_1	-0.088	1.000	-0.824
r_2	0.433	-0.824	1.000

where [481]

$$V_\mu = \langle V(p, \varepsilon) | \bar{q} \gamma^\mu c | D(p') \rangle = \frac{2V(q^2)}{m_D + m_V} \varepsilon_{\mu\nu\rho\sigma} \varepsilon^{*\nu} p'^\rho p^\sigma \quad (197)$$

$$\begin{aligned} A_\mu = \langle V(p, \varepsilon) | -\bar{q} \gamma^\mu \gamma^5 c | D(p') \rangle = & -i(m_D + m_V) A_1(q^2) \varepsilon_\mu^* \\ & + i \frac{A_2(q^2)}{m_D + m_V} (\varepsilon^* \cdot q) (p' + p)_\mu \\ & + i \frac{2m_V}{q^2} (A_3(q^2) - A_0(q^2)) [\varepsilon^* \cdot (p' + p)] q_\mu. \end{aligned} \quad (198)$$

In this expression, m_V is the daughter meson mass and

$$A_3(q^2) = \frac{m_D + m_V}{2m_V} A_1(q^2) - \frac{m_D - m_V}{2m_V} A_2(q^2). \quad (199)$$

Kinematics require that $A_3(0) = A_0(0)$. The differential partial width is

$$\begin{aligned} \frac{d\Gamma(D \rightarrow V \ell \nu_\ell)}{dq^2 d \cos \theta_\ell} = & \frac{G_F^2 |V_{cq}|^2}{128\pi^3 m_D^2} p^* q^2 \times \\ & \left[\frac{(1 - \cos \theta_\ell)^2}{2} |H_-|^2 + \frac{(1 + \cos \theta_\ell)^2}{2} |H_+|^2 + \sin^2 \theta_\ell |H_0|^2 \right], \end{aligned} \quad (200)$$

where H_\pm and H_0 are helicity amplitudes given by

$$H_\pm = \frac{1}{m_D + m_V} [(m_D + m_V)^2 A_1(q^2) \mp 2m_D p^* V(q^2)] \quad (201)$$

$$\begin{aligned} H_0 = & \frac{1}{|q| 2m_V (m_D + m_V)} \times \\ & \left[\left(1 - \frac{m_V^2 - q^2}{m_D^2} \right) (m_D + m_V)^2 A_1(q^2) - 4p^{*2} A_2(q^2) \right]. \end{aligned} \quad (202)$$

Table 175: Results for the form factor normalization $f_+^K(0)|V_{cs}|$ and $f_+^\pi(0)|V_{cd}|$. Results from the different collaborations have been corrected, if needed, using values from PDG 2010. Prior to 2006, and apart for BESII, experiments measure the ratio $(f_+^\pi(0)|V_{cd}|/f_+^K(0)|V_{cs}|)^2$. Corresponding values given in this Table for $f_+^\pi(0)|V_{cd}|$ are obtained by assuming that $f_+^K(0)|V_{cs}| = 0.714 \pm 0.009$. Results of the combined fit include measurements from 2006 and later for experiments measuring $f_+(0)|V_{cq}|$, r_1 and r_2 . Results of CLEO (2008) (untagged) only refer to the D^0 channel. Results from LQCD are given in the last line [496] [497]. Results quoted for LQCD are obtained by multiplying the values computed for $f_+^K(0)$ and $f_+^\pi(0)$ from lattice by $|V_{cs}| = 0.9729$ and $|V_{cd}| = 0.2253$ respectively. These values of $|V_{cs(d)}|$ correspond to present estimates assuming the unitarity of the CKM matrix. Values entering in the combination explained before are marked with a *.

Experiment	Ref.	$f_+^K(0) V_{cs} $	$f_+^\pi(0) V_{cd} $
E691 (1989)	[498]	$0.69 \pm 0.05 \pm 0.05$	
CLEO (1991)	[499]		
CLEOII (1993)	[500]	$0.76 \pm 0.01 \pm 0.04$	
CLEOII (1995)	[501]		$0.163 \pm 0.031 \pm 0.011$
E687 (1995)	[502]	$0.69 \pm 0.03 \pm 0.03$	
E687 (1996)	[503]		$0.160 \pm 0.018 \pm 0.004$
BESII (2004)	[504]	$0.78 \pm 0.04 \pm 0.03$	$0.164 \pm 0.032 \pm 0.014$
CLEOIII (2005) *	[493]		$0.139_{-0.013}^{+0.011} \text{ }_{-0.006}^{+0.009}$
FOCUS (2005)	[494]		$0.137 \pm 0.008 \pm 0.008$
Belle (2006) *	[488]	$0.692 \pm 0.007 \pm 0.022$	$0.140 \pm 0.004 \pm 0.007$
BABAR (2007) *	[489]	$0.720 \pm 0.007 \pm 0.007$	
CLEO-c (2008)(untagged) *	[491]	$0.747 \pm 0.009 \pm 0.009$	$0.139 \pm 0.007 \pm 0.003$
CLEO-c (2009) (tagged) *	[490]	$0.719 \pm 0.006 \pm 0.005$	$0.150 \pm 0.004 \pm 0.001$
BESIII (2012)(prel.) *	[492]	$0.729 \pm 0.008 \pm 0.007$	$0.144 \pm 0.005 \pm 0.002$
Combined fit		0.728 ± 0.005	0.146 ± 0.003
HPQCD	[497] [496]	0.727 ± 0.018	0.150 ± 0.007

p^* is the three-momentum of the $K\pi$ system, measured in the D rest frame. The left-handed nature of the quark current manifests itself as $|H_-| > |H_+|$. The differential decay rate for $D \rightarrow V\ell\nu$ followed by the vector meson decaying into two pseudoscalars is

$$\begin{aligned}
\frac{d\Gamma(D \rightarrow V\ell\nu, V \rightarrow P_1P_2)}{dq^2 d \cos \theta_V d \cos \theta_\ell d\chi} &= \frac{3G_F^2}{2048\pi^4} |V_{cq}|^2 \frac{p^*(q^2)q^2}{m_D^2} \mathcal{B}(V \rightarrow P_1P_2) \times \\
&\{ (1 + \cos \theta_\ell)^2 \sin^2 \theta_V |H_+(q^2)|^2 \\
&+ (1 - \cos \theta_\ell)^2 \sin^2 \theta_V |H_-(q^2)|^2 \\
&+ 4 \sin^2 \theta_\ell \cos^2 \theta_V |H_0(q^2)|^2 \\
&+ 4 \sin \theta_\ell (1 + \cos \theta_\ell) \sin \theta_V \cos \theta_V \cos \chi H_+(q^2) H_0(q^2) \\
&- 4 \sin \theta_\ell (1 - \cos \theta_\ell) \sin \theta_V \cos \theta_V \cos \chi H_-(q^2) H_0(q^2) \\
&- 2 \sin^2 \theta_\ell \sin^2 \theta_V \cos 2\chi H_+(q^2) H_-(q^2) \}, \quad (203)
\end{aligned}$$

where the angles θ_ℓ , θ_V , and χ are defined in Fig. 68.

Ratios between the values of the hadronic form factors expressed at $q^2 = 0$ are usually introduced:

$$r_V \equiv V(0)/A_1(0), \quad r_2 \equiv A_2(0)/A_1(0). \quad (204)$$

Table 176 lists measurements of r_V and r_2 from several experiments. Most of measurements assume that the q^2 dependence of hadronic form factors is given by the simple pole ansatz. The measurements are plotted in Fig. 69 which shows that they are all consistent.

Table 176: Results for r_V and r_2 from various experiments.

Experiment	Ref.	r_V	r_2
$D^+ \rightarrow \overline{K}^{*0} l^+ \nu$			
E691	[505]	$2.0 \pm 0.6 \pm 0.3$	$0.0 \pm 0.5 \pm 0.2$
E653	[506]	$2.00 \pm 0.33 \pm 0.16$	$0.82 \pm 0.22 \pm 0.11$
E687	[507]	$1.74 \pm 0.27 \pm 0.28$	$0.78 \pm 0.18 \pm 0.11$
E791 (e)	[508]	$1.90 \pm 0.11 \pm 0.09$	$0.71 \pm 0.08 \pm 0.09$
E791 (μ)	[509]	$1.84 \pm 0.11 \pm 0.09$	$0.75 \pm 0.08 \pm 0.09$
Beatrice	[510]	$1.45 \pm 0.23 \pm 0.07$	$1.00 \pm 0.15 \pm 0.03$
FOCUS	[511]	$1.504 \pm 0.057 \pm 0.039$	$0.875 \pm 0.049 \pm 0.064$
$D^0 \rightarrow \overline{K}^0 \pi^- \mu^+ \nu$			
FOCUS	[512]	$1.706 \pm 0.677 \pm 0.342$	$0.912 \pm 0.370 \pm 0.104$
BABAR	[513]	$1.493 \pm 0.014 \pm 0.021$	$0.775 \pm 0.011 \pm 0.011$
$D_s^+ \rightarrow \phi e^+ \nu$			
BABAR	[514]	$1.636 \pm 0.067 \pm 0.038$	$0.705 \pm 0.056 \pm 0.029$
$D^0, D^+ \rightarrow \rho e \nu$			
CLEO	[515]	$1.40 \pm 0.25 \pm 0.03$	$0.57 \pm 0.18 \pm 0.06$

8.2.6 S -wave component

In 2002 FOCUS reported [516] an asymmetry in the observed $\cos(\theta_V)$ distribution. This is interpreted as evidence for an S -wave component in the decay amplitude as follows. Since H_0 typically dominates over H_\pm , the distribution given by Eq. (203) is, after integration over χ , roughly proportional to $\cos^2 \theta_V$. Inclusion of a constant S -wave amplitude of the form $A e^{i\delta}$ leads to an interference term proportional to $|AH_0 \sin \theta_\ell \cos \theta_V|$; this term causes an asymmetry in $\cos(\theta_V)$. When FOCUS fit their data including this S -wave amplitude, they obtained $A = 0.330 \pm 0.022 \pm 0.015 \text{ GeV}^{-1}$ and $\delta = 0.68 \pm 0.07 \pm 0.05$ [511].

More recently, both BABAR [514] and CLEO-c [517] have also found evidence for an f_0 component in semileptonic D_s decays.

8.2.7 Model-independent form factor measurement

Subsequently the CLEO-c collaboration extracted the form factors $H_+(q^2)$, $H_-(q^2)$, and $H_0(q^2)$ in a model-independent fashion directly as functions of q^2 [518] and also determined the S -wave

form factor $h_0(q^2)$ via the interference term, despite the fact that the $K\pi$ mass distribution appears dominated by the vector $K^*(892)$ state. Their results are shown in Figs. 71 and 70. Plots in Fig. 71 clearly show that $H_0(q^2)$ dominates over essentially the full range of q^2 , but especially at low q^2 . They also show that the transverse form factor $H_t(q^2)$ (which can be related to $A_3(q^2)$) is small (compared to Lattice Gauge Theory calculations) and suggest that the form factor ratio $r_3 \equiv A_3(0)/A_1(0)$ is large and negative.

The product $H_0(q^2) \times h_0(q^2)$ is shown in Fig. 70 and clearly indicates the existence of $h_0(q^2)$, although it seems to fall faster with q^2 than $H_0(q^2)$. The other plots in that figure show that D - and F -wave versions of the S -wave $h_0(q^2)$ are not significant.

8.2.8 Detailed measurements of the $D^+ \rightarrow K^- \pi^+ e^+ \nu_e$ decay channel

BABAR [513] has selected a large sample of 244×10^3 signal events with a ratio $S/B \sim 2.3$ from an analyzed integrated luminosity of 347 fb^{-1} . With four particles emitted in the final state, the differential decay rate depends on five variables. In addition to the four variables defined in previous sections there is m^2 , the mass squared of the $K\pi$ system. Apart for this last variable, the reconstruction algorithm does not provide a high resolution on the other measured quantities and a multi-dimensional unfolding procedure is not used to correct for efficiency and resolution effects. Meanwhile these limitations still allow an essentially model independent measurement of the differential decay rate. This is because, apart for the q^2 and mass dependence of the form factors, angular distributions are fixed by kinematics. In addition, present accurate measurements of $D \rightarrow P \bar{\ell} \nu_\ell$ decays have shown that the q^2 dependence of the form factors can be well described by several models as long as the corresponding model parameter(s) are fitted on data. This is even more true in $D \rightarrow V \bar{\ell} \nu_\ell$ decays because the q^2 range is reduced. To analyze the $D^+ \rightarrow K^- \pi^+ e^+ \nu_e$ decay channel it is assumed that all form factors have a q^2 variation given by the simple pole model and the effective pole mass value, $m_A = (2.63 \pm 0.10 \pm 0.13) \text{ GeV}/c^2$, is fitted for the axial vector form factors. This value is compatible with expectations when comparing with the mass of $J^P = 1^+$ charm mesons. Data are not sensitive to the effective mass of the vector form factor for which $m_V = (2.1 \pm 0.1) \text{ GeV}/c^2$ is used, nor to the effective pole mass of the scalar component for which m_A is used. For the mass dependence of the form factors, a Breit-Wigner with a mass dependent width and a Blatt-Weisskopf damping factor is used. For the S-wave amplitude, considering what was measured in $D^+ \rightarrow K^- \pi^+ \pi^+$ decays, a polynomial variation below the $\bar{K}_0^*(1430)$ and a Breit-Wigner distribution, above are assumed. For the polynomial part, a linear term is sufficient to fit data.

It is verified that the variation of the S-wave phase is compatible with expectations from elastic $K\pi$ scattering, according to the Watson theorem. At variance with elastic scattering, a negative relative sign between the S- and P-waves is measured; this is compatible with the previous theorem. In Fig. 72, the measured S-wave phase is compared with the phase of the elastic, $I = 1/2$, $K\pi$ elastic phase for different values of the $K\pi$ mass.

Contributions from other resonances decaying into $K^- \pi^+$ are considered. A small signal from the $\bar{K}^*(1410)$ is observed, compatible with expectations from τ decays and this component is included in the nominal fit. In total, 11 parameters are fitted in addition to the total number of signal events. They give a detailed description of the differential decay rate versus the 5 variables and corresponding matrices for statistical and systematic uncertainties are provided allowing to evaluate the compatibility of data with future theoretical expectations.

In Fig. 73 are compared measured values from CLEO-c of the products $q^2 H_0^2(q^2)$ and

$q^2 h_0(q^2) H_0(q^2)$ with corresponding results from *BABAR* illustrating the difference in behaviour of the scalar h_0 component and the helicity zero H_0 P-wave form factor. For this comparison, plotted values from *BABAR* for the two distributions are equal to 1 at $q^2 = 0$. The different behaviour of $h_0(q^2)$ and $H_0(q^2)$ can be explained by their different dependence in the p^* variable. Results of this analysis for the rates and few characteristics for S, P and D-waves are given in Table 177.

Table 177: Detailed determination of the properties of the $D^+ \rightarrow K^- \pi^+ e^+ \nu_e$ decay channel from *BABAR*. Values for $\mathcal{B}(D^+ \rightarrow \overline{K}^*(1410)^0 / \overline{K}_2^*(1430)^0 e^+ \nu_e)$ are corrected for their respective branching fractions into $K^- \pi^+$.

Measurement	<i>BABAR</i> result
$m_{K^*(892)^0} (MeV/c^2)$	$895.4 \pm 0.2 \pm 0.2$
$\Gamma_{K^*(892)^0}^0 (MeV/c^2)$	$46.5 \pm 0.3 \pm 0.2$
$r_{BW} (GeV/c)^{-1}$	$2.1 \pm 0.5 \pm 0.5$
r_V	$1.463 \pm 0.017 \pm 0.031$
r_2	$0.801 \pm 0.020 \pm 0.020$
$m_A (GeV/c^2)$	$2.63 \pm 0.10 \pm 0.13$
$\mathcal{B}(D^+ \rightarrow K^- \pi^+ e^+ \nu_e)(\%)$	$4.04 \pm 0.03 \pm 0.04 \pm 0.09$
$\mathcal{B}(D^+ \rightarrow K^- \pi^+ e^+ \nu_e)_{\overline{K}^{*0}}(\%)$	$3.80 \pm 0.04 \pm 0.05 \pm 0.09$
$\mathcal{B}(D^+ \rightarrow K^- \pi^+ e^+ \nu_e)_{S\text{-wave}}(\%)$	$0.234 \pm 0.007 \pm 0.007 \pm 0.005$
$\mathcal{B}(D^+ \rightarrow \overline{K}^*(1410)^0 e^+ \nu_e)(\%)$	$0.30 \pm 0.12 \pm 0.18 \pm 0.06 (< 0.6 \text{ at } 90\% \text{ C.L.})$
$\mathcal{B}(D^+ \rightarrow \overline{K}_2^*(1430)^0 e^+ \nu_e)(\%)$	$0.023 \pm 0.011 \pm 0.011 \pm 0.001 (< 0.05 \text{ at } 90\% \text{ C.L.})$

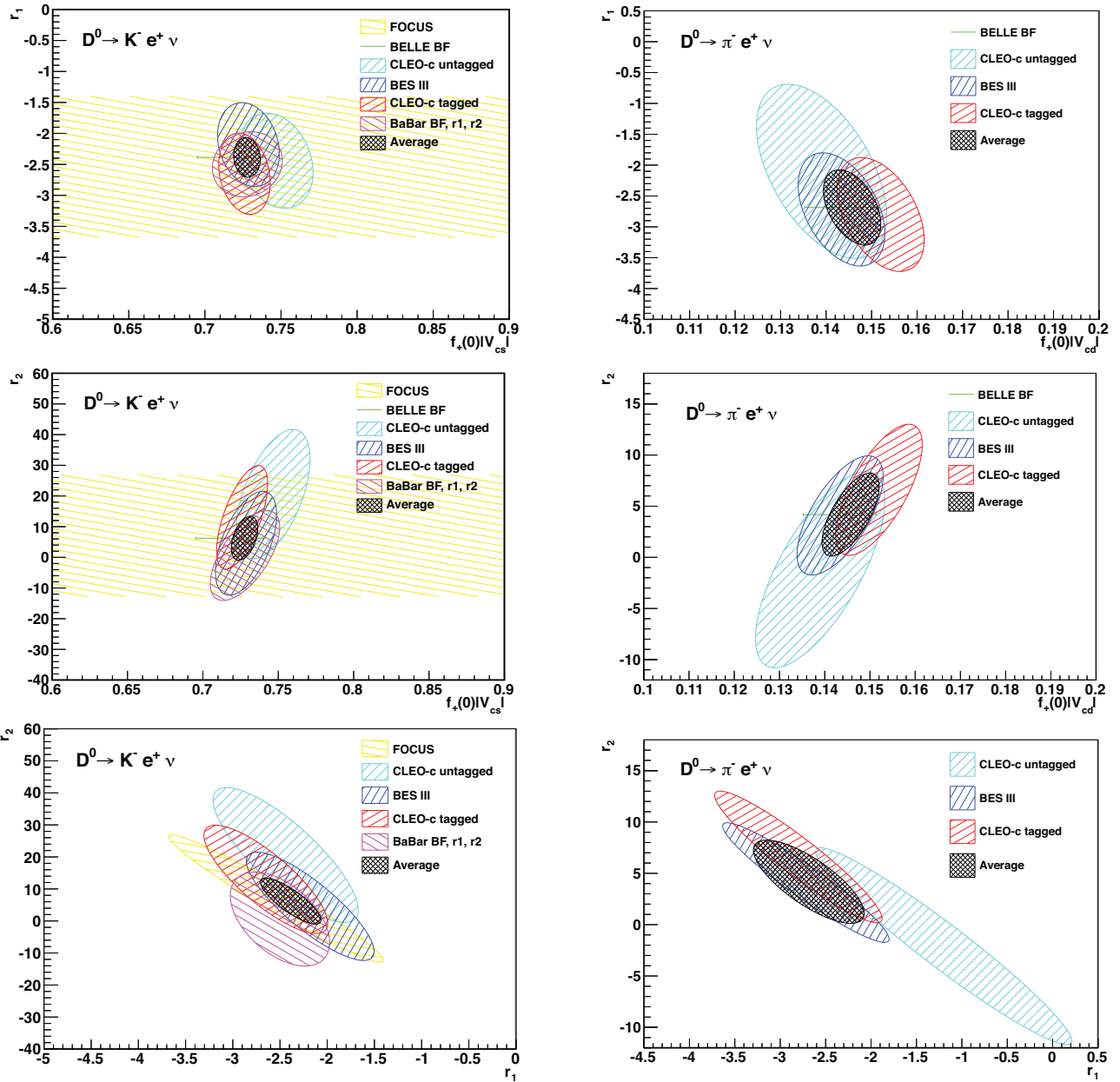


Figure 67: The $D^0 \rightarrow K^- e^+ \nu$ (left) and $D^0 \rightarrow \pi^- e^+ \nu$ (right) 68% C.L. error ellipses from the average fit of the 3-parameter z -expansion results.

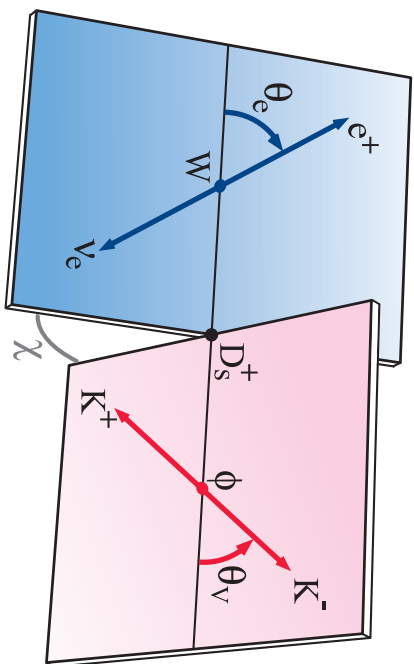
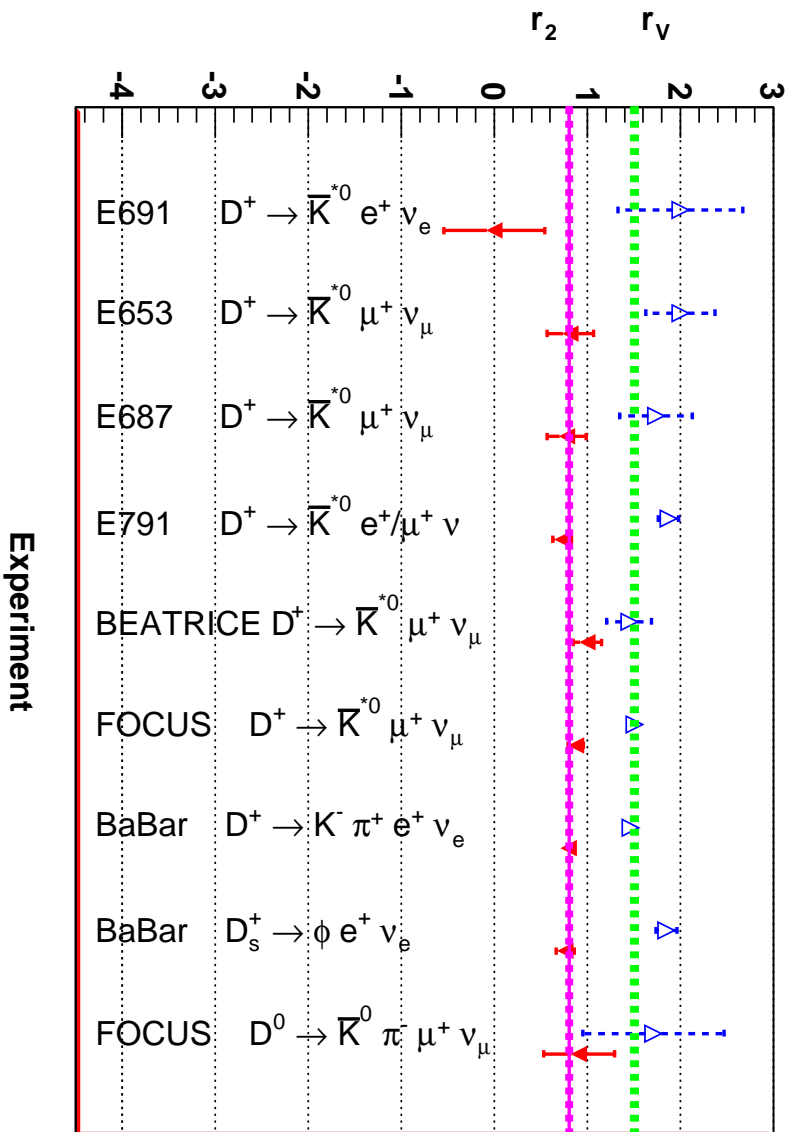


Figure 68: Decay angles θ_V , θ_l and χ . Note that the angle χ between the decay planes is defined in the D -meson reference frame, whereas the angles θ_V and θ_l are defined in the V meson and W reference frames, respectively.



Experiment

Figure 69: A comparison of r_2 and r_V values from various experiments. The first seven measurements are for $D^+ \rightarrow K^- \pi^+ l^+ \nu_l$ decays. Also shown as a line with $1\text{-}\sigma$ limits is the average of these. The last two points are D_s^+ decays and Cabibbo-suppressed D decays.

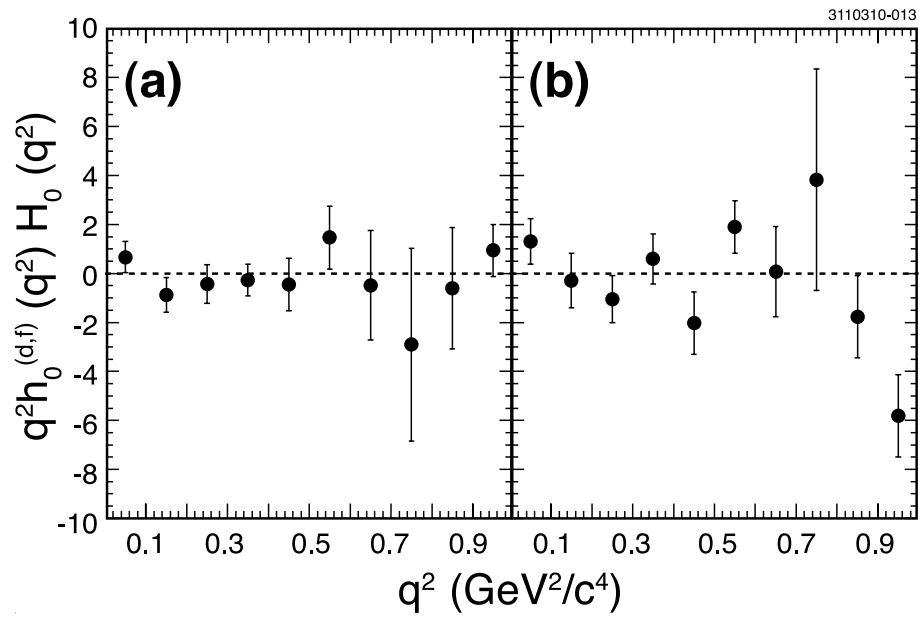
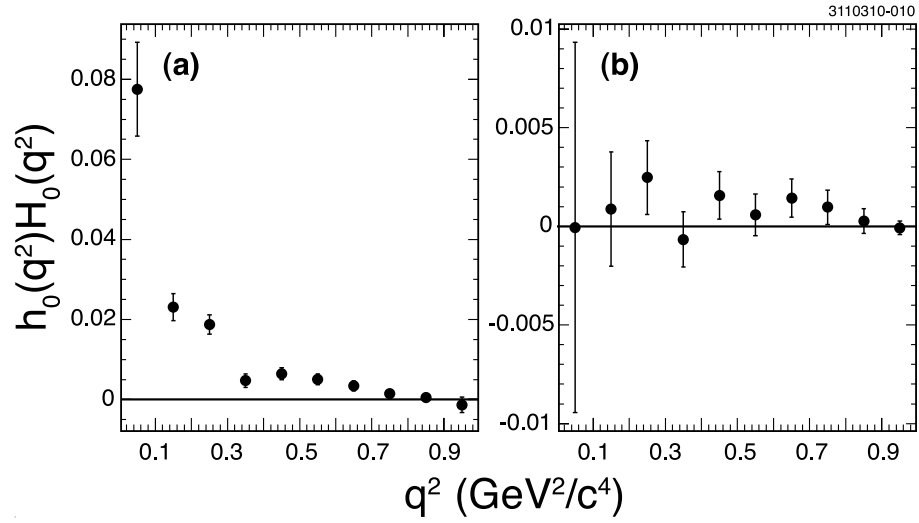


Figure 70: Model-independent form factors $h_0(q^2)$ measured by CLEO-c [518].

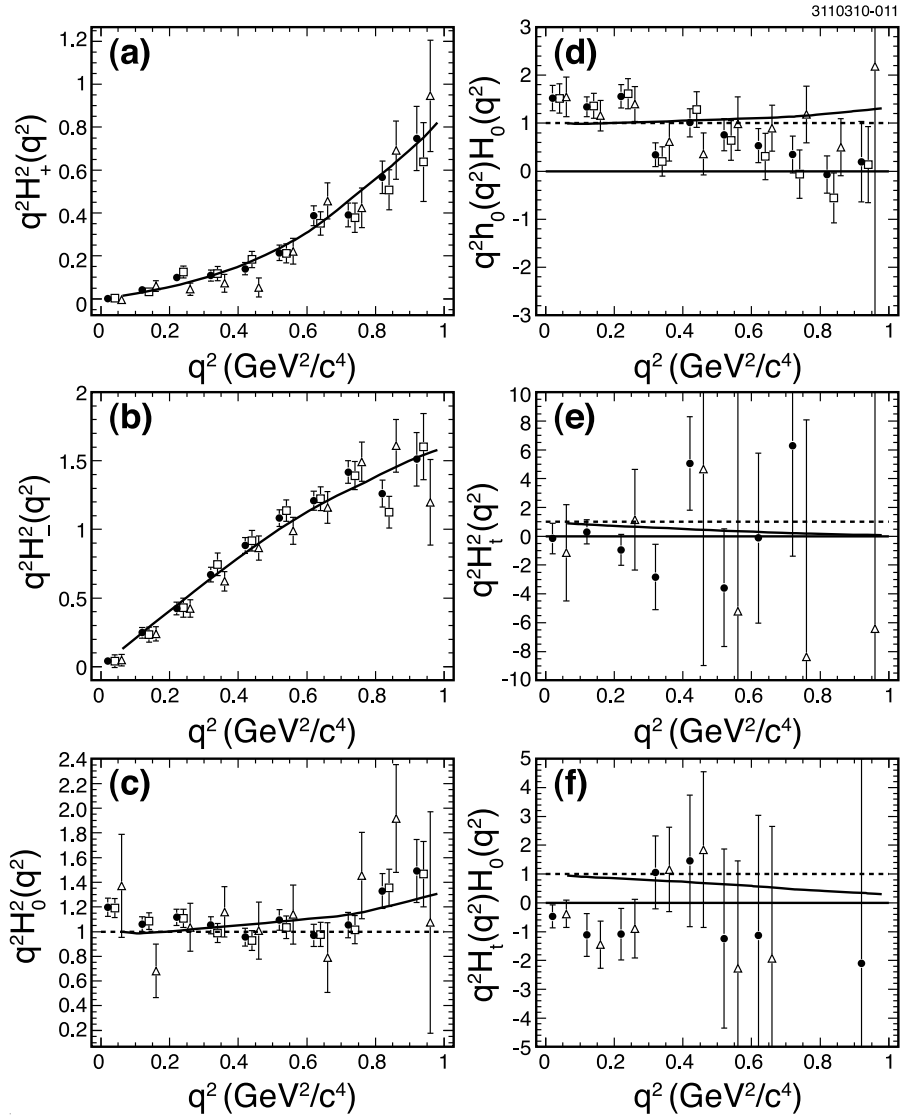


Figure 71: Model-independent form factors $H(q^2)$ measured by CLEO-c [518].

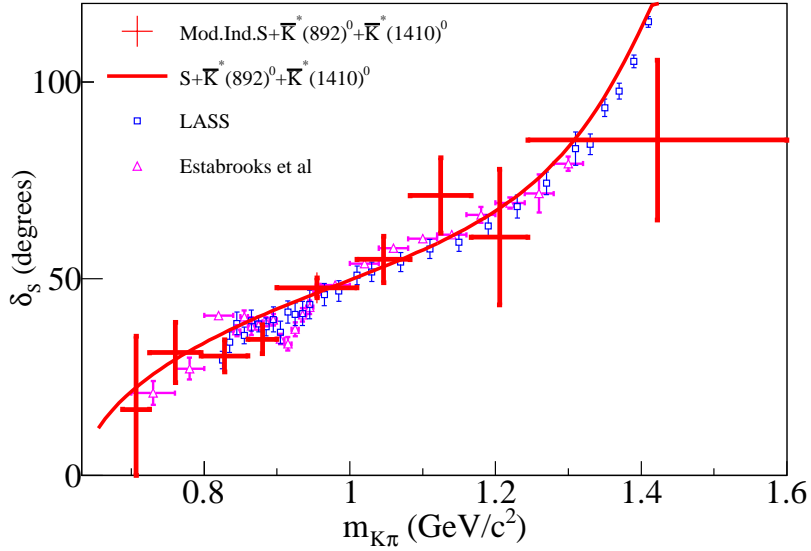


Figure 72: Points (full circles) give the *BABAR* S -wave phase variation assuming a signal containing S -wave, $\bar{K}^*(892)^0$ and $\bar{K}^*(1410)^0$ components. Error bars include systematic uncertainties. The full line corresponds to a parameterized S -wave phase variation fitted on *BABAR* data. The phase variation measured in $K\pi$ scattering by Ref. [519] (triangles) and LASS [270] (squares), after correcting for $\delta^{3/2}$, are given.

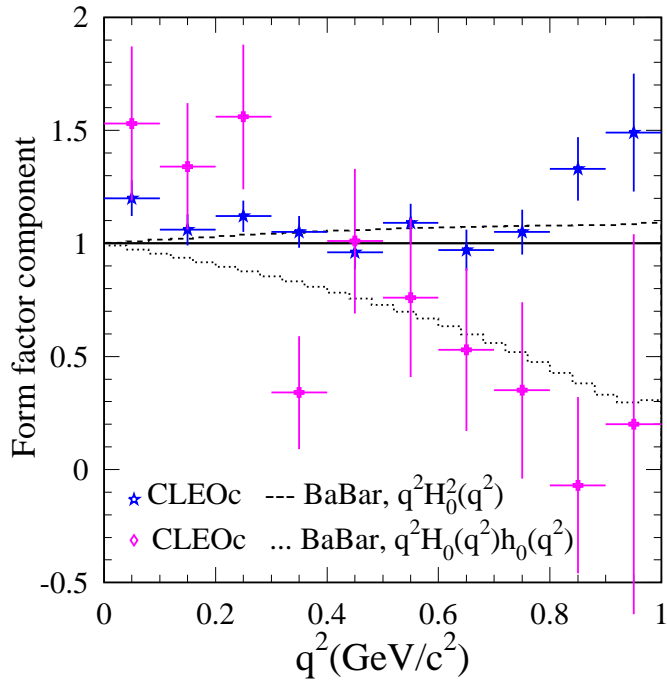


Figure 73: Comparison between CLEO-c measurements and *BABAR* results for the quantities $q^2 H_0^2(q^2)$ and $q^2 H_0(q^2) h_0(q^2)$.

8.3 CP asymmetries

CP violation occurs if the decay rate for a particle differs from that of its CP -conjugate [520]. In general there are two classes of CP violation, termed *indirect* and *direct* [521]. Indirect CP violation refers to $\Delta C = 2$ processes and arises in D^0 decays due to D^0 - \bar{D}^0 mixing. It can occur as an asymmetry in the mixing itself, or it can result from interference between a decay amplitude arising via mixing and a non-mixed amplitude. Direct CP violation refers to $\Delta C = 1$ processes and occurs in both charged and neutral D decays. It results from interference between two different decay amplitudes (e.g., a penguin and tree amplitude) that have different weak (CKM) and strong phases⁴⁷. A difference in strong phases typically arises due to final-state interactions (FSI) [522]. A difference in weak phases arises from different CKM vertex couplings, as is often the case for spectator and penguin diagrams.

The CP asymmetry is defined as the difference between D and \bar{D} partial widths divided by their sum:

$$A_{CP} = \frac{\Gamma(D) - \Gamma(\bar{D})}{\Gamma(D) + \Gamma(\bar{D})}. \quad (205)$$

However, to take into account differences in production rates between D and \bar{D} (which would affect the number of respective decays observed), experiments usually normalize to a Cabibbo-favored mode. In this case there is the additional benefit that most corrections due to inefficiencies cancel out, reducing systematic uncertainties. An implicit assumption is that there is no measurable CP violation in the Cabibbo-favored normalizing mode. The CP asymmetry is calculated as

$$A_{CP} = \frac{\eta(D) - \eta(\bar{D})}{\eta(D) + \eta(\bar{D})}, \quad (206)$$

where (considering, for example, $D^0 \rightarrow K^- K^+$)

$$\eta(D) = \frac{N(D^0 \rightarrow K^- K^+)}{N(D^0 \rightarrow K^- \pi^+)}, \quad (207)$$

$$\eta(\bar{D}) = \frac{N(\bar{D}^0 \rightarrow K^- K^+)}{N(\bar{D}^0 \rightarrow K^+ \pi^-)}. \quad (208)$$

In the case of D^+ and D_s^+ decays, A_{CP} measures direct CP violation; in the case of D^0 decays, A_{CP} measures direct and indirect CP violation combined. Values of A_{CP} for D^+ , D^0 and D_s^+ decays are listed in Tables 178, 179 and 180 respectively.

⁴⁷The weak phase difference will have opposite signs for $D \rightarrow f$ and $\bar{D} \rightarrow \bar{f}$ decays, while the strong phase difference will have the same sign. As a result, squaring the total amplitudes to obtain the decay rates gives interference terms having opposite sign, i.e., non-identical decay rates.

Table 178: CP asymmetries $A_{CP} = [\Gamma(D^+) - \Gamma(D^-)]/[\Gamma(D^+) + \Gamma(D^-)]$ for D^\pm decays.

Mode	Year	Collaboration	A_{CP}
$D^+ \rightarrow \mu^+\nu$	2008	CLEOc [523]	$+0.08 \pm 0.08$
$D^+ \rightarrow \pi^+\pi^0$	2010	CLEOc [524]	$+0.029 \pm 0.029 \pm 0.003$
$D^+ \rightarrow \pi^+\eta$	2010	CLEOc [524]	$-0.020 \pm 0.023 \pm 0.003$
$D^+ \rightarrow \pi^+\eta'$	2010	CLEOc [524]	$-0.040 \pm 0.034 \pm 0.003$
$D^+ \rightarrow K^+\pi^0$	2010	CLEOc [524]	$-0.035 \pm 0.107 \pm 0.009$
$D^+ \rightarrow K_s^0\pi^+$	2011	BABAR [525]	$-0.0044 \pm 0.0013 \pm 0.0010$
	2010	Belle [526]	$-0.0071 \pm 0.0019 \pm 0.0020$
	2010	CLEOc [524]	$-0.013 \pm 0.007 \pm 0.003$
	2002	FOCUS [527]	$-0.016 \pm 0.015 \pm 0.009$
		COMBOS average	-0.0054 ± 0.0014
$D^+ \rightarrow K_s^0K^+$	2010	Belle [526]	$-0.0016 \pm 0.0058 \pm 0.0025$
	2010	CLEOc [524]	$-0.002 \pm 0.015 \pm 0.009$
	2002	FOCUS [527]	$+0.071 \pm 0.061 \pm 0.012$
		COMBOS average	-0.0010 ± 0.0059
$D^+ \rightarrow \pi^+\pi^-\pi^+$	1997	E791 [528]	-0.017 ± 0.042 (stat.)
$D^+ \rightarrow K^-\pi^+\pi^+$	2010	CLEOc [524]	$-0.001 \pm 0.004 \pm 0.009$
$D^+ \rightarrow K_s^0\pi^+\pi^0$	2007	CLEO-c [529]	$+0.003 \pm 0.009 \pm 0.003$
$D^+ \rightarrow K^+K^-\pi^+$	2008	CLEO-c [530]	$-0.0003 \pm 0.0084 \pm 0.0029$
	2005	BABAR [531]	$+0.014 \pm 0.010 \pm 0.008$
	2000	FOCUS [532]	$+0.006 \pm 0.011 \pm 0.005$
	1997	E791 [528]	-0.014 ± 0.029 (stat.)
	1994	E687 [533]	-0.031 ± 0.068 (stat.)
		COMBOS average	$+0.0039 \pm 0.0061$
$D^+ \rightarrow K^-\pi^+\pi^+\pi^0$	2007	CLEOc [529]	$+0.010 \pm 0.009 \pm 0.009$
$D^+ \rightarrow K_s^0\pi^+\pi^+\pi^-$	2007	CLEOc [529]	$+0.001 \pm 0.011 \pm 0.006$
$D^+ \rightarrow K_s^0K^+\pi^+\pi^-$	2005	FOCUS [534]	$-0.042 \pm 0.064 \pm 0.022$

Table 179: CP asymmetries $A_{CP} = [\Gamma(D^0) - \Gamma(\bar{D}^0)]/[\Gamma(D^0) + \Gamma(\bar{D}^0)]$ for D^0, \bar{D}^0 decays.

Mode	Year	Collaboration	A_{CP}
$D^0 \rightarrow \pi^+\pi^-$	2012	CDF [535]	$+0.0022 \pm 0.0024 \pm 0.0011$
	2008	Belle [472]	$+0.0043 \pm 0.0052 \pm 0.0012$
	2008	BABAR [471]	$-0.0024 \pm 0.0052 \pm 0.0022$
	2002	CLEO [467]	$+0.019 \pm 0.032 \pm 0.008$
	2000	FOCUS [532]	$+0.048 \pm 0.039 \pm 0.025$
	1998	E791 [536]	$-0.049 \pm 0.078 \pm 0.030$
			COMBOS average
$D^0 \rightarrow \pi^0\pi^0$	2001	CLEO [537]	$+0.001 \pm 0.048$ (stat. and syst. combined)
$D^0 \rightarrow K_s^0\pi^0$	2011	Belle [538]	$-0.0028 \pm 0.0019 \pm 0.0010$
	2001	CLEO [537]	$+0.001 \pm 0.013$ (stat. and syst. combined)
		COMBOS average	-0.0027 ± 0.0021
$D^0 \rightarrow K_s^0\eta$	2011	Belle [538]	$+0.0054 \pm 0.0051 \pm 0.0016$
$D^0 \rightarrow K_s^0\eta'$	2011	Belle [538]	$+0.0098 \pm 0.0067 \pm 0.0014$
$D^0 \rightarrow K_s^0K_s^0$	2001	CLEO [537]	-0.23 ± 0.19 (stat. and syst. combined)
$D^0 \rightarrow K^+K^-$	2012	CDF [535]	$-0.0024 \pm 0.0022 \pm 0.0009$
	2008	Belle [472]	$-0.0043 \pm 0.0030 \pm 0.0011$
	2008	BABAR [471]	$+0.0000 \pm 0.0034 \pm 0.0013$
	2002	CLEO [467]	$+0.000 \pm 0.022 \pm 0.008$
	2000	FOCUS [532]	$-0.001 \pm 0.022 \pm 0.015$
	1998	E791 [536]	$-0.010 \pm 0.049 \pm 0.012$
	1995	CLEO [539]	$+0.080 \pm 0.061$ (stat.)
	1994	E687 [533]	$+0.024 \pm 0.084$ (stat.)
			COMBOS average
$D^0 \rightarrow \pi^+\pi^-\pi^0$	2008	BABAR [540]	$-0.0031 \pm 0.0041 \pm 0.0017$
	2008	Belle [541]	$+0.0043 \pm 0.0130$
	2005	CLEO [542]	$+0.001^{+0.09}_{-0.07} \pm 0.05$
		COMBOS average	-0.0023 ± 0.0042
$D^0 \rightarrow K^-\pi^+\pi^0$	2007	CLEOc [529]	$+0.002 \pm 0.004 \pm 0.008$
	2001	CLEO [543]	-0.031 ± 0.086 (stat.)
		COMBOS average	$+0.0016 \pm 0.0089$
$D^0 \rightarrow K^+\pi^-\pi^0$	2005	Belle [544]	-0.006 ± 0.053 (stat.)
	2001	CLEO [545]	$+0.09^{+0.25}_{-0.22}$ (stat.)
		COMBOS average	-0.0014 ± 0.0517
$D^0 \rightarrow K_s^0\pi^+\pi^-$	2004	CLEO [546]	$-0.009 \pm 0.021^{+0.016}_{-0.057}$
$D^0 \rightarrow K^+K^-\pi^0$	2008	BABAR [540]	$0.0100 \pm 0.0167 \pm 0.0025$
$D^0 \rightarrow K^+\pi^-\pi^+\pi^-$	2005	Belle [544]	-0.018 ± 0.044 (stat.)
$D^0 \rightarrow K^+K^-\pi^+\pi^-$	2005	FOCUS [534]	$-0.082 \pm 0.056 \pm .047$

Table 180: CP asymmetries $A_{CP} = [\Gamma(D_s^+) - \Gamma(D_s^-)]/[\Gamma(D_s^+) + \Gamma(D_s^-)]$ for D_s^\pm decays.

Mode	Year	Collaboration	A_{CP}
$D_s^+ \rightarrow \mu^+ \nu$	2009	CLEOc [547]	$+0.048 \pm 0.061$
$D_s^+ \rightarrow \pi^+ \eta$	2010	CLEOc [524]	$-0.046 \pm 0.029 \pm 0.003$
$D_s^+ \rightarrow \pi^+ \eta'$	2010	CLEOc [524]	$-0.061 \pm 0.030 \pm 0.003$
$D_s^+ \rightarrow K_s^0 \pi^+$	2010	Belle [526]	$+0.0545 \pm 0.0250 \pm 0.0033$
	2010	CLEOc [524]	$+0.163 \pm 0.073 \pm 0.003$
		COMBOS average	$+0.066 \pm 0.024$
$D_s^+ \rightarrow K^+ \pi^0$	2010	CLEOc [524]	$+0.266 \pm 0.228 \pm 0.009$
$D_s^+ \rightarrow K^+ \eta$	2010	CLEOc [524]	$+0.093 \pm 0.152 \pm 0.009$
$D_s^+ \rightarrow K^+ \eta'$	2010	CLEOc [524]	$+0.060 \pm 0.189 \pm 0.009$
$D_s^+ \rightarrow K^+ K_s^0$	2010	Belle [526]	$+0.0012 \pm 0.0036 \pm 0.0022$
	2010	CLEOc [524]	$+0.047 \pm 0.018 \pm 0.009$
		COMBOS average	$+0.0031 \pm 0.0041$
$D_s^+ \rightarrow \pi^+ \pi^+ \pi^-$	2008	CLEOc [548]	$+0.020 \pm 0.046 \pm 0.007$
$D_s^+ \rightarrow K^+ \pi^+ \pi^-$	2008	CLEOc [548]	$+0.112 \pm 0.070 \pm 0.009$
$D_s^+ \rightarrow K^+ K^- \pi^+$	2008	CLEOc [548]	$+0.003 \pm 0.011 \pm 0.008$
$D_s^+ \rightarrow K_s^0 K^- \pi^+ \pi^+$	2008	CLEOc [548]	$-0.007 \pm 0.036 \pm 0.011$
$D_s^+ \rightarrow K^+ K^- \pi^+ \pi^0$	2008	CLEOc [548]	$-0.059 \pm 0.042 \pm 0.012$

8.4 T -violating asymmetries

T -violating asymmetries are measured using triple-product correlations and assuming the validity of the CPT theorem. Triple-product correlations of the form $\vec{a} \cdot (\vec{b} \times \vec{c})$, where a , b , and c are spins or momenta, are odd under time reversal (T). For example, for $D^0 \rightarrow K^+ K^- \pi^+ \pi^-$ decays, $C_T \equiv \vec{p}_{K^+} \cdot (\vec{p}_{\pi^+} \times \vec{p}_{\pi^-})$ changes sign (i.e., is odd) under a T transformation. The corresponding quantity for \bar{D}^0 is $\bar{C}_T \equiv \vec{p}_{K^-} \cdot (\vec{p}_{\pi^-} \times \vec{p}_{\pi^+})$. Defining

$$A_T = \frac{\Gamma(C_T > 0) - \Gamma(C_T < 0)}{\Gamma(C_T > 0) + \Gamma(C_T < 0)} \quad (209)$$

for D^0 decay and

$$\bar{A}_T = \frac{\Gamma(-\bar{C}_T > 0) - \Gamma(-\bar{C}_T < 0)}{\Gamma(-\bar{C}_T > 0) + \Gamma(-\bar{C}_T < 0)} \quad (210)$$

for \bar{D}^0 decay, in the absence of strong phases either $A_T \neq 0$ or $\bar{A}_T \neq 0$ indicates T violation. In these expressions the Γ 's are partial widths. The asymmetry

$$A_{T \text{ viol}} \equiv \frac{A_T - \bar{A}_T}{2} \quad (211)$$

tests for T violation even with nonzero strong phases (see Refs. [549–553]). Values of $A_{T \text{ viol}}$ for some D^+ , D_s^+ , and D^0 decay modes are listed in Table 181.

Table 181: T -violating asymmetries $A_{T \text{ viol}} = (A_T - \bar{A}_T)/2$.

Mode	Year	Collaboration	$A_{T \text{ viol}}$
$D^0 \rightarrow K^+ K^- \pi^+ \pi^-$	2010	<i>BABAR</i> [554]	$+0.0010 \pm 0.0051 \pm 0.0044$
	2005	FOCUS [534]	$+0.010 \pm 0.057 \pm 0.037$
		COMBOS average	$+0.0011 \pm 0.0067$
$D^+ \rightarrow K_s^0 K^+ \pi^+ \pi^-$	2010	<i>BABAR</i> [555]	$-0.0120 \pm 0.0100 \pm 0.0046$
	2005	FOCUS [534]	$+0.023 \pm 0.062 \pm 0.022$
		COMBOS average	-0.0110 ± 0.0109
$D_s^+ \rightarrow K_s^0 K^+ \pi^+ \pi^-$	2010	<i>BABAR</i> [555]	$-0.0136 \pm 0.0077 \pm 0.0034$
	2005	FOCUS [534]	$-0.036 \pm 0.067 \pm 0.023$
		COMBOS average	-0.0139 ± 0.0084

8.5 World average for the D_s^+ decay constant f_{D_s}

The Heavy Flavor Averaging Group has used measurements of the branching fractions $\mathcal{B}(D_s^+ \rightarrow \mu^+\nu)$ [547,556,557] and $\mathcal{B}(D_s^+ \rightarrow \tau^+\nu)$ [547,556–560] from Belle, *BABAR*, and CLEO to calculate a world average (WA) value for the D_s^+ decay constant f_{D_s} . We do not use older results from the ALEPH [561], BEATRICE [562], OPAL [563], and L3 [564] experiments as the errors are large and these measurements have some unknown systematic errors.

The value for f_{D_s} is calculated using the formula

$$f_{D_s} = \frac{1}{G_F |V_{cs}| m_\ell \left(1 - \frac{m_\ell^2}{m_{D_s}^2}\right)} \sqrt{\frac{8\pi \mathcal{B}(D_s^+ \rightarrow \ell^+\nu)}{m_{D_s} \tau_{D_s}}}, \quad (212)$$

where $\ell^+ = \mu^+$ or τ^+ . For $\mathcal{B}(D_s^+ \rightarrow \ell^+\nu)$ we use the WA values obtained below. The error on f_{D_s} is calculated as follows: values for variables on the right-hand-side of Eq. (212) are sampled from Gaussian distributions having mean values equal to the central values and standard deviations equal to their respective errors. The resulting values of f_{D_s} are plotted, and the r.m.s. of the distribution is taken as the $\pm 1\sigma$ errors on f_{D_s} . The procedure is done separately for $\mathcal{B}(D_s^+ \rightarrow \mu^+\nu)$ and $\mathcal{B}(D_s^+ \rightarrow \tau^+\nu)$; the resulting two values for f_{D_s} are averaged together using COMBOS [565], which accounts for correlations such as the values of $|V_{cs}|$, m_{D_s} , and τ_{D_s} used⁴⁸ in Eq. (212). The result is plotted in Fig. 74. The WA value is

$$f_{D_s} = 255.6 \pm 4.2 \text{ MeV}, \quad (213)$$

where the statistical and systematic errors are combined.

The WA value for $\mathcal{B}(D_s^+ \rightarrow \mu^+\nu)$ is calculated from CLEOc [547], Belle [557], and *BABAR* [556] measurements of absolute branching fractions. These measurements are *not* normalized to $D_s^+ \rightarrow \phi\pi^+$ decays as was done for earlier measurements, and thus they do not have uncertainties due to the non-resonant $D_s^+ \rightarrow K^+K^-\pi^+$ contribution. All input values and the result are plotted in Fig. 75. The WA value is $\mathcal{B}(D_s^+ \rightarrow \mu^+\nu) = (0.554 \pm 0.024)\%$.

The WA value for $\mathcal{B}(D_s^+ \rightarrow \tau^+\nu)$ is also calculated from CLEOc, Belle, and *BABAR* measurements. CLEOc made separate measurements for $\tau^+ \rightarrow e^+\nu\bar{\nu}$ [559], $\tau^+ \rightarrow \pi^+\nu$ [547], and $\tau^+ \rightarrow \rho^+\nu$ [558]; *BABAR* made separate measurements for $\tau^+ \rightarrow \mu^+\nu\bar{\nu}$ [556] and $\tau^+ \rightarrow e^+\nu\bar{\nu}$ [556,560]; and Belle made separate measurements for $\tau^+ \rightarrow \mu^+\nu\bar{\nu}$, $\tau^+ \rightarrow e^+\nu\bar{\nu}$, and $\tau^+ \rightarrow \pi^+\nu$ [557]. All input values and the result are plotted in Fig. 76. The WA value is $\mathcal{B}(D_s^+ \rightarrow e^+\nu) = (5.44 \pm 0.22)\%$.

⁴⁸These values (taken from the PDG [18]) are $|V_{cs}| = 0.97345^{+0.00015}_{-0.00016}$; $m_\tau = (1.77682 \pm 0.00016) \text{ GeV}/c^2$; $m_{D_s} = (1.96847 \pm 0.00033) \text{ GeV}/c^2$; and $\tau_{D_s} = (500 \pm 7) \times 10^{-15} \text{ s}$.

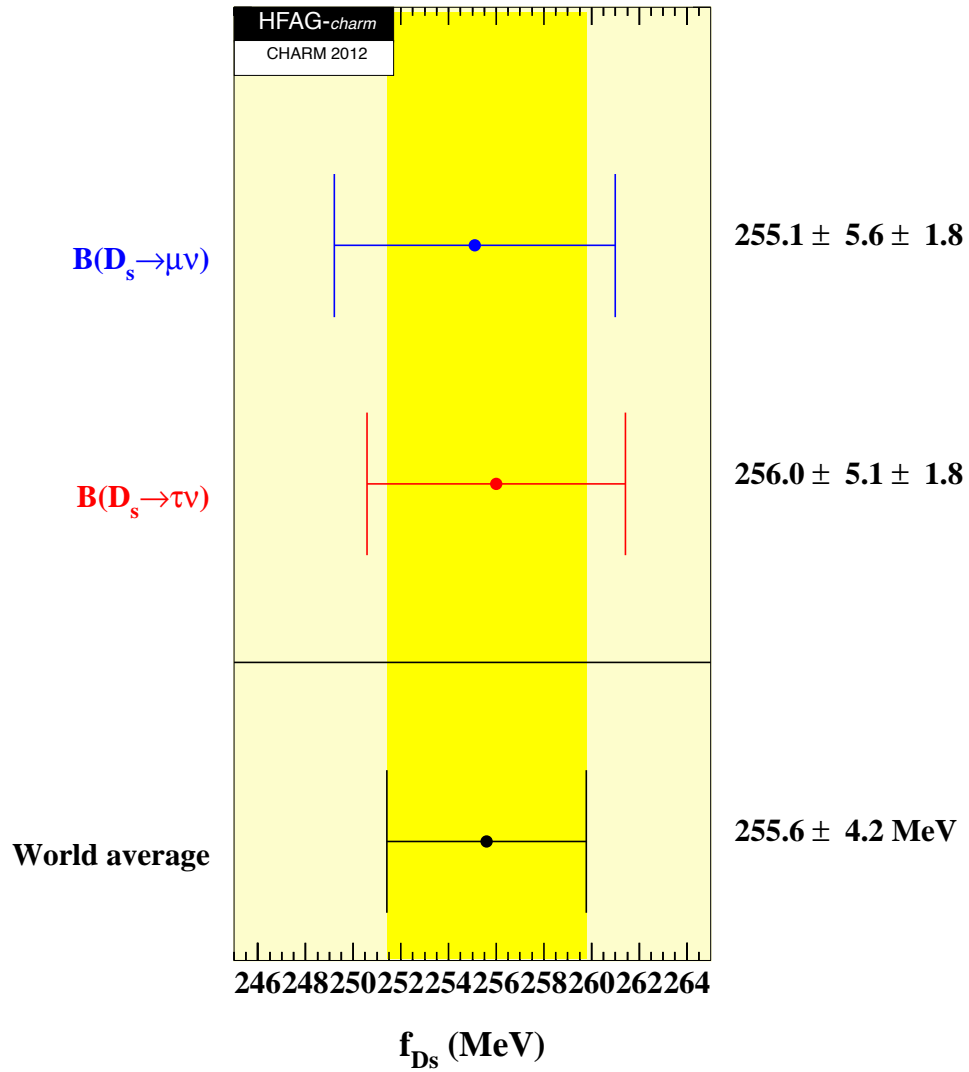


Figure 74: WA value for f_{D_s} . For each measurement, the first error listed is the total uncorrelated error, and the second error is the total correlated error (mostly from τ_{D_s}).

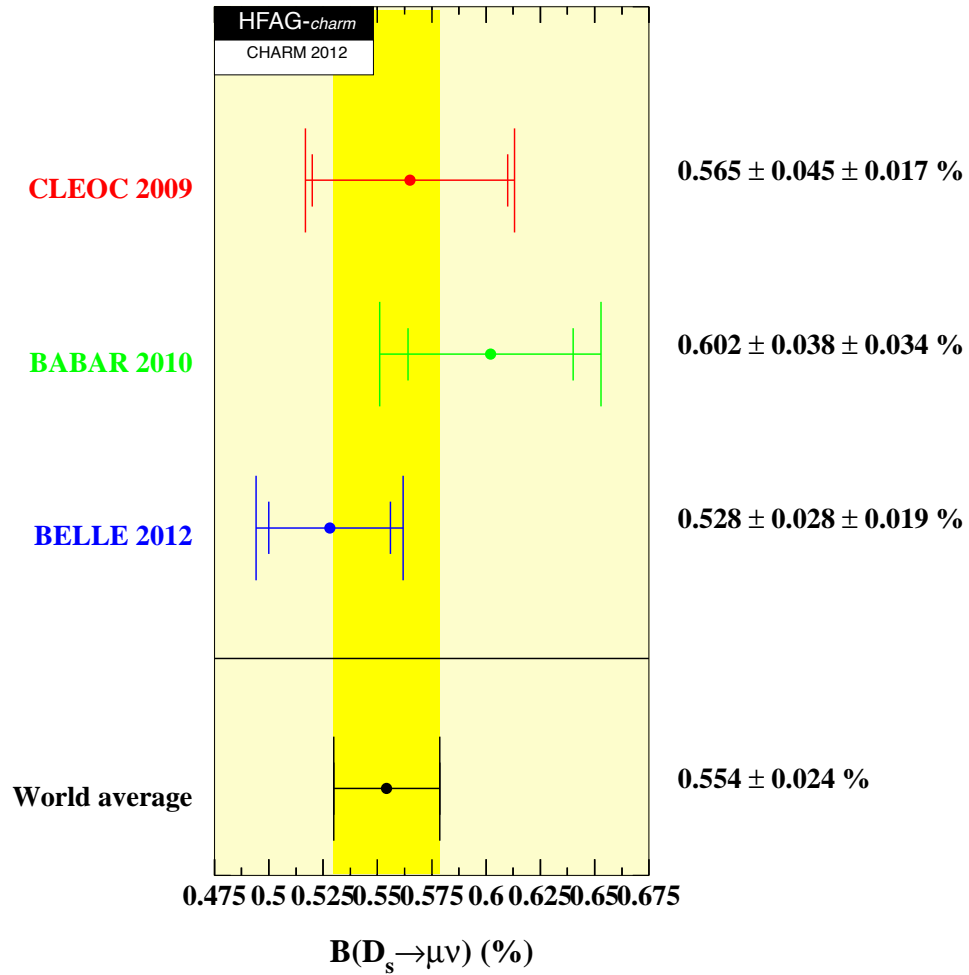


Figure 75: WA value for $\mathcal{B}(D_s^+ \rightarrow \mu^+ \nu)$, as calculated from Refs. [547, 556, 557]. When two errors are listed, the first one is statistical and the second is systematic.

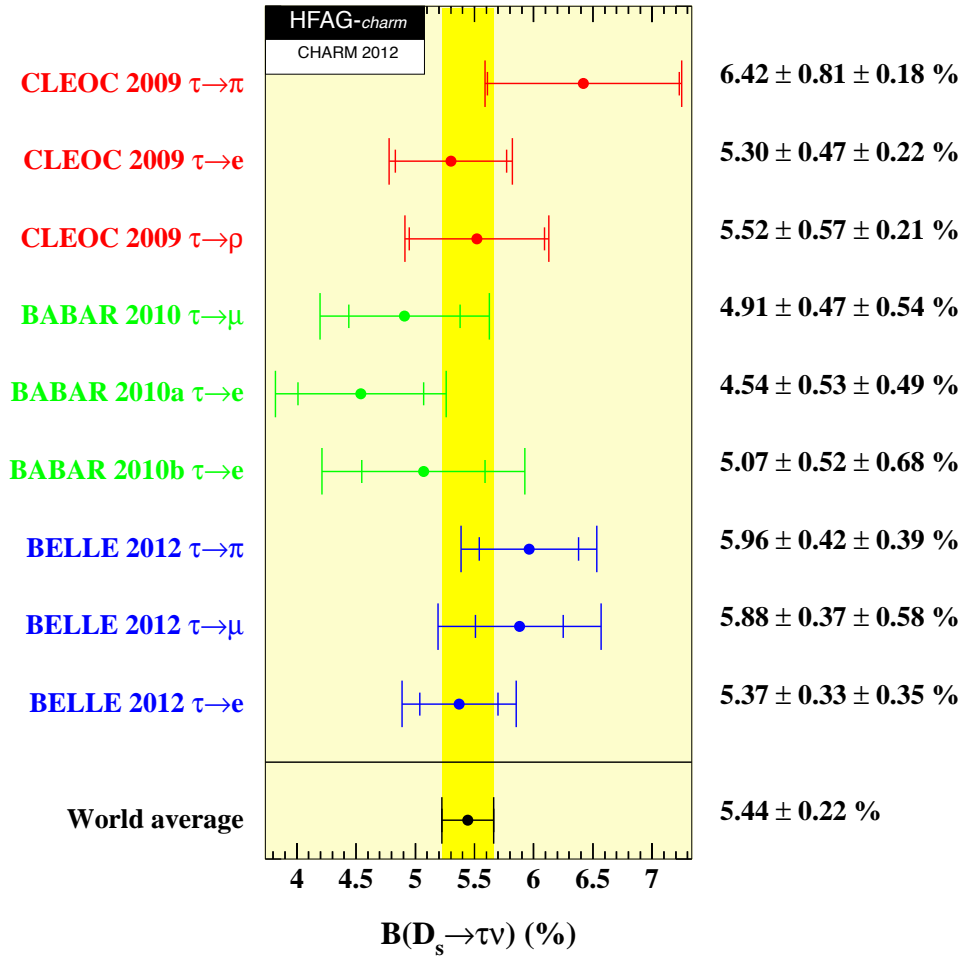


Figure 76: WA value for $\mathcal{B}(D_s^+ \rightarrow \tau^+ \nu)$, as calculated from Refs. [547, 556–560]. When two errors are listed, the first one is statistical and the second is systematic.

8.6 Two-body hadronic D^0 decays and final state radiation

Branching fractions measurements for $D^0 \rightarrow K^-\pi^+$, $D^0 \rightarrow \pi^+\pi^-$ and $D^0 \rightarrow K^+K^-$ have reached sufficient precision to allow averages with $\mathcal{O}(1\%)$ relative uncertainties. At these precisions, Final State Radiation (FSR) must be treated correctly and consistently across the input measurements for the accuracy of the averages to match the precision. The sensitivity of measurements to FSR arises because of a tail in the distribution of radiated energy that extends to the kinematic limit. The tail beyond $E_\gamma \approx 30$ MeV causes typical selection variables like the hadronic invariant mass to shift outside the selection range dictated by experimental resolution (see Fig. 77). While the differential rate for the tail is small, the integrated rate amounts to several percent of the total $h^+h^-(n\gamma)$ rate because of the tail's extent. The tail therefore translates directly into a several percent loss in experimental efficiency.

All measurements that include an FSR correction have a correction based on use of PHOTOS [566–569] within the experiment's Monte Carlo simulation. PHOTOS itself, however, has evolved, over the period spanning the set of measurements. In particular, incorporation of interference between radiation off of the two separate mesons has proceeded in stages: it was first available for particle–antiparticle pairs in version 2.00 (1993), and extended to any two body, all charged, final states in version 2.02 (1999). The effects of interference are clearly visible (Figure 77), and cause a roughly 30% increase in the integrated rate into the high energy photon tail. To evaluate the FSR correction incorporated into a given measurement, we must therefore note whether any correction was made, the version of PHOTOS used in correction, and whether the interference terms in PHOTOS were turned on.

8.6.1 Branching fraction corrections

Before averaging the measured branching fractions, the published results are updated, as necessary, to the FSR prediction of PHOTOS 2.15 with interference included. The correction will always shift a branching fraction to a higher value: with no FSR correction or with no interference term in the correction, the experimental efficiency determination will be biased high, and therefore the branching fraction will be biased low.

Most of the branching fraction analyses used the kinematic quantity sensitive to FSR in the candidate selection criteria. For the analyses at the $\psi(3770)$, the variable was ΔE , the difference between the candidate D^0 energy and the beam energy (*e.g.*, $E_K + E_\pi - E_{\text{beam}}$ for $D^0 \rightarrow K^-\pi^+$). In the remainder of the analyses, the relevant quantity was the reconstructed hadronic two-body mass $m_{h^+h^-}$. To correct we need only to evaluate the fraction of decays that FSR moves outside of the range accepted for the analysis.

The corrections were evaluated using an event generator (EvtGen [570]) that incorporates PHOTOS to simulate the portions of the decay process most relevant to the correction. We compared corrections determined both with and without smearing to account for experimental resolution. The differences were negligible, typically of order of a 1% of the correction itself. The immunity of the correction to resolution effects comes about because most of the long FSR-induced tail in, for example, the $m_{h^+h^-}$ distribution resides well away from the selection boundaries. The smearing from resolution, on the other hand, mainly affects the distribution of events right at the boundary.

For measurements incorporating an FSR correction that did not include interference, we update by assessing the FSR-induced efficiency loss for both the PHOTOS version and configuration used in the analysis and our nominal version 2.15 with interference. For measurements

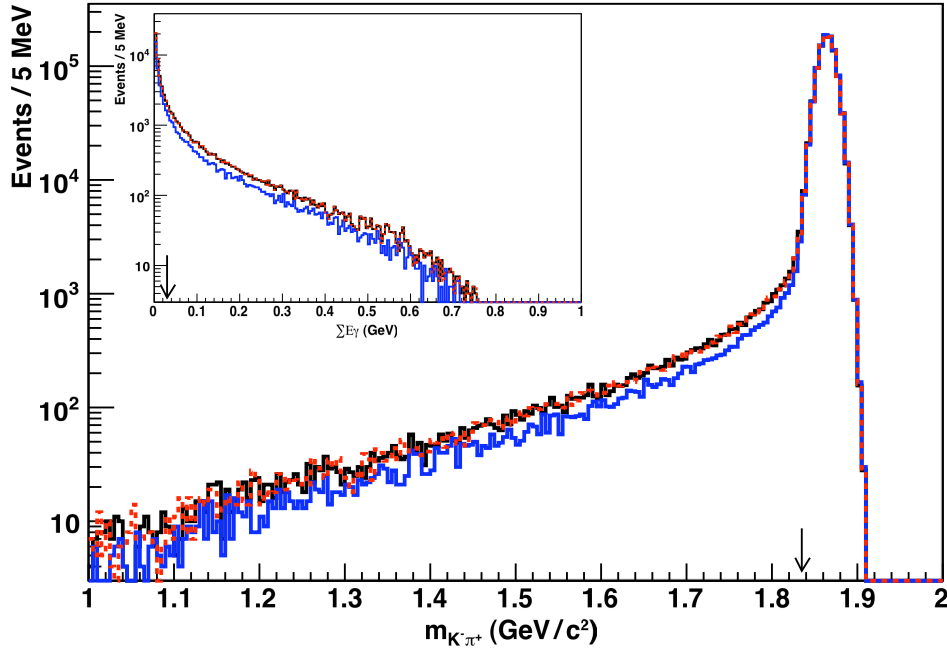


Figure 77: The $K\pi$ invariant mass distribution for $D^0 \rightarrow K^-\pi^+(n\gamma)$ decays. The 3 curves correspond to three different configurations of PHOTOS for modeling FSR: version 2.02 without interference (blue), version 2.02 with interference (red dashed) and version 2.15 with interference (black). The true invariant mass has been smeared with a typical experimental resolution of $10 \text{ MeV}/c^2$. Inset: The corresponding spectrum of total energy radiated per event. The arrow indicates the E_γ value that begins to shift kinematic quantities outside of the range typically accepted in a measurement.

that published their sensitivity to FSR, our generator-level predictions for the original efficiency loss agreed to within a few percent (of the correction). This agreement lends additional credence to the procedure.

Once the event loss from FSR in the most sensitive kinematic quantity is accounted for, the event loss from other quantities is very small. Analyses using D^* tags, for example, showed little sensitivity to FSR in the reconstructed $D^* - D^0$ mass difference: for example, in $m_{K^-\pi^+\pi^+} - m_{K^-\pi^+}$. Because the effect of FSR tends to cancel in the difference of the reconstructed masses, this difference showed a much smaller sensitivity than the two body mass even before a two body mass requirement. In the $\psi(3770)$ analyses, the beam-constrained mass distributions ($\sqrt{E_{\text{beam}}^2 - |\vec{p}_K + \vec{p}_\pi|^2}$) showed little further sensitivity.

The FOCUS [571] analysis of the branching ratios $\mathcal{B}(D^0 \rightarrow \pi^+\pi^-)/\mathcal{B}(D^0 \rightarrow K^-\pi^+)$ and $\mathcal{B}(D^0 \rightarrow K^+K^-)/\mathcal{B}(D^0 \rightarrow K^-\pi^+)$ obtained yields using fits to the two body mass distributions. FSR will both distort the low end of the signal mass peak, and will contribute a signal component to the low side tail used to estimate the background. The fitting procedure is not sensitive to signal events out in the FSR tail, which would be counted as part of the background.

A more complex toy Monte Carlo procedure was required to analyze the effect of FSR on the fitted yields, which were published with no FSR corrections applied. A detailed description of the procedure and results is available on the HFAG web page, and a brief summary is provided here. Determining the correction involved an iterative procedure in which samples of similar

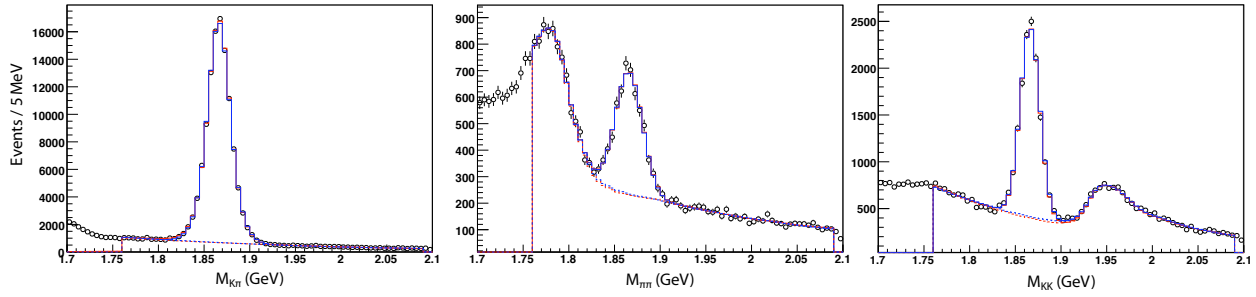


Figure 78: FOCUS data (dots), original fits (blue) and toy MC parameterization (red) for $D^0 \rightarrow K^- \pi^+$ (left), $D^0 \rightarrow \pi^+ \pi^-$ (center) and $D^0 \rightarrow \pi^+ \pi^-$ (right).

size to the FOCUS sample were generated and then fit using the FOCUS signal and background parameterizations. The MC parameterizations were tuned based on differences between the fits to the toy MC data and the FOCUS fits, and the procedure was repeated. These steps were iterated until the fit parameters matched the original FOCUS parameters.

The toy MC samples for the first iteration were based on the generator-level distribution of $m_{K^- \pi^+}$, $m_{\pi^+ \pi^-}$ and $m_{K^+ K^-}$, including the effects of FSR, smeared according to the original FOCUS resolution function, and on backgrounds thrown using the parameterization from the final FOCUS fits. For each iteration, 400 to 1600 individual data-sized samples were thrown and fit. The means of the parameters from these fits determined the corrections to the generator parameters for the following iteration. The ratio between the number of signal events generated and the final signal yield provides the required FSR correction in the final iteration. Only a few iterations were required in each mode. Figure 78 shows the FOCUS data, the published FOCUS fits, and the final toy MC parameterizations. The toy MC provides an excellent description of the data.

The corrections obtained to the individual FOCUS yields were 1.0298 ± 0.0001 for $K^- \pi^+$, 1.062 ± 0.001 for $\pi^+ \pi^-$, and 1.0183 ± 0.0003 for $K^+ K^-$. These corrections tend to cancel in the branching ratios, leading to corrections of 1.031 to $\mathcal{B}(D^0 \rightarrow \pi^+ \pi^-)/\mathcal{B}(D^0 \rightarrow K^- \pi^+)$, and 0.9888 for $\mathcal{B}(D^0 \rightarrow K^+ K^-)/\mathcal{B}(D^0 \rightarrow K^- \pi^+)$.

Table 182 summarizes the corrected branching fractions. The published FSR-related modeling uncertainties have been replaced by with a new, common, estimate based on the assumption that the dominant uncertainty in the FSR corrections come from the fact that the mesons are treated like structureless particles. No contributions from structure-dependent terms in the decay process (eg. radiation off individual quarks) are included in PHOTOS. Internal studies done by various experiments have indicated that in $K\pi$ decay, the PHOTOS corrections agree with data at the 20-30% level. We therefore attribute a 25 uncertainty to the FSR prediction from potential structure-dependent contributions. For the other two modes, the only difference in structure is the final state valence quark content. While radiative corrections typically come in with a $1/M$ dependence, one would expect the additional contribution from the structure terms to come in on time scales shorter than the hadronization time scale. In this case, you might expect LambdaQCD to be the relevant scale, rather than the quark masses, and therefore that the amplitude is the same for the three modes. In treating the correlations among the measurements this is what we assume. We also assume that the PHOTOS amplitudes and any missing structure amplitudes are relatively real with constructive interference. The

Table 182: The experimental measurements relating to $\mathcal{B}(D^0 \rightarrow K^-\pi^+)$, $\mathcal{B}(D^0 \rightarrow \pi^+\pi^-)$ and $\mathcal{B}(D^0 \rightarrow K^+K^-)$ after correcting to the common version and configuration of PHOTOS. The uncertainties are statistical and total systematic, with the FSR-related systematic estimated in this procedure shown in parentheses. Also listed are the percent shifts in the results from the correction, if any, applied here, as well as the original PHOTOS and interference configuration for each publication.

Experiment	result (rescaled)	correction [%]	PHOTOS
$D^0 \rightarrow K^-\pi^+$			
CLEO-c 07 (CC07) [529]	$3.891 \pm 0.035 \pm 0.065(27)\%$	–	2.15/Yes
BABAR 07 (BB07) [572]	$4.035 \pm 0.037 \pm 0.074(24)\%$	0.69	2.02/No
CLEO II 98 (CL98) [573]	$3.920 \pm 0.154 \pm 0.168(32)\%$	2.80	none
ALEPH 97 (AL97) [574]	$3.930 \pm 0.091 \pm 0.125(32)\%$	0.79	2.0/No
ARGUS 94 (AR94) [575]	$3.490 \pm 0.123 \pm 0.288(24)\%$	2.33	none
CLEO II 93 (CL93) [576]	$3.960 \pm 0.080 \pm 0.171(15)\%$	0.38	2.0/No
ALEPH 91 (AL91) [577]	$3.730 \pm 0.351 \pm 0.455(34)\%$	3.12	none
$D^0 \rightarrow \pi^+\pi^-/D^0 \rightarrow K^-\pi^+$			
CLEO-c 10 (CC10) [524]	$0.0370 \pm 0.0006 \pm 0.0009(02)$	–	2.15/Yes
CDF 05 (CD05) [578]	$0.03594 \pm 0.00054 \pm 0.00043(15)$	–	2.15/Yes
FOCUS 02 (FO02) [571]	$0.0364 \pm 0.0012 \pm 0.0006(02)$	3.10	none
$D^0 \rightarrow K^+K^-/D^0 \rightarrow K^-\pi^+$			
CLEO-c 10 [524]	$0.1041 \pm 0.0011 \pm 0.0012(03)$	–	2.15/Yes
CDF 05 [578]	$0.0992 \pm 0.0011 \pm 0.0012(01)$	–	2.15/Yes
FOCUS 02 [571]	$0.0982 \pm 0.0014 \pm 0.0014(01)$	-1.12	none

uncertainties largely cancel in the branching fraction ratios. For the final average branching fractions, the FSR uncertainty on $K\pi$ dominates. Note that because of the relative sizes of FSR in the different modes, the $\pi\pi/K\pi$ branching ratio uncertainty from FSR is positively correlated with that for $K\pi$ branching, while the $KK/K\pi$ branching ratio FSR uncertainty is negatively correlated.

The $\mathcal{B}(D^0 \rightarrow K^-\pi^+)$ measurement of reference [579], the $\mathcal{B}(D^0 \rightarrow \pi^+\pi^-)/\mathcal{B}(D^0 \rightarrow K^-\pi^+)$ measurements of references [536] and [467] and the $\mathcal{B}(D^0 \rightarrow K^+K^-)/\mathcal{B}(D^0 \rightarrow K^-\pi^+)$ measurement of reference [467] are excluded from the branching fraction averages presented here. The measurements appear not to have incorporated any FSR corrections, and insufficient information is available to determine the 2-3% corrections that would be required.

8.6.2 Average branching fractions

The average branching fractions for $D^0 \rightarrow K^-\pi^+$, $D^0 \rightarrow \pi^+\pi^-$ and $D^0 \rightarrow K^+K^-$ are obtained from a single χ^2 minimization procedure, in which the three branching fractions are floating parameters. The central values derive from a fit in which the covariance matrix is the sum of the covariance matrices for the statistical, systematic (excluding FSR) and FSR uncertainties. The statistical uncertainties are obtained from a fit using only the statistical covariance matrix. The systematic uncertainties are obtained from the quadrature uncertainties from a fit with statistical-only and statistical+systematic covariance matrices, and the FSR uncertainties on the averages from the quadrature differences in the uncertainties obtained from the nominal fit

Table 183: The correlation matrix corresponding to the covariance matrix from the sum of statistical, systematic and FSR covariances.

	CC07	BB07	CL98	AL97	AR94	CL93	AL91	FO02	CD05	CC10	FO02	CD05	CC10
CC07	1.000	0.106	0.044	0.064	0.023	0.025	0.018	0.053	0.078	0.052	-0.015	-0.025	-0.065
BB07	0.106	1.000	0.035	0.051	0.019	0.020	0.014	0.042	0.062	0.041	-0.012	-0.019	-0.051
CL98	0.044	0.035	1.000	0.021	0.008	0.298	0.006	0.017	0.026	0.017	-0.005	-0.008	-0.021
AL97	0.064	0.051	0.021	1.000	0.011	0.012	0.116	0.025	0.038	0.025	-0.007	-0.012	-0.031
AR94	0.023	0.019	0.008	0.011	1.000	0.004	0.003	0.009	0.014	0.009	-0.003	-0.004	-0.011
CL93	0.025	0.020	0.298	0.012	0.004	1.000	0.003	0.010	0.015	0.010	-0.003	-0.005	-0.012
AL91	0.018	0.014	0.006	0.116	0.003	0.003	1.000	0.007	0.010	0.007	-0.002	-0.003	-0.009
FO02	0.053	0.042	0.017	0.025	0.009	0.010	0.007	1.000	0.031	0.021	-0.006	-0.010	-0.026
CD05	0.078	0.062	0.026	0.038	0.014	0.015	0.010	0.031	1.000	0.031	-0.009	-0.014	-0.038
CC10	0.052	0.041	0.017	0.025	0.009	0.010	0.007	0.021	0.031	1.000	-0.006	-0.010	-0.025
FO02	-0.015	-0.012	-0.005	-0.007	-0.003	-0.003	-0.002	-0.006	-0.009	-0.006	1.000	0.003	0.007
CD05	-0.025	-0.019	-0.008	-0.012	-0.004	-0.005	-0.003	-0.010	-0.014	-0.010	0.003	1.000	0.012
CC10	-0.065	-0.051	-0.021	-0.031	-0.011	-0.012	-0.009	-0.026	-0.038	-0.025	0.007	0.012	1.000

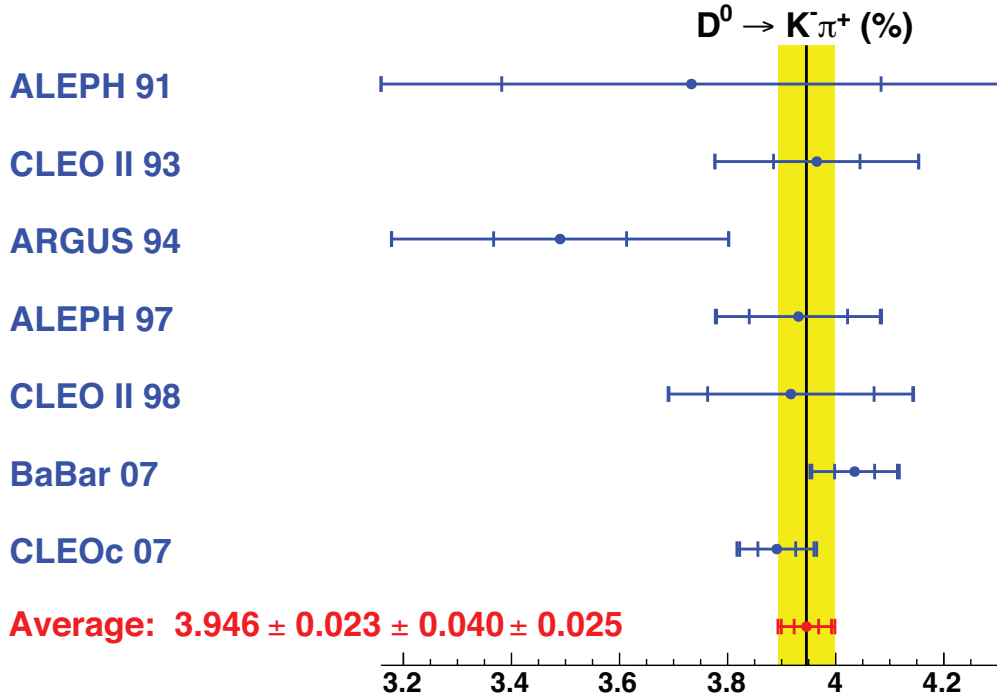


Figure 79: Comparison of measurements of $\mathcal{B}(D^0 \rightarrow K^- \pi^+)$ (blue) with the average branching fraction obtained here (red, and yellow band).

and a fit excluding the FSR uncertainties.

In forming the covariance matrix for the FSR uncertainties, the FSR uncertainties are treated as fully correlated (or anti-correlated) as described above. For the systematic covariance matrix, ALEPH's systematic uncertainties in the θ_{D^*} parameter are treated as fully correlated between the ALEPH 97 and ALEPH 91 measurements. Similarly, the tracking efficiency uncertainties in the CLEO II 98 and the CLEO II 93 measurements are treated as fully correlated. Table 183 presents the correlation matrix for the nominal fit (stat.+syst.+FR).

The averaging procedure results in a final χ^2 of 11.6 for 13-3 degrees of freedom. The branching fractions obtained are

$$\begin{aligned}
 \mathcal{B}(D^0 \rightarrow K^- \pi^+) &= 3.946 \pm 0.023 \pm 0.040 \pm 0.025 \\
 \mathcal{B}(D^0 \rightarrow \pi^+ \pi^-) &= 0.143 \pm 0.002 \pm 0.002 \pm 0.002 \\
 \mathcal{B}(D^0 \rightarrow K^+ K^-) &= 0.398 \pm 0.004 \pm 0.005 \pm 0.002.
 \end{aligned}$$

The uncertainties, estimated as described above, are statistical, systematic (excluding FSR), and FSR modeling. The correlation coefficients from the fit using the total uncertainties are

	$K^- \pi^+$	$\pi^+ \pi^-$	$K^+ K^-$
$K^- \pi^+$	1.00	0.72	0.78
$\pi^+ \pi^-$	0.72	1.00	0.55
$K^+ K^-$	0.78	0.55	1.00

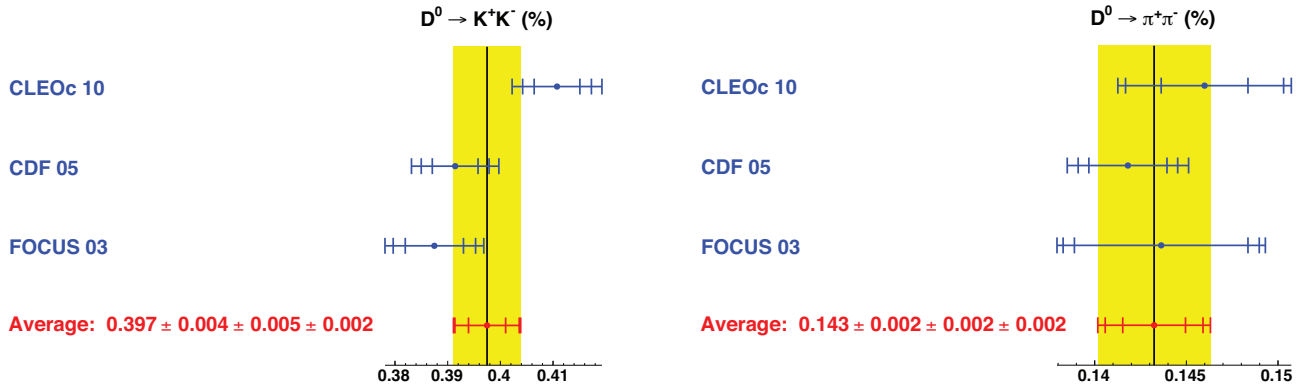


Figure 80: The $\mathcal{B}(D^0 \rightarrow K^+K^-)$ (left) and $\mathcal{B}(D^0 \rightarrow \pi^+\pi^-)$ (right) values obtained by scaling the measured branching ratios with the $\mathcal{B}(D^0 \rightarrow K^-\pi^+)$ branching fraction average obtained here. For the measurements (blue points), the error bars correspond to the statistical, systematic and $K\pi$ normalization uncertainties. The average obtained here (red point, yellow band) lists the statistical, systematics excluding FSR, and the FSR systematic.

As the χ^2 would suggest and Fig. 79 shows, the average value for $\mathcal{B}(D^0 \rightarrow K^-\pi^+)$ and the input branching fractions agree very well. With the estimated uncertainty in the FSR modeling used here, the FSR uncertainty dominates the statistical uncertainty in the average, suggesting that experimental work in the near future should focus on verification of FSR with $E_\gamma \gtrsim 100$ MeV. The $\mathcal{B}(D^0 \rightarrow K^+K^-)$ and $\mathcal{B}(D^0 \rightarrow \pi^+\pi^-)$ measurements inferred from the branching ratio measurements also agree well (Fig. 80).

The $\mathcal{B}(D^0 \rightarrow K^-\pi^+)$ average obtained here is approximately one statistical standard deviation higher than the 2011 PDG update average [5]. Table 184 shows the evolution from a fit similar to the PDG's (no FSR corrections or correlations, reference [579] included) to the average presented here. There are two main contributions to the difference. The branching fraction in reference [579] is low, and its exclusion shifts the result upwards. The FSR corrections also shift the result upwards, as expected, and contribute the dominant shift of +0.019%.

Table 184: Evolution of the $D^0 \rightarrow K^-\pi^+$ branching fraction from a fit with no FSR corrections or correlations (similar to the average in the PDG 2011 update [419]) to the nominal fit presented here.

Modes fit	description	$\mathcal{B}(D^0 \rightarrow K^-\pi^+)$ (%)	$\chi^2 / (\text{d.o.f.})$
$K^-\pi^+$	PDG summer 2011 equivalent	$3.913 \pm 0.022 \pm 0.043$	6.0 / (8-1)
$K^-\pi^+$	drop Ref. [579]	$3.921 \pm 0.023 \pm 0.044$	4.8 / (7-1)
$K^-\pi^+$	add FSR corrections	$3.940 \pm 0.023 \pm 0.041 \pm 0.015$	4.0 / (7-1)
$K^-\pi^+$	add FSR correlations	$3.940 \pm 0.023 \pm 0.041 \pm 0.025$	4.2 / (7-1)
all	–	$3.946 \pm 0.023 \pm 0.040 \pm 0.025$	11.6 / (13-3)

8.7 Direct CP violation

In decays of D^0 mesons, CP asymmetry measurements have contributions from both direct and indirect CP violation as discussed in Sec. 8.1. The contribution from indirect CP violation depends on the decay-time distribution of the data sample [478]. This section describes a combination of measurements that allows the extraction of the individual contributions of the two types of CP violation. At the same time, the level of agreement for a no- CP -violation hypothesis is tested. The observables are:

$$A_\Gamma \equiv \frac{\tau(D^0 \rightarrow h^+h^-) - \tau(\bar{D}^0 \rightarrow h^+h^-)}{\tau(D^0 \rightarrow h^+h^-) + \tau(\bar{D}^0 \rightarrow h^+h^-)}, \quad (214)$$

where h^+h^- can be K^+K^- or $\pi^+\pi^-$, and

$$\Delta A_{\text{CP}} \equiv A_{\text{CP}}(K^+K^-) - A_{\text{CP}}(\pi^+\pi^-), \quad (215)$$

where A_{CP} are time-integrated CP asymmetries. The underlying theoretical parameters are:

$$\begin{aligned} a_{\text{CP}}^{\text{dir}} &\equiv \frac{|A_{D^0 \rightarrow f}|^2 - |A_{\bar{D}^0 \rightarrow f}|^2}{|A_{D^0 \rightarrow f}|^2 + |A_{\bar{D}^0 \rightarrow f}|^2}, \\ a_{\text{CP}}^{\text{ind}} &\equiv \frac{1}{2} \left[\left(\left| \frac{q}{p} \right| + \left| \frac{p}{q} \right| \right) x \sin \phi - \left(\left| \frac{q}{p} \right| - \left| \frac{p}{q} \right| \right) y \cos \phi \right], \end{aligned} \quad (216)$$

where $A_{D \rightarrow f}$ is the amplitude for $D \rightarrow f$ [580]. We use the following relations between the observables and the underlying parameters [581]:

$$\begin{aligned} A_\Gamma &= -a_{\text{CP}}^{\text{ind}} - a_{\text{CP}}^{\text{dir}} y_{\text{CP}}, \\ \Delta A_{\text{CP}} &= \Delta a_{\text{CP}}^{\text{dir}} \left(1 + y_{\text{CP}} \frac{\langle t \rangle}{\tau} \right) + a_{\text{CP}}^{\text{ind}} \frac{\Delta \langle t \rangle}{\tau} + a_{\text{CP}}^{\text{dir}} y_{\text{CP}} \frac{\Delta \langle t \rangle}{\tau}, \end{aligned} \quad (217)$$

$$\Delta a_{\text{CP}}^{\text{dir}} \left(1 + y_{\text{CP}} \frac{\langle t \rangle}{\tau} \right) + a_{\text{CP}}^{\text{ind}} \frac{\Delta \langle t \rangle}{\tau}. \quad (218)$$

The first relation constrains mostly indirect CP violation, and the direct CP violation contribution can differ for different final states. In the second relation, $\langle t \rangle/\tau$ denotes the mean decay time in units of the D^0 lifetime; ΔX denotes the difference in quantity X between K^+K^- and $\pi^+\pi^-$ final states; and X denotes the average for quantity X . We neglect the last term in this relation as all three factors are $\mathcal{O}(10^{-2})$ or smaller, and thus this term is negligible with respect to the other two terms. Note that $\Delta \langle t \rangle/\tau \ll \langle t \rangle/\tau$, and it is expected that $|a_{\text{CP}}^{\text{dir}}| < |\Delta a_{\text{CP}}^{\text{dir}}|$ because $a_{\text{CP}}^{\text{dir}}(K^+K^-)$ and $a_{\text{CP}}^{\text{dir}}(\pi^+\pi^-)$ are expected to have opposite signs.

A χ^2 fit is performed in the plane $\Delta a_{\text{CP}}^{\text{dir}}$ vs. $a_{\text{CP}}^{\text{ind}}$. For the *BABAR* result the difference of the quoted values for $A_{\text{CP}}(K^+K^-)$ and $A_{\text{CP}}(\pi^+\pi^-)$ is calculated, adding all uncertainties in quadrature. This may overestimate the systematic uncertainty for the difference as it neglects correlated errors; however, the result is conservative and the effect is small as all measurements are statistically limited. For all measurements, statistical and systematic uncertainties are added in quadrature when calculating the χ^2 . We use the current world average value $y_{\text{CP}} = (1.064 \pm 0.209)\%$ (see Sec. 8.1) and the measurements listed in Table 185.

The combination plot shows the measurements listed in Table 185 for ΔA_{CP} and A_Γ , where the bands represent $\pm 1\sigma$ intervals. The point of no CP violation (0,0) is shown as a filled circle,

Table 185: Inputs to the fit for direct and indirect CP violation. The first uncertainty listed is statistical, and the second is systematic.

Year	Experiment	Results	$\Delta\langle t \rangle/\tau$	$\langle t \rangle/\tau$	Reference
2007	Belle	$A_\Gamma = (0.01 \pm 0.30 \pm 0.15)\%$	-	-	[448]
2008	BABAR	$A_\Gamma = (0.26 \pm 0.36 \pm 0.08)\%$	-	-	[468]
2011	LHCb	$A_\Gamma = (0.59 \pm 0.59 \pm 0.21)\%$	-	-	[470]
2008	BABAR	$A_{CP}(KK) = (0.00 \pm 0.34 \pm 0.13)\%$			
		$A_{CP}(\pi\pi) = (0.24 \pm 0.52 \pm 0.22)\%$	0.00	1.00	[471]
2008	Belle	$\Delta A_{CP} = (0.86 \pm 0.60 \pm 0.07)\%$	0.00	1.00	[472]
2011	LHCb	$\Delta A_{CP} = (0.82 \pm 0.21 \pm 0.11)\%$	0.10	2.08	[473]
2012	CDF Prelim.	$\Delta A_{CP} = (0.62 \pm 0.21 \pm 0.10)\%$	0.25	2.58	[475]

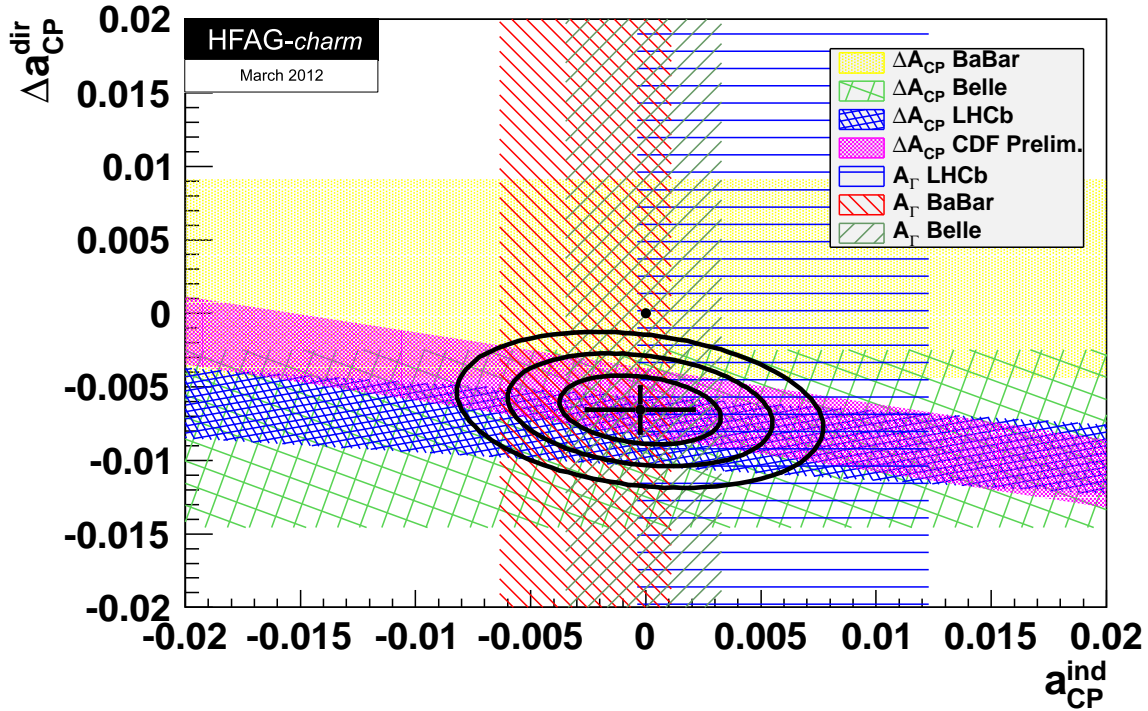


Figure 81: Plot of all data and the fit result. Individual measurements are plotted as bands showing their $\pm 1\sigma$ range. The no- CPV point $(0,0)$ is shown as a filled circle, and the best fit value is indicated by a cross showing the one-dimensional errors. Two-dimensional 68% CL, 95% CL, and 99.7% CL regions are plotted as ellipses.

and two-dimensional 68% CL, 95% CL, and 99.7% CL regions are plotted as ellipses. The best fit value is indicated by a cross showing the one-dimensional errors.

From the fit, the change in χ^2 from the minimum value for the no- CPV point (0,0) is 19.4, which corresponds to a CL of 6.1×10^{-5} for two degrees of freedom. Thus the data are consistent with the no- CP -violation hypothesis at only 0.006% CL. The central values and $\pm 1\sigma$ errors for the individual parameters are

$$\begin{aligned} a_{\text{CP}}^{\text{ind}} &= (-0.025 \pm 0.231)\% \\ \Delta a_{\text{CP}}^{\text{dir}} &= (-0.656 \pm 0.154)\%. \end{aligned} \tag{219}$$

These results indicate that the origin of this CP violation lies in the difference between direct CP violation in the two final states, rather than in a common indirect CP violation.

Table 186: Summary of excited Λ_c^+ baryons family.

Charmed Baryon Excited State	Mode	Mass or ΔM , MeV/c ²	Natural Width, MeV/c ²	J^P
$\Lambda_c(2595)^+$	$\Lambda_c^+ \pi^+ \pi^-$, $\Sigma_c \pi$	2595.4 ± 0.6	$3.6_{-1.3}^{+2.0}$	$1/2^-$
$\Lambda_c(2625)^+$	$\Lambda_c^+ \pi^+ \pi^-$, $\Sigma_c \pi$	2628.1 ± 0.6	< 1.9	$3/2^-$
$\Lambda_c(2765)^+$	$\Lambda_c^+ \pi^+ \pi^-$, $\Sigma_c \pi$	2766.6 ± 2.4	50	??
$\Lambda_c(2880)^+$	$\Lambda_c^+ \pi^+ \pi^-$, $\Sigma_c \pi$, $\Sigma_c(2520)\pi$, $D^0 p$	2881.53 ± 0.35	5.8 ± 1.1	$5/2^+$ (experimental evidence)
$\Lambda_c(2940)^+$	$D^0 p$, $\Sigma_c \pi$	$2939.3_{-1.5}^{+1.4}$	17_{-6}^{+8}	??

8.8 Charm baryons

Here we summarize the present status of excited charm baryons, decaying strongly or electromagnetically: their masses (or mass difference between excited baryon and the corresponding ground state), natural widths, decay modes and presumably assigned quantum numbers. Table 186 summarizes the excited Λ_c^+ 's. First two states, $\Lambda_c(2595)^+$ and $\Lambda_c(2625)^+$ are well established. Based on measured masses they are believed to be orbitally excited Λ_c^+ 's with total momentum of light quarks $L=1$. Therefore, their quantum numbers are assigned to be $J^P = (\frac{1}{2})^-$ and $J^P = (\frac{3}{2})^-$. Recently, their masses were precisely measured by CDF [582]: $M(\Lambda_c(2595)^+) = 2592.25 \pm 0.24 \pm 0.14$ MeV/c², $M(\Lambda_c(2625)^+) = 2628.11 \pm 0.13 \pm 0.14$ MeV/c². Next two states, $\Lambda_c(2765)^+$ and $\Lambda_c(2880)^+$, were discovered by CLEO [583] in $\Lambda_c^+ \pi^+ \pi^-$ final state. They found that $\Lambda_c(2880)^+$ decays also through the $\Sigma_c(2445)^{++/0} \pi^{-/+}$ mode. Later, *BABAR* [584] observed that this state has also $D^0 p$ decay mode. It is the first example where excited charm baryon decays into charm meson and light baryon. (Usually, excited charm baryons decay into charm baryon and light mesons.) In that analysis *BABAR* observed for the first time else one state, $\Lambda_c(2940)^+$, decaying into $D^0 p$. By looking at $D^+ p$ final state, they found no signals which results in the conclusion that the $\Lambda_c(2880)^+$ and $\Lambda_c(2940)^+$ are really Λ_c^+ excited states, not Σ_c . Belle reported the result of an angular analysis that favors the $5/2$ for the $\Lambda_c(2880)^+$ spin hypothesis. Moreover, the measured ratio of branching fractions $\mathcal{B}(\Lambda_c(2880)^+ \rightarrow \Sigma_c(2520)\pi^\pm)/\mathcal{B}(\Lambda_c(2880)^+ \rightarrow \Sigma_c(2455)\pi^\pm) = (0.225 \pm 0.062 \pm 0.025)$ combined with theoretical predictions based on HQS [376, 585] favoring even parity.

The open questions in the present excited Λ_c^+ family are the experimental determination of quantum numbers for almost all states and the nature of $\Lambda_c(2765)^+$ state: whether it is excited Σ_c^+ or Λ_c^+ .

Table 187 summarizes the excited $\Sigma_c^{++,+0}$ baryons. Triplet of $\Sigma_c(2520)^{++,+0}$ baryons is well established. Recently CDF [582] precisely measured the masses and widths of the double charged and neutral members of this triplet to be $M(\Sigma_c(2520)^{++}) = (2517.19 \pm 0.46 \pm 0.14)$ MeV/c², $\Gamma(\Sigma_c(2520)^{++}) = (15.03 \pm 2.52)$ MeV/c² and $M(\Sigma_c(2520)^0) = (2519.34 \pm 0.58 \pm 0.14)$ MeV/c², $\Gamma(\Sigma_c(2520)^0) = (12.51 \pm 2.28)$ MeV/c², respectively. The short list of excited Σ_c baryons completes the triplet of $\Sigma_c(2800)$ states observed by Belle [586]. Based on measured mass and theoretical predictions [587, 588] one can tentatively identify these states as members of the predicted Σ_{c2} $3/2^-$ triplet. From the study of resonant substructure in $B^- \rightarrow \Lambda_c^+ \bar{p} \pi^-$ decays, *BABAR* found significant signal in $\Lambda_c^+ \pi^-$ with the mean value higher by about 3σ from obtained by Belle (see Table 187). The widths from measurements, Belle and *BABAR*, are consistent.

Table 188 summarizes the excited $\Xi_c^{+,0}$ and Ω_c^0 baryons. Recently, the list of excited Ξ_c

Table 187: Summary of excited $\Sigma_c^{++,+,0}$ baryons family.

Charmed Baryon Excited State	Mode	Mass or ΔM , MeV/c ²	Natural Width, MeV/c ²	J^P
$\Sigma_c(2520)^{++}$	$\Lambda_c^+ \pi^+$	231.9 ± 0.6	14.9 ± 1.9	$3/2^+$
$\Sigma_c(2520)^+$	$\Lambda_c^+ \pi^+$	231.0 ± 2.3	< 17 @ 90% CL	$3/2^+$
$\Sigma_c(2520)^0$	$\Lambda_c^+ \pi^+$	231.6 ± 0.5	16.1 ± 2.1	$3/2^+$
$\Sigma_c(2800)^{++}$	$\Lambda_c^+ \pi^+$	$514.5^{+3.4+2.8}_{-3.1-4.9}$	75^{+18+12}_{-13-11}	tentatively identified as members of the predicted Σ_{c2} $3/2^-$ isospin triplet
$\Sigma_c(2800)^+$	$\Lambda_c^+ \pi^0$	$505.4^{+5.8+12.4}_{-4.6-2.0}$	62^{+37+52}_{-23-38}	
$\Sigma_c(2800)^0$	$\Lambda_c^+ \pi^-$	$515.4^{+3.2+2.1}_{-3.1-6.0}$	61^{+18+22}_{-13-13}	
	$\Lambda_c^+ \pi^-$	$560 \pm 8 \pm 10$	86^{+33}_{-22}	

baryons have enriched by several states with masses above 2900 MeV/c² and decaying into $\Lambda_c^+ K^-$ and $\Lambda_c^+ K^{-/0} \pi^{+/-}$. Some of these states are seen by both Belle [589] and BABAR [590] and are believed to be well-established, these are $\Xi_c(2980)^+$ and $\Xi_c(3080)^{+,0}$. All others need to be confirmed or studied in more depth. These are $\Xi_c(2930)^0$ seen in $\Lambda_c^+ K^-$ final state, $\Xi_c(3055)^+$ found in $\Sigma_c(2455)^{++} \pi^-$ final state, and $\Xi_c(3123)^+$ claimed by BABAR [590] in $\Sigma_c(2520)^{++} \pi^-$ final state.

The excited Ω_c^0 double charm baryon are seen by both BABAR [591] and Belle [592], the $\delta M = M(\Omega_c^{*0}) - M(\Omega_c^0)$ are in good agreement in both experiments and consistent with most theoretical predictions [593–596].

Figure 82 shows the levels of excited charm baryons with the corresponding transitions between them or to the charm baryon ground states. Interesting feature recently discovered by BABAR and Belle is that now we know that transitions between families are possible (between Ξ_c and Λ_c^+ families of excited baryons). Also, highly excited Λ_c^+ baryons can decay into charm meson and proton.

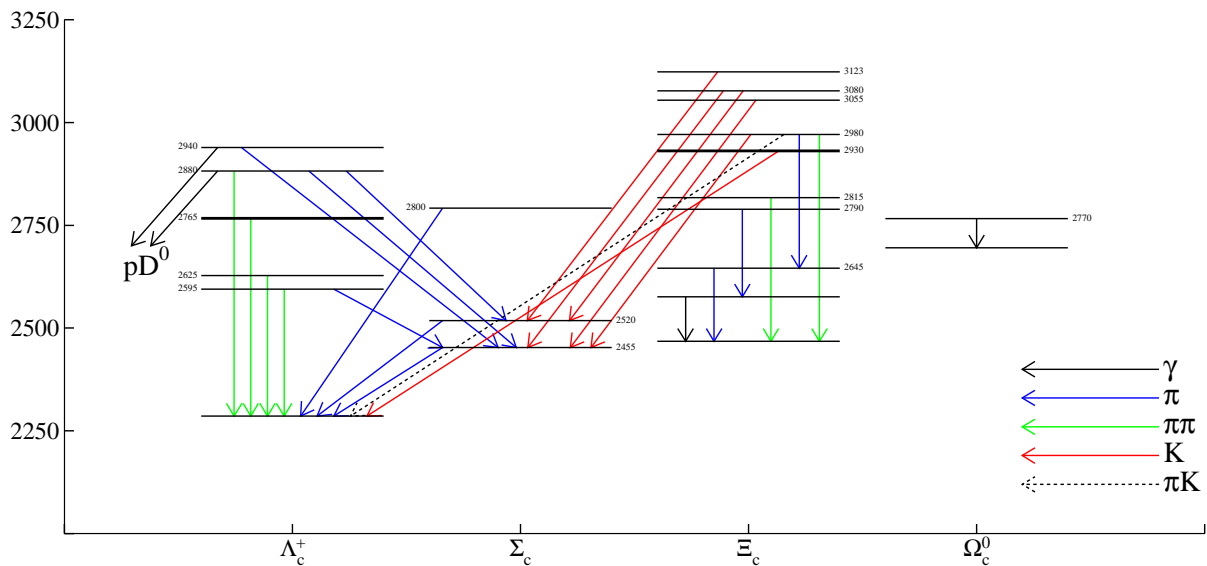


Figure 82: Level diagram for excited charm baryons.

Table 188: Summary of excited $\Xi_c^{+,0}$ and Ω_c^0 baryons families.

Charmed Baryon Excited State	Mode	Mass or ΔM , MeV/c ²	Natural Width, MeV/c ²	J^P
$\Xi_c^{\prime+}$	$\Xi_c^+\gamma$	2575.6 ± 3.1		$1/2^+$
$\Xi_c^{\prime0}$	$\Xi_c^0\gamma$	2577.9 ± 2.9		$1/2^+$
$\Xi_c(2645)^+$	$\Xi_c^0\pi^+$	$2645.9^{+0.6}_{-0.5}$	< 3.1	$3/2^+$
$\Xi_c(2645)^0$	$\Xi_c^+\pi^-$	2645.9 ± 0.5	< 5.5	$3/2^+$
$\Xi_c(2790)^+$	$\Xi_c^{\prime0}\pi^+$	2789.1 ± 3.2	< 15	$1/2^-$
$\Xi_c(2790)^0$	$\Xi_c^{\prime+}\pi^-$	2791.8 ± 3.3	< 12	$1/2^-$
$\Xi_c(2815)^+$	$\Xi_c^+\pi^+\pi^-$, $\Xi_c(2645)^0\pi^+$	2816.6 ± 0.9	< 3.5	$3/2^-$
$\Xi_c(2815)^0$	$\Xi_c^0\pi^+\pi^-$, $\Xi_c(2645)^+\pi^-$	2819.6 ± 1.2	< 6.5	$3/2^-$
$\Xi_c(2930)^0$	$\Lambda_c^+K^-$	2931.6 ± 6	36 ± 13	??
$\Xi_c(2980)^+$	$\Lambda_c^+K^-\pi^+$, $\Sigma_c^{++}K^-$, $\Xi_c(2645)^0\pi^+$	2971.4 ± 3.3	26 ± 7	??
$\Xi_c(2980)^0$	$\Xi_c(2645)^+\pi^-$	2968.0 ± 2.6	20 ± 7	??
$\Xi_c(3055)^+$	$\Sigma_c^{++}K^-$	3054.2 ± 1.3	17 ± 13	??
$\Xi_c(3080)^+$	$\Lambda_c^+K^-\pi^+$, $\Sigma_c^{++}K^-$, $\Sigma_c(2520)^{++}K^-$	3077.0 ± 0.4	5.8 ± 1.0	??
$\Xi_c(3080)^0$	$\Lambda_c^+K_S^0\pi^-$, $\Sigma_c^0K_S^0$, $\Sigma_c(2520)^0K_S^0$	3079.9 ± 1.4	5.6 ± 2.2	??
$\Xi_c(3123)^+$	$\Sigma_c(2520)^{++}K^-$	3122.9 ± 1.3	4 ± 4	??
$\Omega_c(2770)^0$	$\Omega_c^0\gamma$	2765.9 ± 2.0	$70.7^{+0.8}_{-0.9}$	$3/2^+$

8.9 Rare and forbidden decays

This section provides a summary of rare and forbidden charm decays in tabular form. The decay modes can be categorized as flavor-changing neutral currents, lepton-flavor-violating, lepton-number-violating, and both baryon- and lepton-number-violating decays. Figures 83-85 plot the upper limits for D^0 , D^+ , D_s^+ , and A_c^+ decays. Tables 189-192 give the corresponding numerical results. Some theoretical predictions are given in Refs. [597–602].

Table 189: Upper limits at 90% CL for D^0 decays.

Decay	Limit $\times 10^6$	Experiment	Reference
$\gamma\gamma$	26.0	CLEO II	[603]
	2.2	<i>BABAR</i> Preliminary	[604]
e^+e^-	220.0	CLEO	[605]
	170.0	Argus	[606]
	130.0	Mark3	[607]
	13.0	CLEO II	[608]
	8.19	E789	[609]
	6.2	E791	[610]
	1.2	<i>BABAR</i>	[611]
	0.079	Belle	[612]
$\mu^+\mu^-$	70.0	Argus	[606]
	44.0	E653	[613]
	34.0	CLEO II	[608]
	15.6	E789	[609]
	5.2	E791	[610]
	2.0	HERAb	[614]
	1.3	<i>BABAR</i>	[611]
	0.21	CDF	[615]
	0.14	Belle	[612]
	0.011	LHCb Preliminary	[616]
$\pi^0 e^+ e^-$	45.0	CLEO II	[608]
$\pi^0 \mu^+ \mu^-$	540.0	CLEO II	[608]
	180.0	E653	[613]
$\eta e^+ e^-$	110.0	CLEO II	[608]
$\eta \mu^+ \mu^-$	530.0	CLEO II	[608]
$\pi^+ \pi^- e^+ e^-$	370.0	E791	[617]
$\rho e^+ e^-$	450.0	CLEO	[605]
	124.0	E791	[617]
	100.0	CLEO II	[608]

Table 189 – continued from previous page

Decay	Limit $\times 10^6$	Experiment	Reference
$\pi^+\pi^-\mu^+\mu^-$	30.0	E791	[617]
$\rho\mu^+\mu^-$	810.0	CLEO	[605]
	490.0	CLEO II	[608]
	230.0	E653	[613]
	22.0	E791	[617]
ωe^+e^-	180.0	CLEO II	[608]
$\omega\mu^+\mu^-$	830.0	CLEO II	[608]
$K^+K^-e^+e^-$	315.0	E791	[617]
ϕe^+e^-	59.0	E791	[617]
	52.0	CLEO II	[608]
$K^+K^-\mu^+\mu^-$	33.0	E791	[617]
$\phi\mu^+\mu^-$	410.0	CLEO II	[608]
	31.0	E791	[617]
$\overline{K}^0 e^+e^-$	1700.0	Mark3	[618]
	110.0	CLEO II	[608]
$\overline{K}^0\mu^+\mu^-$	670.0	CLEO II	[608]
	260.0	E653	[613]
$K^-\pi^+e^+e^-$	385.0	E791	[617]
$\overline{K}^{*0}(892)e^+e^-$	140.0	CLEO II	[608]
	47.0	E791	[617]
$K^-\pi^+\mu^+\mu^-$	360.0	E791	[617]
$\overline{K}^{*0}(892)\mu^+\mu^-$	1180.0	CLEO II	[608]
	24.0	E791	[617]
$\pi^+\pi^-\pi^0\mu^+\mu^-$	810.0	E653	[613]

Table 189 – continued from previous page

Decay	Limit $\times 10^6$	Experiment	Reference
$\mu^\pm e^\mp$	270.0	CLEO	[605]
	120.0	Mark3	[619]
	100.0	Argus	[606]
	19.0	CLEO II	[608]
	17.2	E789	[609]
	8.1	E791	[610]
	0.81	<i>BABAR</i>	[611]
	0.26	Belle	[612]
$\pi^0 e^\pm \mu^\mp$	86.0	CLEO II	[608]
$\eta e^\pm \mu^\mp$	100.0	CLEO II	[608]
$\pi^+ \pi^- e^\pm \mu^\mp$	15.0	E791	[617]
$\rho e^\pm \mu^\mp$	66.0	E791	[617]
	49.0	CLEO II	[608]
$\omega e^\pm \mu^\mp$	120.0	CLEO II	[608]
$K^+ K^- e^\pm \mu^\mp$	180.0	E791	[617]
$\phi e^\pm \mu^\mp$	47.0	E791	[617]
	34.0	CLEO II	[608]
$\bar{K}^0 e^\pm \mu^\mp$	100.0	CLEO II	[608]
$K^- \pi^+ e^\pm \mu^\mp$	550.0	E791	[617]
$K^{*0}(892) e^\pm \mu^\mp$	100.0	CLEO II	[608]
	83.0	E791	[617]
$\pi^\mp \pi^\mp e^\pm e^\pm$	112.0	E791	[617]
$\pi^\mp \pi^\mp \mu^\pm \mu^\pm$	29.0	E791	[617]
$K^\mp \pi^\mp e^\pm e^\pm$	206.0	E791	[617]
$K^\mp \pi^\mp \mu^\pm \mu^\pm$	390.0	E791	[617]
$K^\mp K^\mp e^\pm e^\pm$	152.0	E791	[617]
$K^\mp K^\mp \mu^\pm \mu^\pm$	94.0	E791	[617]
$\pi^\mp \pi^\mp e^\pm \mu^\pm$	79.0	E791	[617]
$K^\mp \pi^\mp e^\pm \mu^\pm$	218.0	E791	[617]
$K^\mp K^\mp e^\pm \mu^\pm$	57.0	E791	[617]
pe^-	10.0	CLEO	[620]
$\bar{p}e^+$	11.0	CLEO	[620]

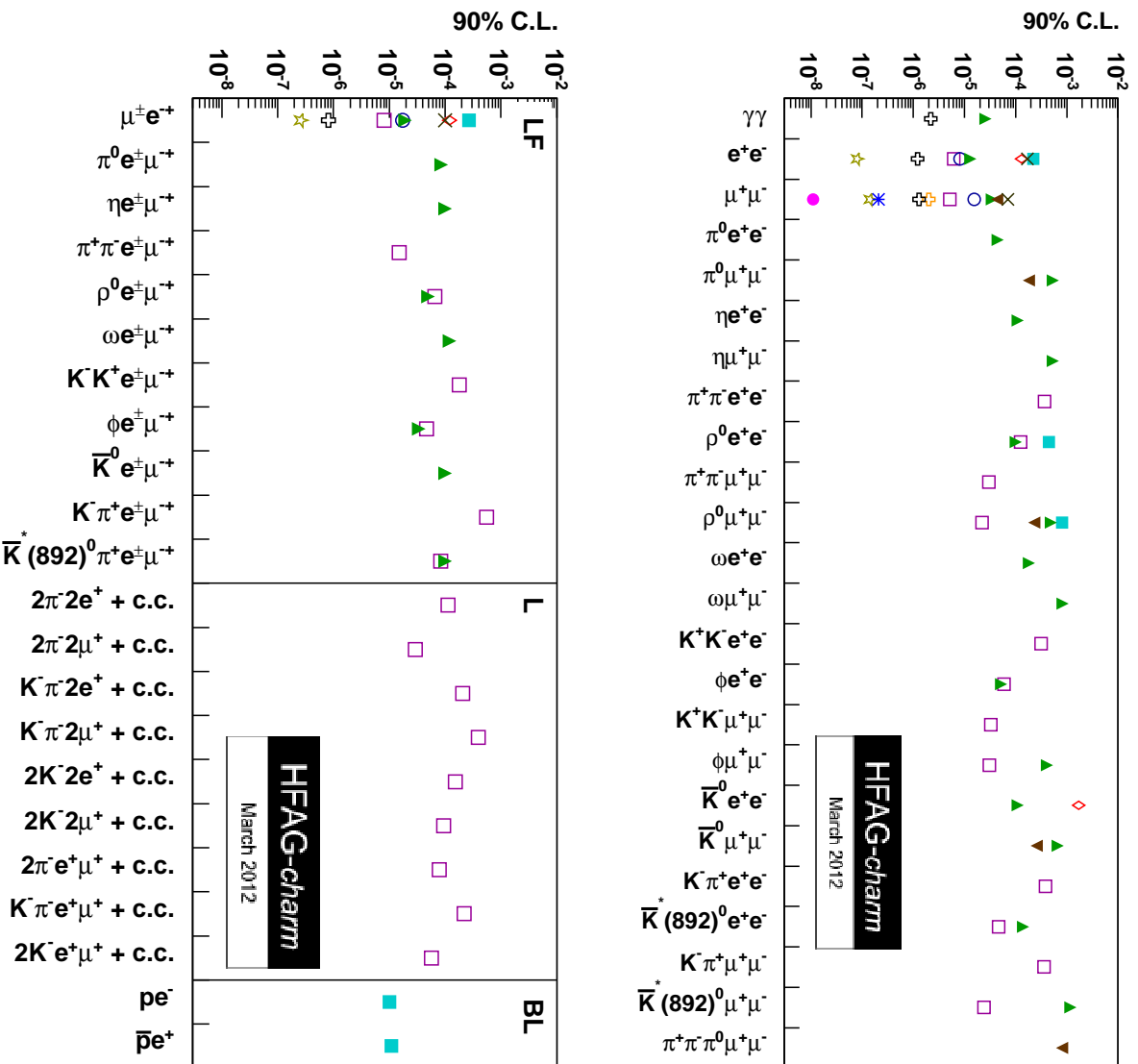


Figure 83: Upper limits at 90% CL for D^0 decays. The top plot shows flavor-changing neutral current decays, and the bottom plot shows lepton-flavor-changing (LF), lepton-number-changing (L), and both baryon- and lepton-number-changing (BL) decays. The legend is given in Fig. 85.

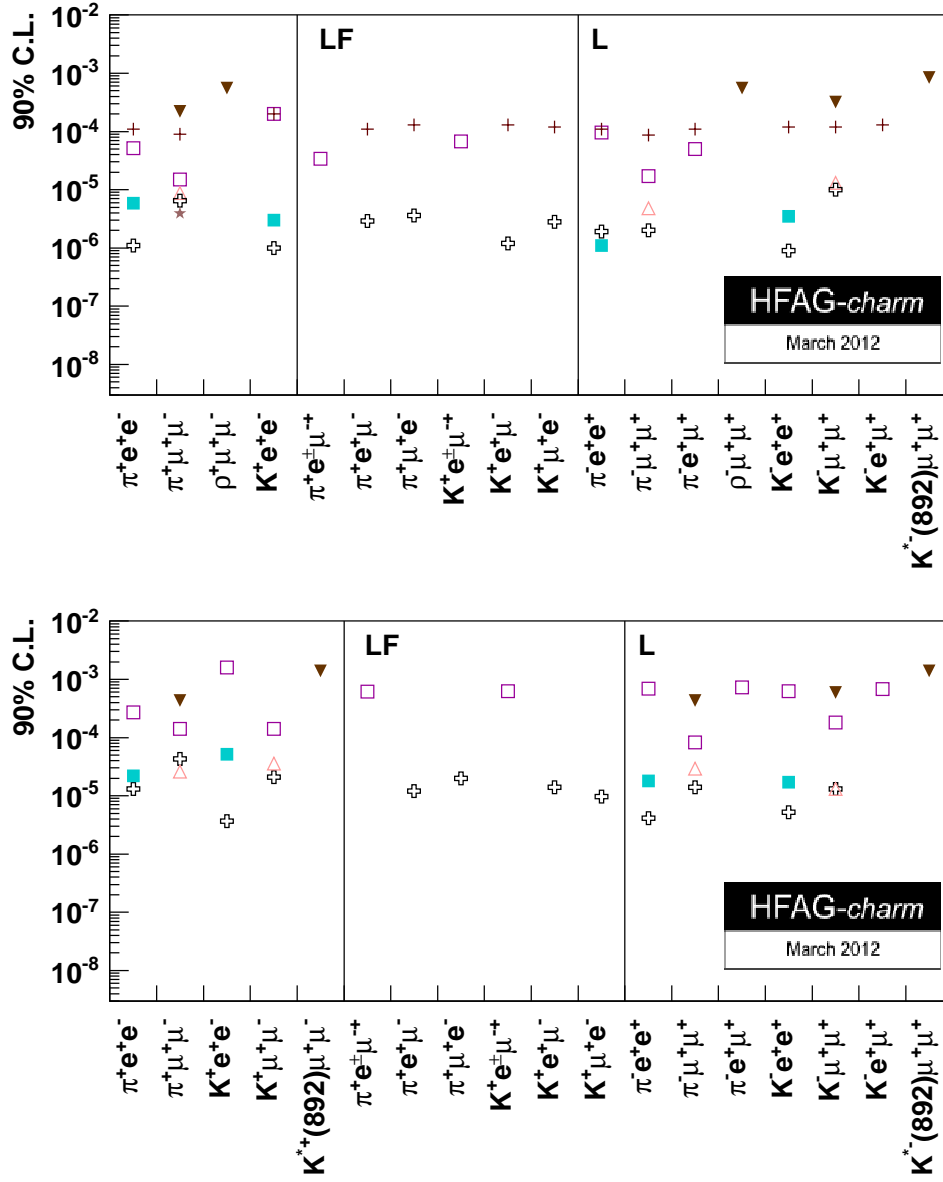


Figure 84: Upper limits at 90% CL for D^+ (top) and D_s^+ (bottom) decays. Each plot shows flavor-changing neutral current decays, lepton-flavor-changing decays (LF), and lepton-number-changing (L) decays. The legend is given in Fig. 85.

Table 190: Upper limits at 90% CL for D^+ decays.

Decay	Limit $\times 10^6$	Experiment	Reference
$\pi^+ e^+ e^-$	110.0	E687	[621]
	52.0	E791	[610]
	5.9	CLEO	[622]
	1.1	<i>BABAR</i>	[623]
$\pi^+ \mu^+ \mu^-$	220.0	E653	[613]
	89.0	E687	[621]

Table 190 – continued from previous page

Decay	Limit $\times 10^6$	Experiment	Reference
	15.0	E791	[610]
	8.8	FOCUS	[624]
	6.5	<i>BABAR</i>	[623]
	3.9	D0	[625]
$\rho^+\mu^+\mu^-$	560.0	E653	[613]
$K^+e^+e^-$	200.0	E687	[621]
	3.0	CLEO	[622]
	1.0	<i>BABAR</i>	[623]
$\pi^+e^\pm\mu^\mp$	34.0	E791	[610]
$\pi^+e^+\mu^-$	110.0	E687	[621]
	2.9	<i>BABAR</i>	[623]
$\pi^+\mu^+e^-$	130.0	E687	[621]
	3.6	<i>BABAR</i>	[623]
$K^+e^\pm\mu^\mp$	68.0	E791	[610]
$K^+e^+\mu^-$	130.0	E687	[621]
	1.2	<i>BABAR</i>	[623]
$K^+\mu^+e^-$	120.0	E687	[621]
	2.8	<i>BABAR</i>	[623]
$\pi^-e^+e^+$	110.0	E687	[621]
	96.0	E791	[610]
	1.9	<i>BABAR</i>	[623]
	1.1	CLEO	[622]
$\pi^-\mu^+\mu^+$	87.0	E687	[621]
	17.0	E791	[610]
	4.8	FOCUS	[624]
	2.0	<i>BABAR</i>	[623]
$\pi^-e^+\mu^+$	110.0	E687	[621]
	50.0	E791	[610]
$\rho^-\mu^+\mu^+$	560.0	E653	[613]
$K^-e^+e^+$	120.0	E687	[621]
	3.5	CLEO	[622]
	0.9	<i>BABAR</i>	[623]
$K^-\mu^+\mu^+$	320.0	E653	[613]
	120.0	E687	[621]
	13.0	FOCUS	[624]
	10.0	<i>BABAR</i>	[623]
$K^-e^+\mu^+$	130.0	E687	[621]
$K^{*-}(892)\mu^+\mu^+$	850.0	E653	[613]

Table 191: Upper limits at 90% CL for D_s^+ decays.

Decay	Limit $\times 10^6$	Experiment	Reference
$\pi^+e^+e^-$	270.0	E791	[610]

Table 191 – continued from previous page

Decay	Limit $\times 10^6$	Experiment	Reference
	22.0	CLEO	[622]
	13.0	<i>BABAR</i>	[623]
$\pi^+\mu^+\mu^-$	430.0	E653	[613]
	140.0	E791	[610]
	43.0	<i>BABAR</i>	[623]
	26.0	FOCUS	[624]
$K^+e^+e^-$	1600.0	E791	[610]
	52.0	CLEO	[622]
	3.7	<i>BABAR</i>	[623]
$K^+\mu^+\mu^-$	140.0	E791	[610]
	36.0	FOCUS	[624]
	21.0	<i>BABAR</i>	[623]
$K^{*+}(892)\mu^+\mu^-$	1400.0	E653	[613]
$\pi^+e^\pm\mu^\mp$	610.0	E791	[610]
$\pi^+e^+\mu^-$	12.0	<i>BABAR</i>	[623]
$\pi^+\mu^+e^-$	20.0	<i>BABAR</i>	[623]
$K^+e^\pm\mu^\mp$	630.0	E791	[610]
$K^+e^+\mu^-$	14.0	<i>BABAR</i>	[623]
$K^+\mu^+e^-$	9.7	<i>BABAR</i>	[623]
$\pi^-e^+e^+$	690.0	E791	[610]
	18.0	CLEO	[622]
	4.1	<i>BABAR</i>	[623]
$\pi^-\mu^+\mu^+$	430.0	E653	[613]
	82.0	E791	[610]
	29.0	FOCUS	[624]
	14.0	<i>BABAR</i>	[623]
$\pi^-e^+\mu^+$	730.0	E791	[610]
$K^-e^+e^+$	630.0	E791	[610]
	17.0	CLEO	[622]
	5.2	<i>BABAR</i>	[623]
$K^-\mu^+\mu^+$	590.0	E653	[613]
	180.0	E791	[610]
	13.0	FOCUS	[624]
$K^-e^+\mu^+$	680.0	E791	[610]
$K^{*-}(892)\mu^+\mu^+$	1400.0	E653	[613]

Table 192: Upper limits at 90% CL for Λ_c^+ decays.

Decay	Limit $\times 10^6$	Experiment	Reference
$p e^+ e^-$	5.5	<i>BABAR</i>	[623]
$p \mu^+ \mu^-$	340.0	E653	[613]
	44.0	<i>BABAR</i>	[623]
$\sigma^+ \mu^+ \mu^-$	700.0	E653	[613]

Table 192 – continued from previous page

Decay	Limit $\times 10^6$	Experiment	Reference
$pe^+\mu^-$	9.9	<i>BABAR</i>	[623]
$p\mu^+e^-$	19.0	<i>BABAR</i>	[623]
$\bar{p}e^+e^+$	2.7	<i>BABAR</i>	[623]
$\bar{p}\mu^+\mu^+$	9.4	<i>BABAR</i>	[623]

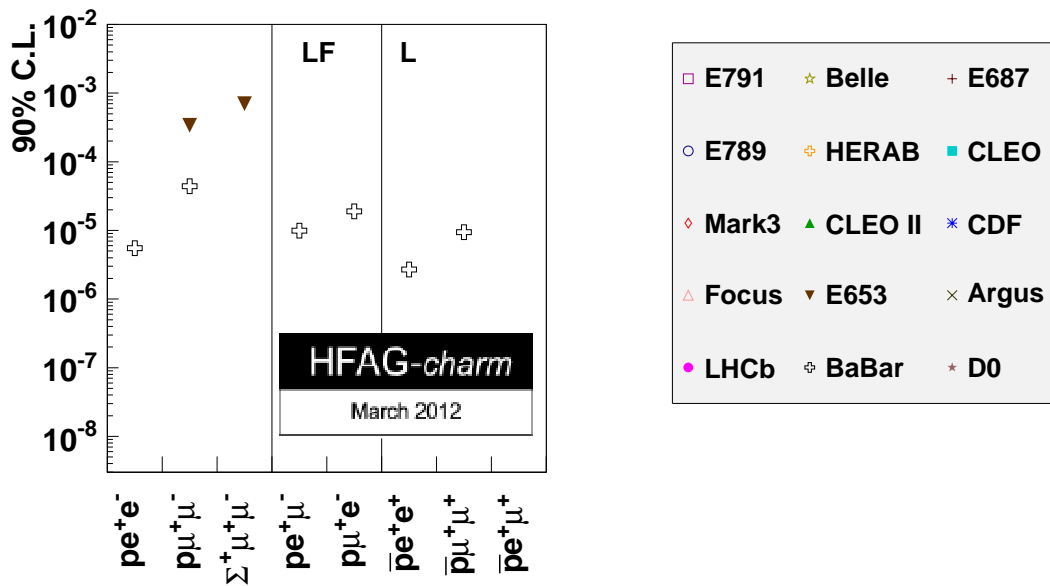


Figure 85: Upper limits at 90% CL for Λ_c^+ decays. Shown are flavor-changing neutral current decays, lepton-flavor-changing (LF) decays, and lepton-number-changing (L) decays.

9 Tau lepton properties

We present averages of a selection of physics quantities related to the tau lepton, where we follow the HFAG methodology [4] to improve the Review of Particle Physics (PDG) [5] results by:

- including a selection of reliable preliminary results, hence obtaining more up-to-date results;
- updating the experimental measurements value and systematic error when it depends on external parameters whose values and uncertainties are updated;
- taking into account the statistical correlation that is induced by the dependence from common systematic contributions.

All published statistical correlations are considered, and a selection of measurements, particularly the most precise and the most recent, were examined to obtain all the significant systematic dependencies. The HFAG techniques are most useful in the global fit of the tau branching fractions (Section 9.1). We use the branching fraction fit results to obtain updated lepton universality tests (Section 9.2) and updated determinations of $|V_{us}|$ with tau measurements (Section 9.4). Finally, we report in Section 9.5 the most up-to-date limits on the lepton-flavour-violating tau branching fractions.

9.1 Branching fractions fit

The measurements listed in Table 193 have been used in a minimum χ^2 fit subject to the equality constraints that are listed either in the same table (where some fitted quantities and experimental measurements are expressed as ratios of fit quantities) or in Section 9.1.2. The fitted quantities and the measurements are labelled using the PDG [5] Γ_n notation, where n is an integer number, which matches the PDG notation for $n < 800$. We use $n \geq 800$ to denote some additional branching fractions, as documented in the former HFAG report [4].

The fitted branching fractions consist on 40 “base nodes” and 45 derived branching fractions, described either as sum of base nodes (see Section 9.1.2) or as ratios of branching fractions (see Table 193). Furthermore, we define (see Section 9.1.2) Γ_{All} as the sum of all the base modes, which correspond to all non-overlapping tau decay modes, $\Gamma_{998} = 1 - \Gamma_{\text{All}}$ and $\Gamma_{110} = X_s^- \nu_\tau$, which is the total branching fraction of the tau to modes with the strangeness quantum number equal to one.

The fitted HFAG-Tau averages are reported in Table 193. The fit has $\chi^2/\text{d.o.f.} = 143.5/118$, corresponding to a confidence level $\text{CL} = 5.5\%$. We use a total of 157 measurements and 47 constraint equations to fit 86 quantities. The fit is statistically consistent with the unitarity constraint, but the unitarity constraint is not applied.

In several cases, when it is statistically equivalent within the HFAG-Tau fitting procedure, for historical reasons the statistical and systematic errors are added in quadrature and are reported in the above table in the location of the statistical error, reporting zero as systematic error. A scale factor of 5.44 (as in the former report [4]) has been applied in the fit to the quoted errors of the two inconsistent measurements of $\Gamma_{96} = \tau \rightarrow KKK\nu$ by *BABAR* and *Belle*.

With respect to the end-of-2009 HFAG report [4], following comments by M. Davier [626], we have included 3 new modes:

$$\begin{aligned}\Gamma_{49} &= \pi^- \pi^0 K^0 \bar{K}^0 \nu_\tau, \\ \Gamma_{804} &= \pi^- K_L^0 K_L^0 \nu_\tau, \\ \Gamma_{805} &= a_1^- (\rightarrow \pi^- \gamma) \nu_\tau\end{aligned}$$

along with the related measurements

$$\begin{aligned}\Gamma_{46} = \pi^- K^0 \bar{K}^0 \nu_\tau &= (0.1530 \pm 0.0340 \pm 0.0000) \cdot 10^{-2} \quad (\text{ALEPH [627]}), \\ \Gamma_{49} = \pi^- \pi^0 K^0 \bar{K}^0 \nu_\tau &= (3.1000 \pm 2.3000 \pm 0.0000) \cdot 10^{-4} \quad (\text{ALEPH [628]}),\end{aligned}$$

the estimate

$$\Gamma_{805} = a_1^- (\rightarrow \pi^- \gamma) \nu_\tau = (4.0000 \pm 2.0000 \pm 0.0000) \cdot 10^{-4} \quad (\text{ALEPH [629]}),$$

and the constraint

$$\Gamma_{46} = \Gamma_{48} + \Gamma_{47} + \Gamma_{804} .$$

Furthermore, the following new measurements were added:

$$\begin{aligned}\Gamma_{128} = K^- \eta \nu_\tau &= (1.4200 \pm 0.1100 \pm 0.0700) \cdot 10^{-4} \quad (\text{BABAR [630]}), \\ \Gamma_{40} = \bar{K}^0 \pi^- \pi^0 \nu_\tau &= (0.3840 \pm 0.0040 \pm 0.0160) \cdot 10^{-2} \quad (\text{Belle [631]}), \\ \Gamma_{42} = K^- \pi^0 K^0 \nu_\tau &= (0.1480 \pm 0.0020 \pm 0.0080) \cdot 10^{-2} \quad (\text{Belle [631]}).\end{aligned}$$

Finally, the constraint parameters (see Section 9.1.2) have been updated to the PDG 2011 results [5].

Table 193: HFAG Winter 2012 branching fractions fit results.

Tau lepton branching fraction	Value	Exp.	Ref.
$\Gamma_3 = \mu^- \bar{\nu}_\mu \nu_\tau$	$(17.392 \pm 0.040) \cdot 10^{-2}$	HFAG	Winter 2012 fit
	$(17.319 \pm 0.077 \pm 0.000) \cdot 10^{-2}$	ALEPH	[629]
	$(17.325 \pm 0.122 \pm 0.000) \cdot 10^{-2}$	DELPHI	[632]
	$(17.342 \pm 0.129 \pm 0.000) \cdot 10^{-2}$	L3	[633]
	$(17.340 \pm 0.108 \pm 0.000) \cdot 10^{-2}$	OPAL	[634]
$\frac{\Gamma_3}{\Gamma_5} = \frac{\mu^- \bar{\nu}_\mu \nu_\tau}{e^- \bar{\nu}_e \nu_\tau}$	0.9761 ± 0.0028	HFAG	Winter 2012 fit
	$0.9970 \pm 0.0532 \pm 0.0000$	ARGUS	[635]
	$0.9796 \pm 0.0039 \pm 0.0005$	BABAR	[636]
	$0.9777 \pm 0.0107 \pm 0.0000$	CLEO	[637]
$\Gamma_5 = e^- \bar{\nu}_e \nu_\tau$	$(17.818 \pm 0.041) \cdot 10^{-2}$	HFAG	Winter 2012 fit
	$(17.837 \pm 0.080 \pm 0.000) \cdot 10^{-2}$	ALEPH	[629]

Table 193 – continued from previous page

Tau lepton branching fraction	Value	Exp.	Ref.
	$(17.760 \pm 0.180 \pm 0.000) \cdot 10^{-2}$	CLEO	[637]
	$(17.877 \pm 0.155 \pm 0.000) \cdot 10^{-2}$	DELPHI	[632]
	$(17.806 \pm 0.129 \pm 0.000) \cdot 10^{-2}$	L3	[633]
	$(17.810 \pm 0.108 \pm 0.000) \cdot 10^{-2}$	OPAL	[638]
$\Gamma_7 = h^- \geq 0K_L^0\nu_\tau$	$(12.020 \pm 0.055) \cdot 10^{-2}$	HFAG	Winter 2012 fit
	$(12.400 \pm 0.990 \pm 0.000) \cdot 10^{-2}$	DELPHI	[639]
	$(12.470 \pm 0.502 \pm 0.000) \cdot 10^{-2}$	L3	[640]
	$(12.100 \pm 0.860 \pm 0.000) \cdot 10^{-2}$	OPAL	[641]
$\Gamma_8 = h^- \nu_\tau$	$(11.507 \pm 0.054) \cdot 10^{-2}$	HFAG	Winter 2012 fit
	$(11.524 \pm 0.105 \pm 0.000) \cdot 10^{-2}$	ALEPH	[629]
	$(11.520 \pm 0.130 \pm 0.000) \cdot 10^{-2}$	CLEO	[637]
	$(11.571 \pm 0.166 \pm 0.000) \cdot 10^{-2}$	DELPHI	[642]
	$(11.980 \pm 0.206 \pm 0.000) \cdot 10^{-2}$	OPAL	[643]
$\Gamma_9 = \pi^- \nu_\tau$	$(10.811 \pm 0.053) \cdot 10^{-2}$	HFAG	Winter 2012 fit
$\frac{\Gamma_9}{\Gamma_5} = \frac{\pi^- \nu_\tau}{e^- \bar{\nu}_e \nu_\tau}$	$(60.675 \pm 0.321) \cdot 10^{-2}$	HFAG	Winter 2012 fit
	$(59.450 \pm 0.574 \pm 0.248) \cdot 10^{-2}$	BABAR	[636]
$\Gamma_{10} = K^- \nu_\tau$	$(0.6955 \pm 0.0096) \cdot 10^{-2}$	HFAG	Winter 2012 fit
	$(0.6960 \pm 0.0287 \pm 0.0000) \cdot 10^{-2}$	ALEPH	[644]
	$(0.6600 \pm 0.1140 \pm 0.0000) \cdot 10^{-2}$	CLEO	[645]
	$(0.8500 \pm 0.1800 \pm 0.0000) \cdot 10^{-2}$	DELPHI	[646]
	$(0.6580 \pm 0.0396 \pm 0.0000) \cdot 10^{-2}$	OPAL	[647]
$\frac{\Gamma_{10}}{\Gamma_5} = \frac{K^- \nu_\tau}{e^- \bar{\nu}_e \nu_\tau}$	$(3.9031 \pm 0.0543) \cdot 10^{-2}$	HFAG	Winter 2012 fit
	$(3.8820 \pm 0.0630 \pm 0.0174) \cdot 10^{-2}$	BABAR	[636]
$\Gamma_{13} = h^- \pi^0 \nu_\tau$	$(25.936 \pm 0.090) \cdot 10^{-2}$	HFAG	Winter 2012 fit
	$(25.924 \pm 0.129 \pm 0.000) \cdot 10^{-2}$	ALEPH	[629]
	$(25.670 \pm 0.010 \pm 0.390) \cdot 10^{-2}$	Belle	[648]
	$(25.870 \pm 0.437 \pm 0.000) \cdot 10^{-2}$	CLEO	[649]
	$(25.740 \pm 0.244 \pm 0.000) \cdot 10^{-2}$	DELPHI	[642]
	$(25.050 \pm 0.610 \pm 0.000) \cdot 10^{-2}$	L3	[640]
	$(25.890 \pm 0.336 \pm 0.000) \cdot 10^{-2}$	OPAL	[643]
$\Gamma_{14} = \pi^- \pi^0 \nu_\tau$	$(25.504 \pm 0.092) \cdot 10^{-2}$	HFAG	Winter 2012 fit
$\Gamma_{16} = K^- \pi^0 \nu_\tau$	$(0.4322 \pm 0.0149) \cdot 10^{-2}$	HFAG	Winter 2012 fit
	$(0.4440 \pm 0.0354 \pm 0.0000) \cdot 10^{-2}$	ALEPH	[644]
	$(0.4160 \pm 0.0030 \pm 0.0180) \cdot 10^{-2}$	BABAR	[650]
	$(0.5100 \pm 0.1221 \pm 0.0000) \cdot 10^{-2}$	CLEO	[645]

Table 193 – continued from previous page

Tau lepton branching fraction	Value	Exp.	Ref.
	$(0.4710 \pm 0.0633 \pm 0.0000) \cdot 10^{-2}$	OPAL	[651]
$\Gamma_{17} = h^- \geq 2\pi^0\nu_\tau$	$(10.803 \pm 0.095) \cdot 10^{-2}$	HFAG	Winter 2012 fit
	$(9.910 \pm 0.411 \pm 0.000) \cdot 10^{-2}$	OPAL	[643]
$\Gamma_{19} = h^- 2\pi^0\nu_\tau$ (ex. K^0)	$(9.3044 \pm 0.0972) \cdot 10^{-2}$	HFAG	Winter 2012 fit
	$(9.2950 \pm 0.1217 \pm 0.0000) \cdot 10^{-2}$	ALEPH	[629]
	$(9.4980 \pm 0.4219 \pm 0.0000) \cdot 10^{-2}$	DELPHI	[642]
	$(8.8800 \pm 0.5597 \pm 0.0000) \cdot 10^{-2}$	L3	[640]
$\frac{\Gamma_{19}}{\Gamma_{13}} = \frac{h^- 2\pi^0\nu_\tau \text{ (ex. } K^0\text{)}}{h^- \pi^0\nu_\tau}$	$(35.874 \pm 0.442) \cdot 10^{-2}$	HFAG	Winter 2012 fit
	$(34.200 \pm 1.709 \pm 0.000) \cdot 10^{-2}$	CLEO	[652]
$\Gamma_{20} = \pi^- 2\pi^0\nu_\tau$ (ex. K^0)	$(9.2414 \pm 0.0997) \cdot 10^{-2}$	HFAG	Winter 2012 fit
$\Gamma_{23} = K^- 2\pi^0\nu_\tau$ (ex. K^0)	$(0.0630 \pm 0.0222) \cdot 10^{-2}$	HFAG	Winter 2012 fit
	$(0.0560 \pm 0.0250 \pm 0.0000) \cdot 10^{-2}$	ALEPH	[644]
	$(0.0900 \pm 0.1044 \pm 0.0000) \cdot 10^{-2}$	CLEO	[645]
$\Gamma_{25} = h^- \geq 3\pi^0\nu_\tau$ (ex. K^0)	$(1.2349 \pm 0.0650) \cdot 10^{-2}$	HFAG	Winter 2012 fit
	$(1.4030 \pm 0.3098 \pm 0.0000) \cdot 10^{-2}$	DELPHI	[642]
$\Gamma_{26} = h^- 3\pi^0\nu_\tau$	$(1.1573 \pm 0.0717) \cdot 10^{-2}$	HFAG	Winter 2012 fit
	$(1.0820 \pm 0.0926 \pm 0.0000) \cdot 10^{-2}$	ALEPH	[629]
	$(1.7000 \pm 0.4494 \pm 0.0000) \cdot 10^{-2}$	L3	[640]
$\frac{\Gamma_{26}}{\Gamma_{13}} = \frac{h^- 3\pi^0\nu_\tau}{h^- \pi^0\nu_\tau}$	$(4.4622 \pm 0.2767) \cdot 10^{-2}$	HFAG	Winter 2012 fit
	$(4.4000 \pm 0.5831 \pm 0.0000) \cdot 10^{-2}$	CLEO	[652]
$\Gamma_{27} = \pi^- 3\pi^0\nu_\tau$ (ex. K^0)	$(1.0322 \pm 0.0749) \cdot 10^{-2}$	HFAG	Winter 2012 fit
$\Gamma_{28} = K^- 3\pi^0\nu_\tau$ (ex. K^0, η)	$(4.1870 \pm 2.1761) \cdot 10^{-4}$	HFAG	Winter 2012 fit
	$(3.7000 \pm 2.3710 \pm 0.0000) \cdot 10^{-4}$	ALEPH	[644]
$\Gamma_{29} = h^- 4\pi^0\nu_\tau$ (ex. K^0)	$(0.1558 \pm 0.0391) \cdot 10^{-2}$	HFAG	Winter 2012 fit
	$(0.1600 \pm 0.0707 \pm 0.0000) \cdot 10^{-2}$	CLEO	[652]
$\Gamma_{30} = h^- 4\pi^0\nu_\tau$ (ex. K^0, η)	$(0.1091 \pm 0.0391) \cdot 10^{-2}$	HFAG	Winter 2012 fit
	$(0.1120 \pm 0.0509 \pm 0.0000) \cdot 10^{-2}$	ALEPH	[629]
$\Gamma_{31} = K^- \geq 0\pi^0 \geq 0K^0 \geq 0\gamma\nu_\tau$	$(1.5481 \pm 0.0310) \cdot 10^{-2}$	HFAG	Winter 2012 fit
	$(1.7000 \pm 0.2247 \pm 0.0000) \cdot 10^{-2}$	CLEO	[645]
	$(1.5400 \pm 0.2400 \pm 0.0000) \cdot 10^{-2}$	DELPHI	[646]
	$(1.5280 \pm 0.0559 \pm 0.0000) \cdot 10^{-2}$	OPAL	[647]
$\Gamma_{33} = K_S^0(\text{particles})^- \nu_\tau$	$(0.8953 \pm 0.0255) \cdot 10^{-2}$	HFAG	Winter 2012 fit
	$(0.9700 \pm 0.0849 \pm 0.0000) \cdot 10^{-2}$	ALEPH	[627]
	$(0.9700 \pm 0.1082 \pm 0.0000) \cdot 10^{-2}$	OPAL	[653]

Table 193 – continued from previous page

Tau lepton branching fraction	Value	Exp.	Ref.
$\Gamma_{34} = h^- \bar{K}^0 \nu_\tau$	$(0.9797 \pm 0.0233) \cdot 10^{-2}$	HFAG	Winter 2012 fit
	$(0.8550 \pm 0.0814 \pm 0.0000) \cdot 10^{-2}$	CLEO	[654]
$\Gamma_{35} = \pi^- \bar{K}^0 \nu_\tau$	$(0.8206 \pm 0.0182) \cdot 10^{-2}$	HFAG	Winter 2012 fit
	$(0.9280 \pm 0.0564 \pm 0.0000) \cdot 10^{-2}$	ALEPH	[644]
	$(0.8400 \pm 0.0040 \pm 0.0230) \cdot 10^{-2}$	BABAR	[655]
	$(0.8080 \pm 0.0040 \pm 0.0260) \cdot 10^{-2}$	Belle	[656]
	$(0.9500 \pm 0.1616 \pm 0.0000) \cdot 10^{-2}$	L3	[657]
	$(0.9330 \pm 0.0838 \pm 0.0000) \cdot 10^{-2}$	OPAL	[658]
$\Gamma_{37} = K^- K^0 \nu_\tau$	$(0.1591 \pm 0.0157) \cdot 10^{-2}$	HFAG	Winter 2012 fit
	$(0.1580 \pm 0.0453 \pm 0.0000) \cdot 10^{-2}$	ALEPH	[627]
	$(0.1620 \pm 0.0237 \pm 0.0000) \cdot 10^{-2}$	ALEPH	[644]
	$(0.1510 \pm 0.0304 \pm 0.0000) \cdot 10^{-2}$	CLEO	[654]
$\Gamma_{38} = K^- K^0 \geq 0\pi^0 \nu_\tau$	$(0.3041 \pm 0.0168) \cdot 10^{-2}$	HFAG	Winter 2012 fit
	$(0.3300 \pm 0.0674 \pm 0.0000) \cdot 10^{-2}$	OPAL	[658]
$\Gamma_{39} = h^- \bar{K}^0 \pi^0 \nu_\tau$	$(0.5099 \pm 0.0146) \cdot 10^{-2}$	HFAG	Winter 2012 fit
	$(0.5620 \pm 0.0693 \pm 0.0000) \cdot 10^{-2}$	CLEO	[654]
$\Gamma_{40} = \pi^- \bar{K}^0 \pi^0 \nu_\tau$	$(0.3649 \pm 0.0108) \cdot 10^{-2}$	HFAG	Winter 2012 fit
	$(0.2940 \pm 0.0818 \pm 0.0000) \cdot 10^{-2}$	ALEPH	[627]
	$(0.3470 \pm 0.0646 \pm 0.0000) \cdot 10^{-2}$	ALEPH	[644]
	$(0.3420 \pm 0.0060 \pm 0.0150) \cdot 10^{-2}$	BABAR	[659]
	$(0.3840 \pm 0.0040 \pm 0.0160) \cdot 10^{-2}$	Belle	[631]
	$(0.4100 \pm 0.1237 \pm 0.0000) \cdot 10^{-2}$	L3	[657]
$\Gamma_{42} = K^- \pi^0 K^0 \nu_\tau$	$(0.1450 \pm 0.0071) \cdot 10^{-2}$	HFAG	Winter 2012 fit
	$(0.1520 \pm 0.0789 \pm 0.0000) \cdot 10^{-2}$	ALEPH	[627]
	$(0.1430 \pm 0.0291 \pm 0.0000) \cdot 10^{-2}$	ALEPH	[644]
	$(0.1480 \pm 0.0020 \pm 0.0080) \cdot 10^{-2}$	Belle	[631]
	$(0.1450 \pm 0.0412 \pm 0.0000) \cdot 10^{-2}$	CLEO	[654]
$\Gamma_{43} = \pi^- \bar{K}^0 \geq 1\pi^0 \nu_\tau$	$(0.3917 \pm 0.0250) \cdot 10^{-2}$	HFAG	Winter 2012 fit
	$(0.3240 \pm 0.0992 \pm 0.0000) \cdot 10^{-2}$	OPAL	[658]
$\Gamma_{44} = \pi^- \bar{K}^0 \pi^0 \pi^0 \nu_\tau$	$(2.6854 \pm 2.3037) \cdot 10^{-4}$	HFAG	Winter 2012 fit
	$(2.6000 \pm 2.4000 \pm 0.0000) \cdot 10^{-4}$	ALEPH	[628]
$\Gamma_{46} = \pi^- K^0 \bar{K}^0 \nu_\tau$	$(0.1562 \pm 0.0209) \cdot 10^{-2}$	HFAG	Winter 2012 fit
	$(0.1530 \pm 0.0340 \pm 0.0000) \cdot 10^{-2}$	ALEPH	[627]
$\Gamma_{47} = \pi^- K_S^0 K_S^0 \nu_\tau$	$(2.3957 \pm 0.5026) \cdot 10^{-4}$	HFAG	Winter 2012 fit
	$(2.6000 \pm 1.1180 \pm 0.0000) \cdot 10^{-4}$	ALEPH	[627]

Table 193 – continued from previous page

Tau lepton branching fraction	Value	Exp.	Ref.
	$(2.3000 \pm 0.5831 \pm 0.0000) \cdot 10^{-4}$	CLEO	[654]
$\Gamma_{48} = \pi^- K_S^0 K_L^0 \nu_\tau$	$(0.1082 \pm 0.0203) \cdot 10^{-2}$	HFAG	Winter 2012 fit
	$(0.1010 \pm 0.0264 \pm 0.0000) \cdot 10^{-2}$	ALEPH	[627]
$\Gamma_{49} = \pi^- K^0 \bar{K}^0 \pi^0 \nu_\tau$	$(3.1000 \pm 2.3000) \cdot 10^{-4}$	HFAG	Winter 2012 fit
	$(3.1000 \pm 2.3000 \pm 0.0000) \cdot 10^{-4}$	ALEPH	[628]
$\Gamma_{53} = \bar{K}^0 h^- h^- h^+ \nu_\tau$	$(2.2224 \pm 2.0236) \cdot 10^{-4}$	HFAG	Winter 2012 fit
	$(2.3000 \pm 2.0248 \pm 0.0000) \cdot 10^{-4}$	ALEPH	[627]
$\Gamma_{54} = h^- h^- h^+ \geq 0 \text{neutrals} \geq 0 K_L^0 \nu_\tau$	$(15.192 \pm 0.060) \cdot 10^{-2}$	HFAG	Winter 2012 fit
	$(15.000 \pm 0.500 \pm 0.000) \cdot 10^{-2}$	CELLO	[660]
	$(14.400 \pm 0.671 \pm 0.000) \cdot 10^{-2}$	L3	[661]
	$(15.100 \pm 1.000 \pm 0.000) \cdot 10^{-2}$	TPC	[662]
$\Gamma_{55} = h^- h^- h^+ \geq 0 \text{neutrals} \nu_\tau$ (ex. K^0)	$(14.574 \pm 0.056) \cdot 10^{-2}$	HFAG	Winter 2012 fit
	$(14.556 \pm 0.130 \pm 0.000) \cdot 10^{-2}$	L3	[663]
	$(14.960 \pm 0.238 \pm 0.000) \cdot 10^{-2}$	OPAL	[664]
$\Gamma_{57} = h^- h^- h^+ \nu_\tau$ (ex. K^0)	$(9.4404 \pm 0.0530) \cdot 10^{-2}$	HFAG	Winter 2012 fit
	$(9.5100 \pm 0.2119 \pm 0.0000) \cdot 10^{-2}$	CLEO	[665]
	$(9.3170 \pm 0.1218 \pm 0.0000) \cdot 10^{-2}$	DELPHI	[642]
$\frac{\Gamma_{57}}{\Gamma_{55}} = \frac{h^- h^- h^+ \nu_\tau \text{ (ex. } K^0\text{)}}{h^- h^- h^+ \geq 0 \text{neutrals} \nu_\tau \text{ (ex. } K^0\text{)}}$	$(64.776 \pm 0.294) \cdot 10^{-2}$	HFAG	Winter 2012 fit
	$(66.000 \pm 1.456 \pm 0.000) \cdot 10^{-2}$	OPAL	[664]
$\Gamma_{58} = h^- h^- h^+ \nu_\tau$ (ex. K^0, ω)	$(9.4099 \pm 0.0531) \cdot 10^{-2}$	HFAG	Winter 2012 fit
	$(9.4690 \pm 0.0958 \pm 0.0000) \cdot 10^{-2}$	ALEPH	[629]
$\Gamma_{60} = \pi^- \pi^- \pi^+ \nu_\tau$ (ex. K^0)	$(9.0018 \pm 0.0510) \cdot 10^{-2}$	HFAG	Winter 2012 fit
	$(8.8337 \pm 0.0074 \pm 0.1267) \cdot 10^{-2}$	BABAR	[666]
	$(8.4200 \pm 0.0033 \pm 0.2588) \cdot 10^{-2}$	Belle	[667]
	$(9.1300 \pm 0.4627 \pm 0.0000) \cdot 10^{-2}$	CLEO3	[668]
$\Gamma_{62} = \pi^- \pi^- \pi^+ \nu_\tau$ (ex. K^0, ω)	$(8.9719 \pm 0.0511) \cdot 10^{-2}$	HFAG	Winter 2012 fit
$\Gamma_{66} = h^- h^- h^+ \pi^0 \nu_\tau$ (ex. K^0)	$(4.6019 \pm 0.0513) \cdot 10^{-2}$	HFAG	Winter 2012 fit
	$(4.7340 \pm 0.0767 \pm 0.0000) \cdot 10^{-2}$	ALEPH	[629]
	$(4.2300 \pm 0.2280 \pm 0.0000) \cdot 10^{-2}$	CLEO	[665]
	$(4.5450 \pm 0.1478 \pm 0.0000) \cdot 10^{-2}$	DELPHI	[642]
$\Gamma_{69} = \pi^- \pi^- \pi^+ \pi^0 \nu_\tau$ (ex. K^0)	$(4.5146 \pm 0.0524) \cdot 10^{-2}$	HFAG	Winter 2012 fit
	$(4.1900 \pm 0.2326 \pm 0.0000) \cdot 10^{-2}$	CLEO	[669]
$\Gamma_{70} = \pi^- \pi^- \pi^+ \pi^0 \nu_\tau$ (ex. K^0, ω)	$(2.7659 \pm 0.0710) \cdot 10^{-2}$	HFAG	Winter 2012 fit
$\Gamma_{74} = h^- h^- h^+ \geq 2\pi^0 \nu_\tau$ (ex. K^0)	$(0.5231 \pm 0.0311) \cdot 10^{-2}$	HFAG	Winter 2012 fit

Table 193 – continued from previous page

Tau lepton branching fraction	Value	Exp.	Ref.
	$(0.5610 \pm 0.1168 \pm 0.0000) \cdot 10^{-2}$	DELPHI	[642]
$\Gamma_{76} = h^- h^- h^+ 2\pi^0 \nu_\tau$ (ex. K^0)	$(0.4911 \pm 0.0310) \cdot 10^{-2}$	HFAG	Winter 2012 fit
	$(0.4350 \pm 0.0461 \pm 0.0000) \cdot 10^{-2}$	ALEPH	[629]
$\frac{\Gamma_{76}}{\Gamma_{54}} = \frac{h^- h^- h^+ 2\pi^0 \nu_\tau \text{ (ex. } K^0\text{)}}{h^- h^- h^+ \geq 0 \text{ neutrals} \geq 0 K_L^0 \nu_\tau}$	$(3.2326 \pm 0.2024) \cdot 10^{-2}$	HFAG	Winter 2012 fit
	$(3.4000 \pm 0.3606 \pm 0.0000) \cdot 10^{-2}$	CLEO	[670]
$\Gamma_{77} = h^- h^- h^+ 2\pi^0 \nu_\tau$ (ex. K^0, ω, η)	$(9.7301 \pm 3.5416) \cdot 10^{-4}$	HFAG	Winter 2012 fit
$\Gamma_{78} = h^- h^- h^+ 3\pi^0 \nu_\tau$	$(3.1986 \pm 0.3124) \cdot 10^{-4}$	HFAG	Winter 2012 fit
	$(2.2000 \pm 0.5000 \pm 0.0000) \cdot 10^{-4}$	CLEO	[671]
$\frac{\Gamma_{80}}{\Gamma_{60}} = \frac{K^- \pi^- h^+ \nu_\tau \text{ (ex. } K^0\text{)}}{\pi^- \pi^- \pi^+ \nu_\tau \text{ (ex. } K^0\text{)}}$	$(4.8482 \pm 0.0808) \cdot 10^{-2}$	HFAG	Winter 2012 fit
	$(5.4400 \pm 0.5701 \pm 0.0000) \cdot 10^{-2}$	CLEO	[672]
$\frac{\Gamma_{81}}{\Gamma_{69}} = \frac{K^- \pi^- h^+ \pi^0 \nu_\tau \text{ (ex. } K^0\text{)}}{\pi^- \pi^- \pi^+ \pi^0 \nu_\tau \text{ (ex. } K^0\text{)}}$	$(1.9323 \pm 0.2660) \cdot 10^{-2}$	HFAG	Winter 2012 fit
	$(2.6100 \pm 0.6155 \pm 0.0000) \cdot 10^{-2}$	CLEO	[672]
$\Gamma_{82} = K^- \pi^- \pi^+ \geq 0 \text{ neutrals} \nu_\tau$	$(0.4801 \pm 0.0147) \cdot 10^{-2}$	HFAG	Winter 2012 fit
	$(0.5800 \pm 0.1845 \pm 0.0000) \cdot 10^{-2}$	TPC	[673]
$\Gamma_{85} = K^- \pi^- \pi^+ \nu_\tau$ (ex. K^0)	$(0.2929 \pm 0.0068) \cdot 10^{-2}$	HFAG	Winter 2012 fit
	$(0.2140 \pm 0.0470 \pm 0.0000) \cdot 10^{-2}$	ALEPH	[674]
	$(0.2726 \pm 0.0018 \pm 0.0092) \cdot 10^{-2}$	BABAR	[666]
	$(0.3300 \pm 0.0013 \pm 0.0166) \cdot 10^{-2}$	Belle	[667]
	$(0.3840 \pm 0.0405 \pm 0.0000) \cdot 10^{-2}$	CLEO3	[668]
	$(0.4150 \pm 0.0664 \pm 0.0000) \cdot 10^{-2}$	OPAL	[651]
$\Gamma_{88} = K^- \pi^- \pi^+ \pi^0 \nu_\tau$ (ex. K^0)	$(8.1122 \pm 1.1680) \cdot 10^{-4}$	HFAG	Winter 2012 fit
	$(6.1000 \pm 4.2950 \pm 0.0000) \cdot 10^{-4}$	ALEPH	[674]
	$(7.4000 \pm 1.3600 \pm 0.0000) \cdot 10^{-4}$	CLEO3	[675]
$\Gamma_{92} = \pi^- K^- K^+ \geq 0 \text{ neutrals} \nu_\tau$	$(0.1496 \pm 0.0033) \cdot 10^{-2}$	HFAG	Winter 2012 fit
	$(0.1590 \pm 0.0566 \pm 0.0000) \cdot 10^{-2}$	OPAL	[676]
	$(0.1500 \pm 0.0855 \pm 0.0000) \cdot 10^{-2}$	TPC	[673]
$\Gamma_{93} = \pi^- K^- K^+ \nu_\tau$	$(0.1435 \pm 0.0027) \cdot 10^{-2}$	HFAG	Winter 2012 fit
	$(0.1630 \pm 0.0270 \pm 0.0000) \cdot 10^{-2}$	ALEPH	[674]
	$(0.1346 \pm 0.0010 \pm 0.0036) \cdot 10^{-2}$	BABAR	[666]
	$(0.1550 \pm 0.0007 \pm 0.0056) \cdot 10^{-2}$	Belle	[667]
	$(0.1550 \pm 0.0108 \pm 0.0000) \cdot 10^{-2}$	CLEO3	[668]
$\frac{\Gamma_{93}}{\Gamma_{60}} = \frac{\pi^- K^- K^+ \nu_\tau}{\pi^- \pi^- \pi^+ \nu_\tau \text{ (ex. } K^0\text{)}}$	$(1.5940 \pm 0.0305) \cdot 10^{-2}$	HFAG	Winter 2012 fit
	$(1.6000 \pm 0.3354 \pm 0.0000) \cdot 10^{-2}$	CLEO	[672]

Table 193 – continued from previous page

Tau lepton branching fraction	Value	Exp.	Ref.
$\Gamma_{94} = \pi^- K^- K^+ \pi^0 \nu_\tau$	$(0.6113 \pm 0.1829) \cdot 10^{-4}$	HFAG	Winter 2012 fit
	$(7.5000 \pm 3.2650 \pm 0.0000) \cdot 10^{-4}$	ALEPH	[674]
	$(0.5500 \pm 0.1844 \pm 0.0000) \cdot 10^{-4}$	CLEO3	[675]
$\frac{\Gamma_{94}}{\Gamma_{69}} = \frac{\pi^- K^- K^+ \pi^0 \nu_\tau}{\pi^- \pi^- \pi^+ \pi^0 \nu_\tau \text{ (ex. } K^0)}$	$(0.1354 \pm 0.0406) \cdot 10^{-2}$	HFAG	Winter 2012 fit
	$(0.7900 \pm 0.4682 \pm 0.0000) \cdot 10^{-2}$	CLEO	[672]
$\Gamma_{96} = K^- K^- K^+ \nu_\tau$	$(2.1774 \pm 0.8005) \cdot 10^{-5}$	HFAG	Winter 2012 fit
	$(1.5777 \pm 0.1300 \pm 0.1231) \cdot 10^{-5}$	BABAR	[666]
	$(3.2900 \pm 0.1694 \pm 0.1962) \cdot 10^{-5}$	Belle	[667]
$\Gamma_{102} = 3h^- 2h^+ \geq 0 \text{ neutrals } \nu_\tau \text{ (ex. } K^0)$	$(0.1022 \pm 0.0037) \cdot 10^{-2}$	HFAG	Winter 2012 fit
	$(0.0970 \pm 0.0121 \pm 0.0000) \cdot 10^{-2}$	CLEO	[677]
	$(0.1020 \pm 0.0290 \pm 0.0000) \cdot 10^{-2}$	HRS	[678]
	$(0.1700 \pm 0.0341 \pm 0.0000) \cdot 10^{-2}$	L3	[663]
$\Gamma_{103} = 3h^- 2h^+ \nu_\tau \text{ (ex. } K^0)$	$(8.2349 \pm 0.3060) \cdot 10^{-4}$	HFAG	Winter 2012 fit
	$(7.2000 \pm 1.5000 \pm 0.0000) \cdot 10^{-4}$	ALEPH	[629]
	$(6.4000 \pm 2.5080 \pm 0.0000) \cdot 10^{-4}$	ARGUS	[679]
	$(8.5600 \pm 0.0500 \pm 0.4200) \cdot 10^{-4}$	BABAR	[680]
	$(7.7000 \pm 1.0300 \pm 0.0000) \cdot 10^{-4}$	CLEO	[677]
	$(9.7000 \pm 1.5810 \pm 0.0000) \cdot 10^{-4}$	DELPHI	[642]
	$(5.1000 \pm 2.0000 \pm 0.0000) \cdot 10^{-4}$	HRS	[678]
	$(9.1000 \pm 1.5230 \pm 0.0000) \cdot 10^{-4}$	OPAL	[681]
$\Gamma_{104} = 3h^- 2h^+ \pi^0 \nu_\tau \text{ (ex. } K^0)$	$(1.9801 \pm 0.2437) \cdot 10^{-4}$	HFAG	Winter 2012 fit
	$(2.1000 \pm 0.9220 \pm 0.0000) \cdot 10^{-4}$	ALEPH	[629]
	$(1.7000 \pm 0.2828 \pm 0.0000) \cdot 10^{-4}$	CLEO	[671]
	$(1.6000 \pm 1.3420 \pm 0.0000) \cdot 10^{-4}$	DELPHI	[642]
	$(2.7000 \pm 2.0120 \pm 0.0000) \cdot 10^{-4}$	OPAL	[681]
$\Gamma_{110} = X_s^- \nu_\tau$	$(2.8746 \pm 0.0498) \cdot 10^{-2}$	HFAG	Winter 2012 fit
$\Gamma_{126} = \pi^- \pi^0 \eta \nu_\tau$	$(0.1386 \pm 0.0072) \cdot 10^{-2}$	HFAG	Winter 2012 fit
	$(0.1800 \pm 0.0447 \pm 0.0000) \cdot 10^{-2}$	ALEPH	[682]
	$(0.1350 \pm 0.0030 \pm 0.0070) \cdot 10^{-2}$	Belle	[683]
	$(0.1700 \pm 0.0283 \pm 0.0000) \cdot 10^{-2}$	CLEO	[684]
$\Gamma_{128} = K^- \eta \nu_\tau$	$(1.5285 \pm 0.0808) \cdot 10^{-4}$	HFAG	Winter 2012 fit
	$(1.4200 \pm 0.1100 \pm 0.0700) \cdot 10^{-4}$	BABAR	[630]
	$(1.5800 \pm 0.0500 \pm 0.0900) \cdot 10^{-4}$	Belle	[683]
$\Gamma_{130} = K^- \pi^0 \eta \nu_\tau$	$(0.4825 \pm 0.1161) \cdot 10^{-4}$	HFAG	Winter 2012 fit
	$(0.4600 \pm 0.1100 \pm 0.0400) \cdot 10^{-4}$	Belle	[683]

Table 193 – continued from previous page

Tau lepton branching fraction	Value	Exp.	Ref.
	$(1.7700 \pm 0.9043 \pm 0.0000) \cdot 10^{-4}$	CLEO	[685]
$\Gamma_{132} = \pi^- \bar{K}^0 \eta \nu_\tau$	$(0.9364 \pm 0.1491) \cdot 10^{-4}$	HFAG	Winter 2012 fit
	$(0.8800 \pm 0.1400 \pm 0.0600) \cdot 10^{-4}$	Belle	[683]
	$(2.2000 \pm 0.7338 \pm 0.0000) \cdot 10^{-4}$	CLEO	[685]
$\Gamma_{136} = \pi^- \pi^- \pi^+ \eta \nu_\tau$ (ex. K^0)	$(1.4921 \pm 0.0968) \cdot 10^{-4}$	HFAG	Winter 2012 fit
	$(1.6000 \pm 0.0500 \pm 0.1100) \cdot 10^{-4}$	BABAR	[686]
	$(2.3000 \pm 0.5000 \pm 0.0000) \cdot 10^{-4}$	CLEO	[671]
$\Gamma_{150} = h^- \omega \nu_\tau$	$(1.9945 \pm 0.0641) \cdot 10^{-2}$	HFAG	Winter 2012 fit
	$(1.9100 \pm 0.0922 \pm 0.0000) \cdot 10^{-2}$	ALEPH	[682]
	$(1.6000 \pm 0.4909 \pm 0.0000) \cdot 10^{-2}$	CLEO	[687]
$\frac{\Gamma_{150}}{\Gamma_{66}} = \frac{h^- \omega \nu_\tau}{h^- h^- h^+ \pi^0 \nu_\tau}$ (ex. K^0)	$(43.340 \pm 1.389) \cdot 10^{-2}$	HFAG	Winter 2012 fit
	$(43.100 \pm 3.300 \pm 0.000) \cdot 10^{-2}$	ALEPH	[688]
	$(46.400 \pm 2.335 \pm 0.000) \cdot 10^{-2}$	CLEO	[665]
$\Gamma_{151} = K^- \omega \nu_\tau$	$(4.1000 \pm 0.9220) \cdot 10^{-4}$	HFAG	Winter 2012 fit
	$(4.1000 \pm 0.9220 \pm 0.0000) \cdot 10^{-4}$	CLEO3	[675]
$\Gamma_{152} = h^- \pi^0 \omega \nu_\tau$	$(0.4049 \pm 0.0418) \cdot 10^{-2}$	HFAG	Winter 2012 fit
	$(0.4300 \pm 0.0781 \pm 0.0000) \cdot 10^{-2}$	ALEPH	[682]
$\frac{\Gamma_{152}}{\Gamma_{76}} = \frac{h^- \omega \pi^0 \nu_\tau}{h^- h^- h^+ 2\pi^0 \nu_\tau}$ (ex. K^0)	$(82.453 \pm 7.575) \cdot 10^{-2}$	HFAG	Winter 2012 fit
	$(81.000 \pm 8.485 \pm 0.000) \cdot 10^{-2}$	CLEO	[670]
$\Gamma_{800} = \pi^- \omega \nu_\tau$	$(1.9535 \pm 0.0647) \cdot 10^{-2}$	HFAG	Winter 2012 fit
$\Gamma_{801} = K^- \phi \nu_\tau$ ($\phi \rightarrow KK$)	$(3.7002 \pm 1.3604) \cdot 10^{-5}$	HFAG	Winter 2012 fit
$\Gamma_{802} = K^- \pi^- \pi^+ \nu_\tau$ (ex. K^0, ω)	$(0.2923 \pm 0.0068) \cdot 10^{-2}$	HFAG	Winter 2012 fit
$\Gamma_{803} = K^- \pi^- \pi^+ \pi^0 \nu_\tau$ (ex. K^0, ω, η)	$(4.1074 \pm 1.4286) \cdot 10^{-4}$	HFAG	Winter 2012 fit
$\Gamma_{804} = \pi^- K_L^0 K_L^0 \nu_\tau$	$(2.3957 \pm 0.5026) \cdot 10^{-4}$	HFAG	Winter 2012 fit
$\Gamma_{805} = a_1^- (\rightarrow \pi^- \gamma) \nu_\tau$	$(4.0000 \pm 2.0000) \cdot 10^{-4}$	HFAG	Winter 2012 fit
	$(4.0000 \pm 2.0000 \pm 0.0000) \cdot 10^{-4}$	ALEPH	[629]
$\Gamma_{998} = 1 - \Gamma_{\text{All}}$	$(0.0704 \pm 0.1060) \cdot 10^{-2}$	HFAG	Winter 2012 fit

9.1.1 Correlation between base nodes uncertainties

The following tables report the correlation coefficients between base nodes, in percent.

Table 194: Base nodes correlation coefficients in percent, section 1

Γ_5	23													
Γ_9	7	5												
Γ_{10}	3	6	1											
Γ_{14}	-13	-14	-12	-3										
Γ_{16}	-0	-1	2	-1	-16									
Γ_{20}	-5	-5	-7	-1	-40	2								
Γ_{23}	0	0	-0	-2	2	-12	-22							
Γ_{27}	-4	-3	-8	-1	0	3	-36	6						
Γ_{28}	0	0	-0	-1	2	-12	4	-19	-29					
Γ_{30}	-5	-4	-11	-2	-9	-0	6	0	-42	0				
Γ_{35}	-0	-1	1	0	-0	2	-1	1	-0	1	-0			
Γ_{37}	0	0	-1	-1	1	-8	3	-12	4	-12	0	-6		
Γ_{40}	-0	-1	1	-0	-0	0	1	-2	-2	-2	-0	0	-3	
	Γ_3	Γ_5	Γ_9	Γ_{10}	Γ_{14}	Γ_{16}	Γ_{20}	Γ_{23}	Γ_{27}	Γ_{28}	Γ_{30}	Γ_{35}	Γ_{37}	Γ_{40}

Table 195: Base nodes correlation coefficients in percent, section 2

Γ_{42}	-0	-0	0	-0	0	-3	1	-5	-1	-5	0	-0	-7	30
Γ_{44}	0	0	-0	0	-0	0	-0	0	0	0	0	-2	-2	-4
Γ_{47}	-0	-0	-0	-0	-0	0	0	0	0	0	0	-0	-0	-0
Γ_{48}	0	0	0	0	0	0	-0	1	-0	0	-0	-4	-3	-3
Γ_{53}	0	0	0	0	0	-0	0	0	0	0	0	-0	-0	-0
Γ_{62}	-3	-5	8	0	-4	5	-7	-1	-5	-1	-5	4	-1	3
Γ_{70}	-6	-6	-7	-1	-9	-1	-1	0	-1	0	3	-1	0	-1
Γ_{77}	-1	-0	-3	-1	-2	-0	-0	0	2	0	2	-0	0	-0
Γ_{78}	1	1	2	0	1	1	-0	-0	-0	-0	0	1	-0	1
Γ_{93}	-1	-1	2	0	-1	2	-1	-0	-1	-0	-1	2	-0	1
Γ_{94}	-0	-0	-0	-0	-0	-0	-0	0	-0	0	0	-0	0	-0
Γ_{103}	0	0	2	0	0	1	-1	-0	-0	-0	-1	1	-0	1
Γ_{104}	-1	-1	-1	-0	-1	0	0	-0	0	-0	-1	0	-0	0
Γ_{126}	0	0	0	0	0	0	-1	-0	0	-0	-2	0	-0	0
	Γ_3	Γ_5	Γ_9	Γ_{10}	Γ_{14}	Γ_{16}	Γ_{20}	Γ_{23}	Γ_{27}	Γ_{28}	Γ_{30}	Γ_{35}	Γ_{37}	Γ_{40}

Table 196: Base nodes correlation coefficients in percent, section 3

Γ_{128}	-0	-0	1	-0	-0	1	-0	-1	-0	-1	-0	1	-0	1
Γ_{130}	0	0	0	0	0	0	-0	-0	0	-0	-0	0	-0	0
Γ_{132}	0	0	-0	0	-0	0	-0	-0	0	-0	-0	0	-0	0
Γ_{151}	-0	-0	-0	-0	-0	0	-0	-0	-0	-0	0	-0	-0	-0
Γ_{152}	-1	-0	-3	-1	-2	-0	-1	0	2	0	2	-0	0	0
Γ_{800}	-2	-2	-2	-0	-3	-0	-0	0	-0	0	1	-0	0	-0
Γ_{801}	-0	-0	0	-0	-0	0	-0	-0	0	-0	-0	-0	-0	-0
Γ_{802}	-1	-1	0	0	-1	-1	-2	0	-2	0	-1	-1	-0	-0
Γ_{803}	-0	-0	-0	-0	-0	-0	-0	0	-0	0	0	-0	-0	-0
Γ_{805}	0	0	0	0	0	0	0	0	0	0	0	0	0	0
	Γ_3	Γ_5	Γ_9	Γ_{10}	Γ_{14}	Γ_{16}	Γ_{20}	Γ_{23}	Γ_{27}	Γ_{28}	Γ_{30}	Γ_{35}	Γ_{37}	Γ_{40}

Table 197: Base nodes correlation coefficients in percent, section 4

Γ_{44}	-2													
Γ_{47}	-0	-0												
Γ_{48}	-2	-5	-19											
Γ_{53}	-0	0	0	-0										
Γ_{62}	1	-0	-0	-0	-0									
Γ_{70}	-0	0	0	-0	-0	-19								
Γ_{77}	0	-0	-0	0	0	-1	-7							
Γ_{78}	0	-0	-0	-0	-0	2	-2	-1						
Γ_{93}	0	-0	-0	-0	-0	14	-4	-0	1					
Γ_{94}	0	0	0	-0	-0	-0	-2	-0	-0	-0				
Γ_{103}	0	-0	-0	-0	-0	3	-1	-0	4	1	-0			
Γ_{104}	-0	-0	0	0	0	-0	0	1	-36	0	0	-11		
Γ_{126}	0	-0	-0	-0	-0	1	-0	-5	0	0	-0	0	0	
	Γ_{42}	Γ_{44}	Γ_{47}	Γ_{48}	Γ_{53}	Γ_{62}	Γ_{70}	Γ_{77}	Γ_{78}	Γ_{93}	Γ_{94}	Γ_{103}	Γ_{104}	Γ_{126}

Table 198: Base nodes correlation coefficients in percent, section 5

Γ_{128}	0	-0	-0	-0	-0	2	-0	-0	0	1	-0	1	0	4
Γ_{130}	0	-0	-0	-0	-0	0	-0	-1	0	0	-0	0	0	1
Γ_{132}	-0	-0	-0	-0	-0	0	-0	-0	0	0	-0	0	-0	2
Γ_{151}	0	0	0	-0	-0	0	12	0	0	0	-0	0	0	0
Γ_{152}	0	-0	-0	0	0	-1	-11	-64	-1	-0	-0	-0	1	-0
Γ_{800}	-0	0	0	-0	-0	-8	-69	-2	-0	-1	0	-0	0	-0
Γ_{801}	-0	-0	-0	-0	-0	-1	-0	-0	0	1	-0	0	0	0
Γ_{802}	-0	0	0	-0	-0	17	-6	-0	-0	-0	-0	-0	-0	-0
Γ_{803}	-0	0	0	0	-0	-1	-19	-0	-0	-0	-2	-0	0	-0
Γ_{805}	0	0	0	0	0	0	0	0	0	0	0	0	0	0
	Γ_{42}	Γ_{44}	Γ_{47}	Γ_{48}	Γ_{53}	Γ_{62}	Γ_{70}	Γ_{77}	Γ_{78}	Γ_{93}	Γ_{94}	Γ_{103}	Γ_{104}	Γ_{126}

Table 199: Base nodes correlation coefficients in percent, section 6

Γ_{130}	1									
Γ_{132}	1	0								
Γ_{151}	0	0	-0							
Γ_{152}	-0	-0	0	0						
Γ_{800}	-0	-0	-0	-14	-3					
Γ_{801}	0	0	-0	-0	-0	-0				
Γ_{802}	-0	-0	-0	-2	-0	-1	1			
Γ_{803}	-1	-0	-0	-58	-0	9	-0	1		
Γ_{805}	0	0	0	0	0	0	0	0	0	
	Γ_{128}	Γ_{130}	Γ_{132}	Γ_{151}	Γ_{152}	Γ_{800}	Γ_{801}	Γ_{802}	Γ_{803}	Γ_{805}

9.1.2 Equality constraints

We use equality constraints that relate a branching fraction to a sum of branching fractions. As mentioned above, the tau branching fractions are denoted with Γ_n labels. In the constraint relations we use the values of some non-tau branching fractions, denoted e.g. with the self-describing notation $\Gamma_{K_S \rightarrow \pi^0 \pi^0}$. We also use probabilities corresponding to modulus square amplitudes describing quantum mixtures of states such as K^0 , \bar{K}^0 , K_S , K_L , denoted with e.g. $\Gamma_{\langle K^0 | K_S \rangle} = |\langle K^0 | K_S \rangle|^2$. In the fit, all non-tau quantities are taken from the PDG 2011 [5] fits (when available) or averages, and are used without accounting for their uncertainties, which are however in general small with respect to the uncertainties on the tau branching fractions. The tau branching fractions are illustrated in Table 193. The equations in the following permit the computation of the values and uncertainties for branching fractions that are not listed in Table 193, once they are expressed as function of the quantities that are listed there. The following list does not include the (non-linear) constraints already introduced in Section 9.1, and illustrated in Table 193, where some measured branching fractions are expressed as ratios of “base” branching fractions.

$$\Gamma_7 = \Gamma_{35} \cdot \Gamma_{\langle \bar{K}^0 | K_L \rangle} + \Gamma_9 + \Gamma_{804} + \Gamma_{37} \cdot \Gamma_{\langle K^0 | K_L \rangle} + \Gamma_{10}$$

$$\Gamma_8 = \Gamma_9 + \Gamma_{10}$$

$$\begin{aligned} \Gamma_{17} = & \Gamma_{128} \cdot \Gamma_{\eta \rightarrow 3\pi^0} + \Gamma_{30} + \Gamma_{23} + \Gamma_{28} + \Gamma_{35} \cdot (\Gamma_{\langle K^0 | K_S \rangle} \cdot \Gamma_{K_S \rightarrow \pi^0 \pi^0}) \\ & + \Gamma_{40} \cdot (\Gamma_{\langle K^0 | K_S \rangle} \cdot \Gamma_{K_S \rightarrow \pi^0 \pi^0}) + \Gamma_{42} \cdot (\Gamma_{\langle K^0 | K_S \rangle} \cdot \Gamma_{K_S \rightarrow \pi^0 \pi^0}) + \Gamma_{20} + \Gamma_{27} \\ & + \Gamma_{47} \cdot (\Gamma_{K_S \rightarrow \pi^0 \pi^0} \cdot \Gamma_{K_S \rightarrow \pi^0 \pi^0}) + \Gamma_{48} \cdot \Gamma_{K_S \rightarrow \pi^0 \pi^0} + \Gamma_{126} \cdot \Gamma_{\eta \rightarrow 3\pi^0} + \Gamma_{37} \cdot (\Gamma_{\langle K^0 | K_S \rangle} \cdot \Gamma_{K_S \rightarrow \pi^0 \pi^0}) \\ & + \Gamma_{130} \cdot \Gamma_{\eta \rightarrow 3\pi^0} \end{aligned}$$

$$\Gamma_{19} = \Gamma_{23} + \Gamma_{20}$$

$$\Gamma_{25} = \Gamma_{128} \cdot \Gamma_{\eta \rightarrow 3\pi^0} + \Gamma_{30} + \Gamma_{28} + \Gamma_{27} + \Gamma_{126} \cdot \Gamma_{\eta \rightarrow 3\pi^0} + \Gamma_{130} \cdot \Gamma_{\eta \rightarrow 3\pi^0}$$

$$\Gamma_{26} = \Gamma_{128} \cdot \Gamma_{\eta \rightarrow 3\pi^0} + \Gamma_{28} + \Gamma_{40} \cdot (\Gamma_{\langle K^0 | K_S \rangle} \cdot \Gamma_{K_S \rightarrow \pi^0 \pi^0}) + \Gamma_{42} \cdot (\Gamma_{\langle K^0 | K_S \rangle} \cdot \Gamma_{K_S \rightarrow \pi^0 \pi^0}) + \Gamma_{27}$$

$$\Gamma_{29} = \Gamma_{30} + \Gamma_{126} \cdot \Gamma_{\eta \rightarrow 3\pi^0} + \Gamma_{130} \cdot \Gamma_{\eta \rightarrow 3\pi^0}$$

$$\begin{aligned} \Gamma_{31} = & \Gamma_{128} \cdot \Gamma_{\eta \rightarrow \text{neutral}} + \Gamma_{23} + \Gamma_{28} + \Gamma_{42} + \Gamma_{16} + \Gamma_{37} + \Gamma_{10} \\ & + \Gamma_{801} \cdot (\Gamma_{\phi \rightarrow K_S K_L} \cdot \Gamma_{K_S \rightarrow \pi^0 \pi^0}) / (\Gamma_{\phi \rightarrow K^+ K^-} + \Gamma_{\phi \rightarrow K_S K_L}) \end{aligned}$$

$$\begin{aligned}
\Gamma_{33} &= \Gamma_{35} \cdot \Gamma_{\langle \bar{K}^0 | K_S \rangle} + \Gamma_{40} \cdot \Gamma_{\langle \bar{K}^0 | K_S \rangle} + \Gamma_{42} \cdot \Gamma_{\langle K^0 | K_S \rangle} + \Gamma_{47} + \Gamma_{48} + \Gamma_{37} \cdot \Gamma_{\langle K^0 | K_S \rangle} \\
&\quad + \Gamma_{132} \cdot (\Gamma_{\langle \bar{K}^0 | K_S \rangle} \cdot \Gamma_{\eta \rightarrow \text{neutral}}) + \Gamma_{44} \cdot \Gamma_{\langle \bar{K}^0 | K_S \rangle} + \Gamma_{801} \cdot \Gamma_{\phi \rightarrow K_S K_L} / (\Gamma_{\phi \rightarrow K^+ K^-} + \Gamma_{\phi \rightarrow K_S K_L}) \\
\Gamma_{34} &= \Gamma_{35} + \Gamma_{37} \\
\Gamma_{38} &= \Gamma_{42} + \Gamma_{37} \\
\Gamma_{39} &= \Gamma_{40} + \Gamma_{42} \\
\Gamma_{43} &= \Gamma_{40} + \Gamma_{44} \\
\Gamma_{46} &= \Gamma_{48} + \Gamma_{47} + \Gamma_{804} \\
\Gamma_{54} &= \Gamma_{128} \cdot \Gamma_{\eta \rightarrow \text{charged}} + \Gamma_{152} \cdot (\Gamma_{\omega \rightarrow \pi^+ \pi^- \pi^0} + \Gamma_{\omega \rightarrow \pi^+ \pi^-}) + \Gamma_{35} \cdot (\Gamma_{\langle K^0 | K_S \rangle} \cdot \Gamma_{K_S \rightarrow \pi^+ \pi^-}) \\
&\quad + \Gamma_{40} \cdot (\Gamma_{\langle K^0 | K_S \rangle} \cdot \Gamma_{K_S \rightarrow \pi^+ \pi^-}) + \Gamma_{42} \cdot (\Gamma_{\langle K^0 | K_S \rangle} \cdot \Gamma_{K_S \rightarrow \pi^+ \pi^-}) + \Gamma_{78} \\
&\quad + \Gamma_{47} \cdot (2 \cdot \Gamma_{K_S \rightarrow \pi^+ \pi^-} \cdot \Gamma_{K_S \rightarrow \pi^0 \pi^0}) + \Gamma_{77} + \Gamma_{48} \cdot \Gamma_{K_S \rightarrow \pi^+ \pi^-} + \Gamma_{94} + \Gamma_{62} + \Gamma_{70} + \Gamma_{93} \\
&\quad + \Gamma_{126} \cdot \Gamma_{\eta \rightarrow \text{charged}} + \Gamma_{37} \cdot (\Gamma_{\langle K^0 | K_S \rangle} \cdot \Gamma_{K_S \rightarrow \pi^+ \pi^-}) + \Gamma_{802} + \Gamma_{803} \\
&\quad + \Gamma_{800} \cdot (\Gamma_{\omega \rightarrow \pi^+ \pi^- \pi^0} + \Gamma_{\omega \rightarrow \pi^+ \pi^-}) + \Gamma_{151} \cdot (\Gamma_{\omega \rightarrow \pi^+ \pi^- \pi^0} + \Gamma_{\omega \rightarrow \pi^+ \pi^-}) + \Gamma_{130} \cdot \Gamma_{\eta \rightarrow \text{charged}} \\
&\quad + \Gamma_{132} \cdot (\Gamma_{\langle \bar{K}^0 | K_L \rangle} \cdot \Gamma_{\eta \rightarrow \pi^+ \pi^- \pi^0}) \\
&\quad + \Gamma_{\langle \bar{K}^0 | K_S \rangle} \cdot \Gamma_{K_S \rightarrow \pi^0 \pi^0} \cdot \Gamma_{\eta \rightarrow \pi^+ \pi^- \pi^0} + \Gamma_{\langle \bar{K}^0 | K_S \rangle} \cdot \Gamma_{K_S \rightarrow \pi^+ \pi^-} \cdot \Gamma_{\eta \rightarrow 3\pi^0}) \\
&\quad + \Gamma_{53} \cdot (\Gamma_{\langle \bar{K}^0 | K_S \rangle} \cdot \Gamma_{K_S \rightarrow \pi^0 \pi^0} + \Gamma_{\langle \bar{K}^0 | K_L \rangle}) \\
&\quad + \Gamma_{801} \cdot (\Gamma_{\phi \rightarrow K^+ K^-} + \Gamma_{\phi \rightarrow K_S K_L} \cdot \Gamma_{K_S \rightarrow \pi^+ \pi^-}) / (\Gamma_{\phi \rightarrow K^+ K^-} + \Gamma_{\phi \rightarrow K_S K_L}) \\
\Gamma_{55} &= \Gamma_{128} \cdot \Gamma_{\eta \rightarrow \text{charged}} + \Gamma_{152} \cdot (\Gamma_{\omega \rightarrow \pi^+ \pi^- \pi^0} + \Gamma_{\omega \rightarrow \pi^+ \pi^-}) + \Gamma_{78} + \Gamma_{77} + \Gamma_{94} + \Gamma_{62} + \Gamma_{70} + \Gamma_{93} \\
&\quad + \Gamma_{126} \cdot \Gamma_{\eta \rightarrow \text{charged}} + \Gamma_{802} + \Gamma_{803} + \Gamma_{800} \cdot (\Gamma_{\omega \rightarrow \pi^+ \pi^- \pi^0} + \Gamma_{\omega \rightarrow \pi^+ \pi^-}) \\
&\quad + \Gamma_{151} \cdot (\Gamma_{\omega \rightarrow \pi^+ \pi^- \pi^0} + \Gamma_{\omega \rightarrow \pi^+ \pi^-}) + \Gamma_{130} \cdot \Gamma_{\eta \rightarrow \text{charged}} \\
&\quad + \Gamma_{801} \cdot \Gamma_{\phi \rightarrow K^+ K^-} / (\Gamma_{\phi \rightarrow K^+ K^-} + \Gamma_{\phi \rightarrow K_S K_L}) \\
\Gamma_{57} &= \Gamma_{62} + \Gamma_{93} + \Gamma_{802} + \Gamma_{800} \cdot \Gamma_{\omega \rightarrow \pi^+ \pi^-} + \Gamma_{151} \cdot \Gamma_{\omega \rightarrow \pi^+ \pi^-} + \Gamma_{801} \cdot \Gamma_{\phi \rightarrow K^+ K^-} / (\Gamma_{\phi \rightarrow K^+ K^-} + \Gamma_{\phi \rightarrow K_S K_L}) \\
\Gamma_{58} &= \Gamma_{62} + \Gamma_{93} + \Gamma_{802} + \Gamma_{801} \cdot \Gamma_{\phi \rightarrow K^+ K^-} / (\Gamma_{\phi \rightarrow K^+ K^-} + \Gamma_{\phi \rightarrow K_S K_L}) \\
\Gamma_{60} &= \Gamma_{62} + \Gamma_{800} \cdot \Gamma_{\omega \rightarrow \pi^+ \pi^-} \\
\Gamma_{66} &= \Gamma_{128} \cdot \Gamma_{\eta \rightarrow \pi^+ \pi^- \pi^0} + \Gamma_{152} \cdot \Gamma_{\omega \rightarrow \pi^+ \pi^-} + \Gamma_{94} + \Gamma_{70} + \Gamma_{803} + \Gamma_{800} \cdot \Gamma_{\omega \rightarrow \pi^+ \pi^- \pi^0} + \Gamma_{151} \cdot \Gamma_{\omega \rightarrow \pi^+ \pi^- \pi^0} \\
\Gamma_{68} &= \Gamma_{152} \cdot \Gamma_{\omega \rightarrow \pi^+ \pi^-} + \Gamma_{40} \cdot (\Gamma_{\langle K^0 | K_S \rangle} \cdot \Gamma_{K_S \rightarrow \pi^+ \pi^-}) + \Gamma_{70} + \Gamma_{800} \cdot \Gamma_{\omega \rightarrow \pi^+ \pi^- \pi^0} \\
\Gamma_{69} &= \Gamma_{152} \cdot \Gamma_{\omega \rightarrow \pi^+ \pi^-} + \Gamma_{70} + \Gamma_{800} \cdot \Gamma_{\omega \rightarrow \pi^+ \pi^- \pi^0} \\
\Gamma_{74} &= \Gamma_{152} \cdot \Gamma_{\omega \rightarrow \pi^+ \pi^- \pi^0} + \Gamma_{78} + \Gamma_{77} + \Gamma_{126} \cdot \Gamma_{\eta \rightarrow \pi^+ \pi^- \pi^0} + \Gamma_{130} \cdot \Gamma_{\eta \rightarrow \pi^+ \pi^- \pi^0} \\
\Gamma_{76} &= \Gamma_{152} \cdot \Gamma_{\omega \rightarrow \pi^+ \pi^- \pi^0} + \Gamma_{77} + \Gamma_{126} \cdot \Gamma_{\eta \rightarrow \pi^+ \pi^- \pi^0} + \Gamma_{130} \cdot \Gamma_{\eta \rightarrow \pi^+ \pi^- \pi^0} \\
\Gamma_{82} &= \Gamma_{128} \cdot \Gamma_{\eta \rightarrow \text{charged}} + \Gamma_{42} \cdot (\Gamma_{\langle K^0 | K_S \rangle} \cdot \Gamma_{K_S \rightarrow \pi^+ \pi^-}) + \Gamma_{802} + \Gamma_{803} + \Gamma_{151} \cdot (\Gamma_{\omega \rightarrow \pi^+ \pi^- \pi^0} + \Gamma_{\omega \rightarrow \pi^+ \pi^-}) \\
&\quad + \Gamma_{37} \cdot (\Gamma_{\langle K^0 | K_S \rangle} \cdot \Gamma_{K_S \rightarrow \pi^+ \pi^-}) \\
\Gamma_{85} &= \Gamma_{802} + \Gamma_{151} \cdot \Gamma_{\omega \rightarrow \pi^+ \pi^-}
\end{aligned}$$

$$\begin{aligned}
\Gamma_{88} &= \Gamma_{128} \cdot \Gamma_{\eta \rightarrow \pi^+ \pi^- \pi^0} + \Gamma_{803} + \Gamma_{151} \cdot \Gamma_{\omega \rightarrow \pi^+ \pi^- \pi^0} \\
\Gamma_{92} &= \Gamma_{94} + \Gamma_{93} \\
\Gamma_{96} &= \Gamma_{801} \cdot \Gamma_{\phi \rightarrow K^+ K^-} / (\Gamma_{\phi \rightarrow K^+ K^-} + \Gamma_{\phi \rightarrow K_S K_L}) \\
\Gamma_{102} &= \Gamma_{103} + \Gamma_{104} \\
\Gamma_{110} &= \Gamma_{10} + \Gamma_{16} + \Gamma_{23} + \Gamma_{28} + \Gamma_{35} + \Gamma_{40} + \Gamma_{128} + \Gamma_{802} + \Gamma_{803} + \Gamma_{151} + \Gamma_{130} + \Gamma_{132} + \Gamma_{44} + \Gamma_{53} + \Gamma_{801} \\
\Gamma_{136} &= \Gamma_{104} \cdot \Gamma_{\eta \rightarrow \pi^+ \pi^- \pi^0} + \Gamma_{78} \cdot \Gamma_{\eta \rightarrow 3\pi^0} \\
\Gamma_{150} &= \Gamma_{800} + \Gamma_{151} \\
\Gamma_{804} &= \Gamma_{47} \cdot (\Gamma_{\langle K^0 | K_L \rangle} \cdot \Gamma_{\langle K^0 | K_L \rangle}) / (\Gamma_{\langle K^0 | K_S \rangle} \cdot \Gamma_{\langle K^0 | K_S \rangle}) \\
\Gamma_{\text{All}} &= \Gamma_3 + \Gamma_5 + \Gamma_9 + \Gamma_{10} + \Gamma_{14} + \Gamma_{16} + \Gamma_{20} + \Gamma_{23} + \Gamma_{27} + \Gamma_{28} + \Gamma_{30} + \Gamma_{35} + \Gamma_{37} + \Gamma_{40} + \Gamma_{42} + \Gamma_{47} \\
&\quad + \Gamma_{48} + \Gamma_{62} + \Gamma_{70} + \Gamma_{77} + \Gamma_{78} + \Gamma_{93} + \Gamma_{94} + \Gamma_{104} + \Gamma_{126} + \Gamma_{128} + \Gamma_{802} + \Gamma_{803} + \Gamma_{800} + \Gamma_{151} \\
&\quad + \Gamma_{130} + \Gamma_{132} + \Gamma_{44} + \Gamma_{53} + \Gamma_{49} + \Gamma_{804} + \Gamma_{805} + \Gamma_{801} + \Gamma_{152} + \Gamma_{103}
\end{aligned}$$

9.1.3 Fit procedure

The fit procedure is functionally equivalent to the one employed in the former HFAG report [4] and consists in a minimum χ^2 fit subject to linear and non-linear constraints. The fit code has been improved to automatize the treatment of non-linear constraints, which are iteratively Taylor-expanded to obtain numerically approximate linear constraints, which permit an analytical solution for the χ^2 minimization when, as it happens in this case, the χ^2 is a quadratic function of the fitted quantities.

9.2 Tests of lepton universality

In the Standard Model, the partial widths of a heavier lepton L decaying to a lighter lepton ℓ are, neglecting neutrino masses and including radiative corrections [689],

$$\Gamma(L \rightarrow \nu_L \ell \bar{\nu}_\ell(\gamma)) = \frac{B(L \rightarrow \nu_L \ell \bar{\nu}_\ell)}{\tau_L} = \frac{G_L G_\ell m_L^5}{192\pi^3} f\left(\frac{m_\ell^2}{m_L^2}\right) r_W^L r_\gamma^L,$$

where

$$\begin{aligned}
G_\ell &= \frac{g_\ell^2}{4\sqrt{2}M_W^2} & f(x) &= 1 - 8x + 8x^3 - x^4 - 12x^2 \ln x \\
r_W^L &= 1 + \frac{3}{5} \frac{m_L^2}{M_W^2} & r_\gamma^L &= 1 + \frac{\alpha(m_L)}{2\pi} \left(\frac{25}{4} - \pi^2 \right)
\end{aligned}$$

We use $r_\gamma^\tau = 1 - 43.2 \cdot 10^{-4}$ and $r_\gamma^\mu = 1 - 42.4 \cdot 10^{-4}$ [689] and M_W from PDG 2011 [5] as usual.

Proper ratios of the above partial widths, corrected by the suitable above-illustrated factors to remove the dependencies from masses and radiative corrections, measure ratios of charged weak lepton coupling constants. Using the HFAG-Tau fit values where available and using

PDG 2011 for the remaining quantities, we measure, accounting for the statistical correlations emerging from the HFAG-Tau fit:

$$\left(\frac{g_\tau}{g_\mu}\right) = 1.0006 \pm 0.0021, \quad \left(\frac{g_\tau}{g_e}\right) = 1.0024 \pm 0.0021, \quad \left(\frac{g_\mu}{g_e}\right) = 1.0018 \pm 0.0014.$$

Tau decays partial widths to hadrons compared to the same hadron decay to muons measure the tau-muon universality of charged weak couplings as follows:

$$\left(\frac{g_\tau}{g_\mu}\right)^2 = \frac{B(\tau \rightarrow h\nu_\tau)}{B(h \rightarrow \mu\bar{\nu}_\mu)} \frac{2m_h m_\mu^2 \tau_h}{(1 + \delta_h) m_\tau^3 \tau_\tau} \left(\frac{1 - m_\mu^2/m_h^2}{1 - m_h^2/m_\tau^2}\right)^2,$$

where $h = \pi$ or K and the radiative corrections are $\delta_\pi = (0.16 \pm 0.14)\%$ and $\delta_K = (0.90 \pm 0.22)\%$ [690]. Using the HFAG-Tau data and PDG 2011 we measure:

$$\left(\frac{g_\tau}{g_\mu}\right)_\pi = 0.9956 \pm 0.0031, \quad \left(\frac{g_\tau}{g_\mu}\right)_K = 0.9852 \pm 0.0072.$$

Similar tests could be performed with decays to electrons, however they are less precise because the hadron two body decays to electrons are helicity-suppressed. Averaging the three g_τ/g_μ ratios we obtain

$$\left(\frac{g_\tau}{g_\mu}\right)_{\tau+\pi+K} = 0.9996 \pm 0.0020,$$

accounting for statistical correlations.

9.3 Universality improved $B(\tau \rightarrow e\nu\bar{\nu})$ and R_{had}

Following Ref. [691], we assume lepton universality to obtain a more precise experimental determination of $B_e = B(\tau \rightarrow e\bar{\nu}_e\nu_\tau)$ using the tau branching fraction to muon and the tau lifetime, by averaging the B_e direct measurement, the B_e determination from assuming that $g_\mu/g_e = 1$ hence (see also Section 9.2) $B_e = B_\mu \cdot f(m_e^2/m_\tau^2)/f(m_\mu^2/m_\tau^2)$, and B_e from assuming that $g_\tau/g_\mu = 1$ hence $B_e = B(\mu \rightarrow e\bar{\nu}_e\nu_\mu) \cdot (\tau_\tau/\tau_\mu) \cdot (m_\tau/m_\mu)^5 \cdot f(m_e^2/m_\tau^2)/f(m_e^2/m_\mu^2) \cdot (\delta_\gamma^\tau \delta_W^\tau)/(\delta_\gamma^\mu \delta_W^\mu)$ where $B(\mu \rightarrow e\bar{\nu}_e\nu_\mu) = 1$. Accounting for statistical correlations, we obtain

$$B_e^{\text{uni}} = (17.839 \pm 0.028)\%.$$

We use B_e^{uni} to obtain the ratio

$$R_{\text{had}} = \frac{\Gamma(\tau \rightarrow \text{hadrons})}{\Gamma(\tau \rightarrow e\nu\bar{\nu})} = 3.6280 \pm 0.0094.$$

Here $\Gamma(\tau \rightarrow \text{hadrons})$ is obtained by summing all tau hadronic decay modes.

9.4 $|V_{us}|$ measurement

The CKM coefficient $|V_{us}|$ can be measured in several ways from the comparison of tau partial widths to strange and non-strange final states.

9.4.1 Inclusive tau partial width to strange

The tau hadronic partial width is the sum of the tau partial width to strange and to non-strange hadronic final states, $\Gamma_{\text{had}} = \Gamma_s + \Gamma_{VA}$. Dividing by the partial width to electron, Γ_e , we obtain partial width ratios (which are equal to the respective branching fraction ratios) for which $R_{\text{had}} = R_s + R_{VA}$. In terms of such ratios, $|V_{us}|$ is measured as

$$|V_{us}| = \sqrt{R_s / \left[\frac{R_{VA}}{|V_{ud}|^2} - \delta R_{\text{theory}} \right]}, \quad (220)$$

where δR_{theory} can be determined in the context of low energy QCD theory, partly relying on experimental low energy scattering data. We use $\delta R_{\text{theory}} = 0.240 \pm 0.032$ [692], which induces a systematic error on $|V_{us}|$ that lies between two more recent estimates [693, 694].

In the following, we use the universality improved B_e^{uni} (see Section 9.3) to compute the R ratios. The most direct experimental determination of R_s and $R_{VA} = R_{\text{had}} - R_s$ come from the tau inclusive branching fractions to hadronic and strange hadronic states, B_{had} and B_s . However often the total hadronic branching fraction has been replaced by the indirect but more precise expression $B_{\text{had}}^{\text{uni}} = 1 - B_e - B_\mu$ (or similar expressions based on B_e^{uni}), using unitarity, see for example the 2009 HFAG report [4]. We depart from this choice here, and we use the most direct determination of R_{had} , for two reasons: first there is no significant statistical gain in the final errors, because of statistical correlations in the R_{had} expression $(1 - B_e - B_\mu)/B_e^{\text{uni}}$, and second the indirect determination of $R_{VA} = R_{\text{had}}^{\text{uni}} - R_s$ would absorb the effect of possible unobserved hadronic states entirely in R_{VA} , while they could also be strange final states.

With the above choices, using $|V_{ud}| = 0.97425 \pm 0.00022$ [695], using HFAG values of this report, including the above-mentioned B_e^{uni} , $B_s = (2.875 \pm 0.050)\%$ (see also Table 200), $B_{VA} = (61.85 \pm 0.11)\%$ and the PDG 2011 averages, we obtain $|V_{us}|_{\tau s} = 0.2173 \pm 0.0022$, which is 3.4σ lower than the unitarity CKM prediction $|V_{us}|_{\text{uni}} = 0.2255 \pm 0.0010$, from $(|V_{us}|_{\text{uni}})^2 = 1 - |V_{ud}|^2$. The $|V_{us}|_{\tau s}$ uncertainty includes a systematic error contribution of 0.0010 from the theory uncertainty on δR_{theory} ,

If we use the alternative above mentioned definitions of B_{had} , the mismatch remains 3.4σ . Using a unitarity-constrained tau branching fraction fit, the mismatch remains 3.4σ . The 3.4σ discrepancy is close to the unconstrained fit result of the 2009 HFAG report, 3.6σ [4], and also to the 3.3σ from the HFAG-Tau 2011 intermediate document [696], based on a unitarity-constrained fit.

9.4.2 $|V_{us}|$ from $B(\tau \rightarrow K\nu)/B(\tau \rightarrow \pi\nu)$ and from $B(\tau \rightarrow K\nu)$

We use the ratio of branching fractions $B(\tau^- \rightarrow K^- \nu_\tau)/B(\tau^- \rightarrow \pi^- \nu_\tau) = 0.0643 \pm 0.0009$ to measure $|V_{us}|$ from the equation

$$\frac{B(\tau^- \rightarrow K^- \nu_\tau)}{B(\tau^- \rightarrow \pi^- \nu_\tau)} = \frac{f_K^2 |V_{us}|^2 (1 - m_K^2/m_\tau^2)^2 r_{\text{LD}}(\tau^- \rightarrow K^- \nu_\tau)}{f_\pi^2 |V_{ud}|^2 (1 - m_\pi^2/m_\tau^2)^2 r_{\text{LD}}(\tau^- \rightarrow \pi^- \nu_\tau)}.$$

In this ratio, the short-distance radiative corrections cancel. The term $r_{\text{LD}}(p) = 1 + \delta_{\text{LD}}(p)$ corresponds to the long-distance electroweak radiative correction factor for the process p . Following Ref. [697], the ratio of radiative correction factors is estimated as $r_{\text{LD}}^{K\pi} = r_{\text{LD}}(\tau^- \rightarrow K^- \nu/K^- \rightarrow \mu^- \nu)/r_{\text{LD}}(\tau^- \rightarrow \pi^- \nu/\pi^- \rightarrow \mu^- \nu) \cdot r_{\text{LD}}(K^- \rightarrow \mu^- \nu)/r_{\text{LD}}(\pi^- \rightarrow \mu^- \nu)$, where the first ratio is

Table 200: HFAG Winter 2012 Tau branching fractions to strange final states.

Branching fraction	HFAG Winter 2012 fit
$\Gamma_{10} = K^- \nu_\tau$	$(0.6955 \pm 0.0096) \cdot 10^{-2}$
$\Gamma_{16} = K^- \pi^0 \nu_\tau$	$(0.4322 \pm 0.0149) \cdot 10^{-2}$
$\Gamma_{23} = K^- 2\pi^0 \nu_\tau$ (ex. K^0)	$(0.0630 \pm 0.0222) \cdot 10^{-2}$
$\Gamma_{28} = K^- 3\pi^0 \nu_\tau$ (ex. K^0, η)	$(0.0419 \pm 0.0218) \cdot 10^{-2}$
$\Gamma_{35} = \pi^- \bar{K}^0 \nu_\tau$	$(0.8206 \pm 0.0182) \cdot 10^{-2}$
$\Gamma_{40} = \pi^- \bar{K}^0 \pi^0 \nu_\tau$	$(0.3649 \pm 0.0108) \cdot 10^{-2}$
$\Gamma_{44} = \pi^- \bar{K}^0 \pi^0 \pi^0 \nu_\tau$	$(0.0269 \pm 0.0230) \cdot 10^{-2}$
$\Gamma_{53} = \bar{K}^0 h^- h^- h^+ \nu_\tau$	$(0.0222 \pm 0.0202) \cdot 10^{-2}$
$\Gamma_{128} = K^- \eta \nu_\tau$	$(0.0153 \pm 0.0008) \cdot 10^{-2}$
$\Gamma_{130} = K^- \pi^0 \eta \nu_\tau$	$(0.0048 \pm 0.0012) \cdot 10^{-2}$
$\Gamma_{132} = \pi^- \bar{K}^0 \eta \nu_\tau$	$(0.0094 \pm 0.0015) \cdot 10^{-2}$
$\Gamma_{151} = K^- \omega \nu_\tau$	$(0.0410 \pm 0.0092) \cdot 10^{-2}$
$\Gamma_{801} = K^- \phi \nu_\tau$ ($\phi \rightarrow KK$)	$(0.0037 \pm 0.0014) \cdot 10^{-2}$
$\Gamma_{802} = K^- \pi^- \pi^+ \nu_\tau$ (ex. K^0, ω)	$(0.2923 \pm 0.0068) \cdot 10^{-2}$
$\Gamma_{803} = K^- \pi^- \pi^+ \pi^0 \nu_\tau$ (ex. K^0, ω, η)	$(0.0411 \pm 0.0143) \cdot 10^{-2}$
$\Gamma_{110} = X_s^- \nu_\tau$	$(2.8746 \pm 0.0498) \cdot 10^{-2}$

$[1 + (0.90 \pm 0.22)\%]/[1 + (0.16 \pm 0.14)\%]$ [698] and the second ratio is $(0.9930 \pm 0.0035)\%$ [699], hence assuming independent errors $r_{\text{LD}}^{K\pi} = 1.0003 \pm 0.0044$. The ratio f_K/f_π is estimated in lattice QCD to be 1.1936 ± 0.0053 [174]. We measure $|V_{us}|_{\tau K/\pi} = 0.2229 \pm 0.0021$, 1.1σ below the CKM unitarity prediction.

We use the branching fraction $B(\tau^- \rightarrow K^- \nu_\tau)$ to measure $|V_{us}|$ from the equation

$$B(\tau^- \rightarrow K^- \nu_\tau) = \frac{G_F^2 f_K^2 |V_{us}|^2 m_\tau^3 \tau_\tau}{16\pi\hbar} \left(1 - \frac{m_K^2}{m_\tau^2}\right)^2 S_{EW} ,$$

where $f_K = 156.1 \pm 1.1 \text{ MeV}$ [174] is the kaon decay constant estimated with lattice QCD, and $S_{EW} = 1.0201 \pm 0.0003$ [700] accounts for the radiative corrections. We obtain $|V_{us}|_{\tau K} = 0.2214 \pm 0.0022$, which is 1.7σ below the CKM unitarity prediction. CODATA 2006 results [701] and PDG 2011 have been used for the physics constants.

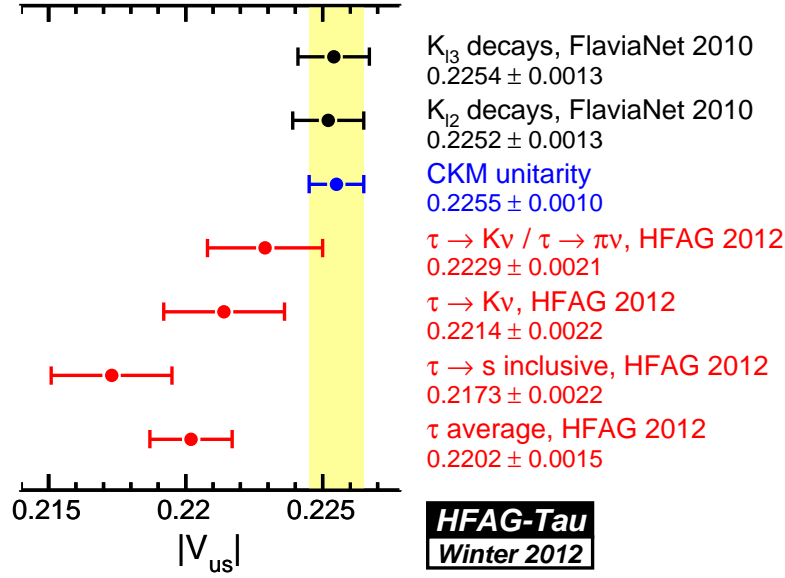


Figure 86: $|V_{us}|$ averages of this document compared with the FlaviaNet results [702].

9.4.3 $|V_{us}|$ from tau summary

We summarize the $|V_{us}|$ results reporting the values, the discrepancy with respect to the $|V_{us}|$ determination from CKM unitarity, and an illustration of the measurement method:

$$\begin{aligned}
 |V_{us}|_{\text{uni}} &= 0.2255 \pm 0.0010 && \text{from } \sqrt{1 - |V_{ud}|^2} \text{ (CKM unitarity) ,} \\
 |V_{us}|_{\tau s} &= 0.2173 \pm 0.0022 && - 3.4\sigma \text{ from } \Gamma(\tau^- \rightarrow X_s^- \nu_\tau) , \\
 |V_{us}|_{\tau K/\pi} &= 0.2229 \pm 0.0021 && - 1.1\sigma \text{ from } \Gamma(\tau^- \rightarrow K^- \nu_\tau) / \Gamma(\tau^- \rightarrow \pi^- \nu_\tau) , \\
 |V_{us}|_{\tau K} &= 0.2214 \pm 0.0022 && - 1.7\sigma \text{ from } \Gamma(\tau^- \rightarrow K^- \nu_\tau) .
 \end{aligned}$$

Thanks to the improved lattice QCD determination of f_K [174], the uncertainty on $|V_{us}|_{\tau K}$ has been significantly reduced with respect to the previous HFAG report. Averaging the three above $|V_{us}|$ determinations we obtain:

$$|V_{us}|_{\tau} = 0.2202 \pm 0.0015 \quad - 2.9\sigma \quad \text{average of 3 } |V_{us}| \text{ tau measurements.}$$

We could not find a published estimate of the correlation of the uncertainties on f_K and f_K/f_π , but even if we assume $\pm 100\%$ correlation, the uncertainty on $|V_{us}|_{\tau}$ does not change more than about $\pm 5\%$. Figure 86 summarizes the $|V_{us}|$ results.

9.5 Upper limits on tau LFV branching fractions

We list in Table 201 the up-to-date upper limits on the tau LFV branching fractions.

Table 201: HFAG Winter 2012 upper limit for the lepton flavor violating τ decay modes. For convenience, the decay modes are grouped in categories labelled according to their particle content. The label “(L)” in the category column means that the decay mode implies lepton number violation as well as the lepton flavor violation.

Decay mode	Category	90% CL Limit	Exp.	Ref.
$\Gamma_{156} = e^- \gamma$	$l\gamma$	$< 12.0 \cdot 10^{-8}$	Belle	[703]
		$< 3.3 \cdot 10^{-8}$	BABAR	[704]
$\Gamma_{157} = \mu^- \gamma$		$< 4.5 \cdot 10^{-8}$	Belle	[703]
		$< 4.4 \cdot 10^{-8}$	BABAR	[704]
$\Gamma_{158} = e^- \pi^0$	lP^0	$< 2.2 \cdot 10^{-8}$	Belle	[705]
		$< 13.0 \cdot 10^{-8}$	BABAR	[706]
$\Gamma_{159} = \mu^- \pi^0$		$< 2.7 \cdot 10^{-8}$	Belle	[705]
		$< 11.0 \cdot 10^{-8}$	BABAR	[706]
$\Gamma_{162} = e^- \eta$		$< 4.4 \cdot 10^{-8}$	Belle	[705]
		$< 16.0 \cdot 10^{-8}$	BABAR	[706]
$\Gamma_{163} = \mu^- \eta$		$< 2.3 \cdot 10^{-8}$	Belle	[705]
		$< 15.0 \cdot 10^{-8}$	BABAR	[706]
$\Gamma_{172} = e^- \eta'(958)$		$< 3.6 \cdot 10^{-8}$	Belle	[705]
		$< 24.0 \cdot 10^{-8}$	BABAR	[706]
$\Gamma_{173} = \mu^- \eta'(958)$		$< 3.8 \cdot 10^{-8}$	Belle	[705]
		$< 14.0 \cdot 10^{-8}$	BABAR	[706]
$\Gamma_{160} = e^- K_S^0$		$< 2.6 \cdot 10^{-8}$	Belle	[707]
		$< 3.3 \cdot 10^{-8}$	BABAR	[708]
$\Gamma_{161} = \mu^- K_S^0$		$< 2.3 \cdot 10^{-8}$	Belle	[707]
		$< 4.0 \cdot 10^{-8}$	BABAR	[708]
$\Gamma_{174} = e^- f_0(980)$	lS^0	$< 3.2 \cdot 10^{-8}$	Belle	[709]
$\Gamma_{175} = \mu^- f_0(980)$		$< 3.4 \cdot 10^{-8}$	Belle	[709]
$\Gamma_{164} = e^- \rho^0$	lV^0	$< 1.8 \cdot 10^{-8}$	Belle	[710]
		$< 4.6 \cdot 10^{-8}$	BABAR	[711]
$\Gamma_{165} = \mu^- \rho^0$		$< 1.2 \cdot 10^{-8}$	Belle	[710]
		$< 2.6 \cdot 10^{-8}$	BABAR	[711]
$\Gamma_{168} = e^- K^*(892)^0$		$< 3.2 \cdot 10^{-8}$	Belle	[710]
		$< 5.9 \cdot 10^{-8}$	BABAR	[711]
$\Gamma_{169} = \mu^- K^*(892)^0$		$< 7.2 \cdot 10^{-8}$	Belle	[710]
		$< 17.0 \cdot 10^{-8}$	BABAR	[711]
$\Gamma_{170} = e^- \bar{K}^*(892)^0$		$< 3.4 \cdot 10^{-8}$	Belle	[710]
		$< 4.6 \cdot 10^{-8}$	BABAR	[711]
$\Gamma_{171} = \mu^- \bar{K}^*(892)^0$		$< 7.0 \cdot 10^{-8}$	Belle	[710]
		$< 7.3 \cdot 10^{-8}$	BABAR	[711]
$\Gamma_{176} = e^- \phi$		$< 3.1 \cdot 10^{-8}$	Belle	[710]
		$< 3.1 \cdot 10^{-8}$	BABAR	[711]
$\Gamma_{177} = \mu^- \phi$		$< 8.4 \cdot 10^{-8}$	Belle	[710]

Table 201 – continued from previous page

Decay mode	Category	90% CL Limit	Exp.	Ref.
		$< 19.0 \cdot 10^{-8}$	<i>BABAR</i>	[711]
$\Gamma_{166} = e^- \omega$		$< 4.8 \cdot 10^{-8}$	Belle	[710]
		$< 11.0 \cdot 10^{-8}$	<i>BABAR</i>	[712]
$\Gamma_{167} = \mu^- \omega$		$< 4.7 \cdot 10^{-8}$	Belle	[710]
		$< 10.0 \cdot 10^{-8}$	<i>BABAR</i>	[712]
$\Gamma_{178} = e^- e^+ e^-$	<i>lll</i>	$< 2.7 \cdot 10^{-8}$	Belle	[713]
		$< 2.9 \cdot 10^{-8}$	<i>BABAR</i>	[714]
$\Gamma_{181} = \mu^- e^+ e^-$		$< 1.8 \cdot 10^{-8}$	Belle	[713]
		$< 2.2 \cdot 10^{-8}$	<i>BABAR</i>	[714]
$\Gamma_{179} = e^- \mu + \mu^-$		$< 2.7 \cdot 10^{-8}$	Belle	[713]
		$< 3.2 \cdot 10^{-8}$	<i>BABAR</i>	[714]
$\Gamma_{183} = \mu^- \mu + \mu^-$		$< 2.1 \cdot 10^{-8}$	Belle	[713]
		$< 3.3 \cdot 10^{-8}$	<i>BABAR</i>	[714]
$\Gamma_{182} = e^- \mu + e^-$		$< 1.5 \cdot 10^{-8}$	Belle	[713]
		$< 1.8 \cdot 10^{-8}$	<i>BABAR</i>	[714]
$\Gamma_{180} = \mu^- e^+ \mu^-$		$< 1.7 \cdot 10^{-8}$	Belle	[713]
		$< 2.6 \cdot 10^{-8}$	<i>BABAR</i>	[714]
$\Gamma_{184} = e^- \pi^+ \pi^-$	<i>lhh</i>	$< 2.3 \cdot 10^{-8}$	Belle	[715]
		$< 12.0 \cdot 10^{-8}$	<i>BABAR</i>	[716]
$\Gamma_{186} = \mu^- \pi^+ \pi^-$		$< 2.1 \cdot 10^{-8}$	Belle	[715]
		$< 29.0 \cdot 10^{-8}$	<i>BABAR</i>	[716]
$\Gamma_{188} = e^- \pi^+ K^-$		$< 3.7 \cdot 10^{-8}$	Belle	[715]
		$< 32.0 \cdot 10^{-8}$	<i>BABAR</i>	[716]
$\Gamma_{194} = \mu^- \pi^+ K^-$		$< 8.6 \cdot 10^{-8}$	Belle	[715]
		$< 26.0 \cdot 10^{-8}$	<i>BABAR</i>	[716]
$\Gamma_{189} = e^- K^+ \pi^-$		$< 3.1 \cdot 10^{-8}$	Belle	[715]
		$< 17.0 \cdot 10^{-8}$	<i>BABAR</i>	[716]
$\Gamma_{195} = \mu^- K^+ \pi^-$		$< 4.5 \cdot 10^{-8}$	Belle	[715]
		$< 32.0 \cdot 10^{-8}$	<i>BABAR</i>	[716]
$\Gamma_{192} = e^- K^+ K^-$		$< 3.4 \cdot 10^{-8}$	Belle	[715]
		$< 14.0 \cdot 10^{-8}$	<i>BABAR</i>	[716]
$\Gamma_{198} = \mu^- K^+ K^-$		$< 4.4 \cdot 10^{-8}$	Belle	[715]
		$< 25.0 \cdot 10^{-8}$	<i>BABAR</i>	[716]
$\Gamma_{191} = e^- K_S^0 K_S^0$		$< 7.1 \cdot 10^{-8}$	Belle	[707]
$\Gamma_{197} = \mu^- K_S^0 K_S^0$		$< 8.0 \cdot 10^{-8}$	Belle	[707]
$\Gamma_{185} = e^+ \pi^- \pi^-$	(L)	$< 2.0 \cdot 10^{-8}$	Belle	[715]
	(L)	$< 27.0 \cdot 10^{-8}$	<i>BABAR</i>	[716]
$\Gamma_{187} = \mu^+ \pi^- \pi^-$	(L)	$< 3.9 \cdot 10^{-8}$	Belle	[715]
	(L)	$< 7.0 \cdot 10^{-8}$	<i>BABAR</i>	[716]
$\Gamma_{190} = e^+ \pi^- K^-$	(L)	$< 3.2 \cdot 10^{-8}$	Belle	[715]
	(L)	$< 18. \cdot 10^{-8}$	<i>BABAR</i>	[716]
$\Gamma_{196} = \mu^+ \pi^- K^-$	(L)	$< 4.8 \cdot 10^{-8}$	Belle	[715]
	(L)	$< 22.0 \cdot 10^{-8}$	<i>BABAR</i>	[716]

Table 201 – continued from previous page

Decay mode	Category	90% CL Limit	Exp.	Ref.
$\Gamma_{193} = e^+ K^- K^-$	(L)	$< 3.3 \cdot 10^{-8}$	Belle	[715]
	(L)	$< 15.0 \cdot 10^{-8}$	BABAR	[716]
$\Gamma_{199} = \mu^+ K^- K^-$	(L)	$< 4.7 \cdot 10^{-8}$	Belle	[715]
	(L)	$< 48.0 \cdot 10^{-8}$	BABAR	[716]
$\Gamma_{211} = \pi^- \Lambda$	$\Lambda \bar{h}$	$< 3.0 \cdot 10^{-8}$	Belle	[717]
		$< 5.8 \cdot 10^{-8}$	BABAR	[718]
$\Gamma_{212} = \pi^- \bar{\Lambda}$		$< 2.8 \cdot 10^{-8}$	Belle	[717]
		$< 5.9 \cdot 10^{-8}$	BABAR	[718]
$\Gamma_{xx} = K^- \Lambda$		$< 4.2 \cdot 10^{-8}$	Belle	[717]
		$< 15. \cdot 10^{-8}$	BABAR	[718]
$\Gamma_{xx} = K^- \bar{\Lambda}$		$< 3.1 \cdot 10^{-8}$	Belle	[717]
		$< 7.2 \cdot 10^{-8}$	BABAR	[718]

Figure 87 summarizes the upper limits on the tau lepton-flavor-violating branching fractions.

10 Summary

This article provides updated world averages for b -hadron properties using results available before the end of 2011. In some sections, results that appeared before the end of April 2012 are also included.

Concerning b -hadron lifetime and mixing averages, the most significant changes in the past two years are due to new results from the CDF, D0 and LHCb experiments, mainly in the B_s^0 sector. While the Tevatron experiments have updated some of their analyses with the full Run II data sample, LHCb has just entered the game and is taking the lead already with results based on the 2010–2011 data samples collected at the LHC. While the updated D0 like-sign dimuon asymmetry still deviates from the Standard Model prediction (with a significance increased to 3.9σ), there is still no evidence of CP violation in either B^0 or B_s^0 mixing, with precisions on the semileptonic asymmetries reaching below the 1% level. However, the most impressive progress was achieved in the analysis of $B_s^0 \rightarrow J/\psi \phi$ decays, where new or significantly improved results became recently available from CDF, D0 and LHCb. The non-zero decay width difference in the $B_s^0 - \bar{B}_s^0$ system is now firmly established, with a relative difference of $(14 \pm 2)\%$. Its sign has also been determined by LHCb: the heavy state of the $B_s^0 - \bar{B}_s^0$ system lives longer than the light state, as expected in the Standard Model. In contrast, and despite the recent efforts from Belle, the relative decay width difference in the $B^0 - \bar{B}^0$ system, which has momentarily reached a slightly better absolute precision, is still consistent with zero. On the other hand, a quantum step has been achieved in the measurement of mixing-induced CP violation in B_s^0 decays proceeding through the $b \rightarrow c\bar{c}s$ transition: the corresponding weak phase has been pinned down to a precision below 0.1 radian and is so far compatible with the Standard Model expectation.

The measurement of $\sin 2\beta \equiv \sin 2\phi_1$ from $b \rightarrow c\bar{c}s$ transitions such as $B^0 \rightarrow J/\psi K_s^0$ has reached $< 3\%$ precision: $\sin 2\beta \equiv \sin 2\phi_1 = 0.679 \pm 0.020$. Measurements of the same parameter using different quark-level processes provide a consistency test of the Standard Model and allow insight into possible new physics. Recent improvements include the use of time-dependent Dalitz plot analyses of $B^0 \rightarrow K_s^0 K^+ K^-$ and $B^0 \rightarrow K_s^0 \pi^+ \pi^-$ to obtain CP violation parameters for ϕK_s^0 , $f_0(980) K_s^0$ and ρK_s^0 . All results among hadronic $b \rightarrow s$ penguin dominated decays are currently consistent with the Standard Model expectations. Among measurements related to the Unitarity Triangle angle $\alpha \equiv \phi_2$, results from the $\rho\rho$ system allow constraints at the level of $\approx 6^\circ$. Knowledge of the third angle $\gamma \equiv \phi_3$ also continues to improve. Notwithstanding the well-known statistical issues in extracting the value of the angle itself, the world average values of the parameters in $B \rightarrow DK$ decays now show significant direct CP violation effects.

Regarding semileptonic B meson decays, the B factories Belle and BABAR continue to dominate the field and a number of results have appeared since the last update. Semileptonic decays remain a focus of interest for theorists: New lattice QCD and light-cone sum rule results help to understand exclusive transitions. Inclusive semileptonic decays are understood at full $\mathcal{O}(\alpha_s^2)$. Still, the experimental situation is not satisfactory: While inclusive and exclusive determinations of $|V_{cb}|$ agree at the level of 2σ , inclusive and exclusive measurements of $|V_{ub}|$ differ by three standard deviations. Clearly more effort on the experimental and theory side is required in the future.

The most important new measurements of rare decays are coming from the LHC. CMS and LHCb both have restrictive limits for the decays $B \rightarrow \mu^+ \mu^-$ and $B_s \rightarrow \mu^+ \mu^-$. The sensitivity is approaching the SM expectations with no significant signals seen yet. LHCb has already

Table 202: Selected world averages from Chapters 3 and 4.

b-hadron lifetimes $\tau(B^0)$ $\tau(B^+)$ $\bar{\tau}(B_s^0) = 1/\Gamma_s$ $\tau(B_c^+)$ $\tau(\Lambda_b^0)$	1.519 ± 0.007 ps 1.642 ± 0.008 ps 1.509 ± 0.012 ps 0.458 ± 0.030 ps 1.413 ± 0.030 ps
b-hadron fractions f^{+-}/f^{00} in $\Upsilon(4S)$ decays f_s in $\Upsilon(5S)$ decays f_s, f_{baryon} in Z decays f_s, f_{baryon} at Tevatron	1.056 ± 0.028 0.199 ± 0.030 $0.103 \pm 0.009, 0.090 \pm 0.015$ $0.103 \pm 0.012, 0.236 \pm 0.067$
B^0 and B_s^0 mixing / CPV parameters Δm_d $ q/p _d$ Δm_s $\Delta\Gamma_s = \Gamma_L - \Gamma_H$ $ q/p _s$ $\phi_s^{c\bar{c}s}$	0.507 ± 0.004 ps ⁻¹ 1.0002 ± 0.0028 17.719 ± 0.043 ps ⁻¹ $+0.095 \pm 0.014$ ps ⁻¹ 1.0052 ± 0.0032 $-0.044^{+0.090}_{-0.085}$
Measurements related to Unitarity Triangle angles $\sin 2\beta \equiv \sin 2\phi_1$ $\beta \equiv \phi_1$ $-\eta S_{\phi K_S^0}$ $-\eta S_{\eta' K^0}$ $-\eta S_{K_S^0 K_S^0 K_S^0}$ $-\eta S_{K^+ K^- K_S^0}$ $-\eta S_{J/\psi \pi^0}$ $S_{K^* \gamma}$ $S_{\pi^+ \pi^-}$ $C_{\pi^+ \pi^-}$ $S_{\rho^+ \rho^-}$ $a(D^{*\pm} \pi^\mp)$ $A_{CP}(B \rightarrow D_{CP^+} K)$ $A_{\text{ADS}}(B \rightarrow D_{K\pi} K)$ $R_{\text{ADS}}(B \rightarrow D_{K\pi} K)$	0.679 ± 0.020 $(21.4 \pm 0.8)^\circ$ $0.74^{+0.11}_{-0.13}$ 0.59 ± 0.07 0.72 ± 0.19 $0.68^{+0.09}_{-0.10}$ 0.93 ± 0.15 -0.16 ± 0.22 -0.65 ± 0.07 -0.36 ± 0.06 -0.05 ± 0.17 -0.039 ± 0.010 0.19 ± 0.03 -0.54 ± 0.12 0.0153 ± 0.0017

Table 203: Selected world averages at the end of 2011 from Chapters 5–7.

Semileptonic B decay parameters	
$\mathcal{B}(\bar{B}^0 \rightarrow D^{*+}\ell^-\bar{\nu})$	$(4.95 \pm 0.11)\%$
$\mathcal{B}(B^- \rightarrow D^{*0}\ell^-\bar{\nu})$	$(5.70 \pm 0.19)\%$
$\mathcal{F}(1) V_{cb} $	$(35.90 \pm 0.45) \times 10^{-3}$
$ V_{cb} $ from $\bar{B} \rightarrow D^*\ell^-\bar{\nu}_\ell$	$(39.54 \pm 0.50_{\text{exp}} \pm 0.74_{\text{th}}) \times 10^{-3}$
$\mathcal{B}(\bar{B}^0 \rightarrow D^+\ell^-\bar{\nu})$	$(2.18 \pm 0.12)\%$
$\mathcal{B}(B^- \rightarrow D^0\ell^-\bar{\nu})$	$(2.26 \pm 0.11)\%$
$\mathcal{G}(1) V_{cb} $	$(42.64 \pm 1.53) \times 10^{-3}$
$ V_{cb} $ from $\bar{B} \rightarrow D\ell^-\bar{\nu}_\ell$	$(39.70 \pm 1.42_{\text{exp}} \pm 0.89_{\text{th}}) \times 10^{-3}$
$\mathcal{B}(\bar{B} \rightarrow X_c\ell^-\bar{\nu}_\ell)$	$(10.51 \pm 0.13)\%$
$\mathcal{B}(\bar{B} \rightarrow X\ell^-\bar{\nu}_\ell)$	$(10.72 \pm 0.13)\%$
$ V_{cb} $ from $\bar{B} \rightarrow X\ell^-\bar{\nu}_\ell$	$(41.88 \pm 0.73) \times 10^{-3}$
$\mathcal{B}(\bar{B} \rightarrow \pi\ell^-\bar{\nu})$	$(1.42 \pm 0.05) \times 10^{-4}$
$ V_{ub} $ from $\bar{B} \rightarrow \pi\ell^-\bar{\nu}$	$(3.23 \pm 0.30) \times 10^{-3}$
$ V_{ub} $ from $\bar{B} \rightarrow X_u\ell^-\bar{\nu}$	$(4.40 \pm 0.15_{\text{exp}} \pm 0.20_{\text{th}}) \times 10^{-3}$
Rare B decays	
$\mathcal{B}(B \rightarrow X_s\gamma)$	$(3.55 \pm 0.24 \pm 0.09) \times 10^{-4}$
$\mathcal{B}(B^+ \rightarrow \tau^+\nu)$	$(1.67 \pm 0.30) \times 10^{-4}$
$A_{\text{FB}}(B^0 \rightarrow K^{*0}\mu^+\mu^-)$ in bins of $q^2 = m^2(\mu^+\mu^-)$	see Table 142
$\mathcal{B}(B_s^0 \rightarrow \mu^+\mu^-)$	$< 1.2 \times 10^{-8}$ (90% C.L.)
$A_{CP}(B^0 \rightarrow K^+\pi^-)$	(-0.087 ± 0.008)
$A_{CP}(B^+ \rightarrow K^+\pi^0)$	(0.037 ± 0.021)
$A_{CP}(B_s^0 \rightarrow K^-\pi^+)$	(0.29 ± 0.07)

produced many other results on a wide variety of decays as indicated in the tables in Sec. 7. Belle and *BABAR* continue to produce new results though their rates are dwindling. It will still be some years before we see new results from upgraded B factories.

Many b to charm results from LHCb are included in our report for the first time this year, combining with results from *BABAR*, Belle and CDF to yield a total of 632 measurements reported in 216 papers. The huge combined sample of b hadrons allows measurements of decays to states with open or hidden charm content with unprecedented precision.

In the charm sector, D^0 - \bar{D}^0 mixing is now well-established. Measurements of 38 separate observables from five experiments are input into a global fit for 10 underlying parameters, and the no-mixing hypothesis is excluded at a confidence level corresponding to 10.2σ . The mixing parameters x and y (see Table 204) differ from zero by 2.7σ and 6.0σ , respectively. The central values are consistent with mixing arising from long-distance processes, as predicted by theory; thus it will probably be difficult to identify new physics from mixing alone. The WA value for the observable y_{CP} is positive, which indicates that the CP -even state is shorter-lived as in

Table 204: Selected world averages at the end of 2011 from Chapters 8 and 9.

D^0 mixing and CPV parameters	
x	$(0.63^{+0.19}_{-0.20})\%$
y	$(0.75 \pm 0.12)\%$
A_D	$(-1.7 \pm 2.4)\%$
$ q/p $	$0.88^{+0.18}_{-0.16}$
ϕ	$(-10.1^{+9.5}_{-8.9})^\circ$
x_{12} (no direct CPV)	$(0.62 \pm 0.19)\%$
y_{12} (no direct CPV)	$(0.75 \pm 0.12)\%$
ϕ_{12} (no direct CPV)	$(4.9^{+7.7}_{-6.5})^\circ$
a_{CP}^{ind}	$(-0.02 \pm 0.23)\%$
$\Delta a_{CP}^{\text{dir}}$	$(-0.66 \pm 0.15)\%$
τ parameters, Lepton Universality, and V_{us}	
g_μ/g_e	1.0018 ± 0.0014
g_τ/g_μ	1.0006 ± 0.0021
g_τ/g_e	1.0024 ± 0.0021
$\mathcal{B}_e^{\text{uni}}$	$(17.839 \pm 0.028)\%$
R_{had}	3.6280 ± 0.0094
$ V_{us} $ from $\mathcal{B}(\tau^- \rightarrow K^- \nu_\tau)$	0.2214 ± 0.0022
$ V_{us} $ from $\mathcal{B}(\tau^- \rightarrow K^- \nu_\tau)/\mathcal{B}(\tau^- \rightarrow \pi^- \nu_\tau)$	0.2229 ± 0.0021
$ V_{us} $ from inclusive sum of strange branching fractions	0.2173 ± 0.0022
$ V_{us} $ tau average	0.2202 ± 0.0015

the $K^0\text{-}\bar{K}^0$ system. However, x also appears to be positive, which implies that the CP -even state is heavier, unlike in the $K^0\text{-}\bar{K}^0$ system. In the $D^0\text{-}\bar{D}^0$ system, there is no evidence for CPV arising from mixing ($|q/p| \neq 1$) or from a phase difference between the mixing amplitude and a direct decay amplitude ($\phi \neq 0$). However, both the LHCb and CDF experiments have obtained evidence for direct CPV in $D^0 \rightarrow K^+K^-$ and $D^0 \rightarrow \pi^+\pi^-$ decays. These experiments measure nonzero values for the *difference* in direct CPV between K^+K^- and $\pi^+\pi^-$ modes, which requires that direct CPV exists in at least one of them. Inputting these measurements into a global fit and also including measurements from Belle and BABAR gives $\Delta a_{CP}^{\text{dir}} \neq 0$ with a significance greater than 4σ .

Concerning tau decays, in this report we include three new tau branching fraction measurements from the B -factories, and we provide more information on the tau branching fraction fit. The $|V_{us}|$ calculation uses now a more complete set of tau branching fractions to strange final states, and thanks primarily to improvements in QCD lattice predictions, two tau determinations of $|V_{us}|$ have reduced errors. For the first time, we compute an average of all $|V_{us}|$ determinations with tau data.

11 Acknowledgments

We are grateful for the strong support of the Belle, *BABAR*, CLEO, CDF, D0 and LHCb collaborations, without whom this compilation of results and world averages would not have been possible. The success of these experiments in turn would not have been possible without the excellent operations of the KEKB, PEP-II, CESR, Tevatron and LHC accelerators, and fruitful collaborations between the accelerator groups and the experiments.

Our averages and this compilation have benefitted greatly from contributions to the Heavy Flavor Averaging Group from numerous individuals. We especially thank David Kirkby, Yoshihide Sakai, Simon Eidelman, Soeren Prell and Gianluca Cavoto for their past leadership of HFAG. We are grateful to Paolo Gambino for assistance with averages that appear in Chapter 5, to David Asner, David Cassel and Milind Purohit for significant contributions to Chapter 8, and to Michel Davier for providing valuable input to Chapter 9.

References

- [1] N. Cabibbo, Phys. Rev. Lett. **10**, 531–533 (1963).
- [2] M. Kobayashi and T. Maskawa, Prog. Theor. Phys. **49**, 652–657 (1973).
- [3] D. Abbaneo *et al.* (ALEPH, CDF, DELPHI, L3, OPAL, and SLD collaborations), arXiv:hep-ex/0009052 (2000), CERN-EP-2000-096; arXiv:hep-ex/0112028 (2001), CERN-EP-2001-050.
- [4] D. Asner *et al.* (Heavy Flavor Averaging Group collaboration) (2010), arXiv:1010.1589 [hep-ex].
- [5] K. Nakamura *et al.* (Particle Data Group), J. Phys. **G37**, 075021 (2010), and 2011 partial update for the 2012 edition.
- [6] B. Aubert *et al.* (BABAR collaboration), Phys. Rev. Lett. **94**, 141801 (2005), arXiv:hep-ex/0412062.
- [7] B. Aubert *et al.* (BABAR collaboration), Phys. Rev. **D65**, 032001 (2002), arXiv:hep-ex/0107025.
- [8] B. Aubert *et al.* (BABAR collaboration), Phys. Rev. **D69**, 071101 (2004), arXiv:hep-ex/0401028.
- [9] J. P. Alexander *et al.* (CLEO collaboration), Phys. Rev. Lett. **86**, 2737–2741 (2001), arXiv:hep-ex/0006002.
- [10] S. B. Athar *et al.* (CLEO collaboration), Phys. Rev. **D66**, 052003 (2002), arXiv:hep-ex/0202033.
- [11] N. C. Hastings *et al.* (Belle collaboration), Phys. Rev. **D67**, 052004 (2003), arXiv:hep-ex/0212033.
- [12] B. Aubert *et al.* (BABAR collaboration), Phys. Rev. Lett. **95**, 042001 (2005), arXiv:hep-ex/0504001.
- [13] B. Aubert *et al.* (BABAR collaboration), Phys. Rev. Lett. **96**, 232001 (2006), arXiv:hep-ex/0604031; A. Sokolov *et al.* (Belle collaboration), Phys. Rev. **D75**, 071103 (2007), arXiv:hep-ex/0611026; B. Aubert *et al.* (BABAR collaboration), Phys. Rev. **D78**, 112002 (2008), arXiv:0807.2014 [hep-ex].
- [14] B. Barish *et al.* (CLEO collaboration), Phys. Rev. Lett. **76**, 1570–1574 (1996).
- [15] A. Drutskoy *et al.* (Belle collaboration), Phys. Rev. **D81**, 112003 (2010), arXiv:1003.5885 [hep-ex].
- [16] G. S. Huang *et al.* (CLEO collaboration), Phys. Rev. **D75**, 012002 (2007), arXiv:hep-ex/0610035; this supersedes the results of Ref. [19].
- [17] A. Drutskoy *et al.* (Belle collaboration), Phys. Rev. Lett. **98**, 052001 (2007), arXiv:hep-ex/0608015.

- [18] J. Beringer *et al.* (Particle Data Group), Phys. Rev. **D86**, 010001 (2012).
- [19] M. Artuso *et al.* (CLEO collaboration), Phys. Rev. Lett. **95**, 261801 (2005), arXiv:hep-ex/0508047.
- [20] K. F. Chen *et al.* (Belle collaboration), Phys. Rev. Lett. **100**, 112001 (2008), arXiv:0710.2577 [hep-ex].
- [21] I. Adachi *et al.* (Belle collaboration), Phys. Rev. Lett. **108**, 032001 (2012), arXiv:1103.3419 [hep-ex].
- [22] R. Louvot, PhD thesis #5213, EPFL, Lausanne (2012), <http://dx.doi.org/10.5075/epfl-thesis-5213>.
- [23] J. P. Lees *et al.* (BABAR collaboration), Phys. Rev. **D85**, 011101 (2012), arXiv:1110.5600 [hep-ex].
- [24] J. Li *et al.* (Belle collaboration), Phys. Rev. Lett. **106**, 121802 (2011), arXiv:1102.2759 [hep-ex].
- [25] R. Louvot *et al.* (Belle collaboration), Phys. Rev. Lett. **102**, 021801 (2009), arXiv:0809.2526 [hep-ex].
- [26] P. Abreu *et al.* (DELPHI collaboration), Phys. Lett. **B289**, 199–210 (1992); P. D. Acton *et al.* (OPAL collaboration), Phys. Lett. **B295**, 357–370 (1992); D. Buskulic *et al.* (ALEPH collaboration), Phys. Lett. **B361**, 221–233 (1995).
- [27] P. Abreu *et al.* (DELPHI collaboration), Z. Phys. **C68**, 375–390 (1995).
- [28] R. Barate *et al.* (ALEPH collaboration), Eur. Phys. J. **C2**, 197–211 (1998).
- [29] D. Buskulic *et al.* (ALEPH collaboration), Phys. Lett. **B384**, 449–460 (1996).
- [30] J. Abdallah *et al.* (DELPHI collaboration), Eur. Phys. J. **C44**, 299–309 (2005), arXiv:hep-ex/0510023.
- [31] P. Abreu *et al.* (DELPHI collaboration), Z. Phys. **C68**, 541–554 (1995).
- [32] R. Barate *et al.* (ALEPH collaboration), Eur. Phys. J. **C5**, 205–227 (1998).
- [33] J. Abdallah *et al.* (DELPHI collaboration), Phys. Lett. **B576**, 29–42 (2003), arXiv:hep-ex/0311005.
- [34] T. Affolder *et al.* (CDF collaboration), Phys. Rev. Lett. **84**, 1663–1668 (2000), arXiv:hep-ex/9909011.
- [35] T. Aaltonen *et al.* (CDF collaboration), Phys. Rev. **D77**, 072003 (2008), arXiv:0801.4375 [hep-ex].
- [36] T. Aaltonen *et al.* (CDF collaboration), Phys. Rev. **D79**, 032001 (2009), arXiv:0810.3213 [hep-ex].

- [37] F. Abe *et al.* (CDF collaboration), Phys. Rev. **D60**, 092005 (1999).
- [38] V. M. Abazov *et al.* (D0 collaboration), Phys. Rev. Lett. **99**, 052001 (2007), arXiv:0706.1690 [hep-ex].
- [39] V. M. Abazov *et al.* (D0 collaboration), Phys. Rev. Lett. **101**, 232002 (2008), arXiv:0808.4142 [hep-ex].
- [40] T. Aaltonen *et al.* (CDF collaboration), Phys. Rev. **D80**, 072003 (2009), arXiv:0905.3123 [hep-ex].
- [41] R. Aaij *et al.* (LHCb collaboration), Phys. Rev. **D85**, 032008 (2012), arXiv:1111.2357 [hep-ex]; the full covariance matrix of the measurements is available at <https://cdsweb.cern.ch/record/1390838>.
- [42] R. Aaij *et al.* (LHCb collaboration), Phys. Rev. Lett. **107**, 211801 (2011), arXiv:1106.4435 [hep-ex].
- [43] S. Schael *et al.* (ALEPH, CDF, DELPHI, L3, OPAL, and SLD collaborations, LEP electroweak working group, SLD electroweak and heavy flavour working groups), Phys. Rept. **427**, 257 (2006), arXiv:hep-ex/0509008; we use the average given in Eq. 5.39 of this paper, obtained from a 10-parameter global fit of all electroweak data where the asymmetry measurements have been excluded.
- [44] V. M. Abazov *et al.* (D0 collaboration), Phys. Rev. **D74**, 092001 (2006), arXiv:hep-ex/0609014.
- [45] CDF collaboration, CDF note 10335, 27 January 2011, <http://www-cdf.fnal.gov/physics/new/bottom/110127.blessed-chibar/>.
- [46] D. Acosta *et al.* (CDF collaboration), Phys. Rev. **D69**, 012002 (2004), arXiv:hep-ex/0309030; this supersedes the $\bar{\chi}$ value of Ref. [176].
- [47] M. A. Shifman and M. B. Voloshin, Sov. Phys. JETP **64**, 698 (1986); J. Chay, H. Georgi, and B. Grinstein, Phys. Lett. **B247**, 399–405 (1990); I. I. Bigi, N. G. Uraltsev, and A. I. Vainshtein, Phys. Lett. **B293**, 430–436 (1992), arXiv:hep-ph/9207214; erratum Phys. Lett. **B297**, 477 (1992).
- [48] I. I. Bigi, arXiv:hep-ph/9508408 (1995); G. Bellini, I. I. Bigi, and P. J. Dornan, Phys. Rept. **289**, 1–155 (1997).
- [49] M. Ciuchini, E. Franco, V. Lubicz, and F. Mescia, Nucl. Phys. **B625**, 211–238 (2002), arXiv:hep-ph/0110375; M. Beneke, G. Buchalla, C. Greub, A. Lenz, and U. Nierste, Nucl. Phys. **B639**, 389–407 (2002), arXiv:hep-ph/0202106; E. Franco, V. Lubicz, F. Mescia, and C. Tarantino, Nucl. Phys. **B633**, 212–236 (2002), arXiv:hep-ph/0203089.
- [50] C. Tarantino, Eur. Phys. J. **C33**, s895–s899 (2004), arXiv:hep-ph/0310241; F. Gabbiani, A. I. Onishchenko, and A. A. Petrov, Phys. Rev. **D68**, 114006 (2003), arXiv:hep-ph/0303235.

- [51] F. Gabbiani, A. I. Onishchenko, and A. A. Petrov, Phys. Rev. **D70**, 094031 (2004), [arXiv:hep-ph/0407004](#).
- [52] L. Di Ciaccio *et al.* (1996), internal note by former *B* lifetime working group, http://lepbos.web.cern.ch/LEPBOSC/lifetimes/ps/final_blife.ps.
- [53] D. Buskulic *et al.* (ALEPH collaboration), Phys. Lett. **B314**, 459–470 (1993).
- [54] P. Abreu *et al.* (DELPHI collaboration), Z. Phys. **C63**, 3–16 (1994).
- [55] P. Abreu *et al.* (DELPHI collaboration), Phys. Lett. **B377**, 195–204 (1996).
- [56] J. Abdallah *et al.* (DELPHI collaboration), Eur. Phys. J. **C33**, 307–324 (2004), [arXiv:hep-ex/0401025](#).
- [57] M. Acciarri *et al.* (L3 collaboration), Phys. Lett. **B416**, 220–232 (1998).
- [58] K. Ackerstaff *et al.* (OPAL collaboration), Z. Phys. **C73**, 397–408 (1997).
- [59] K. Abe *et al.* (SLD collaboration), Phys. Rev. Lett. **75**, 3624–3628 (1995), [arXiv:hep-ex/9511005](#).
- [60] D. Buskulic *et al.* (ALEPH collaboration), Phys. Lett. **B369**, 151–162 (1996).
- [61] P. D. Acton *et al.* (OPAL collaboration), Z. Phys. **C60**, 217–228 (1993).
- [62] F. Abe *et al.* (CDF collaboration), Phys. Rev. **D57**, 5382–5401 (1998).
- [63] ATLAS collaboration, ATLAS note ATLAS-CONF-2011-145, 11 October 2011, <https://cdsweb.cern.ch/record/1389455>.
- [64] R. Barate *et al.* (ALEPH collaboration), Phys. Lett. **B492**, 275–287 (2000), [arXiv:hep-ex/0008016](#).
- [65] D. Buskulic *et al.* (ALEPH collaboration), Z. Phys. **C71**, 31–44 (1996).
- [66] P. Abreu *et al.* (DELPHI collaboration), Z. Phys. **C68**, 13–24 (1995).
- [67] W. Adam *et al.* (DELPHI collaboration), Z. Phys. **C68**, 363–374 (1995).
- [68] P. Abreu *et al.* (DELPHI collaboration), Z. Phys. **C74**, 19–32 (1997).
- [69] M. Acciarri *et al.* (L3 collaboration), Phys. Lett. **B438**, 417–429 (1998).
- [70] R. Akers *et al.* (OPAL collaboration), Z. Phys. **C67**, 379–388 (1995).
- [71] G. Abbiendi *et al.* (OPAL collaboration), Eur. Phys. J. **C12**, 609–626 (2000), [arXiv:hep-ex/9901017](#).
- [72] G. Abbiendi *et al.* (OPAL collaboration), Phys. Lett. **B493**, 266–280 (2000), [arXiv:hep-ex/0010013](#).
- [73] K. Abe *et al.* (SLD collaboration), Phys. Rev. Lett. **79**, 590–596 (1997).

- [74] F. Abe *et al.* (CDF collaboration), Phys. Rev. **D58**, 092002 (1998),
arXiv:hep-ex/9806018.
- [75] D. E. Acosta *et al.* (CDF collaboration), Phys. Rev. **D65**, 092009 (2002).
- [76] T. Aaltonen *et al.* (CDF collaboration), Phys. Rev. Lett. **106**, 121804 (2011),
arXiv:1012.3138 [hep-ex]; these results replace the $\Lambda_b \rightarrow J/\psi \Lambda$ and $B^0 \rightarrow J/\psi K_S$
lifetime measurements of A. Abulencia *et al.* (CDF collaboration),
Phys. Rev. Lett. **98**, 122001 (2007), arXiv:hep-ex/0609021, as well as the
 $B^0 \rightarrow J/\psi K^{*0}$ lifetime measurement of Ref. [258].
- [77] V. M. Abazov *et al.* (D0 collaboration), Phys. Rev. Lett. **102**, 032001 (2009),
arXiv:0810.0037 [hep-ex]; this replaces V. M. Abazov *et al.* (D0 collaboration),
Phys. Rev. Lett. **95**, 171801 (2005), arXiv:hep-ex/0507084.
- [78] V. M. Abazov *et al.* (D0 collaboration), Phys. Rev. **D85**, 112003 (2012),
arXiv:1204.2340 [hep-ex]; this replaces V. M. Abazov *et al.* (D0 collaboration),
Phys. Rev. Lett. **99**, 142001 (2007), arXiv:0704.3909 [hep-ex]; and V. M. Abazov *et al.*
(D0 collaboration), Phys. Rev. Lett. **94**, 102001 (2005), arXiv:hep-ex/0410054.
- [79] B. Aubert *et al.* (BABAR collaboration), Phys. Rev. Lett. **87**, 201803 (2001),
arXiv:hep-ex/0107019.
- [80] B. Aubert *et al.* (BABAR collaboration), Phys. Rev. Lett. **89**, 011802 (2002),
arXiv:hep-ex/0202005; erratum Phys. Rev. Lett. **89**, 169903 (2002).
- [81] B. Aubert *et al.* (BABAR collaboration), Phys. Rev. **D67**, 072002 (2003),
arXiv:hep-ex/0212017.
- [82] B. Aubert *et al.* (BABAR collaboration), Phys. Rev. **D67**, 091101 (2003),
arXiv:hep-ex/0212012.
- [83] B. Aubert *et al.* (BABAR collaboration), Phys. Rev. **D73**, 012004 (2006),
arXiv:hep-ex/0507054.
- [84] K. Abe *et al.* (Belle collaboration), Phys. Rev. **D71**, 072003 (2005),
arXiv:hep-ex/0408111.
- [85] ATLAS collaboration, ATLAS note ATLAS-CONF-2011-092, 5 July 2011,
<https://cdsweb.cern.ch/record/1363779>.
- [86] LHCb collaboration, LHCb note LHCb-CONF-2011-001, 25 March 2011,
<https://cdsweb.cern.ch/record/1328683>.
- [87] T. Aaltonen *et al.* (CDF collaboration), Phys. Rev. **D83**, 032008 (2011),
arXiv:1004.4855 [hep-ex].
- [88] V. M. Abazov *et al.* (D0 collaboration), Phys. Rev. Lett. **94**, 182001 (2005),
arXiv:hep-ex/0410052.

- [89] CDF collaboration, CDF note 7514, 1 March 2005,
<http://www-cdf.fnal.gov/physics/new/bottom/050224.blessed-bsemi-life/>.
- [90] CDF collaboration, CDF note 7386, 23 March 2005,
<http://www-cdf.fnal.gov/physics/new/bottom/050303.blessed-bhadlife/>.
- [91] A. Lenz and U. Nierste (2011), [arXiv:1102.4274](https://arxiv.org/abs/1102.4274) [hep-ph]; this updates the results of A. Lenz and U. Nierste, JHEP **06**, 072 (2007), [arXiv:hep-ph/0612167](https://arxiv.org/abs/hep-ph/0612167).
- [92] M. Beneke, G. Buchalla, C. Greub, A. Lenz, and U. Nierste, Phys. Lett. **B459**, 631–640 (1999), [arXiv:hep-ph/9808385](https://arxiv.org/abs/hep-ph/9808385).
- [93] R. Aaij *et al.* (LHCb collaboration) (2012), [arXiv:1202.4717](https://arxiv.org/abs/1202.4717) [hep-ex], to appear in Phys. Rev. Lett.
- [94] D. Buskulic *et al.* (ALEPH collaboration), Phys. Lett. **B377**, 205–221 (1996).
- [95] F. Abe *et al.* (CDF collaboration), Phys. Rev. **D59**, 032004 (1999), [arXiv:hep-ex/9808003](https://arxiv.org/abs/hep-ex/9808003).
- [96] P. Abreu *et al.* (DELPHI collaboration), Eur. Phys. J. **C16**, 555 (2000), [arXiv:hep-ex/0107077](https://arxiv.org/abs/hep-ex/0107077).
- [97] K. Ackerstaff *et al.* (OPAL collaboration), Phys. Lett. **B426**, 161–179 (1998), [arXiv:hep-ex/9802002](https://arxiv.org/abs/hep-ex/9802002).
- [98] V. M. Abazov *et al.* (D0 collaboration), Phys. Rev. Lett. **97**, 241801 (2006), [arXiv:hep-ex/0604046](https://arxiv.org/abs/hep-ex/0604046).
- [99] T. Aaltonen *et al.* (CDF collaboration), Phys. Rev. Lett. **107**, 272001 (2011), [arXiv:1103.1864](https://arxiv.org/abs/1103.1864) [hep-ex]; we consider that these results supersede those from the old CDF note 7386 [90], although the lifetime analysis of one of the modes ($B_s \rightarrow D_s \pi \pi$) has not been updated.
- [100] R. Barate *et al.* (ALEPH collaboration), Eur. Phys. J. **C4**, 367–385 (1998).
- [101] P. Abreu *et al.* (DELPHI collaboration), Eur. Phys. J. **C18**, 229–252 (2000), [arXiv:hep-ex/0105077](https://arxiv.org/abs/hep-ex/0105077).
- [102] K. Ackerstaff *et al.* (OPAL collaboration), Eur. Phys. J. **C2**, 407–416 (1998), [arXiv:hep-ex/9708023](https://arxiv.org/abs/hep-ex/9708023).
- [103] V. M. Abazov *et al.* (D0 collaboration), Phys. Rev. Lett. **94**, 042001 (2005), [arXiv:hep-ex/0409043](https://arxiv.org/abs/hep-ex/0409043).
- [104] R. Barate *et al.* (ALEPH collaboration), Phys. Lett. **B486**, 286–299 (2000).
- [105] R. Aaij *et al.* (LHCb collaboration), Phys. Lett. **B707**, 349–356 (2012), [arXiv:1111.0521](https://arxiv.org/abs/1111.0521) [hep-ex].
- [106] LHCb collaboration, LHCb note LHCb-CONF-2012-001, 7 March 2012,
<http://cdsweb.cern.ch/record/1422996>.

- [107] T. Aaltonen *et al.* (CDF collaboration), Phys. Rev. **D84**, 052012 (2011), arXiv:1106.3682 [hep-ex].
- [108] K. Hartkorn and H. G. Moser, Eur. Phys. J. **C8**, 381–383 (1999).
- [109] CDF collaboration, CDF note 7757, 13 August 2005, http://www-cdf.fnal.gov/physics/new/bottom/050707.blessed-bs-semi_life/.
- [110] CDF collaboration, CDF note 8524, 7 March 2007, http://www-cdf.fnal.gov/physics/new/bottom/061130.blessed-bh-lifetime_v2/; all these preliminary results are superseded by Ref. [76,258] except those on $B_s^0 \rightarrow J/\psi\phi$.
- [111] D. Tonelli (for the CDF collaboration), arXiv:hep-ex/0605038 (2006).
- [112] F. Abe *et al.* (CDF collaboration), Phys. Rev. Lett. **81**, 2432–2437 (1998), arXiv:hep-ex/9805034.
- [113] CDF collaboration, CDF note 9294, 28 April 2008, http://www-cdf.fnal.gov/physics/new/bottom/080327.blessed-BC_LT_SemiLeptonic/; this replaces A. Abulencia *et al.* (CDF collaboration), Phys. Rev. Lett. **97**, 012002 (2006), arXiv:hep-ex/0603027.
- [114] V. M. Abazov *et al.* (D0 collaboration), Phys. Rev. Lett. **102**, 092001 (2009), arXiv:0805.2614 [hep-ex].
- [115] A. Abulencia *et al.* (CDF collaboration), Phys. Rev. Lett. **96**, 082002 (2006), arXiv:hep-ex/0505076.
- [116] T. Aaltonen *et al.* (CDF collaboration), Phys. Rev. Lett. **100**, 182002 (2008), arXiv:0712.1506 [hep-ex].
- [117] CDF collaboration, CDF note 10533, 21 August 2011, <http://www-cdf.fnal.gov/physics/new/bottom/110804.blessed-bc-lifetime/>.
- [118] D. E. Acosta *et al.* (CDF collaboration), Phys. Rev. Lett. **96**, 202001 (2006), arXiv:hep-ex/0508022.
- [119] D. Buskulic *et al.* (ALEPH collaboration), Phys. Lett. **B365**, 437–447 (1996).
- [120] P. Abreu *et al.* (DELPHI collaboration), Eur. Phys. J. **C10**, 185–199 (1999).
- [121] F. Abe *et al.* (CDF collaboration), Phys. Rev. Lett. **77**, 1439–1443 (1996).
- [122] T. Aaltonen *et al.* (CDF collaboration), Phys. Rev. Lett. **104**, 102002 (2010), arXiv:0912.3566 [hep-ex].
- [123] V. M. Abazov *et al.* (D0 collaboration), Phys. Rev. Lett. **99**, 182001 (2007), arXiv:0706.2358 [hep-ex].
- [124] P. Abreu *et al.* (DELPHI collaboration), Z. Phys. **C71**, 199–210 (1996).
- [125] R. Akers *et al.* (OPAL collaboration), Z. Phys. **C69**, 195–214 (1996).

- [126] M. Beneke, G. Buchalla, and I. Dunietz, Phys. Rev. **D54**, 4419–4431 (1996), arXiv:hep-ph/9605259; Y.-Y. Keum and U. Nierste, Phys. Rev. **D57**, 4282–4289 (1998), arXiv:hep-ph/9710512.
- [127] M. B. Voloshin, Phys. Rept. **320**, 275–285 (1999), arXiv:hep-ph/9901445; B. Guberina, B. Melic, and H. Stefancic, Phys. Lett. **B469**, 253–258 (1999), arXiv:hep-ph/9907468; M. Neubert and C. T. Sachrajda, Nucl. Phys. **B483**, 339–370 (1997), arXiv:hep-ph/9603202; I. I. Bigi, M. A. Shifman, and N. Uraltsev, Ann. Rev. Nucl. Part. Sci. **47**, 591–661 (1997), arXiv:hep-ph/9703290 [hep-ph].
- [128] N. G. Uraltsev, Phys. Lett. **B376**, 303–308 (1996), arXiv:hep-ph/9602324; D. Pirjol and N. Uraltsev, Phys. Rev. **D59**, 034012 (1999), arXiv:hep-ph/9805488; P. Colangelo and F. De Fazio, Phys. Lett. **B387**, 371–378 (1996), arXiv:hep-ph/9604425; M. Di Pierro, C. T. Sachrajda, and C. Michael (UKQCD collaboration), Phys. Lett. **B468**, 143 (1999), arXiv:hep-lat/9906031.
- [129] D. Buskulic *et al.* (ALEPH collaboration), Z. Phys. **C75**, 397–407 (1997).
- [130] P. Abreu *et al.* (DELPHI collaboration), Z. Phys. **C76**, 579–598 (1997).
- [131] J. Abdallah *et al.* (DELPHI collaboration), Eur. Phys. J. **C28**, 155–173 (2003), arXiv:hep-ex/0303032.
- [132] M. Acciarri *et al.* (L3 collaboration), Eur. Phys. J. **C5**, 195–203 (1998).
- [133] K. Ackerstaff *et al.* (OPAL collaboration), Z. Phys. **C76**, 417–423 (1997), arXiv:hep-ex/9707010.
- [134] K. Ackerstaff *et al.* (OPAL collaboration), Z. Phys. **C76**, 401–415 (1997), arXiv:hep-ex/9707009.
- [135] G. Alexander *et al.* (OPAL collaboration), Z. Phys. **C72**, 377–388 (1996).
- [136] F. Abe *et al.* (CDF collaboration), Phys. Rev. Lett. **80**, 2057–2062 (1998), arXiv:hep-ex/9712004; and Phys. Rev. **D59**, 032001 (1999), arXiv:hep-ex/9806026.
- [137] F. Abe *et al.* (CDF collaboration), Phys. Rev. **D60**, 051101 (1999).
- [138] F. Abe *et al.* (CDF collaboration), Phys. Rev. **D60**, 072003 (1999), arXiv:hep-ex/9903011.
- [139] T. Affolder *et al.* (CDF collaboration), Phys. Rev. **D60**, 112004 (1999), arXiv:hep-ex/9907053.
- [140] V. M. Abazov *et al.* (D0 collaboration), Phys. Rev. **D74**, 112002 (2006), arXiv:hep-ex/0609034.
- [141] B. Aubert *et al.* (BABAR collaboration), Phys. Rev. Lett. **88**, 221802 (2002), arXiv:hep-ex/0112044; B. Aubert *et al.* (BABAR collaboration), Phys. Rev. **D66**, 032003 (2002), arXiv:hep-ex/0201020.

- [142] B. Aubert *et al.* (BABAR collaboration), Phys. Rev. Lett. **88**, 221803 (2002), arXiv:hep-ex/0112045.
- [143] Y. Zheng *et al.* (Belle collaboration), Phys. Rev. **D67**, 092004 (2003), arXiv:hep-ex/0211065.
- [144] LHCb collaboration, LHCb note LHCb-CONF-2011-010, 28 April 2011, <https://cdsweb.cern.ch/record/1331124>; this result has been published in Ref. [172].
- [145] CDF collaboration, CDF note 8235, 26 April 2006, http://www-cdf.fnal.gov/physics/new/bottom/060406.blessed-semi_B0mix/.
- [146] CDF collaboration, CDF note 7920, 15 November 2005, http://www-cdf.fnal.gov/physics/new/bottom/050804.hadr_B0mix/.
- [147] H. Albrecht *et al.* (ARGUS collaboration), Z. Phys. **C55**, 357–364 (1992); H. Albrecht *et al.* (ARGUS collaboration), Phys. Lett. **B324**, 249–254 (1994).
- [148] J. E. Bartelt *et al.* (CLEO collaboration), Phys. Rev. Lett. **71**, 1680–1684 (1993).
- [149] B. H. Behrens *et al.* (CLEO collaboration), Phys. Lett. **B490**, 36–44 (2000), arXiv:hep-ex/0005013.
- [150] B. Aubert *et al.* (BABAR collaboration), Phys. Rev. Lett. **92**, 181801 (2004), arXiv:hep-ex/0311037; and Phys. Rev. **D70**, 012007 (2004), arXiv:hep-ex/0403002.
- [151] T. Higuchi *et al.* (Belle collaboration), Phys. Rev. **D85**, 071105 (2012), arXiv:1203.0930 [hep-ex].
- [152] J. Charles *et al.* (CKMfitter group), Phys. Rev. **D84**, 033005 (2011), arXiv:1106.4041 [hep-ph], with updated results and plots available at <http://ckmfitter.in2p3.fr>; similar results are obtained by M. Bona *et al.* (UTfit collaboration), JHEP **10**, 081 (2006), arXiv:hep-ph/0606167, with updated results and plots available at <http://www.utfit.org>.
- [153] CDF collaboration, CDF note 10778, 12 March 2012, <http://www-cdf.fnal.gov/physics/new/bottom/120216.bsjsphi10fb>; this is an update of Ref. [154].
- [154] T. Aaltonen *et al.* (CDF collaboration), Phys. Rev. **D85**, 072002 (2012), arXiv:1112.1726 [hep-ex]; this replaces T. Aaltonen *et al.* (CDF collaboration), Phys. Rev. Lett. **100**, 161802 (2008), arXiv:0712.2397 [hep-ex]; as well as T. Aaltonen *et al.* (CDF collaboration), Phys. Rev. Lett. **100**, 121803 (2008), arXiv:0712.2348 [hep-ex].
- [155] V. M. Abazov *et al.* (D0 collaboration), Phys. Rev. **D85**, 032006 (2012), arXiv:1109.3166 [hep-ex]; this replaces Ref. [77] and V. M. Abazov *et al.* (D0 collaboration), Phys. Rev. Lett. **101**, 241801 (2008), arXiv:0802.2255 [hep-ex]; as well as V. M. Abazov *et al.* (D0 collaboration), Phys. Rev. Lett. **98**, 121801 (2007), arXiv:hep-ex/0701012.

- [156] LHCb collaboration, LHCb note CERN-LHCb-CONF-2012-002, 5 March 2012, <http://cdsweb.cern.ch/record/1423592>; this is an update of Ref. [157].
- [157] R. Aaij *et al.* (LHCb collaboration), Phys. Rev. Lett. **108**, 101803 (2012), [arXiv:1112.3183](https://arxiv.org/abs/1112.3183) [hep-ex].
- [158] R. Fleischer and R. Knegjens, Eur. Phys. J. **C71**, 1789 (2011), [arXiv:1109.5115](https://arxiv.org/abs/1109.5115) [hep-ph].
- [159] S. Esen *et al.* (Belle collaboration), Phys. Rev. Lett. **105**, 201802 (2010), [arXiv:1005.5177](https://arxiv.org/abs/1005.5177) [hep-ex].
- [160] V. M. Abazov *et al.* (D0 collaboration), Phys. Rev. Lett. **102**, 091801 (2009), [arXiv:0811.2173](https://arxiv.org/abs/0811.2173) [hep-ex]; this replaces V. M. Abazov *et al.* (D0 collaboration), Phys. Rev. Lett. **99**, 241801 (2007), [arXiv:hep-ex/0702049](https://arxiv.org/abs/hep-ex/0702049).
- [161] T. Aaltonen *et al.* (CDF collaboration), Phys. Rev. Lett. **100**, 021803 (2008).
- [162] A. Heister *et al.* (ALEPH collaboration), Eur. Phys. J. **C29**, 143–170 (2003).
- [163] F. Abe *et al.* (CDF collaboration), Phys. Rev. Lett. **82**, 3576–3580 (1999).
- [164] J. Abdallah *et al.* (DELPHI collaboration), Eur. Phys. J. **C35**, 35–52 (2004), [arXiv:hep-ex/0404013](https://arxiv.org/abs/hep-ex/0404013).
- [165] G. Abbiendi *et al.* (OPAL collaboration), Eur. Phys. J. **C11**, 587–598 (1999), [arXiv:hep-ex/9907061](https://arxiv.org/abs/hep-ex/9907061).
- [166] G. Abbiendi *et al.* (OPAL collaboration), Eur. Phys. J. **C19**, 241–256 (2001), [arXiv:hep-ex/0011052](https://arxiv.org/abs/hep-ex/0011052).
- [167] K. Abe *et al.* (SLD collaboration), Phys. Rev. **D67**, 012006 (2003), [arXiv:hep-ex/0209002](https://arxiv.org/abs/hep-ex/0209002).
- [168] K. Abe *et al.* (SLD collaboration), Phys. Rev. **D66**, 032009 (2002), [arXiv:hep-ex/0207048](https://arxiv.org/abs/hep-ex/0207048).
- [169] K. Abe *et al.* (SLD collaboration), [arXiv:hep-ex/0012043](https://arxiv.org/abs/hep-ex/0012043) (2000).
- [170] A. Abulencia *et al.* (CDF collaboration), Phys. Rev. Lett. **97**, 242003 (2006), [arXiv:hep-ex/0609040](https://arxiv.org/abs/hep-ex/0609040); this supersedes A. Abulencia *et al.* (CDF collaboration), Phys. Rev. Lett. **97**, 062003 (2006), [arXiv:hep-ex/0606027](https://arxiv.org/abs/hep-ex/0606027).
- [171] D0 collaboration, D0 note 5618-CONF v1.2, 2 May 2008, <http://www-d0.fnal.gov/Run2Physics/WWW/results/prelim/B/B54/>; D0 collaboration, D0 note 5474-CONF, 21 August 2007, <http://www-d0.fnal.gov/Run2Physics/WWW/results/prelim/B/B51/>; D0 collaboration, D0 note 5254-CONF, 24 October 2006, <http://www-d0.fnal.gov/Run2Physics/WWW/results/prelim/B/B46/>; these three notes supersede any previous preliminary results from D0 and replace V. M. Abazov *et al.* (D0 collaboration), Phys. Rev. Lett. **97**, 021802 (2006), [arXiv:hep-ex/0603029](https://arxiv.org/abs/hep-ex/0603029).

- [172] R. Aaij *et al.* (LHCb collaboration), Phys. Lett. **B709**, 177–184 (2012), arXiv:1112.4311 [hep-ex].
- [173] LHCb collaboration, LHCb note LHCb-CONF-2011-050, 28 November 2011, <https://cdsweb.cern.ch/record/1374146>.
- [174] J. Laiho, E. Lunghi, and R. S. Van de Water, Phys. Rev. **D81**, 034503 (2010), arXiv:0910.2928 [hep-ph], updated results and plots available at <http://www.latticeaverages.org>; we use the end-2011 average of ξ obtained by combining the following three unquenched lattice QCD calculations: R. Evans, A. El-Khadra, and E. Gamiz (Fermilab lattice and MILC collaborations), PoS **LATTICE2008**, 052 (2008), http://pos.sissa.it/archive/conferences/066/052/LATTICE%202008_052.pdf; E. Gamiz, C. T. Davies, G. P. Lepage, J. Shigemitsu, and M. Wingate (HPQCD collaboration), Phys. Rev. **D80**, 014503 (2009), arXiv:0902.1815 [hep-lat]; C. Albertus, Y. Aoki, P. Boyle, N. Christ, T. Dumitrescu, *et al.* (RBC and UKQCD collaborations), Phys. Rev. **D82**, 014505 (2010), arXiv:1001.2023 [hep-lat].
- [175] D. E. Jaffe *et al.* (CLEO collaboration), Phys. Rev. Lett. **86**, 5000–5003 (2001), arXiv:hep-ex/0101006.
- [176] F. Abe *et al.* (CDF collaboration), Phys. Rev. **D55**, 2546–2558 (1997).
- [177] CDF collaboration, CDF note 9015, 16 October 2007, <http://www-cdf.fnal.gov/physics/new/bottom/070816.blessed-acp-bsemil/>.
- [178] V. M. Abazov *et al.* (D0 collaboration), Phys. Rev. **D84**, 052007 (2011), arXiv:1106.6308 [hep-ex]; this updates V. M. Abazov *et al.* (D0 collaboration), Phys. Rev. **D82**, 032001 (2010), arXiv:1005.2757 [hep-ex]; as well as V. M. Abazov *et al.* (D0 collaboration), Phys. Rev. Lett. **105**, 081801 (2010), arXiv:1007.0395 [hep-ex]; this paper also supersedes the search for CP violation in B^0 mixing of Ref. [44].
- [179] R. Barate *et al.* (ALEPH collaboration), Eur. Phys. J. **C20**, 431–443 (2001).
- [180] B. Aubert *et al.* (BABAR collaboration), Phys. Rev. Lett. **96**, 251802 (2006), arXiv:hep-ex/0603053; this replaces B. Aubert *et al.* (BABAR collaboration), Phys. Rev. Lett. **88**, 231801 (2002), arXiv:hep-ex/0202041.
- [181] B. Aubert *et al.* (BABAR collaboration) (2006), arXiv:hep-ex/0607091.
- [182] E. Nakano *et al.* (Belle collaboration), Phys. Rev. **D73**, 112002 (2006), arXiv:hep-ex/0505017.
- [183] M. Beneke, G. Buchalla, and I. Dunietz, Phys. Lett. **B393**, 132–142 (1997), arXiv:hep-ph/9609357; I. Dunietz, Eur. Phys. J. **C7**, 197–203 (1999), arXiv:hep-ph/9806521.
- [184] V. M. Abazov *et al.* (D0 collaboration), Phys. Rev. **D76**, 057101 (2007), arXiv:hep-ex/0702030.

- [185] V. M. Abazov *et al.* (D0 collaboration), Phys. Rev. **D82**, 012003 (2010), arXiv:0904.3907 [hep-ex]; this replaces V. M. Abazov *et al.* (D0 collaboration), Phys. Rev. Lett. **98**, 151801 (2007), arXiv:hep-ex/0701007.
- [186] M. Beneke, G. Buchalla, A. Lenz, and U. Nierste, Phys. Lett. **B576**, 173–183 (2003), arXiv:hep-ph/0307344.
- [187] R. Aaij *et al.* (LHCb collaboration), Phys. Lett. **B707**, 497–505 (2012), arXiv:1112.3056 [hep-ex].
- [188] R. Aaij *et al.* (LHCb collaboration) (2012), arXiv:1204.5675 [hep-ex], submitted to Phys. Lett. B; this supersedes the results of Ref. [187].
- [189] R. Aaij *et al.* (LHCb collaboration) (2012), arXiv:1204.5643 [hep-ex], submitted to Phys. Rev. D.
- [190] L.-L. Chau and W.-Y. Keung, Phys. Rev. Lett. **53**, 1802 (1984).
- [191] L. Wolfenstein, Phys. Rev. Lett. **51**, 1945 (1983).
- [192] A. J. Buras, M. E. Lautenbacher, and G. Ostermaier, Phys. Rev. **D50**, 3433–3446 (1994), arXiv:hep-ph/9403384.
- [193] C. Jarlskog, Phys. Rev. Lett. **55**, 1039 (1985).
- [194] C. Jarlskog, Phys. Lett. **B615**, 207–212 (2005), arXiv:hep-ph/0503199.
- [195] J. D. Bjorken, P. F. Harrison, and W. G. Scott, Phys. Rev. **D74**, 073012 (2006), arXiv:hep-ph/0511201.
- [196] P. F. Harrison, S. Dallison, and W. G. Scott, Phys. Lett. **B680**, 328–333 (2009), arXiv:0904.3077 [hep-ph].
- [197] P. H. Frampton and X.-G. He, Phys. Lett. **B688**, 67–70 (2010), arXiv:1003.0310 [hep-ph].
- [198] P. H. Frampton and X.-G. He, Phys. Rev. **D82**, 017301 (2010), arXiv:1004.3679 [hep-ph].
- [199] B. Aubert *et al.* (BABAR collaboration), Phys. Rev. Lett. **86**, 2515–2522 (2001), arXiv:hep-ex/0102030.
- [200] K. Abe *et al.* (Belle collaboration), Phys. Rev. Lett. **87**, 091802 (2001), arXiv:hep-ex/0107061.
- [201] A. B. Carter and A. I. Sanda, Phys. Rev. **D23**, 1567 (1981).
- [202] I. I. Y. Bigi and A. I. Sanda, Nucl. Phys. **B193**, 85 (1981).
- [203] I. Dunietz, R. Fleischer, and U. Nierste, Phys. Rev. **D63**, 114015 (2001), arXiv:hep-ph/0012219.

- [204] B. Aubert *et al.* (*BABAR* collaboration), Phys. Rev. **D79**, 032002 (2009), arXiv:0808.1866 [hep-ex].
- [205] P. Krokovny *et al.* (Belle collaboration), Phys. Rev. Lett. **97**, 081801 (2006), arXiv:hep-ex/0605023.
- [206] B. Aubert *et al.* (*BABAR* collaboration), Phys. Rev. Lett. **99**, 231802 (2007), arXiv:0708.1544 [hep-ex].
- [207] T. E. Browder, A. Datta, P. J. O'Donnell, and S. Pakvasa, Phys. Rev. **D61**, 054009 (2000), arXiv:hep-ph/9905425.
- [208] B. Aubert *et al.* (*BABAR* collaboration), Phys. Rev. **D74**, 091101 (2006), arXiv:hep-ex/0608016.
- [209] J. Dalseno *et al.* (Belle collaboration), Phys. Rev. **D76**, 072004 (2007), arXiv:0706.2045 [hep-ex].
- [210] B. Aubert *et al.* (*BABAR* collaboration), Phys. Rev. Lett. **99**, 161802 (2007), arXiv:0706.3885 [hep-ex].
- [211] Y. Nakahama *et al.* (Belle collaboration), Phys. Rev. **D82**, 073011 (2010), arXiv:1007.3848 [hep-ex].
- [212] J. P. Lees *et al.* (*BABAR* collaboration), arXiv:1201.5897 [hep-ex] (2012).
- [213] A. Garmash *et al.* (Belle collaboration), Phys. Rev. **D71**, 092003 (2005), arXiv:hep-ex/0412066.
- [214] B. Aubert *et al.* (*BABAR* collaboration), Phys. Rev. **D74**, 032003 (2006), arXiv:hep-ex/0605003.
- [215] B. Aubert *et al.* (*BABAR* collaboration), Phys. Rev. **D80**, 112001 (2009), arXiv:0905.3615 [hep-ex].
- [216] J. Dalseno *et al.* (Belle collaboration), Phys. Rev. **D79**, 072004 (2009), arXiv:0811.3665 [hep-ex].
- [217] A. Garmash *et al.* (Belle collaboration), Phys. Rev. Lett. **96**, 251803 (2006), arXiv:hep-ex/0512066.
- [218] B. Aubert *et al.* (*BABAR* collaboration), Phys. Rev. **D72**, 072003 (2005), arXiv:hep-ex/0507004.
- [219] B. Aubert *et al.* (*BABAR* collaboration), Phys. Rev. **D78**, 012004 (2008), arXiv:0803.4451 [hep-ex].
- [220] A. E. Snyder and H. R. Quinn, Phys. Rev. **D48**, 2139–2144 (1993).
- [221] H. R. Quinn and J. P. Silva, Phys. Rev. **D62**, 054002 (2000), arXiv:hep-ph/0001290.

- [222] B. Aubert *et al.* (BABAR collaboration), Phys. Rev. **D76**, 012004 (2007), arXiv:hep-ex/0703008.
- [223] A. Kusaka *et al.* (Belle collaboration), Phys. Rev. Lett. **98**, 221602 (2007), arXiv:hep-ex/0701015.
- [224] A. Kusaka *et al.* (Belle collaboration), Phys. Rev. **D77**, 072001 (2008), arXiv:0710.4974 [hep-ex].
- [225] J. Charles *et al.*, Eur. Phys. J. **C41**, 1–131 (2005), arXiv:hep-ph/0406184, see also online updates, <http://ckmfitter.in2p3.fr/>.
- [226] B. Aubert *et al.* (BABAR collaboration), Phys. Rev. Lett. **99**, 071801 (2007), arXiv:0705.1190 [hep-ex].
- [227] T. Aushev *et al.* (Belle collaboration), Phys. Rev. Lett. **93**, 201802 (2004), arXiv:hep-ex/0408051.
- [228] M. Rohrken *et al.* (Belle collaboration), Phys. Rev. **D85**, 091106 (2012), arXiv:1203.6647 [hep-ex].
- [229] B. Aubert *et al.* (BABAR collaboration), Phys. Rev. Lett. **91**, 201802 (2003), arXiv:hep-ex/0306030.
- [230] C. C. Wang *et al.* (Belle collaboration), Phys. Rev. Lett. **94**, 121801 (2005), arXiv:hep-ex/0408003.
- [231] B. Aubert *et al.* (BABAR collaboration), Phys. Rev. **D73**, 111101 (2006), arXiv:hep-ex/0602049.
- [232] B. Aubert *et al.* (BABAR collaboration), Phys. Rev. **D71**, 112003 (2005), arXiv:hep-ex/0504035.
- [233] O. Long, M. Baak, R. N. Cahn, and D. Kirkby, Phys. Rev. **D68**, 034010 (2003), arXiv:hep-ex/0303030.
- [234] S. Bahinipati *et al.* (Belle collaboration), Phys. Rev. **D84**, 021101 (2011), arXiv:1102.0888 [hep-ex].
- [235] F. J. Ronga *et al.* (Belle collaboration), Phys. Rev. **D73**, 092003 (2006), arXiv:hep-ex/0604013.
- [236] R. Fleischer, Nucl. Phys. **B671**, 459–482 (2003), arXiv:hep-ph/0304027.
- [237] D. Atwood, M. Gronau, and A. Soni, Phys. Rev. Lett. **79**, 185–188 (1997), arXiv:hep-ph/9704272.
- [238] D. Atwood, T. Gershon, M. Hazumi, and A. Soni, Phys. Rev. **D71**, 076003 (2005), arXiv:hep-ph/0410036.
- [239] B. Grinstein, Y. Grossman, Z. Ligeti, and D. Pirjol, Phys. Rev. **D71**, 011504 (2005), arXiv:hep-ph/0412019.

- [240] B. Grinstein and D. Pirjol, Phys. Rev. **D73**, 014013 (2006), [arXiv:hep-ph/0510104](#).
- [241] M. Matsumori and A. I. Sanda, Phys. Rev. **D73**, 114022 (2006), [arXiv:hep-ph/0512175](#).
- [242] P. Ball and R. Zwicky, Phys. Lett. **B642**, 478–486 (2006), [arXiv:hep-ph/0609037](#).
- [243] I. I. Y. Bigi and A. I. Sanda, Phys. Lett. **B211**, 213 (1988).
- [244] M. Gronau and D. London., Phys. Lett. **B253**, 483–488 (1991).
- [245] M. Gronau and D. Wyler, Phys. Lett. **B265**, 172–176 (1991).
- [246] D. Atwood, I. Dunietz, and A. Soni, Phys. Rev. Lett. **78**, 3257–3260 (1997), [arXiv:hep-ph/9612433](#).
- [247] D. Atwood, I. Dunietz, and A. Soni, Phys. Rev. **D63**, 036005 (2001), [arXiv:hep-ph/0008090](#).
- [248] A. Giri, Y. Grossman, A. Soffer, and J. Zupan, Phys. Rev. **D68**, 054018 (2003), [arXiv:hep-ph/0303187](#).
- [249] A. Poluektov *et al.* (Belle collaboration), Phys. Rev. **D70**, 072003 (2004), [arXiv:hep-ex/0406067](#).
- [250] A. Bondar and T. Gershon, Phys. Rev. **D70**, 091503 (2004), [arXiv:hep-ph/0409281](#).
- [251] M. Rama, PoS **FPCP2009**, 003 (2009), [arXiv:1001.2842 \[hep-ex\]](#).
- [252] A. Bondar and A. Poluektov, Eur. Phys. J. **C47**, 347–353 (2006), [arXiv:hep-ph/0510246](#).
- [253] A. Bondar and A. Poluektov, Eur. Phys. J. **C55**, 51 (2008), [arXiv:0801.0840 \[hep-ex\]](#).
- [254] D. Atwood and A. Soni, Phys. Rev. **D68**, 033003 (2003), [arXiv:hep-ph/0304085](#).
- [255] B. Aubert *et al.* (BABAR collaboration), Phys. Rev. Lett. **99**, 251801 (2007), [arXiv:hep-ex/0703037](#).
- [256] B. Aubert *et al.* (BABAR collaboration), Phys. Rev. **D76**, 031102 (2007), [arXiv:0704.0522 \[hep-ex\]](#).
- [257] R. Itoh *et al.* (Belle collaboration), Phys. Rev. Lett. **95**, 091601 (2005), [arXiv:hep-ex/0504030](#).
- [258] D. Acosta *et al.* (CDF collaboration), Phys. Rev. Lett. **94**, 101803 (2005), [arXiv:hep-ex/0412057](#).
- [259] LHCb collaboration, LHCb-CONF-2011-002, 2011, <https://cdsweb.cern.ch/record/1328956?ln=en>.

- [260] B. Aubert *et al.* (BABAR collaboration), Phys. Rev. **D79**, 072009 (2009), arXiv:0902.1708 [hep-ex].
- [261] B. Aubert *et al.* (BABAR collaboration), Phys. Rev. **D69**, 052001 (2004), arXiv:hep-ex/0309039.
- [262] I. Adachi *et al.* (Belle collaboration), Phys. Rev. Lett. **108**, 171802 (2012), arXiv:1201.4643 [hep-ex].
- [263] R. Barate *et al.* (ALEPH collaboration), Phys. Lett. **B492**, 259–274 (2000), arXiv:hep-ex/0009058.
- [264] K. Ackerstaff *et al.* (OPAL collaboration), Eur. Phys. J. **C5**, 379–388 (1998), arXiv:hep-ex/9801022.
- [265] A. A. Affolder *et al.* (CDF collaboration), Phys. Rev. **D61**, 072005 (2000), arXiv:hep-ex/9909003.
- [266] LHCb collaboration, LHCb-CONF-2011-004, 2011, <http://cdsweb.cern.ch/record/1328958?ln=en>.
- [267] Y. Sato *et al.* (Belle collaboration), Phys. Rev. Lett. **108**, 171801 (2012), arXiv:1201.3502 [hep-ex].
- [268] M. Bona *et al.* (UTfit collaboration), JHEP **07**, 028 (2005), arXiv:hep-ph/0501199, see also online updates, <http://www.utfit.org/>.
- [269] I. Dunietz, H. R. Quinn, A. Snyder, W. Toki, and H. J. Lipkin, Phys. Rev. **D43**, 2193–2208 (1991).
- [270] D. Aston *et al.*, Nucl. Phys. **B296**, 493 (1988).
- [271] M. Suzuki, Phys. Rev. **D64**, 117503 (2001), arXiv:hep-ph/0106354.
- [272] B. Aubert *et al.* (BABAR collaboration), Phys. Rev. **D71**, 032005 (2005), arXiv:hep-ex/0411016.
- [273] Y. Grossman and M. P. Worah, Phys. Lett. **B395**, 241–249 (1997), arXiv:hep-ph/9612269.
- [274] R. Fleischer, Phys. Lett. **B562**, 234–244 (2003), arXiv:hep-ph/0301255.
- [275] R. Fleischer, Nucl. Phys. **B659**, 321–355 (2003), arXiv:hep-ph/0301256.
- [276] B. Aubert *et al.* (BABAR collaboration), Phys. Rev. Lett. **99**, 081801 (2007), arXiv:hep-ex/0703019.
- [277] A. Bondar, T. Gershon, and P. Krokovny, Phys. Lett. **B624**, 1–10 (2005), arXiv:hep-ph/0503174.
- [278] R. Fleischer, Int. J. Mod. Phys. **A12**, 2459–2522 (1997), arXiv:hep-ph/9612446.

- [279] D. London and A. Soni, Phys. Lett. **B407**, 61–65 (1997), [arXiv:hep-ph/9704277](#).
- [280] M. Ciuchini, E. Franco, G. Martinelli, A. Masiero, and L. Silvestrini, Phys. Rev. Lett. **79**, 978–981 (1997), [arXiv:hep-ph/9704274](#).
- [281] T. Gershon and M. Hazumi, Phys. Lett. **B596**, 163–172 (2004), [arXiv:hep-ph/0402097](#).
- [282] Y. Grossman, Z. Ligeti, Y. Nir, and H. Quinn, Phys. Rev. **D68**, 015004 (2003), [arXiv:hep-ph/0303171](#).
- [283] M. Gronau and J. L. Rosner, Phys. Lett. **B564**, 90–96 (2003), [arXiv:hep-ph/0304178](#).
- [284] M. Gronau, Y. Grossman, and J. L. Rosner, Phys. Lett. **B579**, 331–339 (2004), [arXiv:hep-ph/0310020](#).
- [285] M. Gronau, J. L. Rosner, and J. Zupan, Phys. Lett. **B596**, 107–115 (2004), [arXiv:hep-ph/0403287](#).
- [286] H.-Y. Cheng, C.-K. Chua, and A. Soni, Phys. Rev. **D72**, 014006 (2005), [arXiv:hep-ph/0502235](#).
- [287] M. Gronau and J. L. Rosner, Phys. Rev. **D71**, 074019 (2005), [arXiv:hep-ph/0503131](#).
- [288] G. Buchalla, G. Hiller, Y. Nir, and G. Raz, JHEP **09**, 074 (2005), [arXiv:hep-ph/0503151](#).
- [289] M. Beneke, Phys. Lett. **B620**, 143–150 (2005), [arXiv:hep-ph/0505075](#).
- [290] G. Engelhard, Y. Nir, and G. Raz, Phys. Rev. **D72**, 075013 (2005), [arXiv:hep-ph/0505194](#).
- [291] H.-Y. Cheng, C.-K. Chua, and A. Soni, Phys. Rev. **D72**, 094003 (2005), [arXiv:hep-ph/0506268](#).
- [292] G. Engelhard and G. Raz, Phys. Rev. **D72**, 114017 (2005), [arXiv:hep-ph/0508046](#).
- [293] M. Gronau, J. L. Rosner, and J. Zupan, Phys. Rev. **D74**, 093003 (2006), [arXiv:hep-ph/0608085](#).
- [294] L. Silvestrini, Ann. Rev. Nucl. Part. Sci. **57**, 405–440 (2007), [arXiv:0705.1624 \[hep-ph\]](#).
- [295] R. Dutta and S. Gardner, Phys. Rev. **D78**, 034021 (2008), [arXiv:0805.1963 \[hep-ph\]](#).
- [296] M. Fujikawa *et al.* (Belle collaboration), Phys. Rev. **D81**, 011101 (2010), [arXiv:0809.4366 \[hep-ex\]](#).
- [297] K. Abe *et al.* (Belle collaboration), [arXiv:0708.1845 \[hep-ex\]](#) (2007).
- [298] K. Abe *et al.* (Belle collaboration), Phys. Rev. **D76**, 091103 (2007), [arXiv:hep-ex/0609006](#).

- [299] B. Aubert *et al.* (*BABAR* collaboration), Phys. Rev. **D71**, 091102 (2005), arXiv:hep-ex/0502019.
- [300] B. Aubert *et al.* (*BABAR* collaboration), Phys. Rev. **D79**, 052003 (2009), arXiv:0809.1174 [hep-ex].
- [301] K. F. Chen *et al.* (Belle collaboration), Phys. Rev. Lett. **98**, 031802 (2007), arXiv:hep-ex/0608039.
- [302] J. Lees *et al.* (*BABAR* collaboration), Phys. Rev. **D85**, 054023 (2012), arXiv:1111.3636 [hep-ex].
- [303] B. Aubert *et al.* (*BABAR* collaboration), Phys. Rev. **D76**, 071101 (2007), arXiv:hep-ex/0702010.
- [304] B. Aubert *et al.* (*BABAR* collaboration), Phys. Rev. **D78**, 092008 (2008), arXiv:0808.3586 [hep-ex].
- [305] R. Fleischer, Phys. Lett. **B459**, 306–320 (1999), arXiv:hep-ph/9903456 [hep-ph].
- [306] LHCb collaboration, LHCb-CONF-2012-007, 2012, <https://cdsweb.cern.ch/record/1426663?ln=en>.
- [307] K. Vervink *et al.* (Belle collaboration), Phys. Rev. **D80**, 111104 (2009), arXiv:0901.4057 [hep-ex].
- [308] B. Aubert *et al.* (*BABAR* collaboration), Phys. Rev. Lett. **101**, 021801 (2008), arXiv:0804.0896 [hep-ex].
- [309] S. E. Lee *et al.* (Belle collaboration), Phys. Rev. **D77**, 071101 (2008), arXiv:0708.0304 [hep-ex].
- [310] Belle collaboration, preliminary results shown at EPS2011, available from <http://belle.kek.jp/belle/talks/EPS11/higuchi.pdf>.
- [311] S. Fratina *et al.* (Belle collaboration), Phys. Rev. Lett. **98**, 221802 (2007), arXiv:hep-ex/0702031.
- [312] B. Aubert *et al.* (*BABAR* collaboration), Phys. Rev. Lett. **97**, 171805 (2006), arXiv:hep-ex/0608036.
- [313] Y. Nakahama *et al.* (Belle collaboration), Phys. Rev. Lett. **100**, 121601 (2008), arXiv:0712.4234 [hep-ex].
- [314] B. Aubert *et al.* (*BABAR* collaboration), Phys. Rev. **D78**, 071102 (2008), arXiv:0807.3103 [hep-ex].
- [315] Y. Ushiroda *et al.* (Belle collaboration), Phys. Rev. **D74**, 111104 (2006), arXiv:hep-ex/0608017.
- [316] B. Aubert *et al.* (*BABAR* collaboration), Phys. Rev. **D79**, 011102 (2009), arXiv:0805.1317 [hep-ex].

- [317] J. Li *et al.* (Belle collaboration), Phys. Rev. Lett. **101**, 251601 (2008), arXiv:0806.1980 [hep-ex].
- [318] H. Sahoo *et al.* (Belle collaboration), Phys. Rev. **D84**, 071101 (2011), arXiv:1104.5590 [hep-ex].
- [319] Y. Ushiroda *et al.* (Belle collaboration), Phys. Rev. Lett. **100**, 021602 (2008), arXiv:0709.2769 [hep-ex].
- [320] B. Aubert *et al.* (BABAR collaboration), Phys. Rev. **D76**, 052007 (2007), arXiv:0705.2157 [hep-ex].
- [321] A. Somov *et al.* (Belle collaboration), Phys. Rev. Lett. **96**, 171801 (2006), arXiv:hep-ex/0601024.
- [322] B. Aubert *et al.* (BABAR collaboration), Phys. Rev. **D78**, 071104 (2008), arXiv:0807.4977 [hep-ex].
- [323] C. C. Chiang *et al.* (Belle collaboration), Phys. Rev. **D78**, 111102 (2008), arXiv:0808.2576 [hep-ex].
- [324] B. Aubert *et al.* (BABAR collaboration), Phys. Rev. Lett. **98**, 181803 (2007), arXiv:hep-ex/0612050.
- [325] B. Aubert *et al.* (BABAR collaboration), Phys. Rev. **D81**, 052009 (2010), arXiv:0909.2171 [hep-ex].
- [326] B. Aubert *et al.* (BABAR collaboration), arXiv:0807.4226 [hep-ex] (2008).
- [327] H. Ishino *et al.* (Belle collaboration), Phys. Rev. Lett. **98**, 211801 (2007), arXiv:hep-ex/0608035.
- [328] A. Somov *et al.* (Belle collaboration), Phys. Rev. **D76**, 011104 (2007), arXiv:hep-ex/0702009.
- [329] M. Gronau and D. London, Phys. Rev. Lett. **65**, 3381–3384 (1990).
- [330] B. Aubert *et al.* (BABAR collaboration), Phys. Rev. **D76**, 091102 (2007), arXiv:0707.2798 [hep-ex].
- [331] B. Aubert *et al.* (BABAR collaboration), Phys. Rev. Lett. **102**, 141802 (2009), arXiv:0901.3522 [hep-ex].
- [332] H. J. Lipkin, Y. Nir, H. R. Quinn, and A. Snyder, Phys. Rev. **D44**, 1454–1460 (1991).
- [333] M. Gronau and J. Zupan, Phys. Rev. **D73**, 057502 (2006), arXiv:hep-ph/0512148.
- [334] B. Aubert *et al.* (BABAR collaboration), Phys. Rev. **D77**, 071102 (2008), arXiv:0712.3469 [hep-ex].
- [335] K. Abe *et al.* (Belle collaboration), arXiv:hep-ex/0307074 (2003).

- [336] P. del Amo Sanchez *et al.* (*BABAR* collaboration), Phys. Rev. **D82**, 072004 (2010), arXiv:1007.0504 [hep-ex].
- [337] Belle collaboration, see T. Gershon, in Proceedings of the Lepton Photon 2011 Conference, to appear in Pramana, available at arXiv:1112.1984 [hep-ex].
- [338] T. Aaltonen *et al.* (CDF collaboration), Phys. Rev. **D81**, 031105 (2010), arXiv:0911.0425 [hep-ex].
- [339] R. Aaij *et al.* (LHCb collaboration), Phys.Lett. **B712**, 203–212 (2012), arXiv:1203.3662 [hep-ex].
- [340] B. Aubert *et al.* (*BABAR* collaboration), Phys. Rev. **D78**, 092002 (2008), arXiv:0807.2408 [hep-ex].
- [341] K. Abe *et al.* (Belle collaboration), Phys. Rev. **D73**, 051106 (2006), arXiv:hep-ex/0601032.
- [342] B. Aubert *et al.* (*BABAR* collaboration), Phys. Rev. **D80**, 092001 (2009), arXiv:0909.3981 [hep-ex].
- [343] P. del Amo Sanchez *et al.* (*BABAR* collaboration), Phys. Rev. **D82**, 072006 (2010), arXiv:1006.4241 [hep-ex].
- [344] Y. Horii *et al.* (Belle collaboration), Phys. Rev. Lett. **106**, 231803 (2011), arXiv:1103.5951 [hep-ex].
- [345] T. Aaltonen *et al.* (CDF collaboration), Phys. Rev. **D84**, 091504 (2011), arXiv:1108.5765 [hep-ex].
- [346] J. P. Lees *et al.* (*BABAR* collaboration), Phys. Rev. **D84**, 012002 (2011), arXiv:1104.4472 [hep-ex].
- [347] B. Aubert *et al.* (*BABAR* collaboration), Phys. Rev. **D80**, 031102 (2009), arXiv:0904.2112 [hep-ex].
- [348] M. Gronau, Phys. Lett. **B557**, 198–206 (2003), arXiv:hep-ph/0211282.
- [349] D. M. Asner *et al.* (CLEO collaboration), Phys. Rev. **D78**, 012001 (2008), arXiv:0802.2268 [hep-ex].
- [350] N. Lowrey *et al.* (CLEO collaboration), Phys. Rev. **D80**, 031105 (2009), arXiv:0903.4853 [hep-ex].
- [351] N. Negishi *et al.* (Belle collaboration), arXiv:1205.0422 [hep-ex] (2012).
- [352] B. Aubert *et al.* (*BABAR* collaboration), Phys. Rev. **D78**, 034023 (2008), arXiv:0804.2089 [hep-ex].
- [353] A. Poluektov *et al.* (Belle collaboration), Phys. Rev. **D81**, 112002 (2010), arXiv:1003.3360 [hep-ex].

- [354] A. Poluektov *et al.* (Belle collaboration), Phys. Rev. **D73**, 112009 (2006),
arXiv:hep-ex/0604054.
- [355] P. del Amo Sanchez *et al.* (BABAR collaboration), Phys. Rev. Lett. **105**, 121801 (2010),
arXiv:1005.1096 [hep-ex].
- [356] B. Aubert *et al.* (BABAR collaboration), Phys. Rev. **D79**, 072003 (2009),
arXiv:0805.2001 [hep-ex].
- [357] E. Barberio *et al.* (Heavy Flavor Averaging Group) (2008),
arXiv:0808.1297 [hep-ex].
- [358] I. Caprini, L. Lellouch, and M. Neubert, Nucl. Phys. **B530**, 153–181 (1998),
arXiv:hep-ph/9712417.
- [359] *B* semileptonic decays common input parameters,
<http://www.slac.stanford.edu/xorg/hfag/semi/EndOfYear11/common/common.param>.
- [360] N. E. Adam *et al.* (CLEO collaboration), Phys. Rev. **D67**, 032001 (2003),
arXiv:hep-ex/0210040.
- [361] B. Aubert *et al.* (BABAR collaboration), Phys. Rev. **D79**, 012002 (2009),
arXiv:0809.0828 [hep-ex].
- [362] B. Aubert *et al.* (BABAR collaboration), Phys. Rev. Lett. **100**, 231803 (2008),
arXiv:0712.3493 [hep-ex].
- [363] D. Buskulic *et al.* (ALEPH collaboration), Phys. Lett. **B395**, 373–387 (1997).
- [364] G. Abbiendi *et al.* (OPAL collaboration), Phys. Lett. **B482**, 15–30 (2000),
arXiv:hep-ex/0003013.
- [365] P. Abreu *et al.* (DELPHI collaboration), Phys. Lett. **B510**, 55–74 (2001),
arXiv:hep-ex/0104026.
- [366] J. Abdallah *et al.* (DELPHI collaboration), Eur. Phys. J. **C33**, 213–232 (2004),
arXiv:hep-ex/0401023.
- [367] W. Dungen *et al.* (Belle collaboration), Phys.Rev. **D82**, 112007 (2010),
arXiv:1010.5620 [hep-ex].
- [368] B. Aubert *et al.* (BABAR collaboration), Phys. Rev. **D77**, 032002 (2008),
arXiv:0705.4008 [hep-ex].
- [369] J. A. Bailey *et al.* (Fermilab Lattice and MILC collaborations collaboration), PoS
LATTICE2010, 311 (2010), arXiv:1011.2166 [hep-lat].
- [370] B. Aubert *et al.* (BABAR collaboration), Phys. Rev. Lett. **100**, 151802 (2008),
arXiv:0712.3503 [hep-ex].
- [371] J. E. Bartelt *et al.* (CLEO collaboration), Phys. Rev. Lett. **82**, 3746 (1999),
arXiv:hep-ex/9811042.

- [372] K. Abe *et al.* (Belle collaboration), Phys. Lett. **B526**, 258–268 (2002), arXiv:hep-ex/0111082.
- [373] B. Aubert *et al.* (BABAR collaboration), Phys. Rev. Lett. **104**, 011802 (2010), arXiv:0904.4063 [hep-ex].
- [374] M. Okamoto *et al.*, Nucl. Phys. Proc. Suppl. **140**, 461–463 (2005), arXiv:hep-lat/0409116.
- [375] D. Liventsev *et al.* (Belle collaboration), Phys. Rev. **D77**, 091503 (2008), arXiv:0711.3252 [hep-ex].
- [376] N. Isgur and M. B. Wise, Phys. Rev. Lett. **66**, 1130–1133 (1991).
- [377] D. Buskulic *et al.* (ALEPH collaboration), Z. Phys. **C73**, 601–612 (1997).
- [378] G. Abbiendi *et al.* (OPAL collaboration), Eur. Phys. J. **C30**, 467–475 (2003), arXiv:hep-ex/0301018.
- [379] A. Anastassov *et al.* (CLEO collaboration), Phys. Rev. Lett. **80**, 4127–4131 (1998), arXiv:hep-ex/9708035.
- [380] V. M. Abazov *et al.* (D0 collaboration), Phys. Rev. Lett. **95**, 171803 (2005), arXiv:hep-ex/0507046.
- [381] B. Aubert *et al.* (BABAR collaboration), Phys. Rev. Lett. **101**, 261802 (2008), arXiv:0808.0528 [hep-ex].
- [382] B. Aubert *et al.* (BABAR collaboration), Phys. Rev. Lett. **103**, 051803 (2009), arXiv:0808.0333 [hep-ex].
- [383] J. Abdallah *et al.* (DELPHI collaboration), Eur. Phys. J. **C45**, 35–59 (2006), arXiv:hep-ex/0510024.
- [384] D. Benson, I. I. Bigi, T. Mannel, and N. Uraltsev, Nucl. Phys. **B665**, 367–401 (2003), arXiv:hep-ph/0302262.
- [385] P. Gambino and N. Uraltsev, Eur. Phys. J. **C34**, 181–189 (2004), arXiv:hep-ph/0401063.
- [386] P. Gambino, JHEP **1109**, 055 (2011), arXiv:1107.3100 [hep-ph].
- [387] C. W. Bauer, Z. Ligeti, M. Luke, A. V. Manohar, and M. Trott, Phys. Rev. **D70**, 094017 (2004), arXiv:hep-ph/0408002.
- [388] B. Aubert *et al.* (BABAR collaboration), Phys. Rev. **D72**, 052004 (2005), arXiv:hep-ex/0508004.
- [389] B. Aubert *et al.* (BABAR collaboration), Phys. Rev. Lett. **97**, 171803 (2006), arXiv:hep-ex/0607071.

- [390] B. Aubert *et al.* (*BABAR* collaboration), Phys. Rev. **D81**, 032003 (2010), arXiv:0908.0415 [hep-ex].
- [391] B. Aubert *et al.* (*BABAR* collaboration), Phys. Rev. **D69**, 111104 (2004), arXiv:hep-ex/0403030.
- [392] C. Schwanda *et al.* (Belle collaboration), Phys. Rev. **D75**, 032005 (2007), arXiv:hep-ex/0611044.
- [393] A. Limosani *et al.* (Belle collaboration), Phys. Rev. Lett. **103**, 241801 (2009), arXiv:0907.1384 [hep-ex].
- [394] P. Urquijo *et al.* (Belle collaboration), Phys. Rev. **D75**, 032001 (2007), arXiv:hep-ex/0610012.
- [395] D. E. Acosta *et al.* (CDF collaboration), Phys. Rev. **D71**, 051103 (2005), arXiv:hep-ex/0502003.
- [396] S. Chen *et al.* (CLEO collaboration), Phys. Rev. Lett. **87**, 251807 (2001), arXiv:hep-ex/0108032.
- [397] S. E. Csorna *et al.* (CLEO collaboration), Phys. Rev. **D70**, 032002 (2004), arXiv:hep-ex/0403052.
- [398] D. Benson, I. I. Bigi, and N. Uraltsev, Nucl. Phys. **B710**, 371–401 (2005), arXiv:hep-ph/0410080.
- [399] B. Dehnadi, A. H. Hoang, V. Mateu, and S. M. Zebarjad (2011), arXiv:1102.2264 [hep-ph].
- [400] C. Schwanda *et al.* (Belle collaboration), Phys. Rev. **D78**, 032016 (2008), arXiv:0803.2158 [hep-ex].
- [401] N. E. Adam *et al.* (CLEO collaboration), Phys. Rev. Lett. **99**, 041802 (2007), arXiv:hep-ex/0703041.
- [402] P. del Amo Sanchez *et al.* (*BABAR* collaboration), Phys. Rev. **D83**, 032007 (2011), arXiv:1005.3288 [hep-ex].
- [403] P. del Amo Sanchez *et al.* (*BABAR* collaboration), Phys. Rev. **D83**, 052011 (2011), arXiv:1010.0987 [hep-ex].
- [404] H. H. *et al.* (Belle collaboration), Phys. Rev. **D83**, 071101 (2011), arXiv:1012.0090 [hep-ex] [hep-ex].
- [405] T. Hokuue *et al.* (Belle collaboration), Phys. Lett. **B648**, 139–148 (2007), arXiv:hep-ex/0604024.
- [406] B. Aubert *et al.* (*BABAR* collaboration), Phys.Rev.Lett. **101**, 081801 (2008), arXiv:0805.2408 [hep-ex].

- [407] B. Aubert *et al.* (*BABAR* collaboration), Phys. Rev. Lett. **97**, 211801 (2006), arXiv:hep-ex/0607089.
- [408] I. Adachi *et al.* (Belle collaboration) (2008), arXiv:0812.1414 [hep-ex].
- [409] A. Khodjamirian, T. Mannel, N. Offen, and Y.-M. Wang, Phys.Rev. **D83**, 094031 (2011), arXiv:1103.2655 [hep-ph].
- [410] P. Ball and R. Zwicky, Phys. Rev. **D71**, 014015 (2005), arXiv:hep-ph/0406232.
- [411] E. Dalgic *et al.*, Phys. Rev. **D73**, 074502 (2006), arXiv:hep-lat/0601021.
- [412] J. A. Bailey, C. Bernard, C. E. DeTar, M. Di Pierro, A. El-Khadra, *et al.*, Phys.Rev. **D79**, 054507 (2009), arXiv:0811.3640 [hep-lat].
- [413] B. H. Behrens *et al.* (CLEO collaboration), Phys. Rev. **D61**, 052001 (2000), arXiv:hep-ex/9905056.
- [414] B. Aubert *et al.* (*BABAR* collaboration), Phys. Rev. **D79**, 052011 (2009), arXiv:0808.3524 [hep-ex].
- [415] R. Gray *et al.* (CLEO collaboration), Phys. Rev. **D76**, 012007 (2007), arXiv:hep-ex/0703042.
- [416] P. Urquijo *et al.* (Belle collaboration), Phys. Rev. Lett. **104**, 021801 (2010), arXiv:0907.0379 [hep-ex].
- [417] J. Lees (*BABAR* collaboration) (2011), arXiv:1112.0702 [hep-ex].
- [418] C. W. Bauer, Z. Ligeti, and M. E. Luke, Phys. Rev. **D64**, 113004 (2001), arXiv:hep-ph/0107074.
- [419] C. Amsler *et al.* (Particle Data Group collaboration), Phys. Lett. **B667**, 1 (2008), and 2009 partial update for the 2010 edition.
- [420] M. Neubert, Phys. Rev. **D49**, 4623–4633 (1994), arXiv:hep-ph/9312311.
- [421] A. K. Leibovich, I. Low, and I. Z. Rothstein, Phys. Rev. **D61**, 053006 (2000), arXiv:hep-ph/9909404.
- [422] B. O. Lange, M. Neubert, and G. Paz, JHEP **10**, 084 (2005), arXiv:hep-ph/0508178.
- [423] B. Aubert *et al.* (*BABAR* collaboration), Phys. Rev. Lett. **96**, 221801 (2006), arXiv:hep-ex/0601046.
- [424] V. B. Golubev, Y. I. Skovpen, and V. G. Luth, Phys. Rev. **D76**, 114003 (2007), arXiv:hep-ph/0702072.
- [425] B. Aubert *et al.* (*BABAR* collaboration), Phys. Rev. **D73**, 012006 (2006), arXiv:hep-ex/0509040.
- [426] R. V. Kowalewski and S. Menke, Phys. Lett. **B541**, 29–34 (2002), arXiv:hep-ex/0205038.

- [427] B. Aubert *et al.* (*BABAR* collaboration), Phys. Rev. Lett. **95**, 111801 (2005), arXiv:hep-ex/0506036.
- [428] A. Bornheim *et al.* (CLEO collaboration), Phys. Rev. Lett. **88**, 231803 (2002), arXiv:hep-ex/0202019.
- [429] A. Limosani *et al.* (Belle collaboration), Phys. Lett. **B621**, 28–40 (2005), arXiv:hep-ex/0504046.
- [430] H. Kakuno *et al.* (Belle collaboration), Phys. Rev. Lett. **92**, 101801 (2004), arXiv:hep-ex/0311048.
- [431] I. Bizjak *et al.* (Belle collaboration), Phys. Rev. Lett. **95**, 241801 (2005), arXiv:hep-ex/0505088.
- [432] B. O. Lange, M. Neubert, and G. Paz, Phys. Rev. **D72**, 073006 (2005), arXiv:hep-ph/0504071.
- [433] S. W. Bosch, B. O. Lange, M. Neubert, and G. Paz, Nucl. Phys. **B699**, 335–386 (2004), arXiv:hep-ph/0402094.
- [434] S. W. Bosch, M. Neubert, and G. Paz, JHEP **11**, 073 (2004), arXiv:hep-ph/0409115.
- [435] M. Neubert, Eur. Phys. J. **C44**, 205–209 (2005), arXiv:hep-ph/0411027.
- [436] M. Neubert, Phys.Lett. **B612**, 13–20 (2005), arXiv:hep-ph/0412241 [hep-ph].
- [437] M. Neubert, Phys.Rev. **D72**, 074025 (2005), arXiv:hep-ph/0506245 [hep-ph].
- [438] J. R. Andersen and E. Gardi, JHEP **01**, 097 (2006), arXiv:hep-ph/0509360.
- [439] P. Gambino, P. Giordano, G. Ossola, and N. Uraltsev, JHEP **10**, 058 (2007), arXiv:0707.2493 [hep-ph].
- [440] U. Aglietti, F. Di Lodovico, G. Ferrera, and G. Ricciardi, Eur. Phys. J. **C59**, 831–840 (2009), arXiv:0711.0860 [hep-ph].
- [441] U. Aglietti, G. Ferrera, and G. Ricciardi, Nucl. Phys. **B768**, 85–115 (2007), arXiv:hep-ph/0608047.
- [442] U. Aglietti, G. Ricciardi, and G. Ferrera, Phys. Rev. **D74**, 034004 (2006), arXiv:hep-ph/0507285.
- [443] U. Aglietti, G. Ricciardi, and G. Ferrera, Phys. Rev. **D74**, 034005 (2006), arXiv:hep-ph/0509095.
- [444] U. Aglietti, G. Ricciardi, and G. Ferrera, Phys. Rev. **D74**, 034006 (2006), arXiv:hep-ph/0509271.
- [445] O. Buchmüller and H. Flächer, Phys. Rev. **D73**, 073008 (2006), arXiv:hep-ph/0507253.

- [446] K. Abe *et al.* (Belle collaboration), Phys. Lett. **B511**, 151–158 (2001),
arXiv:hep-ex/0103042.
- [447] B. Aubert *et al.* (BABAR collaboration), Phys. Rev. **D77**, 051103 (2008),
arXiv:0711.4889 [hep-ex].
- [448] M. Staric *et al.* (Belle collaboration), Phys. Rev. Lett. **98**, 211803 (2007),
arXiv:hep-ex/0703036.
- [449] B. Aubert *et al.* (BABAR collaboration), Phys. Rev. Lett. **98**, 211802 (2007),
arXiv:hep-ex/0703020.
- [450] T. Aaltonen *et al.* (CDF collaboration), Phys. Rev. Lett. **100**, 121802 (2008),
arXiv:0712.1567 [hep-ex].
- [451] I. I. Y. Bigi and N. G. Uraltsev, Nucl. Phys. **B592**, 92–106 (2001),
arXiv:hep-ph/0005089.
- [452] A. A. Petrov (2003), arXiv:hep-ph/0311371.
- [453] A. A. Petrov, Nucl. Phys. Proc. Suppl. **142**, 333–339 (2005), arXiv:hep-ph/0409130.
- [454] A. F. Falk, Y. Grossman, Z. Ligeti, Y. Nir, and A. A. Petrov, Phys. Rev. **D69**, 114021
(2004), arXiv:hep-ph/0402204.
- [455] E. M. Aitala *et al.* (E791 collaboration), Phys. Rev. Lett. **77**, 2384–2387 (1996),
arXiv:hep-ex/9606016.
- [456] C. Cawfield *et al.* (CLEO collaboration), Phys. Rev. **D71**, 077101 (2005),
arXiv:hep-ex/0502012.
- [457] B. Aubert *et al.* (BABAR collaboration), Phys. Rev. **D76**, 014018 (2007),
arXiv:0705.0704 [hep-ex].
- [458] U. Bitenc *et al.* (Belle collaboration), Phys. Rev. **D77**, 112003 (2008),
arXiv:0802.2952 [hep-ex].
- [459] HFAG: charm physics parameters,
<http://www.slac.stanford.edu/xorg/hfag/charm/index.html>.
- [460] L. M. Zhang *et al.* (Belle collaboration), Phys. Rev. Lett. **96**, 151801 (2006),
arXiv:hep-ex/0601029.
- [461] L. M. Zhang *et al.* (Belle collaboration), Phys. Rev. Lett. **99**, 131803 (2007),
arXiv:0704.1000 [hep-ex].
- [462] P. del Amo Sanchez *et al.* (BABAR collaboration), Phys.Rev.Lett. **105**, 081803 (2010),
arXiv:1004.5053 [hep-ex].
- [463] B. Aubert *et al.* (BABAR collaboration), Phys. Rev. Lett. **103**, 211801 (2009),
arXiv:0807.4544 [hep-ex].

- [464] W. M. Sun (CLEO collaboration), Prepared for 30th International Symposium on Physics in Collision (PIC 2010), Karlsruhe, Germany, 1-4 Sep 2010.
- [465] E. M. Aitala *et al.* (E791 collaboration), Phys. Rev. Lett. **83**, 32–36 (1999), [arXiv:hep-ex/9903012](#).
- [466] J. M. Link *et al.* (FOCUS collaboration), Phys. Lett. **B485**, 62–70 (2000), [arXiv:hep-ex/0004034](#).
- [467] S. E. Csorna *et al.* (CLEO collaboration), Phys. Rev. **D65**, 092001 (2002), [arXiv:hep-ex/0111024](#).
- [468] B. Aubert *et al.* (BABAR collaboration), Phys. Rev. **D78**, 011105 (2008), [arXiv:0712.2249 \[hep-ex\]](#).
- [469] A. Zupanc *et al.* (Belle collaboration), Phys. Rev. **D80**, 052006 (2009), [arXiv:0905.4185 \[hep-ex\]](#).
- [470] R. Aaij *et al.* (LHCb collaboration) (2011), [arXiv:1112.4698 \[hep-ex\]](#).
- [471] B. Aubert *et al.* (BABAR collaboration), Phys.Rev.Lett. **100**, 061803 (2008), [arXiv:0709.2715 \[hep-ex\]](#).
- [472] M. Staric *et al.* (Belle collaboration), Phys. Lett. **B670**, 190–195 (2008), [arXiv:0807.0148 \[hep-ex\]](#).
- [473] R. Aaij *et al.* (LHCb collaboration), Phys.Rev.Lett. **108**, 111602 (2012), [arXiv:1112.0938 \[hep-ex\]](#).
- [474] T. Aaltonen *et al.* (CDF collaboration), Phys.Rev. **D85**, 012009 (2012), [arXiv:1111.5023 \[hep-ex\]](#).
- [475] CDF collaboration, CDF note 10784, 28 February 2012, <http://www-cdf.fnal.gov/physics/new/bottom/120216.blessed-CPVcharm10fb/>.
- [476] F. James, MINUIT – Function Minimization and Error Analysis, Reference Manual Version 94.1, CERN Program Library Long Writeup D506, <http://wwwasdoc.web.cern.ch/wwwasdoc/minuit/minmain.html>.
- [477] M. Ciuchini, E. Franco, D. Guadagnoli, V. Lubicz, M. Pierini, *et al.*, Phys.Lett. **B655**, 162–166 (2007), [arXiv:hep-ph/0703204 \[hep-ph\]](#).
- [478] A. L. Kagan and M. D. Sokoloff, Phys.Rev. **D80**, 076008 (2009), [arXiv:0907.3917 \[hep-ph\]](#).
- [479] Y. Grossman, Y. Nir, and G. Perez, Phys.Rev.Lett. **103**, 071602 (2009), [arXiv:0904.0305 \[hep-ph\]](#).
- [480] T. Becher and R. J. Hill, Phys.Lett. **B633**, 61–69 (2006), [arXiv:hep-ph/0509090 \[hep-ph\]](#).
- [481] F. J. Gilman and R. L. Singleton, Phys.Rev. **D41**, 142 (1990).

- [482] R. J. Hill, eConf **C060409**, 027 (2006), [arXiv:hep-ph/0606023](#) [hep-ph].
- [483] D. Becirevic and A. B. Kaidalov, *Phys.Lett.* **B478**, 417–423 (2000), [arXiv:hep-ph/9904490](#) [hep-ph].
- [484] C. G. Boyd, B. Grinstein, and R. F. Lebed, *Phys.Rev.Lett.* **74**, 4603–4606 (1995), [arXiv:hep-ph/9412324](#) [hep-ph].
- [485] C. G. Boyd and M. J. Savage, *Phys.Rev.* **D56**, 303–311 (1997), [arXiv:hep-ph/9702300](#) [hep-ph].
- [486] M. C. Arnesen, B. Grinstein, I. Z. Rothstein, and I. W. Stewart, *Phys. Rev. Lett.* **95**, 071802 (2005).
- [487] C. Bourrely, B. Machet, and E. de Rafael, *Nucl. Phys.* **B189**, 157 (1981).
- [488] L. Widhalm *et al.* (Belle collaboration), *Phys.Rev.Lett.* **97**, 061804 (2006), [arXiv:hep-ex/0604049](#) [hep-ex].
- [489] B. Aubert *et al.* (BABAR collaboration), *Phys.Rev.* **D76**, 052005 (2007), [arXiv:0704.0020](#) [hep-ex].
- [490] D. Besson *et al.* (CLEO collaboration), *Phys.Rev.* **D80**, 032005 (2009), [arXiv:0906.2983](#) [hep-ex].
- [491] S. Dobbs *et al.* (CLEO collaboration), *Phys.Rev.* **D77**, 112005 (2008), [arXiv:0712.1020](#) [hep-ex].
- [492] BESIII collaboration, presented at Charm 2012 conference, 2012, <http://www.phys.hawaii.edu/indico/contributionDisplay.py?contribId=43&confId=338>.
- [493] G. Huang *et al.* (CLEO collaboration), *Phys.Rev.Lett.* **94**, 011802 (2005), [arXiv:hep-ex/0407035](#) [hep-ex].
- [494] J. Link *et al.* (FOCUS collaboration), *Phys.Lett.* **B607**, 233–242 (2005), [arXiv:hep-ex/0410037](#) [hep-ex].
- [495] C. Aubin *et al.* (Fermilab Lattice collaboration, MILC collaboration, HPQCD collaboration collaboration), *Phys.Rev.Lett.* **94**, 011601 (2005), [arXiv:hep-ph/0408306](#) [hep-ph].
- [496] H. Na, C. T. Davies, E. Follana, G. P. Lepage, and J. Shigemitsu, *Phys.Rev.* **D82**, 114506 (2010), [arXiv:1008.4562](#) [hep-lat].
- [497] H. Na, C. T. Davies, E. Follana, J. Koponen, G. P. Lepage, *et al.*, *Phys.Rev.* **D84**, 114505 (2011), [arXiv:1109.1501](#) [hep-lat].
- [498] J. Anjos *et al.* (Tagged Photon Spectrometer collaboration collaboration), *Phys.Rev.Lett.* **62**, 1587–1590 (1989).
- [499] G. D. Crawford *et al.* (CLEO collaboration), *Phys.Rev.* **D44**, 3394–3401 (1991).

- [500] A. Bean *et al.* (CLEO collaboration), Phys.Lett. **B317**, 647–654 (1993).
- [501] F. Butler *et al.* (CLEO collaboration), Phys.Rev. **D52**, 2656–2660 (1995).
- [502] P. Frabetti *et al.* (E687 collaboration), Phys.Lett. **B364**, 127–136 (1995).
- [503] P. Frabetti *et al.* (E687 collaboration), Phys.Lett. **B382**, 312–322 (1996).
- [504] M. Ablikim *et al.* (BES collaboration), Phys.Lett. **B597**, 39–46 (2004),
arXiv:hep-ex/0406028 [hep-ex].
- [505] J. Anjos *et al.* (Fermilab E691 collaboration), Phys.Rev.Lett. **65**, 2630–2633 (1990).
- [506] K. Kodama *et al.* (Fermilab E653 collaboration), Phys.Lett. **B274**, 246–252 (1992).
- [507] P. Frabetti *et al.* (Fermilab E687 collaboration), Phys.Lett. **B307**, 262–268 (1993).
- [508] E. Aitala *et al.* (E791 collaboration), Phys.Rev.Lett. **80**, 1393–1397 (1998),
arXiv:hep-ph/9710216 [hep-ph].
- [509] E. Aitala *et al.* (E791 collaboration), Phys.Lett. **B440**, 435–441 (1998),
arXiv:hep-ex/9809026 [hep-ex].
- [510] M. Adamovich *et al.* (BEATRICE collaboration), Eur.Phys.J. **C6**, 35–41 (1999).
- [511] J. Link *et al.* (FOCUS collaboration), Phys.Lett. **B544**, 89–96 (2002),
arXiv:hep-ex/0207049 [hep-ex].
- [512] J. Link *et al.* (FOCUS collaboration), Phys.Lett. **B607**, 67–77 (2005),
arXiv:hep-ex/0410067 [hep-ex].
- [513] P. del Amo Sanchez *et al.* (BABAR collaboration), Phys.Rev. **D83**, 072001 (2011),
arXiv:1012.1810 [hep-ex].
- [514] B. Aubert *et al.* (BABAR collaboration), Phys. Rev. **D78**, 051101 (2008),
arXiv:0807.1599 [hep-ex].
- [515] H. Mahlke, eConf **C0610161**, 014 (2006), arXiv:hep-ex/0702014 [hep-ex].
- [516] J. Link *et al.* (FOCUS collaboration), Phys.Lett. **B535**, 43–51 (2002),
arXiv:hep-ex/0203031 [hep-ex].
- [517] K. M. Ecklund *et al.* (CLEO collaboration), Phys. Rev. **D80**, 052009 (2009),
arXiv:0907.3201 [hep-ex].
- [518] R. A. Briere *et al.* (CLEO collaboration), Phys.Rev. **D81**, 112001 (2010),
arXiv:1004.1954 [hep-ex].
- [519] P. Estabrooks, R. Carnegie, A. D. Martin, W. Dunwoodie, T. Lasinski, *et al.*,
Nucl.Phys. **B133**, 490 (1978).
- [520] I. I. Y. Bigi and A. I. Sanda, Camb. Monogr. Part. Phys. Nucl. Phys. Cosmol. **9**, 1–382
(2000).

- [521] Y. Nir (1999), [arXiv:hep-ph/9911321](#).
- [522] F. Buccella, M. Lusignoli, G. Miele, A. Pugliese, and P. Santorelli, *Phys. Rev.* **D51**, 3478–3486 (1995), [arXiv:hep-ph/9411286](#).
- [523] B. I. Eisenstein *et al.* (CLEO collaboration), *Phys. Rev.* **D78**, 052003 (2008), [arXiv:0806.2112 \[hep-ex\]](#).
- [524] H. Mendez *et al.* (CLEO collaboration), *Phys. Rev.* **D81**, 052013 (2010), [arXiv:0906.3198 \[hep-ex\]](#).
- [525] P. del Amo Sanchez *et al.* (BABAR collaboration), *Phys. Rev.* **D83**, 071103 (2011), [arXiv:1011.5477 \[hep-ex\]](#).
- [526] B. R. Ko, E. Won, *et al.* (Belle collaboration), *Phys. Rev. Lett.* **104**, 181602 (2010), [arXiv:1001.3202 \[hep-ex\]](#).
- [527] J. M. Link *et al.* (FOCUS collaboration), *Phys. Rev. Lett.* **88**, 041602; 159903(E) (2002), [arXiv:hep-ex/0109022](#).
- [528] E. M. Aitala *et al.* (E791 collaboration), *Phys. Lett.* **B403**, 377–382 (1997), [arXiv:hep-ex/9612005](#).
- [529] S. Dobbs *et al.* (CLEO collaboration), *Phys. Rev.* **D76**, 112001 (2007), [arXiv:0709.3783 \[hep-ex\]](#).
- [530] P. Rubin *et al.* (CLEO collaboration), *Phys. Rev.* **D78**, 072003 (2008), [arXiv:0807.4545 \[hep-ex\]](#).
- [531] B. Aubert *et al.* (BABAR collaboration), *Phys. Rev.* **D71**, 091101 (2005), [arXiv:hep-ex/0501075](#).
- [532] J. M. Link *et al.* (FOCUS collaboration), *Phys. Lett.* **B491**, 232–239 (2000), [arXiv:hep-ex/0005037](#).
- [533] P. L. Frabetti *et al.* (E687 collaboration), *Phys. Rev.* **D50**, 2953–2956 (1994).
- [534] J. M. Link *et al.* (FOCUS collaboration), *Phys. Lett.* **B622**, 239–248 (2005), [arXiv:hep-ex/0506012](#).
- [535] T. Aaltonen *et al.* (CDF collaboration), *Phys. Rev.* **D85**, 012009 (2012), [arXiv:1111.5023 \[hep-ex\]](#).
- [536] E. M. Aitala *et al.* (E791 collaboration), *Phys. Lett.* **B421**, 405–411 (1998), [arXiv:hep-ex/9711003](#).
- [537] G. Bonvicini *et al.* (CLEO collaboration), *Phys. Rev.* **D63**, 071101 (2001), [arXiv:hep-ex/0012054](#).
- [538] B. R. Ko *et al.* (Belle collaboration), *Phys. Rev. Lett.* **106**, 211801 (2011), [arXiv:1101.3365 \[hep-ex\]](#).

- [539] J. E. Bartelt *et al.* (CLEO collaboration), Phys. Rev. **D52**, 4860–4867 (1995).
- [540] B. Aubert *et al.* (*BABAR* collaboration), Phys. Rev. **D78**, 051102 (2008),
arXiv:0802.4035 [hep-ex].
- [541] K. Arinstein (Belle collaboration), Phys. Lett. **B662**, 102–110 (2008),
arXiv:0801.2439 [hep-ex].
- [542] D. Cronin-Hennessy *et al.* (CLEO collaboration), Phys. Rev. **D72**, 031102 (2005),
arXiv:hep-ex/0503052.
- [543] S. Kopp *et al.* (CLEO collaboration), Phys. Rev. **D63**, 092001 (2001),
arXiv:hep-ex/0011065.
- [544] X. C. Tian *et al.* (Belle collaboration), Phys. Rev. Lett. **95**, 231801 (2005),
arXiv:hep-ex/0507071.
- [545] G. Brandenburg *et al.* (CLEO collaboration), Phys. Rev. Lett. **87**, 071802 (2001),
arXiv:hep-ex/0105002.
- [546] D. M. Asner *et al.* (CLEO collaboration), Phys. Rev. **D70**, 091101 (2004),
arXiv:hep-ex/0311033.
- [547] J. Alexander *et al.* (CLEO collaboration), Phys. Rev. **D79**, 052001 (2009),
arXiv:0901.1216 [hep-ex].
- [548] J. P. Alexander *et al.* (CLEO collaboration), Phys. Rev. Lett. **100**, 161804 (2008),
arXiv:0801.0680 [hep-ex].
- [549] E. Golowich and G. Valencia, Phys. Rev. **D40**, 112 (1989).
- [550] I. I. Y. Bigi (2001), arXiv:hep-ph/0107102.
- [551] W. Bensalem, A. Datta, and D. London, Phys. Rev. **D66**, 094004 (2002),
arXiv:hep-ph/0208054.
- [552] W. Bensalem and D. London, Phys. Rev. **D64**, 116003 (2001), arXiv:hep-ph/0005018.
- [553] W. Bensalem, A. Datta, and D. London, Phys. Lett. **B538**, 309–320 (2002),
arXiv:hep-ph/0205009.
- [554] P. del Amo Sanchez *et al.* (*BABAR* collaboration), Phys. Rev. **D81**, 111103 (2010),
arXiv:1003.3397 [hep-ex].
- [555] J. P. Lees *et al.* (*BABAR* collaboration), Phys. Rev. **D84**, 031103 (2011),
arXiv:1105.4410 [hep-ex].
- [556] P. del Amo Sanchez *et al.* (*BABAR* collaboration), Phys. Rev. **D82**, 091103 (2010),
arXiv:1008.4080 [hep-ex].
- [557] Belle collaboration, presented at Charm 2012, 2012,
<http://www.phys.hawaii.edu/indico/contributionDisplay.py?contribId=45&confId=338>.

- [558] P. Onyisi *et al.* (CLEO collaboration), Phys.Rev. **D79**, 052002 (2009), arXiv:0901.1147 [hep-ex].
- [559] P. Naik *et al.* (CLEO collaboration), Phys.Rev. **D80**, 112004 (2009), arXiv:0910.3602 [hep-ex].
- [560] J. Lees *et al.* (BABAR collaboration) (2010), arXiv:1003.3063 [hep-ex].
- [561] A. Heister *et al.* (ALEPH collaboration), Phys.Lett. **B528**, 1–18 (2002), arXiv:hep-ex/0201024 [hep-ex].
- [562] Y. Alexandrov *et al.* (BEATRICE collaboration), Phys.Lett. **B478**, 31–38 (2000).
- [563] G. Abbiendi *et al.* (OPAL collaboration), Phys.Lett. **B516**, 236–248 (2001), arXiv:hep-ex/0103012 [hep-ex].
- [564] M. Acciarri *et al.* (L3 collaboration), Phys.Lett. **B396**, 327–337 (1997).
- [565] 1999, <http://www.slac.stanford.edu/xorg/hfag/docs/combo.ps>.
- [566] E. Barberio, B. van Eijk, and Z. Was, Comput. Phys. Commun. **66**, 115–128 (1991).
- [567] E. Barberio and Z. Was, Comput. Phys. Commun. **79**, 291–308 (1994).
- [568] P. Golonka and Z. Was, Eur. Phys. J. **C45**, 97–107 (2006), arXiv:hep-ph/0506026.
- [569] P. Golonka and Z. Was, Eur. Phys. J. **C50**, 53–62 (2007), arXiv:hep-ph/0604232.
- [570] A. Ryd *et al.* (2005), EVTGEN-V00-11-07.
- [571] J. M. Link *et al.* (FOCUS collaboration), Phys. Lett. **B555**, 167–173 (2003), arXiv:hep-ex/0212058.
- [572] B. Aubert *et al.* (BABAR collaboration), Phys. Rev. Lett. **100**, 051802 (2008), arXiv:0704.2080 [hep-ex].
- [573] M. Artuso *et al.* (CLEO collaboration), Phys. Rev. Lett. **80**, 3193–3197 (1998), arXiv:hep-ex/9712023.
- [574] R. Barate *et al.* (ALEPH collaboration), Phys. Lett. **B403**, 367–376 (1997).
- [575] H. Albrecht *et al.* (ARGUS collaboration), Phys. Lett. **B340**, 125–128 (1994).
- [576] D. S. Akerib *et al.* (CLEO collaboration), Phys. Rev. Lett. **71**, 3070–3074 (1993).
- [577] D. Decamp *et al.* (ALEPH collaboration), Phys. Lett. **B266**, 218–230 (1991).
- [578] D. E. Acosta *et al.* (CDF collaboration), Phys. Rev. Lett. **94**, 122001 (2005), arXiv:hep-ex/0504006.
- [579] T. E. Coan *et al.* (CLEO collaboration), Phys. Rev. Lett. **80**, 1150–1155 (1998), arXiv:hep-ex/9710028.

- [580] Y. Grossman, A. L. Kagan, and Y. Nir, Phys.Rev. **D75**, 036008 (2007), arXiv:hep-ph/0609178 [hep-ph].
- [581] M. Gersabeck, M. Alexander, S. Borghi, V. Gligorov, and C. Parkes, J.Phys.G **G39**, 045005 (2012), arXiv:1111.6515 [hep-ex].
- [582] T. Aaltonen *et al.* (CDF collaboration), Phys.Rev. **D84**, 012003 (2011), arXiv:1105.5995 [hep-ex].
- [583] M. Artuso *et al.* (CLEO collaboration), Phys.Rev.Lett. **86**, 4479–4482 (2001), arXiv:hep-ex/0010080 [hep-ex].
- [584] B. Aubert *et al.* (BABAR collaboration), Phys.Rev.Lett. **98**, 012001 (2007), arXiv:hep-ex/0603052 [hep-ex].
- [585] H.-Y. Cheng and C.-K. Chua, Phys.Rev. **D75**, 014006 (2007), arXiv:hep-ph/0610283 [hep-ph].
- [586] R. Mizuk *et al.* (Belle collaboration), Phys.Rev.Lett. **94**, 122002 (2005), arXiv:hep-ex/0412069 [hep-ex].
- [587] L. Copley, N. Isgur, and G. Karl, Phys.Rev. **D20**, 768 (1979).
- [588] D. Pirjol and T.-M. Yan, Phys.Rev. **D56**, 5483–5510 (1997), arXiv:hep-ph/9701291 [hep-ph].
- [589] R. Chistov *et al.* (Belle collaboration), Phys.Rev.Lett. **97**, 162001 (2006), arXiv:hep-ex/0606051 [hep-ex].
- [590] B. Aubert *et al.* (BABAR collaboration), Phys.Rev. **D77**, 012002 (2008), arXiv:0710.5763 [hep-ex].
- [591] B. Aubert *et al.* (BABAR collaboration), Phys.Rev.Lett. **97**, 232001 (2006), arXiv:hep-ex/0608055 [hep-ex].
- [592] E. Solovieva, R. Chistov, I. Adachi, H. Aihara, K. Arinstein, *et al.*, Phys.Lett. **B672**, 1–5 (2009), arXiv:0808.3677 [hep-ex].
- [593] J. L. Rosner, Phys.Rev. **D52**, 6461–6465 (1995), arXiv:hep-ph/9508252 [hep-ph].
- [594] L. Y. Glozman and D. Riska, Nucl.Phys. **A603**, 326–344 (1996), arXiv:hep-ph/9509269 [hep-ph].
- [595] E. E. Jenkins, Phys.Rev. **D54**, 4515–4531 (1996), arXiv:hep-ph/9603449 [hep-ph].
- [596] L. Burakovsky, J. T. Goldman, and L. Horwitz, Phys.Rev. **D56**, 7124–7132 (1997), arXiv:hep-ph/9706464 [hep-ph].
- [597] G. Burdman, E. Golowich, J. L. Hewett, and S. Pakvasa, Phys.Rev. **D66**, 014009 (2002), arXiv:hep-ph/0112235 [hep-ph].

- [598] S. Fajfer, A. Prapotnik, S. Prelovsek, P. Singer, and J. Zupan, Nucl.Phys.Proc.Suppl. **115**, 93–97 (2003), [arXiv:hep-ph/0208201](#) [hep-ph].
- [599] S. Fajfer, N. Kosnik, and S. Prelovsek, Phys.Rev. **D76**, 074010 (2007), [arXiv:0706.1133](#) [hep-ph].
- [600] E. Golowich, J. Hewett, S. Pakvasa, and A. A. Petrov, Phys.Rev. **D79**, 114030 (2009), [arXiv:0903.2830](#) [hep-ph].
- [601] A. Paul, I. I. Bigi, and S. Recksiegel, Phys.Rev. **D82**, 094006 (2010), [arXiv:1008.3141](#) [hep-ph].
- [602] A. Borisov (2011), [arXiv:1112.3269](#) [hep-ph].
- [603] T. Coan *et al.* (CLEO collaboration), Phys.Rev.Lett. **90**, 101801 (2003), [arXiv:hep-ex/0212045](#) [hep-ex].
- [604] J. Lees (*BABAR* collaboration) (2011), [arXiv:1110.6480](#) [hep-ex].
- [605] P. Haas *et al.* (CLEO collaboration), Phys.Rev.Lett. **60**, 1614 (1988).
- [606] H. Albrecht *et al.* (ARGUS collaboration), Phys.Lett. **B209**, 380 (1988).
- [607] J. Adler *et al.* (MARK-III collaboration), Phys.Rev. **D37**, 2023 (1988), erratum *ibid* **D40**, 3788 (1989).
- [608] A. Freyberger *et al.* (CLEO collaboration), Phys.Rev.Lett. **76**, 3065–3069 (1996).
- [609] D. Pripstein *et al.* (E789 collaboration), Phys.Rev. **D61**, 032005 (2000), [arXiv:hep-ex/9906022](#) [hep-ex].
- [610] E. Aitala *et al.* (E791 collaboration), Phys.Lett. **B462**, 401–409 (1999), [arXiv:hep-ex/9906045](#) [hep-ex].
- [611] B. Aubert *et al.* (*BABAR* collaboration), Phys.Rev.Lett. **93**, 191801 (2004), [arXiv:hep-ex/0408023](#) [hep-ex].
- [612] M. Petric *et al.* (Belle collaboration), Phys.Rev. **D81**, 091102 (2010), [arXiv:1003.2345](#) [hep-ex].
- [613] K. Kodama *et al.* (E653 collaboration), Phys.Lett. **B345**, 85–92 (1995).
- [614] I. Abt *et al.* (HERA-B collaboration), Phys.Lett. **B596**, 173–183 (2004), [arXiv:hep-ex/0405059](#) [hep-ex].
- [615] T. Aaltonen *et al.* (CDF collaboration), Phys.Rev. **D82**, 091105 (2010), [arXiv:1008.5077](#) [hep-ex].
- [616] LHCb-CONF-2012-005, 2012, <https://cdsweb.cern.ch/record/1426268?ln=en>.
- [617] E. Aitala *et al.* (E791 collaboration), Phys.Rev.Lett. **86**, 3969–3972 (2001), [arXiv:hep-ex/0011077](#) [hep-ex].

- [618] J. Adler *et al.* (MARK-III collaboration), Phys.Rev. **D40**, 906 (1989).
- [619] J. Becker *et al.* (MARK-III collaboration), Phys.Lett. **B193**, 147 (1987).
- [620] P. Rubin *et al.* (CLEO collaboration), Phys.Rev. **D79**, 097101 (2009),
arXiv:0904.1619 [hep-ex].
- [621] P. Frabetti *et al.* (E687 collaboration), Phys.Lett. **B398**, 239–244 (1997).
- [622] P. Rubin *et al.* (CLEO collaboration), Phys.Rev. **D82**, 092007 (2010),
arXiv:1009.1606 [hep-ex].
- [623] J. Lees *et al.* (BABAR collaboration), Phys.Rev. **D84**, 072006 (2011),
arXiv:1107.4465 [hep-ex].
- [624] J. Link *et al.* (FOCUS collaboration), Phys.Lett. **B572**, 21–31 (2003),
arXiv:hep-ex/0306049 [hep-ex].
- [625] V. Abazov *et al.* (D0 collaboration), Phys.Rev.Lett. **100**, 101801 (2008),
arXiv:0708.2094 [hep-ex].
- [626] M. Davier. Private communication, 2011.
- [627] R. Barate *et al.* (ALEPH collaboration), Eur.Phys.J. **C4**, 29–45 (1998),
<http://cdsweb.cern.ch/record/346304>.
- [628] R. Barate *et al.* (ALEPH collaboration), Eur.Phys.J. **C11**, 599–618 (1999),
arXiv:hep-ex/9903015 [hep-ex].
- [629] S. Schael *et al.* (ALEPH collaboration), Phys.Rept. **421**, 191–284 (2005),
arXiv:hep-ex/0506072 [hep-ex], HFAG-tau uses measurements of $\tau \rightarrow hX$ and
 $\tau \rightarrow KX$ and obtains $\tau \rightarrow \pi X$ by difference; the measurement of
 $\mathcal{B}(\tau^- \rightarrow 3h^-2h^+\pi^0\nu_\tau)$ (ex. K^0) has been read as $(2.1 \pm 0.7 \pm 0.6) \times 10^{-4}$ whereas
PDG11 uses $(2.1 \pm 0.7 \pm 0.9) \times 10^{-4}$.
- [630] P. del Amo Sanchez *et al.* (BABAR collaboration), Phys.Rev. **D83**, 032002 (2011),
arXiv:1011.3917 [hep-ex].
- [631] S. Ryu (Belle collaboration), “Measurement of the branching fractions for
 $\tau^- \rightarrow \pi^- K_S \pi^0 \nu_\tau$ and $\tau^- \rightarrow K^- K_S \pi^0 \nu_\tau$.” Presented at the International Workshop on
 e^+e^- collisions from phi to psi (PHIPSI11), Novosibirsk, 19-22 Sep, 2011.
http://q2c.snu.ac.kr/sryu/phipsi2011_sryu.pdf. To be published in Nucl. Phys.
B Proceedings Supplement.
- [632] P. Abreu *et al.* (DELPHI collaboration), Eur.Phys.J. **C10**, 201–218 (1999).
- [633] M. Acciarri *et al.* (L3 collaboration), Phys.Lett. **B507**, 47–60 (2001),
arXiv:hep-ex/0102023 [hep-ex].
- [634] G. Abbiendi *et al.* (OPAL collaboration), Phys.Lett. **B551**, 35–48 (2003),
arXiv:hep-ex/0211066 [hep-ex].

- [635] H. Albrecht *et al.* (ARGUS collaboration), Z.Phys. **C53**, 367–374 (1992).
- [636] B. Aubert *et al.* (BABAR collaboration), Phys.Rev.Lett. **105**, 051602 (2010), arXiv:0912.0242 [hep-ex].
- [637] A. Anastassov *et al.* (CLEO collaboration), Phys.Rev. **D55**, 2559–2576 (1997), erratum ibid **D58**, 119903 (1998).
- [638] G. Abbiendi *et al.* (OPAL collaboration), Phys.Lett. **B447**, 134–146 (1999), arXiv:hep-ex/9812017 [hep-ex].
- [639] P. Abreu *et al.* (DELPHI collaboration), Z.Phys. **C55**, 555–568 (1992).
- [640] M. Acciarri *et al.* (L3 collaboration), Phys.Lett. **B345**, 93–102 (1995).
- [641] G. Alexander *et al.* (OPAL collaboration), Phys.Lett. **B266**, 201–217 (1991).
- [642] J. Abdallah *et al.* (DELPHI collaboration), Eur.Phys.J. **C46**, 1–26 (2006), arXiv:hep-ex/0603044 [hep-ex].
- [643] K. Ackerstaff *et al.* (OPAL collaboration), Eur.Phys.J. **C4**, 193–206 (1998), arXiv:hep-ex/9801029 [hep-ex].
- [644] R. Barate *et al.* (ALEPH collaboration), Eur.Phys.J. **C10**, 1–18 (1999), arXiv:hep-ex/9903014 [hep-ex].
- [645] M. Battle *et al.* (CLEO collaboration), Phys.Rev.Lett. **73**, 1079–1083 (1994), arXiv:hep-ph/9403329 [hep-ph].
- [646] P. Abreu *et al.* (DELPHI collaboration), Phys.Lett. **B334**, 435–449 (1994).
- [647] G. Abbiendi *et al.* (OPAL collaboration), Eur.Phys.J. **C19**, 653–665 (2001), arXiv:hep-ex/0009017 [hep-ex].
- [648] M. Fujikawa *et al.* (Belle collaboration), Phys.Rev. **D78**, 072006 (2008), arXiv:0805.3773 [hep-ex].
- [649] M. Artuso *et al.* (CLEO collaboration), Phys.Rev.Lett. **72**, 3762–3766 (1994), arXiv:hep-ph/9404310 [hep-ph].
- [650] B. Aubert *et al.* (BABAR collaboration), Phys.Rev. **D76**, 051104 (2007), arXiv:0707.2922 [hep-ex].
- [651] G. Abbiendi *et al.* (OPAL collaboration), Eur.Phys.J. **C35**, 437–455 (2004), arXiv:hep-ex/0406007 [hep-ex].
- [652] M. Procaro *et al.* (CLEO collaboration), Phys.Rev.Lett. **70**, 1207–1211 (1993).
- [653] R. Akers *et al.* (OPAL collaboration), Phys.Lett. **B339**, 278–292 (1994).
- [654] T. Coan *et al.* (CLEO collaboration), Phys.Rev. **D53**, 6037–6053 (1996).

- [655] B. Aubert *et al.* (*BABAR* collaboration), Nucl. Phys. Proc. Suppl. **189**, 193–198 (2009), arXiv:0808.1121 [hep-ex], contributed to 34th International Conference on High Energy Physics (ICHEP 2008), Philadelphia, Pennsylvania, 30 Jul - 5 Aug 2008.
- [656] D. Epifanov *et al.* (Belle collaboration), Phys.Lett. **B654**, 65–73 (2007), arXiv:0706.2231 [hep-ex].
- [657] M. Acciarri *et al.* (L3 collaboration), Phys.Lett. **B352**, 487–497 (1995).
- [658] G. Abbiendi *et al.* (OPAL collaboration), Eur.Phys.J. **C13**, 213–223 (2000), arXiv:hep-ex/9911029 [hep-ex].
- [659] S. Paramesvaran (*BABAR* collaboration) (2009), arXiv:0910.2884 [hep-ex], contributed to the proceedings of Meeting of the Division of Particles and Fields of the American Physical Society (DPF 2009), Detroit, Michigan, 26-31 Jul 2009.
- [660] H. Behrend *et al.* (CELLO collaboration), Phys.Lett. **B222**, 163 (1989).
- [661] B. Adeva *et al.* (L3 collaboration), Phys.Lett. **B265**, 451–461 (1991).
- [662] H. Aihara *et al.* (TPC/Two Gamma collaboration), Phys.Rev. **D35**, 1553 (1987).
- [663] P. Achard *et al.* (L3 collaboration), Phys.Lett. **B519**, 189–198 (2001), arXiv:hep-ex/0107055 [hep-ex].
- [664] R. Akers *et al.* (OPAL collaboration), Z.Phys. **C68**, 555–568 (1995).
- [665] R. Balest *et al.* (CLEO collaboration), Phys.Rev.Lett. **75**, 3809–3813 (1995).
- [666] B. Aubert *et al.* (*BABAR* collaboration), Phys.Rev.Lett. **100**, 011801 (2008), arXiv:0707.2981 [hep-ex].
- [667] M. Lee *et al.* (Belle collaboration), Phys.Rev. **D81**, 113007 (2010), arXiv:1001.0083 [hep-ex], HFAG-tau uses more detailed and numerically precise information on errors and correlations that has been privately provided by the Belle collaboration; the errors have been symmetrized.
- [668] R. A. Briere *et al.* (CLEO collaboration), Phys.Rev.Lett. **90**, 181802 (2003), arXiv:hep-ex/0302028 [hep-ex].
- [669] K. Edwards *et al.* (CLEO collaboration), Phys.Rev. **D61**, 072003 (2000), arXiv:hep-ex/9908024 [hep-ex].
- [670] D. Bortoletto *et al.* (CLEO collaboration), Phys.Rev.Lett. **71**, 1791–1795 (1993).
- [671] A. Anastassov *et al.* (CLEO collaboration), Phys.Rev.Lett. **86**, 4467–4471 (2001), arXiv:hep-ex/0010025 [hep-ex].
- [672] S. Richichi *et al.* (CLEO collaboration), Phys.Rev. **D60**, 112002 (1999), arXiv:hep-ex/9810026 [hep-ex].
- [673] D. A. Bauer *et al.* (TPC/Two Gamma collaboration), Phys.Rev. **D50**, 13–17 (1994).

- [674] R. Barate *et al.* (ALEPH collaboration), *Eur.Phys.J.* **C1**, 65–79 (1998).
- [675] K. E. Arms *et al.* (CLEO collaboration), *Phys.Rev.Lett.* **94**, 241802 (2005), [arXiv:hep-ex/0501042](#) [[hep-ex](#)].
- [676] G. Abbiendi *et al.* (OPAL collaboration), *Eur.Phys.J.* **C13**, 197–212 (2000), [arXiv:hep-ex/9908013](#) [[hep-ex](#)].
- [677] D. Gibaut *et al.* (CLEO collaboration), *Phys.Rev.Lett.* **73**, 934–938 (1994).
- [678] B. Bylsma, S. Abachi, P. S. Baringer, R. DeBonte, D. Koltick, *et al.*, *Phys.Rev.* **D35**, 2269 (1987).
- [679] H. Albrecht *et al.* (ARGUS collaboration), *Phys.Lett.* **B202**, 149 (1988).
- [680] B. Aubert *et al.* (BaBar collaboration), *Phys.Rev.* **D72**, 072001 (2005), [arXiv:hep-ex/0505004](#) [[hep-ex](#)].
- [681] K. Ackerstaff *et al.* (OPAL collaboration), *Eur.Phys.J.* **C8**, 183–189 (1999), [arXiv:hep-ex/9808011](#) [[hep-ex](#)].
- [682] D. Buskulic *et al.* (ALEPH collaboration), *Z.Phys.* **C74**, 263–273 (1997).
- [683] K. Inami *et al.* (Belle collaboration), *Phys.Lett.* **B672**, 209–218 (2009), [arXiv:0811.0088](#) [[hep-ex](#)].
- [684] M. Artuso *et al.* (CLEO collaboration), *Phys.Rev.Lett.* **69**, 3278–3281 (1992).
- [685] M. Bishai *et al.* (CLEO collaboration), *Phys.Rev.Lett.* **82**, 281–285 (1999), [arXiv:hep-ex/9809012](#) [[hep-ex](#)].
- [686] B. Aubert *et al.* (BABAR collaboration), *Phys.Rev.* **D77**, 112002 (2008), [arXiv:0803.0772](#) [[hep-ex](#)].
- [687] P. S. Baringer *et al.* (CLEO collaboration), *Phys.Rev.Lett.* **59**, 1993 (1987).
- [688] D. Buskulic *et al.* (ALEPH collaboration), *Z.Phys.* **C70**, 579–608 (1996).
- [689] W. Marciano and A. Sirlin, *Phys.Rev.Lett.* **61**, 1815–1818 (1988).
- [690] R. Decker and M. Finkemeier, *Phys.Lett.* **B334**, 199–202 (1994).
- [691] M. Davier, A. Hocker, and Z. Zhang, *Rev.Mod.Phys.* **78**, 1043–1109 (2006), [arXiv:hep-ph/0507078](#) [[hep-ph](#)].
- [692] E. Gamiz, M. Jamin, A. Pich, J. Prades, and F. Schwab, *Nucl. Phys. Proc. Suppl.* **169**, 85–89 (2007), [arXiv:hep-ph/0612154](#).
- [693] E. Gamiz, M. Jamin, A. Pich, J. Prades, and F. Schwab, *PoS KAON*, 008 (2008), [arXiv:0709.0282](#) [[hep-ph](#)].
- [694] K. Maltman (2010), [arXiv:1011.6391](#) [[hep-ph](#)].

- [695] J. C. Hardy and I. S. Towner, Phys. Rev. **C79**, 055502 (2009),
arXiv:0812.1202 [nucl-ex].
- [696] S. Banerjee, K. Hayasaka, H. Hayashii, A. Lusiani, J. Roney, *et al.*,
Nucl. Phys. Proc. Suppl. **218**, 329–334 (2011), arXiv:1101.5138 [hep-ex].
- [697] S. Banerjee (*BABAR* collaboration) (2008), arXiv:0811.1429 [hep-ex], presented at
ICHEP08, Philadelphia, USA, July, 2008.
- [698] R. Decker and M. Finkemeier, Nucl. Phys. **B438**, 17–53 (1995),
arXiv:hep-ph/9403385.
- [699] W. J. Marciano, Phys. Rev. Lett. **93**, 231803 (2004), arXiv:hep-ph/0402299.
- [700] J. Erler, Rev. Mex. Fis. **50**, 200–202 (2004), arXiv:hep-ph/0211345.
- [701] P. J. Mohr, B. N. Taylor, and D. B. Newell, Rev.Mod.Phys. **80**, 633–730 (2008),
arXiv:0801.0028 [physics.atom-ph].
- [702] M. Antonelli, V. Cirigliano, G. Isidori, F. Mescia, M. Moulson, *et al.*,
Eur.Phys.J. **C69**, 399–424 (2010), arXiv:1005.2323 [hep-ph].
- [703] K. Hayasaka *et al.* (*Belle* collaboration), Phys.Lett. **B666**, 16–22 (2008),
arXiv:0705.0650 [hep-ex].
- [704] B. Aubert *et al.* (*BABAR* collaboration), Phys.Rev.Lett. **104**, 021802 (2010),
arXiv:0908.2381 [hep-ex].
- [705] K. Hayasaka (*Belle* collaboration), J.Phys.Conf.Ser. **335**, 012029 (2011).
- [706] B. Aubert *et al.* (*BABAR* collaboration), Phys.Rev.Lett. **98**, 061803 (2007),
arXiv:hep-ex/0610067 [hep-ex].
- [707] Y. Miyazaki *et al.* (*Belle* collaboration), Phys.Lett. **B692**, 4–9 (2010),
arXiv:1003.1183 [hep-ex].
- [708] B. Aubert *et al.* (*BABAR* collaboration), Phys.Rev. **D79**, 012004 (2009),
arXiv:0812.3804 [hep-ex].
- [709] Y. Miyazaki *et al.* (*Belle* collaboration), Phys.Lett. **B672**, 317–322 (2009),
arXiv:0810.3519 [hep-ex].
- [710] Y. Miyazaki (*Belle* collaboration), Phys.Lett. **B699**, 251–257 (2011),
arXiv:1101.0755 [hep-ex].
- [711] B. Aubert *et al.* (*BABAR* collaboration), Phys.Rev.Lett. **103**, 021801 (2009),
arXiv:0904.0339 [hep-ex].
- [712] B. Aubert *et al.* (*BABAR* collaboration), Phys.Rev.Lett. **100**, 071802 (2008),
arXiv:0711.0980 [hep-ex].

- [713] K. Hayasaka, K. Inami, Y. Miyazaki, K. Arinstein, V. Aulchenko, *et al.*, Phys.Lett. **B687**, 139–143 (2010), arXiv:1001.3221 [hep-ex].
- [714] J. Lees *et al.* (BABAR collaboration), Phys.Rev. **D81**, 111101 (2010), arXiv:1002.4550 [hep-ex].
- [715] Y. Miyazaki *et al.* (Belle collaboration) (2012), arXiv:1206.5595 [hep-ex].
- [716] B. Aubert *et al.* (BABAR collaboration), Phys.Rev.Lett. **95**, 191801 (2005), arXiv:hep-ex/0506066 [hep-ex].
- [717] K. Hayasaka (Belle collaboration), “Recent LFV results on tau lepton from Belle.” Presented at the International Workshop on e^+e^- collisions from phi to psi (PHIPSI11), Novosibirsk, 19-22 Sep, 2011.
http://phipsi11.inp.nsk.su/talks/phipsi11_hayasaka.pdf. To be published in Nucl. Phys. B Proceedings Supplement.
- [718] G. Lafferty (BABAR collaboration), Nucl.Phys.Proc.Suppl. **169**, 186–191 (2007).